THE GEOLOGY OF THE RAS ED DOM AND ABU DOM IGNEOUS RING-COMPLEXES BAYUDA DESERT, SUDAN

DESMOND ANTHONY O'HALLORAN
B.A. NAT. SCI. (HONS)

A thesis submitted for the Degree of Doctor
of Philosophy of the Council of National
Academic Awards

School of Geology, Kingston Polytechnic

June, 1982

frontispiece : The curved outcrop of the Syenite 3 ring-dyke, north west Abu Dom complex. Viewed facing south westwards.

This thesis is dedicated to my mother and father.

THE GEOLOGY OF THE RAS ED DOM AND ABU DOM IGNEOUS RING-COMPLEXES BAYUDA DESERT, SUDAN.

Ras ed Dom and Abu Dom are two anorogenic ring-complexes, of Triassic age, emplaced into the Precambrian gneisses of the central Bayuda Desert in northern Sudan. The two complexes are closely similar lithologically and are composed of early-formed subaluminous syenites, and later peralkaline syenites and granites. The intrusions are emplaced as sub-volcanic stocks and ring-dykes and both complexes are partly girdled by acid cone-sheet swarms. Minor occurrences of acid volcanic rocks are also present. Ras ed Dom is a striking example of a migrating ring-complex, and in it the focus of magmatism migrated eastwards, and declined in strength, with time. Field relations indicate that the sequence early syenite → alkali syenite → alkali granite constitutes a recurrent fractionation series in the complexes. The early syenites occasionally contain early-formed plagioclase, but in general the suite is typically hypersolvus. Feldspar bulk compositions cluster close to Or38 Ab62, and the most calcic composition (An 7 mol%) is from an early syenite. Pyroxenes in the subaluminous units are zoned from cores of ferrohedenbergite to rims of aegirine-augite, and are enclosed within later ferroedenite. Amphiboles in the peralkaline rocks range from ferrorichterite through arfvedsonite compositions to riebeckite. Late aegirine typically replaces alkali amphibole, especially in the granites. Aenigmatite is an additional mafic phase in some of the syenites. Minor late albite is common in the peralkaline rocks. The principal cryptic variation in the mafic phases is the substitution of Na and Fe^{3+} for Mg, Ca and Fe^{2+}. Major element variation in the rocks supports the proposed fractionation sequence, and it is apparent that the main changes with fractionation are enrichment in SiO_2 and Fe_2O_3 relative to FeO, together with an increase in alkalinity due to Al_2O_3 depletion relative to the alkalies. Relations to alkali-rich analogues of the 'granite system' confirm a magmatic origin , and trends in terms of SiO_2 - Al_2O_3 - (Na_2O + K_2O) suggest that fractionation of alkali-feldspar is the major process in the evolution of the rock-series. Major depletions in Sr and Ba support this hypothesis, as does the variation in Rb/Sr ratios. In

common with other alkaline provinces the Bayuda rocks exhibit strong enrichment in incompatibile elements such as Zr, Nb, Rb, Y and the LREE group. Concentrations are highest in the granites and this may reflect in part the overprinting by late sodic residual fluids. Partial REE trends are characterised by LREE enrichment, and are consistent with a cogenetic origin for the rocks. The parental melt is believed to have been similar in composition to the early syenites, and is considered to have been generated by lower crustal partial melting. Ras ed Dom and Abu Dom, together with some eighteen or so similar ring-complexes in the Bayuda area, belong to the Younger Granite Association which occurs widely throughout the Sudan, and shows many features in common with the Nigerian Younger Granite province.

CONTENTS

LIST OF FIGURES

CHAPTER 3 : STRUCTURE OF THE YOUNGER GRANITE ROCKS

CHAPTER 4 : PETROGRAPHY OF THE YOUNGER GRANITE ROCKS

CHAPTER 5 : MINERAL CHEMISTRY

pages

CHAPTER 6 : GEOCHEMISTRY

CHAPTER 7 : PETROGENESIS

CHAPTER 8 : SUMMARY AND CONCLUSIONS

LIST OF TABLES

pages

CHAPTER 1 : INTRODUCTION AND REGIONAL GEOLOGY

CHAPTER 2 : FIELD RELATIONS OF THE YOUNGER GRANITE ROCKS

CHAPTER 3 : STRUCTURE OF THE YOUNGER GRANITE ROCKS

CHAPTER 4 : PETROGRAPHY OF THE YOUNGER GRANITE ROCKS

CHAPTER 5 : MINERAL CHEMISTRY

CHAPTER 6 : GEOCHEMISTRY

APPENDIX III : WHOLE-ROCK ANALYSES

LIST OF PLATES

CHAPTER 4 : PETROGRAPHY OF THE YOUNGER GRANITE ROCKS

ACKNOWLEDGEMENTS

This work was carried out under the tenure of an Overseas Development Authority research studentship (research scheme R 2986) which is gratefully acknowledged. I am indebted to the staff of the Geological and Mineral Resources Department of the Democratic Republic of the Sudan, and of the Geology Department, University of Khartoum, for their cooperation and assistance. Especial thanks are due to Mr. Y. Suleiman and Dr. F. Ahmed for assistance in undertaking field work.

The research was supervised by Prof. D. C. Almond (University of Khartoum, formerly of Kingston Polytechnic) and Prof. J. R. Vail (Portsmouth Polytechnic) and I should like to express my thanks for their guidance and encouragement, and for introducing me to the African continent and its geology.

X.R.F. whole-rock analysis was undertaken at Portsmouth Polytechnic and thanks are due to Dr. D. J. Hughes for instruction in X.R.F. techniques. I am grateful to Dr. P. Treloar of the Department of Earth Sciences, Cambridge University, for instruction in electron microprobe machine procedures.

In addition,I should like to thank all my colleagues at Kingston and Portsmouth for their advice and camraderie, especially P. Curtis, M. McCormac, W. Iles, P. J. Hill and D. K. Wright. Much credit is due to L. Parry and D. Bayliss for the cartographic and photographic standards achieved in this work, and that debt is gratefully acknowledged. I am indebted to Christine Sparrow for the excellent quality of the final typed text.

Finally I must express my appreciation for the support shown by my mother and father, and my sister Sheila, during the period of my research. Also deserving of mention are my flatmates, Garry and Pete, without whose support, friendship and tolerance completion of this work would have been considerably less enjoyable. Likewise, the kindness and interest shown by David and Greta Almond over the years, is sincerely appreciated.

LIST OF ABBREVIATIONS

N, S, E, W, : points of the compass
loc. : field locality
S : syenite
IT : intrusive trachyte
G : granite
MG : microgranite
ASF : Abu Siba felsite
RED : Ras ed Dom
AD : Abu Dom
p.f.u. : per formula unit
pH_2O : partial water vapour pressure
pO_2 : partial pressure of oxygen
fO_2 : oxygen fugacity
aNa_2O : activity of Na_2O
$aSiO_2$: activity of SiO_2
WM : magnetite-wustite
QFM : quartz-fayalite-magnetite
HM : haematite-magnetite
MI : magnetite-iron
IW : iron-wustite
NNO : nickel-nickel oxide
ag. ratio : agpaitic ratio
$>$; $\geqslant$: greater than; greater than or equal to.
$<$; $\leqslant$: less than; less than or equal to.

c ; $\sim$: circa ; approximately about.
HREE ; LREE : heavy and light rare earth element groupings.

CHAPTER 1 : INTRODUCTION AND REGIONAL GEOLOGY

1.1. : Location and Extent

The Ras ed Dom and Abu Dom Younger Granite ring-complexes are located in the central part of the Bayuda Desert of northern Sudan (Fig. 1.1). Ras ed Dom (18° 12'N; 32° 57'E) covers an area of 61km^2, and is part of a larger multiphase massif that also embraces Ban Gidid, Muweilih and Sultaniyat complexes (McCormac, in prep.; Curtis, 1979; Map 3 rear pocket). Within this massif igneous activity has followed an anti-clockwise arcuate path, terminating in Ras ed Dom. Abu Dom (17° 57'N.; 32° 57'E) is a smaller, isolated complex, 35km^2 in size, positioned 25km due S. of Ras ed Dom. It is believed that, following local cessation of activity in Muweilih complex, the magmatic focus shifted south probably to Abu Dom (see Map 3 inset). If this is correct then Abu Dom antedates both Sultaniyat and Ras ed Dom.

1.2. : Physiography and Settlement

1.2.A. : Climate

The following brief account of the climate largely relies on that of Barbour (1961).

The winter season in Bayuda lasts from November to early March, and is cool and dry. Atbara (Fig. 1.1) has a mean daily temperature of 16°C at this time, but away from the Nile a high diurnal range in temperature is encountered. The hot season extends from March to July and maximum temperatures at Atbara can reach 43°C in June, although again the desert experiences higher temperatures. The rainy season brings 50 - 100mm of rain to the region, mostly in July and August. However, in the dry areas of northern Sudan mean annual rainfall figures can be misleading, as they take no account of the variability, which is very high. At Abu Hamed (Fig. 1.1), for example, variability, expressed as a percentage of the mean annual rainfall, is eighty percent. A recent instance of the effects of such variability, was the failure of the rains in 1976 which obliged some of the nomad youth to travel to Atbara in search of an alternative livelihood.

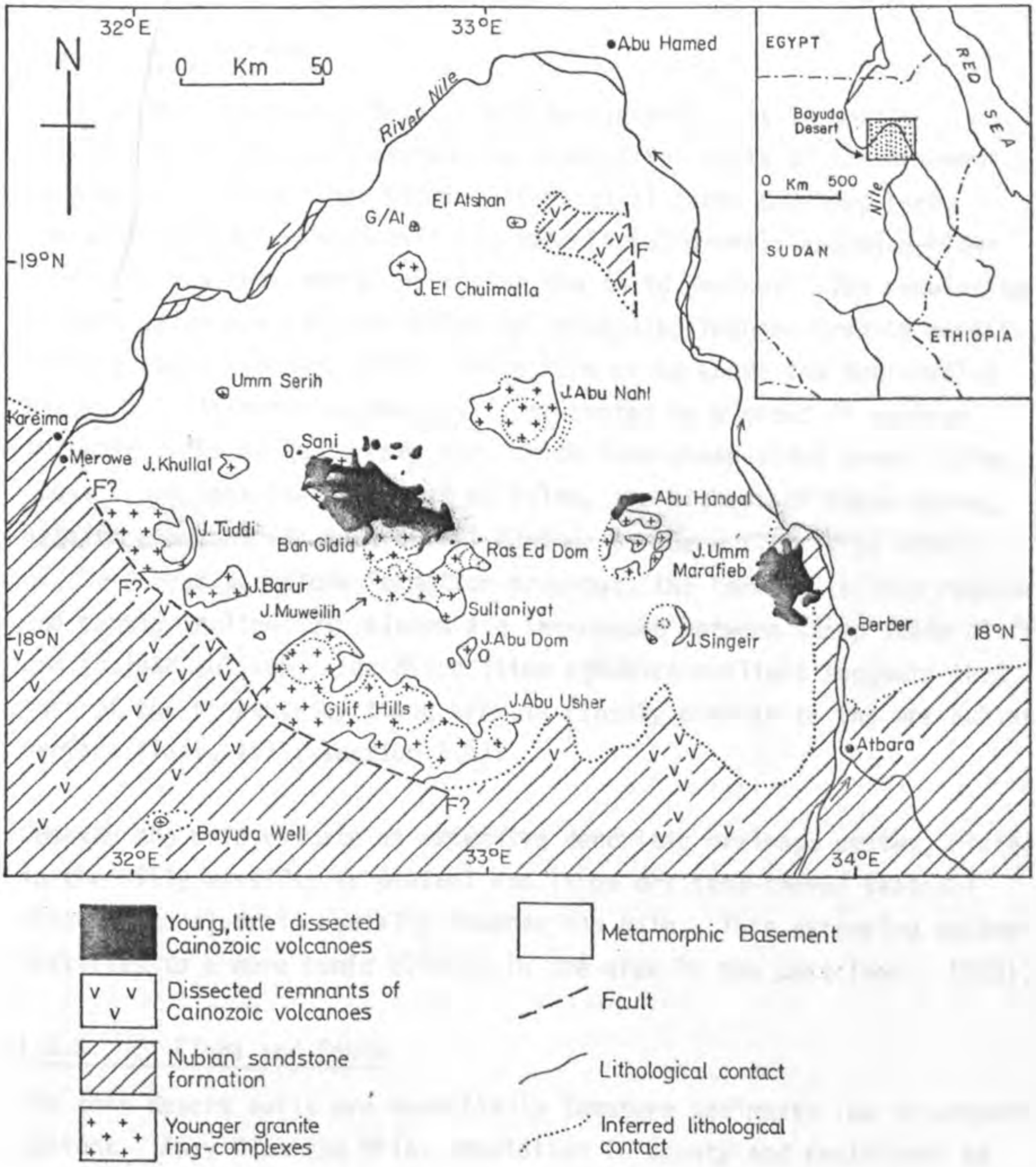

Fig 1.1 : DISTRIBUTION OF YOUNGER GRANITE RING-COMPLEXES IN THE BAYUDA DESERT, SUDAN.

1.2.B. : Topography

Most of the Bayuda Desert is formed by a broad, flat to gently undulating peneplain, underlain by crystalline rocks of the Basement Complex (for definitions of the lithological terms employed here, see section 1.4). Unconsolidated superficial gravels and wind-blown sands, form a thin veneer obscuring the solid geology. The regularity of this landscape is interrupted by upstanding Younger Granite massifs, forming rugged, broken hills rising 200m or so above the surrounding plains. A different morphology is presented by a group of younger volcanic rocks of Quaternary age, which form steep-sided cones rising above broad lava fields. Hosh ed Dalam, the highest of these cones, attains a height of about 400m. Further S. where flat-lying strata of the Nubian Sandstone Formation crop-out, the terrain is less regular, and gently inclined dip slopes are interposed between steep scarp bluffs and incised gullies. The disposition of Nubian outliers suggests that much of the present-day topography is closely similar to the pre-Nubian surface (Vail, 1971; section 2.5).

Despite the arid climate an extensive dendritic drainage system, rising in the hilly massifs, is present and large dry sand-choked seasonal rivers (khors) drain radially towards the Nile. This extensive system testifies to a more humid climate in the area in the past (Vail, 1978).

1.2.C. : Flora and Fauna

The thin desert soils are essentially immature sediments low in organic content. Away from the Nile, vegetation is scanty and restricted to the wadis or in the hills, to narrow ravines. The plants are xerophytic types including thorny acacia trees, tussocky grasses and occasional herbs.

In the open expanses gazelles are the only commonly seen wildlife, birds being sparse. Foxes, hares, lizards, scorpions and locusts constitute the fauna in the hills.

1.2.D. : Settlement

The arid climate does not favour agricultural endeavour, and the scanty population of Hassaniya tribesmen pursue a nomadic existence. Choosing to live in isolated, grass-built homesteads they tend to their sheep, goat and camel herds and migrate in pursuit of the best pastures during the'kharif' or rainy season. Trees destroyed during the flash floods of the 'kharif' are burnt for charcoal, which is then traded to passing market ('sukh') lorries in exchange for essentials such as salt, flour and tea.

Water is obtained from deep stone-lined wells some of which are of a permanent nature, e.g. Bir Ras ed Dom (18° 3'N. ; 32° 50'E) in northern Sultaniyat. Many of the wells are located in the coarse mantle of pervious detritus within or adjacent to the Younger Granite massifs. Others, situated in wadi courses, are temporary, being destroyed annually during the succeeding wet season.

1.3. : Access and Mapping Procedure

The Bayuda Desert is most readily accessible from the town of Atbara on the Nile. Atbara lies some 250km N. of the capital, Khartoum, and the two are linked by air, train and road. Roads are not asphalted for any great distance outside the larger towns,and they usually consist of dirt tracks which are deeply rutted in places or cut across the fine sands of the wadis. During the wet season such tracts are frequently impassable. Crossing the Nile is facilitated by numerous ferry points such as Atbara, Berber and Merowe.

In the desert reasonably well defined routes used by the sukh lorries connect the towns of Berber, Atbara and Shendi in the E. with those of Merowe and Kareima in the W. Several of these routes intersect near Jebel Abu Usher (Fig. 1.1), 10km S.W. of Abu Dom Complex, and are thus convenient approach roads to the study area. Away from such main routes trackways are impersistent but repeated journeys by Land Rover enable good tracks to be forged across the desert plains. In Ras ed Dom it was possible, after several hours removing stones, to drive up Wadi el Widian (see Fig. 2.2) right into the heart of the complex.

Likewise access into Abu Dom was possible by car along Wadi el Milega and Wadi el Guna (Fig. 2.8).

Within the hills, which are unpopulated, the only paths are those created by goats and sheep. Gorges and occasional broader valleys, however, provide access to most areas.

The constraints imposed by the difficult climate are such that field work is feasible only during the cool winter season, and in the present instance was undertaken during two visits to the Sudan - from January to March 1976 and from November of that year until February 1977. Base camps were established near the wells of Ban Gidid (18° 12'N. ; 32° 43'E) and Sultaniyat (18° 3'N. ;32° 47'E) respectively during the successive field seasons, and daily excursions were made to the mapping areas. During the second visit the writer found that fly-camping in wadis within the two complexes was most effective, enabling as it did, all but the most remote areas to be mapped entirely on foot. Fortnightly visits were made to Atbara for petrol and provisions, whilst water supplies were obtained from the local wells.

Most of the Younger Granite complexes of Bayuda lie in the northern part of the desert, near the junction of the Dongola-Merowe, Shendi and Berber administrative districts. The only published maps of the vicinity are the 1:250,000 topographical sheets of the Sudan Survey Department. The majority of the ring-complexes lie in the area covered by the following sheets, Baiyuda (sheet 45-J), Atbara (45-K) and Merowe (45-F). The small scale of these maps and the fact that away from the Nile the information recorded on them tends to be sparse and approximate, means that they are of limited use. Indeed for mapping purposes aerial photographs provide better base maps. Preliminary evaluation of the geology and the location of outcrops of Basement, Younger Granite, Nubian Formation and Quaternary basaltic rocks was accomplished using blackand white Landsat satellite images on a 1:250000 scale. Photogeological maps of individual ring-complexes were also prepared prior to field work,from interpretations of 1:40000 and 1:38000 aerial photographs obtained from the Sudan

Survey Department. In the field, observations were mapped directly on to the photographs by means of transparent overlays. The same photographs were used to construct uncontrolled print laydowns, and the resultant photomosaics (see rear pocket) formed the base maps for Maps 1 and 2 (rear pocket). A problem encountered in Ras ed Dom was the existence of a gap in the photo-cover. The extent of this gap was established by field triangulation. Ground measurements made to determine the scale of the photographs are inevitably of limited precision, and so accordingly are the quoted scales on the maps.

1.4. : Regional Geology and History of Research

1.4.A. : Introduction

The geology of Sudan has been reviewed in two publications, Whiteman (1971) and Vail (1978). The latter writer has remarked upon the relative simplicity of the geological column for Sudan, owing to the paucity of Phanerozoic deposits. This observation is also true of the Bayuda area, the geology of which is summarised in table 1.1, and in map form in Fig. 1.1.

1.4.B. : Basement Complex

Andrew (1948) defined the term Basement Complex to include "all igneous and sedimentary rocks, whether metamophic or not, out of which the platform was carved on which the quasi-horizontal continental sediments rest". The continental sediments referred to comprise mainly the Nubian Sandstone Formation. Field relations indicate that the Younger Granite ring-complexes in Bayuda underlie the Nubian beds, and accordingly belong to the Basement Complex *sensu stricto*. In this thesis this definition is respected although the term basement is also used loosely to refer to the country rocks of the Younger Granite intrusions.

The Basement Complex in Bayuda comprises five main units as follows (Fig. 1.2; Vail, 1979).

superficial deposits	
Basaltic volcanic activity	(Cainozoic)
Uplift and erosion; exhumation of the pre-Nubian surface; faulting	
Deposition of the Nubian Sandstone Formation	(Lower Cretaceous ?)
Erosion and peneplanation	
Emplacement of Younger Granite ring-complexes; extrusion of related volcanic rocks	(Silurian - Jurassic)
End of tectonism; uplift and erosion	
Multistage formation of the metamorphic rocks of the Basement Complex.	(Precambrian)
Batholithic Granites	
Greenschist Assemblage	
Metasedimentary Group	
Grey Gneiss Group	

Table 1.1 : Sequence of geological events in the Bayuda Desert (adapted from Vail,1978; Vail,1979 and Barth and Meinhold,1979)

The oldest unit, according to Vail (1979),is the Grey Gneiss Group, which crops-out over the central part of the desert and forms the country rocks for the two Younger Granite complexes discussed in this thesis. It consists of granite-, biotite- and muscovite-gneisses, and is unconformably overlain by the Metasedimentary Group which comprises psammitic gneisses, impure quartzites, graphitic and micaceous schists, marbles and amphibolites. Near to the present study area quartzite, unconformably overlying the grey gneisses and synformally disposed, was reported by Almond et al. (1969) from a locality 6km S. of Sani (Fig. 1.1). Poorly foliated quartz-mica schists, unconformably lying on the gneisses are known to form an extensive outcrop a few kilometres S. of Muweilih Complex (McCormac, Pers. comm.). According to Kabesh (1959, 1960, 1962a, 1962b) and Vail (1971, 1978) three fold phases are present in the two early basement units, and the regional metamorphic grade is amphibolite facies.

In the E. of the desert between Shereik and Berber (Fig. 1.2), a third and uppermost unit, lying unconformably upon the metasediments, constitutes a supercrustal Greenschist Assemblage (Vail, 1979) of predominantly volcanic nature. E. of Bayuda it is the most widely exposed basement unit in the northern Red Sea Hills. The assemblage consists of andesites, some basalts and thin rhyolites, with interbedded sediments that include chloritic shales and limestones. Only F2 and F3 fold-phases are recorded in these lower-grade rocks.

All the preceeding units are intruded by the Batholithic Granite, a calc-alkali suite of granodioritess, adamellites and diorites.

At this juncture it is relevant to note that a radically different interpretation of the basement in Bayuda has been proposed by Meinhold (1979a). Meinhold maintains that the Greenschist Assemblage is the oldest of the units, while the Grey Gneisses are the youngest. Two objections may be made to such a proposition. Firstly, it is necessary to explain the lower grade of metamorphism

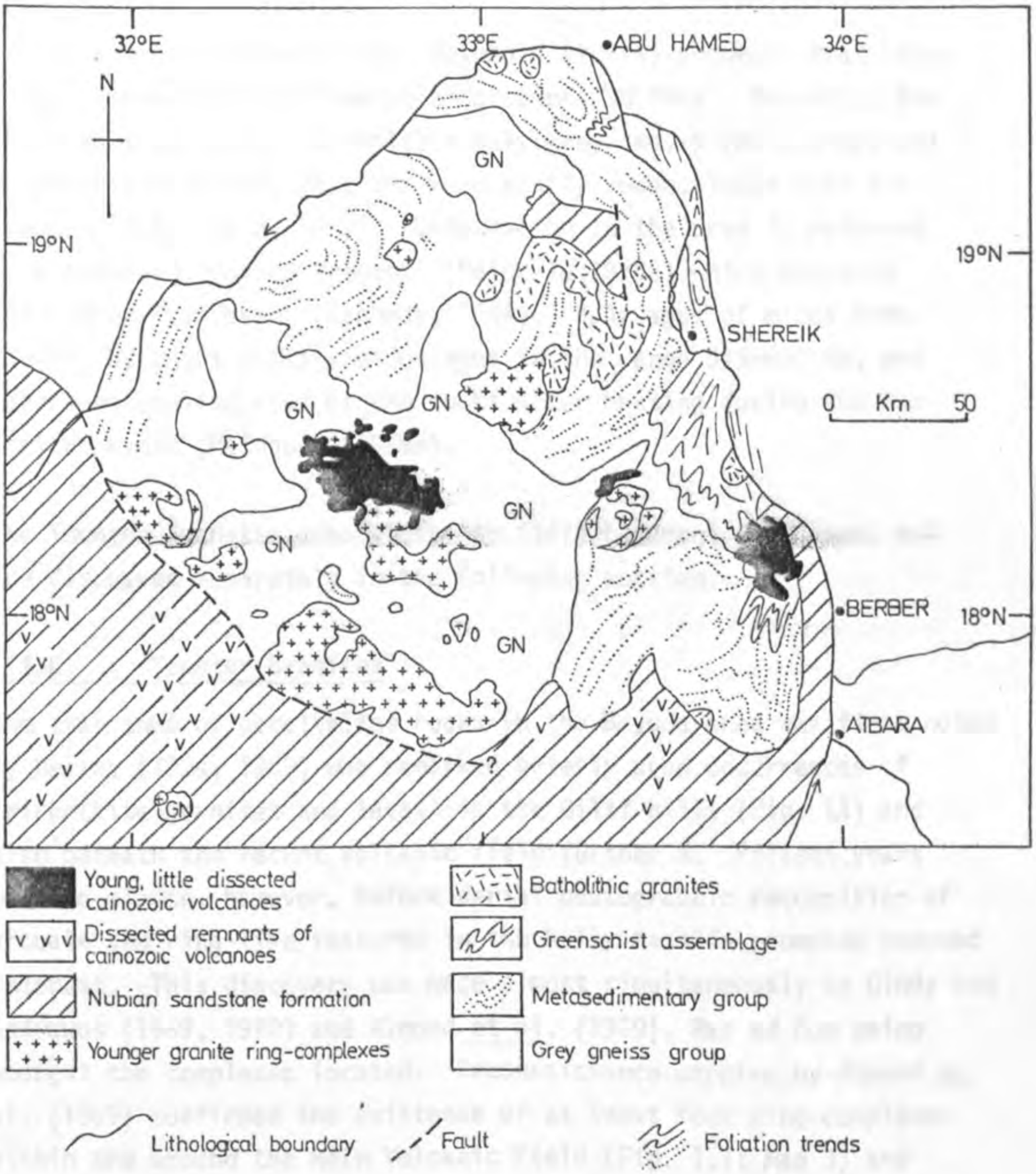

Fig. 1.2 GEOLOGY OF THE BAYUDA DESERT, SHOWING SUBDIVISIONS AND FOLIATION TRENDS IN THE BASEMENT COMPLEX. (after Vail, 1979)

in the supposed older group. Meinhold (1979a) suggests that late-stage retrogressive metamorphism accounts for this. Secondly, the Rb/Sr ages quoted by Meinhold, namely grey gneiss (874±33 Ma) and greenschists (757±29 Ma), are more easily reconcilable with the ideas of Vail (1978, 1979). Deformation in the area is referred to a proposed 'Bayuda Orogeny' (Meinhold,1979a) which predates the Pan-African event (Kennedy, 1964). K/Ar ages of micas from several basement units yielded ages in the range 519-680 Ma, and represent cooling ages of the rocks after heating during the Pan-African event (Meinhold, 1979a).

The Younger Granites constitute the fifth basement component, and are discussed separately in the following section.

1.4.C. : Younger Granites

The existence of peralkaline rocks in the Bayuda area was first noted by Delany (1954, 1958) who remarked briefly upon occurrences of 'riebeckite granites and lavas' in the Gilif hills (Fig. 1.1) and also beneath the recent volcanic field further N. Fifteen years were to elapse, however, before aerial photographic recognition of arcuate and ring-like features in the hilly massifs prompted renewed interest. This discovery was made almost simultaneously by Gindy and Andrawos (1969, 1970) and Almond et al. (1969), Ras ed Dom being amongst the complexes located. Reconnaissance mapping by Almond et al. (1969) confirmed the existence of at least four ring-complexes within and around the Main Volcanic Field (Fig. 1.1; Map 3) and these comprise what is now known as the Ban Gidid - Ras ed Dom chain. Related dyke swarms were also found. The field relations and sodic character of these 'Younger Granites' led Almond et al. (1969) to compare them with the better known Younger Granites of Nigeria (Jacobson et al., 1958). Subsequently Vail (1971) provided summary accounts of three more ring-complexes further to the N. and E. Continued air-photo interpretation and reconnaissance mapping has increased the number of known Younger Granite rings in the area in to over twenty, as described in a review by Almond et al.(1976). The rings are part of a larger Younger Granite association that occurs widely in Sudan (Almond, 1979) and is discussed further in

Chapter 8. The association is characterised by high-level, anorogenic ring intrusions and associated caldera-preserved early volcanic rocks. Basic rocks are scarce and peralkaline granites and syenites prevail over biotite-bearing rock-types (map 3, rear pocket).

Rb-Sr whole-rock ages, supplemented by K-Ar data, are quoted by Meinhold (1979b) and Barth and Meinhold (1979). It appears that magmatism started in Silurian-Devonian times in the S. of the Desert and moved northwards with time. Ban Gidid is Devonian (397±18 Ma) in age, whilst Abu Dom, Sultaniyat and Ras ed Dom are Permo-Triassic (234±6 Ma). The more northerly complexes date from the Jurassic. The latter dates agree with the K-Ar age of 209±5 Ma, published by Vail (1976) for a sample from the Jebel Abu Nahl complex (Fig. 1.1).

1.4.D. : Nubian Sandstone Formation

The nature and occurrence of the Nubian Sandstone Formation in the Sudan has been reviewed by Whiteman (1971) and Vail (1974, 1978). Diagnostic fossils and useful marker horizons are rare, and in practice the unit is identified on lithological criteria. These considerations, together with the fact that the unit crops-out over one-third of the Sudan and also widely beyond, have raised problems as to nomenclature, origin and age range. However, limited fossil evidence from Darfür Province indicates an early Cretaceous (Neocomian-Barremian) age (Edwards, 1926). The earliest beds at the type locality in Egypt are younger, dating from the Upper Cretaceous (early Maastrichtian) according to Issawi (1973).

The Nubian Sandstone comprises sub-horizontal brown sandstones, mudstones and conglomerates, formed under sub-aqueous, continental conditions such as occur in braided stream and playa environments (Whiteman, 1971; Vail, 1974). Palaeocurrent evidence indicates transport directions from S.E.-N., over the northern half of Sudan (Kheiralla, 1966).

In the Bayuda area the Nubian Sandstone is largely absent N. of an E.-W. line through Atbara. To the S. of this line it forms an extensive blanket covering the older rocks (Fig.1.1). The N.W. limit of this cover, between Kareima and the Gilif hills, may be in part faulted (Almond et al, 1976). N. of this line, e.g. in the Abu Dom area, numerous minor outliers of the sandstone, lying unconformably on the Basement Complex and Younger Granite rocks (Fig. 1.1), testify to its former greater extent in the area.

1.4.E. : Cainozoic Volcanic Rocks

Gregory (1920) observed from the air the existence of young extinct volcanoes in the Bayuda desert, and the volcanic cones have been subsequently visited by Grabham (1920), Delany (1954), Putzer (1958) and Almond et al. (1969). The Main Volcanic Field ($520km^2$) straddles the older Younger Granite rocks of the Sani and Ban Gidid complexes, partly obscuring them. Smaller fields occur at Jebel Umm Marafieb, near Berber, and elsewhere in the desert (Fig. 1.1).

The most detailed investigation on these rocks was that undertaken by Almond et al. (1969) and largely concerned the Main Volcanic Field. This field consists of 100 or so small, monogenetic, 'strombolian' volcanoes. Hosh ed Dalam is the highest example, standing about 400m above the adjacent plains. The cones are formed of bedded pyroclastic deposits, and broad lava-flows extend from them over the surrounding countryside. Some centres display late-stage explosion craters. Compositionally the basalts are strongly undersaturated basanites and nepheline trachybasalts (Almond, 1974).

1.5. : Aims and Scope of the Research

A brief outline of the intentions behind this work is appropriate, before embarking upon the main body of the text. Broadly speaking, the aims of the project were fivefold.

i. To map Ras ed Dom and Abu Dom ring-complexes on a scale of 1:40,000 and to produce maps illustrating the geology and structure of the two complexes. The results are presented as Maps 1 and 2 (rear pocket).

ii. To establish, through petrographic observation, the nature and range of rock-types present in the complexes, and to describe the mineralogical variation encountered in them.

iii. To undertake an investigation into the mineral chemistry, in order to establish the range of variation present, and to elucidate upon the physio-chemical conditions governing the assemblages found.

iv. To investigate the variation in whole-rock chemistry, and from the results to interpret the petrogenesis of the rocks.

v. More broadly, to contribute to the understanding of the nature of the Bayuda Younger Granites by means of the above-mentioned research, and through such characterisation, facilitate comparison with other alkaline provinces.

CHAPTER 2 : FIELD RELATIONS OF THE YOUNGER GRANITE ROCKS

2.1. : The Metamorphic Basement Rocks

Detailed study of the basement rocks falls beyond the scope of this investigation, but as they form the country rocks to the Younger Granites a brief discussion is appropriate.

In the area mapped the basement rocks consist almost exclusively of quartzo-feldspathic gneisses (section 1.4.B; plate 2.1). Thin remnants of the Nubian cover rocks locally overlie them, but for the most part the peneplained gneisses are obscured beneath a mantle of unconsolidated sands and gravels. Exposure is consequently poor, with the gneisses tending to crop-out only where shielded by the resistant Younger Granite emplacements. Even in the latter instances, however, the contrast in topography between the two rock-types is such that the contacts are generally buried beneath scree. As a result the precise role played by basement structures, such as jointing, in guiding the emplacement of the ring-complexes remains unknown. The Younger Granite intrusions are, however, normally discordant towards the local gneissose foliation.

Few measurements of basement trends were obtained because of poor exposure and rather variable development of the foliation. None the less the available data indicate that, near Abu Dom, the foliation strikes N.E. and dips about 40°E. (Map 5). Further north, around Ras ed Dom the strike is E.N.E. and the value and sense of dip more variable (Map 4). These observations are in accord with the known regional trends for Bayuda (Vail, 1972b;Barth and Meinhold, 1979; see fig. 1.2).

Around Abu Dom leucocratic, medium to coarse-grained biotite gneiss predominates. Feldspar augen (to 4cm; plate 2.2) are present in some of the finer types, along with migmatitic bands that parallel the foliation. In thin section the main constituents are seen to be alkali-feldspar, oligoclase, quartz and biotite, together with lesser amounts of apatite, Fe-Ti oxide, zircon and epidote. The biotite is commonly partially choritised. Sericite, saussurite and epidote are alteration products of the feldspars. The quartz is highly strained and segregated into lenses (to 4mm). At loc.684 (Fig.2.10) an intercalation of rare hornblende-gneiss is found. The amphibole is pleochroic in pale greens, and forms poikiloblasts, containing small quartz inclusions, and recrystallised random aggregates. The plagioclase (An 48) is more basic, and the quartz content lower than is the case in the biotite gneisses, reflecting the more basic composition of this rock.

On the S. flank of Ras ed Dom similar biotite gneisses occur, but to the N. garnet-bearing varieties are found. The garnet occurs as small cracked grains (1mm), sheathed by biotite, and also as the cores to larger corona structures (to 5cm), in which biotite and Fe-Ti oxides form successive outer zones.

The mineral assemblages present in these rocks indicate amphibolite facies of regional metamorphism.

A few folded 'old dykes' of granitic composition that predate the Younger Granite episode are present.

Enclosures and screens of gneiss are common within the ring-complexes, and such occurrences are discussed where appropriate in succeeding chapters.

Recrystallisation of quartz, late quartz, alteration of feldspars to sericite and saussurite, deformed plagioclase twins, kinked biotite and mortar texture between adjacent feldspars are features seen in the gneisses. However, they are also known to occur in areas away from the Younger Granites (Barth and Meinhold, 1979) and thus their presence near the ring-complexes is of no special significance. However at loc. 1005 (Fig. 2.3), in the Widian basement block, unequivocal evidence of minor transformation of the gneiss by Younger Granite derived fluids does occur. Veinlets and pods (to 3cm) of quartz and arfvedsonite invade the gneiss, and granophyric texture, of evident recrystallisation and perhaps replacement origin, is developed along the vein margins (plate 4.8B). Contact alteration of the older rocks on any sizeable scale is not however characteristic of the ring-complexes.

2.2. : Ras Ed Dom Complex

2.2.A. : Introduction

The geology of Rad ed Dom is shown on Map 1 (rear pocket), and in figures 2.3. - 2.7., interspersed through the following discussion. The reader is also invited to refer to the structural cross-sections provided in chapter 3 (figures. 3.3. - 3.6.).

The intrusive units are grouped into eight structural centres (Fig. 2.1), as explained in section 3.2.B. There are four recurrent rock-types namely, Syenite (S; 15 units in all), Intrusive Trachyte (IT; 3 units), Granite (G; 2 units) and Microgranite (MG; 3 units). The capital letters in brackets are the respective abbreviations used throughout the text. A simple system of labelling is employed. For any one rock-type the numeration is chronologically consistent e.g.Syenite 13 postdates Syenite 12. This observation does not hold between the different categories e.g. G2 is not emplaced between S1 and S3. Table 2.1 summarises the intrusive chronology and outcrop areas of the various intrusions.

The term felsite, as in Abu Siba Felsite (ASF), is used as a synonym for intrusive rhyolite. This felsite can be only fitted provisionally into the succession.

Place names (fig. 2.2) are generally used to identify specific features such as faults. The petrography of the Younger Granites is the subject of Chapter 4. For convenience the area, full name and colour index (M) are quoted in brackets after the first mention of each unit. The grain size limits used are given in section 4.1. The rocks are classified according to Streckeisen (1967, 1976; see section 4.1).

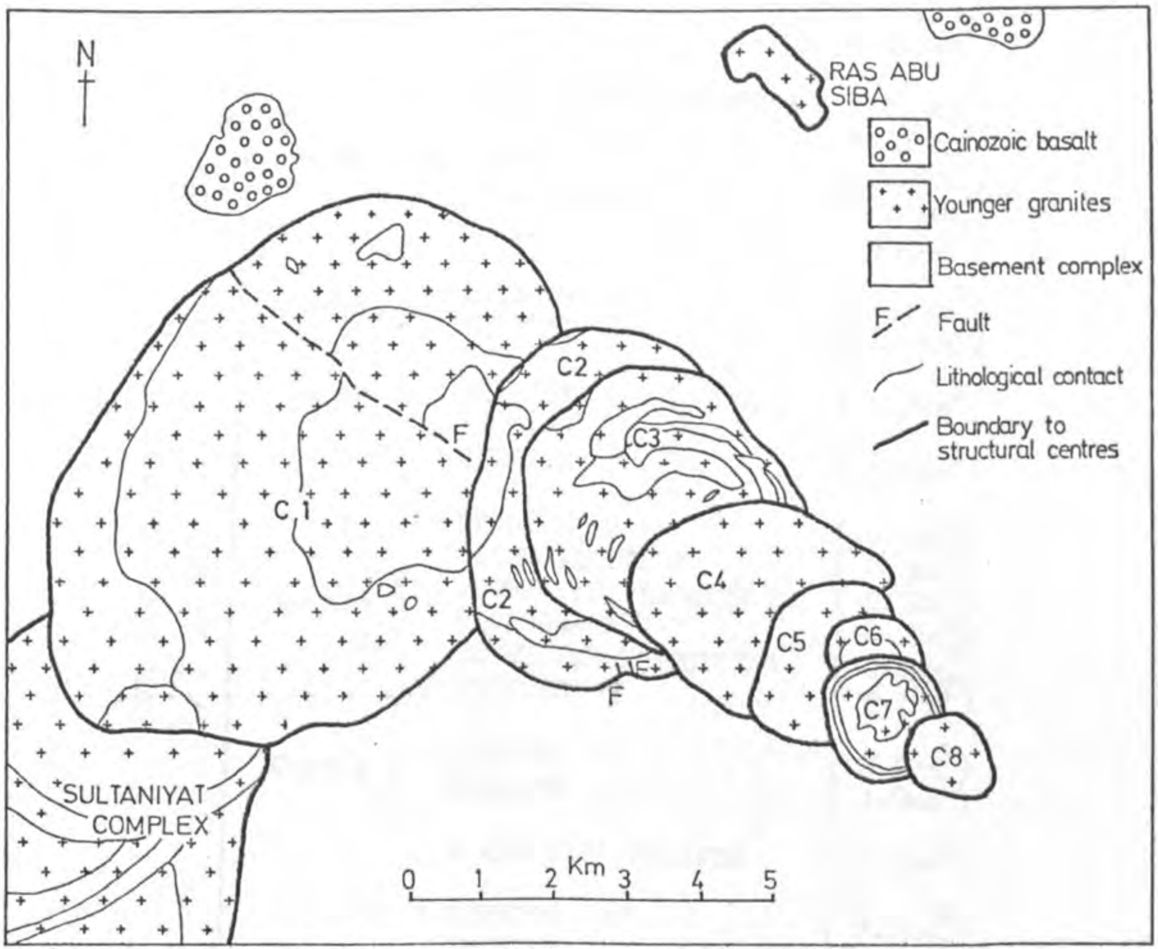

Fig. 2.1. STRUCTURAL CENTRES (C1-C8) TOGETHER WITH THE OUTLYING RAS ABU SIBA CENTRE, RAS ED DOM COMPLEX

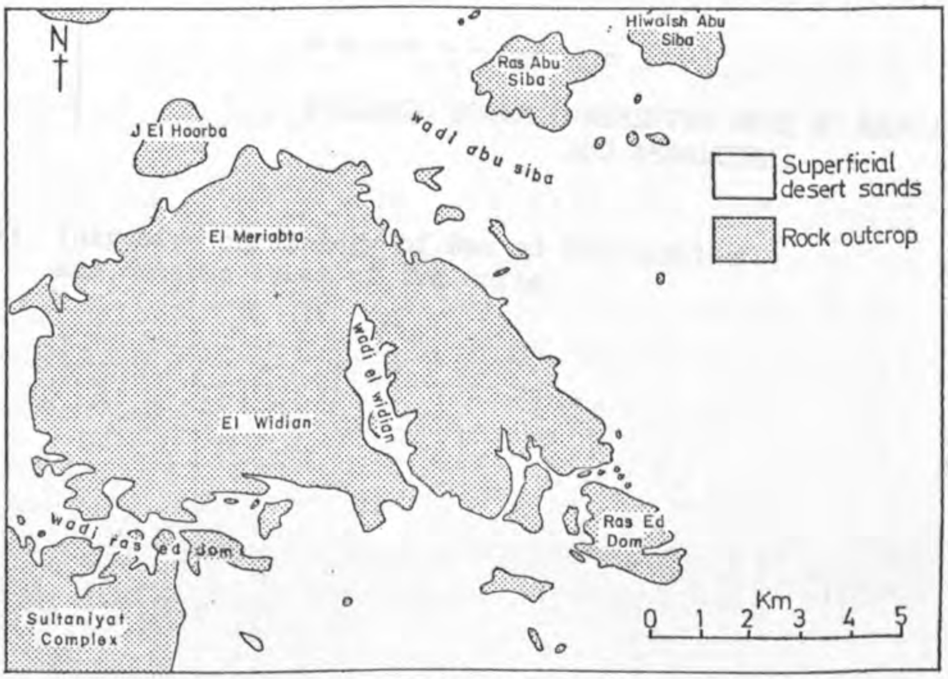

Fig. 2.2. PLACE NAMES IN THE RAS ED DOM VICINITY

YOUNGER	Centre 8	SYENITE 15	(1.2km^2)
	Centre 7	INTRUSIVE TRACHYTE 3	(0.5km^2)
		SYENITE 14	(.04km^2)
		SYENITE 13	(0.8km^2)
		SYENITE 12	(0.3km^2)
		SYENITE 11	(0.5km^2)
	Centre 6	SYENITE 10	(0.2km^2)
		SYENITE 9	(0.4km^2)
	Centre 5	SYENITE 8	(2.2km^2)
INTRUSIVE SEQUENCE	Centre 4	SYENITE 7	(5.7km^2)
	Centre 3	GRANITE 2	(0.9km^2)
		MICROGRANITE 2	(0.3km^2)
		INTRUSIVE TRACHYTE 2	(0.5km^2)
		MICROGRANITE 1	(0.2km^2)
		INTRUSIVE TRACHYTE 1	(0.6km^2)
		SYENITE 6	(5.7km^2)
	Centre 2	SYENITE 5	(3.2km^2)
		SYENITE 4	(1.8km^2)
		? ABU SIBA FELSITE	(1.0km^2)
	Centre 1	SYENITE 3	(7.7km^2)
		GRANITE 1	(22.4km^2)
		SYENITE 2	(5.0km^2)
		SYENITE 1	(0.7km^2)
OLDER		VOLCANIC ROCKS (PRESERVED ONLY AS RAFTS AND XENOLITHS)	

Table 2.1: Intrusive chronology of Ras ed Dom Complex and outcrop areas of the units.

2.2.B. : Volcanic Rocks

Volcanic rocks are uncommon in Ras ed Dom. Two volcanic remnants occur in the high-level intrusions of Centre 3 (figures 2.4 and 2.5). The largest is at loc. 307 in IT2 (Fig. 2.5C) and is a raft, about 2m long, composed of thinly bedded (av.~ 0.3m) pyroclastic tuff and breccia. The bedding dips 12°S.W. and is discordant to the attitude of the raft, which inclines 47° N. The second remnant consists of rounded fragments of crystal tuff, sometimes enclosed in overgrowths of alkali-feldspar, at loc. 399 in MG2 (fig. 2.5D). Volcanic xenoliths also occur in IT3 (fig. 2.7) and include clasts of crystal-lithic tuff, trachyte, flow-banded rhyolite and sundry other haematised fragments.

A detailed reconstruction of the volcanic episode on the basis of such meagre evidence is not possible, but several facts are clear.

1. Ras ed Dom was once the site of a Younger Granite related volcanic superstructure.
2. The volcanic episode produced both lavas and pyroclastic rocks.
3. The fine-grained, high-level intrusions in which the xenoliths are found, were probably feeders to the volcanic pile.

An insight into the probable nature of the early volcanic phase at Ras ed Dom, is provided by the extensive caldera-preserved volcanic sequences of the adjacent Sultaniyat and Muweilih complexes (Map 3). In Sultaniyat, the volcanic pile is 3000m thick and in it pyroclastic rocks predominate over lavas. Occasional basic-intermediate clasts occur but the majority of the volcanic rocks are acid and peralkaline (Curtis, 1979). A more complete early sequence is reported from Muweilih complex (McCormac, pers.comm.) where lavas spanning a broad compositional range (hawaiite-mugearite-benmoreite-alkali feldspār trachyte) are known to occur.

2.2.C. : Centre 1

Centre 1 is the largest structural centre (35km^2) in the complex and comprises S1, S2, S3 and G1 (fig. 2.3). These units record a E.N.E. shift in magmatism with time.

The earliest intrusion is Syenite 1 (0.7km^2;ferro-augite syenite; M = 16), a small unit located in the S.W. of the centre. In hand-specimen it is typically a coarse-grained, greenish syenite. In thin section, granulation (with development of strained extinction) and recrystallisation of alkali-feldspar occur along shears, but these cataclastic features are not generally apparent in hand-specimen. The cataclasis testifies to the disruption of the unit and its original form and extent are consequently unknown. Wadi Ras ed Dom isolates S1 from the Sultaniyat complex to the south, but the steady northward displacement of magmatism in that complex (Curtis, 1979) indicates that it predates S1.

Syenite 2 (5km^2 ; quartz-syenite; M = 14) forms a crescentic ridge of hills, bounded on the W. by a smoothly curving margin believed to follow a ring-fracture. In the S., the intrusion and associated dykes swing E. rather abruptly, evidently deflected by the earlier Sultaniyat massif (fig. 2.3). The outer contact of the unit is scree-obscured but is unaffected by topography and must be steep in attitude. Grain-size is rather variable within the intrusion varying from medium- to coarse-grained, but it does not noticeably chill against the enclosing gneisses. The unit is lithologically heterogeneous, consisting of hedenbergite-bearing syenite in the S., whereas sodic pyriboles predominate in the N. A porphyritic facies, with large pink feldspar phenocrysts, is sporadically present in the interior (fig. 2.3). The emplacement of G1 must have caused foundering of part of S2. It also induced recrystallisation of the syenite to medium-grain size in places e.g. loc. 131 and 132 (fig. 2.3). As with S1 the original form is a matter of conjecture but a broad, though perhaps incomplete ring-dyke is tentatively suggested.

Granite 1 (22.5 km^2; aegirine-arfvedsonite granite; M = 11), the largest unit in Ras ed Dom, is a broad annular intrusion the eastern portion of which has foundered (fig. 2.3). The bounding ring-fracture is smoothly arcuate where it cuts through the gneisses but is somewhat sinuous where it cuts S2. In the S. the fracture is step-like,

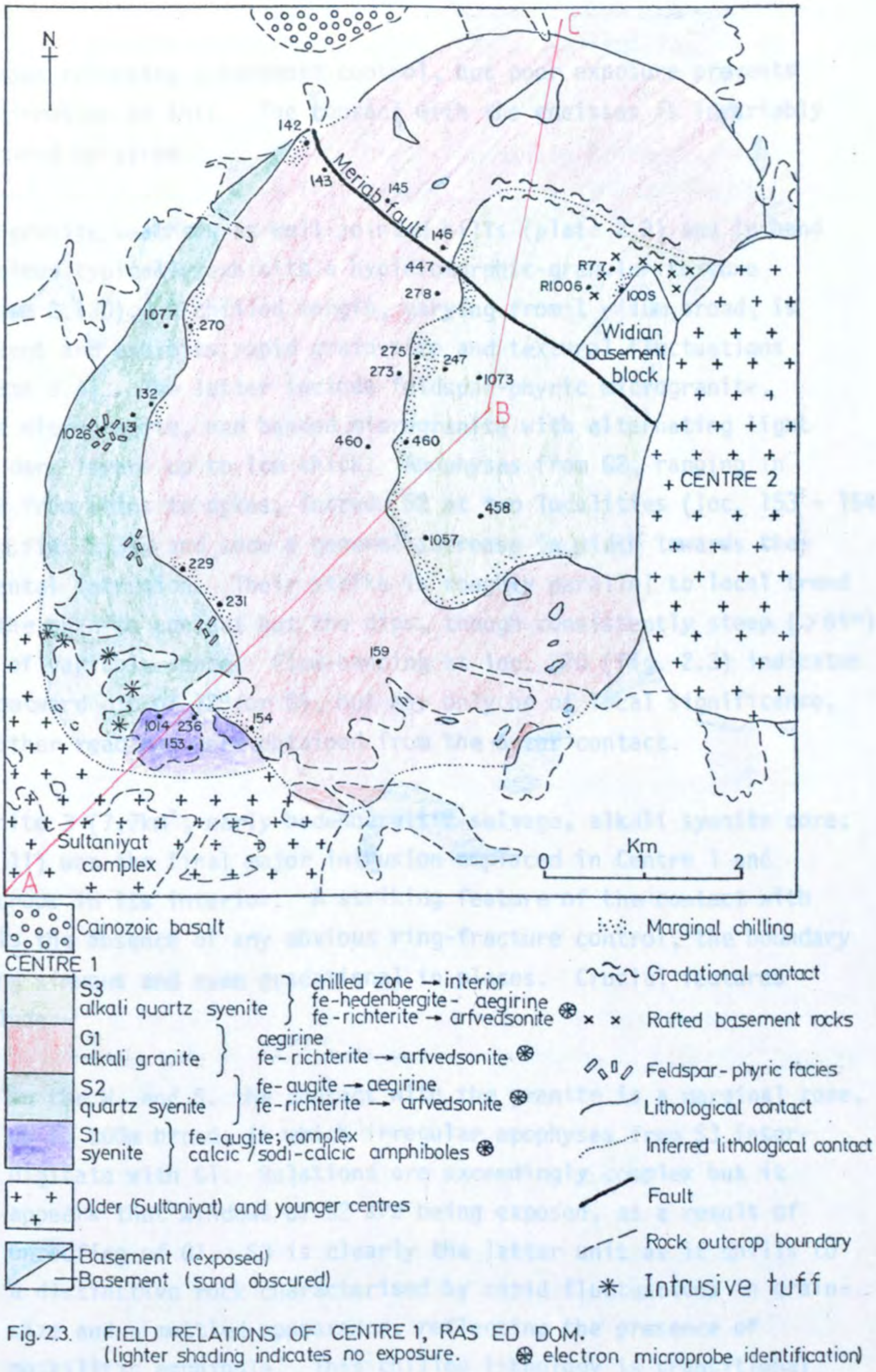

Fig. 2.3. FIELD RELATIONS OF CENTRE 1, RAS ED DOM.
(lighter shading indicates no exposure. ⊛ electron microprobe identification)

perhaps refecting a basement control, but poor exposure prevents confirmation of this. The contact with the gneisses is invariably obscured by scree.

The granite weathers as well jointed hills (plate 2.3) and in hand specimen typically exhibits a hypidiomorphic-granular texture (plate 2.13D). A chilled margin, varying from 1 - 10m broad, is present and exhibits rapid grain-size and textural fluctuations (plate 2.4). The latter include feldspar-phyric microgranite, dark microgranite, and banded microgranite with alternating light and dark layers up to 1cm thick. Apophyses from G2, ranging in size from veins to dykes, intrude S2 at two localities (loc. 153 - 154, 229; fig. 2.3), and show a general increase in width towards the parental intrusion. Their strike is roughly parallel to local trend of the granite contact but the dips, though consistently steep (>65°), are of variable sense. Flow-banding at loc. 270 (fig. 2.3) indicates an outward dip of 72° for G1, but may only be of local significance. No other readings were obtained from the outer contact.

Syenite 3 (7.7km^2; early hedenbergitic selvage, alkali syenite core; M = 11) was the final major intrusion emplaced in Centre 1 and outcrops in its interior. A striking feature of the contact with G1 is the absence of any obvious ring-fracture control, the boundary being sinuous and even gradational in places. Crucial features include:-

a. in the W. and S. the contact with the granite is a marginal zone, up to 300m broad, in which irregular apophyses from S3 interdigitate with G1. Relations are exceedingly complex but it appears that windows of S2 are being exposed, as a result of unroofing of G1. S3 is clearly the latter unit as it chills to a distinctive rock characterised by rapid fluctuations in grain-size and a mottled appearance, reflecting the presence of poikilitic amphibole. This chilled lithology is transitional between typical hedenbergite-syenite and the alkali syenite that comprises the core of the unit (plate 2.13B).

b. N. of the Meriab fault continuous gradation from syenite to granite is common (fig. 2.3).

c. Enclosures of basement, of which the Widian basement block (0.9km^2;plate 2.5) is the largest, occur in the N.E. of S3 (fig. 2.3). Basement rafts,often of considerable size,are also abundant at loc. R77 and 1006. Although the rafts can be of irregular form their long axes tend to dip south at about 45°(plate 2.6).

A problem in interpreting these observed relations is deciding what original form characterised G1. Two alternative interpretations are suggested, as follows:-

a. G1 was originally a large stock, the interior of which foundered permitting the emplacement of S3. If this was the case then the Widian basement block and smaller basement rafts may be part of the foundered roof rocks to G1.

b. G1 was originally a broad ring-dyke, enclosing a piston-like core of basement rocks. This basement core became mechanically unstable, and consequently foundered permitting emplacement of S3. In such a model the Widian basement block and smaller basement rafts are remnants of the basement piston.

On the available evidence, it is not possible to discriminate between the two models with confidence. The writer, however, favours the second model, as illustrated in the cross-section provided in fig. 3.3. In support of this it is relevant to note that broad ring-dykes, comparable in width to G1, are common in the Nigerian Younger Granites (Turner, 1972). Moreover the smooth arcuate trace of G1 against the enclosing country rocks along the N. margin of the complex, suggests that it is probably a ring-fault.

Whichever interpretation is correct, it seems necessary that G1 and S2 were emplaced closely in time, while G1 was still hot and plastic, in order to account for the gradational contacts seen between them in the N.

Post-emplacement faulting further complicatesthe picture. Centre 1 is transected by the Meriab fault, with the Widian basement block faulted out to the S. (fig. 2.3). Clearly substantial vertical movement has occurred along the fault, and it is suggested in fig.3.3 that downfaulting has occurred to the S. Exposure of a higher structural level S. of the fault would account for several of the observed features, as follows:-

a. chilling in S3, reflecting cooler higher-level conditions.

b. the greater diameter and breadth of G1 to the S. is though to reflect less steeply dipping contacts at a higher structural level.

c. the complex interdigitation of G1 and S1 in the marginal zone is at least partly due to unroofing of the granite, a feature also reflecting shallower inclinations of the contacts.

2.2.D. : Centre 2.

Centre 2 (5km^2) comprises S4 and S5, and is a crescentic structure which displays re-entrants where it tuncates Centre 1. It records a major eastwards shift in magmatism (fig. 2.4). Although much of the centre has been destroyed by S6, the marginal ring-fault is remarkably complete, extending through 240° of arc, and acting as a common outer boundary to both S4 and S5.

Syenite 4 (1.7km^2; ferro-augite syenite; M = 15) is the earlier unit and is divided by S5 into two isolated outcrops. The southern segment is an arcuate ridge rising 40m above the basement gneisses, and cross-cutting their foliation. The contact with G1 has been sculpted into a valley along which the granite shows unusually intense weathering, perhaps attributable to alteration along a fault. Confirmation of ring-faulting is seen further north where the margin of the Widian basement block is brecciated adjacent to S4,with gneiss fragments set in a vitreous-looking quartzose matrix (loc. R96, R99, R1000; Fig. 2.4). In hand-specimen S4 is a dark, feldspar-phyric rock with resorbed perthite phenocrysts (up to 7mm long) set in a medium-grained groundmass.

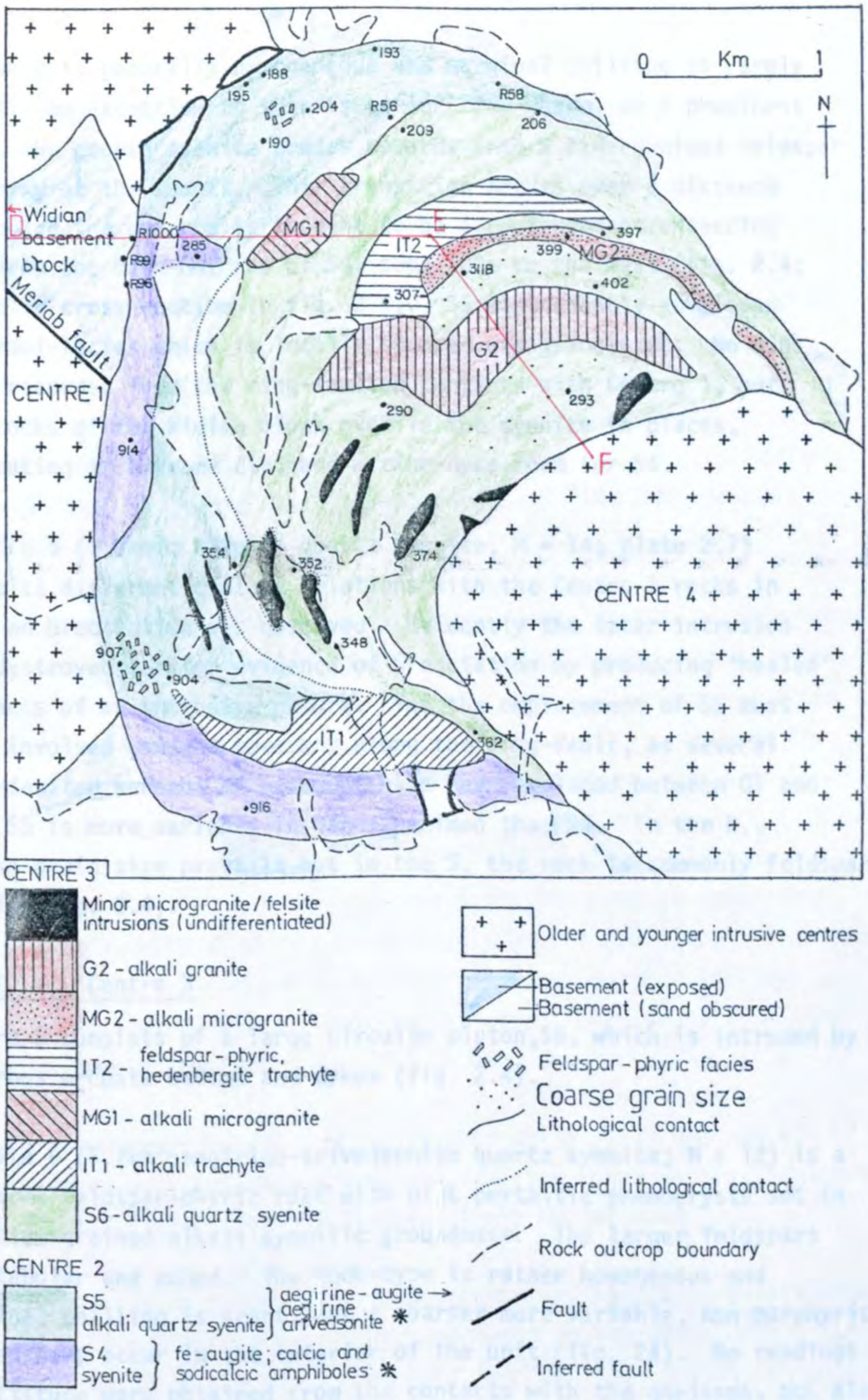

Fig 2.4 FIELD RELATIONS OF CENTRES 2 AND 3, RAS ED DOM.
(lighter shading indicates no exposure. ✱ electron microprobe identification)

The unit is generally homogeneous and marginal chilling is rarely found. An exception to this is at loc. 285 where, on a prominent hill, the coarse syenite grades upwards into a fine-grained feldspar porphyry at the summit. This transition occurs over a distance of 1m and the outcrop is thought to be a roof-pendant extending out from the main outcrop of S4, some 100m to the west (fig. 2.4; see also cross-section in fig. 3.4). S5 discordantly envelopes the roof-facies which is locally sheared and granulated. No dips were recorded from the ring-faulted contacts with Centre 1, but the rocks of the Widian block overlie the syenite in places, indicating an outward dip, and a ring-dyke form for S4.

Syenite 5 (3.2km^2; alkali quartz syenite; M = 14; plate 2.7) exhibits different contact relations with the Centre 1 rocks in that no brecciation was observed. Evidently the later intrusion has destroyed earlier evidence of brecciation by producing 'healed' contacts of an intrusive nature. Yet the emplacement of S5 must have involved renewed movement along the ring-fault, as several down-faulted screens of basement have been emplaced between G1 and S5. S5 is more variable in hand-specimen than S4. In the N., coarse-grain size prevails but in the S. the rock is commonly feldspar-phyric (fig. 2.4).

2.2.E. : Centre 3

Centre 3 consists of a large circular pluton,S6, which is intruded by numerous arcuate bodies and dykes (fig. 2.4).

Syenite 6 (5.7km^2;aegirine-arfvedsonite quartz syenite; M = 12) is a handsome feldspar-phyric rock with pink perthitic phenocrysts set in a medium-grained alkali syenitic groundmass. The larger feldspars are tabular and zoned. The rock-type is rather homogenous and marginal chilling is scant, but a coarser more variable, non-porphyritic facies does occur in the interior of the unit (fig. 2.4). No readings of attitude were obtained from the contacts with the gneisses, but along the contact with S5 two readings of 53°and 70°(loc.206 and 354 respectively) establish outward dipping contacts. Sporadic xenoliths of S5 occur along the contacts whilst a raft of hedenbergite-syenite occurs at loc. 209 (fig. 2.4). This latter occurrence suggests that an early syenite body, perhaps akin to S4 in Centre 2, may have formerly existed in Centre 3. The overall form of S6 is of a broad cylindrical stock with outwarding dipping contacts.

Considering the smaller intrusions of Centre 3, the crosscutting intrusive relationships, where seen, indicate that the more easterly the unit the younger it is. Two such units MG1 and IT1 straddle the S5/S6 boundary (fig. 2.4).

Microgranite 1 (0.16 km^2; aegirine microgranite; M = 7) is an arcuate body of blue felsite, locally feldspar-phyric. Flow-banding, which in places is convolute (plate 2.8), and autobrecciation occur along its margins. It constitutes a sheet with vertical to easterly dips on the west side, and a less inclined lobate eastern roof structure (fig. 2.5A). Intrusive trachyte 1 (0.6km^2;alkali trachyte; M = 22) forms a ridge that tapers out laterally. It is grey in colour and feldspar-phyric with a finer, aphyric selvage. Contacts with host rocks are gradational with a transitional hybrid zone (up to 6m broad) in which the older rocks are fluidised to form coarse tuffisite. Topographic considerations indicate a steeper outer and a shallower inner contact, rather like MG1 (fig. 2.5B).

In the interior of Centre 3 three further units (IT2, MG2 and G2) display curving forms that are parallel to the outer margin, implying that joints within S6 have influenced their emplacement.

Intrusive Trachyte 2 (0.6 km^2; feldspar-phyric, hedenbergite trachyte; M = 32) is a crescentic body that tapers out to the east but is truncated by G2 in the west. The unit is often flow-banded and the dips recorded (fig. 2.5C) are consistent with a steep, partially roofed, incomplete ring-dyke form. At loc. 307 the presence of a raft of volcanic rocks supports the idea that this intrusion has attained a high structural level.

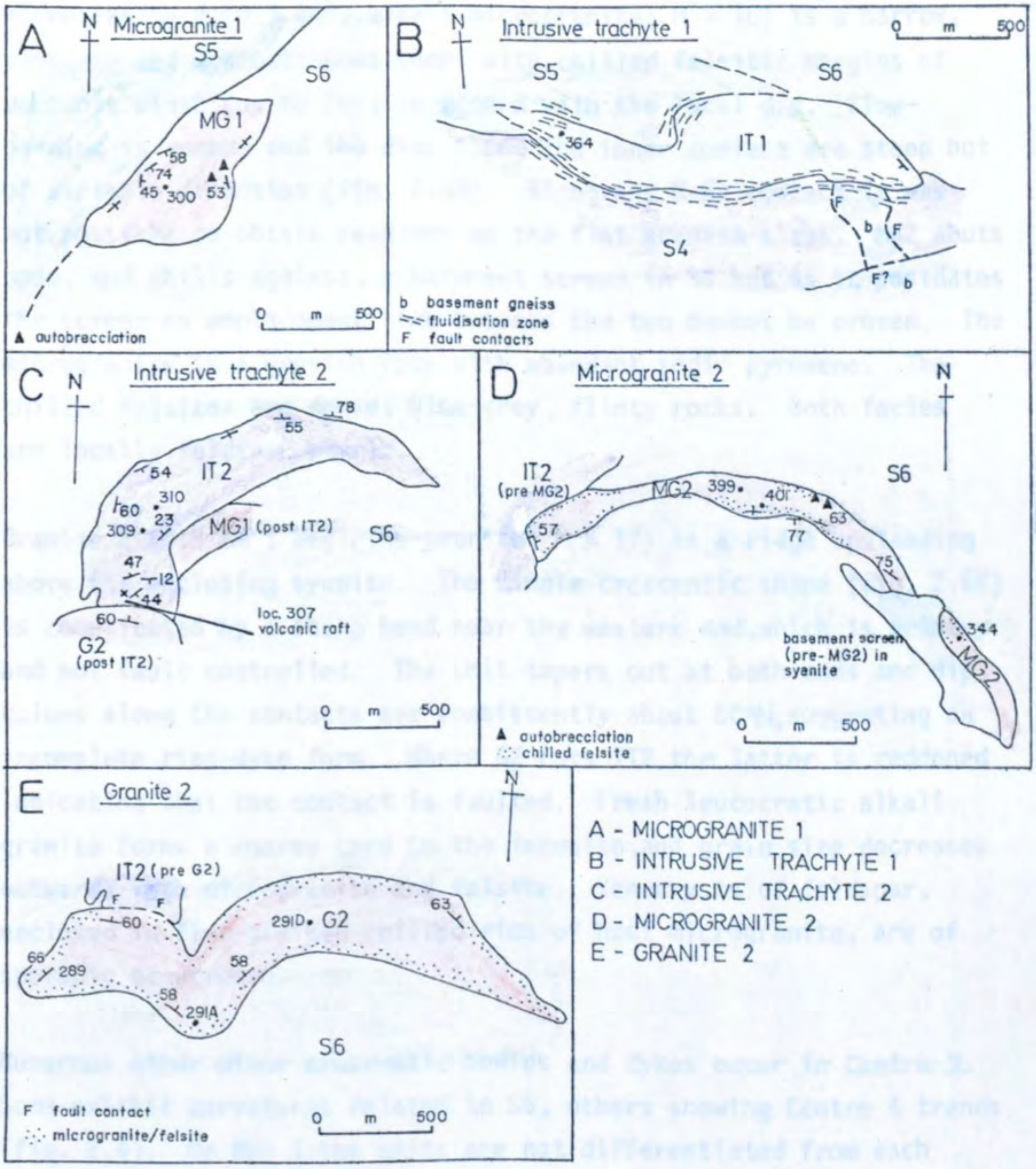

Fig. 2.5. FIELD RELATIONS AND STRUCTURE OF THE LESSER INTRUSIONS OF CENTRES 2 AND 3, RAS ED DOM.

Microgranite 2 (0.3 km^2; alkali microgranite; M = 16) is a narrow, elongate and discontinuous sheet with chilled felsitic margins of variable width (up to 2m), in accord with the local dip. Flow-banding is common and the dips along the inner contact are steep but of variable direction (fig. 2.5D). Along the N.E. contact it was not possible to obtain readings on the flat granite slabs. MG2 abuts upon, and chills against, a basement screen in S6 but as it postdates the screen an emplacement link between the two cannot be proven. The microgranite is a greyish rock with abundant sodic pyroxene. The chilled felsites are dense, blue-grey, flinty rocks. Both facies are locally feldspar phyric.

Granite 2 (0.9 km^2; aegirine-granite; M = 17) is a ridge upstanding above the enclosing syenite. The simple crescentic shape (fig. 2.5E) is complicated by a sharp bend near the western end,which is primary and not fault controlled. The unit tapers out at both ends and dip values along the contacts are consistently about 60°N,suggesting an incomplete ring-dyke form. Where G2 cuts IT2 the latter is reddened indicating that the contact is faulted. Fresh leucocratic alkali granite forms a coarse core to the intusion,and grain size decreases outwards into microgranite and felsite. Xenocrysts of feldspar, enclosed in fine-grained chilled rims of host microgranite, are of sporadic occurrence.

Numerous other minor crescentic bodies and dykes occur in Centre 3. Some exhibit curvatures related to S6, others showing Centre 4 trends (fig. 2.4). On Map 1 the units are not differentiated from each other, but are grouped together as 'minor microgranite intrusions'. A number of them are truncated by S7 and it is likely that the others predate it too. All are thoroughly acid and peralkaline in nature.

2.2.F. : Centre 4

Centre 4 is a simple entity, consisting of a single,sub-circular intrusion, S7. The unit's relief is saucer shaped, being low in the interior but rising by about 70m towards the margins. This is due to a combination of numerous granitic dykes along the margin,

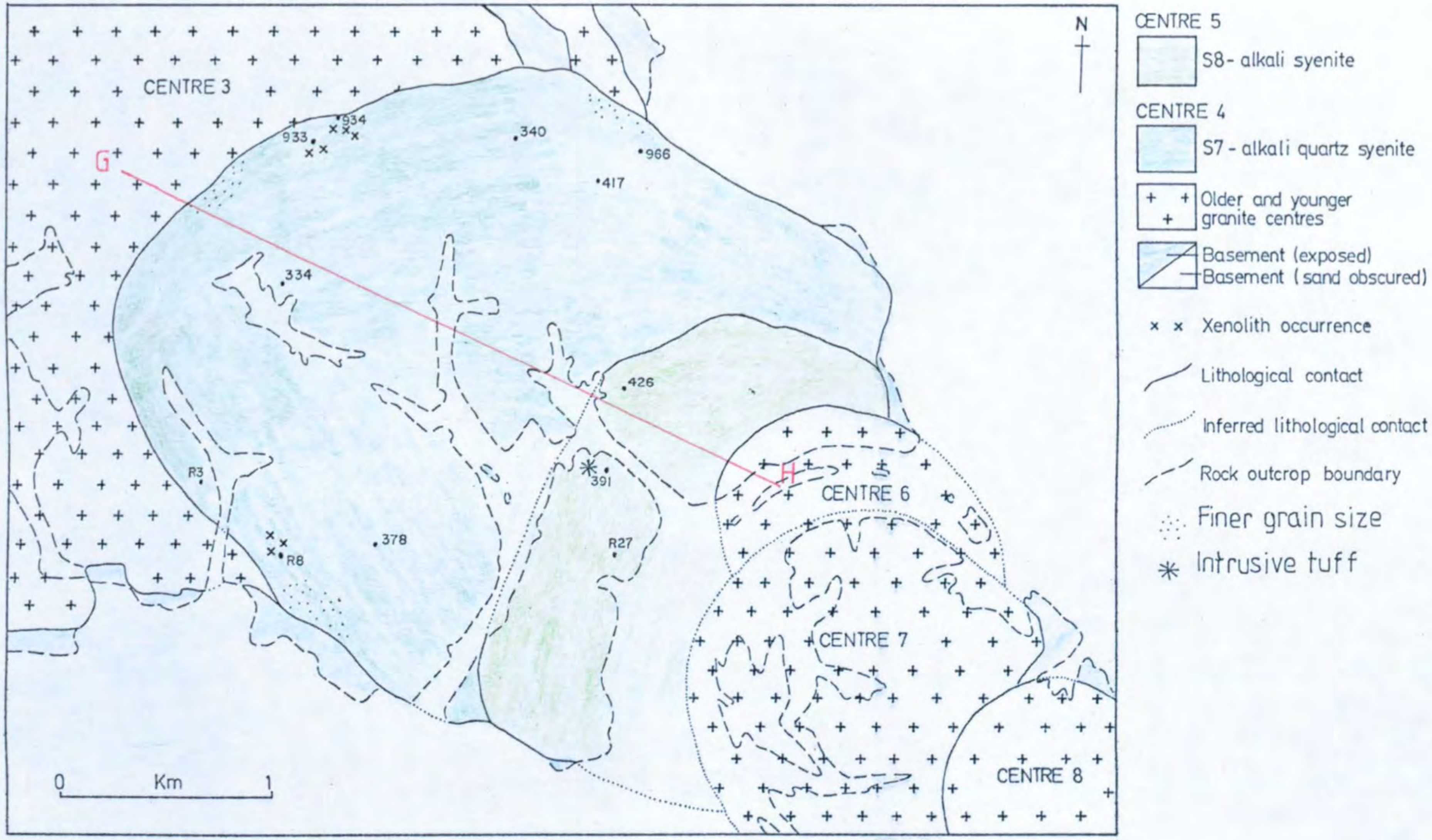

Fig. 2.6 FIELD RELATIONS OF CENTRES 4 AND 5, RAS ED DOM.
(lighter shading indicates no exposure)

and in places the protective shadow afforded by S6, both of which have led to resistant terrain. Syenite 7 (2.7 km^2; alkali quartz syenite; M = 15) is typically a medium-grained,leucocratic, hypidiomorphic rock with cream-coloured feldspar tablets, anhedral quartz, and interstitial sodic pyriboles. The unit is somewhat homogeneous and only towards the outer contact does it become uneven grained, with finer variants present locally (fig. 2.6). It is distinct on aerial photographs by virtue of its closely spaced jointing, and since the contact is little affected by changes in relief it must be steep. The form is that of a broad stock and the absence of basement xenoliths is in accord with passive intrusion along a near vertical, circular fracture.

Concentrations of xenoliths of hedenbergite syenite occur at two localities, both less than 100m in from the contact with S6 (fig. 2.6). At loc. 933-934 the xenoliths are aggregated into three slightly curved layers, up to 2m broad, one of which is traceable for 4m. The xenoliths (2-3cm) are irregular in shape and show no preferred orientation. Although densely packed they are separated by slivers of enclosing chilled syenite (plate 4.15). Since the latter grades into adjacent average syenite the layers are clearly primary, and not dykes. Partial digestion of the xenoliths has given rise to a concentric zonation in them (plate 4.15), and accounts for the absence of any preferred alignment, which might otherwise be expected (Balk, 1937, p.17). The layers are sub-parallel to the margin of the syenite and an outward dip of 75° was obtained from one of them. The second occurrence, at loc. R8 (fig. 2.6), is similar to the first,but less regular in form and it cannot definitely be said to constitute a layer as such.

2.2.G. : Centre 5

Like the preceeding centre, Centre 5 is a single unit (S8) and continues the progressive eastwards shift in magmatism in Ras ed Dom.

Syenite 8 (2.2 km^2; arfvedsonite aegirine-augite syenite; M = 16) forms a ridge of hills in the N., cutting a re-entrant into the outline of Centre 4. Elsewhere relief is low and exposure poor, with only concentric dykes eroding as upstanding features (photomosaic A). In hand-specimen the syenite is a typical, medium-grained, alkali quartz syenite. To the east the unit is truncated by Centres 6 and 7, but extrapolation of its circular form suggests that initially it may have been twice its present size.

2.2.H. : Centre 6

Centre 6 is small and comprises two nested semi-circular intrusions, truncated by Centre 7 to the S.E. (fig. 2.7.A). The outer ring (S9) is assumed to be the earlier although lack of exposure prohibits confirmation of this.

Syenite 9 (0.4 km^2; aegirine-augite syenite;M = 14) is medium-grained and chilling enabled the margin with S8 to be located, but no structural readings were obtained along it. Syenite 10 (0.22 km^2; aegirine-augite arfvedsonite syenite; M = 11) crops-out as a narrow discontinuous ridge isolated from adjacent units by wadi sands. It is a medium- to coarse-grained syenite with the mafic minerals commonly rotted away. As with S9 quartz is uncommon. Lack of exposure along its contacts means that little can be inferred as to its original form.

2.2.I. : Centre 7

The nested annular intrusions of Centre 7 are closely similar to the classic example of the Amo Complex, Nigeria (Buchanan et al., 1971). The three earliest units (S11, S12 and S13) are almost perfectly concentric (plate 2.9), with decreasing ages inwards. S14 is a small boss emplaced eccentrically and slightly to the N.E. The youngest unit, IT3, is a central cone-like structure (fig. 2.7B).

S11 and S12 are narrow, discontinuously exposed rings of markedly coarse grain size overall. Syenite 11 (0.45km^2; hedenbergite syenite; M = 7) is poorly exposed along inner and outer contacts, but does not appear to chill along them. Syenite 12 (0.34km^2; arfvedsonite syenite; M = 7) is a coarsely pegmatitic rock which has undergone intense weathering and tends to crumble in the hand. Syenite 13 (0.8km^2; alkali syenite; M = 13) is the largest intrusion and forms a stock. It is less coarse-grained than the two preceeding units and has a leucocratic appearance. An outer chill zone, up to 2m wide, is present within which the grain size fluctuates considerably. Syenite 14 (0.04km^2;biotite alkali syenite; M = 15) is a small boss similar in appearance and composition to S13, though of finer grain size overall.

No dips were obtained from the contacts of these units, but it is evident that the three earliest units are symmetrical about a vertical axis, and the independence of their forms from topographic controls is consistent with near vertical attitudes. Unlike the above mentioned Amo Complex, basement screens do not occur between the units as far as can be determined. It is thus not possible to decide whether S11 and S12 were emplaced as ring-dykes similar in width to their present form, or were originally stocks pierced co-axially by subsequent intrusions. In either instance, the absence of xenoliths suggests the successive emplacement of the units by permissive cauldron subsidence along steeply inclined ring-faults.

Intrusive Trachyte 3 (0.5km^2; alkali trachyte) consists of a series of inclined sheets disposed centripetally about a central point (fig. 2.7B). The trachyte is a flinty, blue-black, fine-grained rock. Xenoliths ranging in size from about 1cm to over 7cm abound within it. These include hedenbergite syenite, alkali syenite, trachyte, rhyolite and pyroclastic rocks. The volcanic xenoliths presumably derive from a former roof-structure, downfaulted during cauldron subsidence in this centre, and together with the fine grain size suggest that the trachyte is a hypabyssal structure. Basement xenoliths also occur and may have been derived from higher levels also, or alternatively if carried up from below may suggest that the accompanying nested

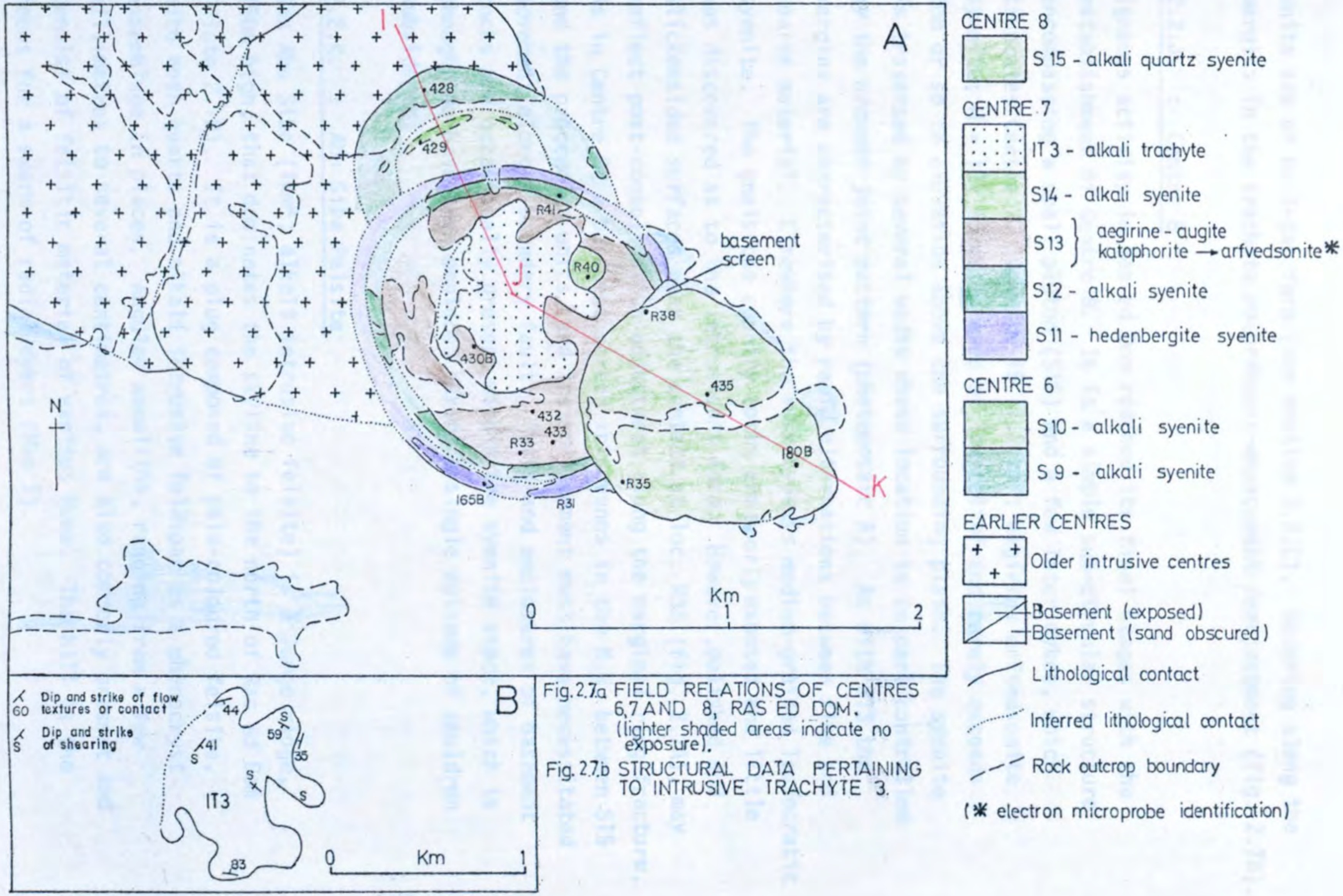

Fig. 2.7a FIELD RELATIONS OF CENTRES 6, 7 AND 8, RAS ED DOM.
(lighter shaded areas indicate no exposure).

Fig. 2.7b STRUCTURAL DATA PERTAINING TO INTRUSIVE TRACHYTE 3.

units are of bell-jar form (see section 3.2.C). Shearing along the margins in the trachyte records post-empacement readjustment (fig. 2.7B).

2.2.J. : Centre 8

Igneous activity in Ras ed Dom reached its final stages with the establishment of Centre 8. It is a simple sub-circular structure encompassing a small pluton (S15) and a few later dykes, which truncates Centre 7. Syenite 15 (1.2 km^2; aegirine arfvedsonite syenite; M = 13) forms an area of low relief and rarely exceeds 20m or so in elevation above the surrounding plain. The syenite is traversed by several wadis whose location is in part controlled by the arcuate joint pattern (photomosaic A). As with S13 the margins are characterised by rapid alternations between fine and coarse material. Elsewhere the rock-type is medium-grained leucocratic syenite. The gneissose country rocks are poorly exposed and little was discovered as to the intrusion's form. However, polished and slickensided surfaces near the contact at loc. R38 (fig. 2.7A), may reflect post-consolidation adjustment along the marginal ring-fracture. As in Centre 2, a basement screen intervenes in the N.W. between S15 and the preceeding units, and its emplacement must have necessitated movement along a boundary fault. Rafts and enclosures of basement rocks are occasionally present within the syenite stock, which is thought to have been emplaced during a single episode of cauldron subsidence.

2.2.K. : Abu Siba Felsite

Ras Abu Siba (1km^2; alkali intrusive felsite) is a large ridge, 150m high, that dominates the skyline to the north of Ras ed Dom (plate 2.10). It is a plug composed of pale-coloured felsite, with both quartz and alkali intrusive feldspar as a phenocryst assemblage in places. Angular xenoliths, ranging from a few millimetres to several centimetres, are also commonly present and consist of felsitic material of various hues. The hill is the focus for a swarm of radial dykes (Map 1).

Owing to its geographical isolation the felsite cannot be firmly fitted into the intrusive chronology, but it could conceiveably be a continuation of the northward migrating magmatism of Centre 1. The peralkaline mineralogy of the felsite proves its affinities with the Younger Granite episode.

2.2.L. : Minor Intrusions

Within and around Ras ed Dom, minor intrusions (plate 2.11) abound in such profusion that systematic mapping of them was not possible in the available time. Their distribution based on a combination of air-photo interpretation and field observation is depicted on Map 4 (rear pocket). Shallow inclinations are relatively rare, most of these intrusions being dykes.

1. Internal Dykes (emplaced with the ring-complex)

A consideration of strike and dip reveals the existence of four major types, as follows:-

a. Cone-sheets : inward dipping.

b. Minor ring-dykes : vertical to outward dipping.

c. Radial dykes.

d. Linear dykes : these follow major E-W joint fractures, and characteristically persist for long distances, e.g. 25km. They are the youngest dykes in the complex.

The concentric or radial disposition exhibited by the first three categories can be commonly related to the intrusive forms of the major units, and like them, record the eastwards progression of magmatism with time that characterises Ras ed Dom (fig. 2.1). In contrast to the larger plutons, acidic compositions predominate over intermediate ones. Lithologies observed include microgranites, felsites, microsyenites and intrusive trachytes. Peralkaline types prevail everywhere, but a few early hedenbergite-bearing syenite dykes are known from S1 and S2 of Centre 1, and also from Centres 7 and 8.

Some of the dykes are intrusive tuffs, and a cluster of such bodies occurs along the outer S-W margin of S2 (fig. 2.3). They occur in steep dykes veins and pipes, but apart from some gas-streamed banding no regular zonal or concentric features were noted. The pipe form is best exemplified by an elliptical body (100m) of tuffisite which intrudes S8, at loc. 391 (fig. 2.6). In hand-specimen the tuffisites are characterised by fluidised feldspar fragments and mafic clots, whilst in the coarser breccias angular to rounded syenite clasts, up to 5cm in size, are set in a tuffisitic matrix.

2. External Dykes (emplaced into adjacent basement rocks)

Younger Granite dykes, now present as upstanding ridges in the gneisses, form a girdle about Ras ed Dom (Map 4;photomosaic A). Cross-cutting relations amongst these dykes enables the recognition of local dyke chronologies, but correlation of these different local sequences is difficult for several reasons, as listed below.

a. Repetition of similar lithologies : most of the dykes are fine-grained, peralkaline, acid intrusives, with syenitic types less in evidence as compared to the internal dykes. Spherulitic quartz-feldspar-phyric types are especially common. Affinities are consequently unclear, e.g. N.E. of Centre 1 a set of quartz-feldspar porphyries occurs which could belong to the Abu Siba swarm, or equally to the similar swarm that runs parallel to the Centre 1 margin just east of J. el Hoorba (Map 4).

b. Extrapolation of curving strikes is highly subjective.

c. Fracture patterns once established may be exploited by dykes of more than one age. For instance, the cone-sheets south of Centres 7 and 8 exhibit a curvature related to those centres and are evidently relatively young, yet adopt an earlier E-W trend at their westerly ends (Map 4).

Nevertheless, the observed age relationships suggest that, broadly speaking, three main types of swarm are present, although more than one age of each probably occurs.

a. Rectilinear dykes tangential or oblique to the local strike of the margin of the complex generally predate it (e.g. Area A on Map 4).

b. Dykes radial to the complex edge usually postdate it (e.g. Abu Siba swarm, Map 4).

c. Dykes that strike parallel to the edge of the complex and display a curvature in sympathy with it, postdate both aforementioned types. Dips are generally inward suggesting a cone-sheet structure. In one instance the dips on a series of such sheets increase steadily inwards in the classic fashion (Area B, Map 4). Generally however such an ideal pattern of dips is absent, probably because most of the swarms are multiple i.e. contain dykes emplaced at different times.

2.3. : Abu Dom Complex

2.3.A. : Introduction

The naming of the intrusive units in Abu Dom follows the same principles applied earlier to Ras ed Dom (section 2.2.A). However as only seven major intrusions are present in Abu Dom sub-grouping into structural centres is not attempted. The intrusive chronology is presented in table 2.2. Place names are illustrated in fig. 2.8. The overall geology of the complex is presented on Map 2 (rear pocket), but local maps are also interspersed with the text. Structural cross-sections are presented in the succeeding chapter (figs. 3.7 - 3.9).

2.3.B. : Abu Dom Volcanic Group

The Abu Dom Volcanic Group comprises a small outcrop (0.1km^2) in the S.E. of the complex (fig. 2.10).

YOUNGER	INTRUSIVE SEQUENCE ↑	GRANITE 2	(3.8km^2)
		SYENITE 5	(4.3km^2)
		SYENITE 4	(5.2km^2)
		SYENITE 3	(4.6km^2)
		GRANITE 1	(10.3km^2)
		SYENITE 2	(5.3km^2)
		SYENITE 1	(1.2km^2)
OLDER		ABU DOM VOLCANIC GROUP	(0.1km^2)

Table 2.2 : Intrusive chronology of Abu Dom Complex, and outcrop areas of the units.

Fig. 2.8 PLACE NAMES IN THE JEBEL ABU DOM VICINITY.

The volcanic rocks consist of ignimbrite and rhyolitic lavas, interbedded with agglomerate. Convolutions in the flow-banding of the lavas complicate the structural picture, but the overall dips are 45-50°N.W. Intrusive rocks are also present in the S. of the outcrop. A small granite body separates the volcanic rocks from a hedenbergite-syenite (plate 2.13A), both intrusions being exposed only in a few small outcrops. The granite postdates both the syenite and the volcanic rocks and on grounds of petrographic similarity is attributed to G1. For similar reasons the syenite is considered part of S1.

Basement gneisses crop-out in places between the volcanic rocks and Abu Dom to the W. Conceivably the volcanic rocks might be thought to occupy a depression on the pre-Younger Granite basement surface, but this would not account for their dip, nor for the presence of associated intrusive rocks. More probably the outcrop is fault controlled, with the volcanic rocks down-faulted against the intrusives. Sparse exposure makes this difficult to confirm but indirect evidence is present. Firstly,the granite was fluidised, with shears healed by late-crystallised groundmass, suggesting fluidisation during emplacement. Secondly, immediately E. of the outcrop, the strike in adjacent Nubian sandstones swings abruptly from N.S. to E.W., evidently about an unexposed fault (Map 2; fig. 2.13; section 3.4). If this fault was active in pre-Nubian times also then it may partly control the location of the preserved volcanic rocks.

As at Ras ed Dom sparse evidence of a volcanic episode is found. In this instance its early-stage occurrence is suggested by the fact that it appears to predate S1.

2.3.C. : Syenite 1

Syenite 1 (1.2km^2; hedenbergite syenite; M = 16) comprises several isolated outcrops of early hedenbergite syenite scattered about Abu Dom, and identified by place names as indicated in fig. 2.9. The

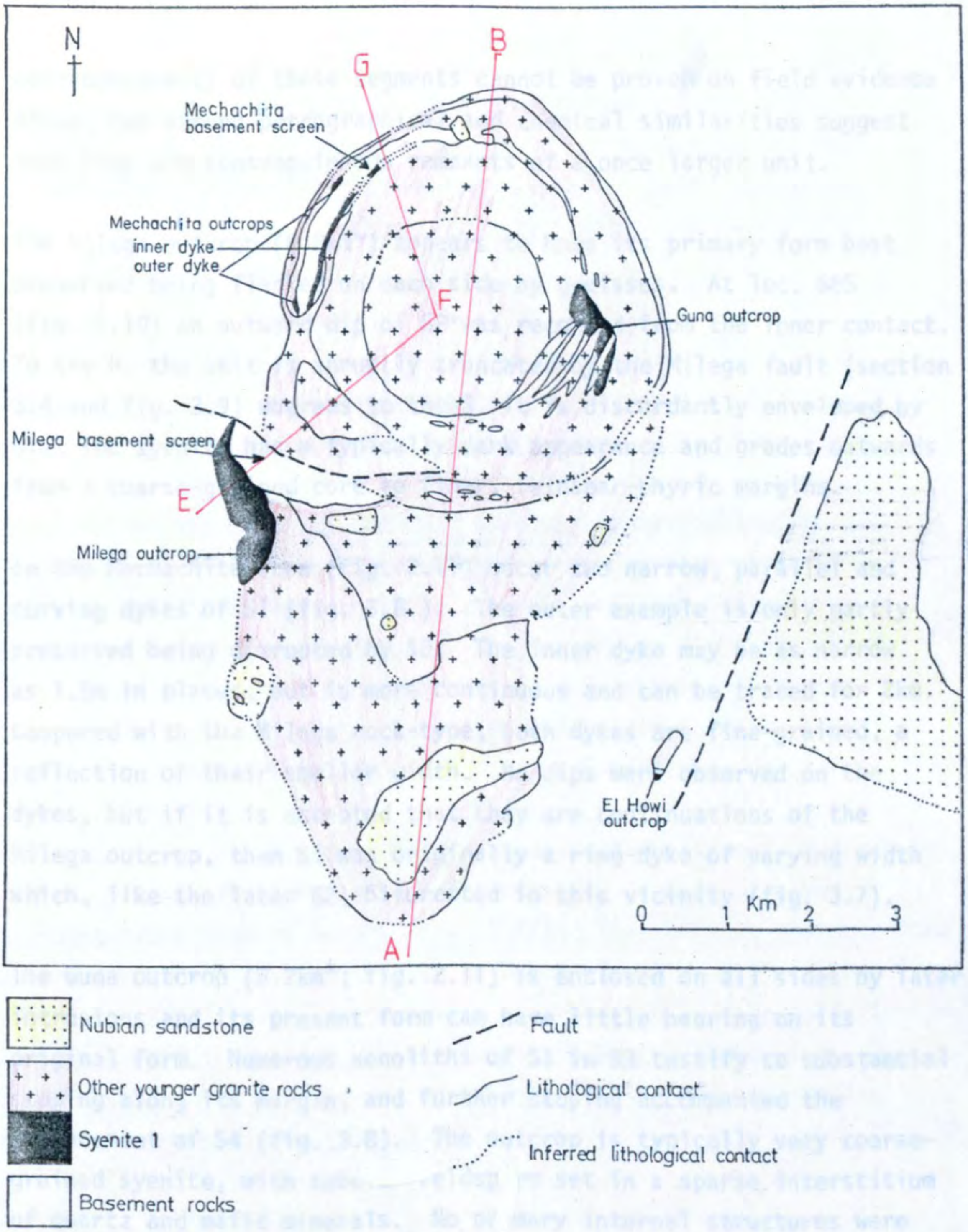

Fig. 2.9 LOCATION AND DESIGNATION OF THE VARIOUS OUTCROPS OF SYENITE 1, ABU DOM COMPLEX.
(For further explanation see text)

contemporaneity of these segments cannot be proven on field evidence alone, but strong petrographical and chemical similarities suggest that they are consanguineous remnants of a once larger unit.

The Milega outcrop (0.8km^2) appears to have its primary form best preserved being flanked on each side by gneisses. At loc. 685 (fig. 2.10) an outward dip of 68° was recorded from the inner contact. To the N. the unit is abruptly truncated by the Milega fault (section 3.4 and fig. 3.9) whereas to the S. it is discordantly enveloped by G1. The syenite has a typically dark appearance and grades outwards from a coarse-grained core to finer, feldspar-phyric margins.

In the Mechachita area (fig. 2.11) occur two narrow, parallel and curving dykes of S1 (fig. 3.8.). The outer example is only partly preserved being disrupted by S3. The inner dyke may be as narrow as 1.5m in places, but is more continuous and can be traced for 2km. Compared with the Milega rock-type, both dykes are fine-grained, a reflection of their smaller width. No dips were observed on the dykes, but if it is accepted that they are continuations of the Milega outcrop, then S1 was originally a ring-dyke of varying width which, like the later G2, bifurcated in this vicinity (fig. 3.7).

The Guna outcrop (0.2km^2; fig. 2.11) is enclosed on all sides by later intrusions and its present form can have little bearing on its original form. Numerous xenoliths of S1 in S3 testify to substantial stoping along its margin, and further stoping accompanied the emplacement of S4 (fig. 3.8). The outcrop is typically very coarse-grained syenite, with tabular feldspars set in a sparse interstitium of quartz and mafic minerals. No primary internal structures were found.

The fourth occurrence of early syenite is the El Howi outcrop that borders the Abu Dom Volcanic Group (fig. 2.10). The outcrop is less than 2m in size but is closely similar in appearance to the Milega type.

To summarise, it seems that S1 once constituted a major early ring-dyke. As with the early syenites of Ras ed Dom it has been disrupted by faulting and foundering related to later intrusive events, but S1 documents these events in greater detail than is found in that complex.

2.3.D. : Syenite 2

Syenite 2 (5.3km^2; aegirine-arfvedsonite syenite; M = 15) is a broad irregularly shaped intrusion located to the S. of Wadi el Milega (fig. 2.10). Relief throughout is low, rarely exceeding 2m in height and although the unit is bordered by gneisses to E. and N.W., the contacts are not exposed. The position of S2 in the intrusive chronology rests on indirect evidence. Firstly it exhibits a more evolved mineralogy as compared to S1. Secondly, although G2 intervenes between it and S3,the latter does appear to truncate S2. Its only well-exposed contact is with the later G1 intrusion to the S.

For much of its areal extent S2 is composed of monotonous, moderately coarse-grained alkali syenite, but in the N.E. a belt of paler, medium-grained syenite occurs (fig. 2.10). This belt is characterised by cream-coloured prismatic perthite and trends E.W, a direction roughly parallel to the contact with the gneisses in that vicinity. S3 cuts across this trend, suggesting it to be the later unit. To conclude, S2 forms a stock but the attitude of its margins remains a matter for conjecture (fig. 3.7).

2.3.E. : Granite 1

Granite 1 (10.3km^2; arfvedsonite-aegirine granite; M = 12) is the largest unit in Abu Dom, forming a V-shaped body in the S. of the complex.

In the W. and S. exposure is rather limited, and basement/granite relations are obscured by a thin veneer of Nubian sandstone or by recent wadi alluvium. In the S.E. exposure is better and the gneiss/

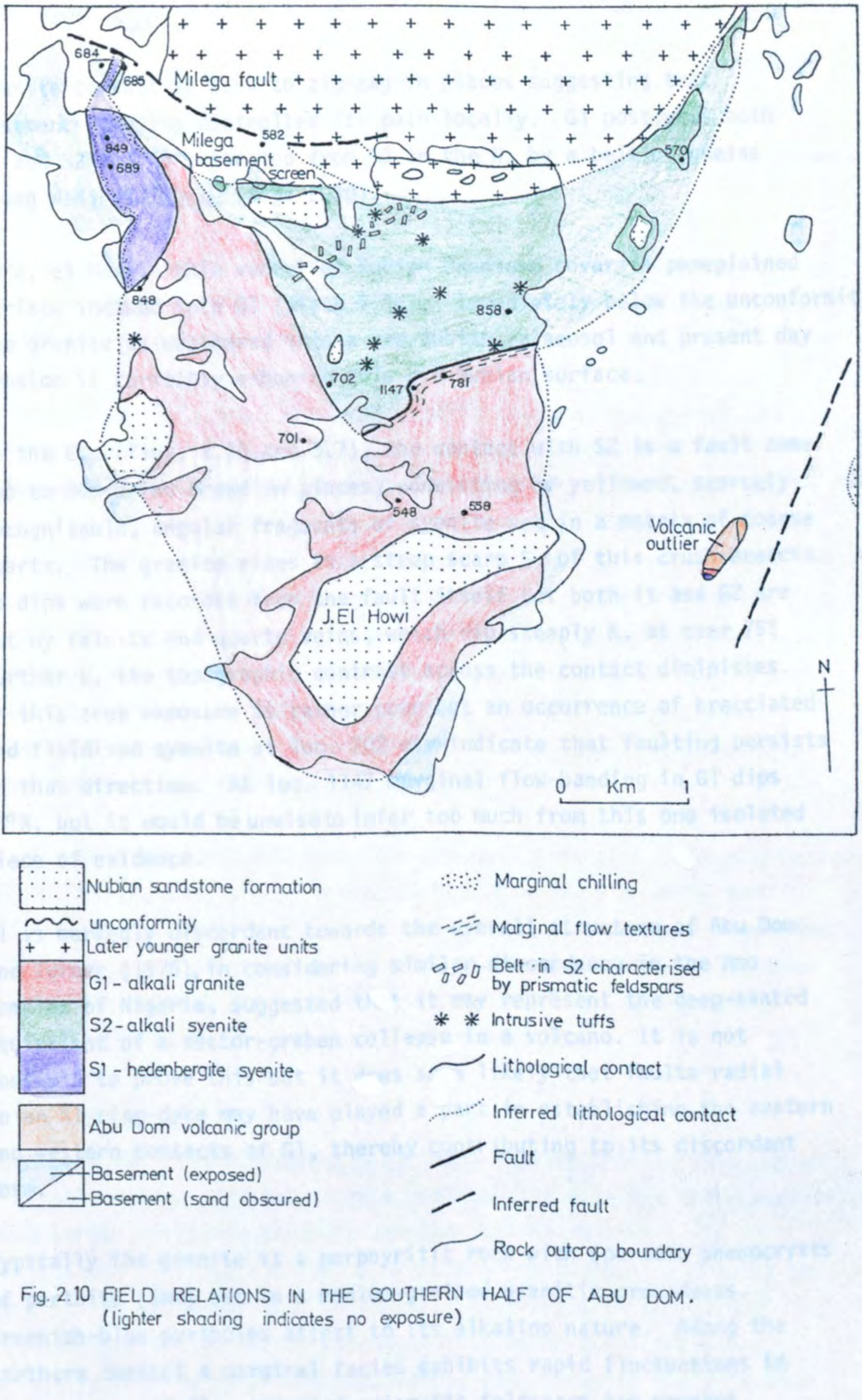

Fig. 2.10 FIELD RELATIONS IN THE SOUTHERN HALF OF ABU DOM.
(lighter shading indicates no exposure)

granite contact is seen to zig-zag in places suggesting that basement jointing controlled its path locally. G1 postdates both S1 and S2 and is separated from G2 in the N. by a belt of gneiss along Wadi el Milega (fig. 2.10).

At J. el Howi a thin veneer of Nubian Sandtone covers a peneplained surface incised into G1 (plate 2.14). Immediately below the unconformity the granite is weathered into a pre-Nubian palaeosol and present day erosion is currently exhuming this pre-Nubian surface.

In the E. (figs. 2.10 and 3.7), the contact with S2 is a fault zone (up to 20m or so broad in places) consisting of yellowed, scarcely recognisable, angular fragments of syenite set in a matrix of coarse quartz. The granite rises as a steep scarp S. of this crush-breccia. No dips were recorded from the fault itself but both it and G2 are cut by felsite and quartz veins, which dip steeply N. at over 75°. Further W. the topographic contrast across the contact diminishes. In this area exposure is rather poor but an occurrence of brecciated and fluidised syenite at loc. 702 may indicate that faulting persists in that direction. At loc. 1147 marginal flow-banding in G1 dips 45°N. but it would be unwise to infer too much from this one isolated piece of evidence.

G1 is markedly discordant towards the overall structure of Abu Dom and Turner (1976), in considering similar discordancy in the Amo Complex of Nigeria, suggested that it may represent the deep-seated equivalent of a sector-graben collapse in a volcano. It is not possible to prove this but it does seem likely that faults radial to an S1 ring-dyke may have played a part in establishing the eastern and western contacts of G1, thereby contributing to its discordant form.

Typically the granite is a porphyritic rock with sporadic phenocrysts of perthite (5mm) set in a medium-grained granitic groundmass. Greenish-blue pyriboles attest to its alkaline nature. Along the northern contact a marginal facies exhibits rapid fluctuations in grain-size, and flow-oriented prismatic feldspars are present.

2.3.F. : Syenite 3

Syenite 3 (4.6km^2; aegirine-arfvedsonite syenite; M = 16) is the oldest and outermost of the three nested syenites located in northern Abu Dom (fig. 2.11).

In the S. and E. S3 forms a broad ring-dyke (av. width 0.6km) but in the N.W. it narrows to form an upstanding arcuate ridge (see frontespiece) which follows the earlier S1 trend in this area.

Although everywhere a leucocratic quartz syenite, grain size and textures vary from place to place. In the E. (fig. 2.11) it is typically medium-grained although coarser types occur in places away from the margins. Feldspar-phyric types are developed locally near the outer contacts. Where the unit narrows in the N. it becomes consistently porphyritic with tabular feldspars (7mm but occasionally as large as 2cm) set in a medium-grained groundmass. The S.W. outcrop is again typically porphyritic but the matrix grain size is variable and fluctuates between fine and medium grade. Xenoliths are common both here and adjacent to the S1 Guna outcrop, testifying to the importance of stoping.

No dip readings were obtained from the unit's margins, primarily because of the emplacement of the later G2, accompanied by shearing and hybridisation, along them. However in the N.W. a screen of basement gneiss is preserved on the inner side of S3, suggesting a ring-dyke form (frontespiece and figs. 2.11 and 3.9). There, the gneisses underlie the S3 rocks, indicating an outward dip.

2.3.G. : Syenite 4

Syenite 4 (5.1km^2; arfvedsonite aegirine syenite;M = 12) is a second ring-shaped body of 0.6km average width,emplaced on the inner side of S3. Large exfoliated boulders are the typical physiographic expression. A broad chilled outer zone is ubiquitous (fig.2.11) and consists of medium-grained leucocratic syenite, with occasional segregations of pegmatitic syenite. This outer zone coarsens gradually inwards into a darker looking rock in which the feldspars become larger, greenish, tabular perthites (5-8cm).

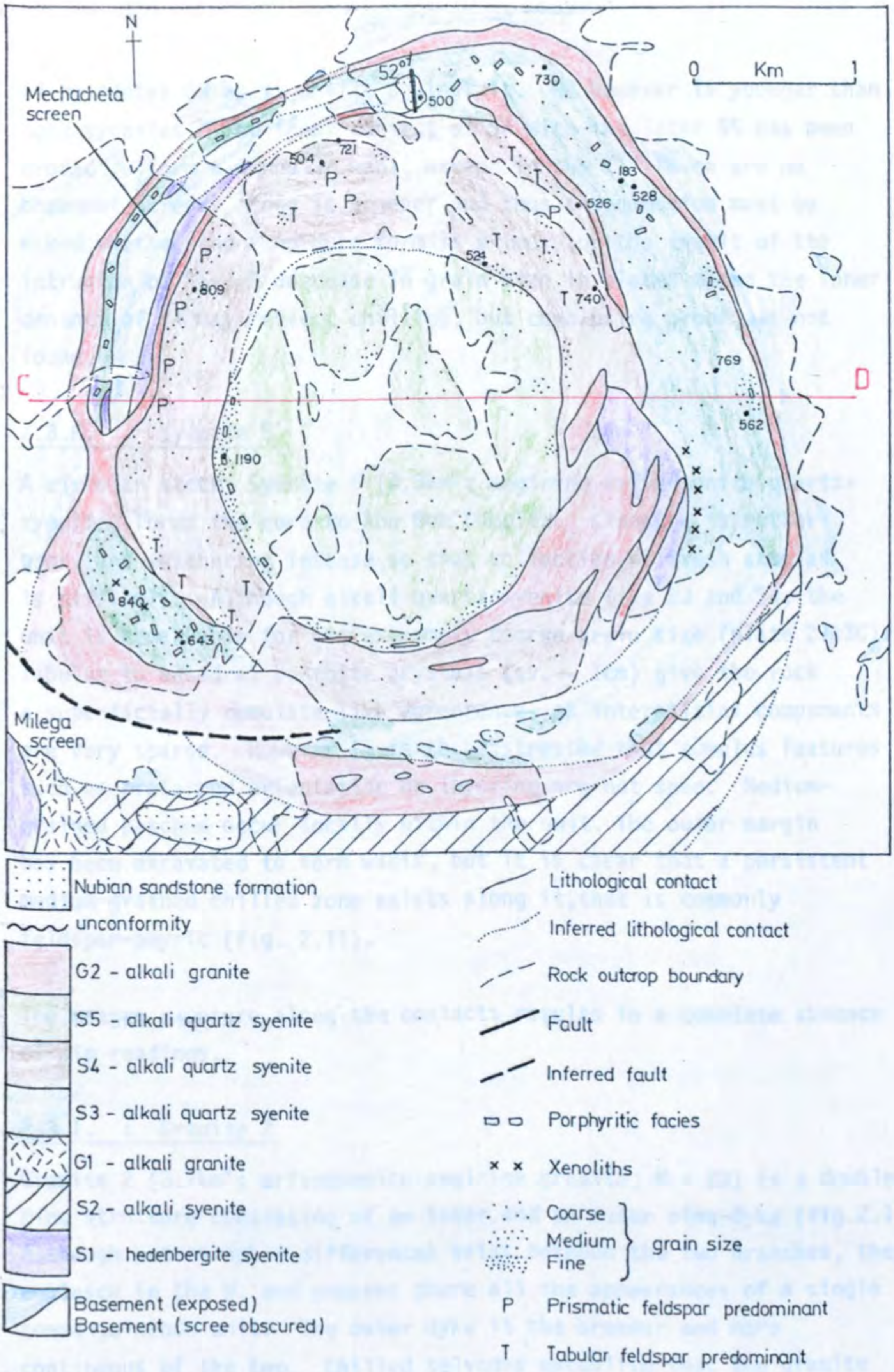

Fig. 2.11 FIELD RELATIONS IN THE NORTHERN HALF OF ABU DOM.
(lighter shading indicates no exposure)

S4 postdates S3 as it chills against it. G2 however is younger than both syenites. The inner contact of S4 with the later S5 has been eroded to form a circular wadi, except in the E. There are no basement screens along it however and thus the question must be asked whether the ring-dyke form is primary,or the result of the intrusion of S5. A decrease in grain size in places along the inner contact of S4 may reflect chilling, but conclusive proof was not found.

2.3.H. : Syenite 5

A circular stock, Syenite 5 (4.3km^2; aegirine arfvedsonite quartz-syenite) forms the core to Abu Dom Complex. Exposure is rather poor, and weathering intense so that collection of fresh samples is difficult. Although alkali quartz-syenite like S3 and S4, the unit is remarkable for its extremely coarse grain size (plate 2.13C). Tabular to anhedral perthite crystals (av. ~ 1cm) give the rock a superficially cumulate-like appearance, as interstitial components are very sparse. However it is to be stressed that cumulus features such as preferred orientation or layering are not seen. Medium-grained patches occur locally within the unit. The outer margin has been excavated to form wadis, but it is clear that a persistent medium-grained chilled zone exists along it,that is commonly feldspar-phyric (fig. 2.11).

The meagre exposure along the contacts results in a complete absence of dip readings.

2.3.I. : Granite 2

Granite 2 (3.7km^2; arfvedsonite aegirine granite; M = 23) is a double ring structure consisting of an inner and an outer ring-dyke (fig.2.12). Although petrographic differences exist between the two branches, they coalesce in the W. and present there all the appearances of a single consanguineous unit. The outer dyke is the broader and more continuous of the two. Chilled selvages establish that the granite postdates syenites 1-5 inclusive and is therefore the final major igneous event to occur in the complex.

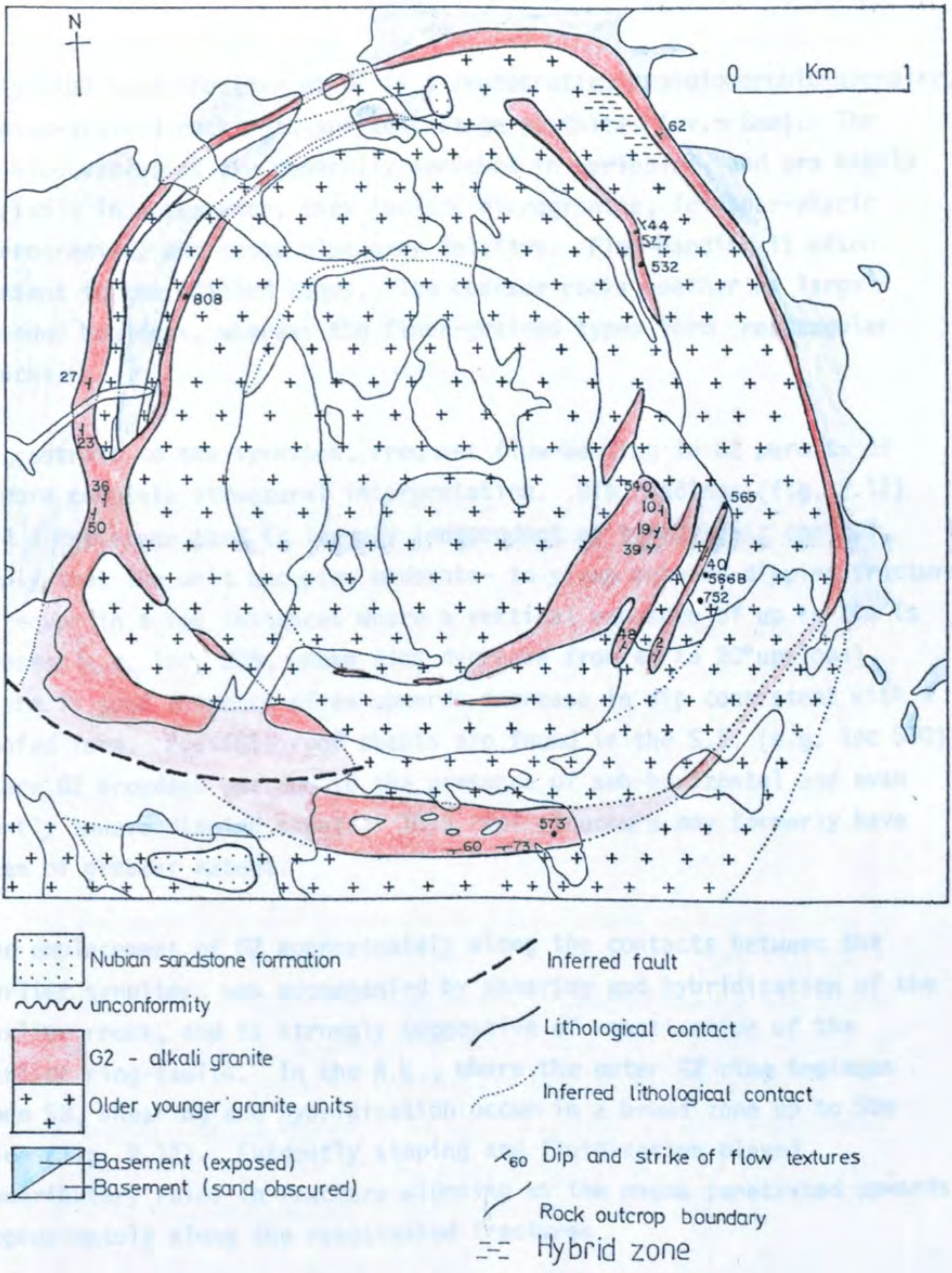

Fig. 2.12 STRUCTURAL DATA FOR GRANITE 2, ABU DOM.
(lighter shading indicates no exposure)

A typical hand-specimen of G2 is a leucocratic, hypidiomorphic-granular, medium-grained rock with sporadic large perthites (av.~ 8mm). The chilled varieties are generally enriched in pyriboles, and are highly variable in appearance; they include microgranite, feldspar-phyric microgranite, and dense blue-grey felsites. Flow-banding is often present in the chilled zones. The coarser rocks weather as large rounded boulders, whereas the finer-grained types form rectangular blocks.

In contrast to the syenites, frequent flow-banding in G2 permits of a more complete structural interpretation. Dip readings (fig. 2.12) and a curvature that is largely independent of topographic control, imply that the unit occupies moderate- to steep outward-dipping fractures. Moreover in a few instances where a vertical exposure of up to 20m is present (e.g. loc. 808, where dips decrease from 44° to 20° upslope), there is good evidence of an upwards decrease in dip consistent with a roofed form. Possible roof sheets are found in the S.E. (e.g. loc 540) where G2 broadens out due to the presence of sub-horizontal and even gently inward dipping sheets. This roof structure may formerly have been of greater extent.

The emplacement of G2 approximately along the contacts between the earlier syenites, was accompanied by shearing and hybridisation of the earlier rocks, and is strongly suggestive of reactivation of the earlier ring-faults. In the N.E., where the outer G2 ring impinges upon S3, shearing and hybridisation occur in a broad zone up to 50m wide (fig. 2.12). Evidently stoping and fluidisation played contributary roles in fracture widening as the magma penetrated upwards approximately along the reactivated fractures.

2.3.J. : Minor Intrusions

1. Internal Dykes (emplaced within the ring-complex)

As in Ras ed Dom it is possible to recognise cone-sheets, minor ring-dykes and radial dykes. Acidic compositions prevail over intermediate types. Peralkaline mineralogies are the rule, although two hedenbergite syenite dykes in the Mechachita screen are known, and thought to belong to S1. A small dyke of dolerite intrudes S3 at loc. 183 (fig. 2.11) and has the distinction of being the only basic rock-type known from either complex (section 4.6).

Intrusive tuffs, all of dyke form, are present in several places. A major cluster occurs in S2 (fig. 2.10), as is probably related to the faulting along the S2/G2 contact. Most of the dykes are coarse intrusive breccias with gas-streamed matrices.

2. External Dykes (emplaced into the adjacent gneisses)

A major cone-sheet swarm partly girdles the Abu Dom complex. The swarm is assymetric and most fully developed in the N.W. where it strikes N.E. (Map 5; photomosaic B). Further S. the swarm swings approximately S.S.E., whilst on the eastern side of the complex a complimentary swarm is weakly developed. The main swarm is multiple and several elements can be distinguished as follows:-

a. various dykes of felsite that are roughly radial to Abu Dom antedate the main swarm.

b. the swarm is present in the Mechachita screen in the N.W. but does not cut S4 or any later unit. In the S. it does intrude S1, S2 and G1. Thus it's emplacement occurred during the hiatus in which the focus of magmatism moved into the norther sector of the complex. In detail this picture may be something of an oversimplification however, as several cross-cutting sub-trends are present within the swarm, suggesting that it is a composite feature, including dykes of more than one age.

With very few exceptions the dykes display inward-dipping contacts, and are thus cone-sheets. No regular variation in the dips was found however, probably because of the swarm's multiple nature. On a larger scale the asymmetry of the swarm is intriguing. The country rocks are homogeneous gneisses and the reason can scarcely lie therein. An asymmetrically shaped magma chamber might account for it (Koide and Bhattacharji, 1975), but is unlikely in view of the perfect symmetry displayed by the major units in north Abu Dom. Other factors such as asymmetry of the horizontal regional stress at the time of emplacement may have been responsible.

Lithologically the cone-sheets are mainly microgranites and felsites. They often display devitrification textures such as spherulites (as large as 4cm across, plate 2.12).

2.4. Summary

From theforegoing descriptions it is clear that lithologically Ras ed Dom and Abu Dom are closely similar. 3 main rock-types are recognised as follows. These are, calcic-clinopyroxene bearing syenites, alkali syenites and alkali granites (plate 2.13A-D). The mafic colour index declines in that order also, although locally the chilled margins of the alkali rocks are enriched in sodic pyriboles. Markedly coarse grain size occurs in some of the later units in Ras ed Dom (e.g. S11 and S12 in centre 7 of Ras ed Dom; S5 of Abu Dom) and also in the chilled margins in some instances (e.g. S4, Abu Dom). Volcanic rocks are poorly preserved in both complexes. Syenitic compositions predominate in the major intrusions, whilst the dykes are predominantly acid in composition.

Details of the petrography and structure are discussed in subsequent chapters.

2.5. : Nubian Sandstone Formation

Several outliers of Nubian Sandstone Formation lie unconformably on the basement and Younger Granite rocks in the Abu Dom area (fig. 2.13). No such deposits occur in the vicinity of Sultaniyat or Ras ed Dom.

These residual deposits nowhere exceed 10m in thickness and are usually less than 1m. The thickest succession is on Jebel el Howi in the south of Abu Dom. The elevation of the base of the Nubian varies by as much as 30m over short distances,a fact that cannot always be accounted for by invoking intervening faults. Rather, it appears that the present topography is a largely exhumed landscape closely similar in profile to that of the pre-Nubian surface.

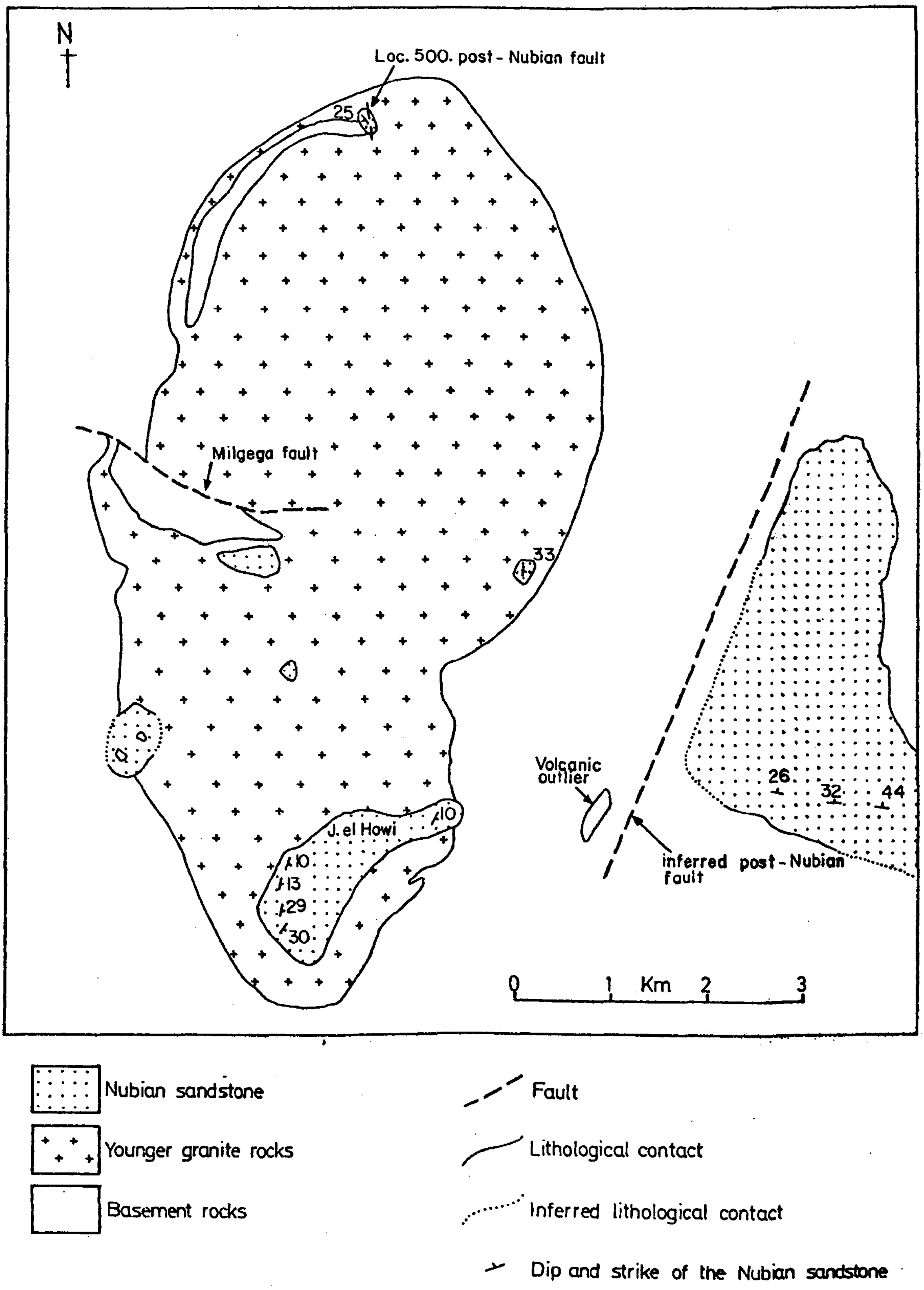

Fig. 2.13 DISTRIBUTION AND ATTITUDE OF THE NUBIAN SANDSTONE FORMATION ABOUT ABU DOM COMPLEX.

At J. el Howi the latter is seen to be a peneplain (plate 2.14) locally incised by gullies. As mentioned earlier (section 2.3.E), G1 was exposed and degraded to a palaeosol prior to deposition of the Nubian strata.

Lithologically, three main facies of Nubian are present, as follows:-

1. Basal pebble conglomerate : This facies infills gullies in the pre-Nubian surface, and is not present everywhere. The boulder conglomerate reported from elsewhere in Bayuda (Barth and Meinhold, 1979) was not found. Quartz fragments predominate and the absence of readily identifiable Younger Granite clasts is noteworthy (op.cit. ; Vail, 1974).

2. Sandstones : these are the commonest lithologies, and both red and white (silicified) types occur. Variants include thin homogeneous beds (0.3m), finely laminated sandstones with purple and white bands (1-5mm), and coarsely cross-bedded horizons (e.g. 15cm, see plate 2.15). In thin section highly strained quartz occurs as single and polycrystalline fragments. Minor amounts of orthoclase, zircon, bent muscovite flakes, and sundry other haematised fragments are present. The matrix is generally of silt-clay grade.

3. Shales : The shales occur as white, kaolinitic bands and lenses intercalcated with the sandstones in places, e.g. J. el Howi and loc. 500 (fig. 2.13).

Both the sandstones and shales belong to the lower argillaceous sandstones and gritstones recognised by Barth and Meinhold (1979).

A marked change in strike occurs to the E. of the Abu Dom Volcanic Group (fig. 2.13). To the W. the strata strike roughly N.S. and dip 10-20°E., whilst E. of the volcanic rocks the beds strike E.W., and dip 10-44°N. Barth and Meinhold (1979) related deviations from the horizontal in the Nubian to tilting of fault blocks, and the writer proposes that an unexposed N.E.-trending fault is present in this area, as indicated on Map. 2.

2.6. : Cainozoic Basalts

2 small composite volcanoes, J. el Hoorba and Hiwaish Abu Siba, are situated in close proximity to Ras ed Dom (Map 1; fig. 2.14). Both cones are of youthful appearance and are outlying parts of the Main Volcanic Field, which lies to the N.W. and has been shown to be Pleistocene in age (Barth and Meinhold, 1979).

J. el Hoorba ($1.7km^2$) consists of a N.E.-trending ridge with a breached cone at its northern end, from which two lava-flows have debouched northwards (fig. 2.14). The upper flow is the less extensive but more vesicular of the two.

At Hiwaish Abu Siba ($1.8km^2$) the primary circular form of the cone is preserved intact. A thin veneer of salt deposits covers the crater floor. A single lava flow has erupted westwards from the cone onto the alluvial sands of the plains.

The lava flows show typically rough aa surfaces, composed of jagged clinker, but behind the hummocky lava fronts smoother ropy surfaces exist locally (fig. 2.14). The latter are characterised by concentric ribbing which is transverse to the flow direction and reflects ramping behind the fronts. The cones consist of bedded pyroclastic fragments including ash, cinder and volcanic bombs (up to 1m; plate 2.16).

Both occurrences are of alkali olivine basalt. Olivine and titanaugite constitute the phenocryst phases. The groundmass is composed of flow-oriented basic plagioclase laths, smaller olivine and clinopyroxene grains, together with Fe-Ti oxides. At Hiwaish Abu Siba oxyhornblende, rimmed by magnetite grains, also occurs. Zenoliths and zenocrysts of basement derivation are common. Calcite occurs as secondary infill of the vesicles. In terms of chemistry, the lavas are undersaturated nepheline-trachybasalts (Almond, 1974). 2 analyses of the basalts are presented in Appendix IIIF.

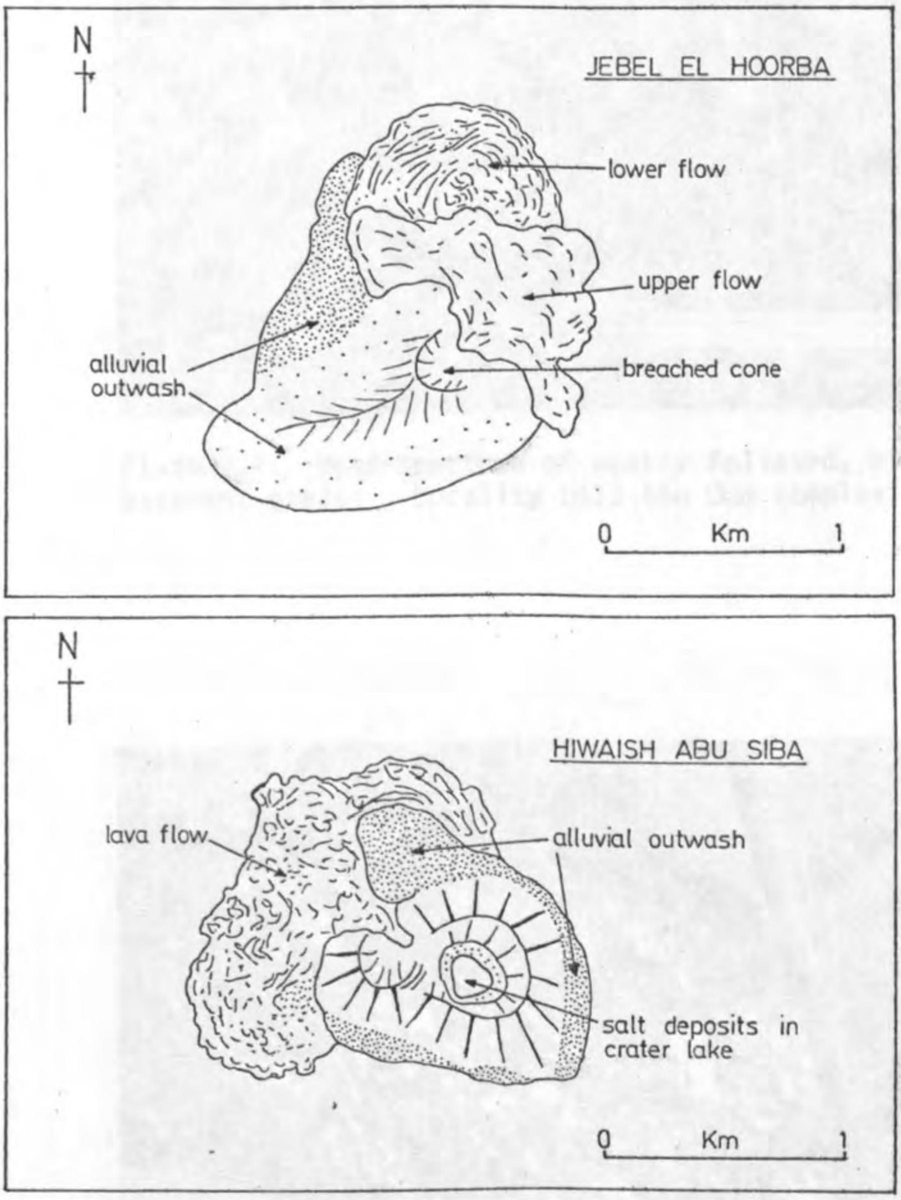

Fig. 2.14 MORPHOLOGY OF THE QUATERNARY VOLCANOES OF JEBEL EL HOORBA AND HIWAISH ABU SIBA.

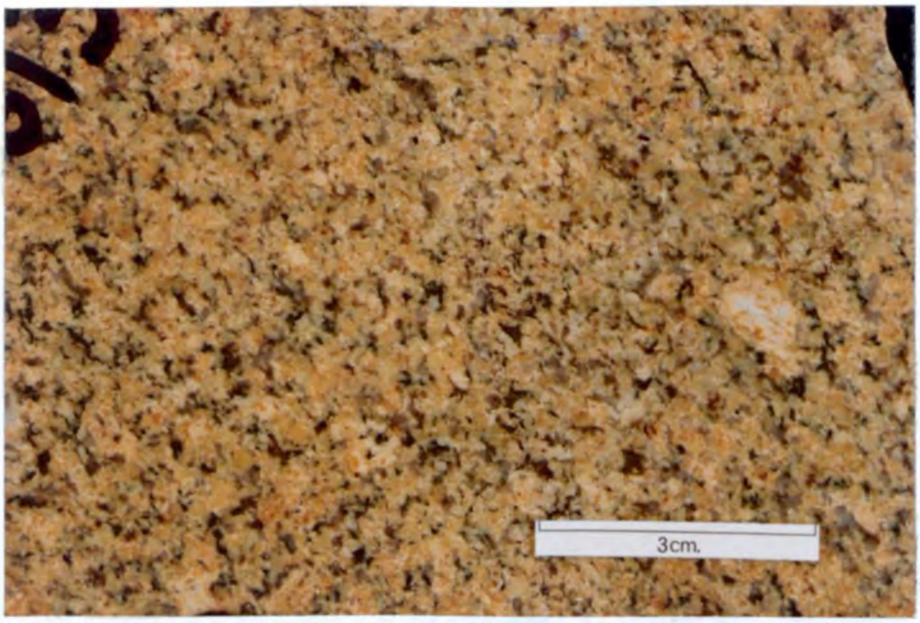

Plate 2.1: Hand-specimen of weakly foliated, biotite-bearing, basement gneiss. Locality D613 Abu Dom complex.

Plate 2.2: Coarsely foliated augen gneiss. Locality D853 Abu Dom complex.

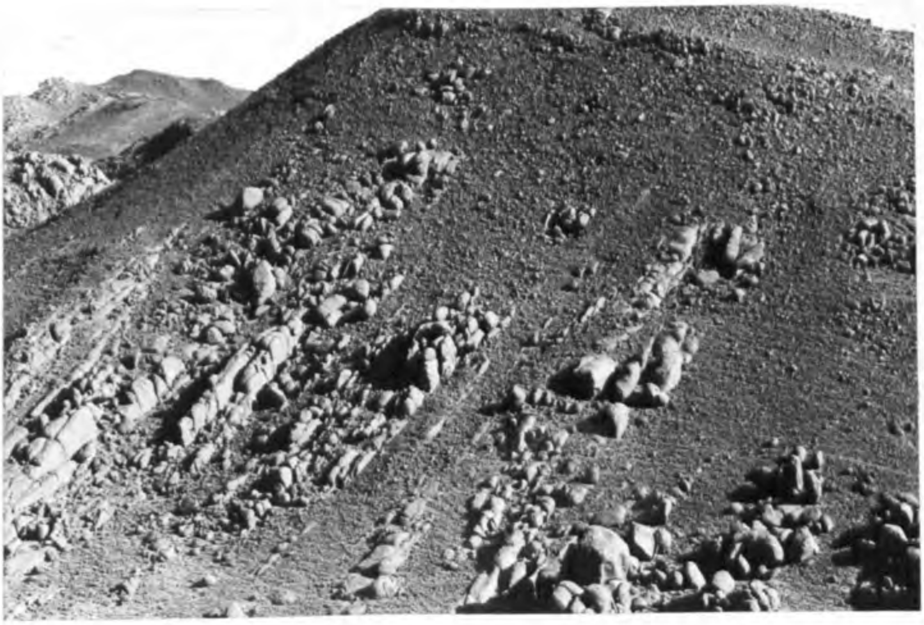

Plate 2.3: Prominently jointed hillside, Granite 1 Ras ed Dom complex. Locality D231, viewed facing east.

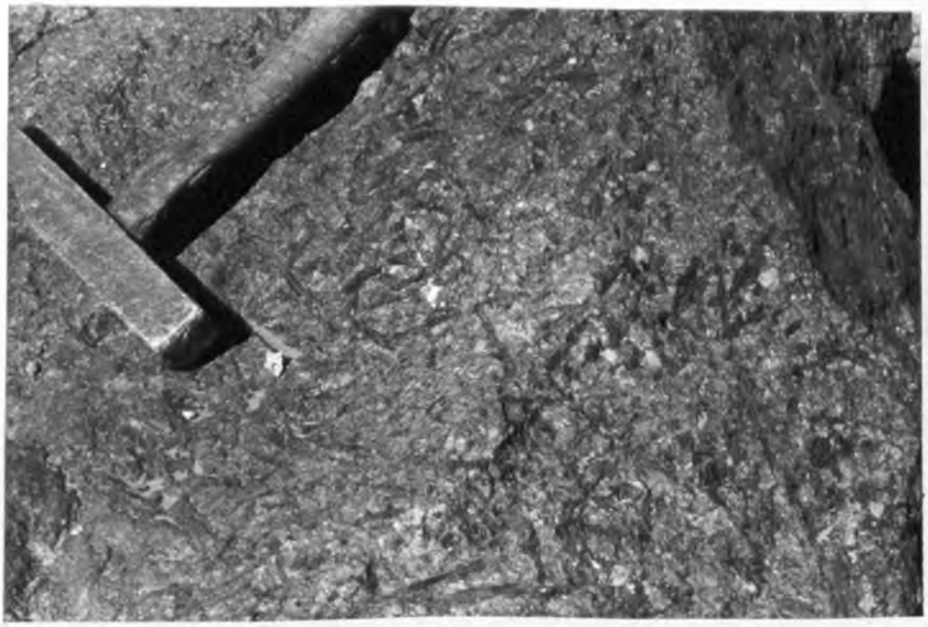

Plate 2.4: Large randomly oriented arfvedsonite prisms in alkali granite. Locality D455, near western margin of Granite 1, Ras ed Dom complex.

Plate 2.5: View looking south across the low terrain of the Widian Basement Block. The prominent valley feature marks the line of the Meria'b fault. Photograph taken 0.4km east of locality R77, Syenite 3, Ras ed Dom complex.

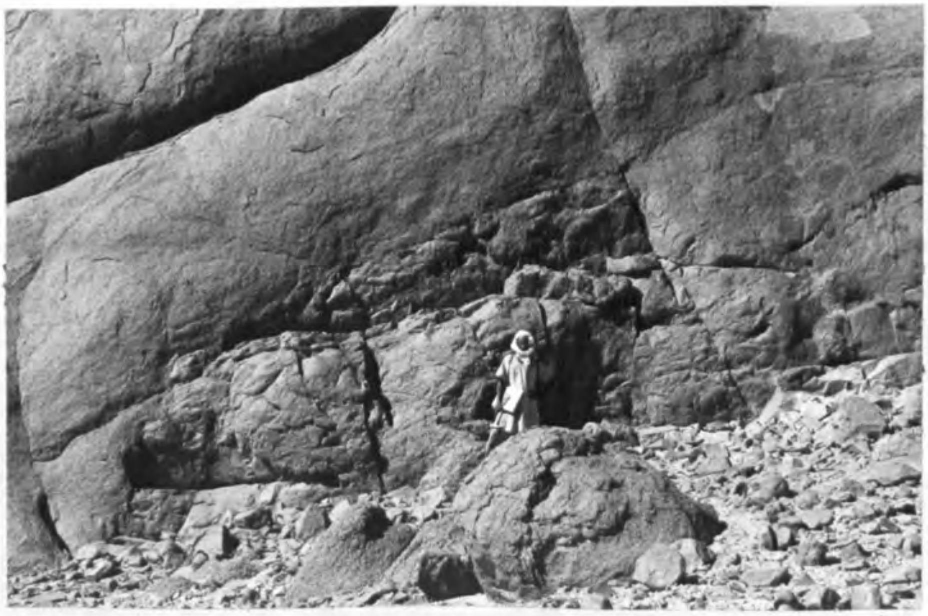

Plate 2.6: Large basement raft at locality R77 in Syenite 3, Ras ed Dom complex. The closely jointed gneiss contrasts with the smoother syenite rock-faces.

Plate 2.7: View looking south-south-west across Wadi el Widian towards the ridge of Syenite 5. Locality D285 in Syenite 4, Ras ed Dom complex.

Plate 2.8: Convolute flow-banding in chilled facies of Microgranite 1, near locality D300, Ras ed Dom complex.

Plate 2.9: Curved outcrop of Syenite 11, Ras ed Dom complex. The hill on the right is Syenite 13, whilst part of Syenite 12 is just visible at the foot of the hill. Rocks in the immediate foreground belong to Syenite 15. The hills in the far distance are Suitaniyat complex. View facing south west.

Plate 2.10: View taken from Syenite 7, looking northwards across Syenite 6 towards the Abu Siba Felsite in the distance. Ras ed Dom complex.

Plate 2.11: Two cross-cutting dykes in Syenite 1, Ras ed Dom complex. The jaggedly weathering acid dykes contrast with the smoother syenite surfaces. The dyke traversing the photograph from east to west is the earlier one. Field notebook provides approximate scale.

Plate 2.12: Spherulites in devitrified acid cone-sheet. Locality D938, north west of Abu Dom complex.

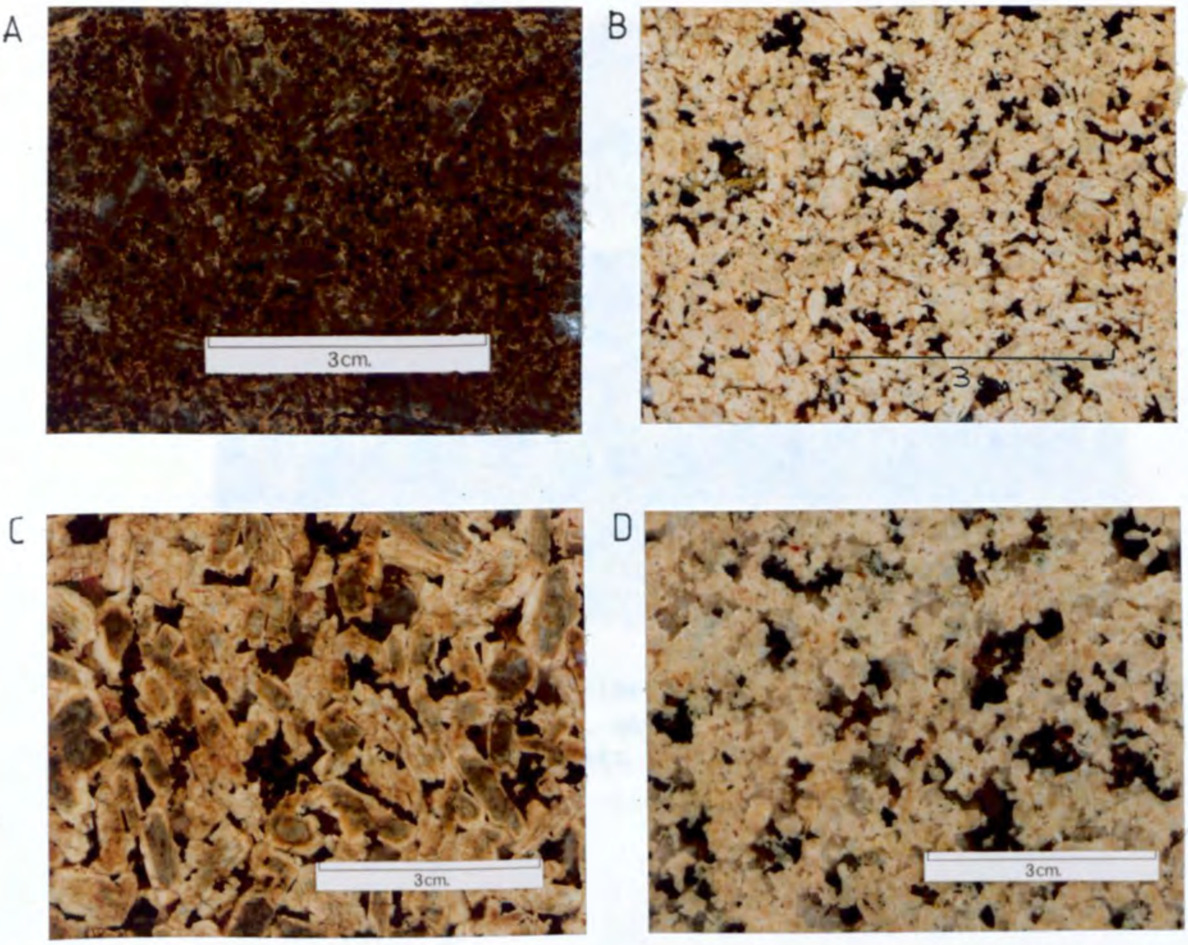

Plate 2.13: Polished hand-specimens of the principal rock-types of Ras ed Dom and Abu Dom.

A: early syenite, locality D596, Abu Dom complex.

B: alkali syenite, locality D1057, Syenite 3, Ras ed Dom complex.

C: coarse alkali syenite. Locality D800, Syenite 5, Abu Dom complex.

D: alkali granite. Locality D186, Granite 1, Ras ed Dom complex.

Plate 2.14: Nubian sediments overlying peneplained Granite 1 surface, locality D853, southern Abu Dom complex. The foreground slope consists of basement gneiss. View facing west.

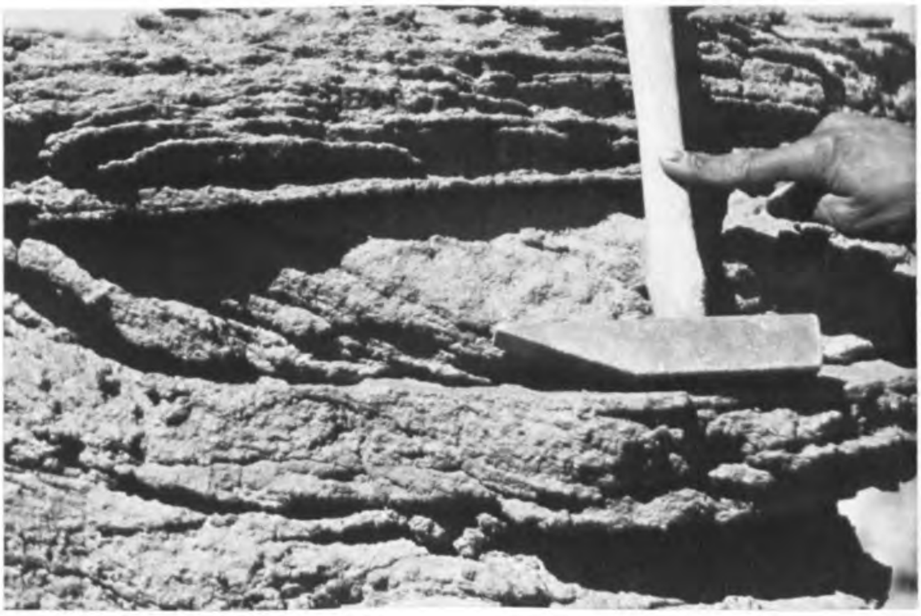

Plate 2.15: Cross-bedding in the Nubian Sandstone. Detail of Nubian beds shown in plate 2.17.

Plate 2.16: Volcanic bomb in the Cainozoic basaltic crater of Jebel Hiwaish Abu Siba, north of Ras ed Dom complex.

CHAPTER 3 : STRUCTURE OF THE YOUNGER GRANITE RING-COMPLEXES

3.1. : Introductory Review

3.1.A. : Introduction

In the early years of this century, mapping of the Scottish Tertiary intrusive centres of Skye (Harker, 1904), Mull (Bailey et al., 1924), Ardnamurchan (Richey et al., 1930), and of the older Glen Coe centre (Clough et al., 1909) revealed that these subvolcanic centres were characterised by distinctive annular intrusions. The now familiar terms cone-sheet, ring-dyke, and cauldron subsidence, were coined to describe these and related structures. Since then numerous further instances have come to light including, to mention but a few, those of New Hampshire (Kingsley, 1931; Chapman, 1935; Billings, 1943,) Oslo (Oftedahl, 1952), and Nigeria (Bain, 1934; Jacobson et al., 1958).

Structural interpretation of ring-complexes has proceeded along several lines, as detailed below.

3.1.B. : Experimental Modelling

Several authors (Jeffreys, 1936; Durrance, 1967; Hills, 1972) have noted the resemblance between cone-sheets and the percussion cones produced in glass by impact pressure at a point. Durrance (1967) elegantly interpreted the Ardnamurchan cone-sheets in terms of logarithmic spirals, but the required outcrop patterns are not duplicated elsewhere (Roberts, 1970).

By far the most successful models are those of Ramberg (1967, 1970) who modelled the permissive rise of 'magma' ($KMnO_4$ soln.) along potential fractures, with results resembling cone-sheets and ring-dykes.

3.1.C. : Mechanistic Modelling

The geometric regularity and radial symmetry about a vertical axis, often present in ring-complexes, might be said to invite mathematical treatment, and the earliest such attempt is that of Anderson (in Bailey et al., 1924, p11-12; also 1936; see fig. 3.1A). His model simulates the stress fields arising from a 'point dilation' and a 'point push' and proposes that cone-sheets occupy tensile fractures

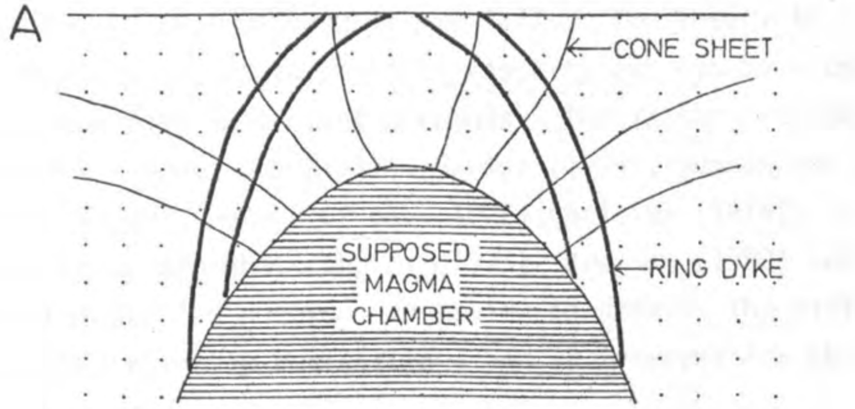

DISPOSITION OF RING DYKES AND CONE SHEETS
ABOUT SUPPOSED MAGMA CHAMBER (after Anderson, 1936)

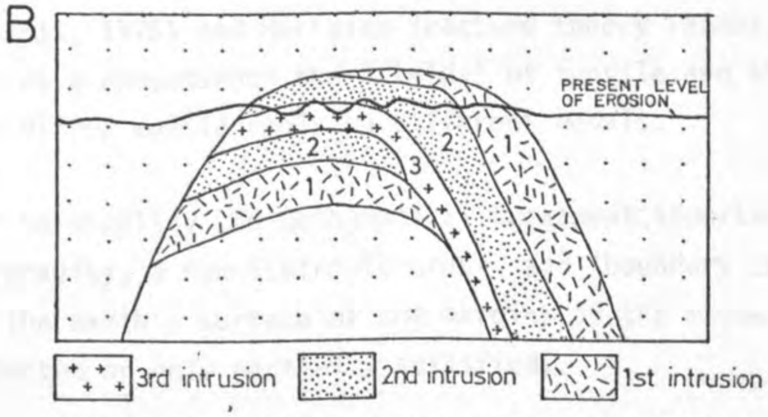

ROOFED NESTED RING-DYKES, MOURNE MOUNTAINS (after Richey, 1928)

Fig. 3.1 COMPARISON OF MECHANICAL AND ACTUALISTIC MODELS
OF RING-STRUCTURE FORMATION

formed in response to increased magmatic pressure, while ring-dykes invade shears formed when magma pressure falls. The theory is 'only a first approximation to reality' (op.cit.) but has been the starting point for most subsequent attempts. The latter include those of Jeffreys (1936), Ode (1957), Garson (1959), Robson and Barr (1964), Roberts (1970), Petrov et al. (1972), Phillips (1974), Walker (1975), Koide and Bhattacharji (1975), Kresten (1980) and Bahat (1979), but are too numerous to review in detail. The differing theories are often directly conflicting, and the reasons for this lack of unanimity include;

1. The 'criteria for failure' employed differ greatly according to the dominant conceptual influence, e.g. Coulomb-Navier theory of internal friction (Robson and Barr, 1964); Griffith Crack theory (Roberts, 1970); effective stress considerations (Anderson, 1936; Roberts, 1970; Phillips, 1974), hydraulic fracturing (Phillips, 1974); Bradley's isopiestic surfaces (Walker, 1975); hydrothermal fluid pressure and elasticity theory (Koide and Bhattacharji, 1975) and Hertzian fracture theory (Bahat, 1979 ; 1980). As a consequence the 'fields' of tensile and shear fracture differ considerably on different models.

2. In order to simplify the mathematical treatment, important factors such as gravity, a non-isotropic crust, and 'boundary conditions' such as the earth's surface or the margins of the magma chamber, are neglected or only partially satisfied.

3. With the exceptions of Koide and Bhattacharji (1975) and Bahat (1979), the models are two-dimensional and expansion into the third dimension involves untestable assumptions.

4. The chosen shape for the magma chamber exerts considerable influence on the outcome for a given model. Anderson (1936) invoked 'an inverted flower-pot' shape, Robson and Barr (1964) a cylindrical one, while Roberts (1970), using a spherical magma chamber, admitted that problems of scale necessitated it to be 'very small' in size. Koide and Bhattacharji (1975) envisaged a vertically elongate spheroid and found that the stress pattern was dependent on the aspect ratio of the apex of the reservoir.

These problems aside, geological observation often provides a test of the relative merits of the rival theories. For instance, Robson and Barr (1964) envisaged tensile fracture as restricted to the uppermost parts of the crust. However dykes occupying such fractures are known to extend to much greater depth (Roberts, 1970). Likewise, Pitcher (1979) observed that the flat tops seen in many plutons are not in concurrence with the Koide and Bhattacharji apical magma chamber.

3.1.D. : Actualistic Approach

The limited usefulness of the mechanistic models described above, brings us to a consideration of more actualistic approaches, perhaps best exemplified by Reynolds (1956), in which field observations form the basis for inferences as to the three dimensional form of ring-complexes.

Contrary to the Andersonian model, outward dipping contacts on ring-dykes are rare, and vertical or inward dips are commonly encountered (Billings, 1943; Reynolds, 1956; Turner, 1972). Thus while the role of cauldron subsidence in ring-dyke formation may be all important in some cases, the attitude of the ring-fracture has a crucial bearing on the 'space' problem. Where dips are indeed outward cauldron subsidence provides cavities for the magma to invade, but where dips are vertical or inwards subsidence alone creates no such cavities. In the latter instances fracture widening processes must have acted to make the space for the ring-dykes. Piecemeal stoping (Billings, 1943), gas-coring (Reynolds, 1956) and marginal deformation of the country rocks (Bailey et al., 1924) are amongst possible processes and are attested to by xenoliths, intrusive breccias and marginal folds respectively.

Where ring fractures reach the surface calderas may be formed, but where subsidence is subterranean, a roofing cross-fracture can form and if subsequently invaded by magma a roofed pluton or 'bell-jar' (Du Toit, 1920; fig. 3.1B) intrusion results. If subsidence is repeated, nested plutons may be formed, although Roberts (1970) has pointed out that one major subsidence followed by spalling-off of domical roof shells would produce a similar result (fig. 3.1B). It is widely accepted that calderas, bell-jars and deeper plutons constitute a denudation series (Reynolds, 1956; Knox, 1974; Pitcher, 1979).

In ensuing sections further variants on ring-structure will be introduced where appropriate.

3.2. : Structural Features of Ras Ed Dom and Abu Dom

3.2.A. : Introduction

By way of introduction a few general comments on the respective structures of Abu Dom and Ras ed Dom are appropriate. Although there is an overall northward shift in the focus of magmatism with time in Abu Dom, the most immediately striking feature is the sustained concentricity exhibited by the intrusions in the northern half of the complex (Map 2; fig. 2.11). These nested plutons were evidently emplaced above an essentially stationary magma chamber. In contrast, the essential structure of Ras ed Dom is one of semi-circular intrusions, successively overlapping each other and younging eastwards (Map 1; Fig. 3.2). The diameters of the units decrease in the same direction so that E.W. variation reflects both migration of the centre of activity and decline in its strength with time (table 3.1).

Ras ed Dom constitutes the final phase of activity of a larger horseshoe shaped massif (Map 3) which embraces the adjacent complexes of Ban Gidid, Muweilih and Sultaniyat. The precise chronological position of Abu Dom in such a sequence is difficult to confirm, in view of its isolated geographical position, but it probably predates the Sultaniyat and Ras ed Dom complexes (see inset, Map 3). The massif constitutes a single multi-phase complex in which the focus of magmatism has progressed in an anti-clockwise direction (Almond et al, 1976; Almond et al., 1982. This massif is comparable in scale to the well documented migrating magmatic centres of Sara-Fier (Turner, 1963) and Ningi-Burra (Turner and Bowden, 1979) in Nigeria.

	INTRUSIVE UNIT	DIAMETER
CENTRE 1	SYENITE 1	-
	SYENITE 2	-
	GRANITE 1*	5.3km
	SYENITE 3	-
CENTRE 2	SYENITE 4 & 5*	4.4km
CENTRE 3	SYENITE 6*	3.5km
CENTRE 4	SYENITE 7*	2.7km
CENTRE 5	SYENITE 8*	2.2km
CENTRE 6	SYENITE 9*	1.4km
	SYENITE 10*	0.9km
CENTRE 7	SYENITE 11	1.8km
	SYENITE 12	1.7km
	SYENITE 13	1.4km
	SYENITE 14	-
CENTRE 8	SYENITE 15	1.2km

Table 3.1 : Diameters of units where bounded by inferred ring-fractures, Ras ed Dom.
*original diameter estimated by extrapolation of incompletely preserved ring-fractures.

In the following discussion, and in subsequent chapters, the abbreviations (RED) and (AD) are used when referring to particular units of Ras ed Dom and Abu Dom, respectively.

3.2.B. : Recognition of Structural Centres

Within Ras ed Dom, eight structural centres are recognised (fig. 3.2), whilst the Abu Siba Felsite cannot be firmly fitted into the intrusive chronology. Recognition of these distinct centres is based on several criteria (see table 3.2), as follows:-

1. migration of the focus of activity results in the formation of new boundary ring-fractures displaying major re-entrants against earlier centres, e.g. between Centres 1 and 2. Each centre tends to have its own concentric set of minor intrustions (Map 1).

2. adjacent centres are sometimes partially separated by screens of basement rocks, e.g. Centres 1 and 2; Centres 7 and 8 (Map 1).

3. initiation of a new centre was commonly accompanied by intrusion of subaluminous hedenbergite-syenite. These 'early' syenites are variably preserved, often as disrupted units (S1 and S4), rafts (in S6) or xenoliths (in S7).

Inevitably an element of subjectivity remains in the recognition of structural centres. For instance, in Centre 1 magmatism shifted north-eastwards with time and consequently the outer boundary is composite, including portions of the boundary ring-fractures of S2 and G1. Likewise the recognition of Centre 3 as separate from Centre 2 is equivocal in that the magmatic shift involved (0.7km) is less than the internal shift (3.7km) in Centre 1. However, the occurrence of rafts of early syenite is considered to outweigh in importance the smallness of the shift (fig. 3.2).

As regards Abu Dom, subdivision into structural centres is unwarranted in view of the relatively few component intrusions, and the limited migration of magmatism.

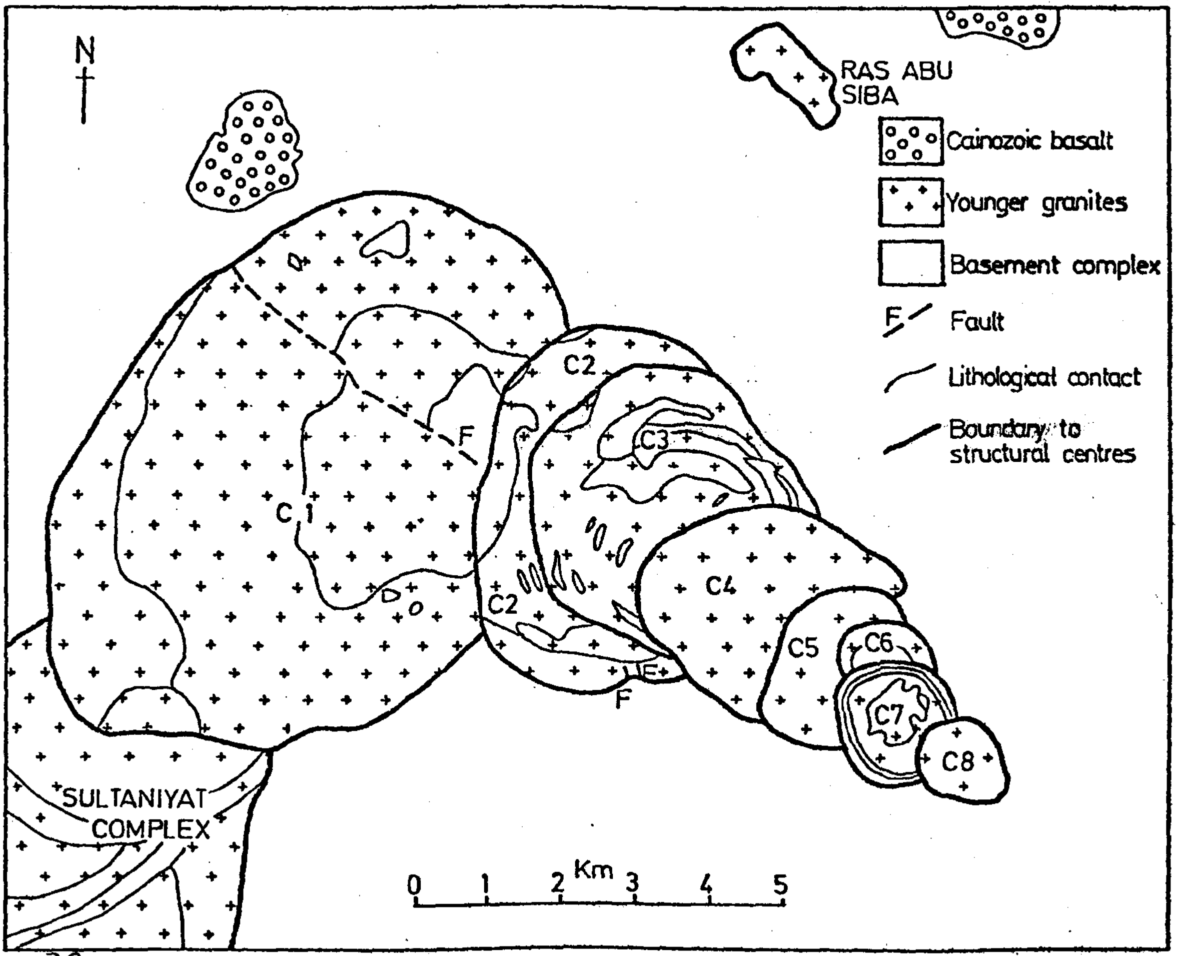

Fig. 3.2: STRUCTURAL CENTRES (C1-C8) TOGETHER WITH THE OUTLYING RAS ABU SIBA CENTRE, RAS ED DOM COMPLEX

STRUCTURAL CENTRE	Evidence of an 'Early' Syenite unit	Inferred boundary ring-fracture	Scale of magmatic shift (in km) to subsequent centre	Presence of intervening Basement screens
Centre 1	+ Syenite 1	+	2.8km	-
Centre 2	+ Syenite 4	+	0.7km	+
Centre 3	+ raft	+	2.0km	-
Centre 4	+ xenoliths	+	1.4km	-
Centre 5	-	+	0.5km	-
Centre 6	-	+	0.7km	-
Centre 7	+ Syenite 11	+	1.1km	-
Centre 8	-	+	-	+

Table 32 : Criteria used in the recognition of structural centres, Ras ed Dom.

3.2.C. : Forms of Intrusions and Emplacement Mechanisms

Schematic cross-sections of Ras ed Dom and Abu Dom (figs. 3.3 - 3.9) illustrate the overall structure of the two complexes.

Although it is believed that most of the intrusions were emplaced along ring-faults, evidence for such faulting is rarely seen and for this reason the more neutral term 'ring-fracture' is used. Perhaps the best example of a faulted margin is where S4(RED) truncates Centre 1 (fig. 2.4 and 3.4). The effects of faulting in this case can be seen in both the basement gneisses of the Widian block, and in the Centre 1 units (section 2.2.D). Significantly, fault evidence is absent where S5(RED) is bordered by the same ring fracture, indicating that the later intrusion has destroyed any traces of faulting, with the production of 'healed' intrusive contacts. This 'healing' process is believed to be typical of the complexes in general, and accounts for the paucity of obviously faulted contacts. Recrystallisation of adjacent units also results in some instances, e.g. locs.131 and 132 in S2(RED) near the contact with the later G1 unit (section 2.2.C). The second major instance of faulted contacts is the northern margin to G1(AD) but relations here are complicated by the fact that G2 has been emplaced along a reactivated S2 margin (fig. 2.10 and fig. 3.7).

Several different intrusive forms are present in the complexes, and in Ras ed Dom the dominant type is one of broad, and sub-circular stocks, (e.g. S6, S7, S8 in Ras ed Dom, Map 1). These units display smoothly curving contacts with the surrounding gneisses that evidently follow ring-fractures. Where successive Younger Granite units are contiguous however (e.g. S1/G1(RED), S2/G1(AD), contacts are less regular indicating that the ring-fractures were more readily propagated within the colder, anisotropic gneisses are compared with the Younger Granite rocks, which were still relatively hot and perhaps semi-plastic. The interiors of the stocks are massive, devoid of primary structures, and although they may constitute roofed 'bell-jars' at depth (see e.g. S7 in fig. 3.5), no evidence of this is seen at the present level of erosion. Where visible, contacts are vertical or outward dipping, and subterranean block subsidence would account for the present form.

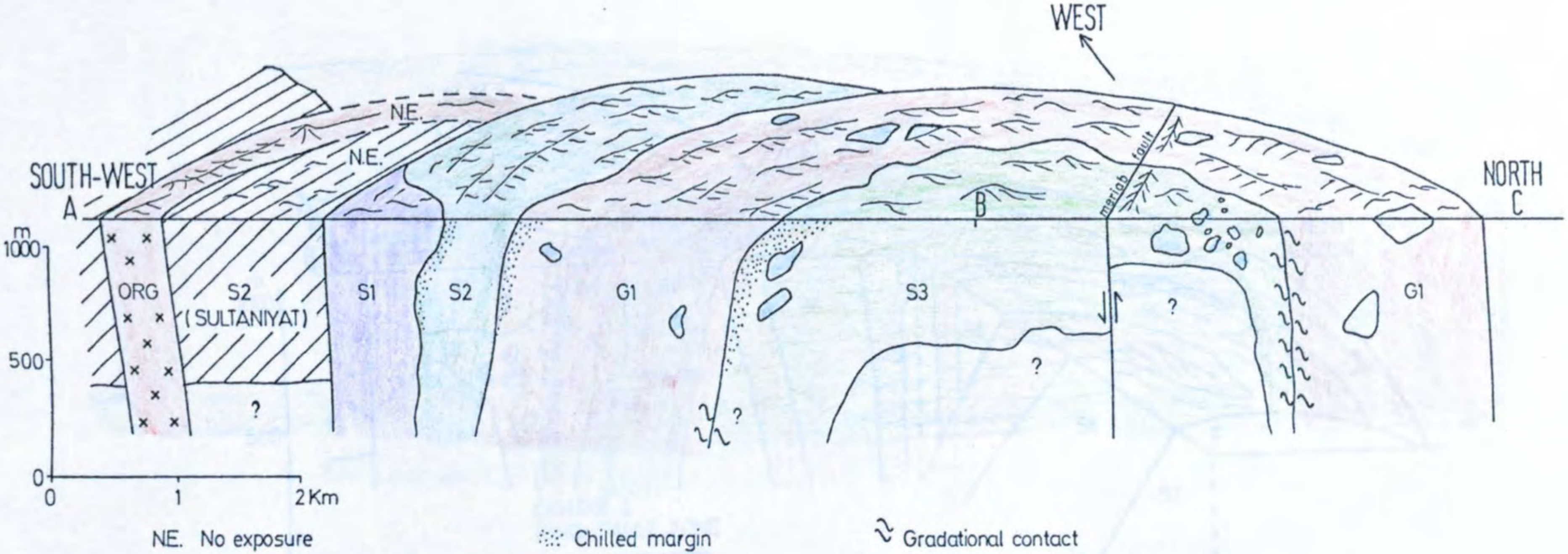

Fig. 3.3 INTERPRETATIVE SECTION ACROSS CENTRE 1. Ras ed Dom.
For location of line ABC see fig. 2.3.
The relationship between centres 1 and 2 is illustrated in fig. 3.4

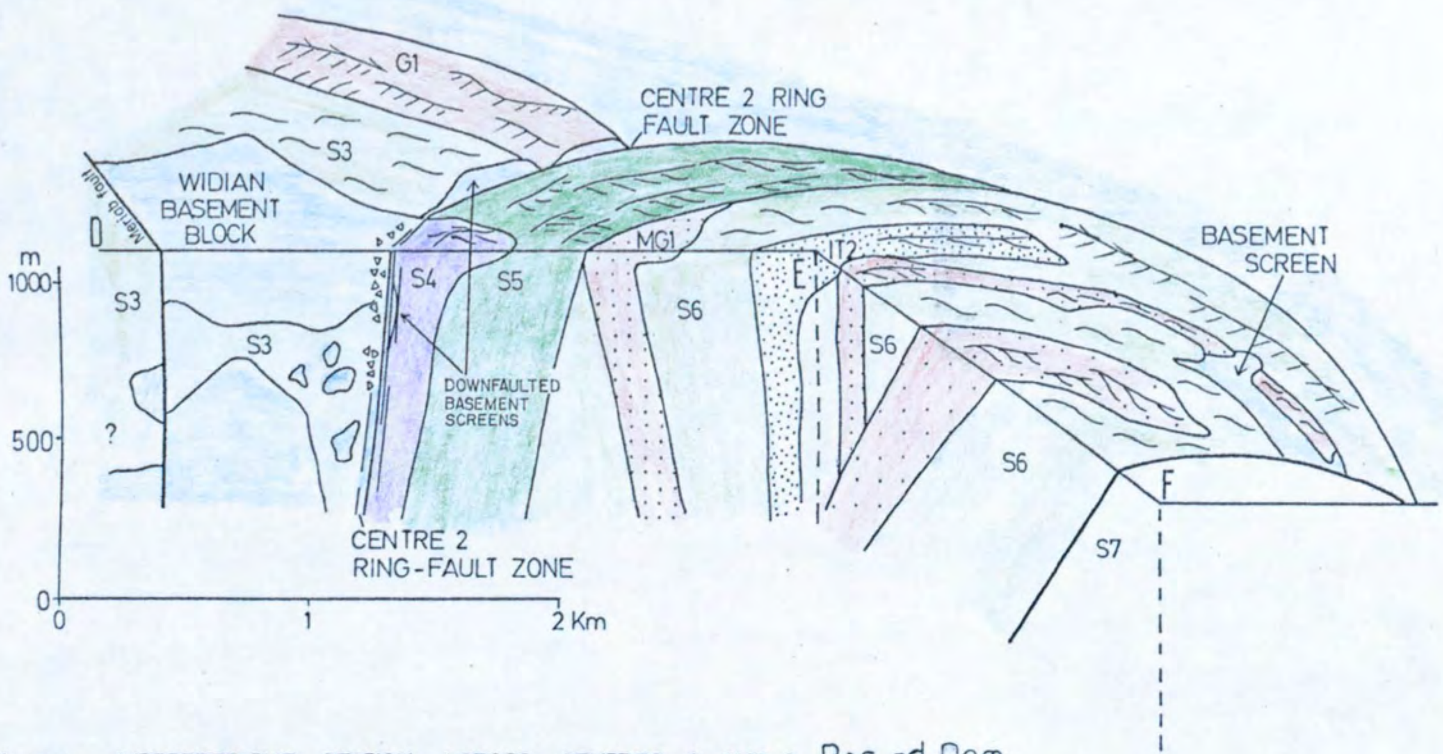

Fig. 3.4 INTERPRETATIVE SECTION ACROSS CENTRES 2 AND 3, Ras ed Dom.
For location of line DEF see fig. 2.4

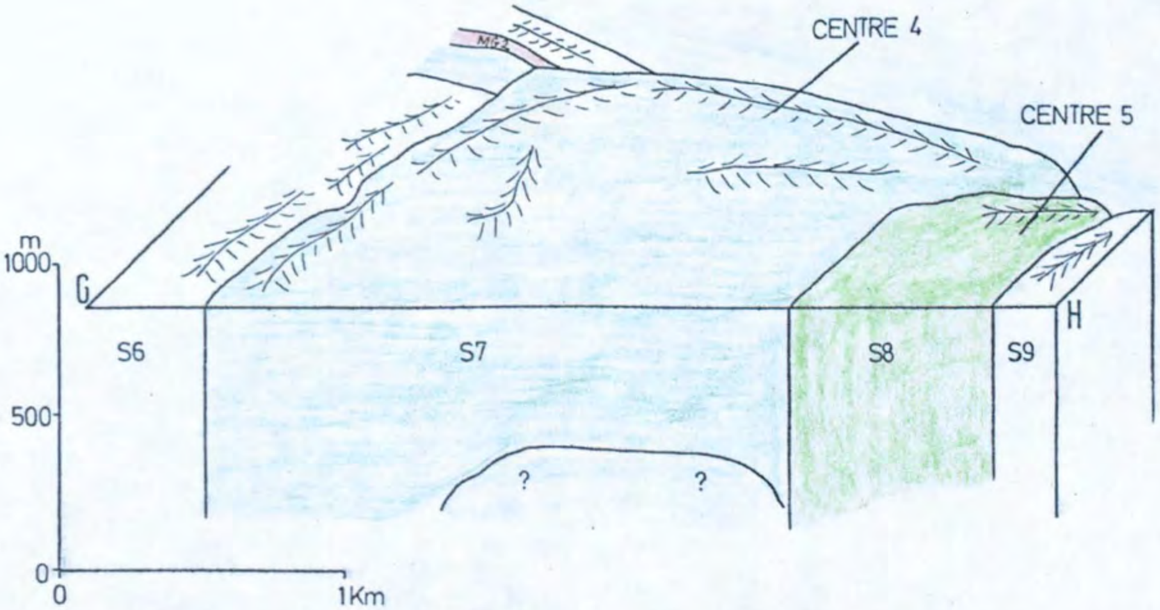

Fig. 3.5 SECTION ACROSS CENTRES 4 AND 5. Ras ed Dom.
For location of line GH see fig.2.6

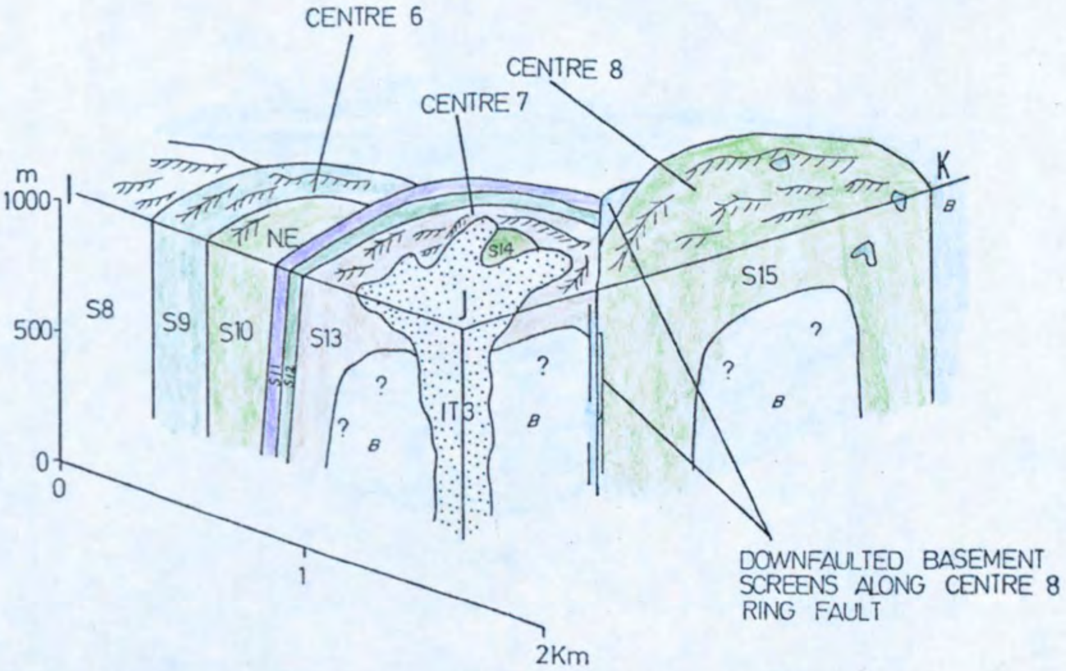

Fig. 3.6 INTERPRETATIVE SECTION ACROSS CENTRES 6,7 AND 8.
For location of line IJK see fig.2.7 Ras ed Dom.

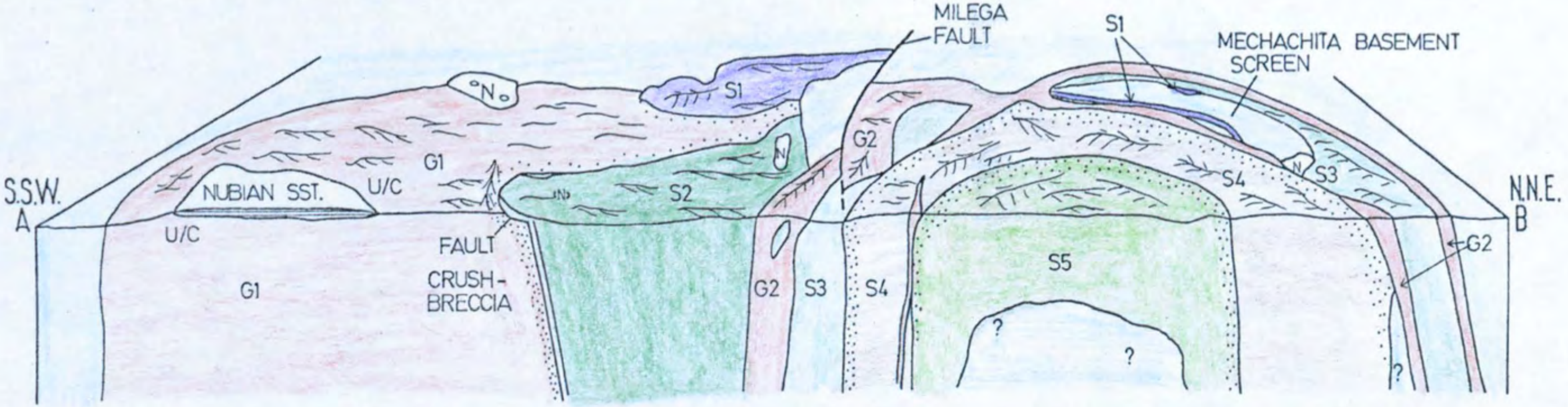

Fig. 3.7 INTERPRETATIVE SECTION ACROSS ABU DOM COMPLEX
For location of line AB see fig. 2.9

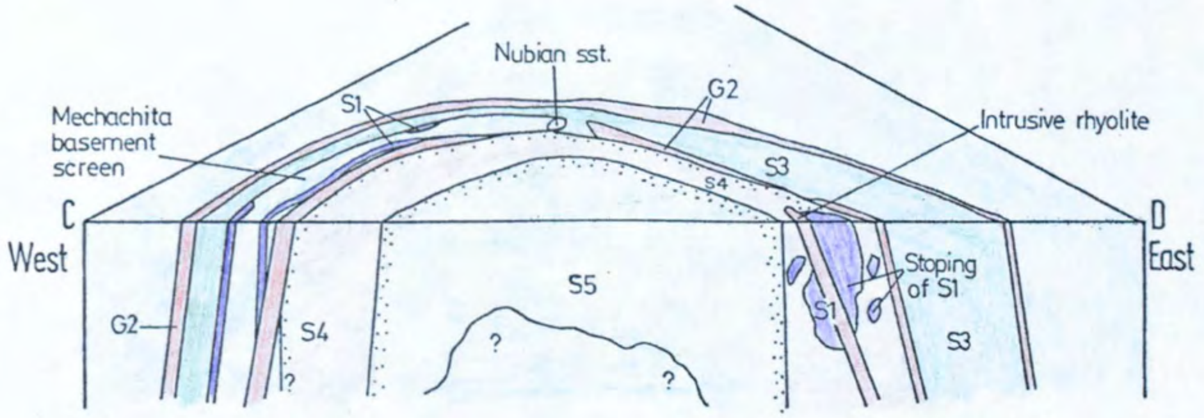

Fig. 3.8 INTERPRETATIVE SECTION ACROSS THE NORTHERN HALF OF ABU DOM
For location of the line CD see fig. 2.11

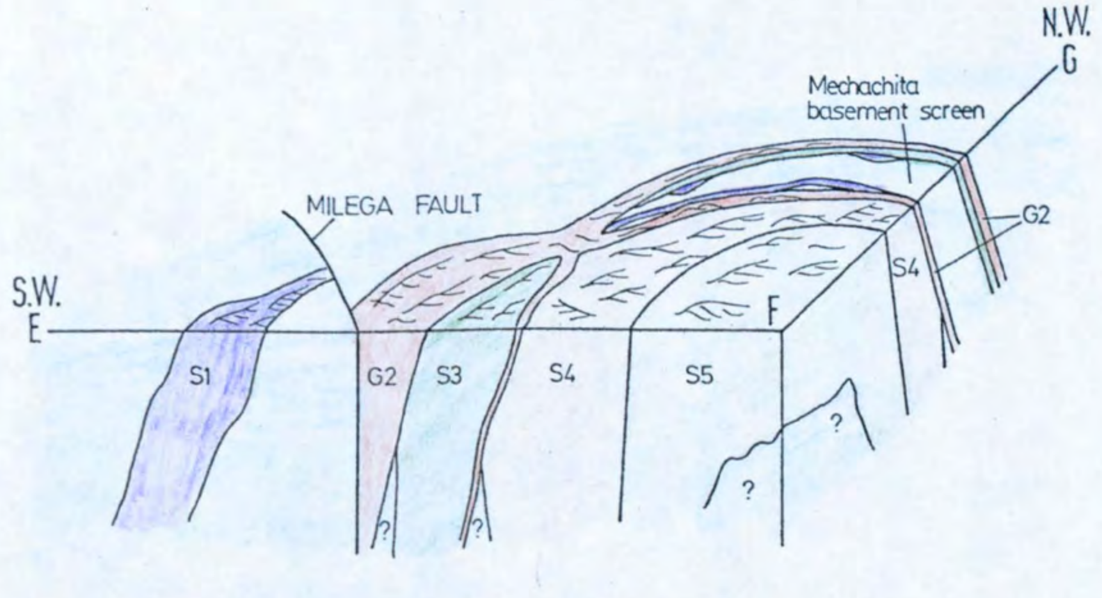

Fig. 3.9 INTERPRETATIVE SECTION ACROSS THE MILEGA FAULT
For location of the line EFG see fig. 2.9

Abu Dom.

Outward dips (e.g. S6(RED) section 2.2.E) are at variance with the vertical attitudes more normally associated with ring-dykes (Reynolds, 1956) but evidently reflect a shallowing of contacts at a high structural level. Their attitude at depth remains problematical. The local presence of zenoliths e.g. S7(RED, fig. 2.6) attests to a subsidiary role played by stoping.

A variant upon the stock form is that of nested plutons e.g. Centres 6 and 7 (RED, fig. 3.6) and S3 to S5 (AD, fig. 3.8). In each case both the diameters and the ages of the units decrease inwards and all contacts, be they against basement or other syenites, define regular ring shapes. No intervening basement screens are found and the question therefore must be asked as to whether the outermost rings were originally of annular form, or whether they are merely the outer parts of now foundered stocks. The question remains open but the occurrence of basement xenoliths in IT3 (Centre 7, RED, fig. 3.6) suggests that the former hypothesis is more likely. In Abu Dom the nested units include a large body of foundered S1 (fig. 3.8) but no equivalent basement blocks, suggestingthat different processes have contributed, in varying degrees, to the development of each centre.

A third type of structure seen in the complexes involves narrow crescentic sheets of microgranite and intrusive trachyte. In Ras ed Dom these typically wedge out laterally e.g. Centre 3 (figure 3.4), but in Abu Dom the G2 unit forms a double, bifurcating ring (fig. 3.7). Steep outward dips are commonly seen often together with inward facing roof pendants. Locally in G2(AD) the outward dips are seen to decrease upwards and the roof structure, where preserved, consists of several thin parallel sub-horizontal sheets (see discussion in section 2.3.I).

This multiple structure may result from intrusion along several domical fractures, or by spalling along such fractures, rather like the structures depicted in fig. 3.1B. The incomplete arcuate form typical of Centre 3 (RED, fig. 3.4) is probably due to tilting of earlier blocks on their inner side. Sparse xenoliths suggest that stoping was of minor importance in the formation of these units, but in two instances, IT1 (RED, fig. 2.5B) and G2 (AD, fig. 2.12) fluidisation and hybridisation of the adjacent rocks played an essential part in the fracture widening process.

The form of G1(RED) is somewhat unique (figs. 2.3 and 3.3), the unit forming a broad ring, widest in the south where it appears to roof S3(RED). Relations between these two intrusions are complex (see section 2.2.C), and transitional contacts in the north suggest their emplacement closely in time, possibly due to the foundering of a central core of basement within the granite ring. The numerous rafts and enclosures of gneiss within the northern half of the syenite are believed to be remnants of that core.

A feature with important consequences for the evolution of individual centres is the existence of basement screens that partially intervene between adjacent centres, e.g. Centres 1/2, 7/8(RED), G1/G2 (Milega vicinity, AD). Truncation of one centre by another obviously involves partial destruction of the earlier one, and accordingly the basement screens are not in situ, but rather occupy the position of former Younger Granite units. Such structures are well known in the Nigerian ring-complexes (Turner, 1963; 1972), and their emplacement must accompany formation of the later centre's ring-fault (or more correctly, ring-fault zone), and involve down-faulting of basement rocks that roofed the earlier centre.

The early hedenbergite-syenites tend to be structurally distinct in that, excepting S11 (RED, fig. 3.6), they have been variably disrupted during the emplacement of subsequent units. Shearing and cataclasis locally attest to this and it seems that the early units were prone to foundering, presumably due to renewed movement along their boundary faults. Disrupted segments of these early units give little or no evidence as to their original form, but the undisturbed segments consist of narrow ring-dykes (e.g. S1(AD), fig. 3.9), with a roof pendant in one instance (S4, RED, fig. 3.4) suggesting a 'bell-jar' form.

3.2.D. : Migration of Activity with Time

A limited northward migration of magmatism is evident between S2 and later units in Abu Dom, but for much of the duration activity was stationary under the northern part of the complex. A more dramatic migration is seen in the plots of foci of magmatic centres for Ras ed Dom (fig. 3.10). There, magmatism followed a broad arc from W. to E. with time. Two sub-trends are present, the first of which, in Centre 2, is a continuation of the N-N.E. trend established in Sultaniyat to the S. The Abu Siba felsite may be the extreme northern termination of this trend, or alternatively may represent an independent or satellite centre. The second trend extends from Centre 2 to Centre 8, and within it activity proceeded steadily S.E. with only minor deviations.

Curtis (1979) noted a deepening in the intrusive level exposed northwards in Sultaniyat, and proposed a slight regional tilting towards the S., about an E.W. axis, to explain it. Certainly the stocks of northern Sultaniyat and Ras ed Dom provide a contrast in structural style with the caldera-preserved volcanics and narrow ring-dykes seen in southern Sultaniyat (Map 3), but such a juxtaposition is thought more likely to be due to a combination of factors, including:-

1. different relative movement along the boundary faults in adjacent centres. The presence of intervening basement screens supports such a notion.

2. contrasting volumes of magma in different centres. This might reflect different absolute volumes supplied from depth, or different relative volumes available for intrusion, as concommittant volcanicity waxed and waned.

3. contrasting original levels of emplacement. For instance the confinement of high-level arcuate units to Centre 3(RED, fig. 3.4) is thought to reflect relatively large down-faulting of that centre.

3.2.E. : The Role of Volcanism and the Nature of the Magma Chambers

Volcanic rocks are associated with both complexes, but are preserved in rather small volumes. In the case of Ras ed Dom volcanic xenoliths are preserved in the intrusions of Centre 3 (IT2, MG2) and Centre 7

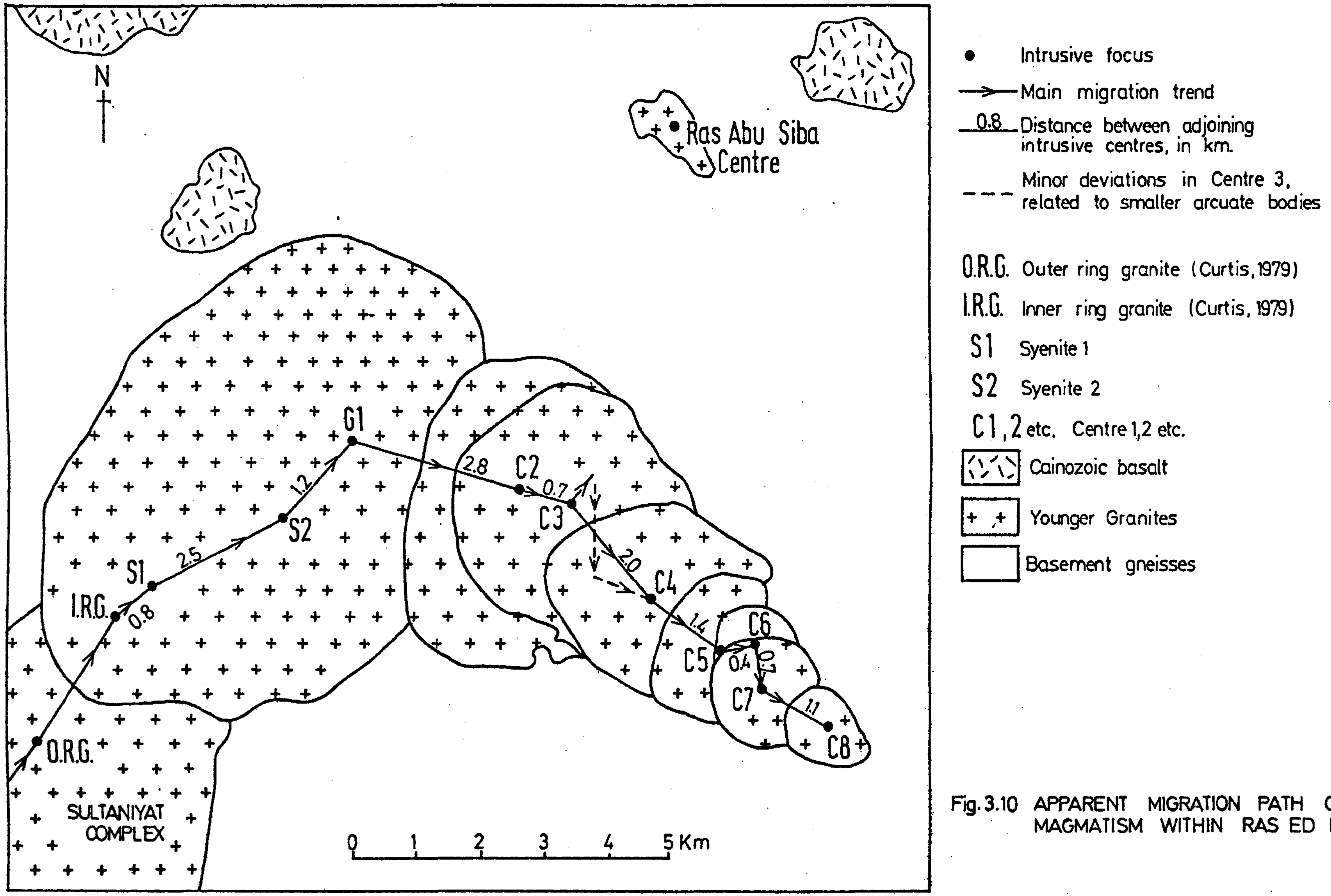

Fig. 3.10 APPARENT MIGRATION PATH OF MAGMATISM WITHIN RAS ED DOM

(fig. 3.6; IT3), indicating that the complex was formerly roofed by a volcanic edifice of unknown extent. Caldera preservation of volcanic rocks is absent, however, unlike the Sultaniyat complex, perhaps reflecting deeper structural levels in Ras ed Dom, but also the likelihood that as magmatism waned so surface volcanism became less extensive. The cone-like IT3 unit of Centre 7 (fig. 3.6), which opens upwards into sill-like sheets, may well have acted as a conduit to the volcanic superstructure. In Abu Dom volcanic rocks are found in a small down-faulted block to the E. of the complex proper, but the meagre exposure limits structural interpretation.

Although the ring-complexes had links with surface volcanism, they in turn must have been supplied by deeper-level magma chambers. As the bulk of possible volcanic feeder pipes seem restricted to within the ring-complexes (the Abu Siba structure is an exception) it is tempting to follow Turner (1963) in concluding that the deeper chambers were similarly limited in size. Thus it is possible to reconcile the nested plutons (fig. 2.7A) with solidification of a magma chamber at depth from the walls inwards, as the resultant volume reduction in successive magma batches would account for the observed decrease in diameters of the intrusions. Such a model is attractive for northern Abu Dom, but is difficult to apply to Ras ed Dom as the repeated occurrence of early syenites in new centres would necessitate multiple chambers. Moreover the possibility that each fresh magma batch arrived anew from the source region cannot be discounted.

3.3. : Jointing

3.3.A. : Introduction

The Younger Granite rocks are characterised by abundant joint sets (figs. 3.11 - 3.12; Photomosaics A and B in rear folder). However, the scale of mapping, together with time restrictions, prohibited detailed single-intrusion studies, and air-photographic interpretation forms the basis for much of the ensuing discussion. It is clear from the mosaics that, in terms of scale, two fundamentally different types of joints, namely minor and major joints, are present in both complexes.

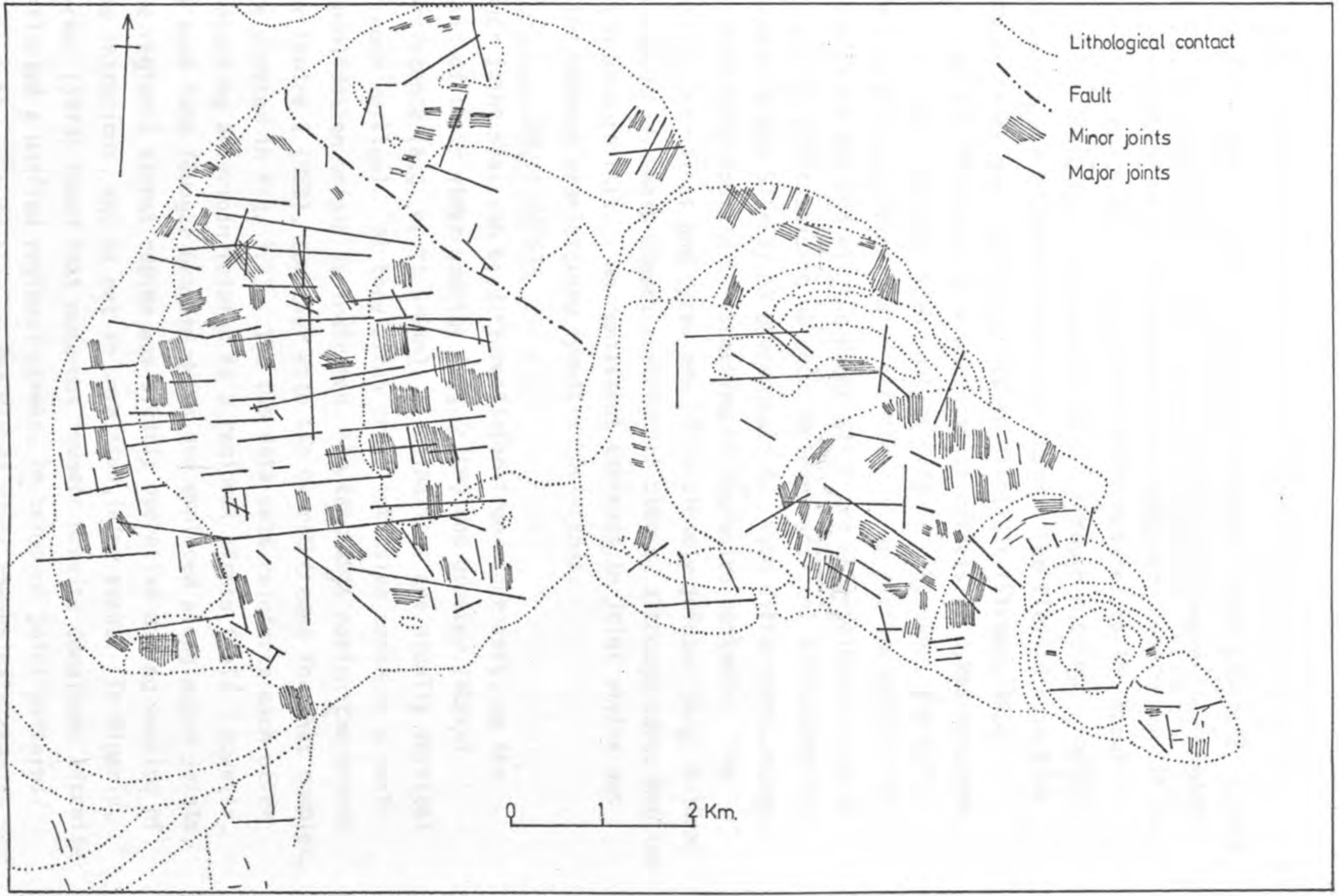

Fig. 3.11 JOINT PATTERNS IN RAS ED DOM COMPLEX

3.3.B. : Minor Joints

Minor joint sets are seen both on the outcrop scale (plate 2.3), and on the air-photographs, but variable geomorphic expression hinders the recognition of an integrated areal pattern. Nonetheless it is clear that the form of the sets is often related to the local intrusive pattern, indicating an origin through cooling. Radial, concentric and diagonal joints are found. The field distinction between shear and tension joints is difficult (Firman, 1960; Hobbs et al., 1976) and only where minor offsets of dykes occurred along joints was their shear nature evident. However, the bulk are thought to be tensional. Lithology is an obvious control on joint character and all the major units are well-jointed. Subtle changes in joint spacing do occur between adjacent intrusions e.g. compare S6 and S7(RED) on photomosaic A. Such differences proved an invaluable tool in the locating of intrusive contacts. The smaller intrusions and dykes are often closely jointed (e.g. 5-10cm) and weather as sharp-edged, rectangular blocks, although scree mantles often obscure this. No consistent contrast in joint styles was noted between granitic and syenitic rock-types.

3.3.C. : Major Joints

Major joint sets can be differentiated from minor sets, on the basis of their wider spacing (e.g. > 1km) and greater lateral persistence (e.g. up to 5-6km). Inclinations are usually vertical or near vertical. As they often cross intrusive contacts a post-consolidation origin is indicated. To test this notion the trends for Centre 1 (RED), together with the overall trends for that complex, are plotted in fig. 3.13. The two data sets reinforce each other indicating an origin related to a regional stress field. However, as some late Younger Granite dykes are emplaced along major joints, the regional stress regime was clearly operative during cooling of the intrusions, and is not an unrelated, later event. In Nigeria, Turner (1973) found that numerous Younger Granite complexes likewise reflected a unified regional stress, in terms of joint patterns. Whether the same is true of the Bayuda rings cannot be tested as yet as the data are not available.

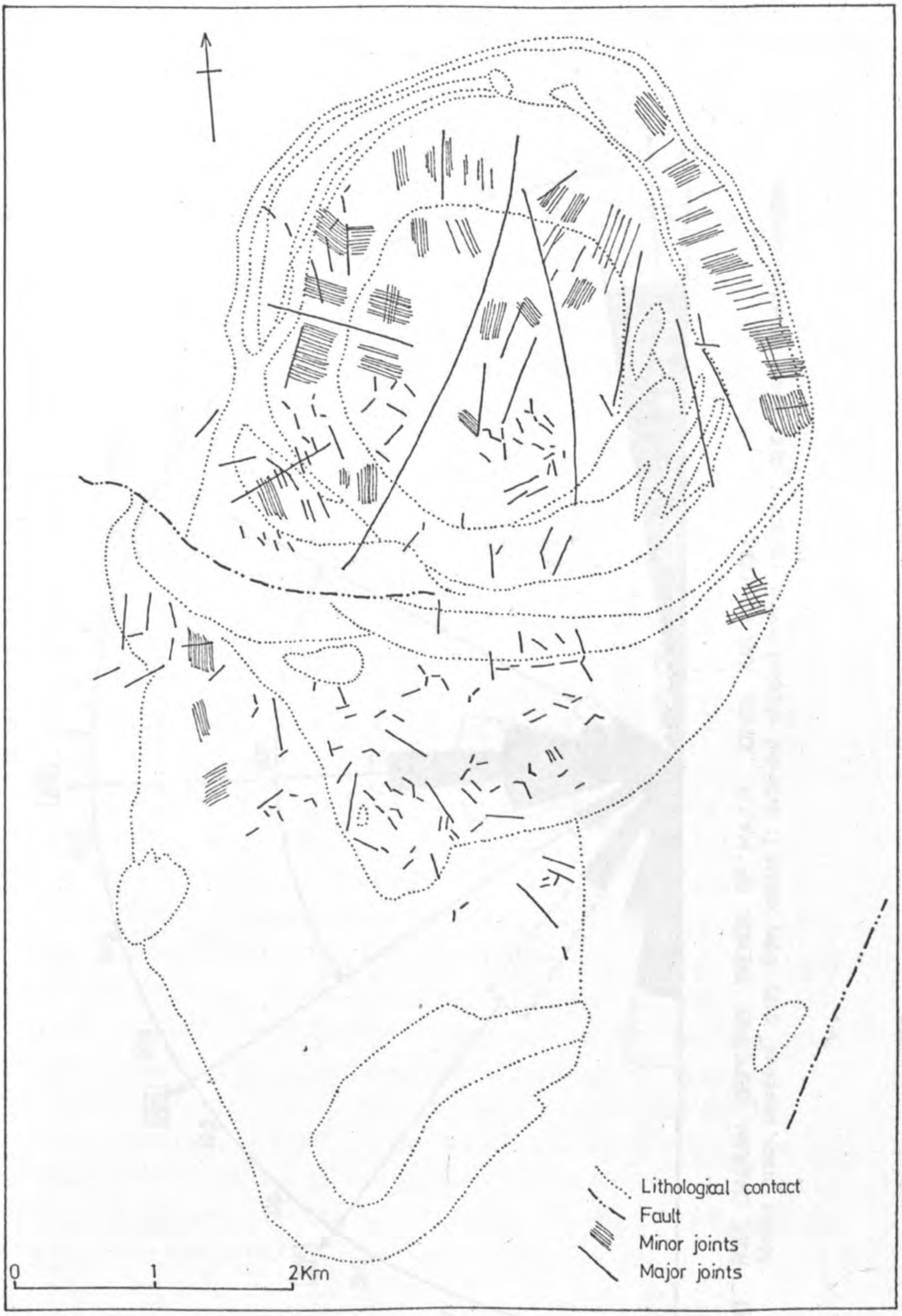

Fig. 3.12 JOINT PATTERNS IN ABU DOM COMPLEX

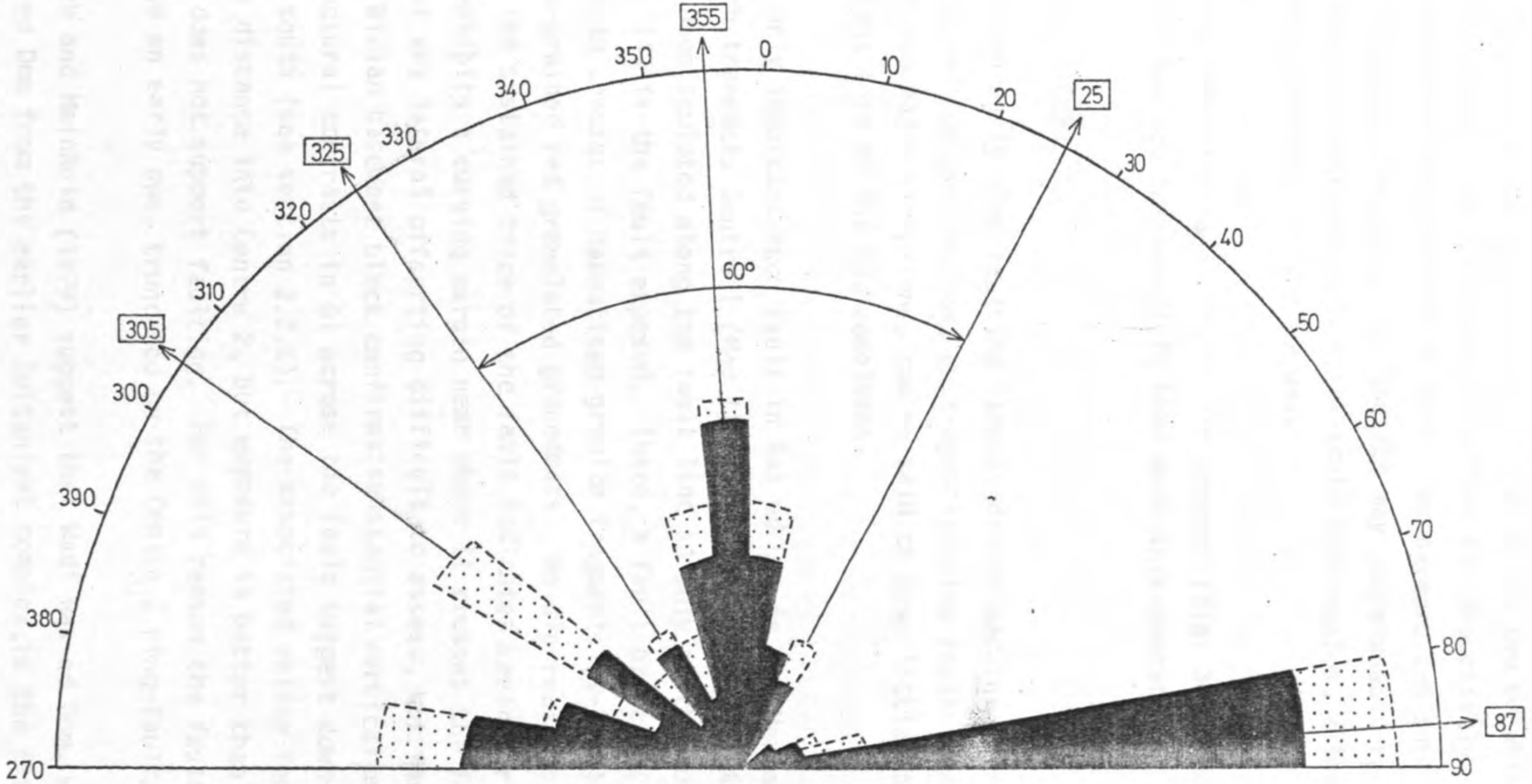

Fig. 3.13 ROSE DIAGRAM DEPICTING TRENDS OF MAJOR JOINTS, RAS ED DOM.
Shaded areas represent data from centre 1; extended stippled areas represent data from the entire complex.

Three major trends are evident in fig. 3.13, two of which constitute an orthogonal set, striking at 175°and 87°respectively. A third independent trend strikes at 125° Furthermore two subordinate complimentary trends at 145°and 25°, may conceiveably record conjugate shearing in response to a north-south compression, although the evidence for this is rather weak.

In Abu Dom a few major joints are present (fig. 3.12 and Photomosaic B) but are too infrequent to bear much interpretation.

3.4. : Faulting

Although early ring-faulting largely determined the intrusive styles of Ras ed Dom and Abu Dom, post-consolidation faults are rare and, with two major exceptions, can be said to have little modified the present form of the two complexes.

The only important such fault in Ras ed Dom is the Meriab fault, which transects Centre 1 (Map 1; plate 2.5;fig. 2.3). A major valley has been sculpted along the fault line so only in the north-west, at loc. 143 is the fault exposed. There, a fault breccia (10m wide) is seen to consist of haematised granite fragments (1-10cm) set in a fine-grained red granulated groundmass. No dip readings were obtained but the sustained trace of the fault indicates a near vertical attitude. S3 exhibits a curving margin near where it crosses the fault, and this makes any lateral offsetting difficult to assess, but faulting-out of the Widian basement block confirms substantial vertical movement. Structural contrasts in G1 across the fault suggest down-faulting to the south (see section 2.2.C). The associated valley feature persists some distance into Centre 2, but exposure is better than in Centre 1 and does not support faulting. For this reason the fault is believed to be an early one, truncated by the Centre 2 ring-fault.

Barth and Meinhold (1979) suggest that Wadi Ras ed Dom, which separates Ras ed Dom from the earlier Sultaniyat complex,is the site of a major E-W shear, but the continuation of G1 across the wadi disproves such a contention.

The Milega fault is the main post-emplacement structural break in Abu Dom (Map 2; fig. 2.10), which has also been excavated to form a major wadi. The fault abruptly truncates the Milega outcrop of S1(AD) and transects G2 causing alteration of the granite over a broad zone up to 100m in width. In addition at loc. 582 a small outcrop of fault breccia is present. Further E. exposure is poor, but the sustained curvature of G2 suggests that the fault does not persist far in that direction. The faulting-out of S1 indicates a downthrow to the N. probably with a dextral lateral component.

A small outcrop of Nubian Sandstone in the N. of Abu Dom (loc. 500) provides proof of post-Nubian faulting in the area. Although outcrop relations to the adjacent basement and syenitic rocks are unclear, the sandstone itself is cut by a N-S. fault, that dips 52°E. The fault gouge is less than 1m wide and is a locus of brecciation and silicification. Beds to the W. of the fault dip W., contrary to regional trends, and fault tilting probably accounts for this.

An abrupt change in strike of the Nubian rocks to the E. of Abu Dom is the reason for invoking a N.E. trending fault in that area (see section 2.5).

CHAPTER 4 : PETROGRAPHY OF THE YOUNGER GRANITE ROCKS

4.1. : Introduction

The petrography of the Younger Granite rocks is the subject of this chapter. In figs. 4.1. and 4.2. the rocks of Ras ed Dom and Abu Dom are plotted onto the Streckeisen (1967) QAP triangle, and are seen to be compositionally restricted to the syenite, quartz-syenite and granite fields of the alkali-feldspar category. In addition most of the rocks may be described as 'alkali', as they contain sodic amphibole and/or pyroxene (Streckeisen, 1967, 1976). This usage of the term 'alkali' corresponds with the chemical condition of peralkalinity.

The alkaline rocks are characterised by specialised and often obscure local names (Sorenson, 1974). In the present context the alkali granites might be described as ekerites (Brogger, 1906), and the alkaline and subalkaline syenites might be grouped together as nordmarkites (Brogger, 1890). The present writer prefers the self-explanatory terminology of Streckeisen (1967), e.g. alkali-granite, accompanied by a more specific designation, such as aegirine-arfvedsonite granite, where appropriate (see Maps 1 and 2).

The groundmass grain size divisions used are; fine (1mm), medium (1-5mm) and coarse (5mm). The corresponding names for the intermediate rocks are intrusive trachyte, microsyenite and syenite, and for the acid rocks intrusive rhyolite, microgranite and granite. The field term felsite is retained for convenience in describing the intrusive rhyolite of Ras Abu Siba.

For brevity in the text mineralogical details are reported separately in Appendix I. Quoted plagioclase compositions were determined by Michel-Levy statistical method using extinction angles, or by microprobe analysis. The species names for the pyriboles are based on the microprobe identifications reported in Chapter 5. In this chapter they are used as 'umbrella' terms. For example, the 'ferroedenite' of the early syenites ranges from ferroedenite through to katophorite and ferrorichterite.

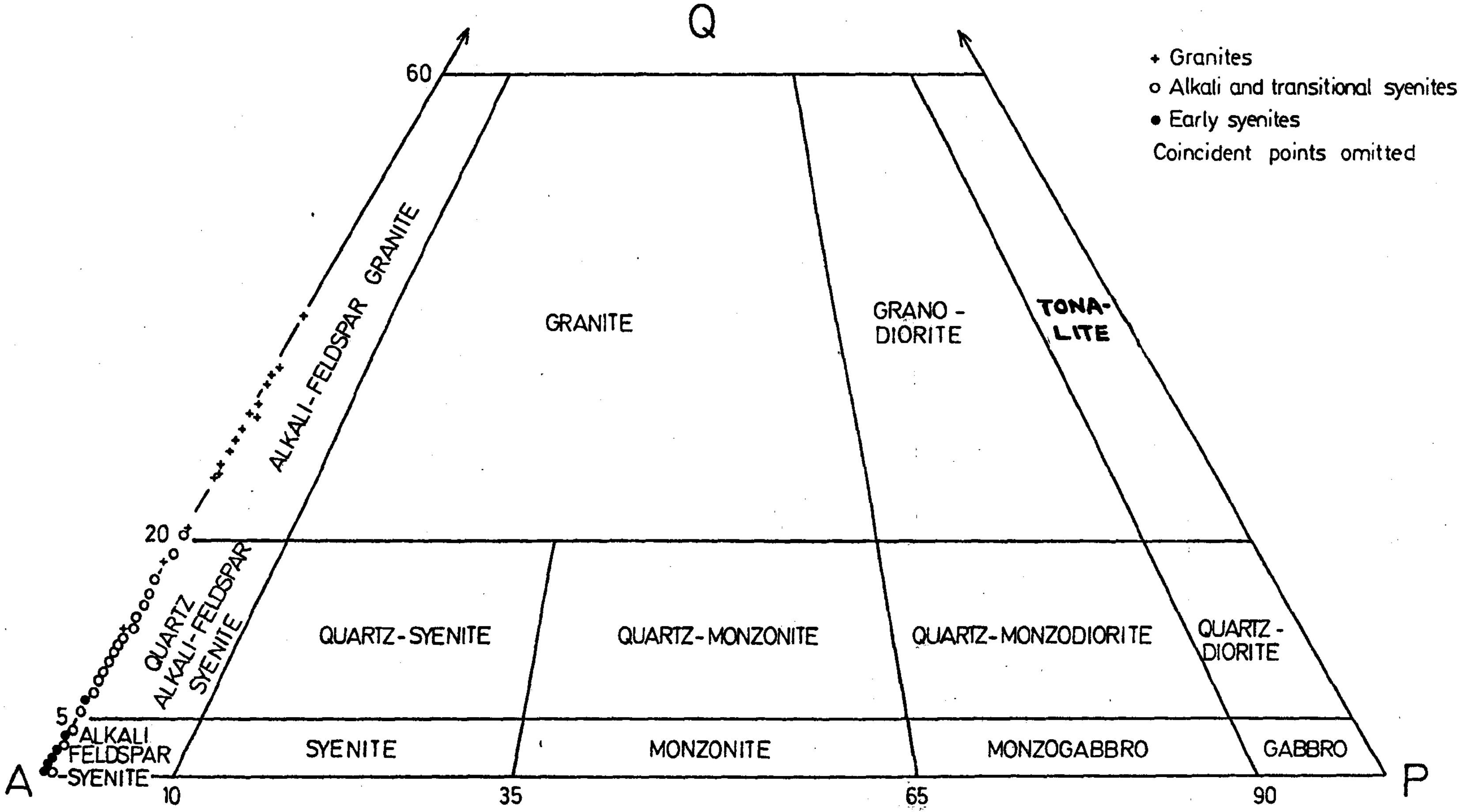

Fig. 4.1 : MODAL ANALYSES FROM RAS ED DOM, PLOTTED ONTO THE Q-A-P COMPOSITIONAL FIELDS OF STRECKEISEN, 1976.

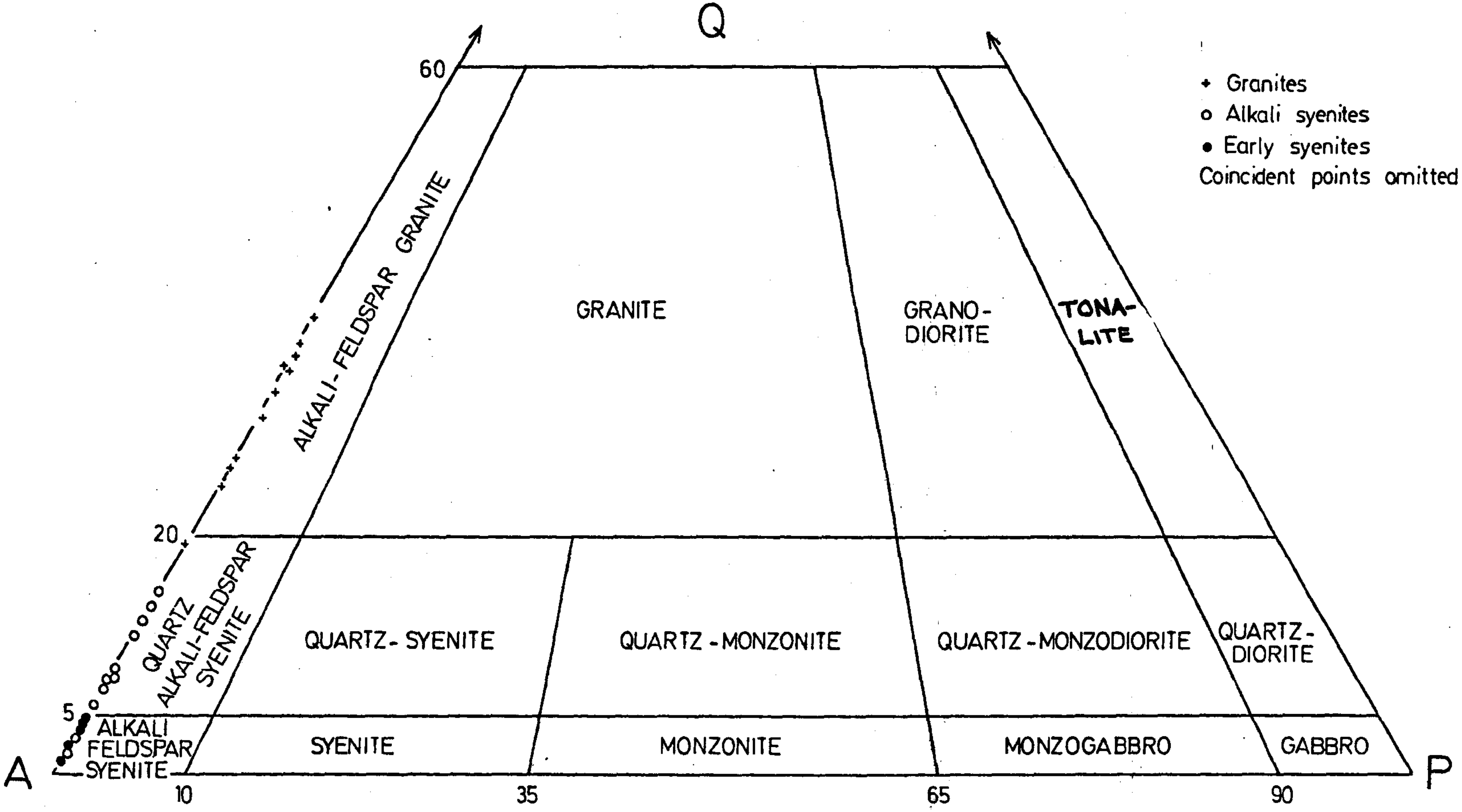

Fig. 4.2 : MODAL ANALYSES FROM ABU DOM, PLOTTED ONTO THE Q-A-P COMPOSITIONAL FIELDS OF STRECKEISEN, 1976

A major division into volcanic rocks, major intrusions and minor intrusions is followed, although most of the account pertains to the major intrusions. The latter are in turn divided into three categories, largely on the basis of the ferromagnesian assemblages (fig. 4.3), as follows:-

1. Early Syenites : containing hedenbergitic pyroxene enclosed in edenitic amphibole. These rocks account for 5.7% and 3.5% of the total area of intrusive rocks of Ras ed Dom and Abu Dom respectively.

2. Transitional Syenites : containing aegirine-augite enclosed in ferrorichterite. They are essentially mildly alkaline varieties of the early syenite type, and are not abundant (see below).

3. Alkali Syenites and Granites : containing arfvedsonite replaced by late aegirine. In terms of the total area of intrusive rocks the syenites (54% RED, 55% AD) are more abundant than the granites (40% RED and AD).

Representative modal analyses are given in table 4.1., and further modes are listed in Appendix I.

Several syenite units are heterogeneous as regards rock-type. For instance S2(RED) is typically transitional syenite (as defined above) in the south, whereas the northern part consists of alkali syenite. S3(RED) exhibits a transitional syenite selvage whilst the more slowly cooled interior contains aegirine and arfvedsonite, thereby providing an excellent example of <u>in-situ</u> fractionation. Evidence is presented below that such heterogeneity reflects the action of late peralkaline residual fluids upon the largely consolidated crystal mush. Similar heterogeneous units occur in the Nigerian Younger Granites (Bowden <u>et al</u>., 1976). A striking example from that province, is the Amo riebeckite-biotite granite ring-dyke. This unit has a dominantly peralkaline outer zone, a volatile-rich middle zone, and a metaluminous inner zone (Bowden <u>et al</u>., 1976)

EARLY SYENITE		TRANSITIONAL SYENITE		ALKALI SYENITE AND GRANITE	DOMINANT PHASE	ORDER OF CRYSTALL-ISATION
Fayalite (?)	abundant Apatite and Fe-Ti oxide	Fayalite (relict)	sparse Apatite and Fe-Ti oxide		FAYALITE (?)	PLUMASITIC magmatic
Ferroaugite Ferrohedenbergite		Ferroaugite and Ferrohedenbergite ↓ Aegirine-augite		Ferrohedenbergite (relict, rare in the granites) ↓	EARLY PYROXENE	
Ferroedenite Ferrorichterite (rare)		Ferrorichterite Aenigmatite		↓ Ferrorichterite and minor Katophorite Aenigmatite ↓ Arfvedsonite ↓ Riebeckite	AMPHIBOLE	?
Ferrowinchite and ferrobarroisite + Biotite + Fe-Ti oxide				Aegirine-augite (rare) Aegirine Aegirine-Augite + Biotite + Fe-Ti oxide	LATE PYROXENE	AGPAITIC late-post magmatic

Fig. 4.3. : Mafic mineral reaction relations in the principal rock types.

Related hydrothermal alteration assemblages are quoted in dotted boxes.

After discussing each main rock-type in turn, more general observations are made in section 4.7. All comments, unless otherwise specified, apply equally to Ras ed Dom and Abu Dom, the two complexes being closely similar lithologically.

Early Syenites

1.	D1014,	Syenite 1,	Ras ed Dom.
2.	D914,	Syenite 4,	Ras ed Dom.
3.	R31,	Syenite 11,	Ras ed Dom.
4.	D689,	Syenite 1,	Abu Dom, Milega outcrop.
5.	D685,	Syenite 1,	Abu Dom, Milega outcrop.

Alkali Syenites

1.	D374A,	Syenite 6,	Ras ed Dom.
2.	D378,	Syenite 7,	Ras ed Dom.
3.	D858,	Syenite 2,	Abu Dom.
4.	D528,	Syenite 3,	Abu Dom.

Alkali Granites

1.	D145,	Granite 1,	Ras ed Dom.
2.	D447,	Granite 1,	Ras ed Dom, albitised sample.
3.	D289,	Granite 2,	Ras ed Dom.
4.	D701,	Granite 1,	Abu Dom.
5.	D828,	Granite 2,	Abu Dom.

Table 4.1. (Opposite): Selected Modal Analyses of the Principal Rock-Types of Ras Ed Dom and Abu Dom.

EARLY SYENITES

	1	2	3	4	5
Alkali-feldspar	80.1	76.7	84.9	82.5	81.2
phenocrysts	-	31.2	-	-	26.7
groundmass	-	45.5	-	-	54.5
Albite*	3.1	-	2.6	+	-
Quartz	1.1	5.3	1.3	0.7	2.8
Edenite	2.7	-	4.9	6.0	-
Fe-winchite	10.9	7.7	0.5	6.2	7.9
Hedenbergite	0.9	3.4	0.8	-	1.5
Biotite	+	+	-	-	-
Fe-Ti oxides	2.8	5.4	2.0	2.5	2.5
Apatite	1.0	1.0	0.5	0.5	0.4
Other minerals	+	0.8	+	+	+

ALKALI SYENITES

	1	2	3	4
Alkali-feldspar	74.1	71.6	83.8	65.4
Albite*	1.0	6.4	3.0	3.4
Quartz	9.2	8.7	1.4	10.4
Arfvedsonite	9.8	1.8	7.1	10.5
Aegirine	5.2	10.3	4.0	9.4
Fe-Ti oxides	0.5	0.4	0.2	0.5
Apatite	0.2	+	0.3	0.4
Zircon	-	+	-	+
Other minerals	+	1	+	-

ALKALI GRANITES

	1	2	3	4	5
Alkali-feldspar	54.6	54.6	59.3	57.1	59.3
Albite*	4.9	10.5	0.2	2.9	3.7
Quartz	25.9	22.8	22.7	31.5	15.2
Arfvedsonite	9.0	7.9	2.1	1.3	7.5
Aegirine	4.7	3.2	14.5	6.1	12.8
Fe-Ti oxides	+	+	+	0.6	+
Apatite	+	+	+	+	+
Zircon	+	-	+	-	+
Other minerals	-	-	-	+	+

Table 4.1 : Selected Modal Analyses of the Principal Rock-Types of Ras ed Dom and Abu Dom (explanation opposite). Albite* refers to discrete grains of exsolution or metasomatic origin.

4.2. : Volcanic Rocks

As described in sections 2.2.B., and 2.3.B., volcanic rocks are not abundant in either complex.

At loc.307 in Ras ed Dom a crystal-lithic tuff consists of trachytic clasts and angular crystals of quartz, perthitic feldspar and rare plagioclase (oligoclase), set in a fine grained feldspathic matrix. In the Abu Dom Volcanic Group ignimbrites and rhyolitic lavas are present. In the ignimbrites fiamme-like structures are visible as eutaxitic foliation on weathered surfaces, but in thin sections are seen to be coarsely recrystallised and occupied by quartz, alkali feldspar or radiating zeolites. The groundmass is also recrystallised and shards are rarely preserved. The phenocryst content is low and where they do occur resorbed quartz grains predominate. The acid lavas are more phyric, with abundant quartz and alkali-feldspar phenocrysts. The groundmass is invariably recrystallised, but flow-banding is often preserved. Subordinate phenocrysts of mafic minerals occur in almost all the above instances, but are haematised and calcitised beyond recognition.

4.3. : Early Syenites

4.3.A. : Introduction

The term 'early syenite' refers to a distinctive group of syenites characterised by hedenbergitic pyroxene. They are emplaced at an early stage in the evolution of the structural centre to which they belong (see Maps 1 and 2, rear pocket). However, as will be shown subsequently, they are also mineralogically and chemically 'early', i.e. less fractionated, as compared to later units.

Typically, the early syenites are dark, rather basic-looking rocks in hand specimen (plate 2.13A). Texturally they range from feldspar-phyric instrusive trachytes to coarse syenites. The latter consist of large tabular feldspars separated by a sparse, finer-grained, mafic-rich interstitium.

Usually the units have been disrupted by the emplacement of subsequent intrusions, and their often discontinuous outcrops are attributable to localised foundering (section 2.3.C). Further evidence of post-intrusive deformation is provided by the localised occurrence of shearing and cataclasis.

The early syenites of Ras ed Dom embrace units SI, S4, SII, IT2, IT3, a raft in S6 and xenoliths in S7 (see Chapter 2), as well as dykes intruding S1. In Abu Dom only one early syenite, SI, is present, although the widely scattered outcrops could represent the remnants of more than one such unit.

The major mineral phases are reviewed in turn below, and petrographic features are depicted in figs. 4.4 and 4.5. Representative modes are given in table 4.1 and in Appendix I.

4.3.B. : Alkali-feldspars

The most striking feature of the alkali-feldspars is the varying degree of turbidity even within one grain. In particular the cores, or more rarely the entire grain, tend to be clear whilst the enclosing rim is highly clouded (fig. 4.4.-C; plate 4.10-A+B). Coarseness of exsolution also increases towards the grain margins (plate 4.10-B). Inwards encroachment of turbity along cleavage planes is also commonly seen (fig. 4.4.-B).

In the larger grains a primary zonation characterised by a sharp core-rim boundary is sometimes visible (fig. 4.4.-C+D). More rarely repeated concentric zoning is expressed by varying turbidity and degree of exsolution (fig. 4.4-A). The cores of such grains often contain oriented inclusions of hedenbergite and Fe-Ti oxide.

Under crossed polars fine perthitic structures are just discernable in the core areas. Moreover, fine deformation lamellae produce an effect akin to diffuse, incipient microcline twinning. Proper cross-hatched twinning is not seen. Microprobe analysis indicate orthoclase bulk compositions up to An7 MOL.% (section 5.2).

Fig. 4.4. (opposite) : Feldspars in the early syenites

A - Primary zonation in alkali-feldspar. D165B, Syenite II, Ras ed Dom.

B - The relationship of turbidity to cleavage and cracks in alkali-feldspar. R31, Syenite II, Ras ed Dom.

C - Inclusions of hedenbergite and Fe-Ti oxide in core of alkali-feldspar grain. Note turbid rim with complex outer margin, indicating recrystallisation and interdigitation with groundmass perthites (not shown). Feldspar-phyric rock, D914, Syenite 4, Ras ed Dom.

D - As C above, but with a sharp boundary separating the core and rim areas. D914, Syenite 4, Ras ed Dom.

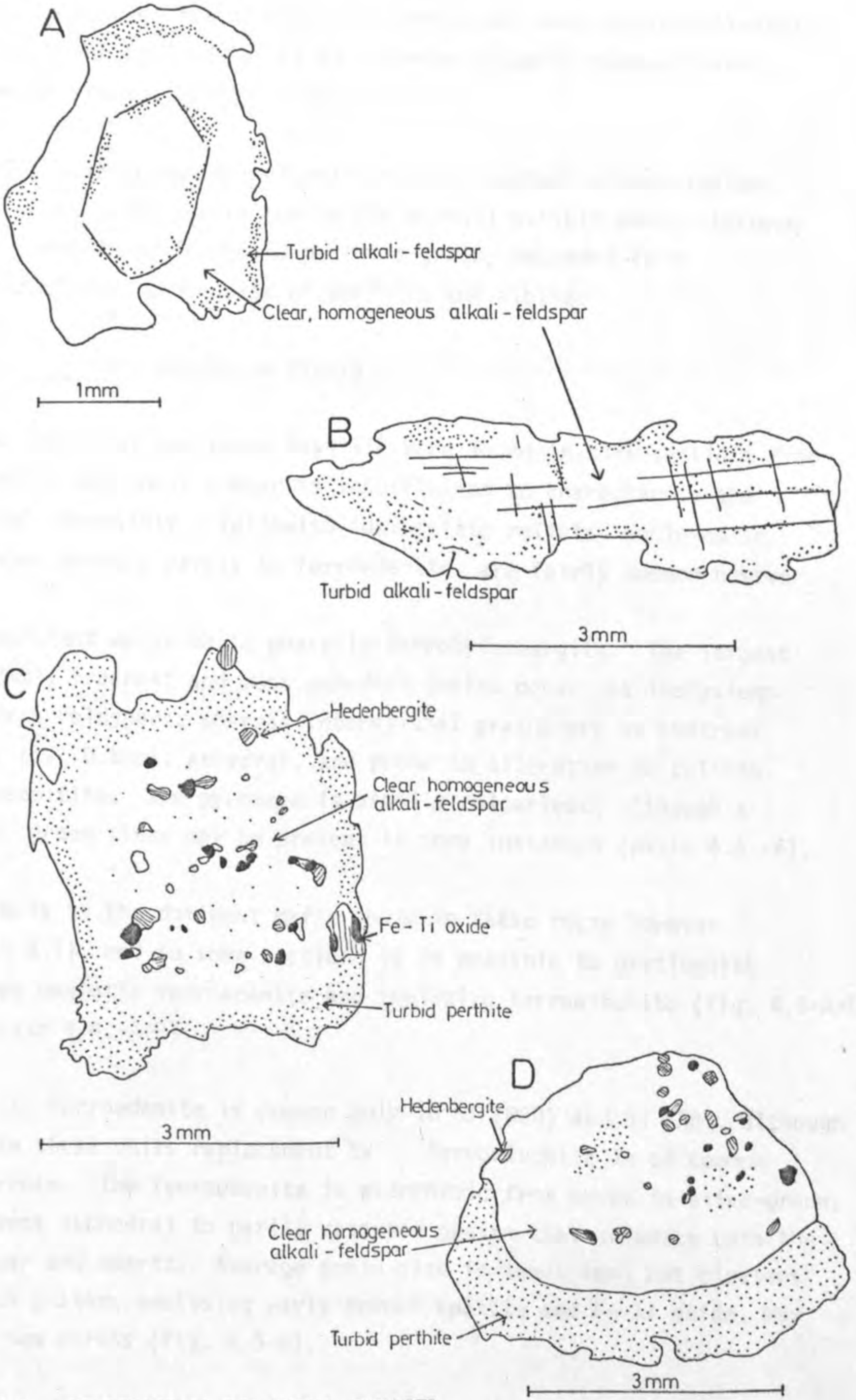

Fig. 4.4 : FELDSPARS IN THE EARLY SYENITES

Grain boundaries are straight to gently scalloped (plate 4.11-A+B). In the finer-grained varieties primary trachytic textures are commonly present (plate 4.2-A).

Locally post-intrusive deformation has resulted in shearing and cataclasis. The shears (up to 5mm across) exhibit mortar texture with rounded and fractured perthite grains embedded in a recrystallised groundmass of perthite and albite.

4.3.C. : Ferromagnesian Minerals

A few grains of unaltered fayalite were found in thin-sections from SI (RED), but their number is insufficient to characterise the mineral adequately. Yellowish iddingsitic relicts, enclosed in feldspar or more rarely in ferroedenite, are fairly common however.

The earliest major mafic phase is ferrohedenbergite. The largest (to 2mm), freshest and most euhedral grains occur as inclusions in large feldspars, whereas interstitial grains are by contrast small (av. 0.5mm), anhedral, and prone to alteration to calcite and haematite. The pyroxene is usually colourless, although a faint green tinge may be present in some instances (plate 4.6.-A).

Amphibole is the dominant mafic phase in these rocks however (table 4.1), and in some sections it is possible to distinguish between magmatic ferroedenite and replacive ferrowinchite (fig. 4.5-A+D, and plate 4.4.-A+B).

Magmatic ferroedenite is common only in SI (RED) and SI (AD), although even in those units replacement by ferrowinchite is of common occurrence. The ferroedenite is pleochroic from brown to olive-green, and forms subhedral to partly resorbed grains that antedate both the feldspar and quartz. Average grain size is about 1mm, but clusters of such grains, enclosing early formed apatite and Fe-Ti oxide, may reach 5mm across (fig. 4.5-B).

Fig. 4.5. (opposite) : Mafic mineral relations in the early syenites

A - Early formed ferro-edenite, with inclusions of apatite and early Fe-Ti oxide, enclosed in later ferro-winchite. Granules of late Fe-Ti oxide have formed along the rim of the ferro-edenite. D1014, Syenite 1, Ras ed Dom.

B - Early formed ferro-edenite, with inclusions of apatite and resorbed Fe-Ti oxide. Later ferro-winchite forms prisms, bottom left. D1014, Syenite 1, Ras ed Dom.

C - Late biotite mantling Fe-Ti oxide. D236, Syenite 1, Ras ed Dom.

D - Late ferro-winchite rimming and pseudomorphing ferro-edenite. The ferro-winchite forms needles in quartz. Minor secondary Fe-Ti oxide also present. D1014, Syenite 1, Ras ed Dom.

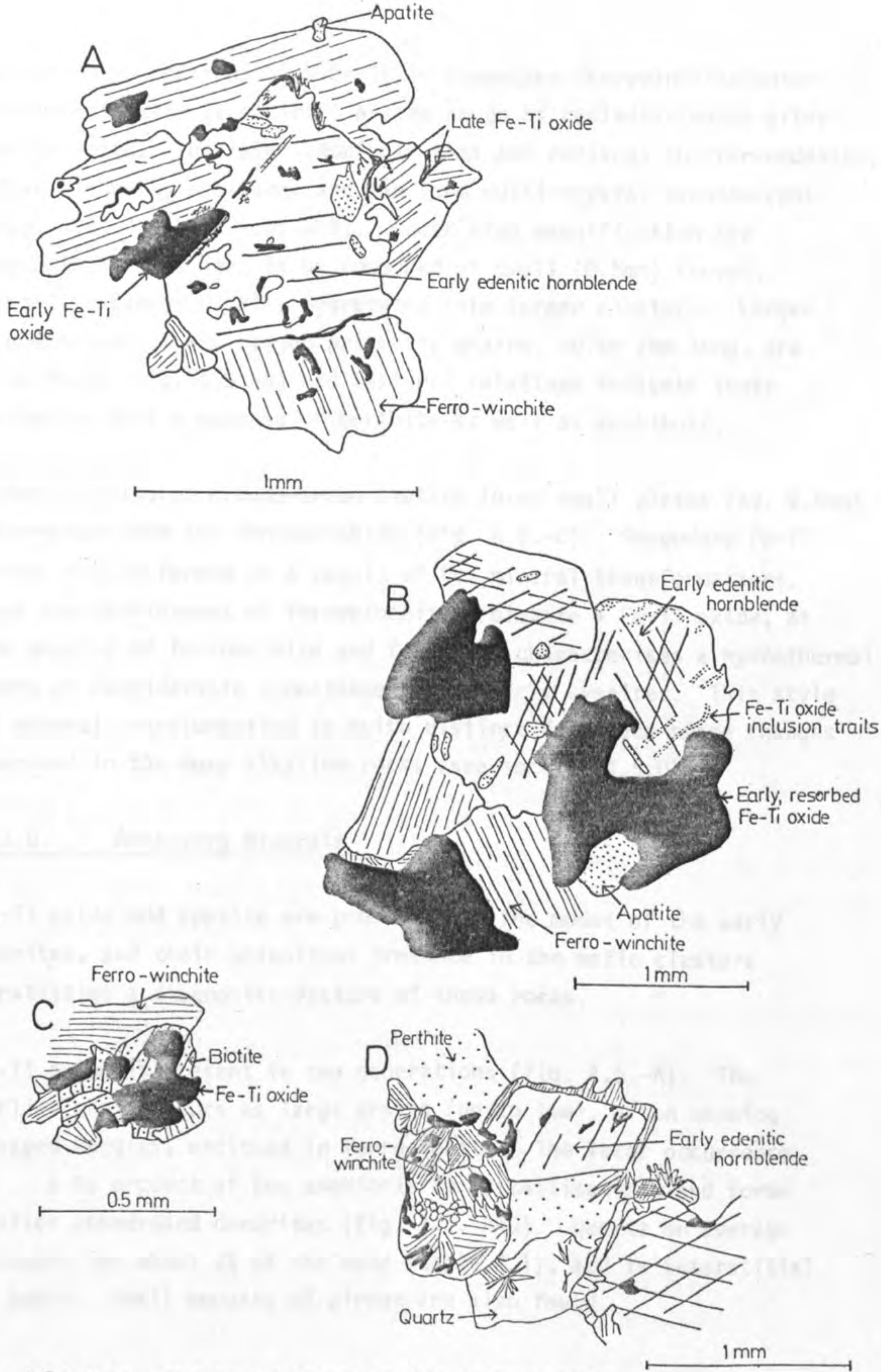

Fig. 4.5 : MAFIC MINERAL RELATIONS IN THE EARLY SYENITES

In most thin-sections however it is secondary ferrowinchite which predominates and it exhibits a wide range of replacive modes after ferroedenite. The later amphibole rims and replaces the ferroedenite, often along the cleavage, and can form multi-crystal pseudomorphs (fig. 4.5.-D; plate 4.4.-A+B). Under high magnification the ferrowinchite is seen to be composed of small (0.5mm) curved, wisp-like fibres usually aggregated into larger clusters. Larger pseudohexagonal and ragged prismatic grains, up to 2mm long, are also found (fig. 4.5.-A) and textural relations indicate their formation at the expense of perthite as well as amphibole.

Strongly-coloured orange-brown biotite forms small plates (av. 0.8mm) intergrown with the ferrowinchite (fig. 4.5.-C). Secondary Fe-Ti oxide is also formed as a result of the mineral transformations. Thus the development of ferrowinchite + biotite + Fe-Ti oxide, at the expense of ferroedenite and feldspar, characterises a hydrothermal event of considerable importance in the early syenites. This style of mineral transformation is quite distinct from late-stage changes observed in the more alkaline rocks (see section 4.5.D).

4.3.D. : Accessory Minerals

Fe-Ti oxide and apatite are prominent in the modes of the early syenites, and their ubiquitous presence in the mafic clusters constitutes a diagnostic feature of these rocks.

Fe-Ti oxide is present in two generations (fig. 4.5.-A). The earlier phase occurs as large grains (up to 1mm), often showing embayed margins, enclosed in ferroedenite. The later occurrence is a by product of the amphibole recrystallisation, and forms smaller anhedra and dendrites (fig. 4.5.-A+D). Quartz on average accounts for about 2% of the mode (table 4.1), and is interstitial in habit. Small amounts of zircon are also found.

4.4. : Transitional Syenites

4.4.A. : Introduction

The early syenites, characterised by calcic pyroxene enclosed in calcic amphibole, and the peralkaline rocks, in which sodic amphibole is rimmed by sodic pyroxene, together account for the bulk of the lithologies present in the two complexes (Maps 1 and 2). However, the S2 and S3 units of Ras ed Dom exhibit mineralogies that link these two extremes. For this reason the adjective 'transitional' is employed in describing these units, which are characterised by early formed sodic-calcic pyroxene enclosed in sodic-calcic amphibole.

The field relations of S2 are described in section 2.2.C. The unit consists of a transitional (as defined above) southern part and a dominantly alkaline northern portion. A similar heterogeneity occurs in S3 (section 2.2.C) but there it is concentrically disposed with the earlier transitional mineral assemblage preserved only in the rapidly chilled selvage, whereas it has been effectively obliterated in the more slowly cooled, alkaline core. The S3 unit thus records in-situ fractionation, and provides crucial evidence that the sequence early syenite → transitional syenite → alkali syenite → alkali granite represents a fractionation sequence.

Broad chilled margins are rare in the Bayuda syenites, and the occurrence of such a feature in S3 is probably due to the rather unique emplacement history of this intrusion (see section 2.2.C). To generalise, the writer suggests that transitional mineralogies are preserved only in somewhat unusual circumstances, such as rapid chilling, and this may account for their rarity.

The important petrographic features of the transitional syenites are summarised below, and are illustrated in figs. 4.6 and 4.7.

4.4.B. : Alkali-feldspars

The transitional syenites are typically felspar-phyric and, as suggested above, a degree of chilling may be essential for the preservation of their mineral assemblages in an unmodified state. The feldspars themselves are not especially distinctive. Those of S2 (RED) have clear, non-turbid cores, reminiscent of the early syenite feldspars (fig. 4.6.-A and plate 4.3.-A), whereas those of S3 (RED) are ubiquitously perthitic. In the latter unit tabular perthites exhibit overgrowth rims (fig. 4.6.-C+D), containing numerous amphibole inclusions and interdigitating with the groundmass in a manner clearly indicative of recrystallisation. As discussed in section 4.7. a distinctive type of albitisation sometimes occurs in these rocks.

As in the early syenites, primary zonation in the feldspars may be reflected by variations in the degree of turbidity and coarseness of exsolution within individual grains (fig. 4.6-B). Bulk compositions are less calcic (~3 mol.% An) than those of the early syenites.

4.4.C. ; Ferromagnesian Minerals

Possible relicts after fayalite are more frequent than in the early syenites, probably because the transitional syenites are free from hydrothermal alteration. The relicts are typically small (av. 0.5mm), of rounded appearance, and consist of weakly pleochroic yellow 'iddingsite' (fig. 4.7.-D+E). They occur enclosed in aegirine-augite, ferrorichterite and aenigmatite.

The early-formed pyroxene occurs as small grains (av. 0.5mm), which are commonly zoned from almost colourless cores to bright green rims (fig. 4.7-A+B+F). The zoning is usually concentrically disposed and can be discontinuous, or more rarely continuous or even oscillatory. Early formed inclusions in feldspar are typically colourless ferrohedenbergite, whereas late interstitial grains are of green

Fig. 4.6. (opposite) : Feldspars from the transitional syenites

A - Irregular distribution of turbidity and exsolution in a grain of alkali-feldspar. D462, Syenite 3, Ras ed Dom.

B - Primary zonation, now reflected as zones of variable turbidity and degree of exsolution, in an alkali-feldspar grain. Note antiperthitic outer rim. D247, Syenite 3, Ras ed Dom.

C - Tabular perthite grain, with straight margin where it abuts upon quartz. The contact with the groundmass perthites is scalloped and recrystallised. A central core that is only partly turbid can be distinguished from an outer zone where turbidity and exsolution is more marked. For simplicity exsolution details are omitted. Arfvedsonite inclusions characterise the outer zone. D259A, Syenite 3, Ras ed Dom.

D - Increase in turbidity and degree of exsolution outwards in perthite grain. D259A, Syenite 3, Ras ed Dom.

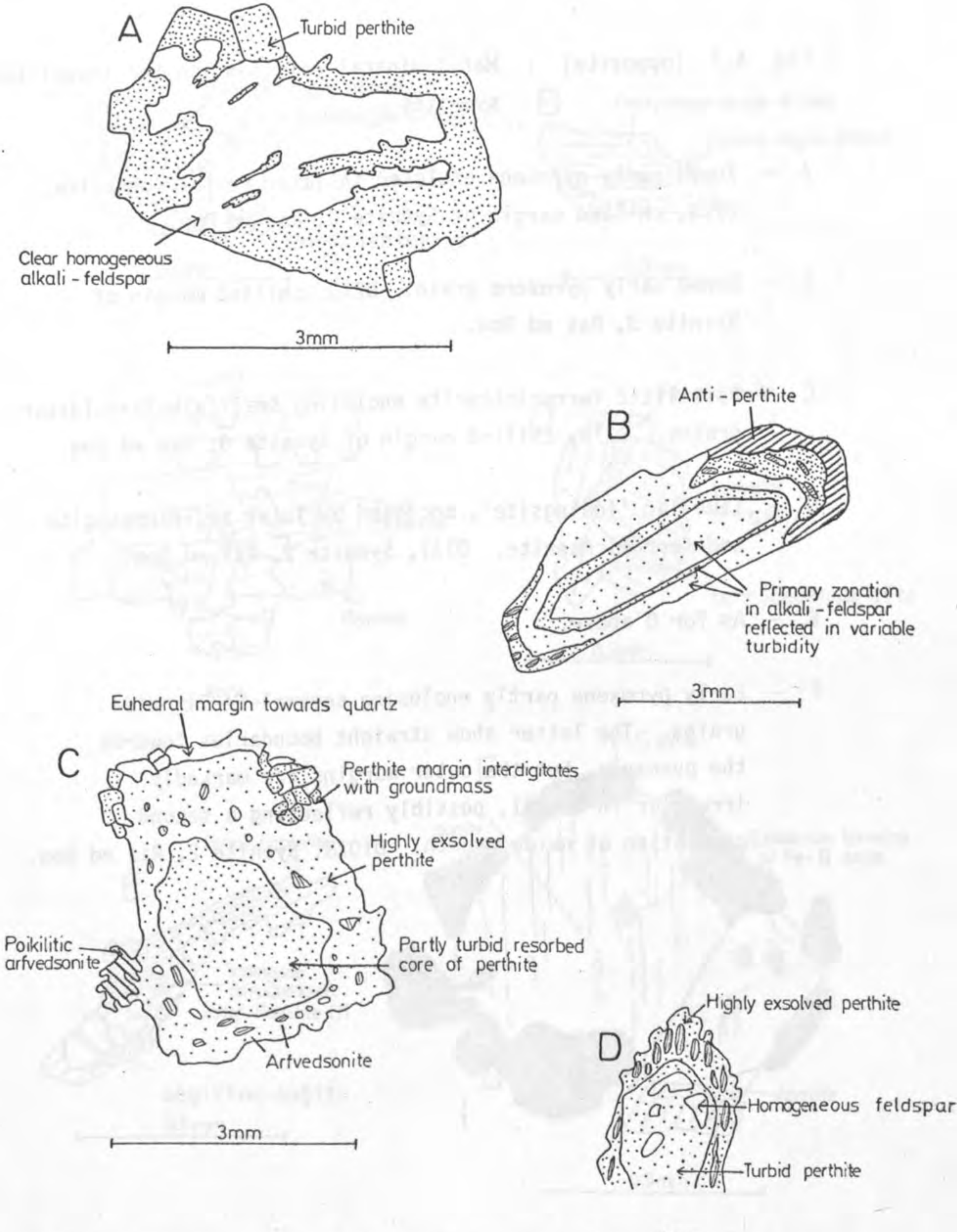

Fig. 4.6 : FELDSPARS FROM THE TRANSITIONAL SYENITES

Fig. 4.7. (opposite) : Mafic mineral relations in the transitional syenites

A - Zoned early pyroxene enclosed in later ferro-richterite. D275, chilled margin of Syenite 3, Ras ed Dom.

B - Zoned early pyroxene grain. D275, chilled margin of Syenite 3, Ras ed Dom.

C - Poikilitic ferrorichterite enclosing small alkali-feldspar grains. D275, chilled margin of Syenite 3, Ras ed Dom.

D - Lamellar 'iddingsite', enclosed by later aegirine-augite and ferrorichterite. D131, Syenite 2, Ras ed Dom.

E - As for D above.

F - Early pyroxene partly enclosing several Fe-Ti oxide grains. The latter show straight boundaries towards the pyroxene, but the outer margins are markedly irregular in detail, possibly reflecting a second generation of oxide growth. D1028, Syenite 2, Ras ed Dom.

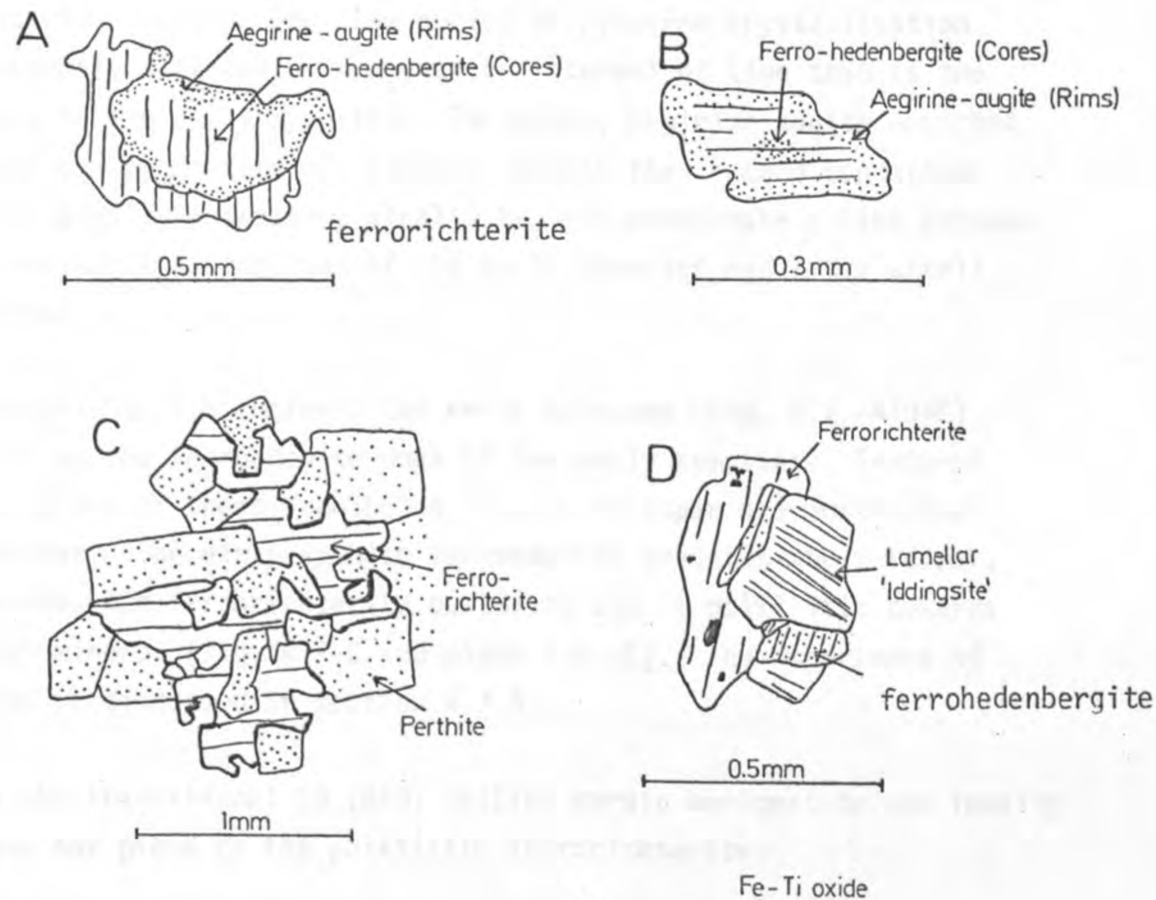

Fig. 4.7 : MAFIC MINERAL RELATIONS IN THE TRANSITIONAL SYENITES

aegirine-augite. Thus the period of pyroxene crystallisation evidently extended over a greater interval of time than is the case in the early syenites. The green, aegirine-augite enriched rims are especially significant in that they record conditions of gradually increasing alkalinity, and constitute a link between the mineral assemblages of the early syenites and later alkali rocks.

Ferrorichterite encloses the early pyroxene (fig. 4.7.-A+D+E), much as the ferroedenite does in the early syenites. Textural relations of these amphiboles towards feldspar are contrasted however. The early syenite ferroedenite predates the feldspar, whereas the ferrorichterite postdates and is poikilitic towards that mineral (fig. 4.7-C and plate 4.4.-C). The importance of this is discussed in section 4.7.A.

In the transitional S3 (RED) chilled margin aenigmatite can locally take the place of the poikilitic ferrorichterite.

4.4.D. : Accessory Minerals

Quartz is rather variable in abundance (table 4.1), but the variation is not of any major significance. Fe-Ti oxide and apatite are present in some of the mafic clusters, but in smaller amounts than in the early syenites. Late interstitial zircon is also present.

4.5. : Alkali Syenites and Granites

4.5.A. : Introduction

The petrography of the alkali rocks - syenites, quartz-syenites, granites and their finer grained equivalents (e.g. intrusive trachytes, microgranites and felsites) - is discussed. Although the intermediate and acid rocks span a wide range of quartz contents their mineral assemblages reflect the importance of two shared processes. The first of these is the late crystallisation of quartz, postdating feldspar (fig. 4.8), whilst the second is the replacement of sodic amphibole by sodic pyroxene (fig. 4.9). Both processes have occurred most extensively in the granites.

The separation between granite and syenite at Q = 20 (Streckeisen, 1967) corresponds well with the field distinction between these rock-types. Locally the divisions may be blurred, e.g. where a syenite may become so enriched locally in quartz as to be technically granitic, but such overlap serves to reinforce the impression of consanguineity in these rocks.

4.5.B. : Alkali-feldspar

The transparent orthoclases of the early and transitional syenites are rarely seen in the alkali rocks, and instead the feldspars are characteristically densely turbid perthites (plate 4.3.-B+C).

The degree of unmixing is often very variable, even within one intrusion. In general however the coarseness of the exsolution intergrowths increases with increasing grain size, and with increasing quartz content. In the syenitic units fine scale stringlet perthites predominate (plate 4.10.-E), and coarser patches are rather randomly located. In the microgranites regular ribbon textures prevail. The coarsest textures are the braid, plume and patch types of the granites (plate 4.10.-C). In the granites exsolution can be highly advanced and antiperthites, with the albitic component showing chess-board textures (plate 4.10.-D), are often developed. In these instances the albite is clear, and turbidity is concentrated in the potassic component.

Grain boundary modifications are common, but where subhedral grains are preserved a primary tabular habit is indicated. In feldspar-phyric units, such as S6 (RED), the phenocrysts are tabular to anhedral in form. Overgrowths of later feldspar upon such phenocrysts contain inclusions of sodic pyriboles and interdigitate with the groundmass. Such overgrowths evidently record recrystallisation under sub-solidus conditions.

Perthite mutual boundaries are typically lobate, scalloped and pleated (the 'swapped rims' of Parsons, 1980; see plate 4.11.-C), and testify to partial adjustment along grain boundaries. Where recrystallisation is advanced a wide range of grain size is sometimes encountered. This results from recrystallisation of large primary grains to form 'domains' or clusters of smaller grains which are characterised by highly complex boundaries (plate 4.11.-D).

The significance of these features, together with an account of the accompanying albitisation, is discussed in section 4.7.B.

4.5.C. : Quartz

The quartz content of these rocks can be very variable, even within one unit (table 4.1.), and as is to be expected from relations in the Granite System (Tuttle and Bowen, 1958) the quartz postdates the alkali-feldspar. In the syenites quartz has crystallised along perthite grain boundaries, evidently occupying all available spaces in the largely solid crystal mush. In the granites the quartz is again interstitial, and sometimes replacive towards the feldspar. As quartz grain size increases the feldspar is reduced to wispy shreds and 'islands' (fig. 4.8.-C+D). 'Tongues' of quartz extend inwards into perthite grains (fig. 4.8.-D). Where the quartz is aggregated into clusters (up to 5mm across) the individual anhedra commonly show mutual triple junctions (fig. 4.8-E) and are evidently recrystallised. Late aegirine is often developed along such interfaces (fig. 4.8.-E). The general textural effect of the relatively late crystallisation of quartz in the alkali rocks is thus to promote xenomorphism in the feldspars.

4.5.D. : Ferromagnesian Minerals

Relicts (av. 1mm) after hedenbergite and early amphibole are sometimes seen in the alkali syenites, but are less frequently encountered in the granites. Usually the relicts are haematised and calcitised. For the most part however the mafic assemblages are dominated by sodic

Fig. 4.8. (opposite) : Quartz-Alkali feldspar relations in the Younger Granite rocks

A - Interstitial quartz. The grains have evidently crystallised along perthite grain boundaries. D1057, Syenite 3, Ras ed Dom.

B - As A above. D1028, Syenite 2, Ras ed Dom.

C - Larger aggregates of quartz, as compared to A and B above. D1077, Syenite 2, Ras ed Dom.

D - Quartz, showing complex boundary relations with alkali-feldspar in places. D132, Granite 1, Ras ed Dom.

E - Aggregated large quartz grains. Note the nucleation of late aegirine along quartz boundaries. D231, Granite 1, Ras ed Dom.

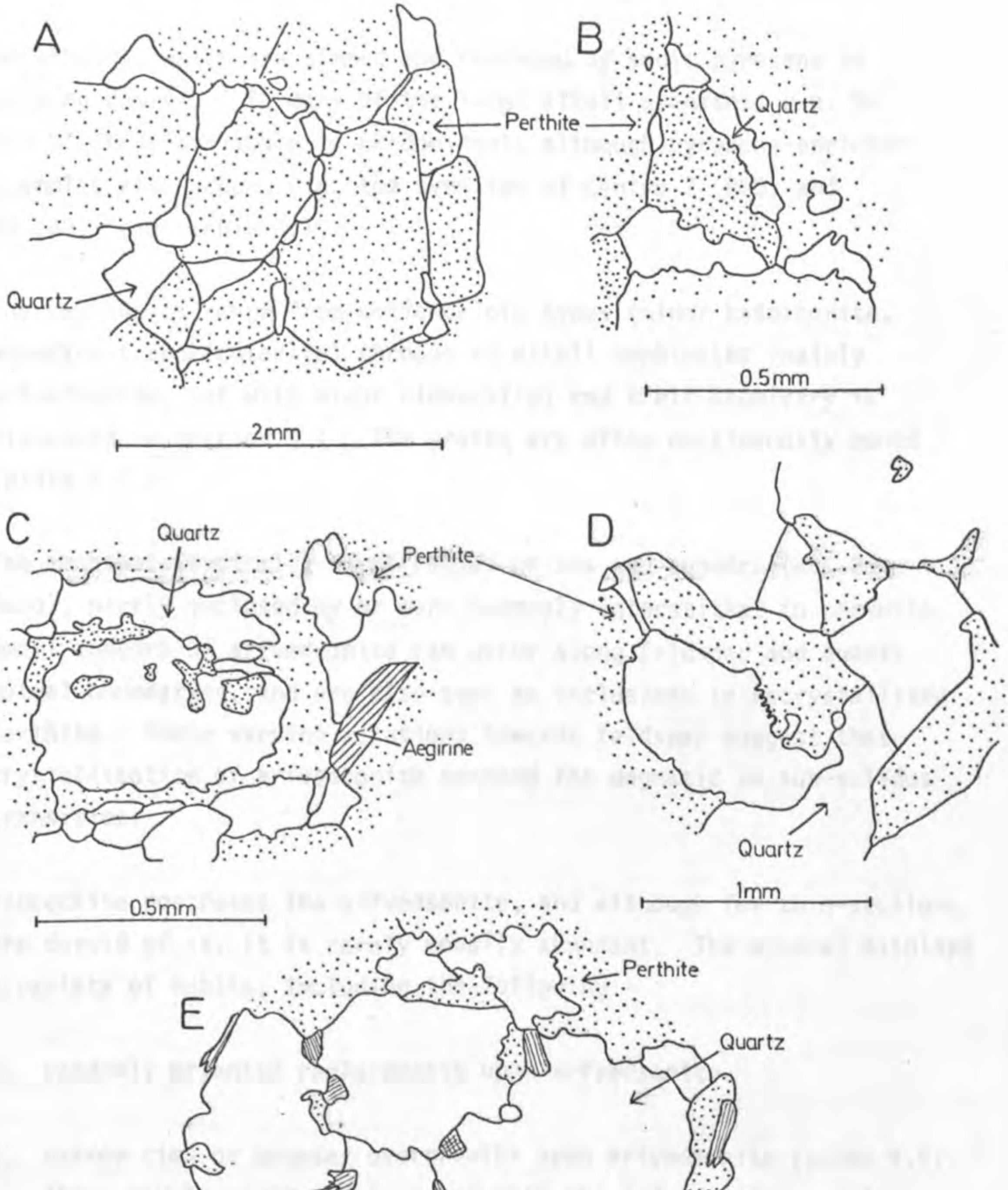

Fig. 4.8 : QUARTZ - ALKALI FELDSPAR RELATIONS IN THE YOUNGER GRANITE ROCKS

amphiboles, which are rimmed and replaced by sodic pyroxene to varying degrees. In many of the large alkali syenites, e.g. S6 and S7 (RED) amphibole is predominant, although pyroxene-enriched examples also occur, e.g. the syenites of Centre 7 (RED) and S4 (AD), (see table 4.1).

The amphiboles range from sodic-calcic types (minor katophorite, abundant ferrorichterite) through to alkali amphiboles (mainly arfvedsonite, but with minor riebeckite) and their chemistry is discussed in section 5.4. The grains are often continuously zoned (plate 4.5.).

The amphibole typically forms ragged prisms and anhedra (av. 2mm long), partly enclosed by or more commonly interstitial to perthite. Small anhedra of arfvedsonite can occur along feldspar and quartz mutual boundaries, and are also seen as inclusions in recrystallised perthite. These varying relations towards feldspar suggest that crystallisation of arfvedsonite spanned the magmatic to sub-solidus transition.

Riebeckite postdates the arfvedsonite, and although few thin-sections are devoid of it, it is rarely modally abundant. The mineral displays a variety of habits, including the following:-

1. randomly oriented replacements upon arfvedsonite.

2. narrow rims or broader overgrowths upon arfvedsonite (plate 4.5). These may be continuously zoned with the arfvedsonite, or form discrete grains, and may themselves show internal zoning (fig. 4.10.-A). Sometimes small peg-like outgrowths extend into adjacent perthite, which evidently the riebeckite can replace also (fig. 4.10.-B).

3. small bundles of curved riebeckite fibres and needles, located within quartz (fig. 4.10.-C+E), and postdating adjacent aegirine. Minute grains also occur along perthite grain boundaries (fig. 4.10.-D).

Several of the above habits (e.g. fig. 4.10.-B+C+D) are consistent with sub-solidus growth.

The replacement of arfvedsonite by sodic pyroxene constitutes a major late-stage mineral adjustment in the alkali rocks, and is especially characteristic of the granites (table 4.1). The pyroxene ranges in composition from aegirine-augite to aegirine (see section 5.3.).

In the initial stages the pyroxene forms a narrow rim mantling the amphibole, but with progressive replacement pervades inwards along the amphibole cleavage (fig. 4.9.-C+D). At an advanced stage a mosaic of pyroxene grains may pseudomorph the amphibole, which forms dispersed but optically continuous remnant shreds (fig. 4.9.-E). The initial pyroxene growths tend to be rather ragged but euhedral prisms are developed as the amphibole is eliminated (plate 4.6.-B). Such grains grow at the expense of both perthite and arfvedsonite, and are thus probably of sub-solidus rather than magmatic origin (see description accompanying plate 4.6.-C). In general however subhedral prisms (up to 2.5mm long) are a commoner expression. Where growth has been especially rapid, stellate clusters are formed (fig. 4.9.-F). Nucleation of the pyroxene along perthite and quartz mutual boundaries is also consistent with sub-solidus growth (fig. 4.8.-E).

Euhedral inclusions of aegirine in quartz often show pointed acmitic terminations (fig. 4.9.-G+H and plate 4.6.-C), and could clearly be magmatic in origin. In the case of plate 4.6.-C, however, a replacive origin has been already been described for the adjacent aegirine prism, and by extension might be applied to the inclusions in quartz. Textures alone are thus equivocal, and it must be concluded that formation of aegirine probably spans the late-to post-magmatic interval.

Zonation from cores of aegirine-augite, which are pleochroic in rich greens, to rims of aegirine exhibiting more delicate tints, is a common feature. The zonation varies from a concentric disposition to irregular patchy examples (fig. 4.9-G+H), and is best exemplified by the late euhedral grains (plate 4.6.-B+C).

Fig. 4.9. (opposite) : Mafic mineral relations in the alkali syenites and granites.

A & B - Late spongy growth of aegirine-augite, with associated Fe-Ti oxide and minor biotite. Recrystallised assemblage, D433, Syenite 13, Ras ed Dom.

C - Aegirine, rimming arfvedsonite and replacing it along the cleavage. D146, Granite 1, Ras ed Dom.

D - Aegirine replacing arfvedsonite. D397, Syenite 6, Ras ed Dom.

E - Aegirine, with relict inclusions of optically continuous arfvedsonite. D231, Granite 1, Ras ed Dom.

F - Radiating growth of late aegirine. Minor associated haematite also present. D180, Syenite 15, Ras ed Dom.

G - Zoned aegirine, with pointed acmitic terminations. D340, Syenite 7, Ras ed Dom.

H - Zoned aegirine. R35, Syenite 15, Ras ed Dom.

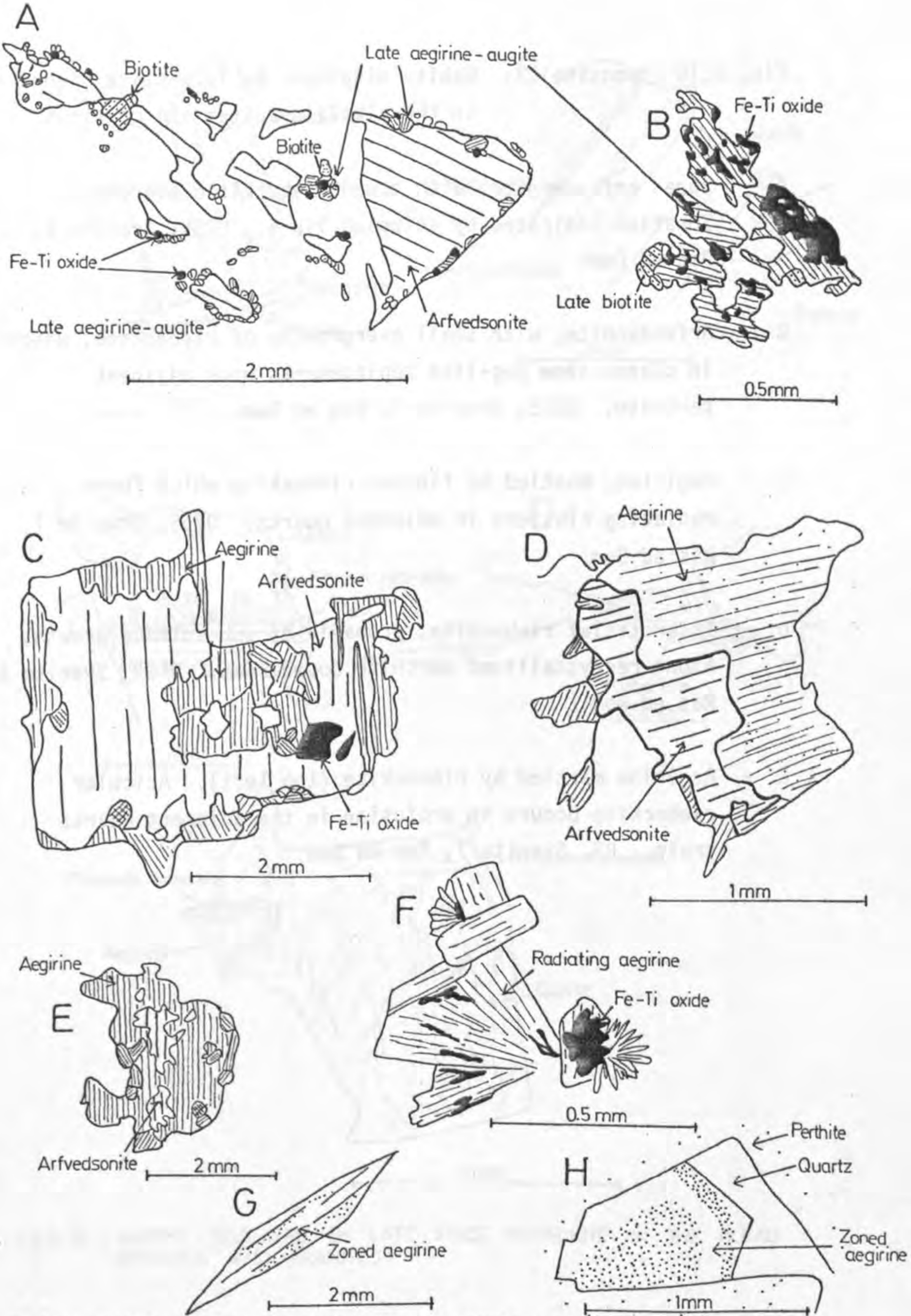

Fig. 4.9 : MAFIC MINERAL RELATIONS IN THE ALKALI SYENITES AND GRANITES

Fig. 4.10 (opposite) : Habits displayed by late-stage riebeckite in the alkali syenites and granites.

A - Zoned arfvedsonite, with zoned riebeckitic overgrowth. Zonation indicated by stippled lines. D255, Granite 1, Ras ed Dom.

B - Arfvedsonite, with small overgrowths of riebeckite, which in places show peg-like replacements upon adjacent perthite. D255, Granite 1, Ras ed Dom.

C - Aegirine, mantled by fibrous riebeckite which forms radiating clusters in adjacent quartz. D255, Granite 1, Ras ed Dom.

D - Interstitial riebeckite, probably of sub-solidus growth, along recrystallised perthite boundaries. D402, Syenite 6, Ras ed Dom.

E - Aegirine mantled by riebeckite (top left). Acicular riebeckite occurs in profusion in the adjacent quartz grain. R3, Syenite 7, Ras ed Dom.

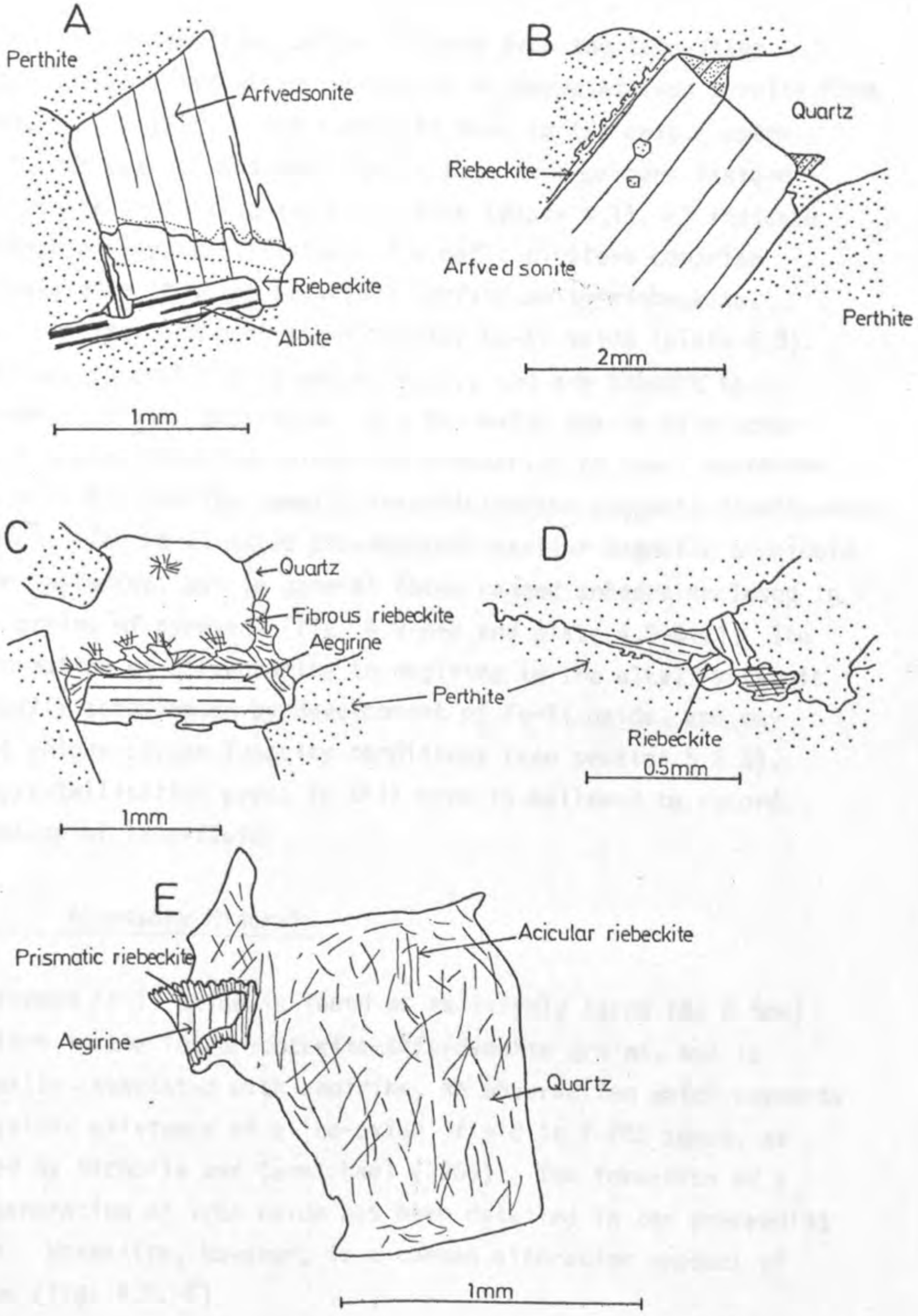

Fig.4.10 : HABITS DISPLAYED BY LATE-STAGE RIEBECKITE IN THE ALKALI SYENITES AND GRANITES

A sub-solidus assemblage, quite distinct from the late-stage adjustments described above, occurs in a recrystallised syenite from loc.D433 in S13 (RED). The sample is near to the unit's outer contact, but even if the small grain size is a primary feature, the intricate perthite grain boundaries (plate 4.11.-E) indicate considerable recrystallisation. The mafic clusters comprise aegirine-augite (but not aegirine), arfvedsonite-riebeckite, amintic biotite, and most significantly Fe-Ti oxide (plate 4.9). They occupy interstitia (plate 4.11.-E), and are thought to pseudomorph earlier amphibole. All the mafic phases also occur as small grains developed along the boundaries to small perthites (plate 4.11-E), and the complex interdigitation suggests simultaneous formation. The Fe-Ti oxide pseudomorphs earlier magmatic amphibole in some instances, but in general forms ragged anhedra enclosed in spongy grains of pyroxene (fig. 4.9-A+B and plate 4.9-B+C). The transformation of arfvedsonite to aegirine in the alkali rocks is not usually accompanied by development of Fe-Ti oxide, and may reflect unique oxygen fugacity conditions (see section 5.3.D). The recrystallisation event in this rock is believed to record the passage of late-fluids.

4.5.E. : Accessory Minerals

Early formed Fe-Ti oxide is found as relatively large (to 0.5mm) inclusions in the ferrorichterite-arfvedsonite grains, but is not usually associated with aegirine, an observation which supports the possible existence of a 'no-oxide' field in T-fO2 space, as reported by Nicholls and Carmichael (1969). The formation of a later generation of iron oxide has been detailed in the preceeding section. Haematite, however, is a common alteration product of aegirine (fig. 4.9.-F).

Apatite is the earliest formed accessory and is found as slender rods within feldspar. Shorter, stouter prisms (to 2mm) occur in the early iron oxide and amphibole, but are rarely preserved in the aegirine.

Zircon is of sporadic occurrence, but where present tends to be gregarious, forming clusters and chains of tiny grains (av. 0.25mm; plate 4.7-C). Both fresh and metamict brown types are seen. The mineral is characteristically associated with quartz and late aegirine.

Calcite is found as a hydrothermal-stage infill of cavities, and is interstitial to quartz and aegirine. A yellowish tinge may reflect iron-enrichment, and colloform intergrowths with a red opaque oxide occur in S7 (RED). Flourite sporadically accompanies the calcite. At loc.175, in S13 (RED), calcite and quartz infill cavities in pegmatitic syenite. Both minerals contain euhedral prisms and needles of aegirine (plate 4.8.-C).

4.6. : Minor Intrusions

The mineral assemblages encountered in the plutonic rocks are present also in dyke rocks, and accordingly it is the petrographic differences which are emphasised in the ensuing discussion. The important categories of dykes are discussed in turn below.

1. Dolerite, Abu Dom

Only one such dyke is known, from loc. 183 in Abu Dom, and it has no known plutonic equivalent. In hand-specimen it is a dark green, fine-medium grained rock with small plagioclase laths. In thin-section (plate 4.1.-B) the randomly oriented plagioclase laths (up to 2mm long) are traversed by cracks and are partially turbid. The grains are normally zoned from cores of labradorite to oligoclase rims (see section 5.2.B). Olivine is absent. Ilmenite, of slightly skeletal habit is fairly abundant, and is partly enclosed by the plagioclase. The original texture was perhaps ophitic, but the pyroxene has been thoroughly altered to an assemblage of ferrowinchite, annitic biotite and secondary Fe-Ti oxide. The style of alteration recalls that found in the early syenites (section 4.3.C).

2. Hedenbergite-Biotite Syenite

Only a few such dykes are known, and they are restricted to Centre 7 (RED). Clear orthoclase, with inclusions of hedenbergite, forms phenocrysts (plate 4.1.-C) whilst discrete hedenbergite phenocrysts, mantled by biotite, also occur. The groundmass feldspars are more perthitic and partly recrystallised. Biotite, of possible sub-solidus growth, is developed along perthite junctions. The rock-type resembles the larger intrusions of biotite-granite from Muweilih complex (McCormac, pers.comm. and Map 3).

3. Early and Transitional Microsyenites

These lithologies are not abundant, the only examples from Abu Dom being those pertaining to S1. In Ras ed Dom several such dykes intrude S1 and S2. As with their plutonic counterparts the salient feature is the occurrence of calcic clinopyroxene, commonly zoned to rims of aegirine-augite. The feldspars exhibit clear, resorbed cores which pass outwards abruptly into rims of ribbon perthite, densely packed with hedenbergite inclusions. Feldspar and hedenbergite, but not amphibole, constitute the phenocryst phases.

4. Alkali Microsyenites and Microgranites

The microsyenites, microgranites and their finer-grained equivalents, the intrusive trachytes and rhyolites, show the same assemblages that characterise the larger alkali plutonics, but some points of note include:-

- One of the commonest lithologies is the quartz-feldspar porphyry (plate 4.2.-B), which is acid in composition. The feldspar phenocrysts are almost invariably albitised (see 4.7.B below). Another interesting feature is that the perthite phenocrysts are often mantled by micrographic intergrowths of presumed eutectic origin.

- The finer-grained dykes are often devitrified glasses and spherulitic textures are common. The spherulitic (up to 3cm across exceptionally) consist not only of radially disposed quartz and feldspar, but also contain needles of aegirine and sodic amphibole. This indicates that devitrification does not invariably involve loss of alkalies.

- Aegirine is the most abundant groundmass mafic phase in the dykes, and appears to coexist stably with subordinate sodic amphibole, contrary to the replacive relations observed in the plutonic counterparts.

- Trachytic textures occur in many of the intermediate dykes, whilst flow-oriented pyriboles and feldspars are common in the microgranites.

- Alkali-feldspar forms phenocrysts in the microsyenites, and is accompanied by quartz phenocrysts in the microgranitic rocks. Aeigirine and arfvedsonite never occur as phenocrysts, although both do occur as late groundmass poikiloblasts.

In summary, although the dyke rocks exhibit textural features unique to them alone, mineralogically they are closely similar to the larger intrusive bodies, and the processes involved in the formation of both are evidently broadly the same.

4.7. : Sundry Petrographic Features

4.7.a. : Recognition of a Fractionation Series

Four principal rock-types, namely early syenite, transitional syenite, alkali syenite and alkali granite, characterise Ras ed Dom and Abu Dom. Two lines of field evidence, as follows, indicate that these four categories (in the order quoted) constitute a fractionation series.

1. The early syenites are commonly the oldest rocks in a particular structural centre.
2. In-situ fractionation from a chilled transitional syenite margin to a core of alkali syenite, is observed in S3 (RED).

A major contrast between the early and alkali rocks is the relative order of crystallisation of the felsic and mafic minerals. Two contrasting sequences of crystallisation can be recognised (c.f. Goldschmidt, 1954; Bowden and van Breeman, 1972) as follows:-

1. a plumasitic sequence, in which the mafic phases (fayalite, apatite, Fe-Ti oxide, ferrohedenbergite, ferroedenite) crystallise early, followed by alkali-feldspar and quartz. This sequence characterises the early syenites.

2. In the alkali rocks an agpaitic order of appearance (alkali-feldspar, quartz, ferrorichterite-arfvedsonite-riebeckite, aenigmatite, aegirine and zircon) is present.

The transitional syenites are of interest in that they show textures transitional between two sequences. The early pyroxenes may be enclosed in feldspar (plumasitic order), or interstitial, and the ferrorichterite is often poikilitic towards feldspar (agpaitic order of appearance). The two sequences are depicted in fig. 4.3., and it can be seen that the plumasitic sequence characterises the earlier magmatic stages, whilst the agpaitic sequence characterises the more evolved magmas. It was suggested in section 4.5.D. that the later stages of the agpaitic sequence may be partly sub-solidus in origin, and this is indicated in fig. 4.3.

Fig. 4.3. also shows that two distinct episodes of pyroxene crystallisation, one predating and the other postdating amphibole, are present in the mafic reaction series.

4.7.B. : Feldspar Exsolution and Albitisation

The syenites and granites of Ras ed Dom and Abu Dom are hypersolvus 'one-feldspar' rocks, characterised by the absence of plagioclase except as a component of perthite (Tuttle and Bowen, 1958; but see also section 4.7.D.). As a hypersolvus rock cools equilibrium can be re-established by a combination of perthitic exsolution, short range migration of the albitic component beyond the border of the original grain, and Si-Al ordering. An aqueous fluid is probably needed for the latter two processes (Martin and Bonin, 1976), and may leave an indelible imprint on the feldspar textures (Parsons, 1978). The exsolution features of the Bayuda rocks, already described in sections 4.3.B., 4.4.B., and 4.5.B., are now considered in this light.

Two major feldspar variants are recognised. The first consists of clear, transparent orthoclase, most commonly found in the early and transitional syenites, where it forms the cores or more rarely the entirety of feldspar grains (plate 4.10-A). Turbidity is concentrated towards grain borders, but can be seen encroaching inwards along the cleavage in places (plate 4.10-A + B). The second type of feldspar is highly turbid micro- and macroperthite, which typifies the alkali rocks (plate 4.10-E). There is a general coarsening of exsolution textures, and a decrease in the regularity of the intergrowths, on passing from syenite to granite. The syenites exhibit string and ribbon textures whereas coarser patch, braid and plume types are found in the granites (plate 4.10-C). This coarsening is accompanied by an increase in turbidity, which is usually concentrated in the potassic component, the plagioclase being relatively clear (plate 4.10-D). The above mentioned changes are also accompanied by an increase in complexity of grain boundaries, which change from straight or gently lobate in the early rocks to intensely sutured, dentate and swapped rim types in the alkali rocks (plate 4.11-A+B+C).

The variation described above may reflect several factors.

1. Anothite content : Mol.% An declines from 7.0 in the early rocks to 0.0 in the alkali syenites (section 5.2.A). However, this variation is slight, and would not account for variable exsolution in different parts of one intrusion, or irregular variation in one grain. Primary compositional zoning does exercise a regular control on later exsolution in certain instances (e.g. see fig. 4.6.-B), but these are of infrequent occurrence. Parsons (1978 and 1980) concludes that the effects of An content and aqueous fluids may act in parallel in promoting exsolution.

2. Rate of Cooling : There is no systematic variation in grain size on passing from the early to alkali rocks. Some microgranite units have finer-scale perthitic textures than those found in the granites, but exceptions are common. One possible example of such a control occurs in the small concentric intrusions of Centre 7 (RED), where the degree of coarseness of exsolution increases from SII to SI4 (see fig. 2.7.A.). The absence of turbidity in the feldspars of SII may reflect emplacement of magma into cold brittle crust, with consequent rapid loss of heat and fluids, whereas the later units were insulated from such losses along their outer margins by the preceeding intrusions.

3. Presence of fluids : The grain boundary changes (plate 4.II), the relation of turbidity to cleavage (plate 4.10.-A), and the coarsening of exsolution towards grain edges (plate 4.10.-B) are readily comprehensible in terms of fluid migration along grain interfaces. Other indirect evidence of late aqueous fluids is provided by:-

   a. the presence of biotite in some of the later syenites of Centre 7 (RED),

   b. the occurrence of pegmatitic facies, of either widespread (e.g. S12 RED) or more local extent (e.g. S5 AD),

   c. Miarolitic cavities, druses and coarse pegmatitic patches occur in GI (RED) and G2 (AD).

Structural state studies (Parsons, 1980), have established a correlation between increasing turbidity and exsolution, and greater Si-Al ordering, and this feature is enhanced when the fluids involved are peralkaline (Martin, 1969). Structural state studies which might confirm this correlation for the rocks under discussion have not been attempted, but McCormac (1979) has reported an increase in ordering with fractionation in the peralkaline sequences of nearby Muweilih complex (Map 3). An intriguing feature of the feldspars is the general absence of microcline twinning, the only exception being in a vein assemblage from Abu Dom (plate 4.8.-A). McCormac (1979) attributes this scarcity to the fact although levels approach maximum microcline in the aegirine-granites, the increase in ordering is still on a relatively short range.

It was noted earlier (section 4.5.B) that advanced exsolution can result in the development of antiperthite in the alkali granites. In addition discrete grains of non-turbid albite are often present, and the term albitisation is used to describe their development. A range of habits are present including the following:-

1. minute grains exsolved in necklace fashion along recrystallised perthite boundaries (plate 4.11.-C). At a more advanced stage the albite forms broad zones (up to 1-2mm wide) between perthite grains, and such 'channels' (plate 4.12.-A+B) are thought to record the passage of aqueous fluids (Parsons, 1980).

2. as tiny grains distributed in patch fashion throughout perthite grains, but not necessarily related to the periphery of the grains. This is believed to represent more pervasive fluid activity. The best examples are found in the marginal zones of S3(RED) and GI(RED), and in the quartz-feldspar porphyry dykes (plate 4.12.-C+D).

3. as somewhat larger grains (exceptionally up to 2.5mm) occupying the interstices between perthite grains, or occurring where perthite abuts upon quartz. They often display straight crystal edges suggesting free growth into a cavity (plate 4.12.-E+F).

Although late albite may account locally for as much as 10.5% of the mode (e.g. GI, RED) the average value in the syenites and granites is 1-2%. Compared with values between 13-49% from the albitised granites of Nigeria (Jacobson and MacLeod, 1977) these values are small and indicate the limited degree of albitisation in the Bayuda rocks.

To summarise the exsolution and alibitisation features of the alkali rocks are consistent with the activity of late-stage fluids.

4.7.C. : Mafic Minerals and the Late- to Post-Magmatic Stages

In this section vein assemblages and recrystallised assemblages are reviewed in an attempt to characterise the transition from the late magmatic to post-magmatic conditions in these rocks.

Two main types of vein assemblage are found. The first type is granitic, and in these elongate, narrow prisms of aegirine are the dominant mafic phase. Introduction of silica into the adjacent host rock is indicated by granophyric intergrowths replacing host-rock feldspar (plate 4.8.-B). The only known occurrence of microcline in either complex is from one such vein, at loc. 603 in S2 of Abu Dom (plate 4.8.-A; section 4.7.B). The second category of veins are mafic-rich, with aegirine, subordinate arfvedsonite-riebeckite and minor quartz and feldspar. Where the pyroxene is aegirine-augite, Fe-Ti oxide is also commonly present, an example being the veins at loc. D129 in S2 of Ras ed Dom (fig. 2.3). There, over an area of several tens of square metres, the host syenite is metasomatised by both discrete veins and more diffuse alteration. This metasomatism is discussed further in section 6.4.

Also relevant in this context is the occurrence of calcite and flourite as cavity infills in the alkali rocks, and the association of zircon with aegirine.

The vein assemblages thus provide evidence of residual liquids of both 'normal' granitic and more extreme mafic-rich composition. Fluids similar in composition to the latter may be responsible for the sub-solidus changes described in the feldspars(previous section), and would also account for the sub-solidus appearance of aegirine and riebeckite in certain instances (section 4.5.D). A slightly different assemblage characterises the recrystallised syenite at loc. D433 (S13, RED), in that arfvedsonite-riebeckite is accompanied by aegirine-augite, Fe-Ti oxide and annite (section 4.5.C). This assemblage is also thought to reflect the passage of late fluids. The chemistry of such fluids is considered in section 6.4.

4.7.D. : Early Plagioclase

The Younger Granite rocks are typically hypersolvus 'one-feldspar' rocks. Plagioclase of magmatic as distinct from exsolution origin does occur, however, in two situations as follows:-

i. As rare cores (up to 5mm long) to alkali-feldspar grains in the early syenite units S1 and S4 of Ras ed Dom (plate 4.14.-C). Compositions in the oligoclase-andesine range were obtained by the Michel-Levy method. It is believed that they record an early two-feldspar stage in a syeno-monzonitic magma.

ii. As a sparse phenocryst phase in the hedenbergite-biotite syenite dykes of Centre 7, Ras ed Dom. The grains are usually sericitised and are too few in number to permit compositional determination by optical means. They are however normally zoned and rather narrow twin lamellae suggest fairly sodic compositions. Whether they record a two-feldspar stage, as in (i) above, or are xenocrystic is difficult to assess on such sparse evidence.

4.7.E. : Pseudomorphs after Magnesian Olivine

In contrast to the iddingsitic replacements of fayalite of the early and transitional syenites (sections 4.3.C., and 4.4.C.) olivines of a more magnesian nature are indicated by complex corona structures found in S4 (RED , plate 4.14-A+B). The commonest type is a triple structure, comprising from core to rim, greenish bowlingite, colourless to pale green actinolite and yellowish biotite. The coronas indicate marked disequilibrium between xenocryst and host melt, and basic precursors, either plutonic or volcanic, are the probable source of the olivine.

4.7.F. : Xenoliths and Hybrid Rocks

Xenoliths are of rather sparse occurrence in Ras ed Dom (but see section 2.2.F), but are very common in Abu Dom (fig. 2.11). The term hybrid rock is applied to those instances where net-veining and partial assimilation of an earlier rock by a later unit have resulted in a xenolith-rich rock. Apart from basement xenoliths, and olivine xenocrysts (previous section), the xenoliths range from early syenite to alkali granite compositions, i.e. the range of variation found in the complexes as a whole. In most instances partial digestion of the xenolith, in the form of a fine-grained enclosing 'skin' or corona (plate 4.15), has occurred. The three most important occurrences are as follows:-

a. The xenolith-rich layers of loc. 933 and R8 in S7, RED (section 2.2.F and fig. 2.6).

b. Early syenite xenoliths in the younger rocks adjacent to the Guna outcrop of S1,AD (section 2.3.G-H and fig. 2.11).

c. The hybrid zone (up to 50m broad in places) where G2 intrudes S3, in N.E. Abu Dom (section 2.3.1 and fig. 2.11)

In these instances a concentric zonation, with some or all of the ensuing features, is present about the xenolith (plate 4.15). The core is usually composed of large (5mm-2cm) subhedral tabular or resorbed grains of alkali-feldspar. Where the xenolith is of early syenite type non-turbid orthoclase, hedenbergite and pseudomorphs after early amphibole (biotite + ferrowinchite + Fe-Ti oxide) are found. Alkali xenoliths consist of perthite and haematised mafic clusters. Overgrowths of perthite on the core interdigitate with the groundmass perthite of the digestion zone.

A fine-grained digestion zone, composed of perthite and sodic pyriboles, envelops the core area (plate 4.15), and in it grain size and quartz content typically increase outwards. Orbs (up to 1mm in radius) consisting of radiating perthite and sodic pyriboles may be present. Whether these represent small digested xenoliths or merely record conditions of rapid crystallisation is not always clear.

The digestion zône is separated from the enclosing syenite or granite by a sharp boundary, and the host-rock feldspars commonly show columnar impingement upon the xenolith (plate 4.15).

Evidently digestion was of limited efficacy in these magmas. Moreover the paucity of basic xenoliths suggests that basic magma was never voluminous, and that the early syenites may approximate closely in composition to the parental magma.

4.7.G. : Occurrences of Aenigmatite

Accessory aenigmatite occurs in two intrusions in Ras ed Dom complex, as follows:-

a. In the chilled 'transitional syenite' margin to S3 (fig. 2.3 and section 4.3.C.). Ferrorichterite forms poikilitic grains enclosing earlier pyroxene and feldspar, and its place is taken locally by aenigmatite.

b. At loc. 204 in the alkali syenite, S5 (fig. 2.4). Aenigmatite forms largish (av. 1mm) slightly elongate or rounded grains, partly enclosed by or interstitial to perthite (plate 4.7-B). The mineral is traversed by cracks which are occupied by a yellowish material, riebeckite and aegirine. The yellow material is finely crystalline, pleochroic and somewhat micaceous in appearance. The aenigmatite is strongly pleochroic from brown-red to opaque (plate 4.7.-A). It is enclosed in sodic amphibole (arfvedsonite-riebeckite), which in turn is prone to replacement by a mosaic aggregate of aegirine (plate 4.7-B).

Aenigmatite co-exists with ferrorichterite in S3, and predates arfvedsonite in S5. This suggests that like ferrorichterite (section 4.7.A) the mineral appears at the transition from a plumasitic order of crystallisation to an agpaitic order (fig. 4.3).

Plate 4.1. (opposite) : Principal rock-types of Ras ed Dom and Abu Dom.

A - Partly recrystallised eutaxitic foliation in ignimbrite, loc. D597, Abu Dom Volcanic Group. PPL, x 30.

B - Strongly zoned plagioclase laths (e.g. upper left) in the dolerite dyke, loc. D183, Abu Dom. Interstitial pyroxene has been replaced by ferrowinchite (?) and biotite. Both large primary Fe-Ti oxide grains and smaller ragged secondary growths are distinguishable. CN, x 30.

C - Biotite and Fe-Ti oxide in a mealuminous hedenbergite-biotite syenite dyke rock. The feldspar phenocryst is composed of clear cryptoperthite. Loc. D172, Centre 7, Ras ed Dom. PPL, x 30.

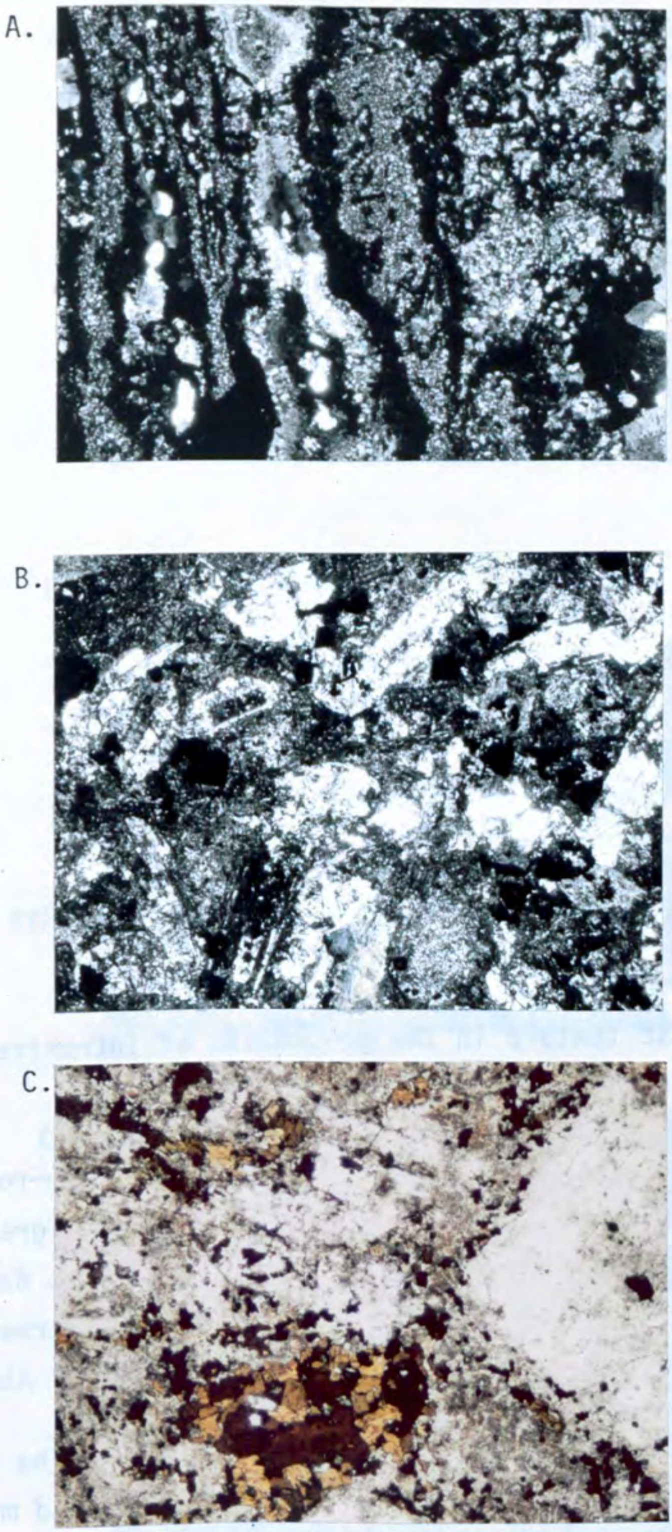

Plate 4.1. : Principal rock-types of Ras ed Dom and Abu Dom, (explanation opposite).

Plate 4.2. (opposite) : Principal rock-types of Ras ed Dom and Abu Dom, continued.

A - Trachytic texture in the groundmass of intrusive trachyte 3, D167, Centre 7 Ras ed Dom. CN, x 75.

B - Typical view of quartz-feldspar porphyry dyke-rock. The phenocrysts show varying degrees of resorbtion. Complex granophryic intergrowths are also visible. The felsitic groundmass is densely crowded with flow-oriented acicular alkali-pyriboles, not readily discernable at this magnification. D1121, cone-sheet N.W. of Abu Dom. CN, x 30.

C - Typical view of porphyritic early syenite. The feldspar phenocrysts contain patches of clear orthoclase and turbid microperthite. The groundmass feldspars are ubiquitously perthitic. The dark interstitial areas consist of secondary ferrowinchite and Fe-Ti oxide. D685, Milega outcrop of Syenite 1, Abu Dom. CN, x 30.

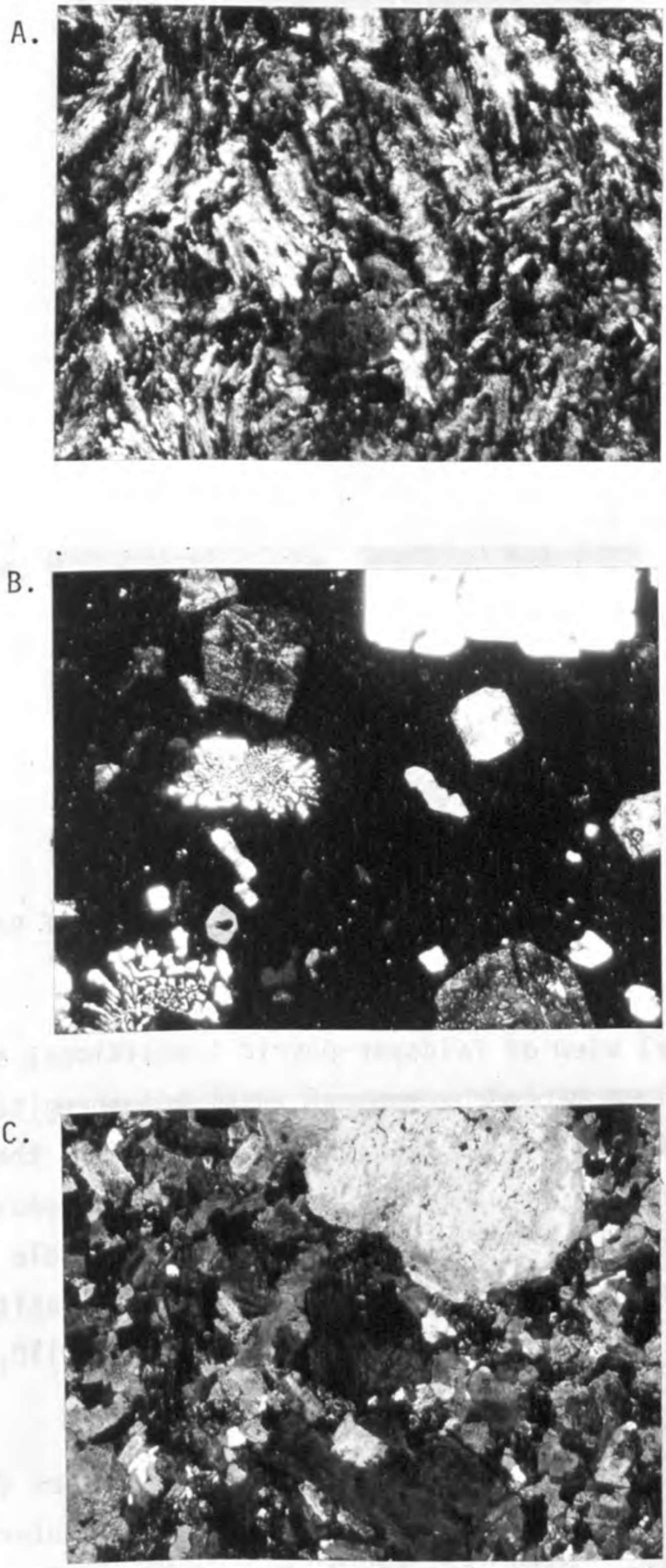

Plate 4.2. : Principal rock-types of Ras ed Dom and Abu Dom, continued (explanation opposite).

Plate 4.3. (opposite) : Principal rock-types of Ras ed Dom and Abu Dom, continued.

A - Typical view of feldspar-phyric transitional syenite. Anhedral zonation, marked by rows of small hedenbergite inclusions, testifies to the complex growth history of these feldspar grains. The orthoclase cores are clear and homogeneous, whilst the rims and interstitial grains are turbid fine-scale perthites. Hedenbergite (H), Fe-Ti oxide (FTO) and apatite (A) occur enclosed within poikilitic ferrorichterite (FR). D110, southern part of Syenite 2, Ras ed Dom. PPL, x 30.

B - Typical view of alkali syenite. The tabular feldspar grains are densely turbid microperthites. The dark interstitial grains are aegirine. D417, Syenite 7, Ras ed Dom. CN, x 30.

C - Typical view of alkali-granite. The feldspars are coarsely exsolved, many being antiperthitic. Discrete albite laths are visible in places. The interstitial mafic minerals consist of aegirine and arfvedsonite, but are not readily distinguishable in this view. Quartz shows up as clear, bright grains. D145, Granite 1, Ras ed Dom. CN, x 30.

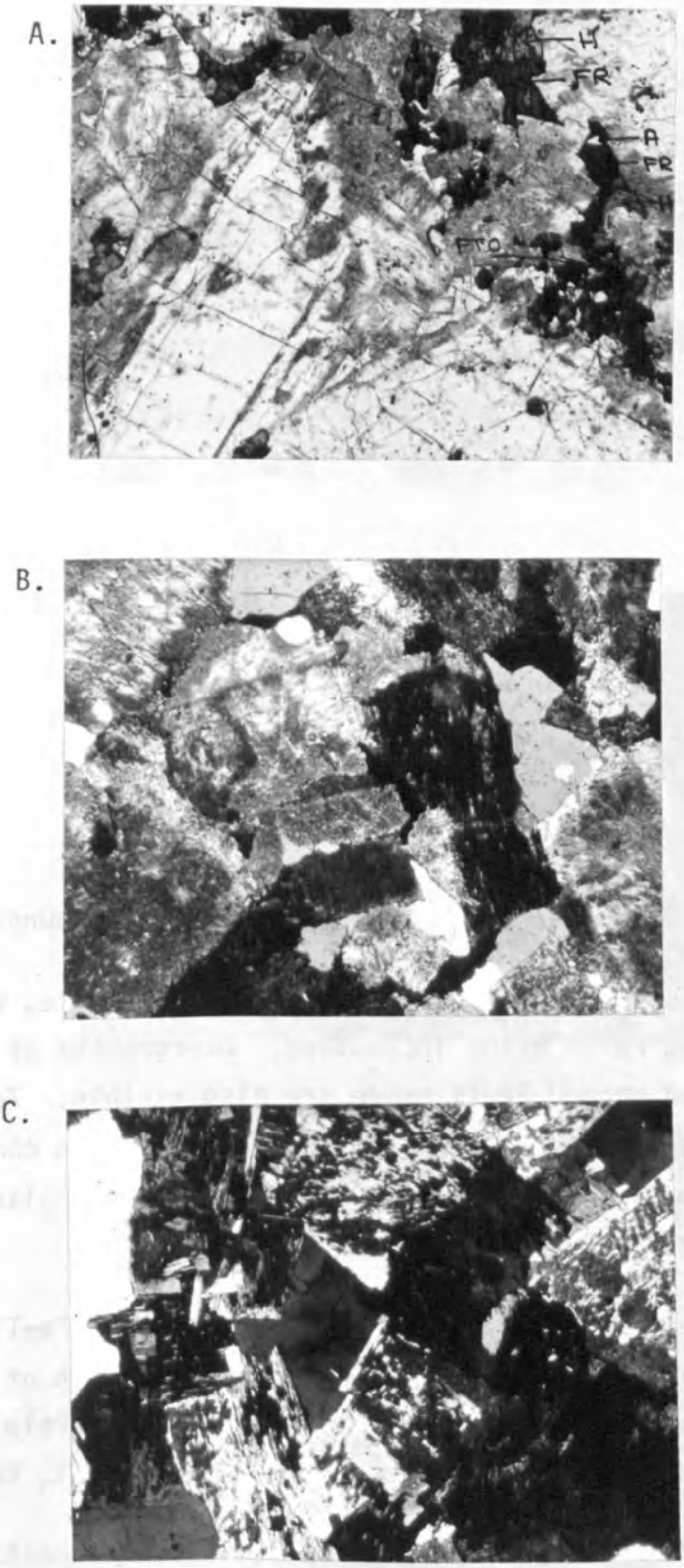

Plate 4.3. : Principal rock-types of Ras ed Dom and Abu Dom, continued (explanation opposite).

Plate 4.4. (opposite) : Amphiboles of the Younger Granite rocks.

A - Rounded grains of pale-brown ferroedenite, with numerous apatite and Fe-Ti oxide inclusions. Overgrowths of pale-green ferrowinchite and ragged Fe-Ti oxide are also visible. Turbid alkali-feldspar is easily distinguishable. The light areas comprise calcite (bottom left) and quartz, both crowded with acicular ferrowinchite. D1014, Syenite 1, Ras ed Dom. PPL, x 75.

B - Ferroedenite enclosing large grains of Fe-Ti oxide. The latter have ragged edges in places due to overgrowth of secondary oxide. Apatite inclusions are also visible. A large grain of pale green ferrowinchite is present (top left). D1014, Syenite 1, Ras ed Dom. PPL, x 75.

c - Green poikilitic ferrorichterite in transitional syenite. The feldspars are turbid microperthite (grey), but albitisation (colourless areas) is extensive. D275, chilled margin to Syenite 3, Ras ed Dom. PPL, x 75.

A.

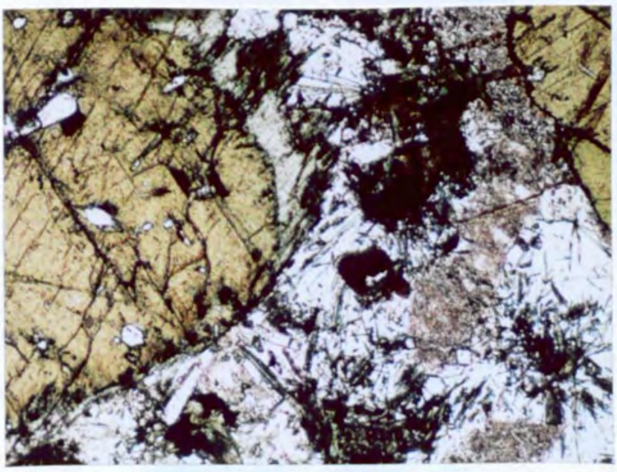

B.

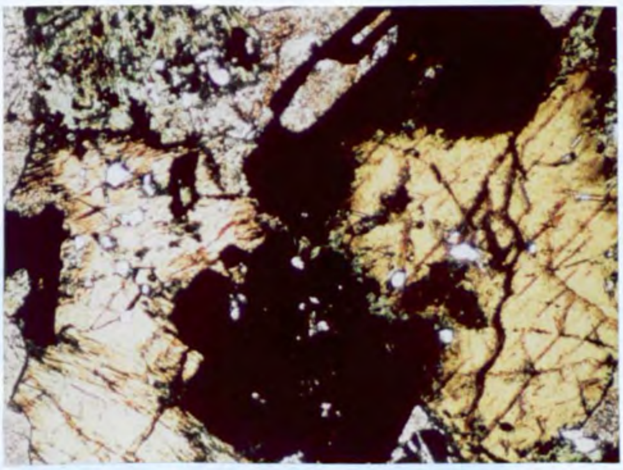

C.

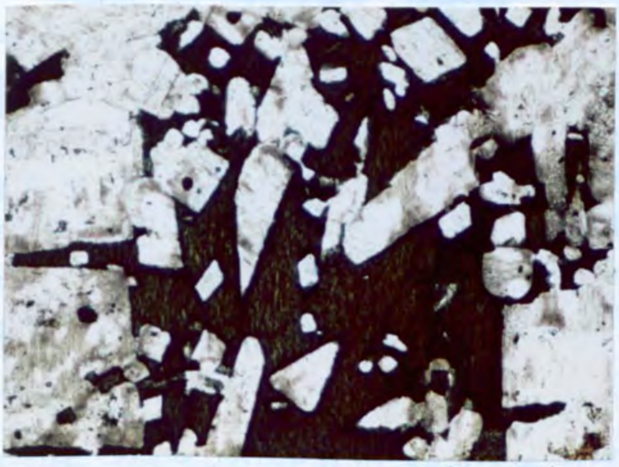

Plate 4.4. : Amphiboles of the Younger Granite rocks (explanation opposite).

Plate 4.5. (opposite) : Amphiboles of the Younger Granite rocks, continued.

A - Interstitial sodic amphibole. The paler green core is ferrorichterite which is continuously zoned outwards to darker green arfvedsonite. Close examination reveals a further overgrowth of blue riebeckite (see also B below). D1057, interior facies of Syenite 3, Ras ed Dom. PPL, x 75.

B - The same grain as in A above, under crossed nicols. The continuous nature of the zoning is now apparent, as is the riebeckite overgrowth. CN, x 75.

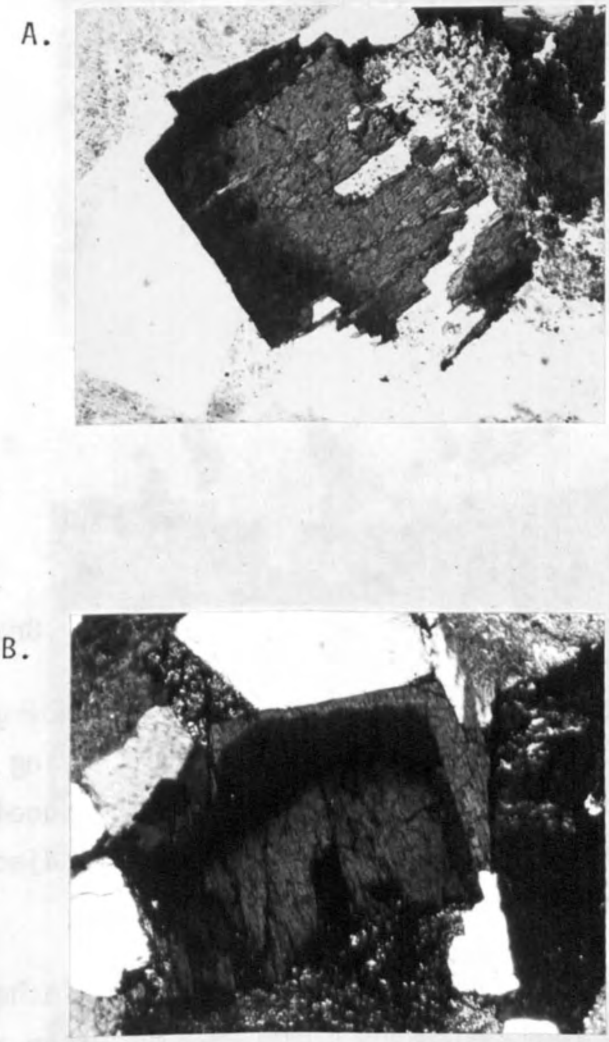

Plate 4.5. : Amphiboles of the Younger Granite rocks, continued (explanation opposite).

Plate 4.6. (opposite) : Pyroxenes of the Younger Granite rocks.

A - Two large grains of faintly green ferrohedenbergite, with numerous apatite and Fe-Ti oxide inclusions. Shattering of some of the apatites during section preparation has produced the low relief gaps visible in places. D596B, Syenite 1, adjacent to the Abu Dom Volcanic Group, Abu Dom. PPL, x 75.

B - Large prismatic grain of aegirine. The grain has a grass green core and is zoned outwards through paler green zones, to colourless acmitic rims. The aegirine is replacive towards arfvedsonite (not visible), and encloses perthite towards which it is also patchily replacive (bottom right). Despite its euhedral shape, the grain is thought to be of late, sub-solidus origin. D781, Granite 1, Abu Dom. PPL, x 75.

C - Small aegirine grains with pointed acmitic terminations, in quartz. Minute grains of aegirine (arrowed) are also visible overgrowing perthite (top margin). The aegirine grain along the bottom margin is the same as that shown in B above. D781, Granite 1, Abu Dom. PPL, x 75.

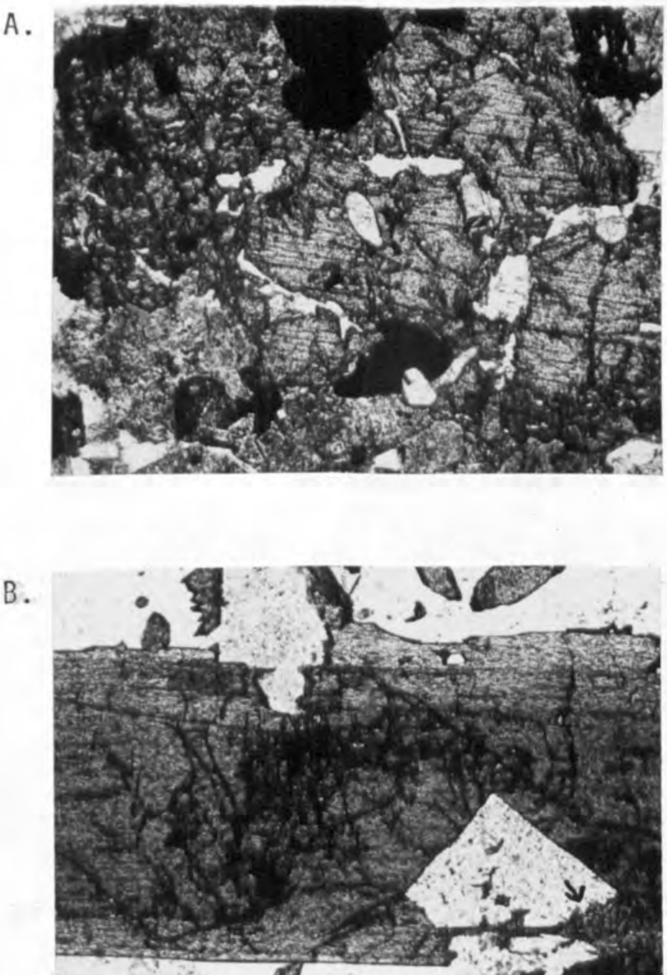

Plate 4.6. : Pyroxenes of the Younger Granite rocks (explanation opposite).

Plate 4.7. (opposite) : Aenigmatite and zircon in the Younger Granite rocks.

A - Large grain of blood-red aenigmatite, rimmed by grains of aegirine. The dark cracks in the aenigmatite are occupied by a secondary alteration product (see text). D204, Syenite 5, Ras ed Dom. CN x 30.

B - Large grain of aenigmatite (dark), traversed by numerous cracks, and enclosed in a mosaic intergrowth of arfvedsonite and aegirine (dark grey). Alkali-feldspar (light grey) and quartz are also discernable. D204, Syenite 5, Ras ed Dom. PPL, x 30.

C - Interstitial cluster of zircon grains, associated with aegirine (upper left). D247, Granite 1, Ras ed Dom. PPL, x 75.

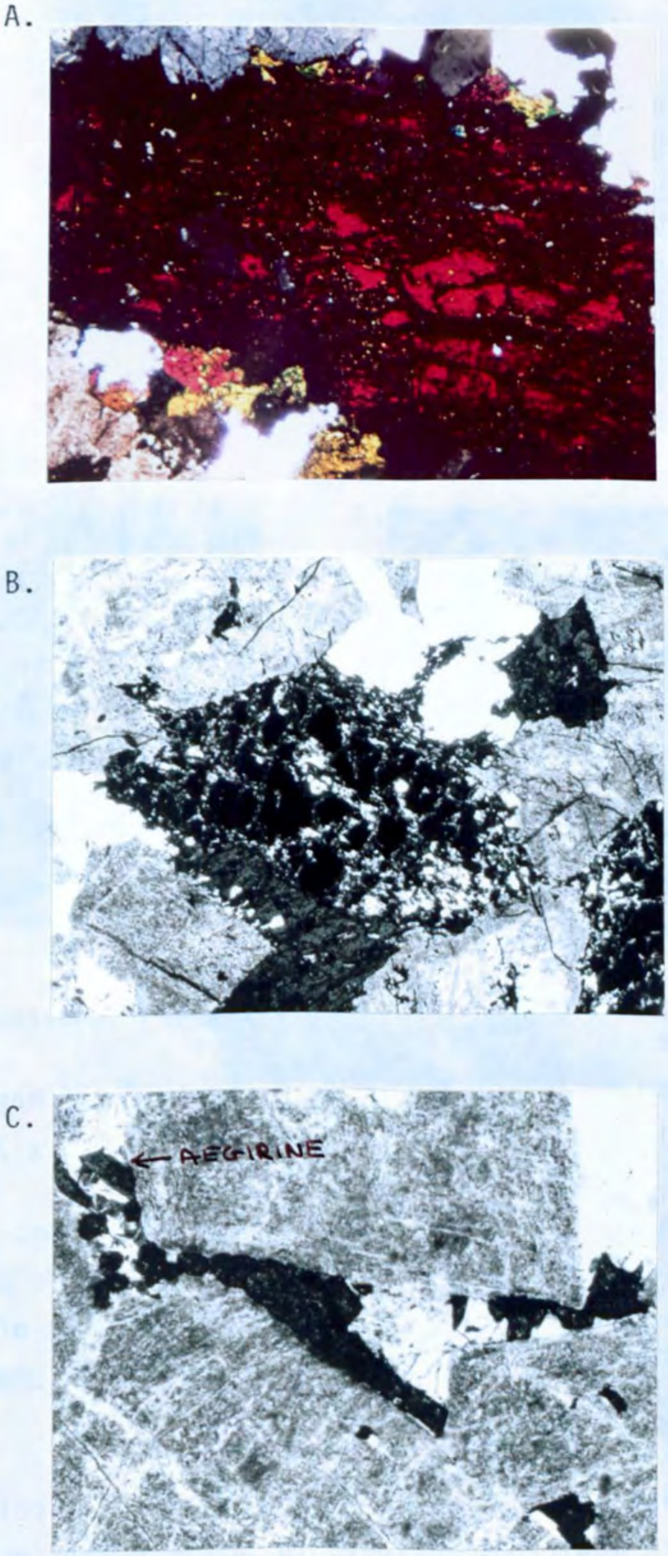

Plate 4.7. : Aenigmatite and zircon in the Younger Granite rocks.

Plate 4.8. (opposite) : Vein assemblages and textures.

A - Microcline perthites together with quartz and aegirine (dark prisms). Vein at loc. D603 in Syenite 2, Abu Dom. CN, x 75.

B - Small-scale metasomatism of the basement gneiss. The gneiss consists of turbid perthite and biotite (right-hand side of view). The replacive assemblage (left-hand side) consists of granophyric intergrowths and arfvedsonite (darker patches). D1005, Meriab basement block, Centre 1, Ras ed Dom. CN, x 30.

C - Pegmatitic patch in alkali syenite. The dark prismatic and acicular grains are aegirine, enclosed in larger grains of quartz and calcite. D175, Syenite 13, Centre 7, Ras ed Dom. CN, x 100.

D - Vein of aegirine-augite, with subordinate quartz and Fe-Ti oxide. Feldspar grains belonging to the host syenite are visible to the left and right. D129, Syenite 2, Ras ed Dom. CN, x 30.

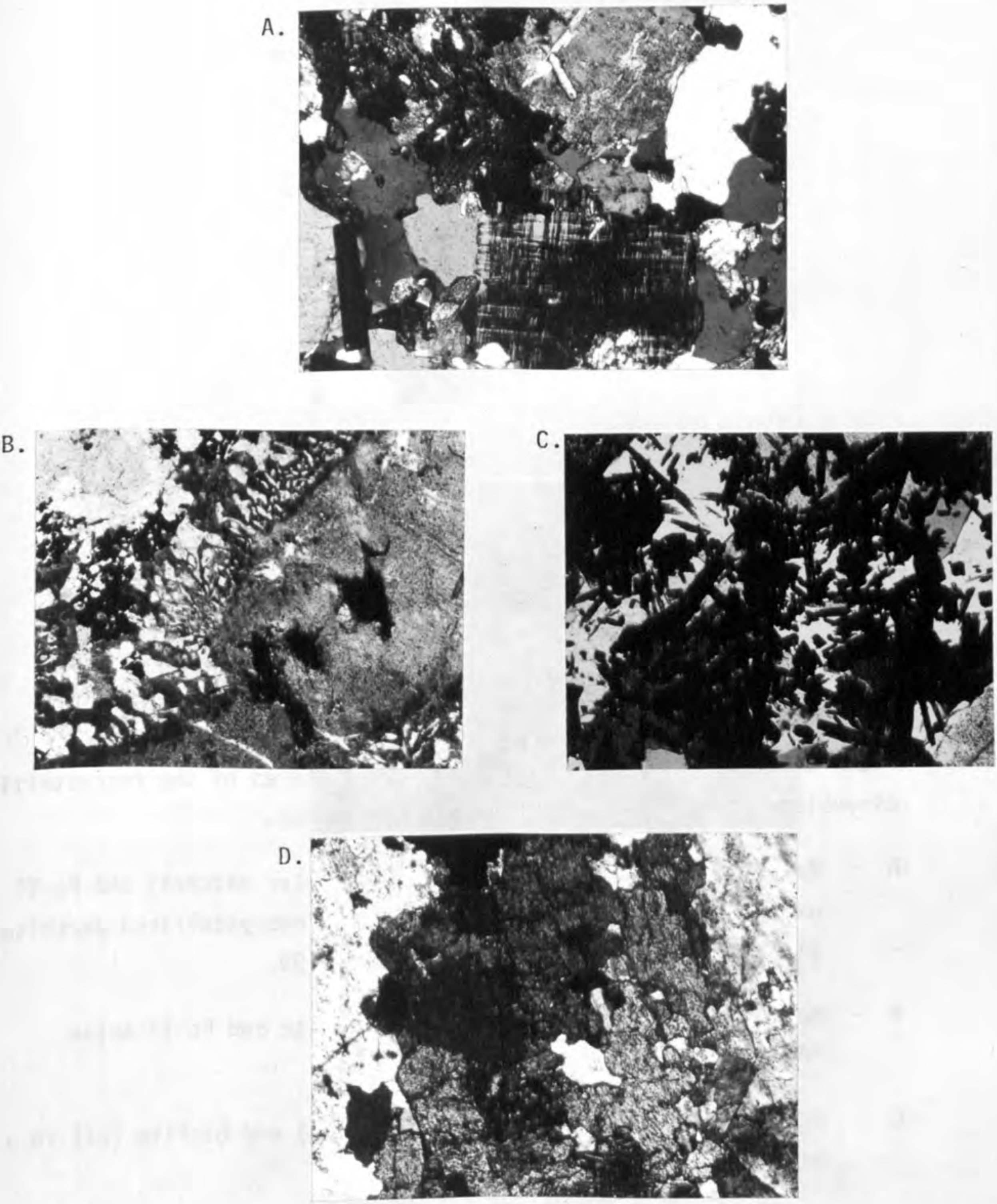

Plate 4.8. : Vein assemblages and textures (explanation opposite).

Plate 4.9. (opposite) : Mineralogy and textures of the recrystallised assemblage at loc. D433, Syenite 13, Ras ed Dom.

A - Mafic clusters of aegirine-augite (lighter patches) and Fe-Ti oxide (dark), interdigitating with the recrystallised perthite (light grey) grain boundaries. PPL, x 30.

B - Mafic clusters of aegirine-augite, annite and Fe-Ti oxide. PPL, x 30.

C - Arfvedsonite (ARF), aegirine-augite (AA) and biotite (BI) in a mafic cluster. PPL, x 75.

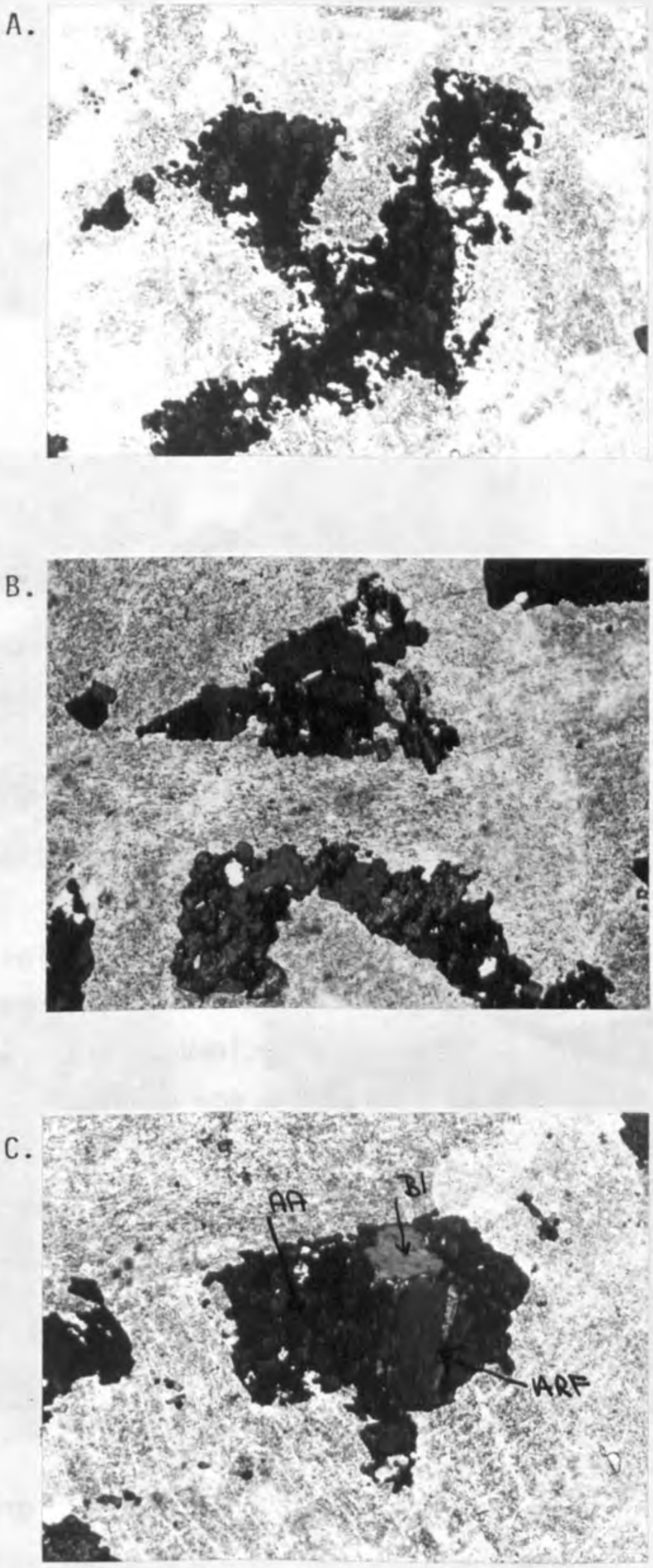

Plate 4.9. : Mineralogy and textures of the recrystallised assemblage at loc. 433, Syenite 13, Ras ed Dom (explanation opposite).

Plate 4.10. (opposite) : Turbidity and exsolution features in the alkali-feldspars.

A - Tabular grains of clear, homogeneous alkali-feldspar with turbid rims, from an early syenite sample. Inwards encroachment of turbidity is visible along the cleavage and cracks. Towards the right-hand margin an enclosure, now pseudomorphed, of early formed mafic minerals is visible. The dark interstitial wedge above the feldspar grain consists of later alkali amphibole. R31, Syenite II Ras ed Dom. PPL, x 30.

B - Perthite grain in alkali syenite sample. Exsolution lamellae coarsen outwards towards the grain margin. Interstitial quartz is present, bottom left. D378, Syenite 7, Ras ed Dom. CN, x 75.

C - Coarse 'tiger-skin' plume perthite in alkali granite. D278, Granite 1, Ras ed Dom. CN, x 75.

D - Large antiperthitic feldspar phenocryst, exhibiting coarsely exsolved 'chess-board' albite. D423, alkali syenite dyke intruding Syenite 7, Ras ed Dom. CN, x 75.

E - Turbid, finely perthitic feldspars in alkali syenite. D1077, northern part of Syenite 2, Ras ed Dom. CN, x 30.

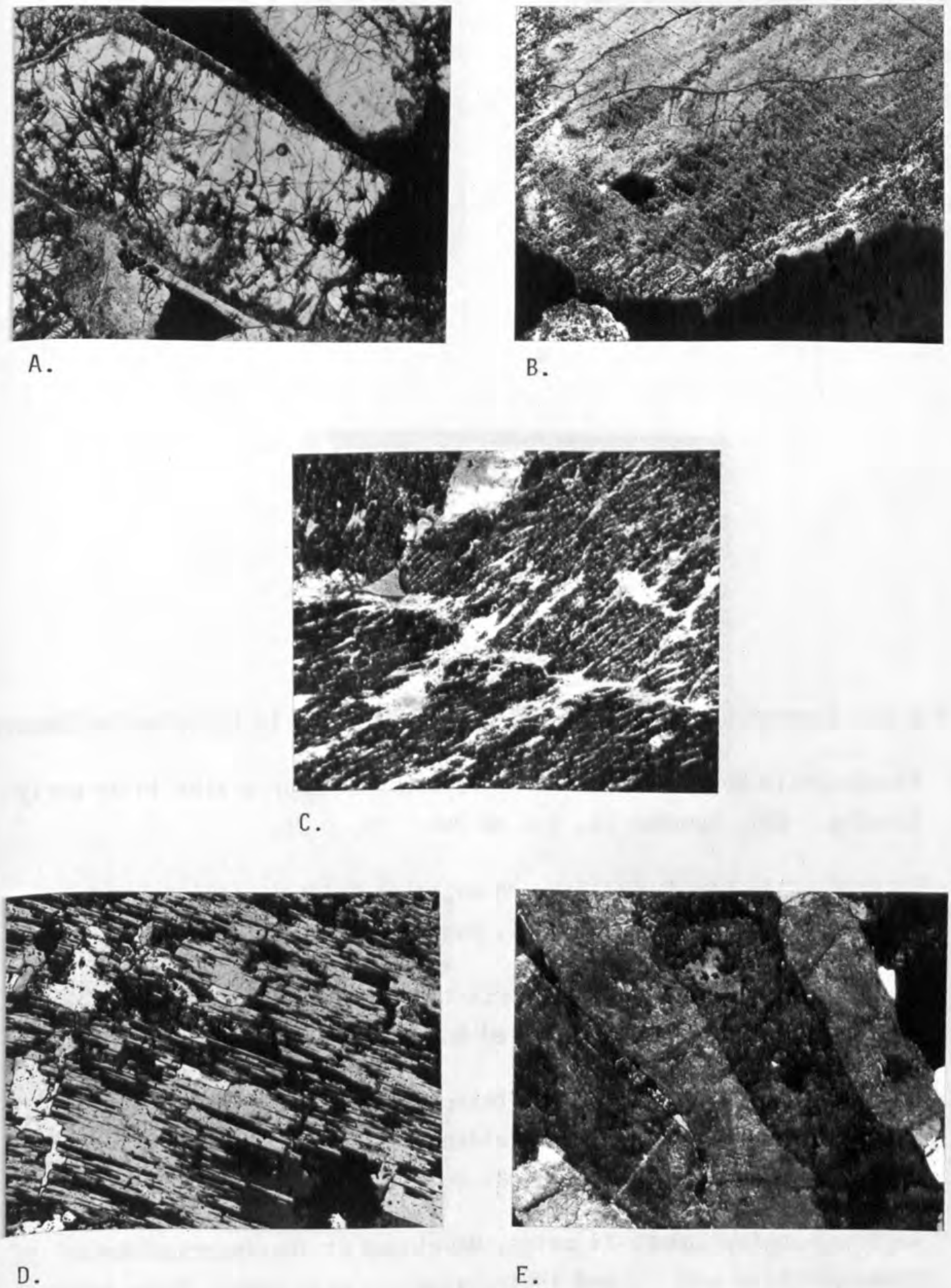

Plate 4.10 : Turbidity and exsolution features in the alkali-feldspars (explanation opposite).

Plate 4.11. (opposite) : Recrystallisation features in the alkali-feldspars.

A - Simple grain boundaries between adjacent feldspar grains in an early syenite. R31, Syenite II, Ras ed Dom. CN, x 75.

B - Sutured grain boundaries between adjacent feldspar grains in an early syenite. R31, Syenite II, Ras ed Dom. CN, x 75.

C - Swapped rims developed along perthite-perthite boundaries in alkali syenite. D966, Syenite 7, Ras ed Dom. CN, 75.

D - Small recrystallised, interdigitating perthite grains, developed at the expense of larger primary feldspars (see E below). Recrystallised assemblage, D433, Syenite 13, Ras ed Dom. CN, x 75.

E - Aegirine-augite and Fe-Ti oxide, developed at the intersection of three perthite grains, and interdigitating with them. Under crossed nicols (see D above) the feldspar grains are seen to consist of numerous recrystallised domains. Recrystallised assemblage, D433, Ras ed Dom. PPL, x 75.

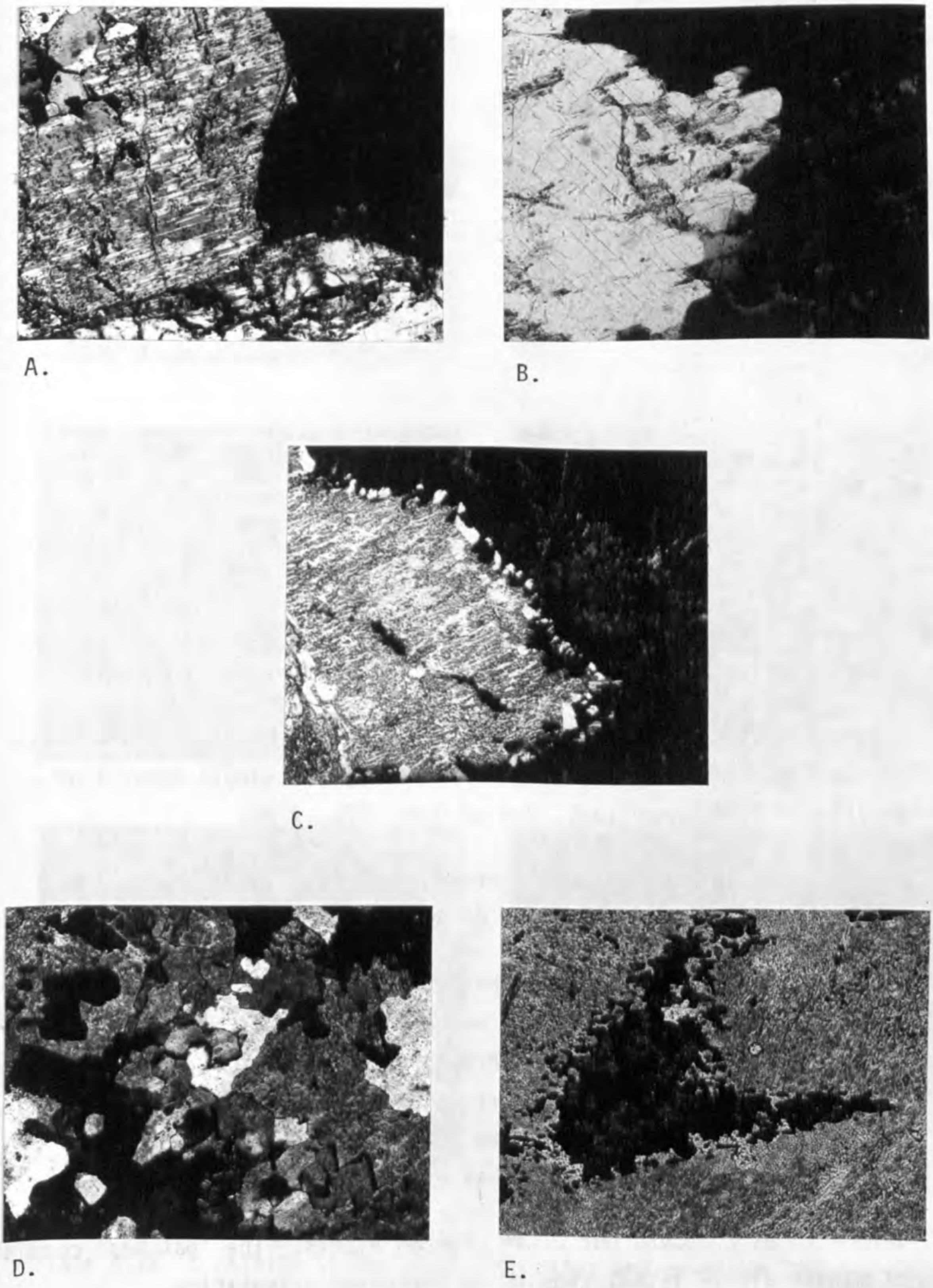

Plate 4.11 : Recrystallisation features in the alkali-feldspars (explanation opposite).

Plate 4.12 (opposite) : Albite in the alkali syenites and granites.

A - 'Channels' of colourless, late albite developed along perthite grain boundaries. The small dark inclusions in the channels consist of aegirine. D278, Granite 1, Ras ed Dom. PPL, x 30.

B - Same view as in A above, under crossed nicols. The 'channels' are seen to consist of minute laths of albite.

C - 'Patch' type albitisation. Although minor 'channels' albite is present, the bulk of the albite occurs as irregular, colourless patches, randomly distributed throughout two large perthite grains. Small, dark inclusions in the patches consist of aegirine. This type is considered to represent a more advanced stage of albitisation than A above. D447, Granite 1 Ras ed Dom. PPL, x 30.

D - Same view as C above, but under crossed nicols. The 'patches' consist of minute albite laths, showing no preferred orientation.

E - Overgrowth of late albite, upon an earlier grain of perthite, suggesting free growth into a cavity. The narrower growth of albite (top right) may be of simple exsolution origin. The enclosing cavity infill is calcite. D340, Syenite 7, Ras ed Dom. CN, x 75.

F - Late albite infilling cavity between perthite grains in alkali syenite. The large dark grain (bottom left) is aegirine. A small acicular prism of aegirine is also present, enclosed in the lower part of the albite grain. D340, Syenite 7, Ras ed Dom. CN, x 75.

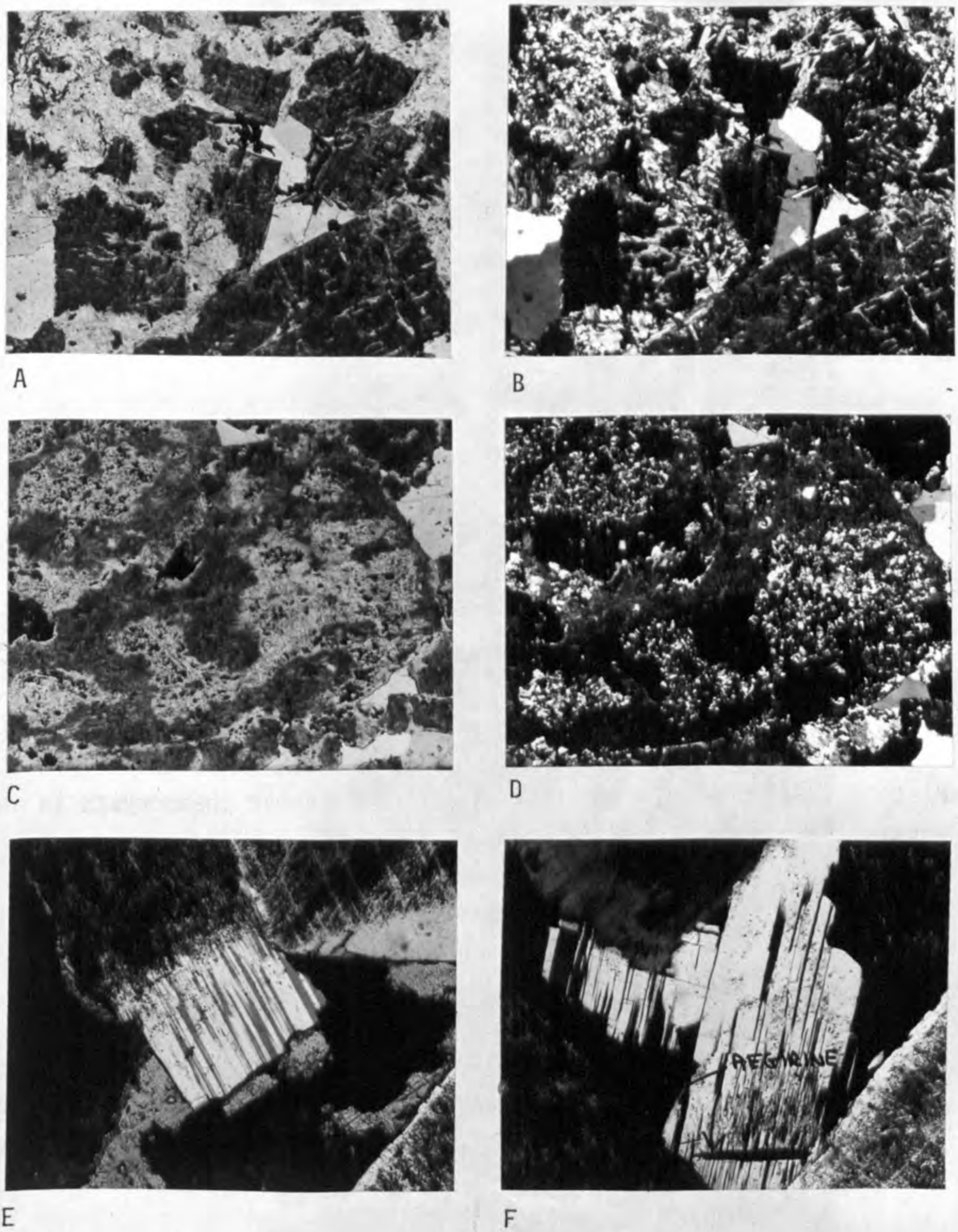

Plate 4.12 : Albite in the alkali syenites and granites (explanation opposite).

Plate 4.13 (opposite) : Albitisation of feldspar phenocrysts in an alkali syenite dyke rock.

A - Advanced alibitisation of alkali-feldspar phenocryst. A small core of primary feldspar is present. R14, alkali syenite dyke to the south of Ras ed Dom. PPL, x 30.

B - Same view as in A above, under crossed nicols. The remnant core is surrounded by radially disposed albite laths. A second phenocryst (left of centre) exhibits 'patch' albitisation characterised by smaller albite laths.

c - Detail of B above. CN, x 75.

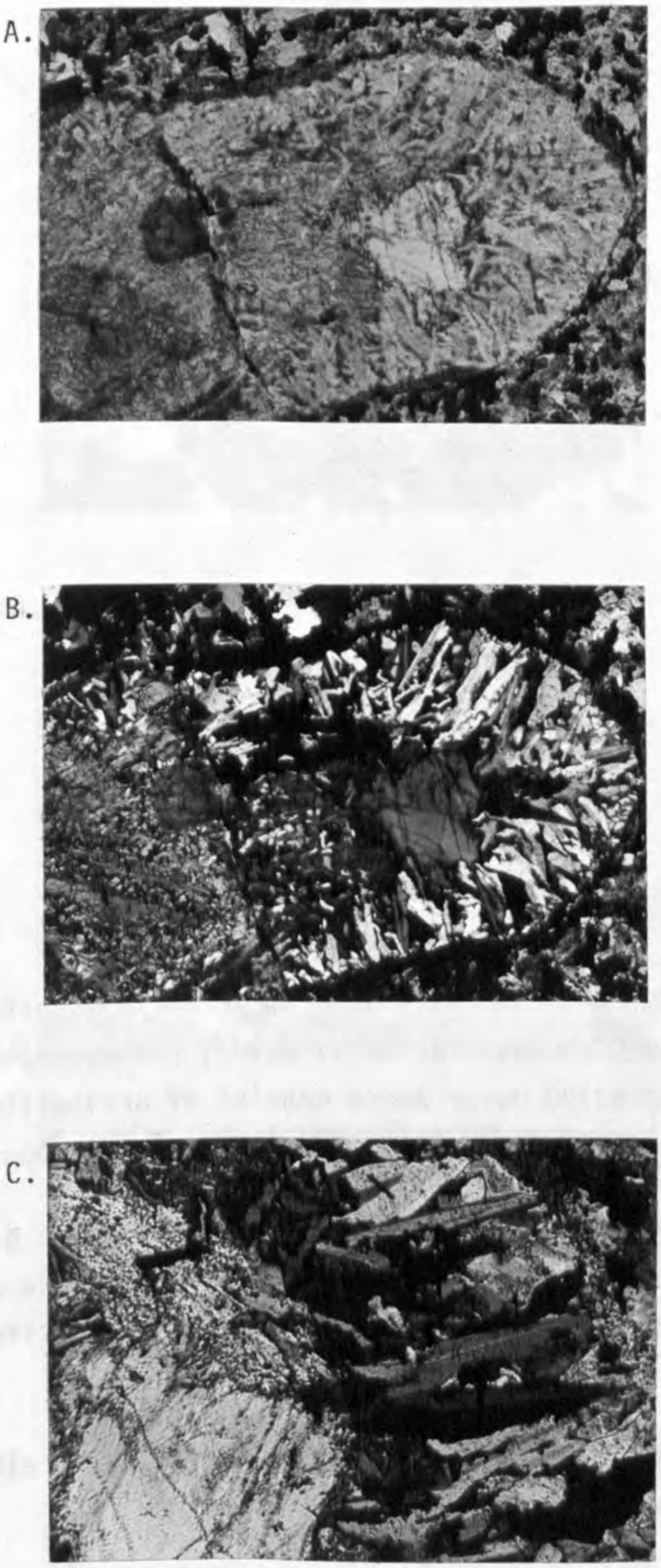

Plate 4.13 : Albitisation of feldspar phenocrysts in an alkali syenite dyke rock (explanation opposite).

Plate 4.14 (opposite) : Relict features in the early syenites.

A - Complex corona structure in an early syenite. The core is mainly composed of Fe-Ti oxide, pseudomorphing magnesian olivine (?) Successive outer zones consist of actinolite, biotite, and biotite + Fe-Ti oxide. D914, Syenite 4, Ras ed Dom. PPL, x 30.

B - Corona structure pseudomorphing magnesian olivine (?) in early syenite. The core consists of Fe-Ti oxide and green bowlingite. Successive outer zones consist of actinolite and biotite. D285A, Syenite 4, Ras ed Dom. PPL, x 30.

C - Plagioclase (oligoclase) core to alkali feldspar grain. D914, Syenite 4, Ras ed Dom. CN, x 75.

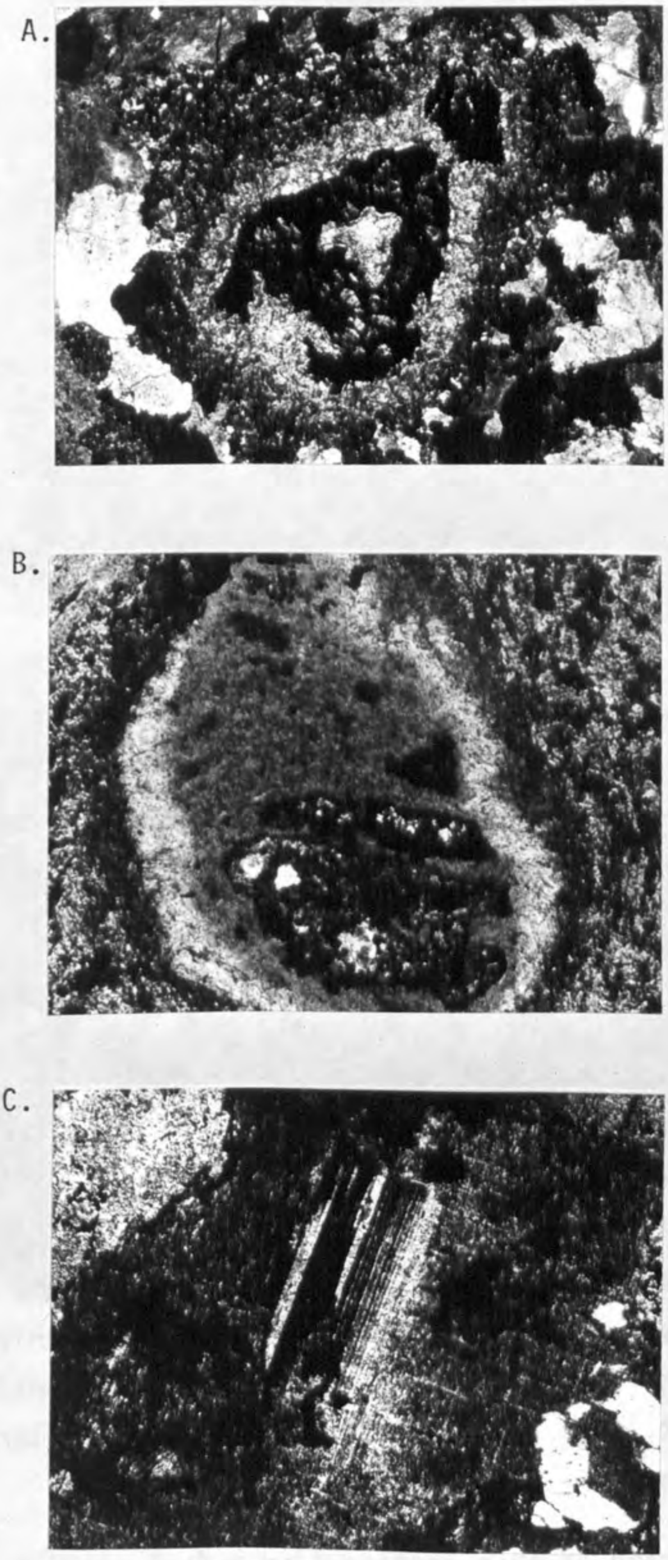

Plate 4.14 : Relict features in the early syenites (explanation opposite).

Plate 4.15 (opposite) : Xenolith partial digestion textures.

A - Photograph of thin-section (7cm x 4cm) showing xenoliths of early syenite in alkali syenite host rock. The xenoliths consist of large grains of orthoclase, which are patchily turbid and variably resorbed, and mafic clots. The latter are now pseudormorphed by annite and sodic amphibole. The xenoliths are enclosed in digestion zones of chilled, alkali syenite in which smaller xenocrysts are discernable. Although of essentially the same composition as the host syenite, the digestion zone commonly exhibits a sharp contact with the host rock. Slivers of the latter interdigitate between the xenoliths and are slightly pegmatitic, with large prisms of aegirine in them. D933, Syenite 7, Ras ed Dom.

B - Photograph of thin-section (7cm x 4cm) showing xenoliths of early syenite in alkali syenite host rock. The textural features are much as in A above, but the boundary between the digestion zone and the host syenite is less sharp. The minerals in the host rock often impinge on the digestion zone in columnar fashion. D767B, Syenite 3, Abu Dom.

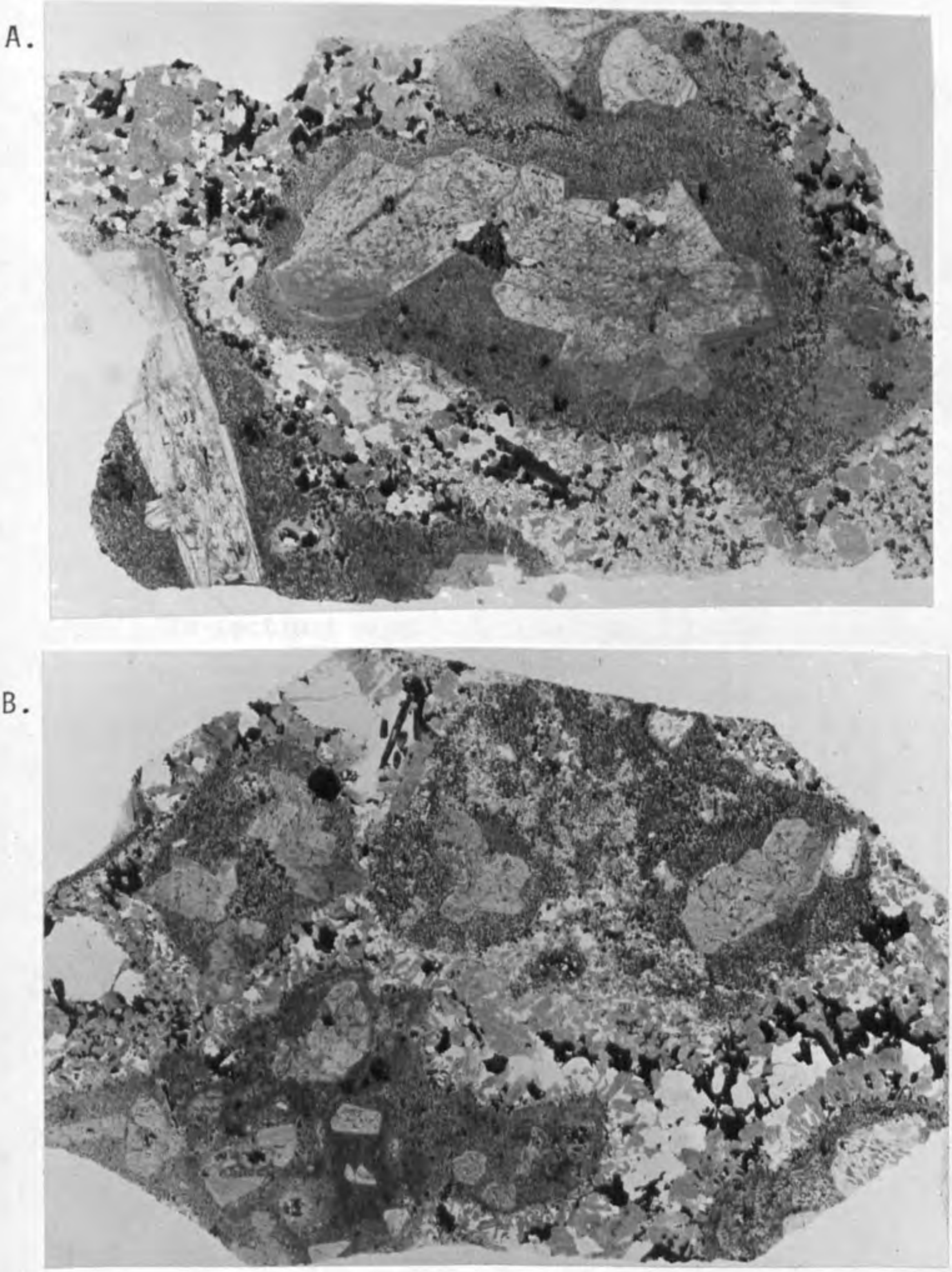

Plate 4.15 : Xenolith partial digestion textures (explanation opposite).

CHAPTER 5 : MINERAL CHEMISTRY

5.1. : Introduction

In this chapter mineral analyses for feldspars, pyroxenes and amphiboles are reported and the cryptic variation displayed by these phases is discussed. The amphibole partial analyses are especially useful as sodic amphiboles are difficult to identify precisely by optical methods, due to their strong dispersion (Ernst, 1962; Borley, 1963; Borg, 1967). Analyses of biotite, aenigmatite and Fe-Ti oxides are also presented.

Ten polished thin-sections were analysed using the elctron microprobe in the department of mineralogy and petrology, Cambridge University (further details are given in Appendix IIA). The rocks are representative of the mineral variation present in the suite. Six of the samples come from CentreI, Ras ed Dom and provide coverage of the four main rock types described in Chapter 4(table 5.I). The four other samples are as follows. D916 is an early syenite from S4, RED. D204 was chosen as it is aenigmatite-bearing. D433 represents a recrystallised assemblage including minor late biotite. D183A is a sample of the dolerite dyke from Abu Dom Complex.

Optical properties of the various mineral phases, where determined, are given in Appendix I.

SAMPLE	UNIT	COMPLEX	COMMENTS
D1014	S1	Ras ed Dom	Early syenite.
D110	S2	Ras ed Dom	Transitional syenite, southern part of S2.
D275	S3	Ras ed Dom	Transitional syenite, chilled margin of S3.
D1057	S3	Ras ed Dom	Alkali syenite, interior of S3.
D145	G1	Ras ed Dom	Alkali granite.
D447	G1	Ras ed Dom	Alkali granite, marginal facies.
D916	S4	Ras ed Dom	Early syenite.
D204	S5	Ras ed Dom	Alkali syenite, aenigmatite-bearing facies.
D433	S13	Ras ed Dom	Alkali syenite, recrystallised.
D183	Dyke in S3	Abu Dom	Basic dyke.

Table 5.1. : Samples Used in Microprobe Analysis.
For sample localities see Maps 4 and 5, rear pocket.

5.2. : Feldspars

5.2.A. : Alkali-feldspars

As microprobe analysis is not ideally suited for obtaining bulk compositions from coarse perthite intergrowths, the analytical programme concentrated on the relatively non-turbid and optically homogeneous orthoclases of the early (D1014, D916) and transitional syenites (D110, D275). The clear feldspars of D204 are the only representatives from the alkali lithologies. In all cases several point analyses (from 2-6 depending on the apparent optical homogeneity) per grain were averaged to give the nineteen bulk compositions listed in Appendix IIB, and table 5.2. Integration of several point analyses, based on accumulated counts for each element, would provide a more statistically valid result, and perthites might be analysed by such an approach (Parsons, 1978). However, in view of the limited analytical time available, this was not attempted. The averaged results quoted are considered to be reasonable estimates of bulk composition as they exhibit smooth, continuous variation. Details of zoning are, of course, lost by the averaging method used.

The alkali-feldspar bulk compositions are plotted onto the ternary Ab-Or-An plot in fig. 5.1, each point representing an average composition for one crystal. The compositional variation (cAb75 Or25 to cAb50 Or50) is restricted, a feature typical of hypersolvus suites (Tuttle and Bowen, 1958; Parsons, 1978), and the points cluster about the low-temperature termination of the plagioclase-alkali feldspar field boundary. Anorthite levels decrease from An7 mol% in the early lithologies to zero in the late-formed rocks (table 5.2).

Eight point analyses of albite from D447 (alkali granite, GI, RED) are also presented in Appendix IIB. The albite is distributed in 'patch' fashion throughout the perthite grains (see section 4.7.B), and is almost pure, six of the eight analyses containing over 99% Ab.

5.2.B. : Plagioclase Feldspars

Seven point analyses, from three plagioclase grains in D183A (basic dyke, Abu Dom) are reported in Appendix IIB. The grains are strongly zoned from cores of labradorite to rims of oligoclase-andesine, and tie-lines indicate the compositional range for individual grains in fig. 5.1. The full range encountered is An59-An21, and is comparable to that reported from the basic rocks of Pantelleria (Villari, 1974), the Ethiopian Rift (Bizouard and Di Paola, 1978), the basic volcanics of Ningi-Burra complex, Nigeria (Turner and Bowden, 1979) and the gabbros and syenogabbros of the Klokken complex, Gardar province (Parsons, 1979).

Rock-type	Sample	Grain	n	1 mol.% OR	 AB	 AN	2 mol.% OR	 AB	 AN
Early syenite	D1014	1	3	36	59	5	28	66	6
		2	5	28	67	5			
		3	2	24	70	6			
		4	4	24	69	7			
Early syenite	D916	1	6	57	41	2	50	47	3
		2	2	44	53	3			
Transitional syenite	D110	1	3	30	67	3	36	62	2
		2	4	43	56	1			
		3	4	41	56	3			
		4	3	29	67	4			
Transitional syenite	D275	1	4	36	64	-	34	66	-
		2	3	31	69	-			
		3	4	40	60	-			
		4	2	30	70	-			
		5	2	35	65	-			
Alkali syenite	D204	1	4	35	63	2	42	57	1
		2	4	44	55	1			
		3	4	40	59	1			
		4	5	48	52	-			

Table 5.2. : Average alkali-feldspar bulk compositions for Ras ed Dom.

Column 1 : averages for individual grains; n = number of point analyses on which the average is based.

Column 2 : averages for individual units.

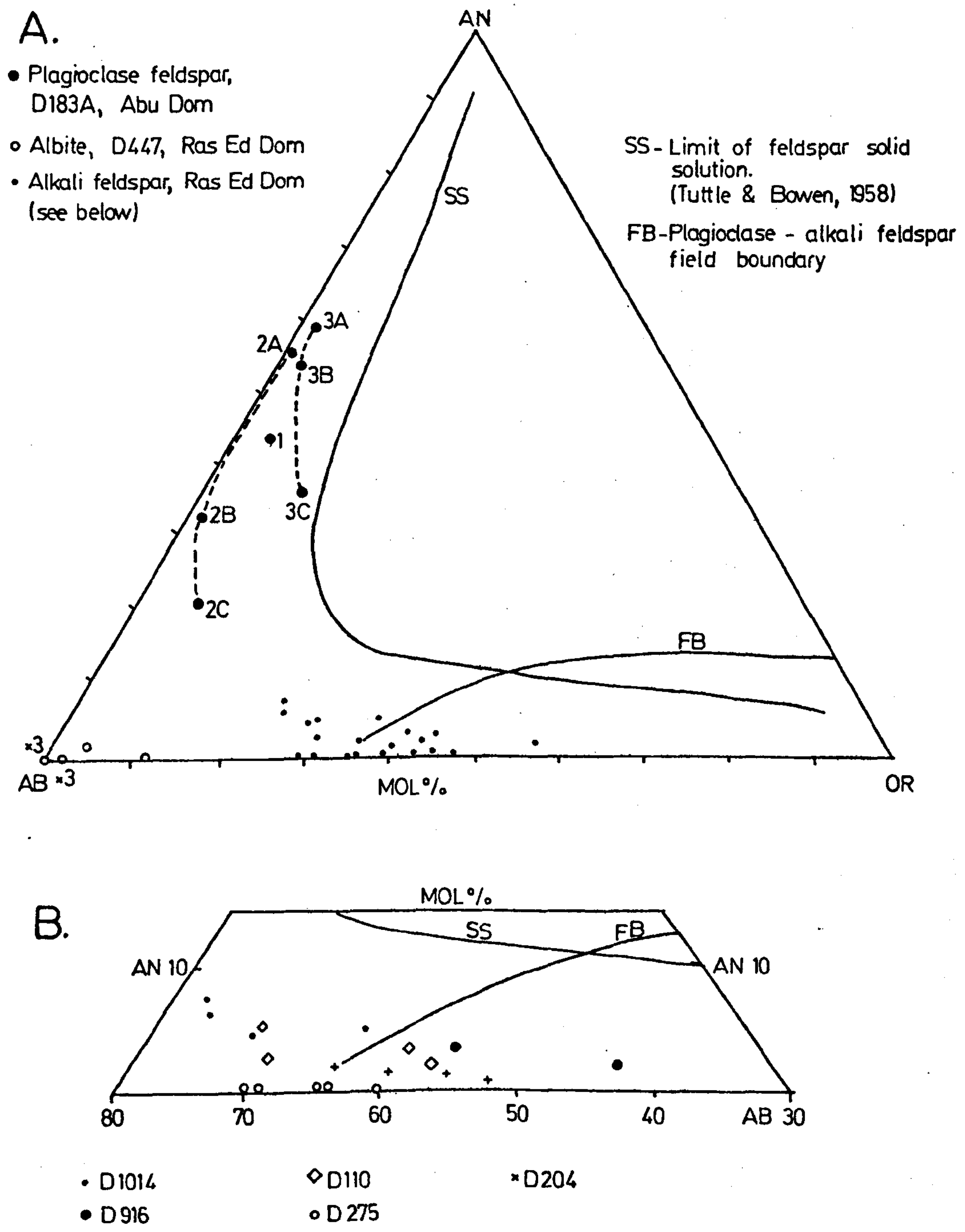

Fig. 5.1 : MICROPROBE ANALYSES OF FELDSPARS.
A. AN-OR-AB PLOT.
B. DETAIL OF A, SHOWING ALKALI FELDSPAR BULK COMPOSITIONS.

5.3. : Pyroxenes

5.3.A. : Introduction and Nomenclature

The clinopyroxenes of the Younger Granites range from calcic, through calcic-sodic, to sodic compositions (tables 5.3 and 5.4). Although in the suite as a whole a continuum of compositions is found, within any one rock sample a textural break, representing an interval of amphibole crystallisation, occurs. Consequently it is possible to distinguish between an 'early' (pre-amphibole) pyroxene group and a 'late' (post-amphibole) category. The early pyroxenes (table 5.3) are those analyses reported from samples D916, D110 and D275, whilst all others fall into the late group (table 5.4).

For the calcic compositions the established nomenclature of Poldevaart and Hess (1951) is observed (fig. 5.2). For more sodic compositions a standardised nomenclature is lacking (Deer et al., 1978). However, following Clark and Papike (1968), the division between calcic phases and aegirine-augite is taken at Na/(Ca+Na) = 0.2 ions p.f.u., and that between aegirine-augite and aegirine at Na/(Ca+Na) = 0.8 ions p.f.u. (see fig. 5.3). The term titanian-aegirine is reserved, in this thesis, for aegirines with 1.0% or more TiO_2. The term acmite is used in a dual sense, firstly to describe aegirines of brown colouration and/or pointed terminations, and secondly to refer to the molecule $NaFe^{3+}Si_2O_6$ (Deer et al., 1978).

5.3.B. : Early Pyroxenes

The early pyroxenes characterise the early and transitional syenites (see sections 4.3.C. and 4.4.C). Twenty nine point analyses are reported (Appendix IIC), the compositional features of which are summarised in table 5.3 .

SAMPLE NUMBER	UNIT	NUMBER OF ANALYSES	PYROXENE COMPOSITION	RANGE OF COMPOSITIONS
D916	S1	1	Ferroaugite	Ca_{43} Mg_{23} Fe_{34}
				Di_{40} Hd_{60} Ac_{0}
D110	S2	9	Ferroaugite ↓	Ca_{45} Mg_{21} Fe_{34} → Ca_{37} Mg_{3} Fe_{60}
		6	Aegirine-augite	Di_{33} Hd_{67} Ac_{0} → Di_{4} Hd_{61} Ac_{35}
D275	S3	4	Ferrohedenbergite ↓	Ca_{43} Mg_{6} Fe_{51} → Ca_{35} Mg_{0} Fe_{65}
		9	Aegirine-Augite	Di_{6} Hd_{85} Ac_{9} → Di_{0} Hd_{37} Ac_{63}
		29 analyses		

Table 5.3. : Compositional variation in the early pyroxenes of Ras ed Dom

SAMPLE NUMBER	UNIT	NUMBER OF ANALYSES	PYROXENE COMPOSITION	RANGE OF COMPOSITIONS
D433	S13	18	Aegirine-augite	Di_8 Hd_{30} Ac_{62} ↓ Di_5 Hd_{19} Ac_{76}
D204	S5	11	Aegirine-augite	Di_0 Hd_{29} Ac_{71}
		8	Aegirine	↓ Di_0 Hd_8 Ac_{92}
D1057	S3	15	Aegirine	Di_0 Hd_3 Ac_{97} ↓ Di_0 Hd_1 Ac_{99}
D447	G1	12	Aegirine	Di_0 Hd_{12} Ac_{88} ↓ Di_0 Hd_1 Ac_{99}
D145	G1	18	Aegirine	Di_0 Hd_{12} Ac_{88} ↓ Di_0 Hd_0 Ac_{100}
		82 analyses		

Table 5.4. : Compositional variation in the late, sodic pyroxenes of Ras ed Dom.

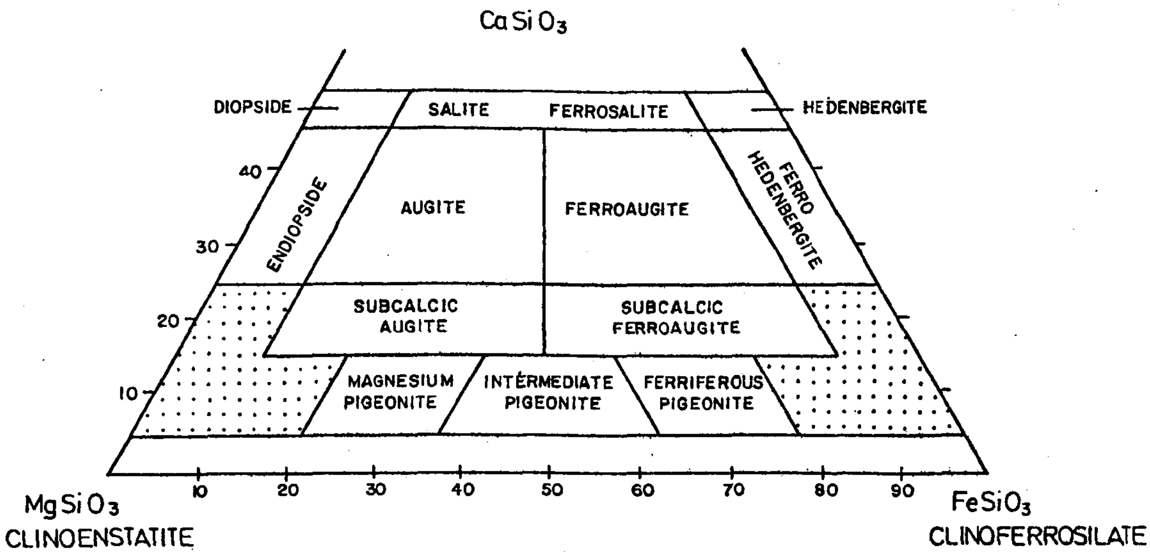

Fig.5.2: NOMENCLATURE OF CLINOPYROXENES IN THE SYSTEM DI-EN-FS-HD (After Poldervaart and Hess, 1951)

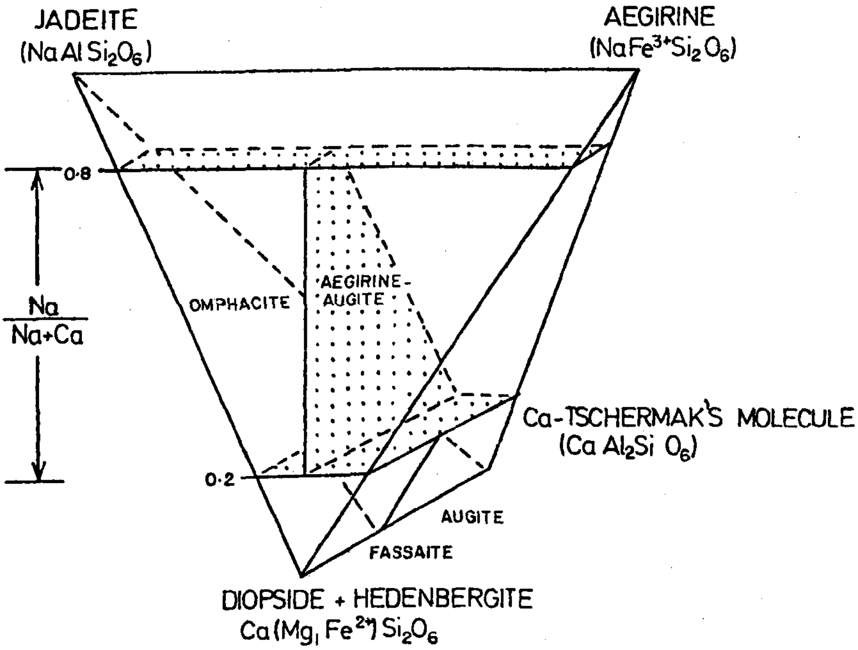

Fig. 5.3 : CLASSIFICATION OF THE SODIC PYROXENES IN THE SYSTEM JD-AC-DI+HE-TSCH (After Clark and Papike, 1968)

Alteration of the pyroxene of the early syenites is common, and the details of this phase remain poorly known. Only one analysis of ferroaugite (from D916) is reported here, and significantly it is the most magnesian of the pyroxenes analysed. Curtis (1979) reported one augite analysis from Sultaniyat complex, whilst ferrosalites occur in the Younger Granite rocks at Sabaloka, near Khartoum (Almond, pers. comm.).

The pyroxenes of D110 and D275 (both transitional syenites) show zoning from cores of ferroaugite and ferrohedenbergite respectively, to rims of aegirine-augite, and from fig. 5.4 it can be seen that this variation is in part accountable for by the substitution of Fe^{2+} for Mg. Strictly speaking the aegirine-augites plot above the plane of the quadrilateral. The concommitant Na-enrichment they record, however, is evident from fig. 5.8., when the analyses are recast in terms of Mg-(Fe^{2+} + Mn)-Na, analogous to the system Di-Hd-Ac (see also table 5.3). It is apparent that D275 shows the greatest enrichment in both hedenbergite and acmite components.

The importance of Ca and Mg depletion, and of enrichment in Na and Fe, is also apparent from the zoning profiles of fig. 5.5., which also shows that Fe^{3+} becomes progressively dominant over Fe^{2+}. Minor reversals in these trends, e.g. grain I (110), correlate with visible fluctuations in the intensity of the green (acmitic) component, and record slight oscillatory zoning. In the case of D275, it is possible to distinguish petrographically between early- and late-formed grains (see section 4.4.C). These observations serve as a basis for erecting the composite zoning profile of fig. 5.5., in which the horizontal axis effectively records time. The profile provides further confirmation of the above-mentioned substitutions.

The early pyroxenes are compared with several documented trends of Fe-enrichment in fig. 5.6., which is analogous to the system Wo-En-Fs. The ferroaugites plot on a line sub-parallel to trends from the Shiant Isles sill (Gibb, 1973) and Iceland (Carmichael, 1960). The ferrohedenbergites are more akin to the pantellerite trend (Nicholls and Carmichael, 1969). The aegirine-augites plot parallel to the Shonkin Sag

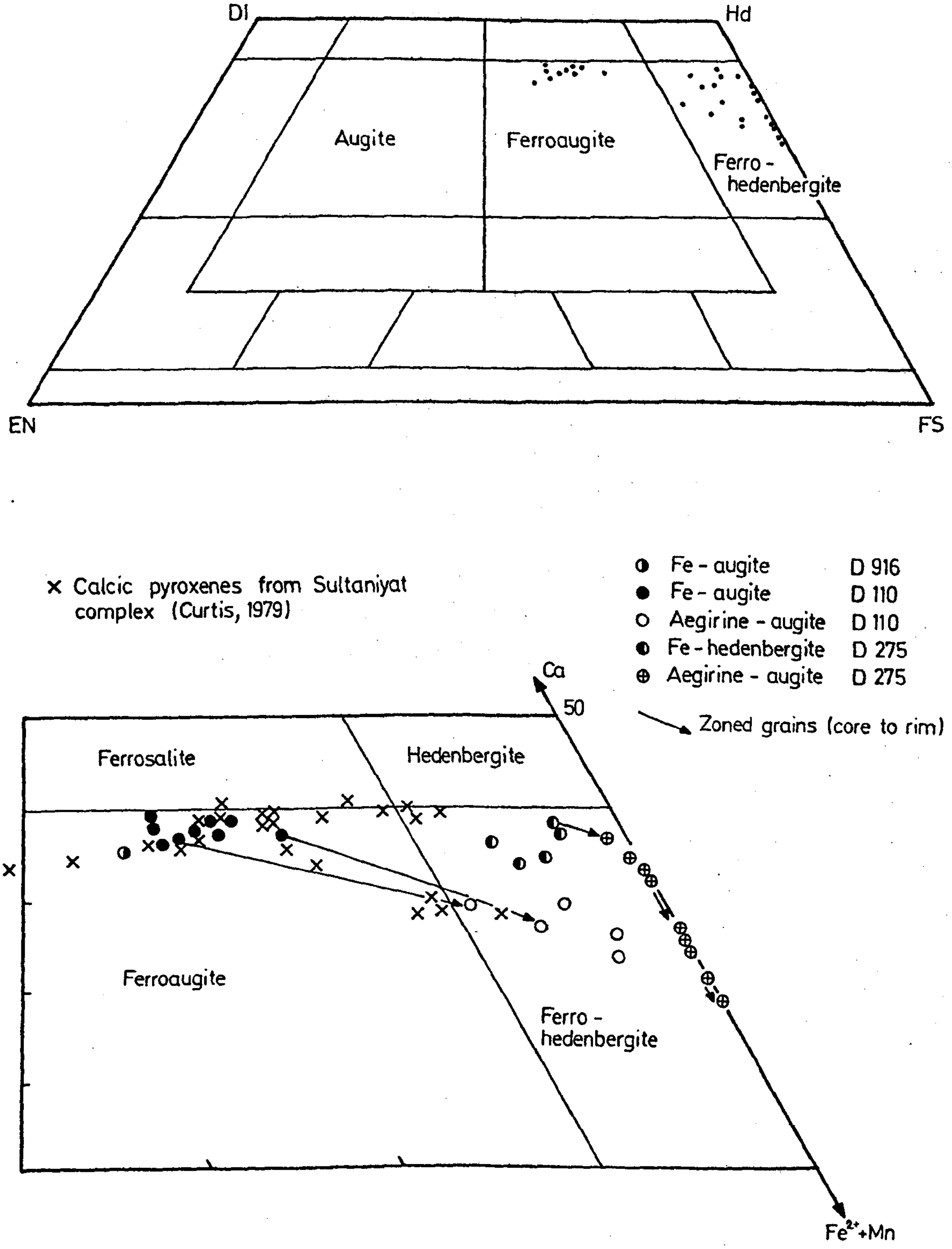

FIG. 54: CALCIC AND SODIC - CALCIC PYROXENES OF RAS ED DOM IN THE SYSTEM Ca Mg Si_2O_6 - Ca Fe Si_2O_6 - $Mg_2Si_2O_6$ - $Fe_2Si_2O_6$ (after Poldervaart and Hess, 1951) THE AEGIRINE - AUGITES PLOT SLIGHTLY ABOVE THE PLANE OF PROJECTION BUT ARE INCLUDED TO ILLUSTRATE ZONING.

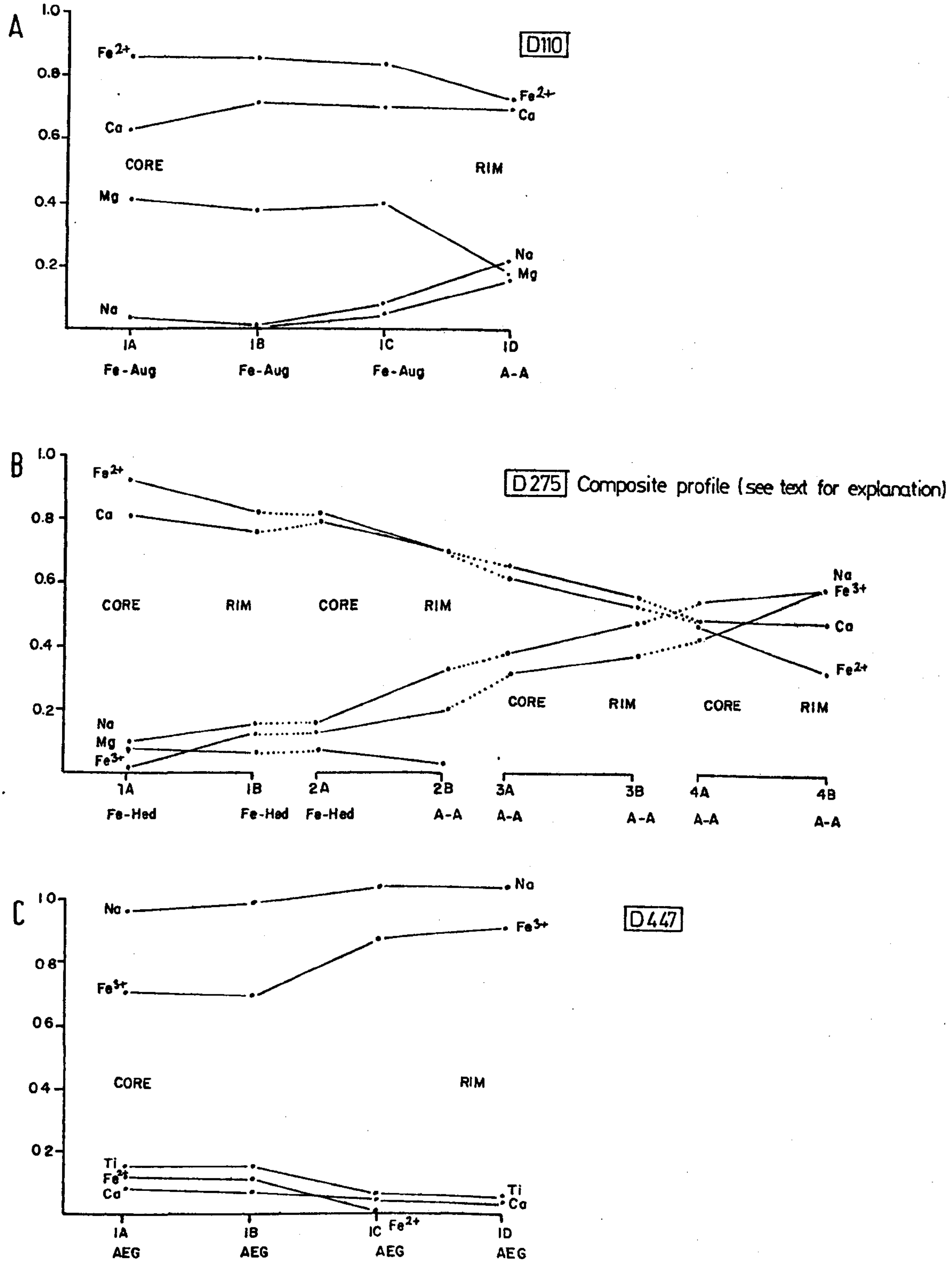

Fig. 55 : ZONING PROFILES FOR RAS ED DOM PYROXENES
Fe-Aug = FERROAUGITE Fe-Hed = FERROHEDENBERGITE
A-A = AEGIRINE-AUGITE AEG = AEGIRINE

Fig. 5.6. (opposite) : Comparative trends for the calcic pyroxenes

1. Morotu, Sakhalin (Yagi, 1953)
2. Shonkin Sag laccolith (Nash and Wilkinson, 1970)
3. Shiant Isles (Gibb, 1973)
4. Pantellerites (Nicholls and Carmichael, 1969)
5. Iceland (Carmichael, 1960)
6. Skaergaard (Brown and Vincent, 1963)

Fig. 5.7. (opposite) : Comparative Ca-levels for the calcic pyroxenes. Triangular plot Wo-En-Fs*, where Fs* equals $Fe^{+2} + Fe^{+3} + Mn - Na$, after Larsen (1976)

1. Uganda nephelinites (Tyler and King, 1967)
2. Shonkin Sag laccolith (Nash and Wilkinson, 1970)
3. Gardar province (Upton, 1964 and Larsen, 1976)
4. Shiant Isles sill (Gibb, 1973)
5. Nandewar volcano (Abbott, 1969)
6. Skaergaard (Brown and Vincent, 1963)
7. Pantellerites (Nicholls and Carmichael, 1969)

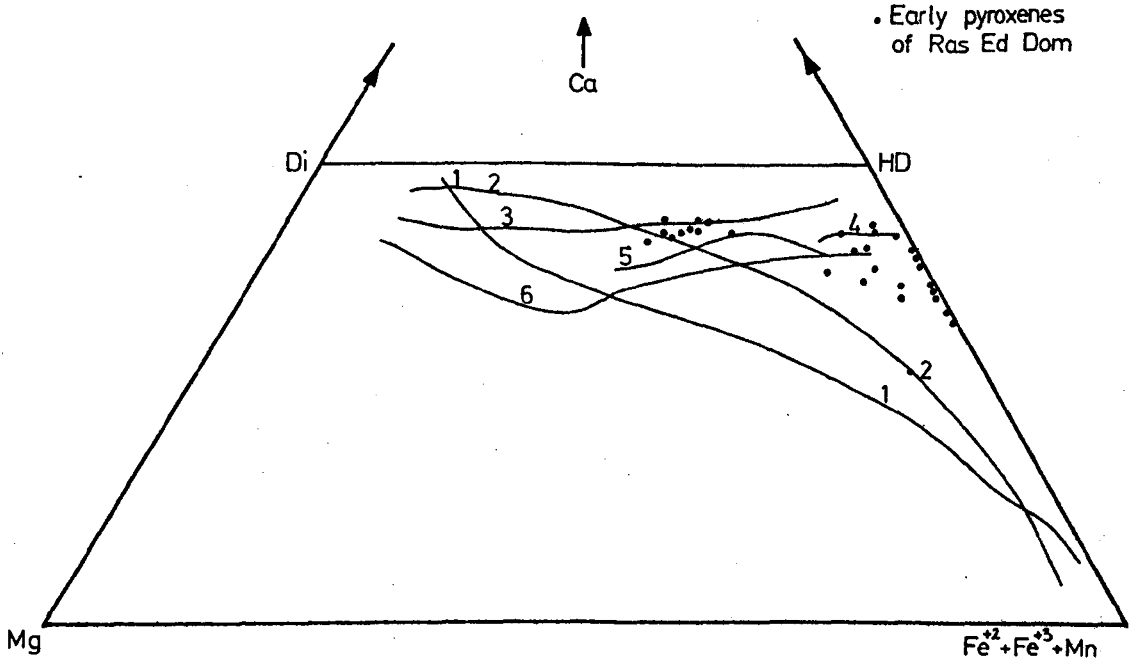

FIG. 5.6: COMPARATIVE TRENDS FOR THE CALCIC PYROXENES (Explanation opposite)

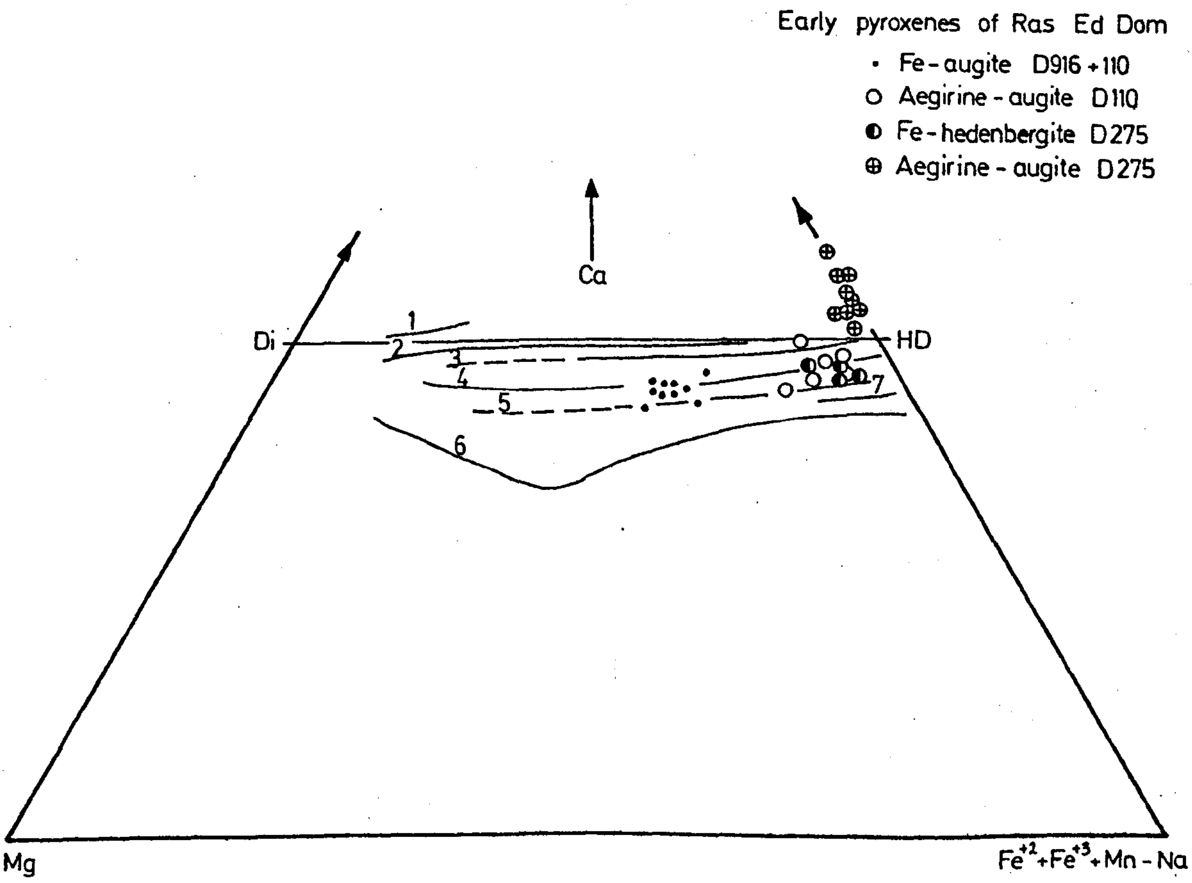

FIG. 5.7: COMPARATIVE Ca LEVELS FOR THE CALCIC PYROXENES (Explanation opposite)

laccolith trend (Nash and Wilkinson, 1970) and, as in that instance, record the onset of alkalinity. Similar trends are present in the Sultaniyat pyroxenes (Curtis, 1979).

The second comparative plot employes the triangular plot Wo-En-Fs* (fig. 5.7), where Fs* = $Fe^{2+} + Fe^{3+} + Mn - Na$, thereby excluding the acmite component (Larsen, 1976). This removes the bend towards the Fs corner, and shifts the trends to slightly higher Ca-levels. Reference to the key in fig. 5.7 shows that higher Ca-levels coincide with decreasing silica activity, and it may be latter factor which controls Ca-levels in the pyroxenes (Larsen, 1976). The Ras ed Dom pyroxenes plot intermediate to the oversaturated and undersaturated trends. The inclusion of the aegirine-augites in the plot shows that any such control ceases once alkalinity in the magma increases.

Comparison of the trends shown by D110 and D275 in terms of the system Di-HD-Ac (fig. 5.8), reveals that neither the initial compositions, nor the end compositions are the same. The samples are from different units (table 5.1), and the differences probably reflect magma compositions, with the greatest Hd and Ac enrichment occurring in the later, more evolved magma (D275). Aegirine-augite is known to become unstable as pH_2O rises, and alkali amphibole follows in a discontinuous reaction relationship (Upton, 1964; Stephenson, 1972). This relation is clear when the early pyroxenes and later amphiboles are superimposed on the analogous plots Mg-Na-(Fe^{2+} + Mn) and Mg-Na-Ca (for pyroxenes and amphiboles respectively) as in fig. 5.8. The Na/Ca ratio in the earliest amphibole should be approximately equal to the Na/(Fe^{2+} + Mn) ratio in the last crystallised pyroxene. This is true for D276, but less apparent for D110, probably due to incomplete sampling.

Also displayed in fig. 5.8 is the extent of <u>in situ</u> fractionation in S3 of Ras ed Dom (section 4.1.). D275 is from the chilled margin,where early pyroxene occurs, whilst D1057 is from the coarser interior. The ferrohedenbergites of D275 are succeeded by ferrorichterite which overlaps in composition with the ferrorichterite-arfvedsonite of D1057. Thereafter the alkali amphibole in D1057 is replaced by late aegirine (fig. 5.8).

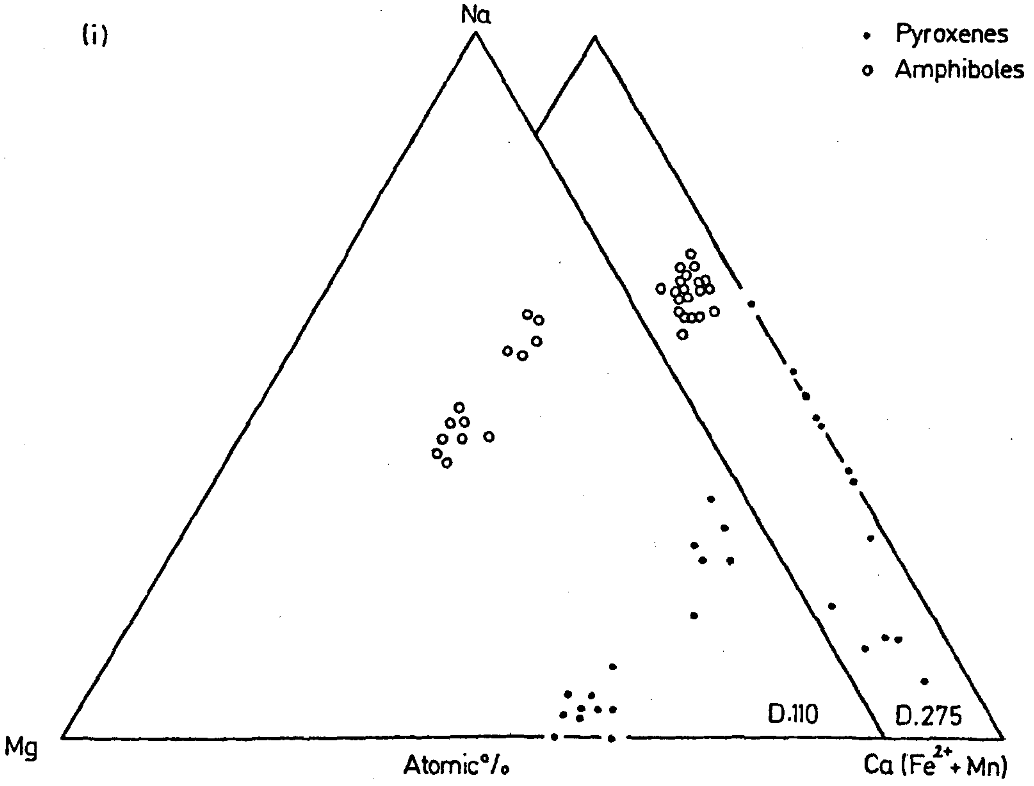

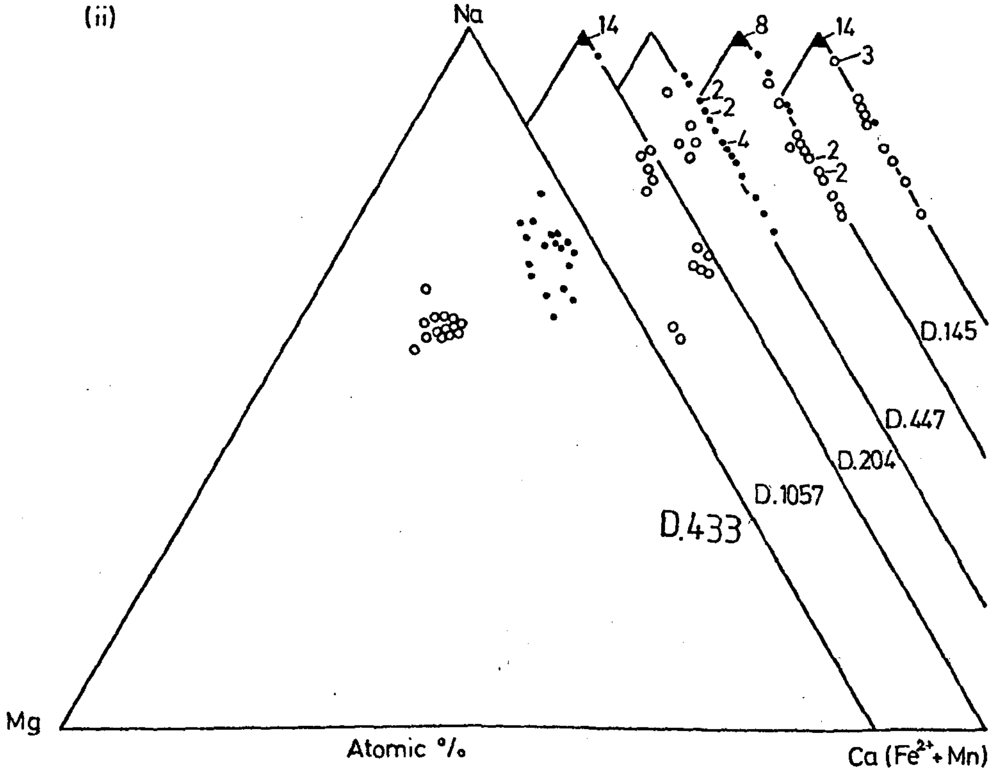

FIG.5.8 : PYROXENES AND AMPHIBOLES FROM INDIVIDUAL ROCK SAMPLES PLOTTED TOGETHER IN THE SYSTEMS Na - Mg - Fe^{2+} + Mn AND Na - Mg - Ca RESPECTIVELY - (i) ROCK TYPES CONTAINING EARLY PYROXENES (ii) ROCK TYPES CONTAINING LATE PYROXENES

Fig. 5.9. (opposite) : Ras ed Dom clinopyroxenes and comparative trends, plotted onto the triangular diagram Na-(Fe^{2+} + Mn)-Mg

Undersaturated provinces

1. Auvergne (Varet, 1969)
2. Lovozero, U.S.S.R. (Bussen and Sakharov, 1972)
3. Itapirapua, Brazil (Gomes, et al., 1970)
4. Uganda (Tyler and King, 1967)
5. Morotu, Sakhalin (Yagi, 1966)
6. South Qoroq, Gardar (Stephenson, 1972)
7. Ilimaussaq (Larsen, 1976)

Oversaturated provinces

8. Japanese alkali-basalts (Aoki, 1964)
9. Pantellerites (Nicholls and Carmichael, 1969)
10. Younger Granites, Nigeria (Borley, 1976)
11. Nandewar volcano (Abbott, 1969)
12. Coldwell syenite, Canada (Mitchell and Platt, 1978)
13. Skaergaard (Brown and Vincent, 1963)

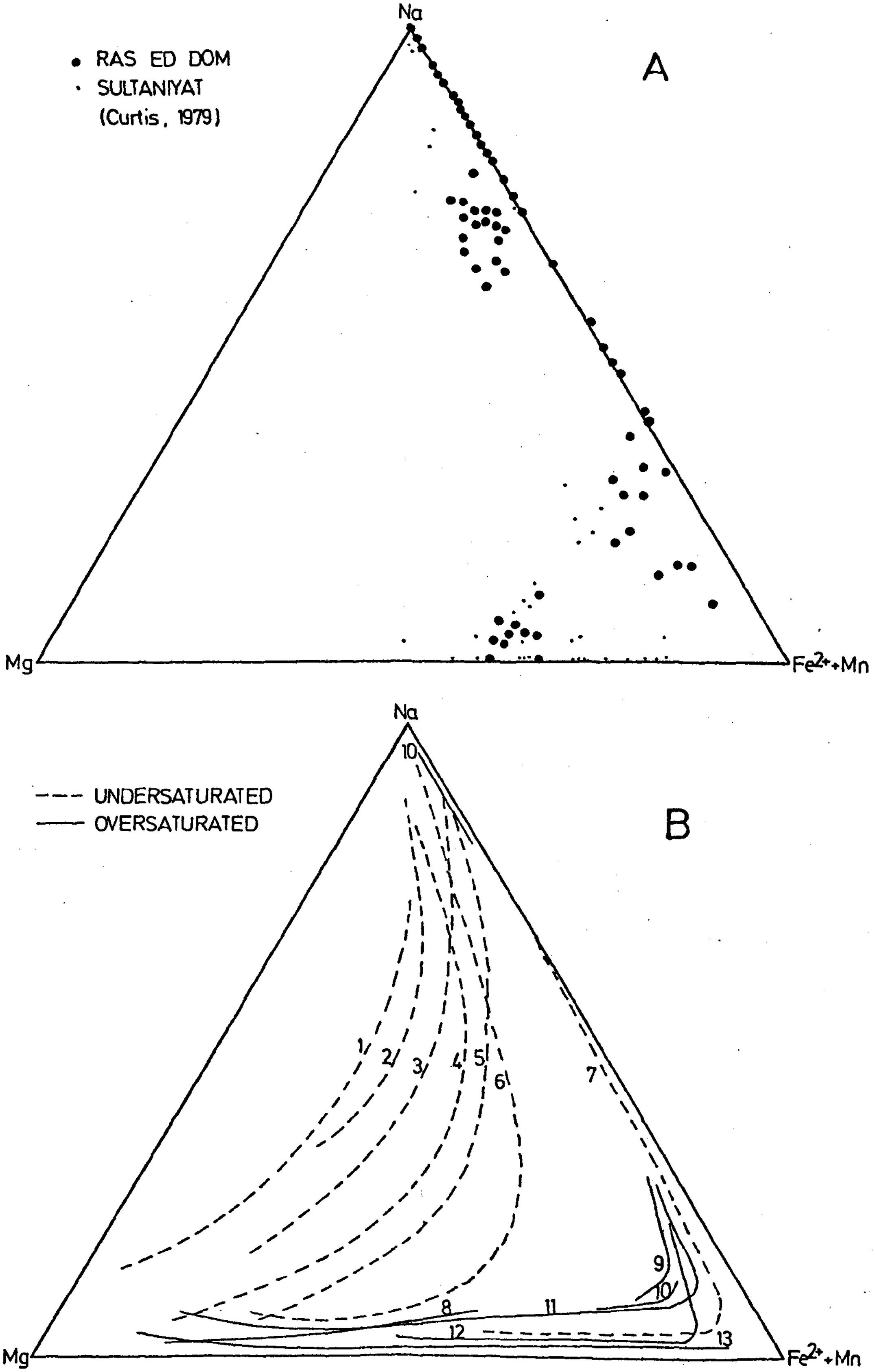

Fig. 5.9 : RAS ED DOM CLINOPYROXENES AND COMPARATIVE TRENDS, PLOTTED ONTO THE TRIANGULAR DIAGRAM Na-(Fe2+ +Mn)-Mg) (SEE EXPLANATION OPPOSITE)

5.3.C. : Late Pyroxenes

The late pyroxenes, which are replacive towards alkali amphibole (section 4.5.D), characterise the alkali syenites and granites. 82 point analyses representing twenty nine aegirine-augites and fifty three aegirines, are presented (Appendix IID), and the compositional ranges are summarised in table 5.4.

Variation in the late pyroxenes reflects progressive enrichment in acmite from the alkali syenites (D1057, D204) to the granites (D447, D145), with numerous points clustering about the Na-apex in the latter (fig. 5.8). The Ras ed Dom Na-enrichment is compared with that found in other provinces as shown by fig. 5.9. From this figure it is apparent that the oversaturated suites show greater degrees of early Fe-enrichment than the undersaturated suites. The Ilimaussaq pyroxenes are exceptional in plotting in the oversaturated field, probably reflecting unusually low Mg-levels in the parent magma (Larsen, 1976). As discussed in the previous section the early pyroxenes show variable substitution of Fe^{2+} for Mg. The late pyroxenes are Mg-depleted, and like their Nigerian counterparts (Borley, 1976) show extreme enrichment in Na.

The zoning profile for D447 (fig. 5.5) illustrates the continued substitution of Na and Fe^{2+}, at the expense of Ca and Fe^{2+}, in the aegirines of the alkali granites.

5.3.D. : Chemical Variation in the Pyroxenes

The parameter Na-Mg (atoms p.f.u.) is used as a fractionation index in fig. 5.10, as it enables the entire pyroxene trend to be represented in a single diagram (Stephenson, 1972; Larsen, 1976). This is because an initial depletion in Mg is followed by a steady increase in Na (Fig. 5.11). The pyroxenes of D433 (recrystallised syenite) are an exception to this, and their behaviour is discussed separately below.

In the early pyroxenes Fe^{2+} increases as Ca falls, recording the substitution CaMg = $CaFe^{2+}$. At a value of Na-Mg of 0.25, an inflection occurs as Ca starts to decrease with increasing Na in 1:1 ratio. Fe^{2+} and Fe^{3+} show a similar relationship, and the dominant substitution thereafter is $CaMgFe^{2+}$ = $NaFe^{3+}$. Na and Fe^{3+} enrichment occurs at an earlier stage in undersaturated suites, e.g. Na-Mg=0.1 for the South Qoroq centre (Stephenson, 1972).

Mn usually follows Fe^{2+} during fractionation in alkaline suites (Gibb , 1973; Stephenson, 1972), and this is true for Ras ed Dom, with the exception of the aegirines where Mn shows an erratic rise (fig. 5.10-iv). Al shows a similar behaviour, and since Si increases steadily with fractionation (not depicted), the Al in the aegirines must enter the Y-site. In contrast Ti, although rising erratically in the aegirines, is low in the less fractionaed pyroxenes reflecting the fact that Fe-Ti oxide crystallised alongside the early pyroxenes (fig. 5.10-vii). Zr is absent from the more augitic compositions, but appears in the aegirine-augites of the early pyroxenes, and in all the late pyroxenes (fig. 5.10 -vi). The distributions are notably erratic even in one rock sample, a feature which may reflect in part the unreliability of the analyses at low concentrations.

The recrystallised aegirine-augites of D433 (see section 4.5.D) are anomalous compared to typical late pryoxenes in being Mg-bearing, and accordingly plot aberantly relative to the Na-Mg index (fig. 5.10). The rock is also chemically distinct in having higher Mg-levels than is usual for the alkali syenites. Mineralogically it is unique in having abundant Fe-Ti oxide. Fe^{2+} values are in the pyroxenes (low) (fig. 5.10-i) and evidently Mg substituted in its place. This may reflect conditions of high fO_2 during the recrystallisation, with oxidation of Fe^{2+} to Fe^{3+}.

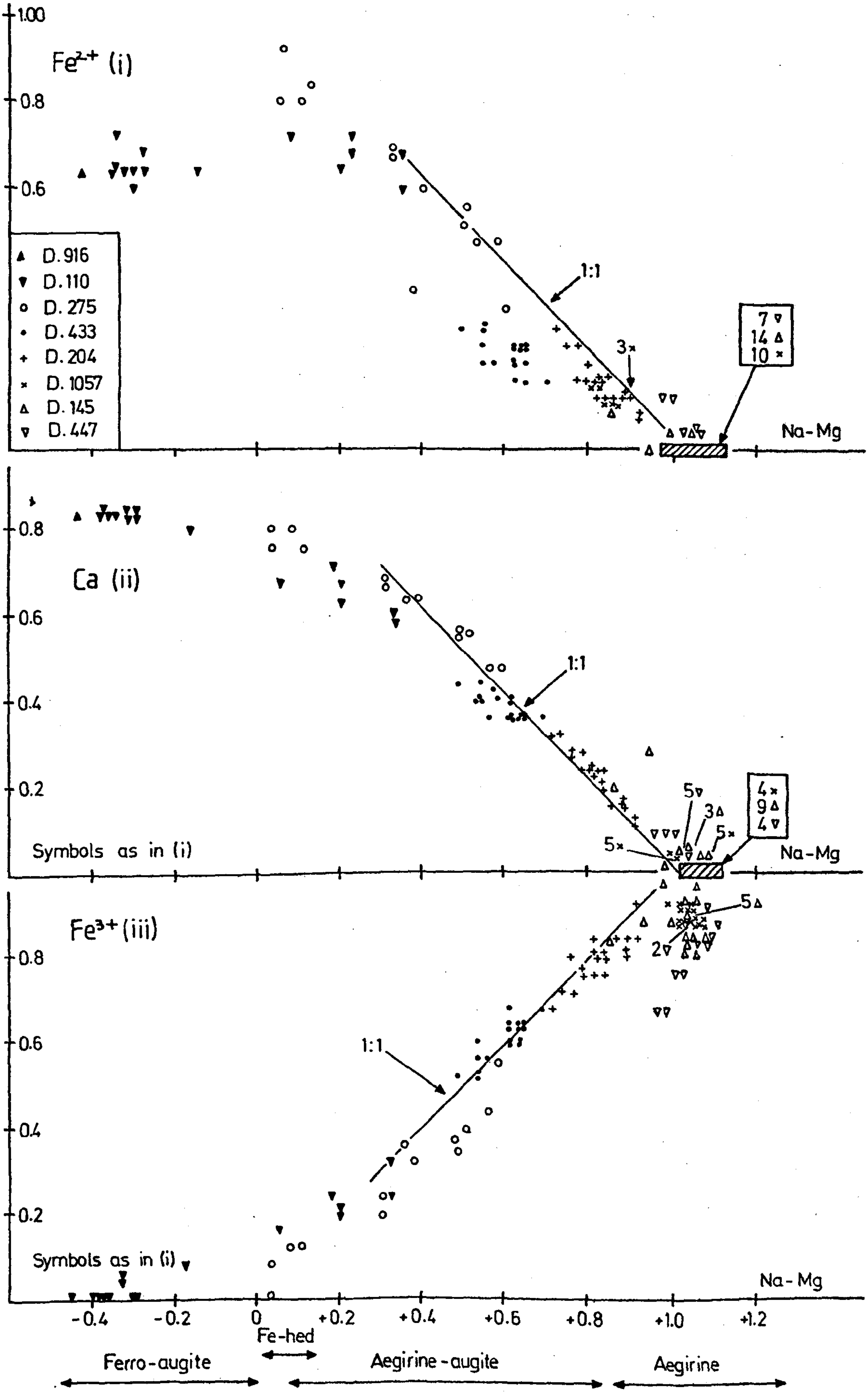

FIG.5.10 : (i), (ii), (iii) CHEMICAL VARIATION OF THE PYROXENES
(All three graphs have a common baseline)

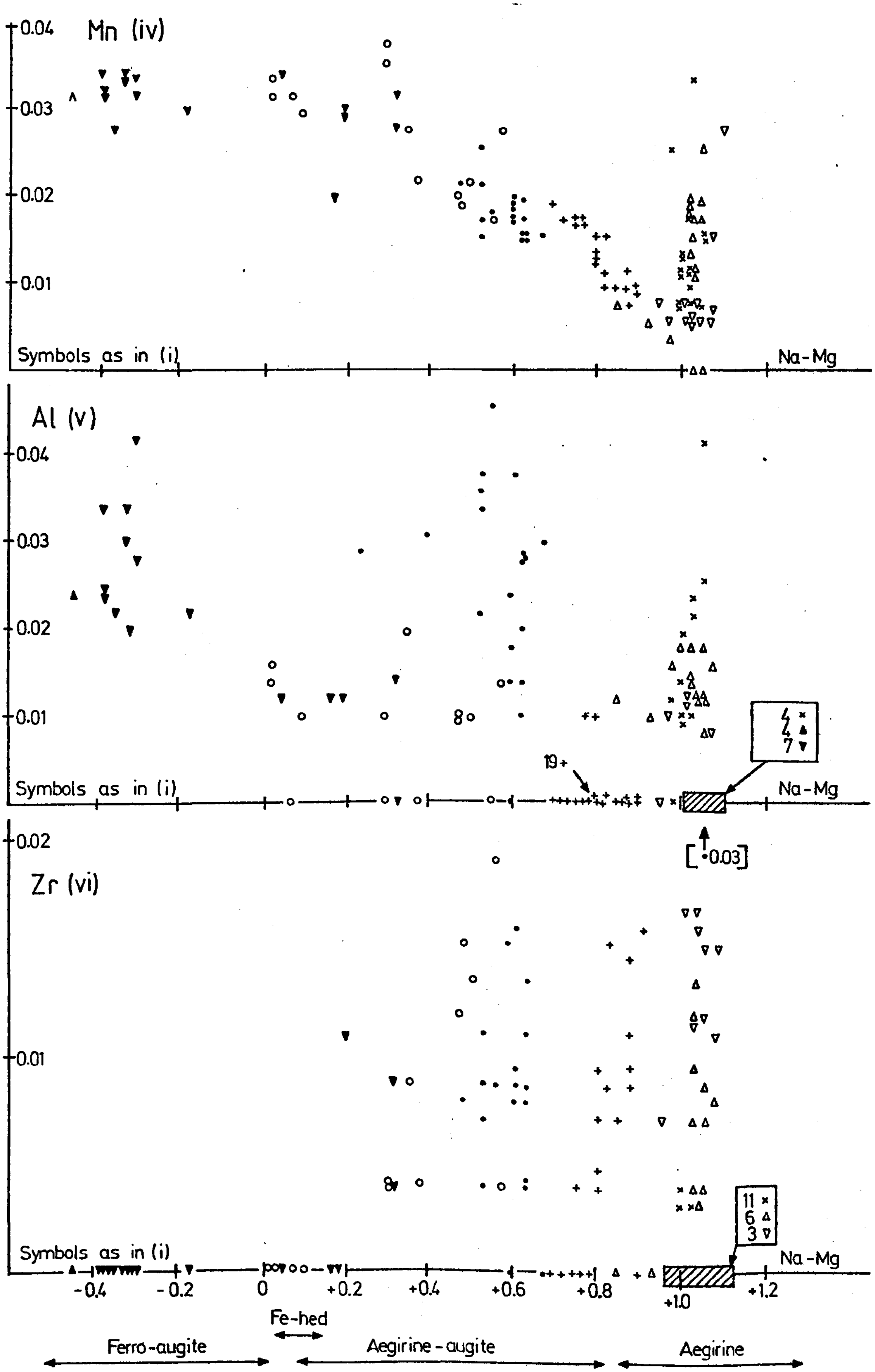

FIG 5.10: (iv), (v), (vi) CHEMICAL VARIATION OF THE PYROXENES
(All three graphs have a common baseline)

FIG.5.10.Cont (vii)

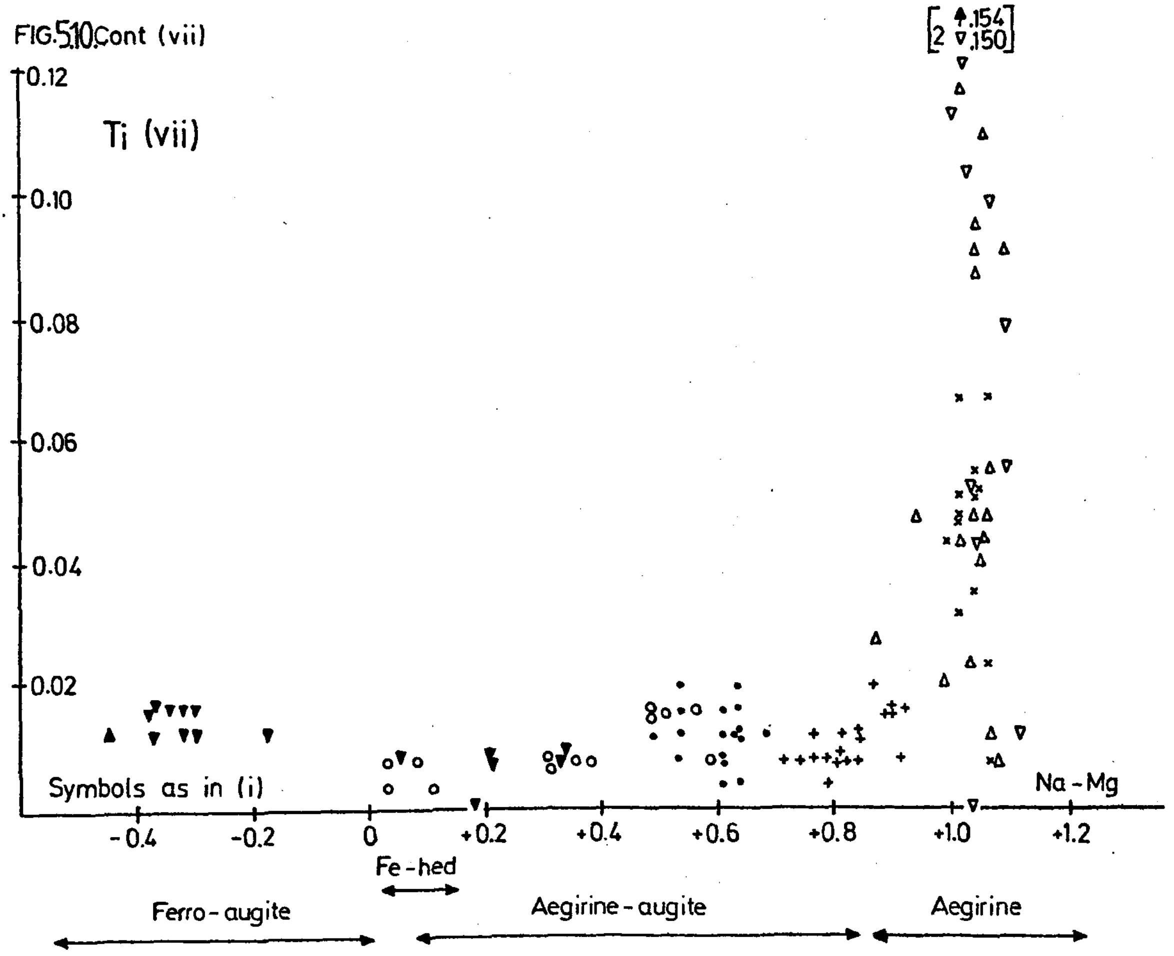

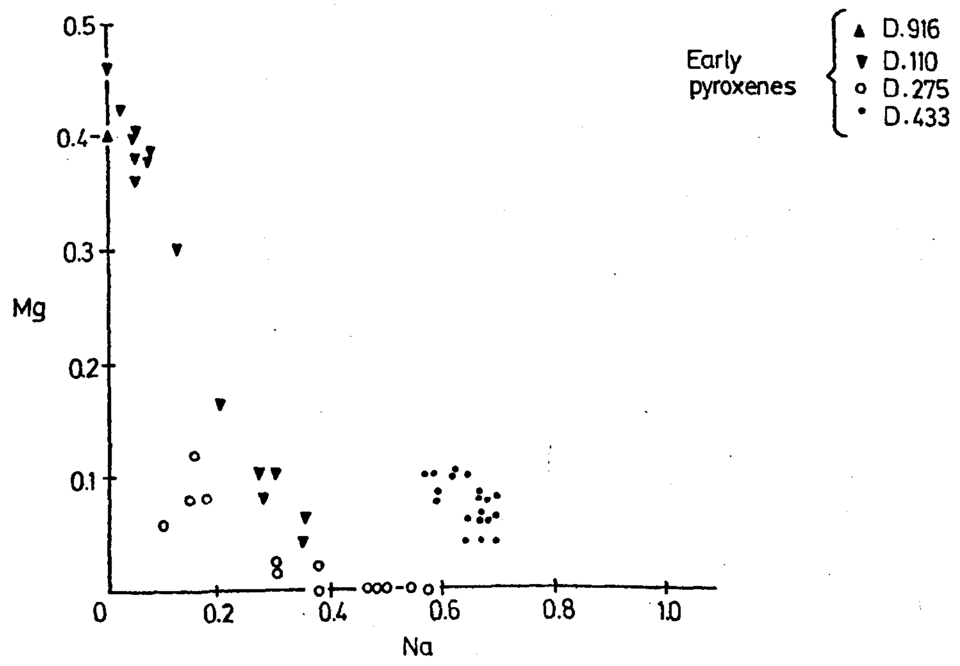

FIG. 5.11: VARIATION OF Mg RELATIVE TO Na FOR THE EARLY PYROXENES AND D.433

5.4. : Amphiboles

5.4.A. : Introduction and Nomenclature

A period of amphibole crystallisation intervenes between the early and late pyroxenes, and the compositional range spans the calcic, sodic-calcic and alkali groups of the I.M.A. classification (Leake , 1978; table 5.5.). One hundred and twenty nine partial amphibole analyses are reported (Appendix IIE), representing a total of ten species as shown in table 5.5., and on figs. 5.12., 5.13., and 5.14. The effects of different recalculation procedures on the analyses are discussed in Appendix IIA.

The calcic amphiboles characterise the early syenites (table 5.5), whilst sodic-calcic types occur in the transitional syenites. The alkali syenites and granites contain amphiboles that are zoned from sodic-calcic cores to alkali rims (table 5.5). This increase in alkalinity with fractionation mirrors that are shown by the pyroxenes.

5.4.B. : Magmatic and Secondary Amphiboles of the Early Syenites

A petrographic distinction between a primary magmatic amphibole and a secondary replacive one can be made in the early syenites (section 4.3.C.). Microprobe analysis reveals the former to be ferroedenite (fig. 5.12), whilst the latter ranges from ferrobarroisite to ferrowinchite (fig. 5.13). However, in the case of the ferroactinolitic hornblendes and ferroactinolites (fig. 5.12) it was not possible to decide optically to which category they belonged. As an aid in further discriminating between the two trends, eight amphibole analyses from the Tuleih syenite of Sabaloka complex (Almond, pers. comm.), ranging from hastingsite to ferroedenite, are employed as a control group in some of the text figures. The justification for this is twofold. Firstly, the Tuleih amphiboles are unequivocally magmatic (Almond, pers.comm.), and secondly their compositions are similar to those characterising the less fractionated lithologies of the Nigerian Younger Granites (Borley, 1963; Ike, 1979).

Amphibole Group	Amphibole Species	Number of analyses	Rock sample number	Rock-type
Calcic group	ferro-edenite	5	D1014	Early syenite
	ferro-actinolitic hornblende	3	D1014	Early syenite
	ferro-actinolite	4	D1014, D916	Early syenite
Sodic-calcic group	ferro-barroisite	5	D1014	Early syenite
	ferro-winchite	14	D1014, D916	Early syenite
	katophorite	6	D1014, D433	Early syenite, alkali syenite*
	ferro-richterite	48	D1014, D916 D110, D275 D1057, D145, D447	Early syenite Tranisitional syenite Alkali syenite and alkali granite
Alkali group	arfvedsonite	40	D204, D433 D1057, D145 D447	Alkali syenite, alkali syenite* and alkali granite
	riebeckite	3	D204, D433	
	crossite	1	D433	Alkali syenite*

Table 5.5. : Amphibole Species from Ras ed Dom

*recrystallised assemblage. Nomenclature after Leake (1978).

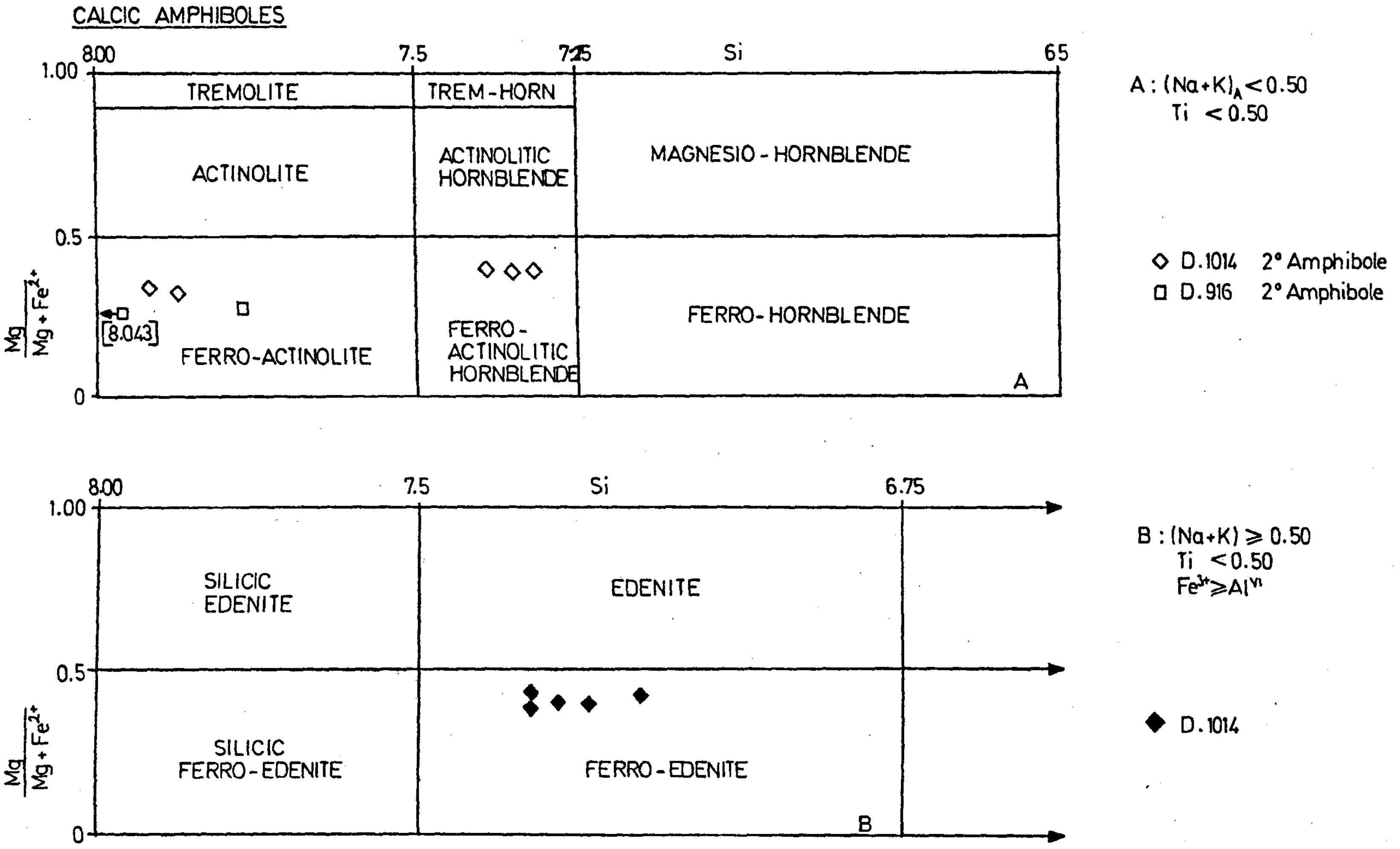

FIG. 5.12 : AMPHIBOLES FROM RAS ED DOM PLOTTED ONTO THE CALCIC COMPOSITIONAL FIELDS [$(Ca+Na)_B \geq 1.34$ $Na_B < 0.67$] OF LEAKE, 1978

SODIC - CALCIC AMPHIBOLES

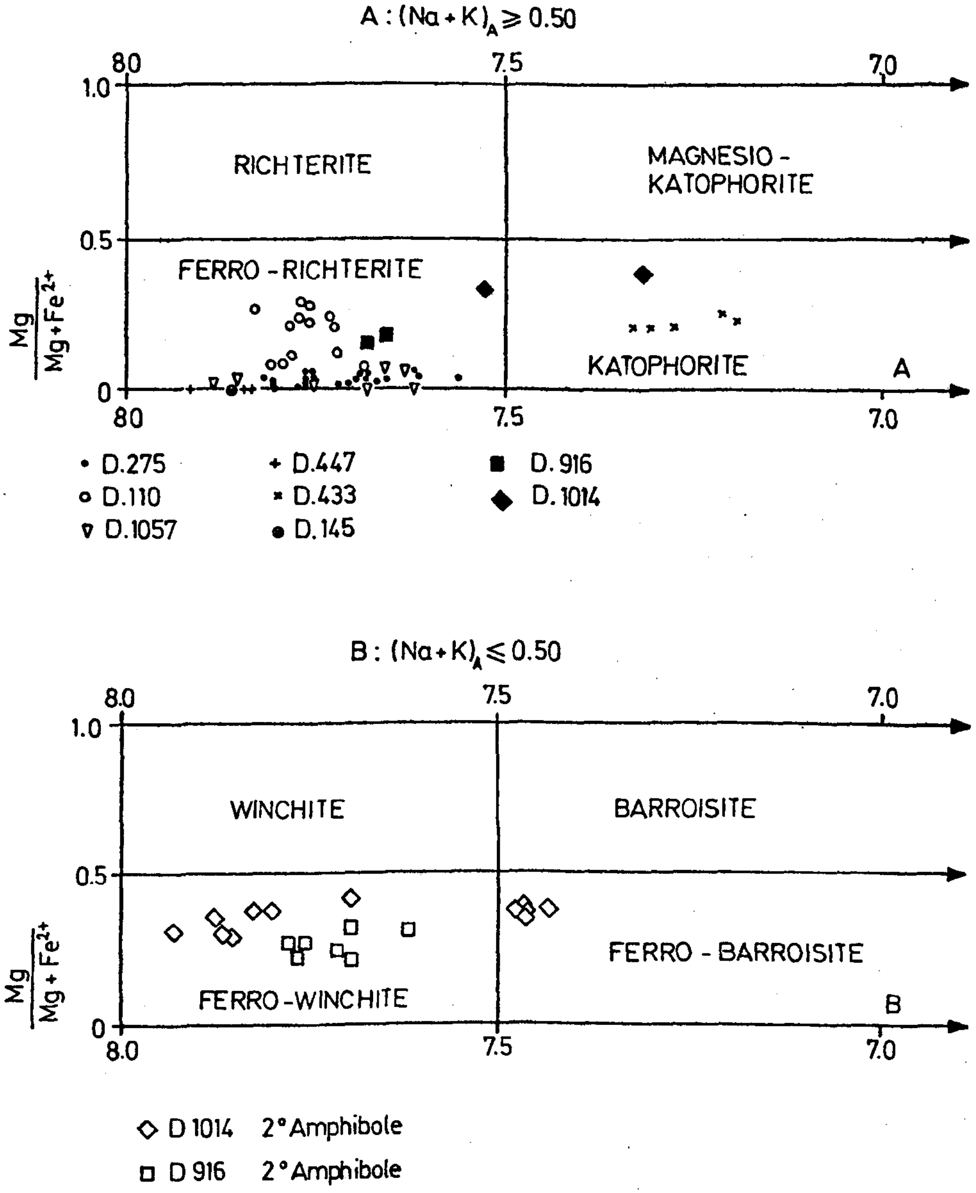

FIG. 5.13: AMPHIBOLES FROM RAS ED DOM PLOTTED ONTO THE SODIC-CALCIC COMPOSITIONAL FIELDS [$(Ca+Na)_B \geq 1.34$; Na_B BETWEEN 0.67 AND 1.34] OF LEAKE, 1978

ALKALI AMPHIBOLES

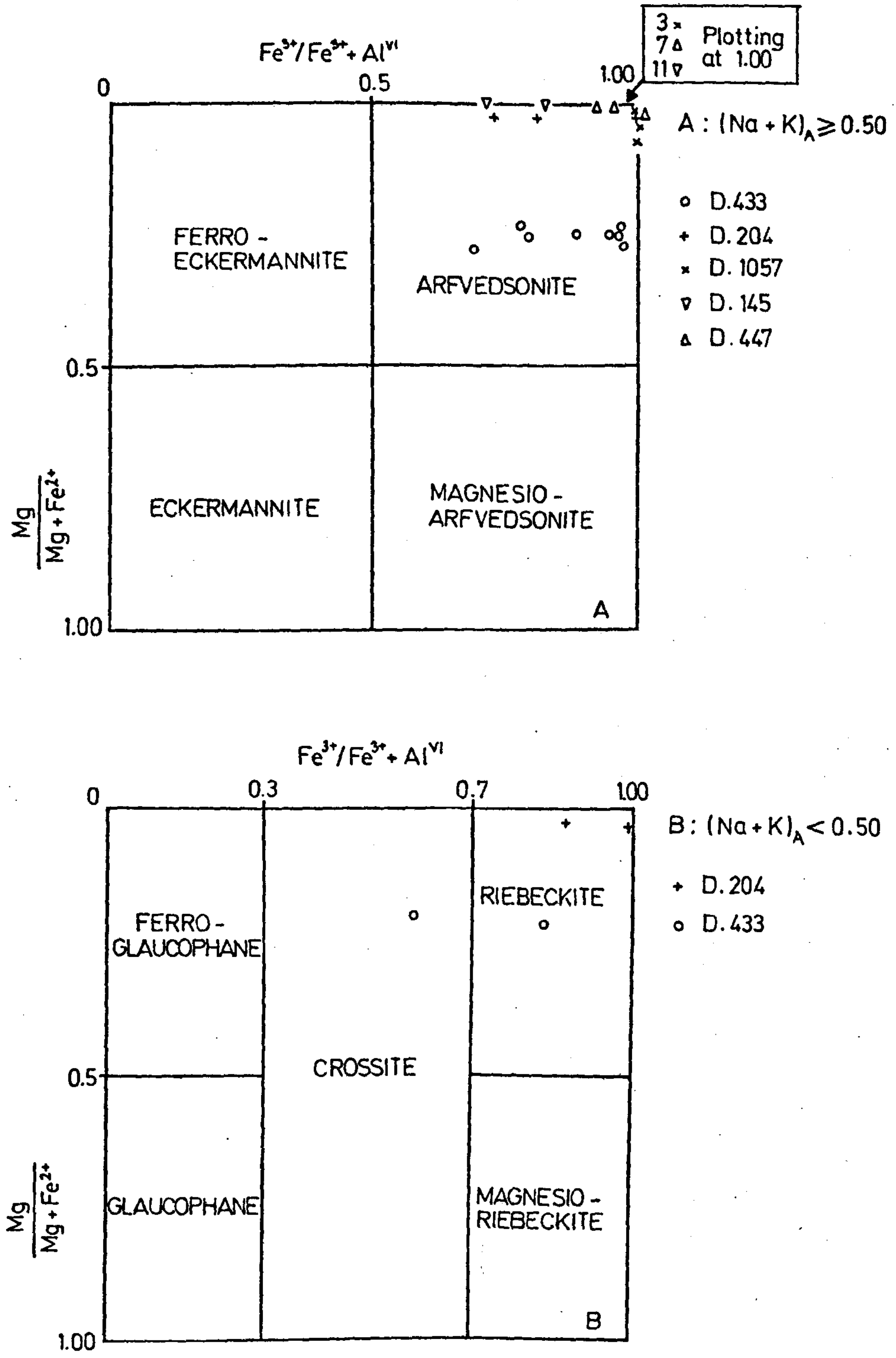

FIG. 5.14 : AMPHIBOLES FROM RAS ED DOM PLOTTED ONTO THE ALKALI COMPOSITIONAL FIELDS ($Na_B \geq 1.34$) OF LEAKE, 1978

From figs. 5.15 - 5.18 inclusive it is apparent that the secondary amphiboles record declining Al^{iv} and alkalies, whilst Si-levels remain unaltered and Ca is constant or increasing (fig. 5.18). In contrast the magmatic amphiboles show a decline in Al^{iv} (fig. 5.15), Mg relative to Fe^{2+} (fig. 5.16), and Ca (fig. 5.18), as the alkalies (especially Na; figs. 5.16 - 5.18 inclusive), and Si increase (fig. 5.17). The distinction between primary and secondary trends is especially clear in figs. 5.17 and 5.18, where the magmatic trends can be projected back to the Tuleih amphiboles, and forward into the alkali amphiboles.

A similar situation occurs in the Coldwell alkali syenites, Ontario (Mitchell and Platt, 1978), where two amphibole trends, one trending towards ferroedenite and the other towards ferroactinolite, are present. However, Mitchell and Platt (1978) believe both trends are magmatic and cannot be linked by simple differentiation, whereas in Ras ed Dom the secondary amphibole is of hydrothermal origin (see section 4.3.C.).

5.4.C. : The Magmatic Amphibole Trend

The bulk of the magmatic sodic-calcic amphiboles are ferrorichterites (fig. 5.13). Until recently this species was considered to be rare (Charles, 1975) but recent microprobe investigations are showing it to be a characteristic mineral in alkali suites (Thompson, 1976; Larsen, 1976; Stull, 1973; Mitchell and Platt, 1978; Curtis, 1979). Ferrorichterite is the dominant amphibole in the transitional syenites, and forms the cores to the arfvedsonite grains in the alkali rocks (table 5.5).

The relation between ferrorichterite and earlier ferroedenite merits comment, as Billings (1928) and Stull (1973) report a discontinuous reaction as occurring at this juncture. Although the hydrothermal overprint in the early syenites obscures the primary amphibole relations, some of the ferroedenites in D1014 are sodian (Appendix IIE), and sporadic ferrorichterite and katophorite occurs. This suggests that alkali enrichment had commenced in the amphiboles of the early syenite magma. Furthermore, on variation diagrams there is continuous variation between the ferroedenites and ferrorichterites (fig. 5.17 and 5.18).

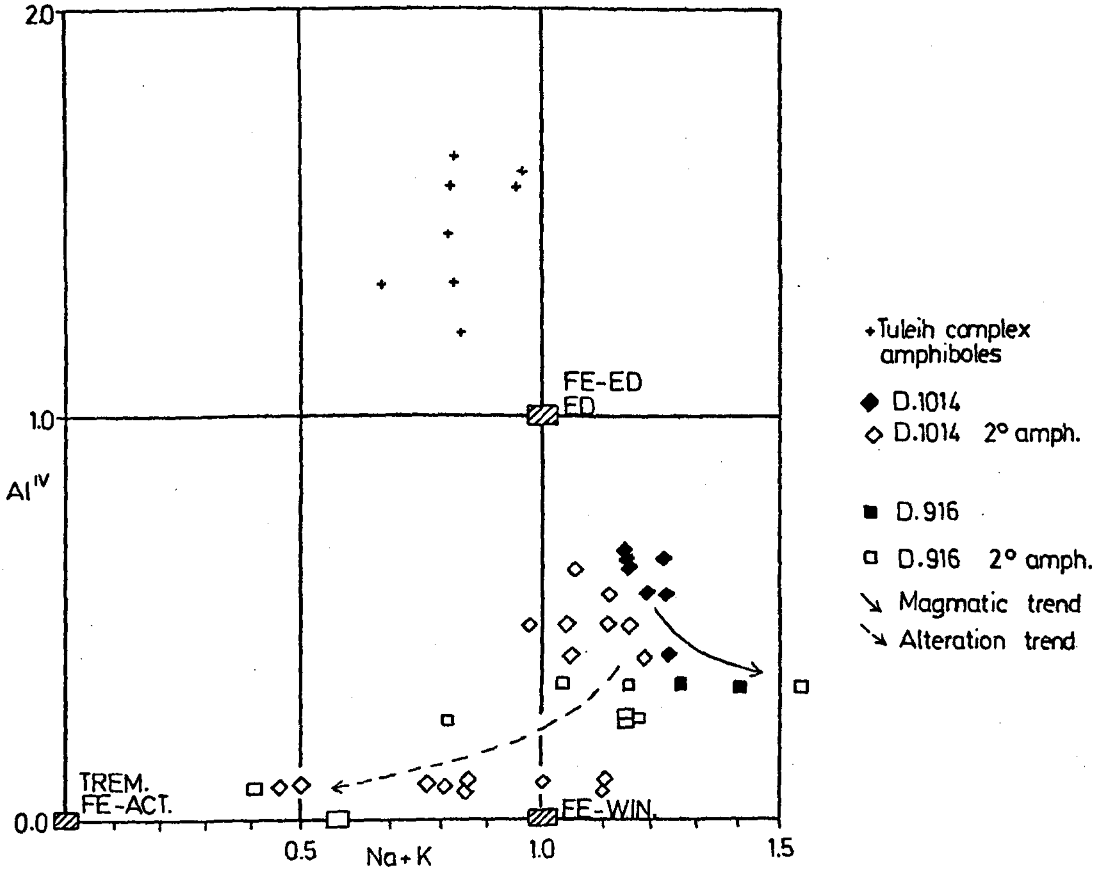

Fig. 5.15 : Al^{IV} VERSUS Na+K FOR THE AMPHIBOLES OF D.916 AND D.1014

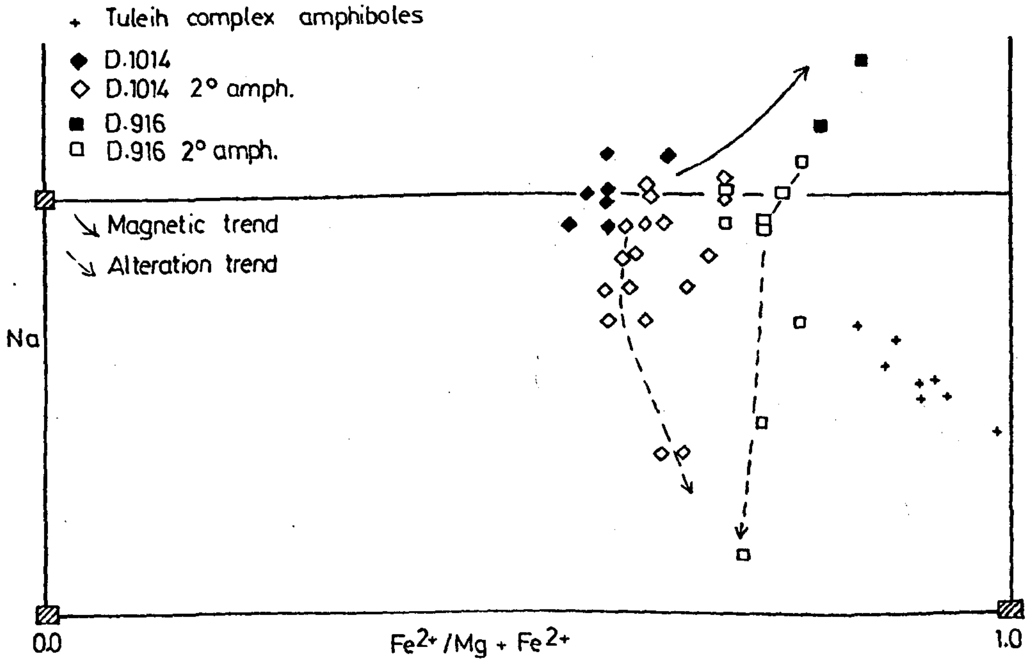

Fig. 5.16 : Na VERSUS Fe^{2+}/ Mg + Fe^{2+} FOR THE AMPHIBOLES OF D.916 AND D.1014

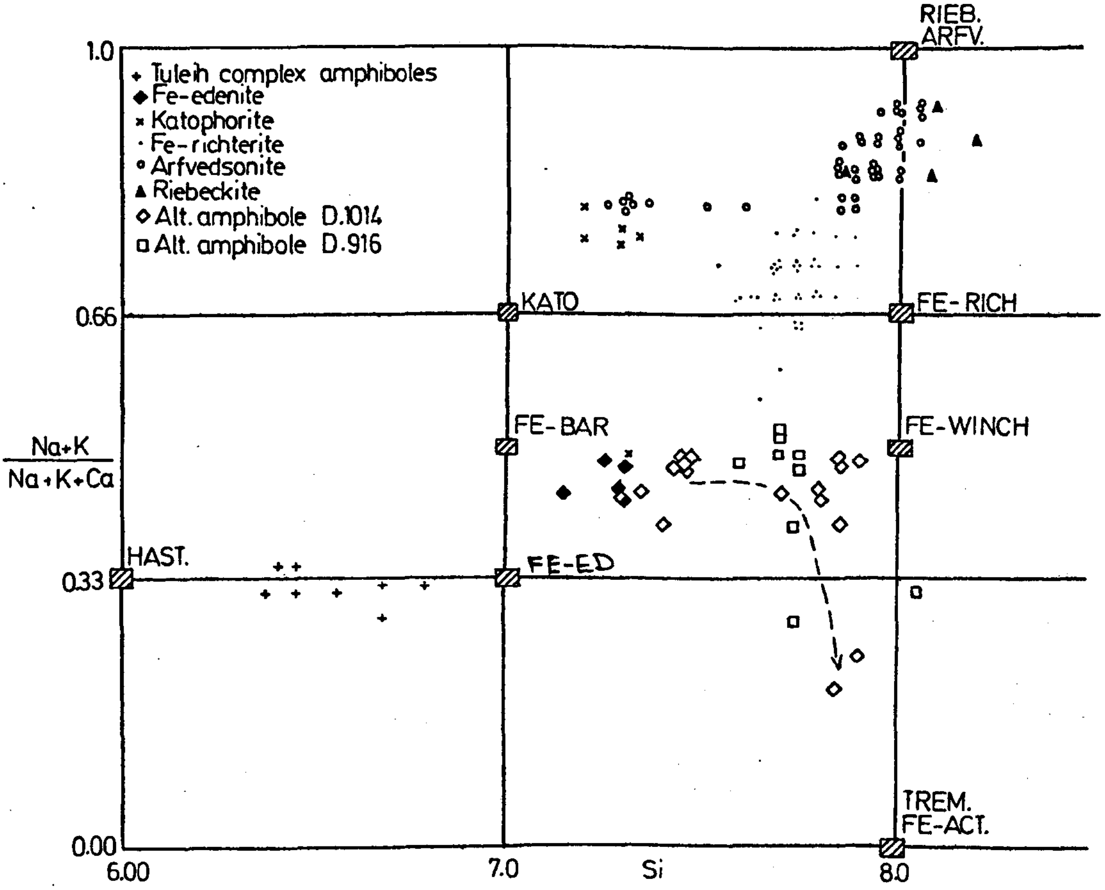

Fig. 517 : Na+K/Na+K+Ca VERSUS Si FOR THE RAS ED DOM AMPHIBOLES

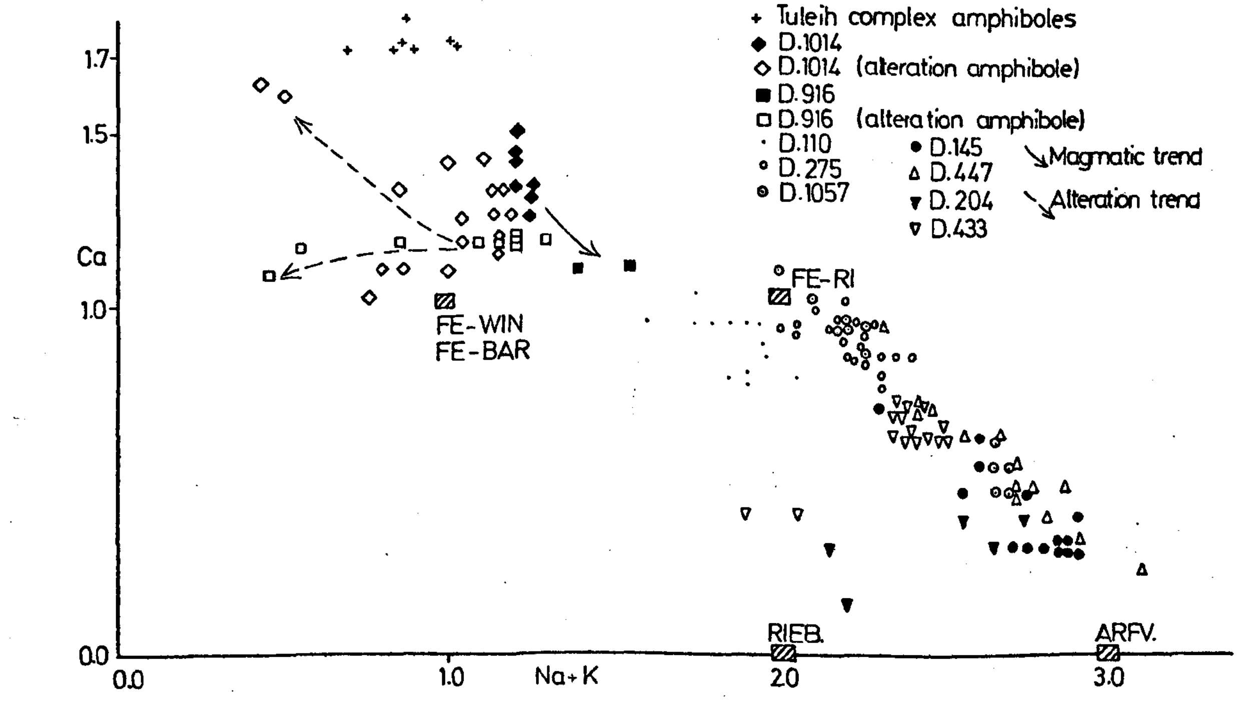

Fig. 518 : Ca RELATIVE TO Na+K FOR THE RAS ED DOM AMPHIBOLES

As mentioned above, the amphiboles of the alkali syenites and granites are zoned from cores of ferrorichterite to arfvedsonite rims (figs. 5.14). Dark blue overgrowths upon arfvedsonite, which can be either continuous or discontinuous (section 4.5.D), were also probed and are riebeckite-crossite in composition (fig. 5.14). The change from arfvedsonite to riebeckite involves continuous solid solution between end-members (fig. 5.17), as expected from the experimental results of Ernst (1962).

The dominant substitution in the series ferroedenite-ferrorichterite-arfvedsonite is that of Na for Ca, as illustrated in the triangular plot Na-Ca-K (fig. 5.19), and also in fig. 5.18 which plots Ca directly against Na+K. This substitution, and to a lesser degree that of Si for Al, is again apparent in fig. 5.20., in which Ca+Al are plotted against Na+K+Si+Ti (Borley, 1963). Both Borley's analyses and those from Ras ed Dom calculated on the basis of C site = thirteen cations, plot lower than,but parallel to,those calculated to a total of sixteen cations. This offset however disappears when the analyses are recalculated to twenty three oxygens only (see Appendix IIA for discussion), indicating it to be an artefact of the recalculation procedures, and there is no reason to doubt that the variation is smoothly continuous.

In fig. 5.21 it can be seen that Fe^{2+} increases from the ferroedenites through to the ferrorichterites (a parallel increase characterises the calcic pyroxenes; see previous section). Thereafter Fe^{3+} becomes progressively dominant in the alkali amphiboles (fig. 5.21).

Zoning in the alkali amphiboles reflects the above-mentioned substitutions but is less regular than in the pyroxenes, especially as regards the Fe^{2+}/Fe^{3+} ratio.

The Fe^{3+}-enrichment is continued into the riebeckites (fig. 5.21), but the accompanying Na-enrichment and K-depletion results in distinct sub-trends towards the riebeckite end-member in figs. 5.18 and 5.19.

The katophorites and arfvedsonites of the recrystallised assemblage of D433 are, like their pyroxene counterparts, relatively magnesian and impoverished in Fe^{2+} (fig. 5.21-B) and Si (Fig. 5.17), and plot slightly off the main magmatic trend.

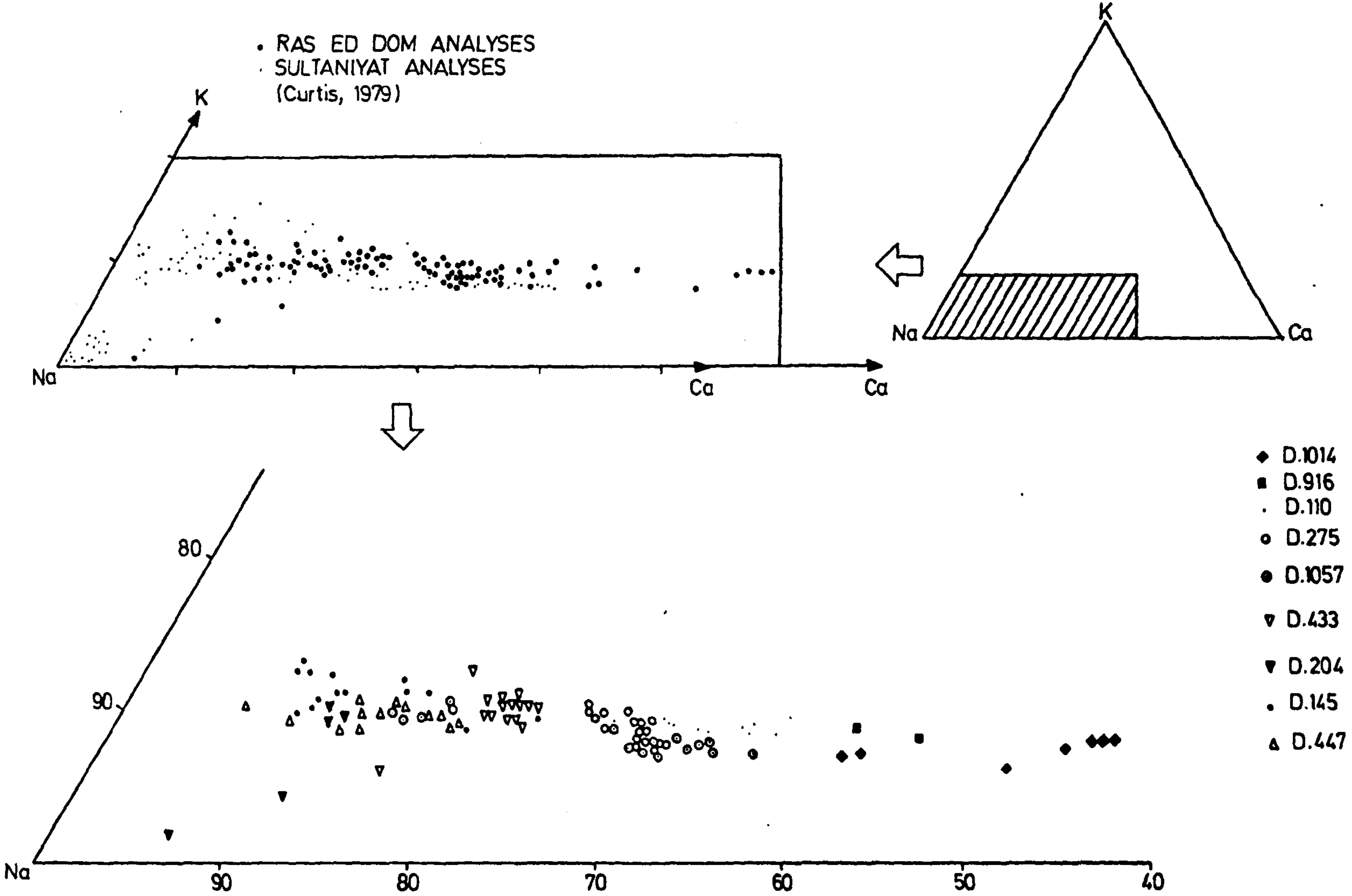

Fig. 5.19 : *AMPHIBOLE ANALYSES IN THE DIAGRAM K - Ca - Na (ATOMIC %)*

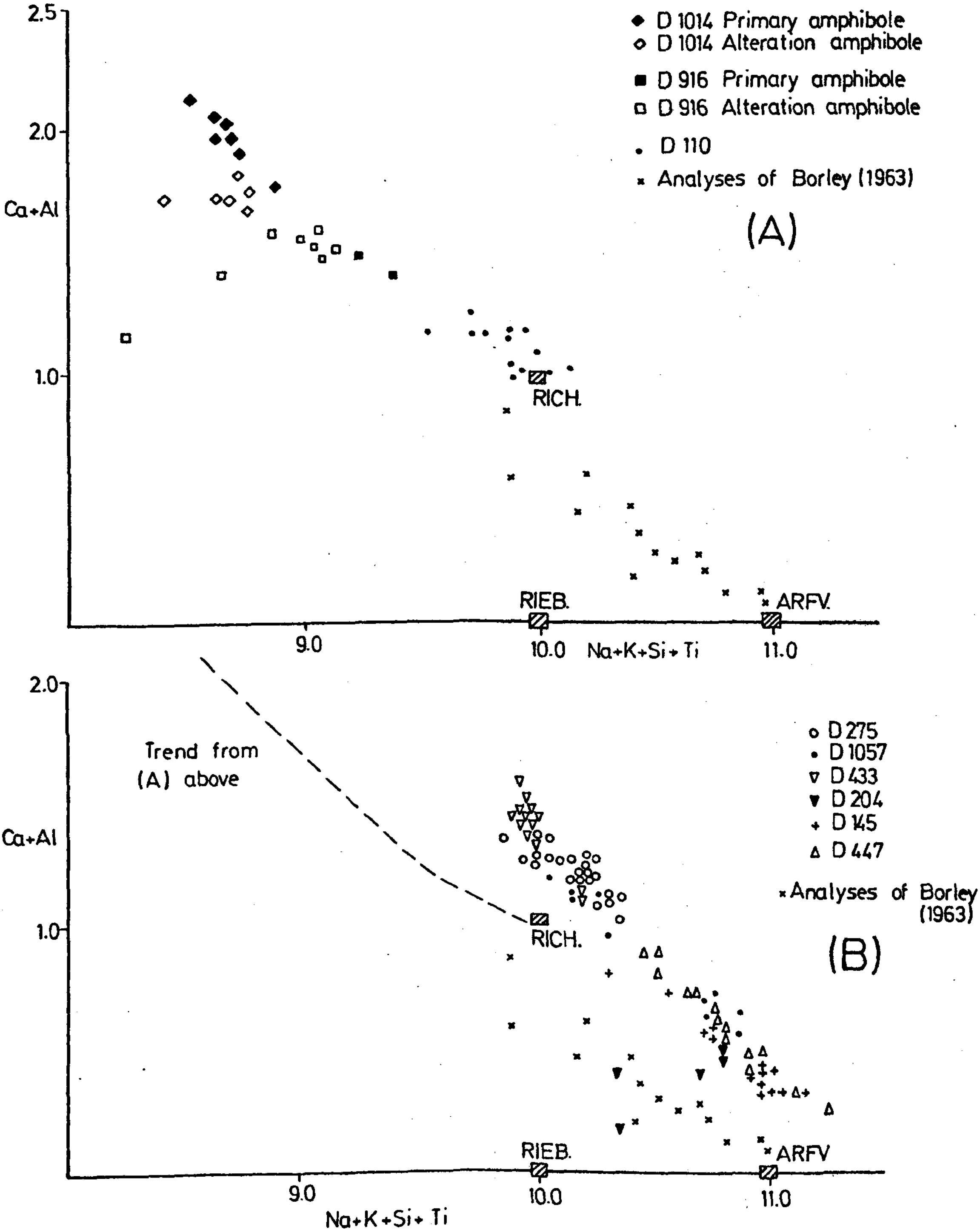

Fig. 5.20 : (Na+K+Si+Ti) VERSUS (Ca+Al) FOR THE RAS ED DOM AMPHIBOLES.
(A) AMPHIBOLES CALCULATED ON THE BASIS OF C+T =13
(B) AMPHIBOLES CALCULATED ON THE BASIS TOTAL CATION = 16;
AND RIEBECKITES C+T=13

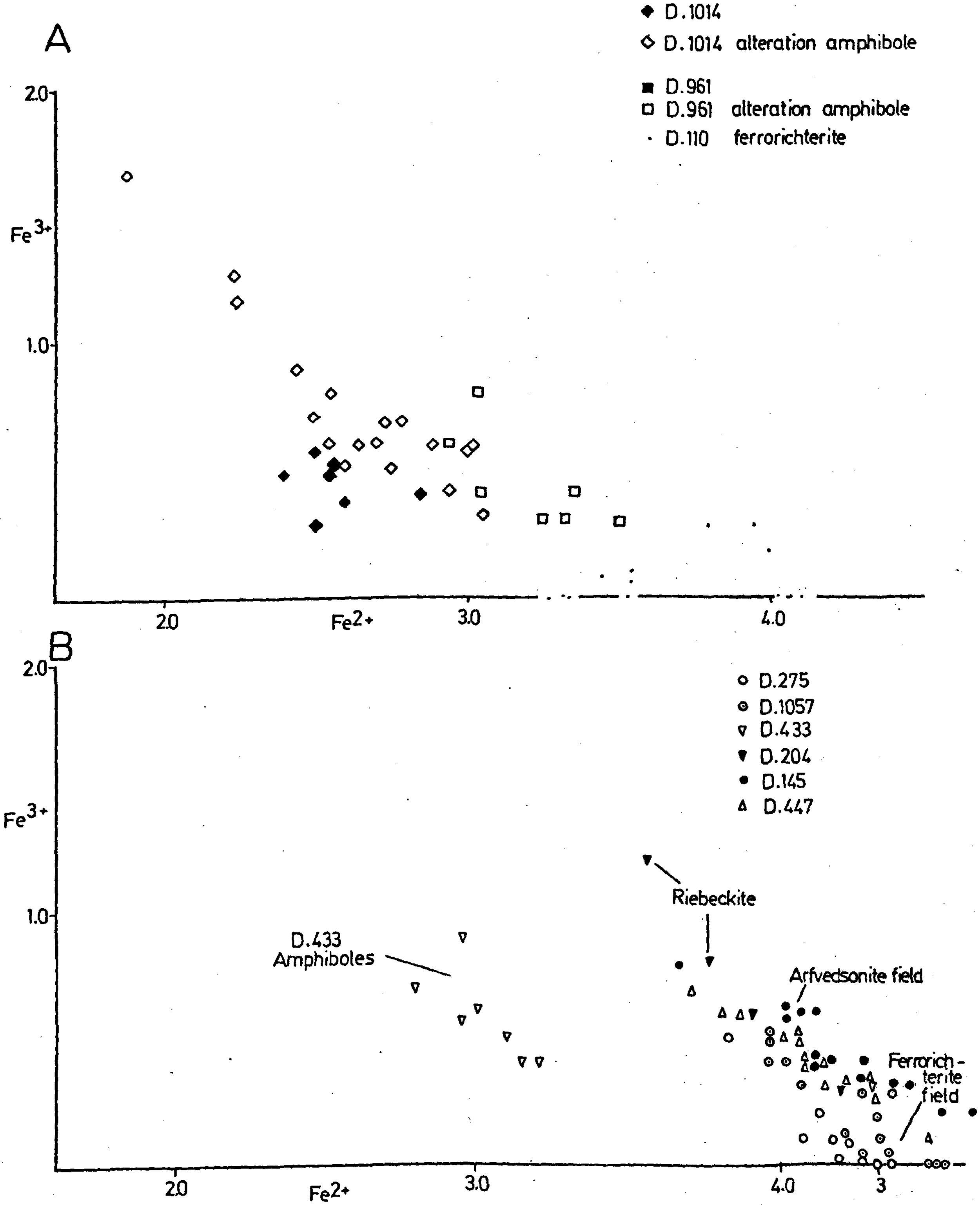

Fig. 5.21 : Fe^{2+} versus Fe^{3+} FOR THE RAS ED DOM AMPHIBOLES
A) AMPHIBOLES ON THE BASIS OF C SITE = 13 CATIONS
B) AMPHIBOLES ON THE BASIS OF TOTAL CATIONS = 16

To summarise, the smooth variation that characterises the magmatic series ferroedenite-ferrorichterite-arfvedsonite-riebeckite records the increasingly alkaline and siliceous nature of the evolving magma. In the Oslo province continuous variation from subcalcic sodian edenite through to arfvedsonite occurs (Neumann, 1976). At Ilimaussaq the range is hastingsite-katophorite-arfvedsonite (Larsen, 1976), whilst Bowden and Turner (1974) report hastingsite cores to arfvedsonite grains in the Nigerian Younger Granites. These compositional ranges are closely similar to that found in Ras ed Dom.

Chlorine in the Ras ed Dom amphiboles is concentrated in the calcic and sodic-calcic amphiboles (Appendix IIE). Values are low (< 0.1 wt.%) compared to similar compositions from Nigeria (mean value 0.7 wt.%, Borley, 1963). The alkali amphiboles are, like their Nigerian counterparts, typically Cl-free; a feature consistent with partitioning of CL into the vapour phase at the late-magmatic stage (Koster Van Groos and Wyllie, 1968; Harris, 1981).

5.5. : Biotites

Six analyses of Fe-rich biotite are presented in Appendix IIF. The analyses are from three grains belonging to the recrystallised assemblage of D433, in S13 RED. Co-existing phases are aegirine-augite, katophorite-arfvedsonite-riebeckite, and Fe-Ti oxide (sections 4.5.D.).

Allocation of elements to lattice sites indicates that either partial vacancies exist in the Z-site (totals range from 7.8 to 7.9), or that Fe^{3+} may substitute into it. Y-site totals (5.6 - 5.9) suggest that the analyses are intermediate between dominant tri-octahedral and sub-ordinate di-octahedral types. X-site vacancies are indicated by a mean site total of 1.83. Sample 3b is distinct in being Na-bearing, having over two atoms in the X-site, and showing a low Ti content compared to other biotites of comparable Fe^{2+} and Mg values.

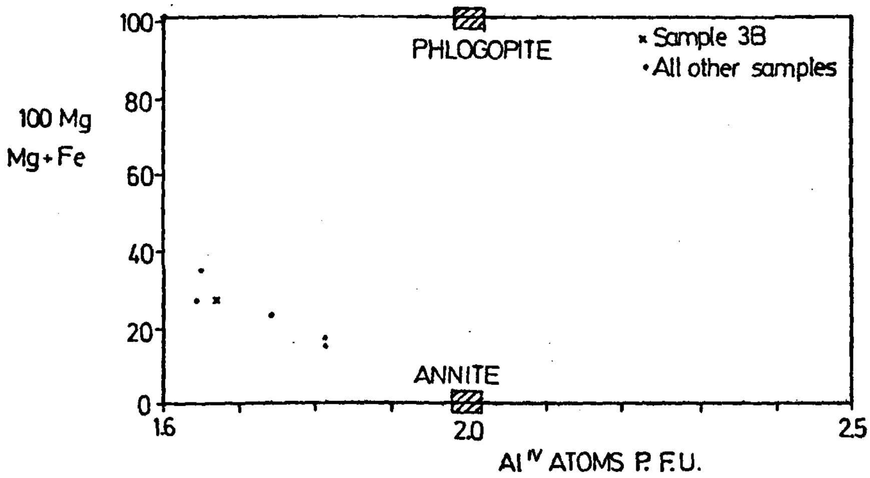

Fig. 5.22 : RAS ED DOM BIOTITES PLOTTED ONTO THE PHLOGOPITE - BIOTITE COMPOSITIONAL FIELDS

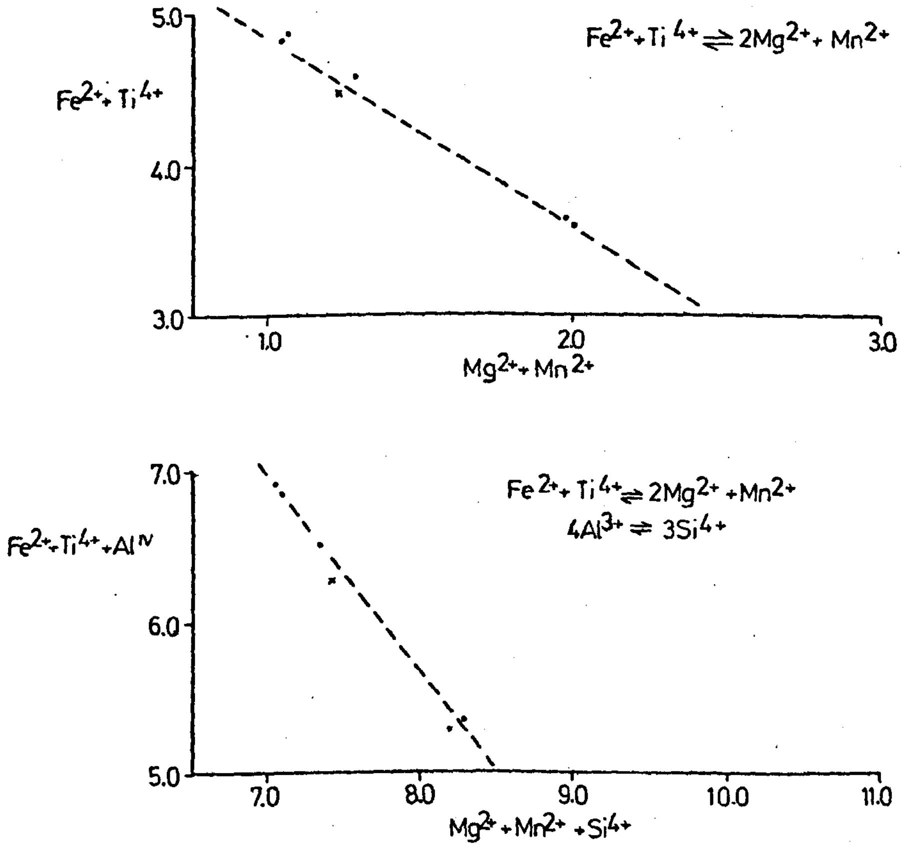

Fig. 5.23 : COUPLED SUBSTITUTIONS IN THE RAS ED DOM BIOTITES
× Sample 3B • All other samples

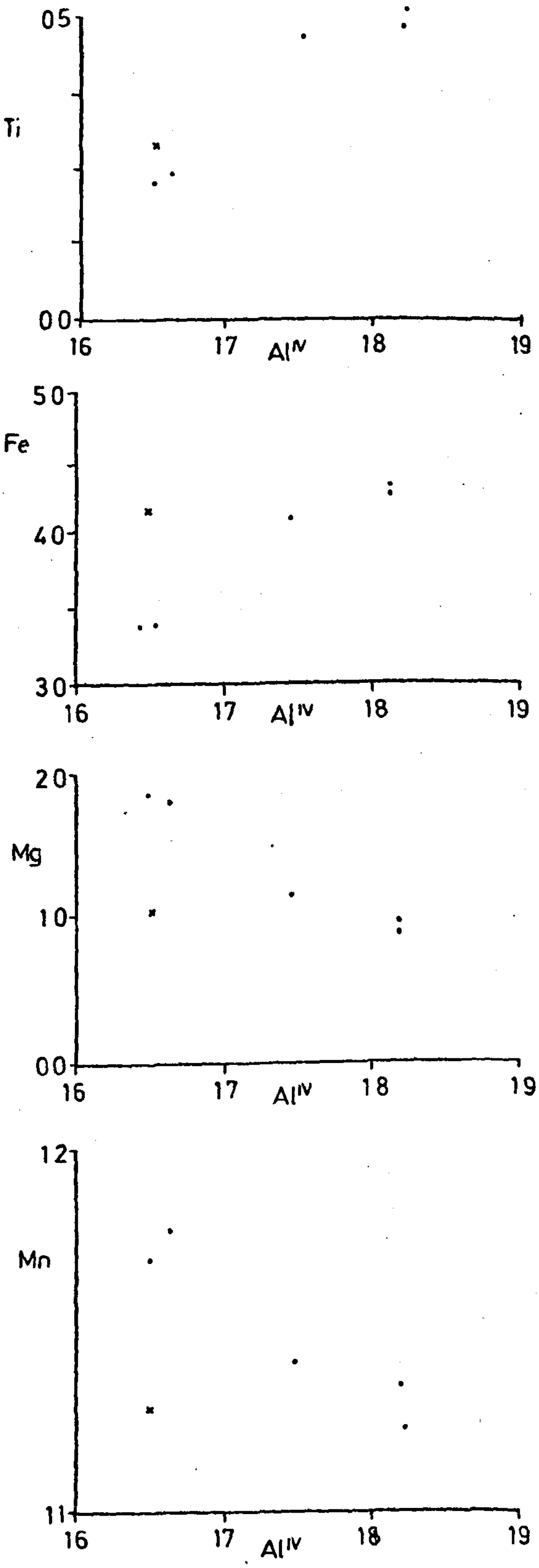

Fig. 5.24 : CHEMICAL VARIATION IN THE RAS ED DOM BIOTITES
×Sample 3B • All other samples

The biotite compositional diagram (fig. 5.22) shows that the biotites are Fe-rich, and fall on the Al-deficient side of the annite end-member. For the purposes of this plot a tri-octahedral nature is assumed. Chambers (1976) has suggested that low Al^{iv} values may indicate a fractionated, low temperature paragenesis, but in the Ras ed Dom occurrence recrystallisation is a complicating factor. The chemistry of the biotites is depicted in figs. 5.23 and 5.24. Si increases as Al^{iv} decreases recording the substitution 3Si = 4Al. Fe^{2+} and Ti decrease, while Mg and Mn increase, with decreasing Al^{iv} (fig. 5.24). The major substitution is $Fe^{2+} + Ti^{4+} = 3Mg^{2+}$, with minor substitution of Mn for Fe^{2+} (fig. 5.23). Minor Ca occurs in the X-site of three of the analyses. As with the amphiboles Cl is low or absent, suggesting partitioning of that element into the vapour phase (Harris, 1981).

5.6. : Aenigmatite

Twelve point-analyses, from two grains of aenigmatite in sample D204, S5 (RED), are presented in Appendix IIG. The textural relations of this occurrence have been discussed in section 4.7.G.

The ideal formula for aenigmatite is $Na_2Fe_5^{2+}TiSi_6O_{20}$ (Kelsey and McKie, 1964) and it has a sapphrine-like structure (Cannillo et al., 1971). The Ras ed Dom aenigmatites are unzoned, and their chemistry is summarised in fig. 5.25 where it is compared with a compilation of thirty seven analyses from oversaturated parageneses, embracing thirty one compiled by Larsen (1977), five from Mitchell and Platt (1978), and one from Ferguson (1978). The Ras ed Dom aenigmatites are depleted in Al, Ca and Mg. Ti levels are average whilst Na and Mn are relatively enriched. Si and Al generally total to less than 6 atoms p.f.u., and Fe^{3+} probably enters the Z-site to compensate (Larsen, 1977). The X-site totals cluster between 2.1 and 2.2, and this may reflect overcorrection for Na in the correction procedures (op.cit.). Ti is consistently less than I atom p.f.u., suggesting a substitution such as $Fe^{2+} + Ti^{4+} = 2Fe^{3+}$. No Zr is present, suggesting low temperatures of formation (Larsen, 1977), and the low Ca and Mg, together with rather high Mn values, suggest crystallisation from a relatively fractionated magma.

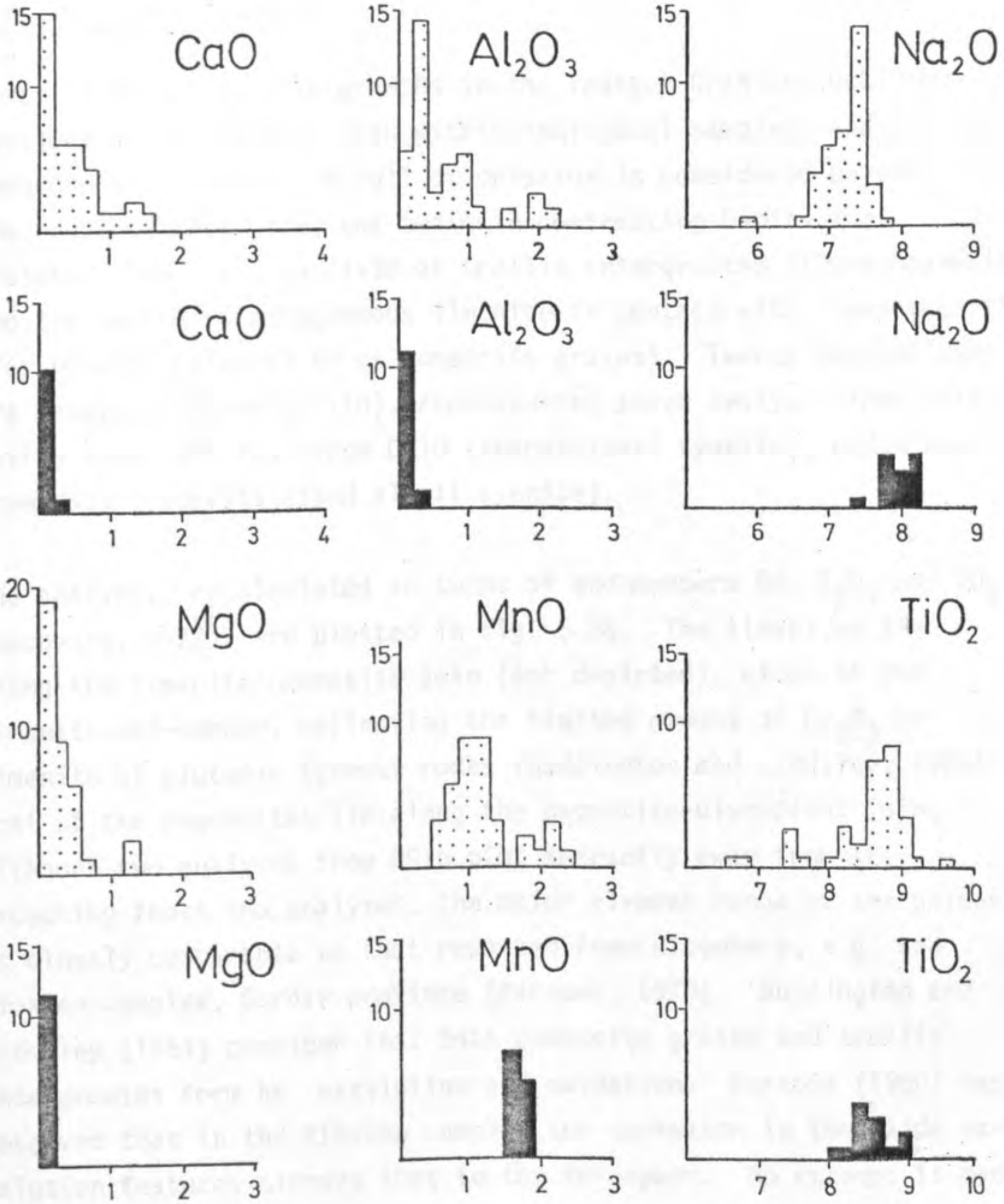

Fig. 5.25 : CHEMISTRY OF RAS ED DOM AENIGMATITES COMPARED WITH A COMPILATION OF AENIGMATITES FROM OVERSATURATED PARAGENESES.

STIPPLED DISTRIBUTIONS = COMPILED, 36 ANALYSIS
SOLID DISTRIBUTION = RAS ED DOM, 12 ANALYSIS

HORIZONTAL AXES = wt%
VERTICAL AXES = FREQUENCY

After Larsen (1977) and others (see text).

5.7. : Fe-Ti Oxides

Ilmenite-magnetite intergrowths in the Younger Granite rocks show considerable diversity, both within individual samples, and throughout the suite. A full description is considered beyond the scope of this work, but two main contrasting habits are present. The first consists of trellis intergrowths (ilmenomagnetite), and the second is homogeneous ilmenite in contact with ilmenomagnetite (for brevity referred to as composite grains). Twenty two analyses are reported (Appendix IIH), representing seven analyses from D916 (early syenite), four from D110 (transitional syenite), and eleven from D433 (recrystallised alkali syenite).

The analyses, recalculated in terms of end-members RO, R_2O_3 and TO_2 (Duchesne, 1972), are plotted in fig. 5.26. The ilmenites lie along the ilmenite-haematite join (not depicted), close to the ilmenite end-member, reflecting the limited amount of Fe_2O_3 in ilmenite of plutonic igneous rocks (Buddington and Lindsley, 1964). Most of the magnetites lie along the magnetite-ulvospinel join, although two analyses from D916 plot aberantly away from it. Excepting these two analyses, the major element range of the oxides is closely comparable to that reported from elsewhere, e.g. the Klokken complex, Gardar province (Parsons, 1979). Buddington and Lindsley (1964) consider that both composite grains and trellis intergrowths form by exsolution and oxidation. Parsons (1980) has observed that in the Klokken complex the variation in the oxide exsolution features mirrors that in the feldspars. No attempt is made to estimate the temperature of formation using the Buddington and Lindsley geothermometer, in view of the complexity of the intergrowths. Moreover, MnO values in excess of 5.0 wt.% characterise the D433 analyses, and the effect of Mn on the stability of ilmenite is not known quantitatively (Neumann, 1976).

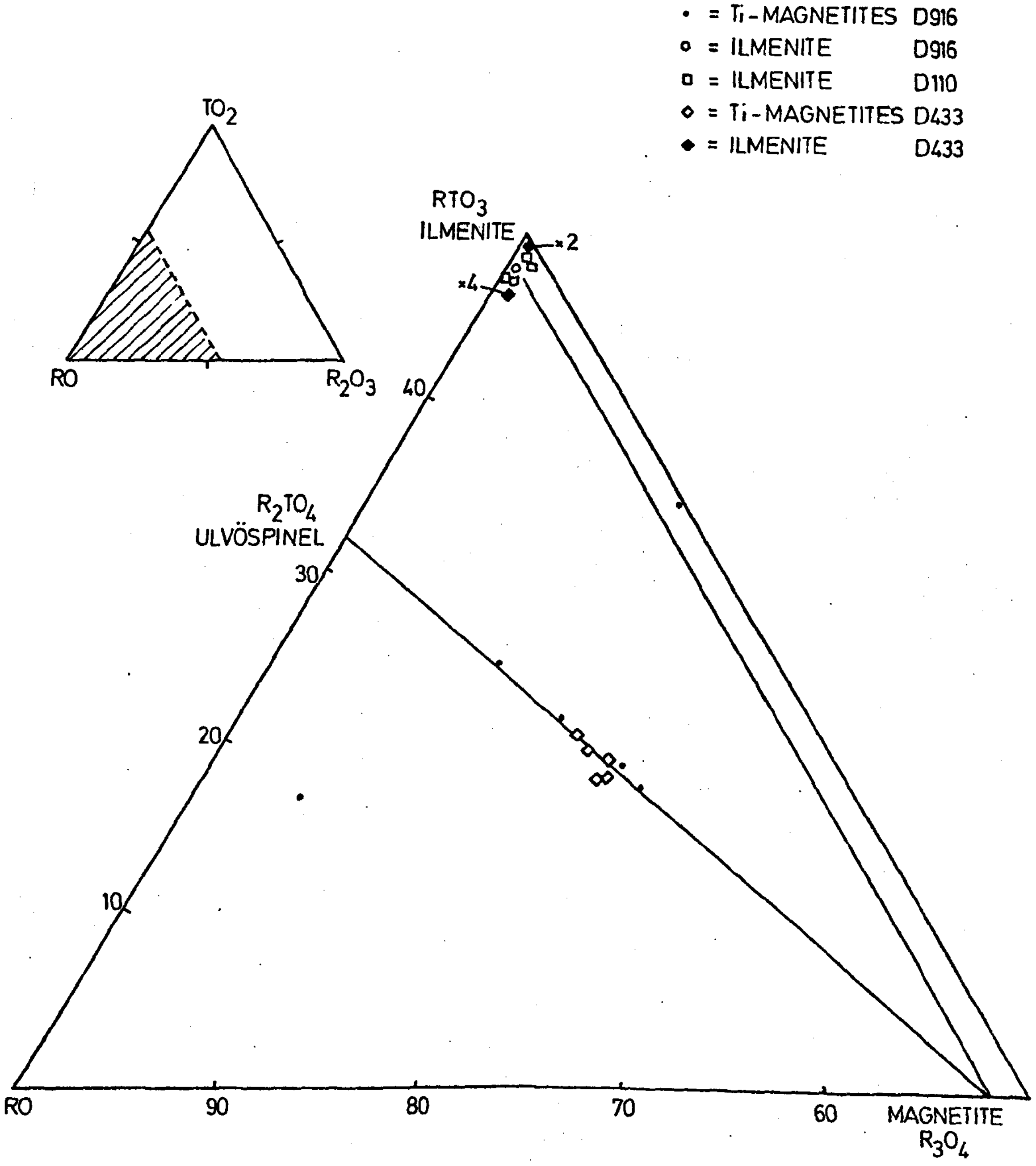

Fig. 5. 26 : Fe-Ti OXIDES FROM RAS ED DOM PLOTTED IN THE TRIANGULAR PLOT RO - TO_2 - R_2O_3 (SEE TEXT FOR DETAILS)

CHAPTER 6 : GEOCHEMISTRY

6.1. : Introduction

6.1.A. : Sampling and Analytical Techniques

One hundred and sixty seven whole-rock analyses are presented in Appendix III, comprising eight analyses of metamorphic basement rocks, one hundred and fifty seven Younger Granite analyses (ninety three from Ras ed Dom, sixty four from Abu Dom) and two from the Cainozoic basalts. Further details of the geochemical coverage are given in table 6.1. below.

Rock-Type	Number of Analyses		
	Ras ed Dom	Abu Dom	Ras ed Dom and Abu Dom
Volcanic Rocks	1	1	2
Early Syenites	9	6	15
Alkali Syenites	40	23	63
Alkali Granites	14	20	34
Dykes - Basic	-	1	1
Dykes - Syenitic	6	6	12
Dykes - Granitic	23	7	30
TOTALS	93	64	157

Table 6.1. : Whole-Rock Analytical coverage for Ras ed Dom and Abu Dom

Ras ed Dom complex has received greater attention than Abu Dom as,

i. a greater number of component intrusions are present there.

ii. the repetition of early syenite units (Map 1), involving successive batches of magma, provided a means of testing fractionation hypotheses.

All localities mentioned in this chapter and in Appendix III are recorded on Maps 4 and 5 (rear pocket).

The number of analyses per unit is roughly proportional to the unit's area, so that the most abundant rock types are best represented. Other sampling criteria included the following:

i. position in the intrusive chronology: the early syenites, as the least evolved rock-types, receive attention disproportionate to their meagre outcrop areas (table 6.2).

ii. internal variation within units: to establish the degree of in situ fractionation, e.g. in the case of S3 (RED) (see section 4.7.A.).

iii. collection of unusual samples, such as weathered or metasomatised rocks, in order to characterise the alteration processes involved.

iv. freshness of samples : sustained searching usually enabled the collection of fresh samples. In a few instances, most notably S5 (AD), this proved difficult.

The samples chosen were powdered and analysed by X-ray flouresence techniques (Brown et. al., 1973) for 10 major oxides (SiO_2, Al_2O_3, total iron as Fe_2O_3, MgO, CaO, Na_2O, K_2O, TiO_2, MnO and P_2O_5) and 10 trace elements (Ga, Rb, Sr, Y, Zr, Nb, Ba, La, Ce, Nd). FeO was determined by wet-chemical analysis. Uranium was determined on thirty samples, by instrumental neutron activation, courtesy of the Institute of Geological Sciences. Further details of the preparation and analysis of samples are presented in Appendix IIIA, together with information on the standard rocks used.

6.1.B. : Choice of Abscissae for Variation Diagrams

The Harker index (SiO_2 as abcissa, fig. 6.8) is used as a simple fractionation index since the rock fractionation series (early syenite → transitional syenite → alkali syenite → alkali granite) proposed in Chapters 4 and 5, corresponds with increasing quartz

	Muweilih		Abu Dom		Sultaniyat		Ras ed Dom		Bayuda averages			Nigeria averages*
	1	2	1	2	1	2	1	2	1	2	3	3
volcanic rocks	82.2	-	0.1	-	54.0	-	-	-	136.3	-	35.9	18.7
peraluminous granites	38.4	51.0	-	-	-	-	-	-	38.4	15.8	10.1	45.1
metaluminous rocks	8.2	10.9	1.2	3.5	16.0	22.2	3.5	5.7	28.9	11.9	7.6	17.8
alkali syenites	-	-	19.4	55.9	20.5	28.5	33.5	54.2	73.4	30.1	19.3	3.8
alkali granites	28.7	38.1	14.1	40.6	35.5	49.3	24.8	40.0	103.1	42.2	27.1	14.0
total area (km^2)	75.3		34.7		72.0		61.8		380.1			

Table 6.2 : Outcrop areas of the principal rock-types in the Ban-Gidid - Ras ed Dom massif.
column 1 : area in km^2.
column 2 : % of total area of intrusive rocks.
column 3 : % of total area of all rock-types. * data from Turner (1976). Does not include the Niger Younger Granites.

content. Macdonald (1968) advocates use of a modified Differention Index (Thornton and Tuttle, 1960), called the Fractionation Index (F.I.), to depict variation in alkaline suites. The F.I. is calculated as the sum or normative Q + Or + Ab + Ac + Ns. In the rocks under discussion the F.I. values are high, consistent with a high degree of fractionation, and the resultant plots are more cluttered. For this reason no figures with the F.I. as abscissa are included in the text.

Zr is used as an abscissa as a positive correlation between acid rock alkalinity (as recorded by the Na_2O+K_2O/Al_2O_3 ratio; see 6.1.D. below) and Zr content has been reported (Siedner, 1965; Bowden, 1966; Curtis, 1979; Watson, 1979). The fact that zircon accompanies late-formed aegirine in some of the rocks suggests that it is also sensitive to late-magmatic processes.

6.1.C. : Range of SiO_2 Values

Histograms of SiO_2 values, for Ras ed Dom and Abu Dom, are presented in fig. 6.1. The distributions for the plutonic rocks are bimodal, with a predominance of syenitic rock-types and a lesser granitic peak. In contrast granitic compositions predominate in nearby Sultaniyat complex (Curtis, 1979). The combined dyke histogram (RED and AD) shows a marked peak for acid compositions, and although based on a smaller number of samples, the predominance is supported by field observations.

A more balanced view of SiO_2 range in the Bayuda Younger Granites is obtained from the histogram of fig. 6.2., which combines data (plutonic, hypabyssal and volcanic) from Ras ed Dom, Abu Dom and Sultaniyat complexes. The result is a bimodal distribution in which acid lithologies are dominant, but less markedly so. The respective frequencies for the intervals 60-70% SiO_2 and 70-80% SiO_2, are one hundred and forty four and one hundred and sixty two respectively. The minimum at 68-72% SiO_2 also occurs in the Garder province (Macdonald, 1969; Upton et al., 1971; Upton, 1974), and might be construed as indicating that the syenites and granites have contrasted origins. Evidence against this is presented in

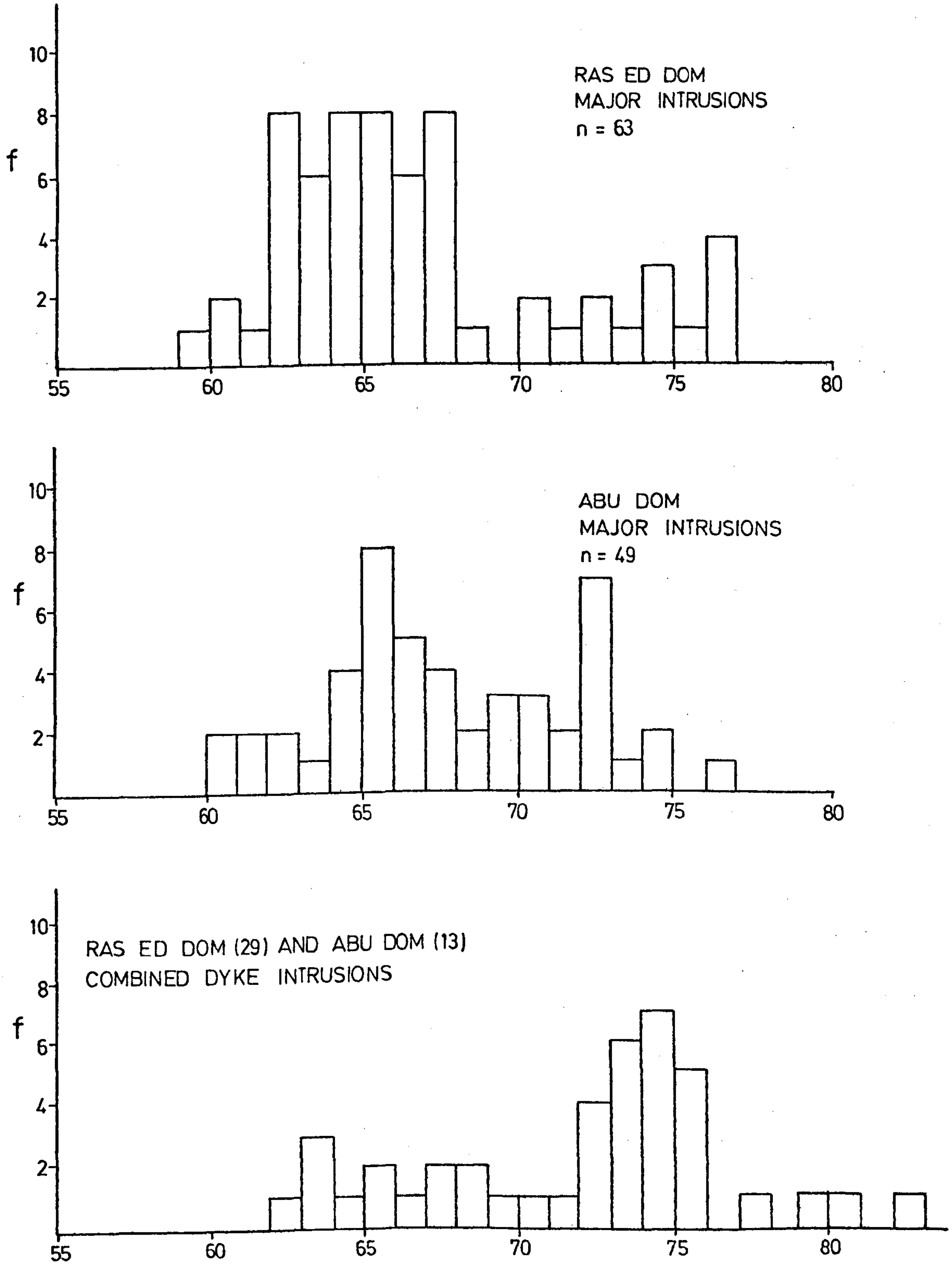

Fig. 6.1 : HISTOGRAMS OF SiO_2 VALUES (wt.%) FOR RAS ED DOM AND ABU DOM

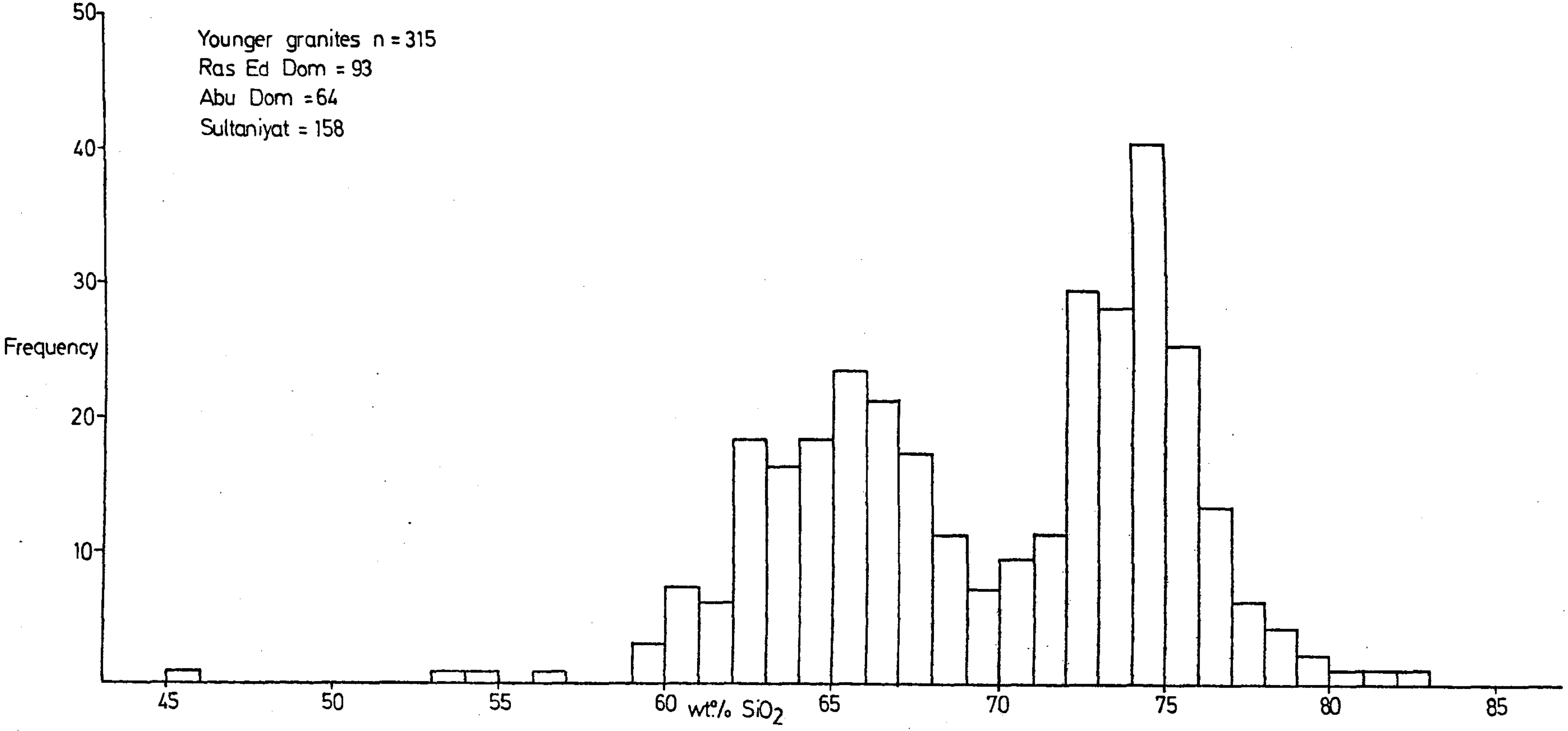

Fig. 6.2 : HISTOGRAM OF SiO_2 (wt.%) VALUES FOR ROCK ANALYSES OF SULTANIYAT, RAS ED DOM AND ABU DOM COMPLEXES.

ensuing sections, and it is more likely that liquids in the minimum compositional range were too viscuous to separate and intrude with facility. This situation would be offset in the more acid compositions by rising volatile and excess alkali content (Upton et. al., 1971).

The basic dyke from loc. 183 in Abu Dom, the only basic rock encountered during the mapping, is included in fig. 6.2. A marked gap separates it from the intermediate rocks, but more data would be needed to substantiate the reality of this gap. The basalt-trachyte series of volcanic rocks present in Muweilih complex (McCormac, pers. comm.) may bridge the gap in part, and would establish whether the so-called Daly gap (53-57% SiO_2), found in some oceanic suites (Chayes, 1963; Baker, 1968) and at Gardar (Upton, 1974), is present in the Bayuda rocks.

An alternative approach to assessing the range of silica levels is consideration of outcrop areas of major rock-types. Table 6.2 shows that in the Ban Gidid - Ras ed Dom chain (Map 3, rear pocket) alkali granites (42%) predominate over alkali syenites (30%), and these proportions suggest that fig. 6.2 is a reasonable estimate of SiO_2 distributions in the suite. Syenites are markedly less common in the Nigerian Younger Granites (table 6.2), but the proportion increases when data from Niger are included (Bowden and Turner, 1974).

6.1.D. : Alkalinity

In chapter 4 the presence of sodic pyriboles was accepted as a modal measure of alkalinity. Chemical parameters of alkalinity are now reviewed.

i. Peralkalinity and the Agpaitic Ratio

Shand (1922) proposed a division of igneous rocks into 4 classes according to the degree of alumina saturation as shown in table 6.3. From the table it is apparent that some of the basement gneisses are peraluminous. The Younger Granites embrace both metaluminous-subaluminous (early syenites) and peralkaline (alkali syenites and granites) rock types.

	PERALUMINOUS	METALUMINOUS	SUBALUMINOUS	PERALKALINE
	$Al_2O_3 > (CaO+Na_2O+K_2O)$ m.p.	$Al_2O_3 < (CaO+Na_2O+K_2O)$ but $Al_2O_3 > (Na_2O+K_2O)$ m.p.	$Al_2O_3 \simeq (Na_2O+K_2O)$ m.p.	$Al_2O_3 < (Na_2O+K_2O)$ m.p.
characteristic normative minerals	corundum (C)	abundant anorthite (An) In current usage little distinction is made between these two categories (Carmichael *et al.*,1974)	minor An	acmite (Ac) sodium silicate (Ns)
typical modal minerals	muscovite topaz	biotite, hornblende		aegirine richterite arfvedsonite riebeckite aenigmatite
rock-types in this study	basement gneisses	basement gneisses and early syenites		alkali syenites and alkali granites

Table 6.3 : Classification of igneous rocks in terms of alumina saturation (Shand, 1922). Note that the petrographic term 'alkali' (Streckeisen, 1967) corresponds with the chemical condition of peralkalinity. m.p. = molecular proportions.

Fig. 6.3. (opposite) : Agpaitic ratios versus SiO_2 wt.% values

A : RAS ED DOM - PLUTONIC ROCKS

▲ S1
▼ S2
△ S3
♦ S4
▽ S5
○ S6
⦶ S7
◓ S8
⊖ S9
◒ S10
▬ S11
⊘ S12
◐ S13
◑ S14
⦸ S15
◇ IT1
● IT2
· IT3
◆ D209 - early syenite raft in S6
+ G1
× G2
✚ MG1
✗ MG2

B : RAS ED DOM AND ABU DOM - DYKE AND VOLCANIC ROCKS

Ras ed Dom

○ syenitic dykes
+ granitic dykes
● rafted sample of tuff, loc. 307

Abu Dom

⊙ syenitic dykes
× granitic dykes
▲ ignimbrite, Abu Dom Volcanic Group, loc. R101

C : ABU DOM - PLUTONIC ROCKS

▲ S1
△ S2
▽ S3
○ S4
⊙ S5
× G1
+ G2

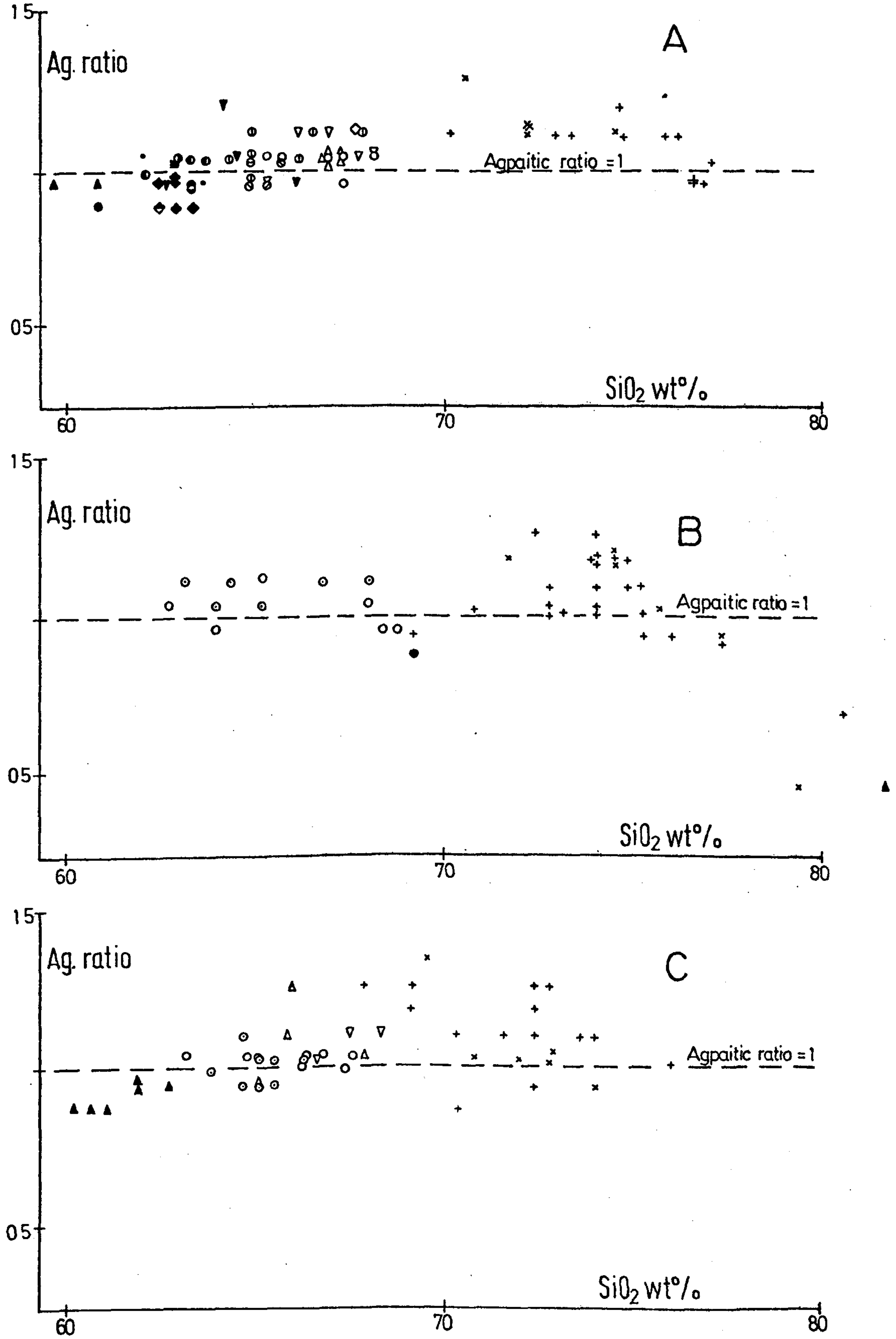

fig.6.3 : Agpaitic ratios versus SiO_2 wt.% values (explanation opposite).

Fig. 6.4. (opposite) : Agpaitic ratios versus Zr.

A : RAS ED DOM - PLUTONIC ROCKS

▲ S1
▼ S2
△ S3
◆ S4
▽ S5
○ S6
⦶ S7
● S8

⊖ S9
◒ S10
▬ S11
⊘ S12
◐ S13
◑ S14
⦸ S15
◇ IT1

• IT2
· IT3
⬘ D209 - early syenite raft in S6
+ G1
× G2
✢ MG1
✗ MG2

B : RAS ED DOM AND ABU DOM - DYKE AND VOLCANIC ROCKS

Ras ed Dom

○ syenitic dykes
+ granitic dykes
• rafted sample of
tuff, loc. 307

Abu Dom

⊙ syenitic dykes
× granitic dykes
▲ ignimbrite, Abu Dom
Volcanic Group, loc. R101

C : ABU DOM - PLUTONIC ROCKS

▲ S1
△ S2
▽ S3
○ S4
⊙ S5
× G1
+ G2

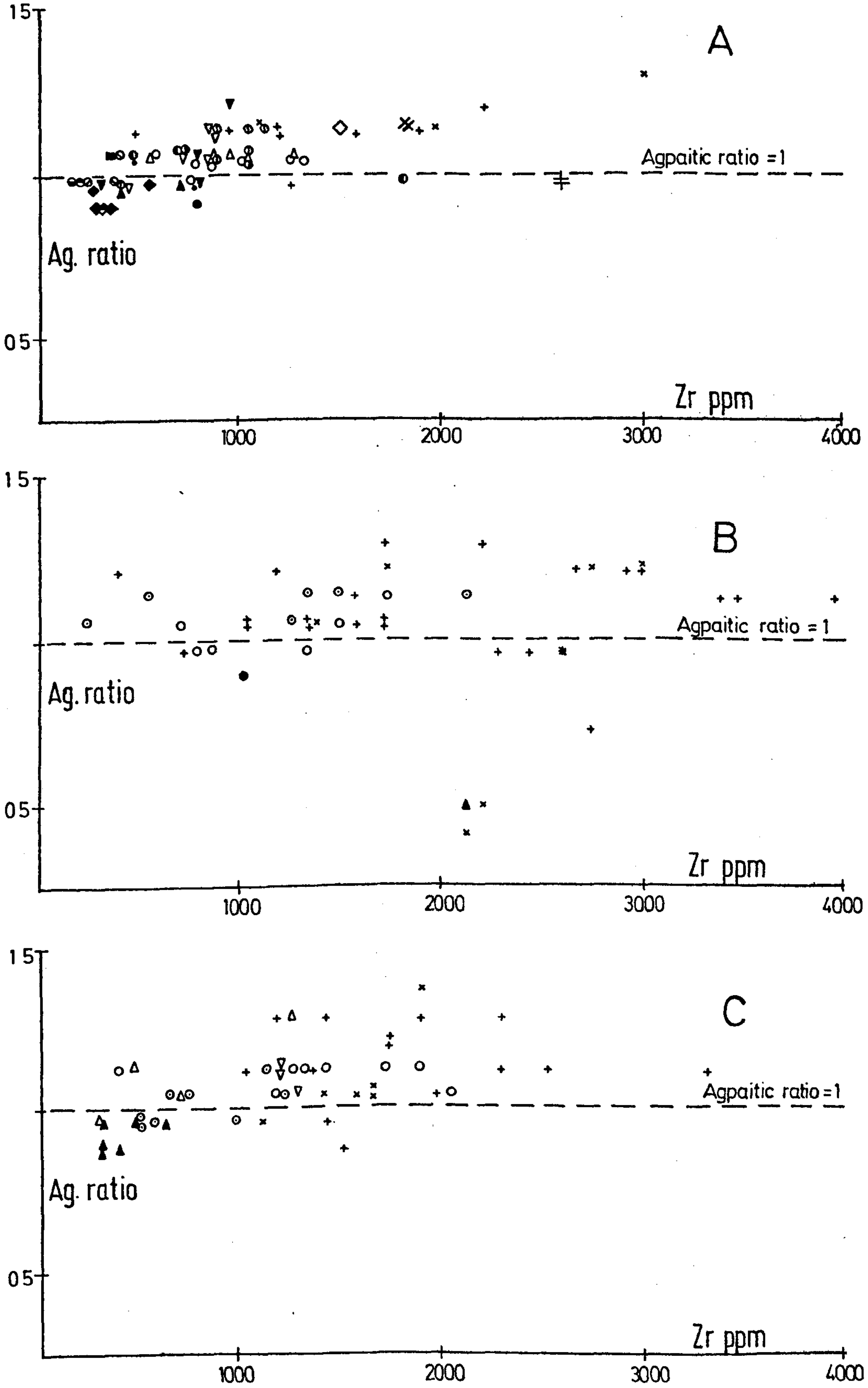

fig.6.4 : Agpaitic ratios versus Zr (explanation opposite).

A closely allied concept is that of agpaicity (Ussing, 1912). The agpatic ratio is defined as $(Na_2O + K_2O)/Al_2O_3$ (molecular proportions). Where the ratio exceeds unity the rock is agpaitic, and where it is less than unity the rock is plumasitic (Goldschmidt, 1930). The implications of this parameter upon the sequence of crystallisation has already been used in chapter 4 to distinguish agpaitic and plumasitic orders of crystallisation (section 4.7.A). The division between plumasitic and agpaitic rocks corresponds with the distinction between aluminous and peralkaline categories on Shand's scheme (table 6.3.).

Agpaitic ratios and normative Ac values for the analysed rocks are quoted in Appendices IIID and IIIE. The ratio increases with fractionation, as recorded by SiO_2 and Zr in figs. 6.3 and 6.4.

ii. Alkalinity Ratio (Wright, 1969)

Wright (1969) has proposed an alkalinity ratio, as follows,

$$\frac{Al_2O_3 + CaO + (Na_2O + K_2O)}{Al_2O_3 + CaO - (Na_2O + K_2O)} \quad \text{wt.\% oxides}$$

In conjunction with wt.% SiO_2 the ratio distinguishes between calc-alkali and alkaline rock series (figs. 6.5 and 6.6). The location of the field boundaries are based on average igneous rock compositions of typical examples (op.cit.). The early syenites fall into the alkaline field, while the alkali rocks range into the peralkaline field. The ratio is less sensitive than the agpaitic ratio, however, in that many of the alkali syenites (which are peralkaline in the original sense of Shand, 1922) plot into the alkaline field. Sample D781A (GI, AD) has the highest value of the alkalinity ratio, and as sodic pyriboles account for 20% of the mode of this rock in this instance, at least, the ratio is sensitive to the modal importance of such minerals.

The metasomatised sample (D129, section 4.5.D) does not plot well into peralkaline field, as the metasomatism has not affected the total alkalies present (see table 6.10). The high agpaitic ratio of 1.17 in contrast, shows that the latter ratio is sensitive to the metasomatism.

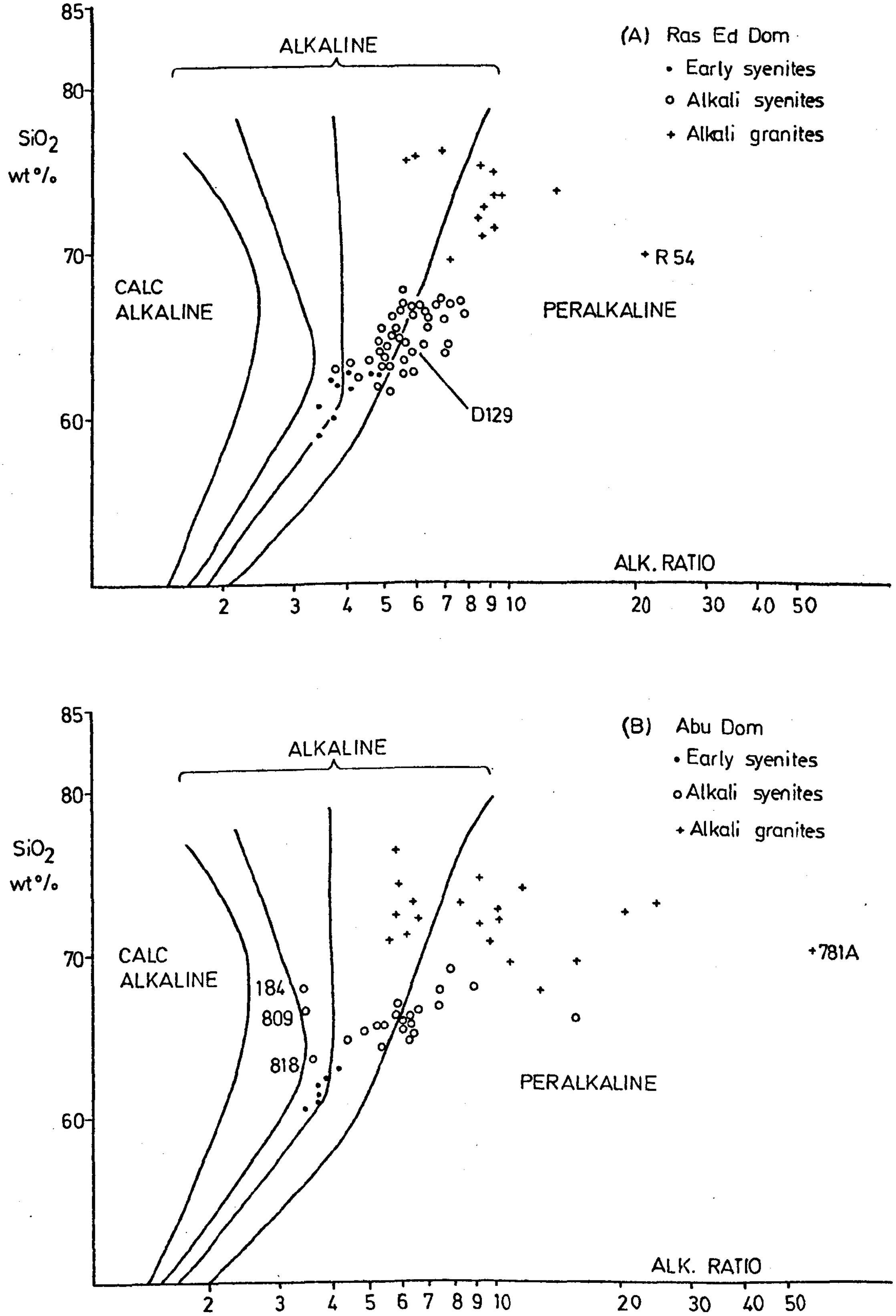

Fig 6.5 : ALKALINITY RATIO VARIATION DIAGRAM (after Wright, 1969) FOR THE PLUTONIC ROCKS OF (A) RAS ED DOM. (B) ABU DOM.

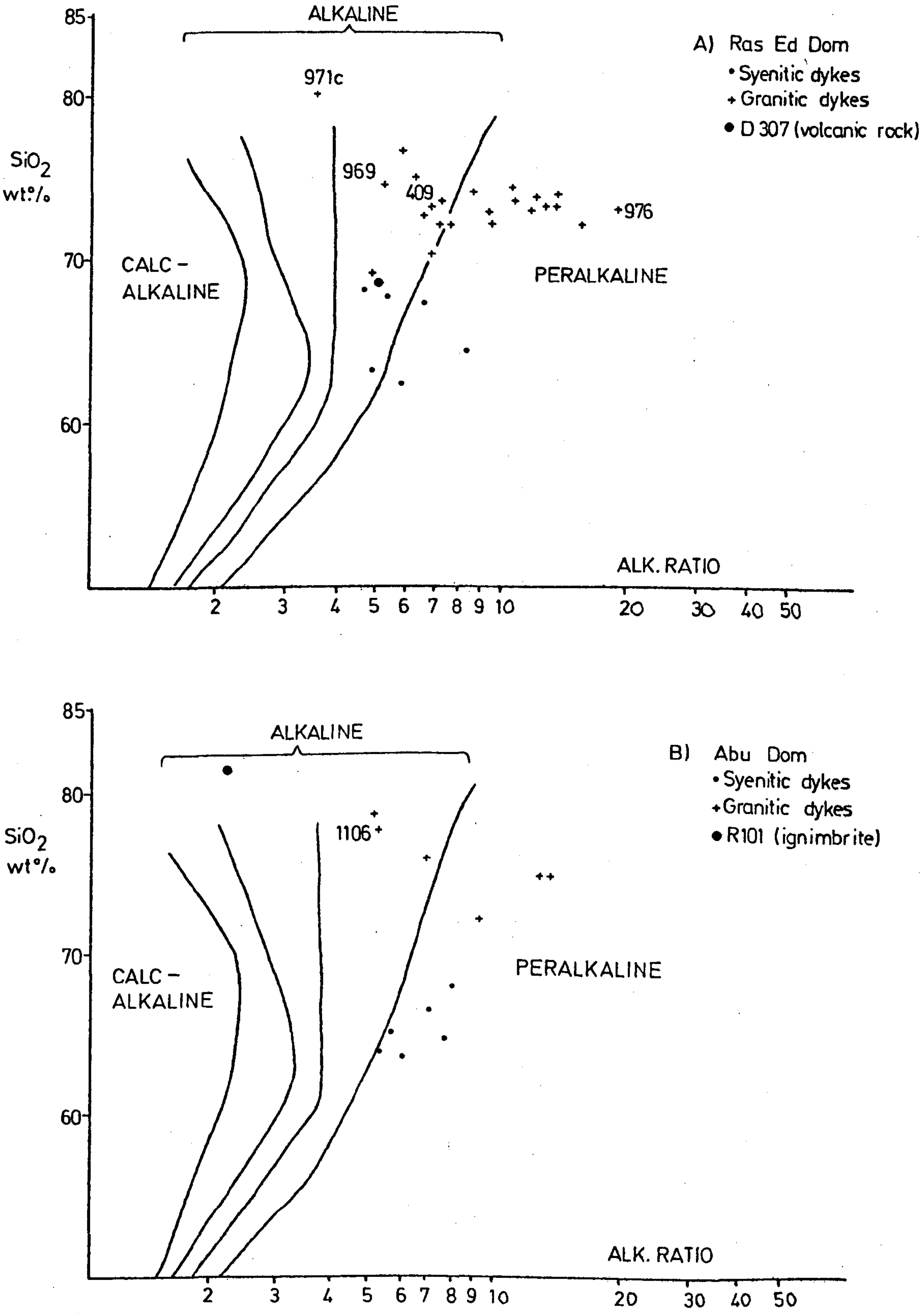

Fig. 6.6 : ALKALINITY RATIO VARIATION DIAGRAM (after Wright, 1969) FOR THE DYKE ROCKS OF (A) RAS ED DOM. (B) ABU DOM.

In fig. 6.6.-A+B, haematised peralkaline granite dykes plot well into the alkaline fields, showing that the alkalinity ratio is sensitive to such alteration processes.

iii. Macdonald and Bailey Classification (1973)

Macdonald and Bailey (1973) have proposed a classification of oversaturated peralkaline volcanic rocks, based on a plot of normative quartz versus normative femics (fig. 6.7). Dyke and volcanic rocks from Ras ed Dom and Abu Dom are plotted according to this scheme in fig. 6.7.

Although the syenitic analyses are few in number there appears to be a continuous transition from intermediate to acid compositions. The syenitic rocks are comenditic , whilst the acid rocks are transitional towards pantellerites. As with the other parameters discussed above, this records an increase in peralkalinity with fractionation.

6.1.E. : Geochemical Characterisation of the Principal Rock-Types

Before embarking upon a detailed discussion of the chemical variation, it is useful to summarise the data in Appendix III in terms of 3 main rock-types, namely early syenite, alkali syenite and alkali granite. The transitional syenites are included in the early syenite category as the few analyses available show strong affinities with that group.

i. Early Syenites

These rocks are notable for their relatively high levels of CaO and MgO, and are characterised by normative An ($\geqslant$ 5). Normative ilmenite, magnetite and apatite are also typically high, in accord with their modal abundances. Ac is absent, the agpaitic ratio is less than unity, and K/Rb ratios are greater than 500.

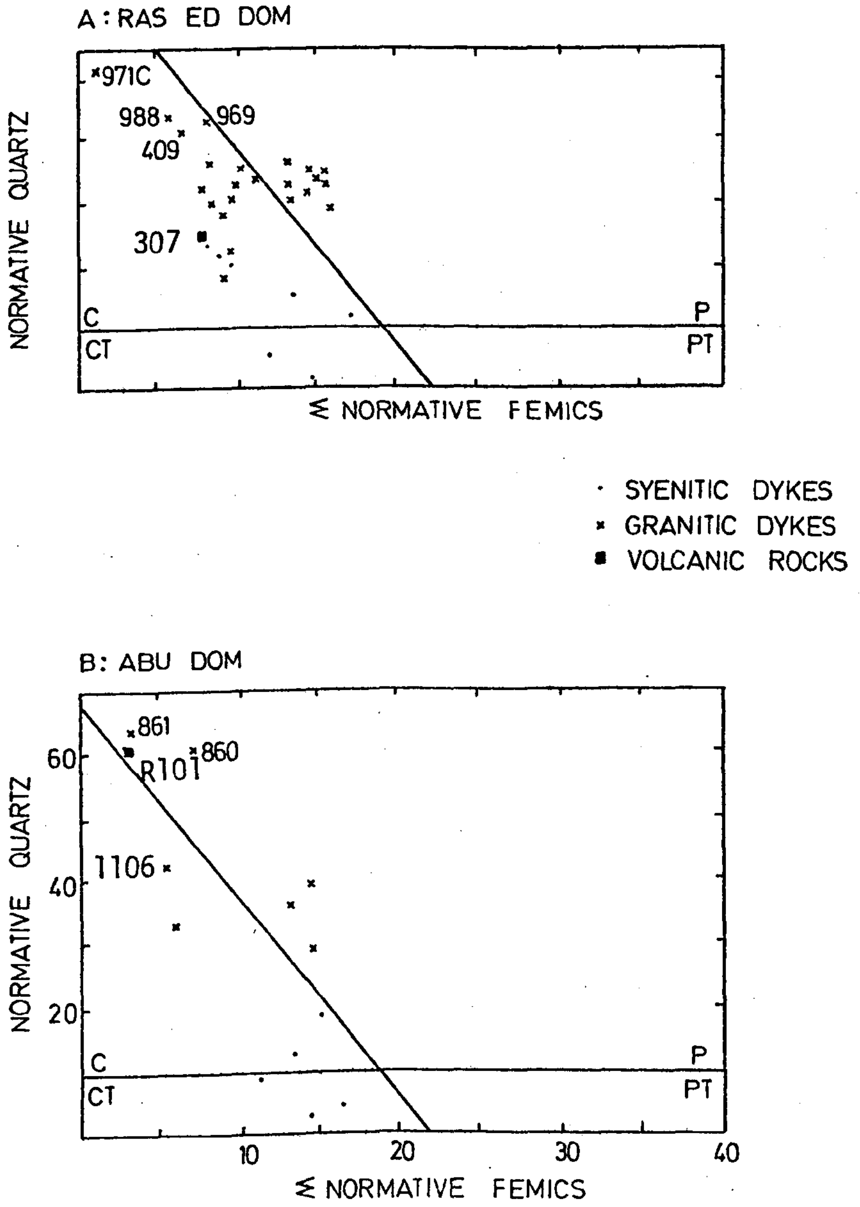

Fig. 6.7 : MINOR INTRUSIONS AND VOLCANIC ROCKS OF RAS ED DOM AND ABU DOM PLOTTED IN THE CLASSIFICATORY SCHEME FOR PERAKALINE, QUARTZ-NORMATIVE EXTRUSIVE ROCKS, AFTER MACDONALD AND BAILEY (1973)

C = Comendite field	CT = Comenditic trachyte field
P = Pantellerite field	PT = Pantelleritic trachyte field

ii. Alkali Syenites

Chemically these rocks are intermediate between the early syenites and the granites. An is low or absent, Ac may reach values of about 8. Mt, Il and Ap are present in the norm, but values are lower than in the early syenites. The agpaitic ratio is above but close to unity. K/Rb ratios are typically about 500.

iii. Alkali Granites

Trends of depletion in MgO, Cao and Al_2O_3 are continued into the granites. Ac is high, averaging about 7-8 but occasionally reaching values of about 14. Ns occurs only rarely in the norm. The agpaitic ratio exceeds unity, except in altered rocks. The total of Mt and Il is less than 3, and Ap is also low, less than 0.1. K/Rb ratios are generally less than 500.

6.1.F. : Effects of Alteration Upon Rock Chemistry

Two examples of alteration, namely haematisation and silification, are discussed.

In table 6.4. sample D132 of GI (RED), in which the mafic minerals have been haematised, is compared with an average GI composition based on eight unaltered samples. The main changes, taking into account standard deviations, are loss of Na_2O and oxidation of iron. Both features are consistent with hydration (Macdonald and Bailey, 1973).

D860 and 861 (table 6.4) are two cone sheets north of Abu Dom, which have been haematised and silicified. In this-section graphic intergrowths of replacement origin are abundant. An average of four fresh acid dyke-rock analyses serves as a basis for comparison. SiO_2 and normative quartz are high in the altered samples, while Na_2O and to a lesser degree K_2O are depleted. The effects of oxidation of iron are difficult to detect, however, in view of the highly oxidised state of the dyke-rocks in general (column 6, table 6.4). As with the previous example corundum may appear in the norm giving an erroneous impression of a peraluminous nature.

wt.%	1	2	3	4	5	6	7
SiO2	76.39	74.18	2.01	79.17	82.90	73.99	1.46
Al2O3	11.10	10.93	0.90	9.60	10.33	10.22	0.92
Fe2O3	3.54	3.61	1.20	6.33	2.67	5.61	1.59
FeO	0.22	1.55	0.83	0.16	0.25	0.60	0.30
MgO	0.15	0.08	0.01	0.10	0.02	0.09	0.02
CaO	0.28	0.36	0.09	0.59	0.05	0.40	0.17
Na2O	3.34	4.43	0.47	1.18	1.14	4.28	0.31
K2O	4.71	4.54	0.24	2.40	2.35	4.45	0.29
TiO2	0.18	0.21	0.12	0.21	0.25	0.22	0.07
MnO	0.07	0.07	0.03	0.23	0.01	0.09	0.04
P2O5	0.02	0.02	0.00	0.02	0.02	0.02	0.00

1. D132; G1, Ras ed Dom; haematised mafic minerals.
2. G1, Ras ed Dom; average of 8
3. Standard deviation for column 2.

4 and 5. D860 and D861; cone-sheets North of Abu Dom; haematised and silicified.
6. Abu Dom; average of 4 fresh acid dykes.
7. Standard deviation for column 6.

Table 6.4 : Effects of Alteration processes on the bulk chemistry of Younger Granite rocks.

Fig. 6.8. (opposite) : Major element variation relative to SiO_2

A : RAS ED DOM - PLUTONIC ROCKS

▲ S1
▼ S2
△ S3
◆ S4
▽ S5
○ S6
⦶ S7
◓ S8

⊖ S9
◒ S10
▬ S11
⊘ S12
◐ S13
◑ S14
⦸ S15
◇ IT1

● IT2
· IT3
⬖ D209 - early syenite raft in S6
+ G1
× G2
✚ MG1
✖ MG2

B : RAS ED DOM AND ABU DOM - DYKE AND VOLCANIC ROCKS

<u>Ras ed Dom</u>

○ syenitic dykes
+ granitic dykes
● rafted sample of tuff, loc. 307

<u>Abu Dom</u>

⊙ syenitic dykes
× granitic dykes
▲ ignimbrite, Abu Dom Volcanic Group, loc. R101

C : ABU DOM - PLUTONIC ROCKS

▲ S1
△ S2
▽ S3
○ S4
⊙ S5
× G1
+ G2

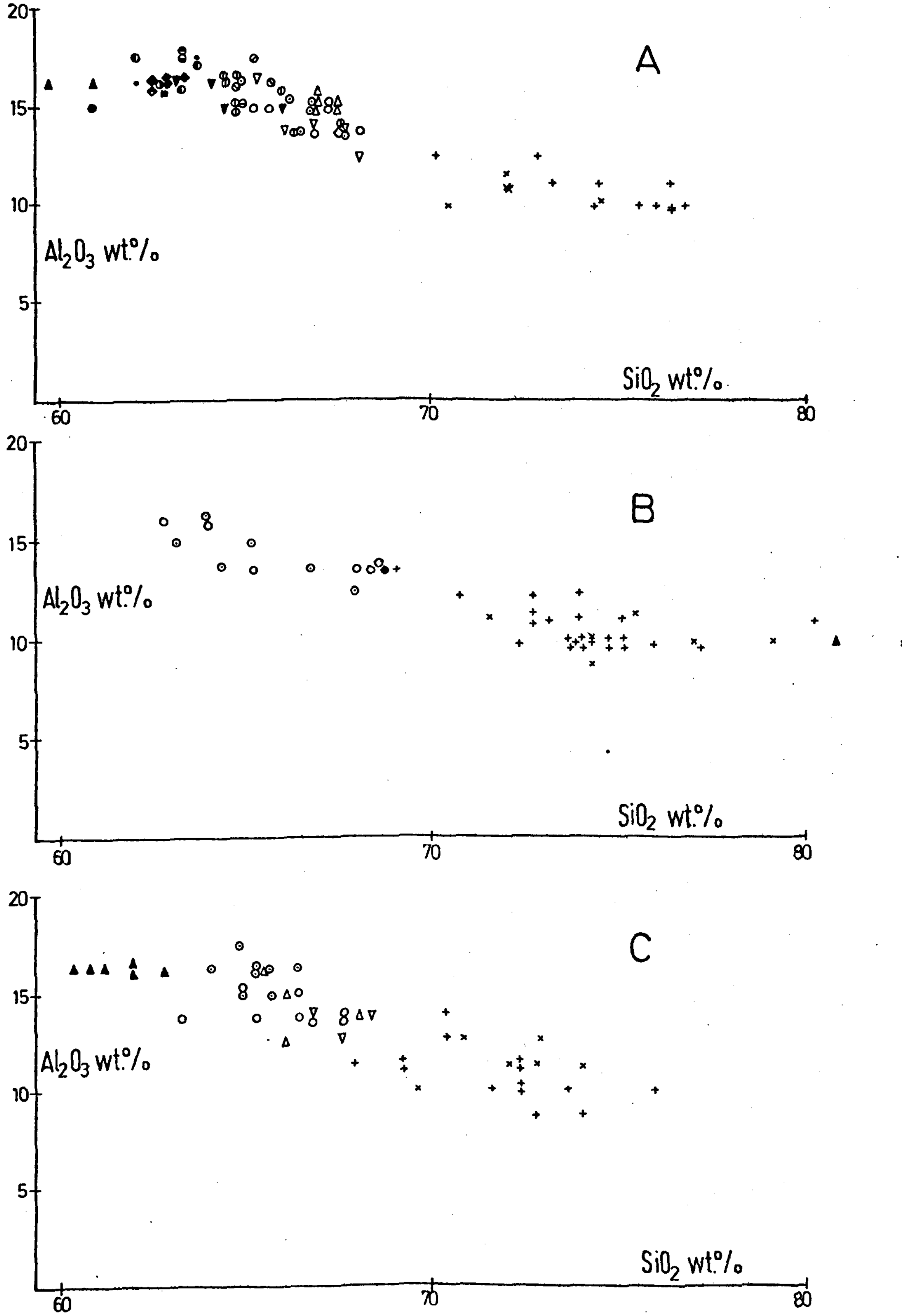

fig.6.8 : Major element variation relative to SiO_2 (explanation opposite).

Fig. 6.8. (opposite) : Major element variation relative to SiO$_2$

A : RAS ED DOM - PLUTONIC ROCKS

▲ S1
▼ S2
△ S3
◆ S4
▽ S5
○ S6
⦶ S7
⊖ S8
⊖ S9
◒ S10
▬ S11
⊘ S12
◐ S13
◑ S14
⦸ S15
◇ IT1
● IT2
· IT3
⬗ D209 - early syenite raft in S6
+ G1
× G2
✚ MG1
✗ MG2

B : RAS ED DOM AND ABU DOM - DYKE AND VOLCANIC ROCKS

Ras ed Dom	Abu Dom
○ syenitic dykes	⊙ syenitic dykes
+ granitic dykes	× granitic dykes
● rafted sample of tuff, loc. 307	▲ ignimbrite, Abu Dom Volcanic Group, loc. R101

C : ABU DOM - PLUTONIC ROCKS

▲ S1
△ S2
▽ S3
○ S4
⊙ S5
× G1
+ G2

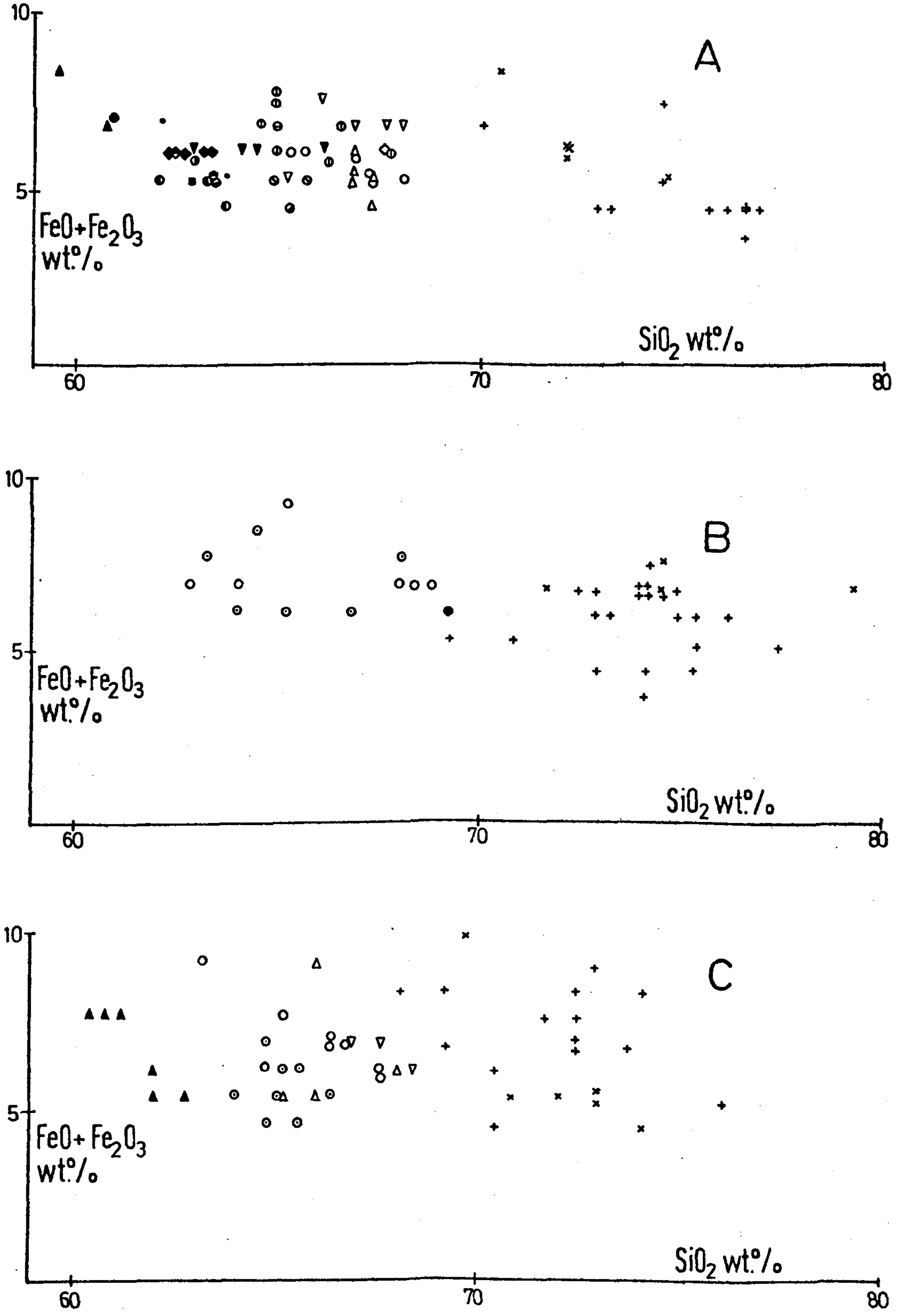

fig.6.8 (contd.) : Major element variation relative to SiO$_2$ (explanation opposite).

Fig. 6.8. (opposite) : Major element variation relative to SiO_2

A : RAS ED DOM - PLUTONIC ROCKS

- ▲ S1
- ▼ S2
- △ S3
- ◆ S4
- ▽ S5
- ○ S6
- ⦶ S7
- ◒ S8
- ⊖ S9
- ◓ S10
- ▬ S11
- ⊘ S12
- ◐ S13
- ◑ S14
- ⦸ S15
- ◇ IT1
- ● IT2
- · IT3
- ⬖ D209 - early syenite raft in S6
- + G1
- × G2
- ✚ MG1
- ✖ MG2

B : RAS ED DOM AND ABU DOM - DYKE AND VOLCANIC ROCKS

Ras ed Dom	Abu Dom
○ syenitic dykes	⊙ syenitic dykes
+ granitic dykes	× granitic dykes
● rafted sample of tuff, loc. 307	▲ ignimbrite, Abu Dom Volcanic Group, loc. R101

C : ABU DOM - PLUTONIC ROCKS

- ▲ S1
- △ S2
- ▽ S3
- ○ S4
- ⊙ S5
- × G1
- + G2

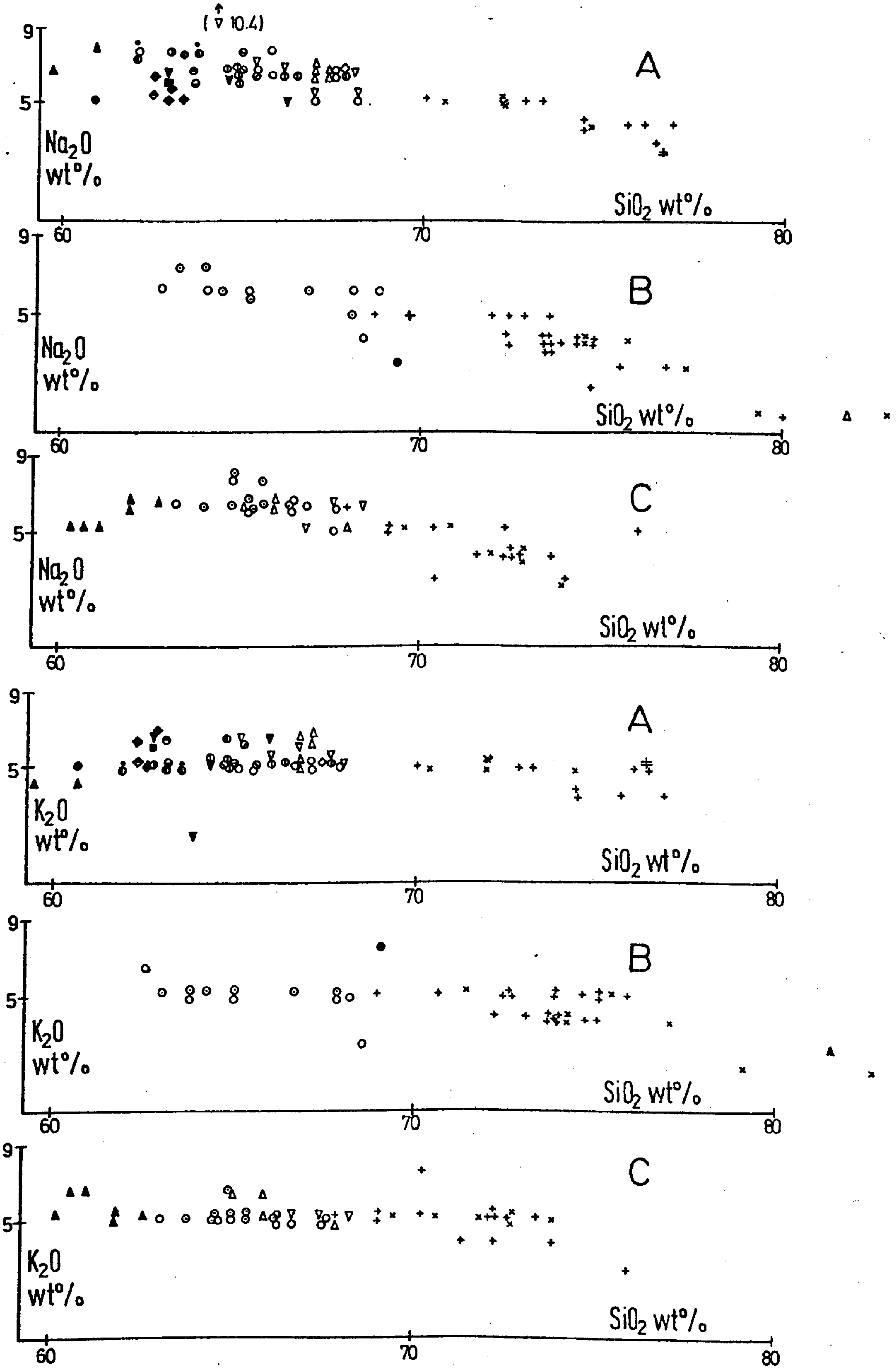

fig.6.8 (contd.) : Major element variation relative to SiO_2 (explanation opposite).

Fig. 6.8. (opposite) : Major element variation relative to SiO_2

A : RAS ED DOM - PLUTONIC ROCKS

- ▲ S1
- ▼ S2
- △ S3
- ◆ S4
- ▽ S5
- ○ S6
- ⦶ S7
- ◓ S8
- ⊖ S9
- ◒ S10
- ▬ S11
- ⊘ S12
- ◐ S13
- ◑ S14
- ⦸ S15
- ◇ IT1
- ● IT2
- · IT3
- ⬘ D209 - early syenite raft in S6
- + G1
- × G2
- ✚ MG1
- ✖ MG2

B : RAS ED DOM AND ABU DOM - DYKE AND VOLCANIC ROCKS

Ras ed Dom	Abu Dom
○ syenitic dykes	⊙ syenitic dykes
+ granitic dykes	× granitic dykes
● rafted sample of tuff, loc. 307	▲ ignimbrite, Abu Dom Volcanic Group, loc. R101

C : ABU DOM - PLUTONIC ROCKS

- ▲ S1
- △ S2
- ▽ S3
- ○ S4
- ⊙ S5
- × G1
- + G2

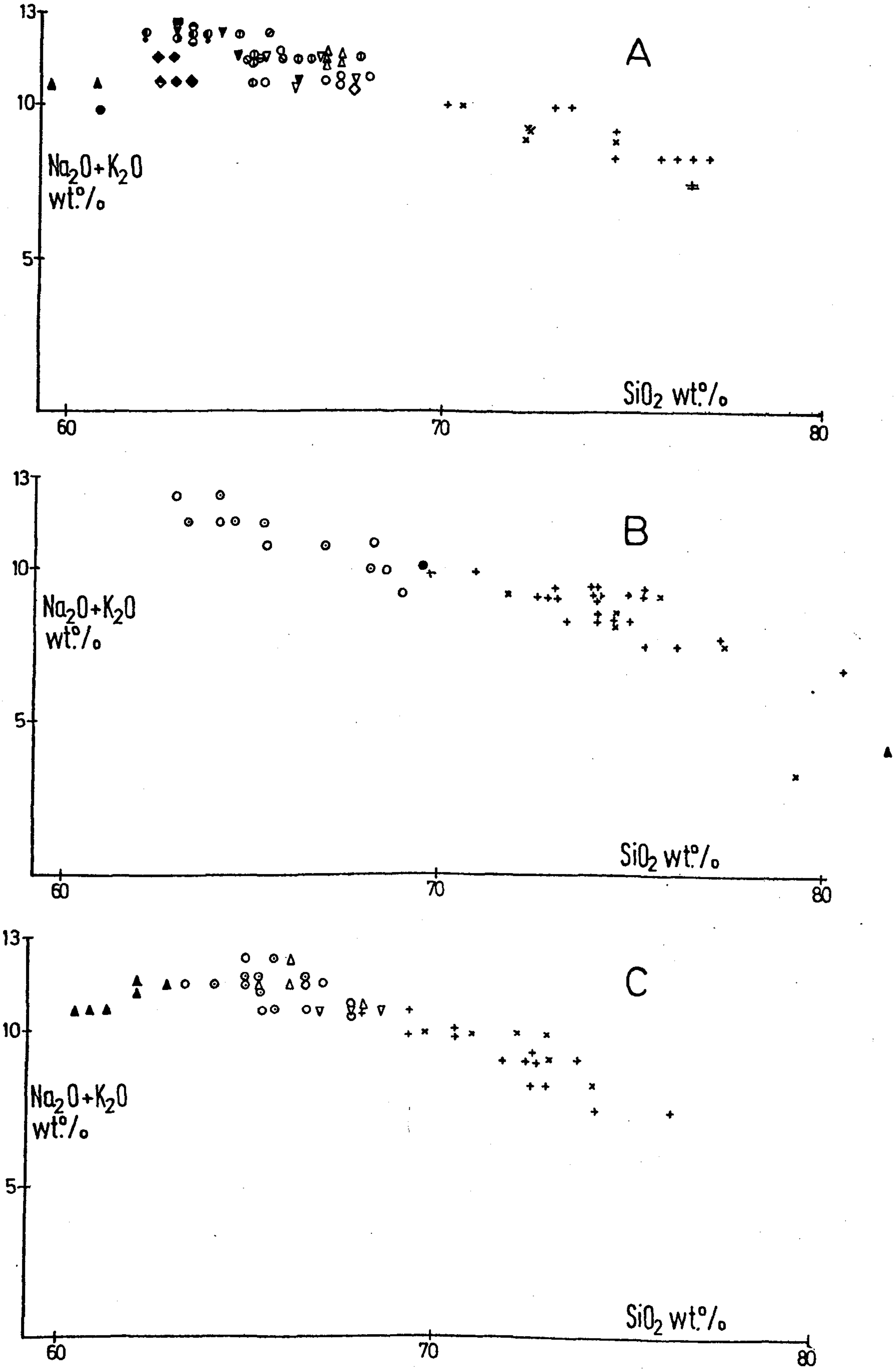

fig.6.8 (contd.) : Major element variation relative to SiO_2 (explanation opposite).

Fig. 6.8. (opposite) : Major element variation relative to SiO_2

A : RAS ED DOM - PLUTONIC ROCKS

▲ S1
▼ S2
△ S3
◆ S4
▽ S5
○ S6
⦶ S7
◓ S8

⊖ S9
◒ S10
▬ S11
⊘ S12
◐ S13
◑ S14
⊘ S15
◇ IT1

● IT2
· IT3
◈ D209 - early syenite raft in S6
+ G1
× G2
+ MG1
✕ MG2

B : RAS ED DOM AND ABU DOM - DYKE AND VOLCANIC ROCKS

Ras ed Dom	Abu Dom
○ syenitic dykes	⊙ syenitic dykes
+ granitic dykes	× granitic dykes
● rafted sample of tuff, loc. 307	▲ ignimbrite, Abu Dom Volcanic Group, loc. R101

C : ABU DOM - PLUTONIC ROCKS

▲ S1
△ S2
▽ S3
○ S4
⊙ S5
× G1
+ G2

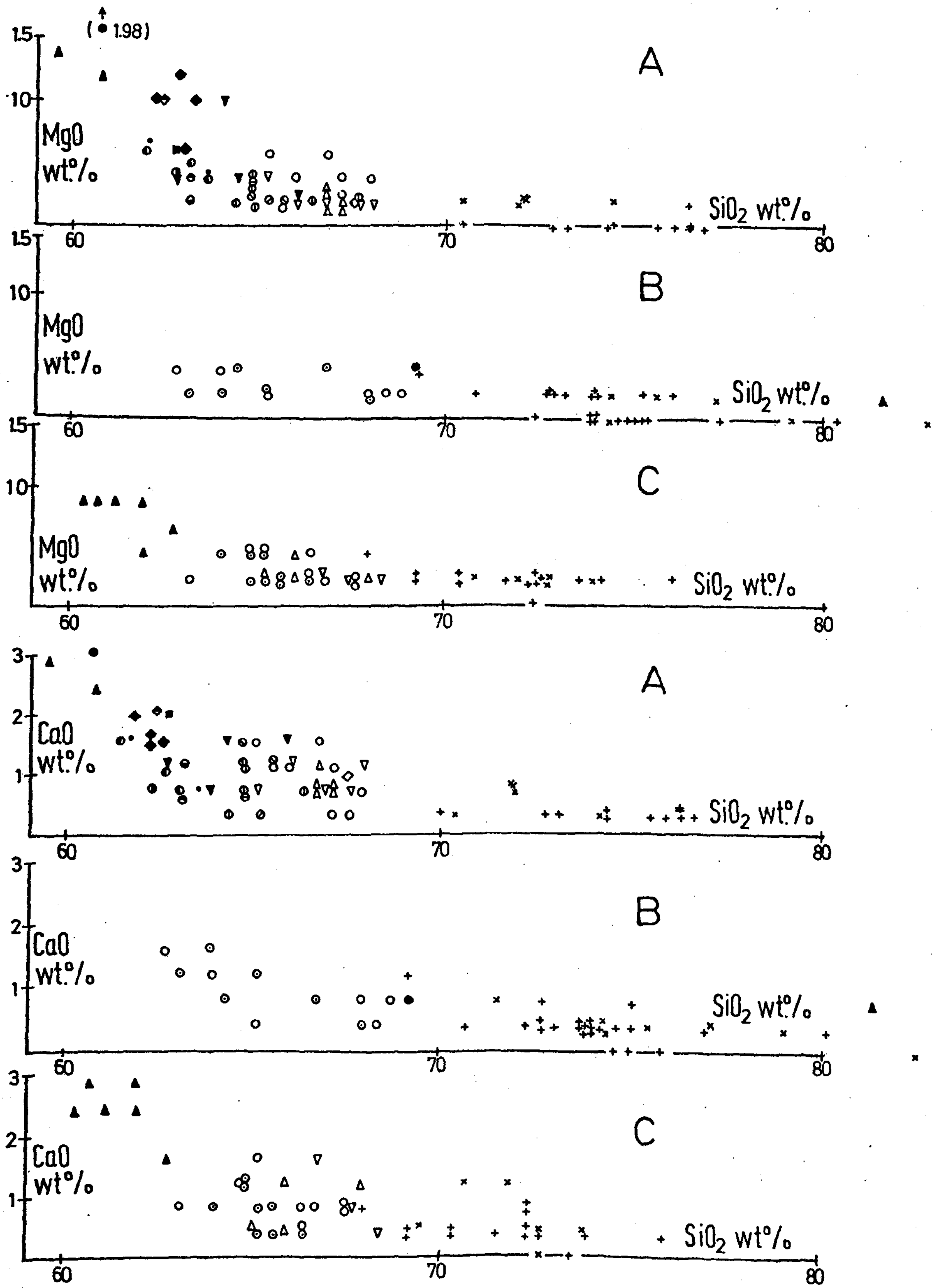

fig.6.8 (contd.) : Major element variation relative to SiO_2 (explanation opposite).

Fig. 6.8. (opposite) : Major element variation relative to SiO_2

A : RAS ED DOM - PLUTONIC ROCKS

▲ S1
▼ S2
△ S3
◆ S4
▽ S5
○ S6
⦶ S7
◍ S8

⊖ S9
◒ S10
▬ S11
⊘ S12
◐ S13
◑ S14
⦸ S15
◇ IT1

● IT2
· IT3
⬖ D209 - early syenite raft in S6
+ G1
× G2
✚ MG1
✖ MG2

B : RAS ED DOM AND ABU DOM - DYKE AND VOLCANIC ROCKS

Ras ed Dom	Abu Dom
○ syenitic dykes	⊙ syenitic dykes
+ granitic dykes	× granitic dykes
● rafted sample of tuff, loc. 307	▲ ignimbrite, Abu Dom Volcanic Group, loc. R101

C : ABU DOM - PLUTONIC ROCKS

▲ S1
△ S2
▽ S3
○ S4
⊙ S5
× G1
+ G2

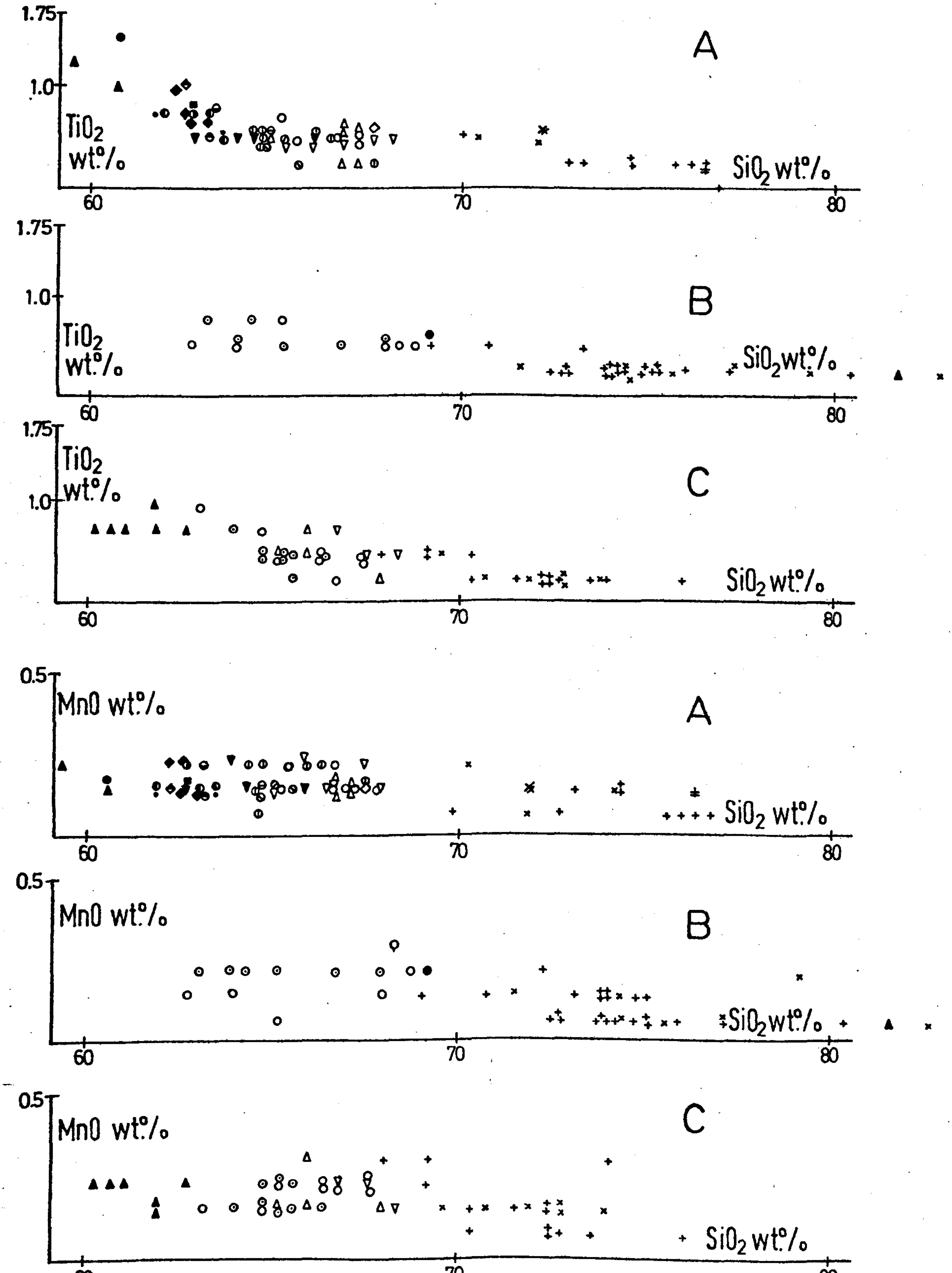

fig.6.8 (contd.) : Major element variation relative to SiO_2 (explanation opposite).

Fig. 6.8. (opposite) : Major element variation relative to SiO_2

A : RAS ED DOM - PLUTONIC ROCKS

- ▲ S1
- ▼ S2
- △ S3
- ◆ S4
- ▽ S5
- ○ S6
- ⦶ S7
- ◓ S8
- ⊖ S9
- ◒ S10
- ▬ S11
- ⊘ S12
- ◐ S13
- ◑ S14
- ⦸ S15
- ◇ IT1
- ● IT2
- · IT3
- ⬘ D209 - early syenite raft in S6
- + G1
- × G2
- ✚ MG1
- ✗ MG2

B : RAS ED DOM AND ABU DOM - DYKE AND VOLCANIC ROCKS

Ras ed Dom	Abu Dom
○ syenitic dykes	⊙ syenitic dykes
+ granitic dykes	× granitic dykes
● rafted sample of tuff, loc. 307	▲ ignimbrite, Abu Dom Volcanic Group, loc. R101

C : ABU DOM - PLUTONIC ROCKS

- ▲ S1
- △ S2
- ▽ S3
- ○ S4
- ⊙ S5
- × G1
- + G2

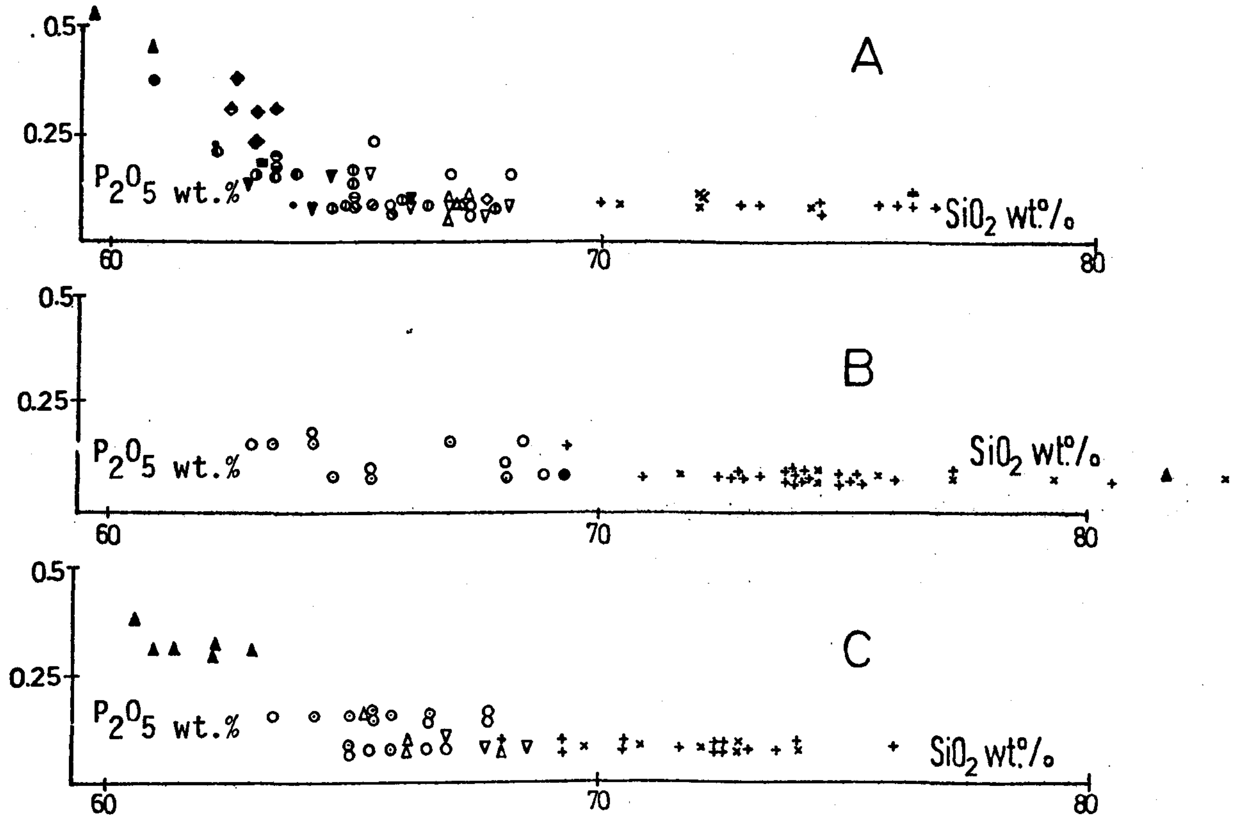

fig.6.8 (contd.) : Major element variation relative to SiO_2 (explanation opposite).

Fig. 6.9. (opposite) : Major element variation relative to **Zr.**

A : RAS ED DOM - PLUTONIC ROCKS

▲ S1
▼ S2
△ S3
◆ S4
▽ S5
○ S6
⦶ S7
◒ S8
⊖ S9
⬬ S10
▬ S11
⊘ S12
◐ S13
◑ S14
⦸ S15
◇ IT1
• IT2
· IT3
◈ D209 - early syenite raft in **S6**
+ G1
× G2
✚ MG1
⋇ MG2

B : RAS ED DOM AND ABU DOM - DYKE AND VOLCANIC ROCKS

Ras ed Dom	Abu Dom
○ syenitic dykes	⊙ syenitic dykes
+ granitic dykes	× granitic dykes
• rafted sample of tuff, loc. 307	▲ ignimbrite, Abu Dom Volcanic Group, loc. R101

C : ABU DOM - PLUTONIC ROCKS

▲ S1
△ S2
▽ S3
○ S4
⊙ S5
× G1
+ G2

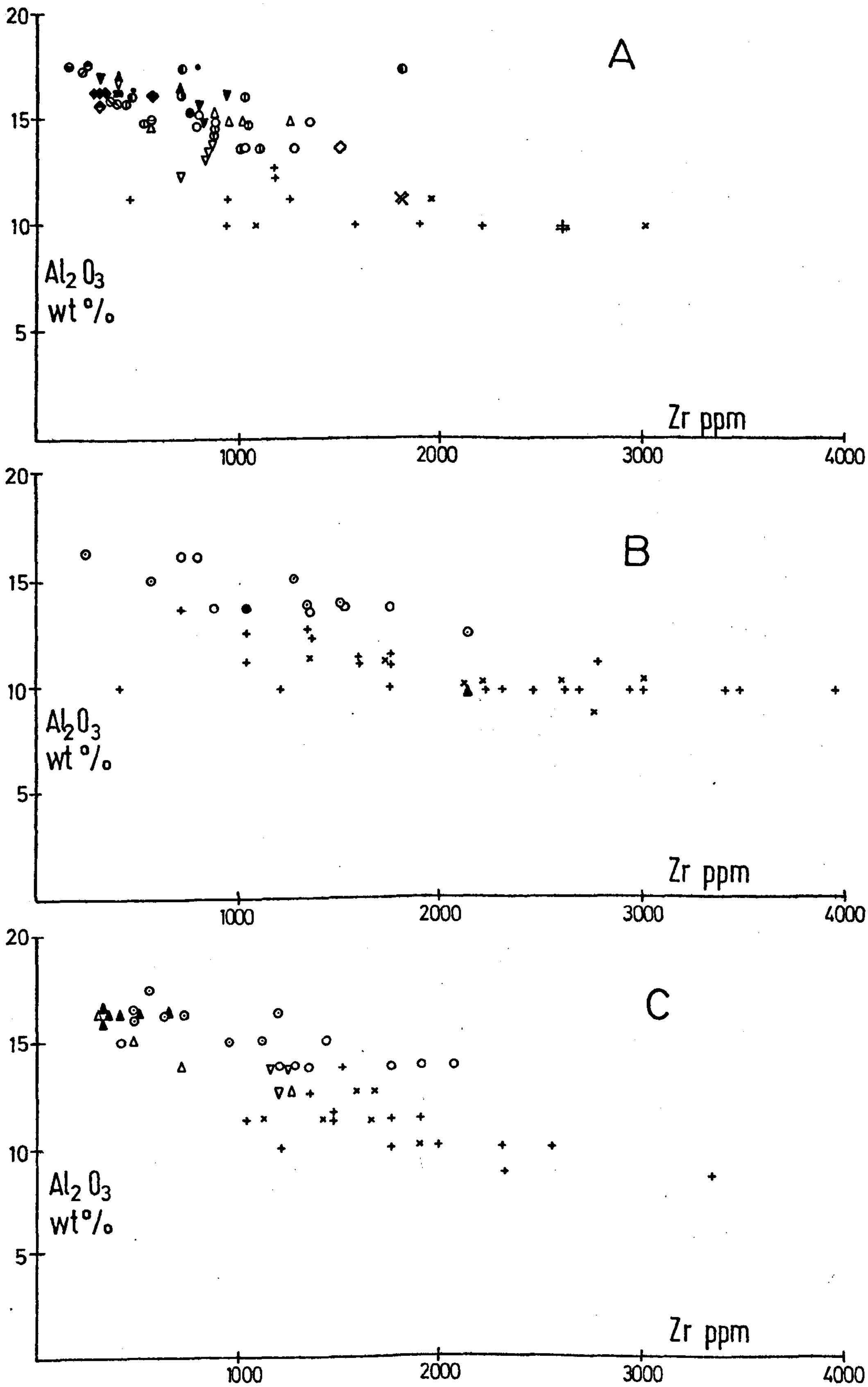

fig.6.9 : Major element variation relative to Zr (explanation opposite).

Fig. 6.9. (opposite) : Major element variation relative to **Zr.**

A : RAS ED DOM - PLUTONIC ROCKS

▲ S1
▼ S2
△ S3
◆ S4
▽ S5
○ S6
⦶ S7
◓ S8
⊖ S9
● S10
▬ S11
⌀ S12
◐ S13
◑ S14
⦸ S15
◇ IT1
• IT2
· IT3
⬘ D209 - early syenite raft in S6
+ G1
× G2
✚ MG1
✖ MG2

B : RAS ED DOM AND ABU DOM - DYKE AND VOLCANIC ROCKS

Ras ed Dom	Abu Dom
○ syenitic dykes	⊙ syenitic dykes
+ granitic dykes	× granitic dykes
• rafted sample of tuff, loc. 307	▲ ignimbrite, Abu Dom Volcanic Group, loc. R101

C : ABU DOM - PLUTONIC ROCKS

▲ S1
△ S2
▽ S3
○ S4
⊙ S5
× G1
+ G2

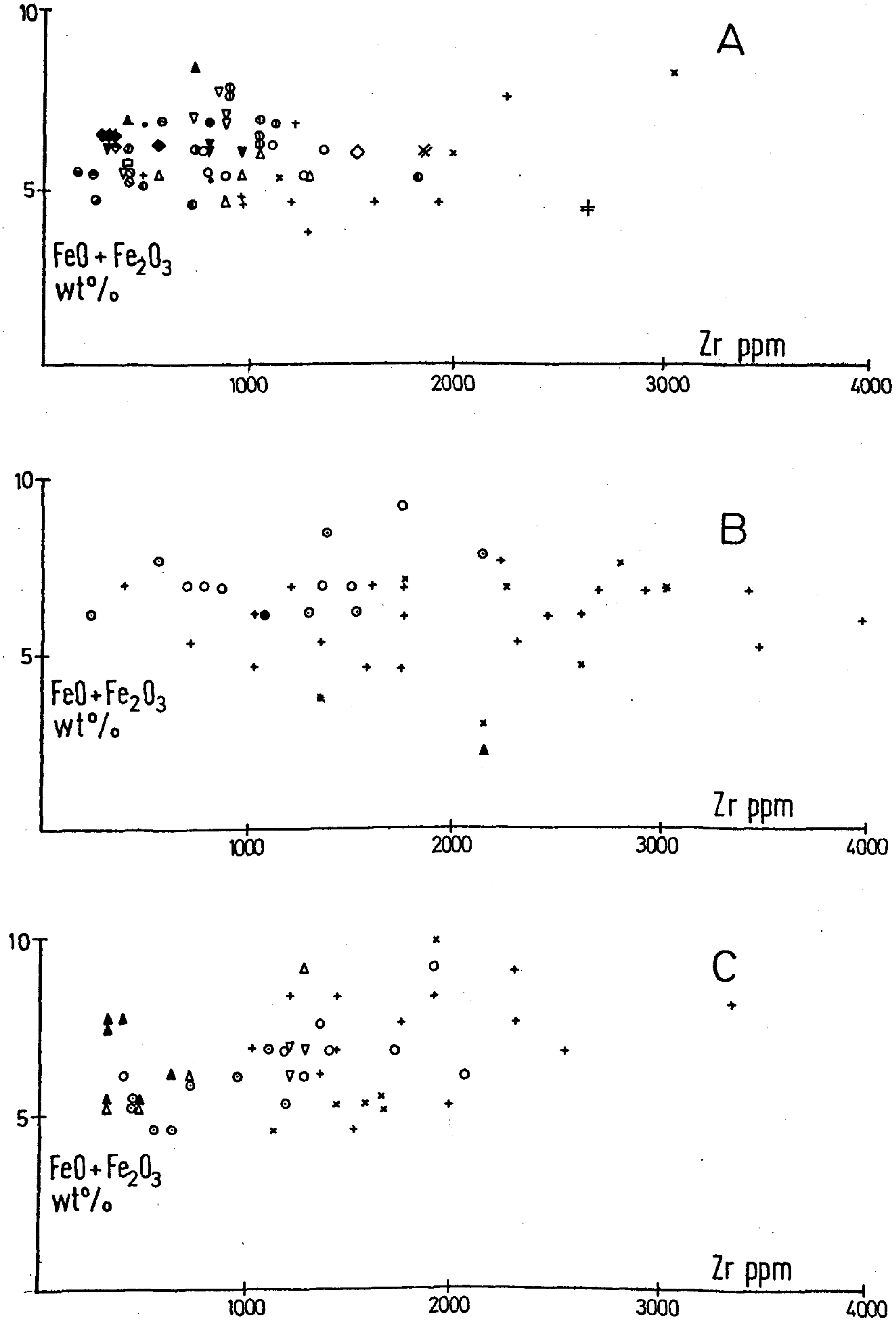

fig.6.9 (contd.) : Major element variation relative to Zr (explanation opposite).

Fig. 6.9. (opposite) : Major element variation relative to **Zr.**

A : RAS ED DOM - PLUTONIC ROCKS

- ▲ S1
- ▼ S2
- △ S3
- ◆ S4
- ▽ S5
- ○ S6
- ⦶ S7
- ◓ S8
- ⊖ S9
- ● S10
- ▬ S11
- ⊘ S12
- ◐ S13
- ◑ S14
- ⦸ S15
- ◇ IT1
- • IT2
- · IT3
- ◆ D209 - early syenite raft in S6
- + G1
- × G2
- ✢ MG1
- ✕ MG2

B : RAS ED DOM AND ABU DOM - DYKE AND VOLCANIC ROCKS

Ras ed Dom	Abu Dom
○ syenitic dykes	⊙ syenitic dykes
+ granitic dykes	× granitic dykes
• rafted sample of tuff, loc. 307	▲ ignimbrite, Abu Dom Volcanic Group, loc. R101

C : ABU DOM - PLUTONIC ROCKS

- ▲ S1
- △ S2
- ▽ S3
- ○ S4
- ⊙ S5
- × G1
- + G2

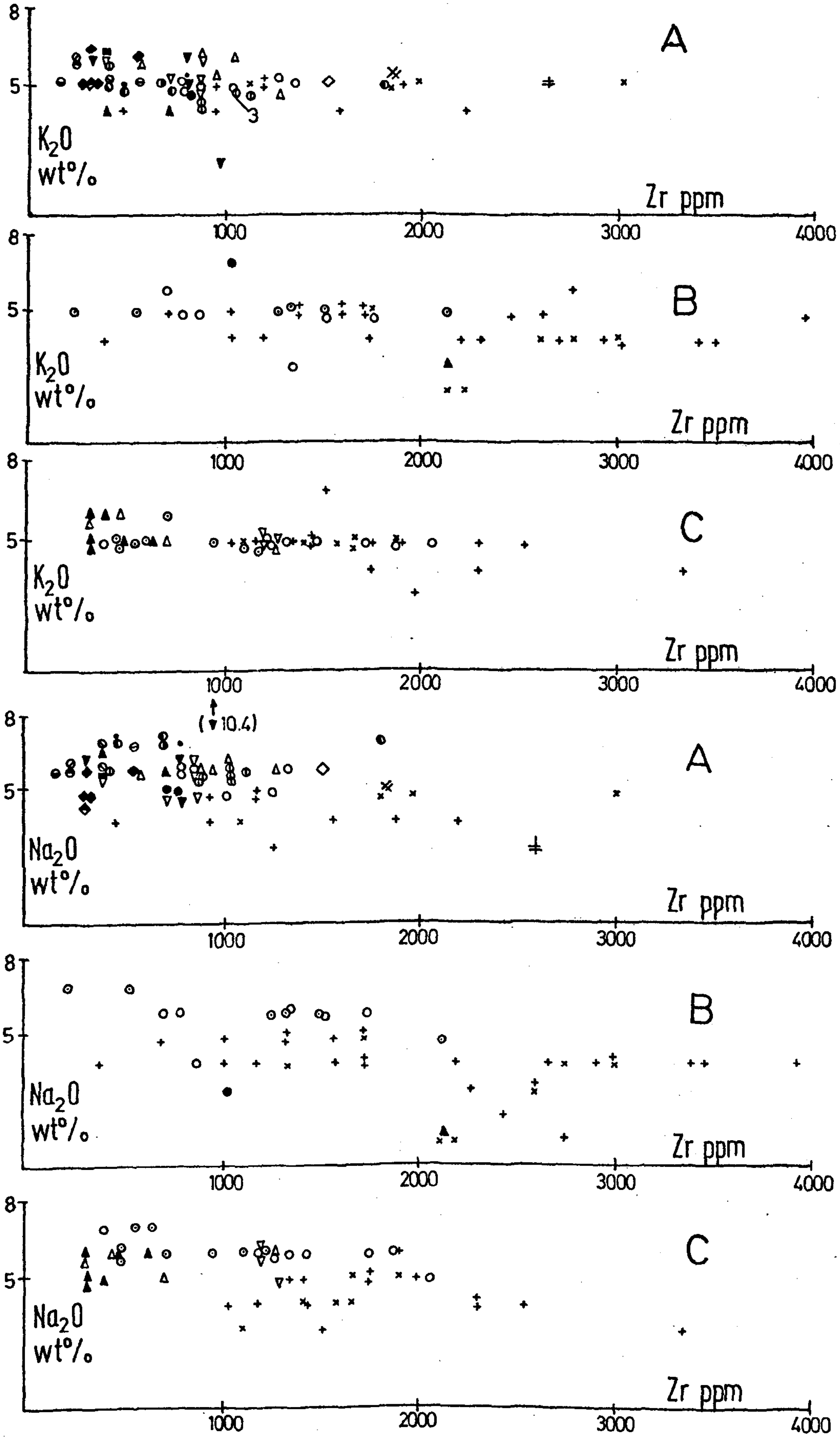

fig 6.9 (contd.) : Major element variation relative to Zr (explanation opposite).

Fig. 6.9. (opposite) : Major element variation relative to Zr.

A : RAS ED DOM - PLUTONIC ROCKS

▲ S1
▼ S2
△ S3
◆ S4
▽ S5
○ S6
⦶ S7
◓ S8
⊖ S9
⬬ S10
▬ S11
⊘ S12
◐ S13
◑ S14
⦸ S15
◇ IT1
● IT2
· IT3
⬘ D209 - early syenite raft in S6
+ G1
× G2
✝ MG1
⋇ MG2

B : RAS ED DOM AND ABU DOM - DYKE AND VOLCANIC ROCKS

Ras ed Dom	Abu Dom
○ syenitic dykes	⊙ syenitic dykes
+ granitic dykes	× granitic dykes
● rafted sample of tuff, loc. 307	▲ ignimbrite, Abu Dom Volcanic Group, loc. R101

C : ABU DOM - PLUTONIC ROCKS

▲ S1
△ S2
▽ S3
○ S4
⊙ S5
× G1
+ G2

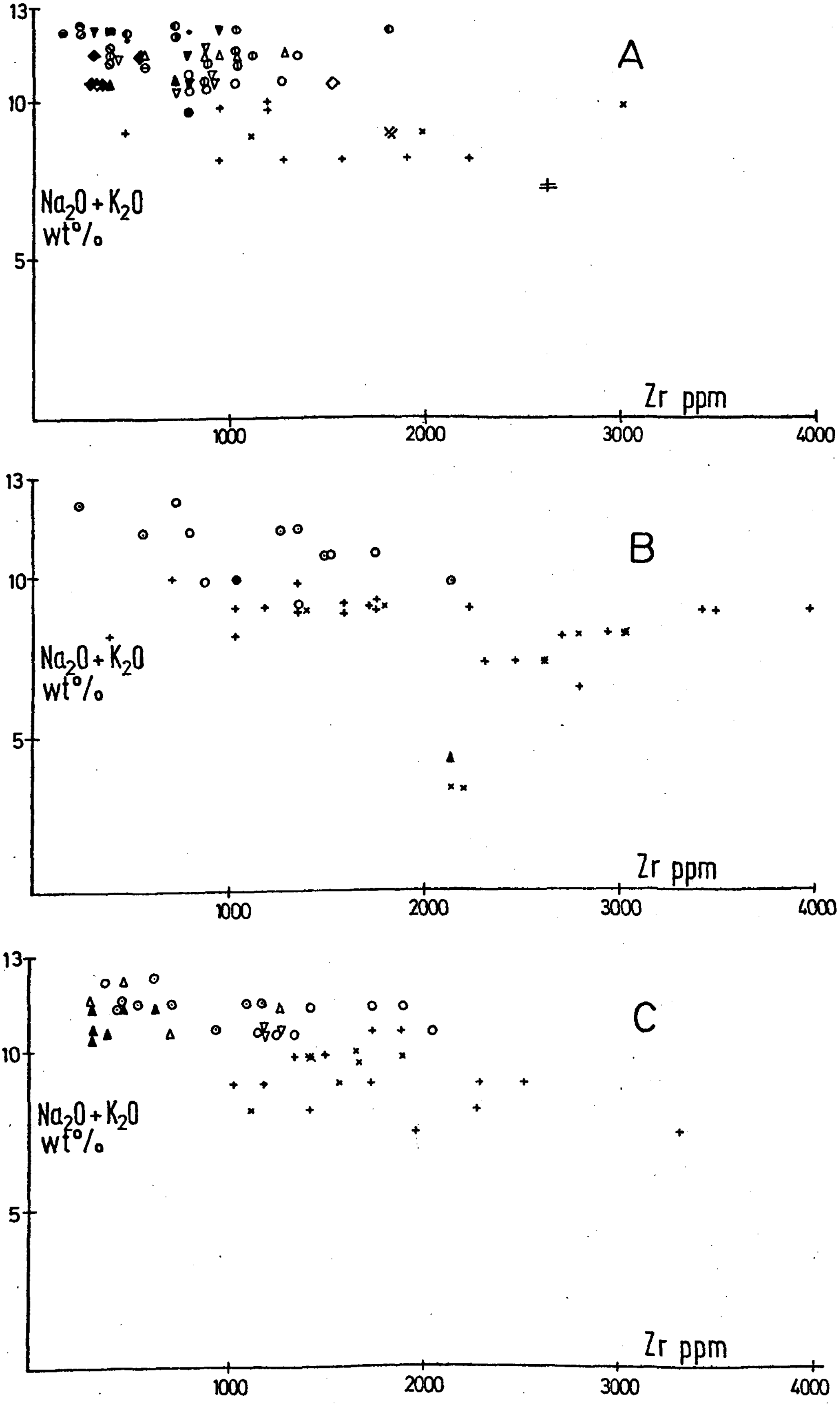

fig.6.9 (contd.) : Major element variation relative to Zr (explanation opposite).

Fig. 6.9. (opposite) : Major element variation relative to **Zr.**

A : RAS ED DOM - PLUTONIC ROCKS

▲ S1
▼ S2
△ S3
◆ S4
▽ S5
○ S6
⦶ S7
◒ S8
⊖ S9
◓ S10
▬ S11
⊘ S12
◐ S13
◑ S14
⦸ S15
◇ IT1
● IT2
· IT3
⬘ D209 - early syenite raft in S6
+ G1
× G2
✛ MG1
✕ MG2

B : RAS ED DOM AND ABU DOM - DYKE AND VOLCANIC ROCKS

Ras ed Dom	Abu Dom
○ syenitic dykes	⊙ syenitic dykes
+ granitic dykes	× granitic dykes
● rafted sample of tuff, loc. 307	▲ ignimbrite, Abu Dom Volcanic Group, loc. R101

C : ABU DOM - PLUTONIC ROCKS

▲ S1
△ S2
▽ S3
○ S4
⊙ S5
× G1
+ G2

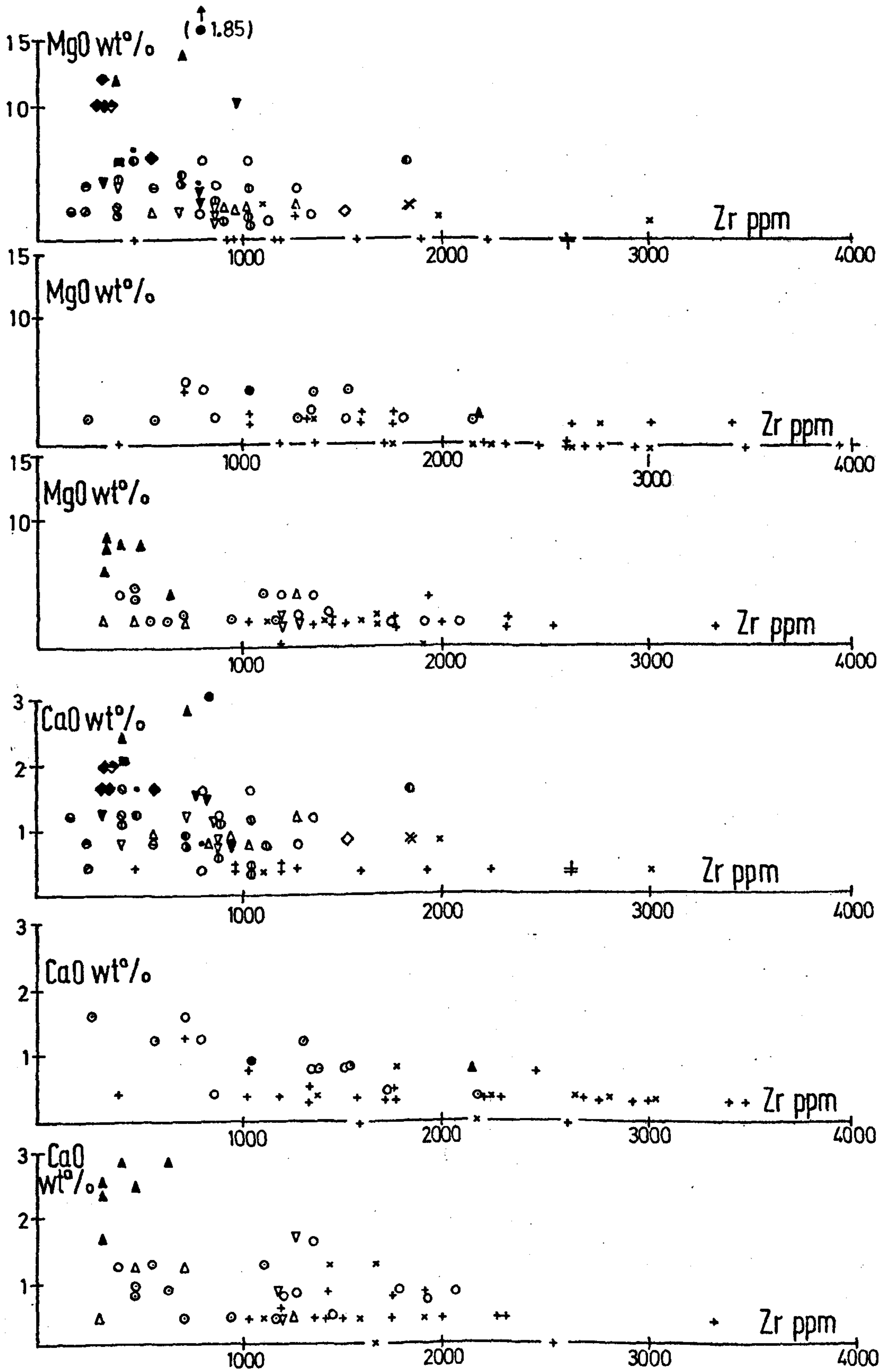

fig.6.9 (contd.) : Major element variation relative to Zr (explanation opposite).

Fig. 6.9. (opposite) : Major element variation relative to Zr.

A : RAS ED DOM - PLUTONIC ROCKS

- ▲ S1
- ▼ S2
- △ S3
- ◆ S4
- ▽ S5
- ○ S6
- ⦶ S7
- ◓ S8
- ⊖ S9
- ◒ S10
- ▬ S11
- ⊘ S12
- ◐ S13
- ◑ S14
- ⦸ S15
- ◇ IT1
- • IT2
- · IT3
- ◆ D209 - early syenite raft in S6
- + G1
- × G2
- ✚ MG1
- ✖ MG2

B : RAS ED DOM AND ABU DOM - DYKE AND VOLCANIC ROCKS

Ras ed Dom

- ○ syenitic dykes
- + granitic dykes
- • rafted sample of tuff, loc. 307

Abu Dom

- ⊙ syenitic dykes
- × granitic dykes
- ▲ ignimbrite, Abu Dom Volcanic Group, loc. R101

C : ABU DOM - PLUTONIC ROCKS

- ▲ S1
- △ S2
- ▽ S3
- ○ S4
- ⊙ S5
- × G1
- + G2

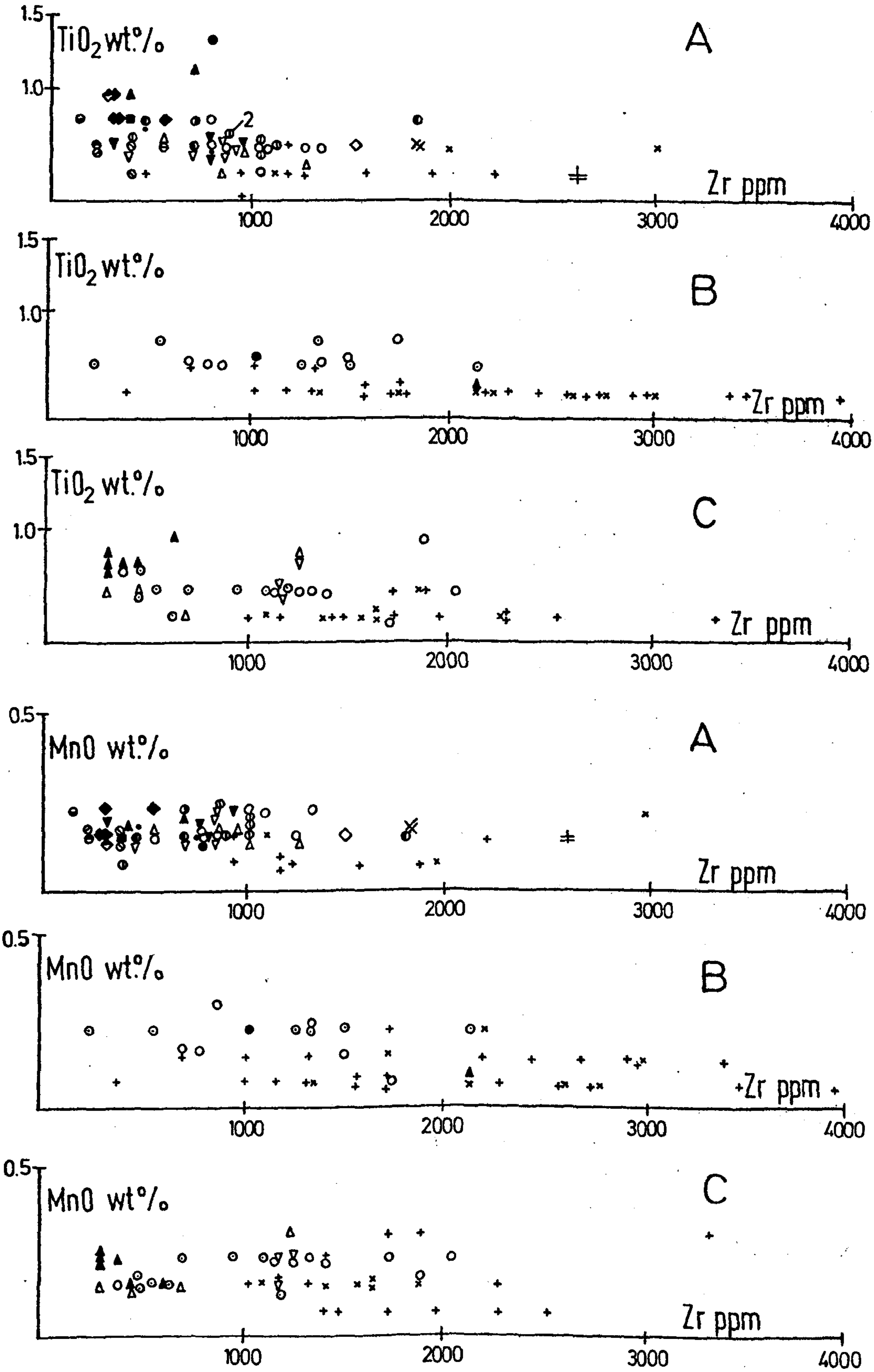

fig.6.9 (contd.) : Major element variation relative to Zr (explanation opposite).

Fig. 6.9. (opposite) : Major element variation relative to Zr.

A : RAS ED DOM - PLUTONIC ROCKS

▲ S1
▼ S2
△ S3
◆ S4
▽ S5
○ S6
⦶ S7
◓ S8
⊖ S9
● S10
▬ S11
⊘ S12
◐ S13
◑ S14
⊗ S15
◇ IT1
• IT2
· IT3
◈ D209 - early syenite raft in S6
+ G1
× G2
+ MG1
× MG2

B : RAS ED DOM AND ABU DOM - DYKE AND VOLCANIC ROCKS

Ras ed Dom	Abu Dom
○ syenitic dykes	⊙ syenitic dykes
+ granitic dykes	× granitic dykes
• rafted sample of tuff, loc. 307	▲ ignimbrite, Abu Dom Volcanic Group, loc. R101

C : ABU DOM - PLUTONIC ROCKS

▲ S1
△ S2
▽ S3
○ S4
⊙ S5
× G1
+ G2

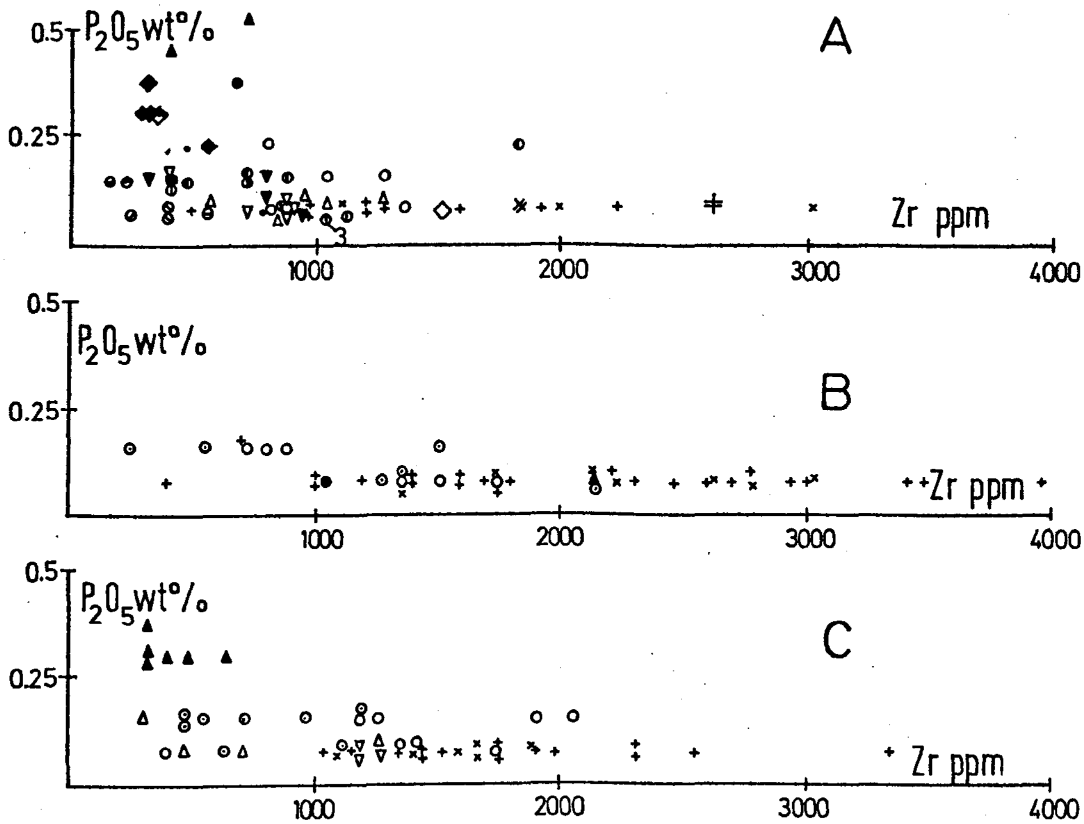

fig.6.9 (contd.) : Major element variation relative to Zr (explanation opposite).

6.2. : Major Element Chemistry

6.2.A. : Recognition of Fractionation Sequences

The major element variation, relative to SiO_2 and Zr, is depicted in figs. 6.8 and 6.9. From these diagrams it is at once apparent that continuous trends link the early syenites, alkali syenites and alkali granites of the two complexes. Thus, in broad terms, the variation in rock chemistry relative to SiO_2 is consistent with the fractionation sequence proposed in chapters 4 and 5.

The partial repetition of this sequence in different structural centres in Ras ed Dom (yielding the overlapping trends in figs. 6.8. and 6.9.), together with its recurrence in Abu Dom and Sultaniyat (Curtis, 1979), emphasises its importance in the differentiation of the Bayuda Younger Granites, and its reproducability in time. The magmas involved evidently varied slightly in chemistry as the syenites S6-S11 of Ras ed Dom are relatively 'basic' in composition (fig. 6.8.A.). Caution is necessary, however, in adducing plutonic rock compositions as representative of magma compositions. The nearest approach to a liquid + phenocryst assemblage is the chilled margin to S3 (RED). Moreover as described in section 4.7.A. the sodic mafic minerals of the alkali rocks are, in part at least, of sub-solidus origin. The dyke-rocks may approximate liquid compositions, but devitrification with attendant changes in chemistry is common in them.

The most complete example of the proposed fractionation sequence is that of Centre I, Ras ed Dom (table 6.5, below). It differs from the intrusive sequence in that S3 postdates GI, but the petrographic, mineralogical and chemical evidence leaves no doubt that GI is the more fractionated lithology.

Gl : alkali granite
↑
S3 : transitional syenite (chilled margin) | alkali syenite (core of unit)
↑
S2 : transitional syenite (south of unit) | alkali syenite (north of unit)
↑
SI : early subaluminous syenite

Table 6.5. : Proposed Fractionation Sequence for Centre I, Ras ed Dom.

6.2.B. : Major Element Variation

Major element variation in the Younger Granite rocks is depicted in figs. 6.8 and 6.9. Trends described below are apparent relative to both SiO_2 and Zr, unless otherwise specified. Although Zr is a reasonable fractionation index, reproducing the trends visible in the Harker plots, the trends are less clearly defined with a greater degree of scatter.

Considering first the major intrusions (plots A and C in figs. 6.8 and 6.9), Al_2O_3 levels are steady in the early syenites, but decline in the alkali rocks. A slight rise in Na_2O occurs from the early to alkali syenites, representing concentration of Na in the residual magma as calcic pyroxene crystallised. Thereafter Na_2O declines with fractionation. Total alkalies decline gradually with fractionation, largely reflecting the fall in Na_2O, as K_2O shows only a slight decrease. MgO and CaO both show an abrupt initial depletion, reflecting incorporation of both into early pyroxene, and of Ca into apatite and feldspar (sections 5.2.A., and 5.3.B.). Thereafter the decrease is more gradual as Ca and Mg are incorporated into amphibole. Mean Mg values in amphibole for the early syenites, transitional syenites, alkali syenites and alkali granites are 1.86, 0.52, 0.10 and 0.0 ions p.f.u. respectively, and Ca levels decline in similar fashion. The late pyroxenes are Mg-free and Ca-poor.

A similar pattern of early abrupt decline, followed by a gradual decrease, is displayed by both TiO_2 and P_2O_5. The fractionating phases in these instances being Fe-Ti oxide and apatite, both of which are abundant in the early syenites (section 4.3.D). MnO levels are constant except in the acid rocks where they fall, apparently in sympathy with Na_2O. Total iron trends relative to SiO_2 are poorly defined, with a wide range of scatter, but appear to be horizontal overall.

Considering the dyke rocks (plot B in figs. 6.8 and 6.9) the trends are closely similar to those for the major intrusives, indicating a co-magmatic origin. The degree of scatter is commonly greater in the dyke plots, however, reflecting the effects of devitrification in many instances.

Average compositions for the principal rock-types are compared with average syenite and granite compositions (Le Maitre, 1976) in table 6.6. Le Maitre's data incorporates a bias towards calc-alkali compositions, and the comparison thus highlights the characteristics of the Bayuda alkaline suite. The early metaluminous syenites have SiO_2, Al_2O_3 and total iron values comparable to Le Maitre's average syenite. Fe_2O_3 is enriched relative to FeO however, and MgO and CaO are somewhat depleted. If, as proposed in section 4.7.F., the parental magma for the Bayuda Younger Granites was close in composition to the early syenites, then it too presumably shared the same characteristics. In the alkali rocks the above features are accompanied by a depletion in Al_2O_3, TiO_2 and P_2O_5 relative to Le Maitre's data. In the granites total iron greatly exceeds Le Maitre's average value, while TiO_2 is not depleted and MnO is slightly enriched. Apart from enrichment in Fe_2O_3, the most striking feature of the comparison is that total alkalies in the Bayuda rocks do not differ significantly from Le Maitre's data, thus emphasising that the peralkaline condition owes more to Al_2O_3 depletion than to alkali enrichment. Na_2O, however, when considered alone, is enriched by about 1% in the Bayuda alkali rocks.

wt.%	1	2	3
SiO_2	59.63	61.95	61.56
Al_2O_3	16.94	16.13	16.37
Fe_2O_3	3.09	3.68	4.80
FeO	3.19	2.61	1.80
MgO	1.90	1.11	0.70
CaO	3.59	2.15	2.46
Na_2O	5.33	5.84	5.50
K_2O	5.04	5.09	5.51
TiO_2	0.86	0.95	0.85
MnO	0.13	0.15	0.16
P_2O_5	0.30	0.32	0.31

1 : average syenite, Le Maitre (1976)

2 : average early syenite, Ras ed Dom

3 : average early syenite, Abu Dom

wt.%	4	5	6
SiO_2	59.63	65.35	65.97
Al_2O_3	16.94	15.31	14.67
Fe_2O_3	3.09	4.44	5.53
FeO	3.19	1.44	0.68
MgO	1.90	0.33	0.28
CaO	3.59	1.01	0.82
Na_2O	5.33	6.16	6.00
K_2O	5.04	5.24	5.23
TiO_2	0.86	0.51	0.54
MnO	0.13	0.15	0.17
P_2O_5	0.30	0.08	0.08

4 : average syenite, Le Maitre (1976)

5 : average alkali syenite, Ras ed Dom

6 : average alkali syenite, Abu Dom

wt.%	7	8	9
SiO_2	71.84	73.92	71.86
Al_2O_3	14.43	10.86	11.00
Fe_2O_3	1.22	4.03	6.25
FeO	1.65	1.42	0.60
MgO	0.72	0.11	0.17
CaO	1.85	0.39	0.48
Na_2O	3.71	4.31	4.36
K_2O	4.10	4.58	4.78
TiO_2	0.31	0.27	0.32
MnO	0.05	0.09	0.13
P_2O_5	0.12	0.03	0.03

7 : average granite, Le Maitre (1976)

8 : average alkali granite, Ras ed Dom

9 : average alkali granite, Abu Dom

Table 6.6. : Average major element compositions for the principal rock-types of Ras ed Dom and Abu Dom compared with the average compositions of Le Maitre (1976)

wt.%	Metaluminous Syenites N	Metaluminous Syenites R	Metaluminous Syenites A	Alkali Syenites N	Alkali Syenites R	Alkali Syenites A	Alkali Granites N	Alkali Granites R	Alkali Granites A
SiO2	61.87	61.95	61.56	62.01	65.35	65.97	71.36	73.92	71.86
Al2O3	17.54	16.13	16.37	14.82	15.31	14.67	11.30	10.86	11.00
Fe2O3	1.83	3.68	4.80	4.59	4.44	5.53	4.30	4.03	6.25
FeO	3.12	2.61	1.80	3.70	1.44	0.68	2.20	1.42	0.60
MgO	0.74	1.11	0.70	0.70	0.33	0.28	0.25	0.11	0.17
CaO	2.40	2.15	2.46	1.88	1.01	0.82	0.84	0.39	0.48
Na2O	5.62	5.84	5.50	6.73	6.16	6.00	4.94	4.31	4.36
K2O	6.00	5.09	5.51	4.68	5.24	5.23	4.21	4.58	4.78
TiO2	0.59	0.95	0.85	0.52	0.51	0.54	0.40	0.27	0.32
MnO	0.09	0.15	0.16	0.20	0.15	0.17	0.11	0.09	0.13
P2O5	0.19	0.32	0.31	0.17	0.08	0.08	0.07	0.03	0.03

N: data from Nockolds (1954), corrected to 100%. metaluminous syenites (11 samples); alkali syenites (47 samples); alkali granites(54 samples).

R: Ras ed Dom averages (n = 9,40,14 for the respective categories).

A: Abu Dom averages (n = 6,23,20 for the respective categories).

Table 6.7 : Average major element compositions for the principal rock-types of Ras ed Dom and Abu Dom, compared with the averages of Nockolds (1954).

Recent compilations of average igneous rock compositions (Le Maitre, 1976; De la Roche et al., 1980) do not differentiate alkali syenites and granites (sensu Streckeisen, 1967; 1976) as separate categories. For this reason recourse is made to the older compilation of Nockolds (1954) in order to compare the Bayuda averages with similar alkaline to peralkaline compositions (table 6.7). The Bayuda suite is typical for most major elements, including the alkalies, but the predominance of Fe_2O_3 over FeO is more marked, especially in the early syenites. The alkali rocks are also rather low in CaO and MgO.

6.2.C. : Magmatic Evolution

i. Major Element Variation and Fractional Crystallisation

No cumulus rocks were recognised in Ras ed Dom and Abu Dom. The coarse syenites that characterise SI (AD), S3 (RED) and, locally, S5 in Abu Dom are superficially cumulus-like in appearance with large tabular perthite grains separated by a sparse mafic-rich interstitium (plate 2.13.-B). Preferred orientation and rhythmic layering, however, are absent. In considering such a feldspar-rich suite the possibility of feldspar fractionation must be critically examined, especially as Al_2O_3 exhibits a sustained decline with increasing SiO_2 (fig. 6.8). The low Ca-levels, however, at once suggest that fractionation of plagioclase, if applicable at all, would apply to precursor lithologies rather than to the observed rock-series. Examples of possible precursor lithologies may be represented in the basic volcanic rocks of Muweilih complex (Map 3; section 2.2.B.). A more probable process for the plutonic rocks is alkali-feldspar fractionation. Although there is no evidence of potash depletion in the later rocks, mean Al_2O_3 values fall from 15-16% in the syenites to 11% in the granites. If this reflects an increase in the Al content of any fractionating assemblage, then it would effectively mean an increase in the feldspar/ferromagnesian ratio of such an assemblage. The role of feldspar-fractionation is returned to below.

An important ferromagnesian reaction series in the plutonic rocks was outlined in chapter 4 (fig. 4.3), and fractionation of such phases may have contributed to the differentiation of the magmas. Although amphibole is not observed as a phenocryst phase in the dyke rocks (section 4.6), this is probably due to volatile loss in the hypabyssal environment (Ferguson, 1978) and fractional removal of amphibole remains a possibility. Considering the major element variation (fig. 6.8) the abrupt fall in TiO_2, P_3O_5 and CaO in the early syenites (see previous section) is consistent with fractionation of Fe-Ti oxide and apatite. Removal of iron oxide would have contributed to a SiO_2 enrichment in the residual magma. Fractionation of Ca and Mg by early pyroxene and amphibole is also consistent with the observed trends (c.f.previous section). Fractionation of the increasingly sodic pyriboles would account for the fall in Na_2O. Such a role cannot, however, be safely extended to include aegirine and riebeckite as the petrographic evidence suggests a possible sub-solidus origin for these minerals. In general, moreover, the mafic phases are modally subordinate to feldspar, and thus the effectiveness of their contribution to fractionation is questionable. Trace element indications of fractional removal of crystallising phases are considered in section 6.3.

ii. The Granite System

An experimental basis for examining granitic compositions is available in the "Granite System" ($NaAlSi_3O_8$-$KAlSi_3O_8$-SiO_2-H_2O) of Tuttle and Bowen (1958). They found a strong coincidence of granitic compositions with experimental minima in the system, indicating a magmatic origin for the rocks. Carmichael and MacKenzie (1963), Bailey and Schairer (1964, 1966) and Thompson and MacKenzie (1967) have attempted to extend the Granite System (in which the ratio of molecular $Na_2O + K_2O/Al_2O_3$ is I.0) to embrace peralkaline acid compositions, by addition of acmite and alkali-silicates. The topic is reviewed by Edgar (1974) and Bailey (1975, 1976).

Carmichael and MacKenzie (1963) added first 4.5%, and then 8.3% each of acmite and sodium metasilicate (Ns; $Na_2 SiO_3$), to the granite system. The effect was to shift the minimum melting compositions, and associated thermal valleys, towards the Or-Q sideline (figs. 6.10 and 6.11). Bailey and Schairer (1964, 1966), however, consider that peralkaline liquids may move away from the Q-Ab-Or plane entirely. Thompson and MacKenzie (1967) envisaged a 'low temperature zone' arising from the thermal valley in Q-Ab-Or, which moves rapidly towards the SiO_2-Al_2O_3-Na_2O plane. Liquids evolve in this zone by precipitating feldspar of restricted

Fig. 6.10 (opposite) : Younger Granite analyses plotted in the Granite System of Tuttle & Bowen (1958)

Plot A : PLUTONIC ROCKS - RAS ED DOM

• early syenite
∘ alkali syenite
+ alkali granite
D129 : metasomatised syenite, S2

Plot B : DYKE AND VOLCANIC ROCKS - RAS ED DOM

∘ syenitic dykes
+ granitic dykes
D307 : volcanic tuff, raft in IT2

A - the liquidus minimum at 3kb pH_2O
B - the liquidus minimum at 2kb pH_2O
C - the liquidus minimum at 1kb pH_2O
D - the liquidus minimum at 0.5kb pH_2O
E - composition of the liquidus minimum at 1kb pH_2O, with 4.5% acmite and 4.5% sodium metasilicate.
F - composition of the liquidus minimum at 1kb pH_2O, with 8% acmite and 8% sodium metasilicate
MI - composition of the liquidus minimum at 1kb and 1% added flourine
M2 - as M1 but with 2% added flourine
M4 - as MI but with 4% added flourine

Points A, B, C, D after Tuttle and Bowen (1958); E and F after Carmichael and Mackenzie (1963); M1, M2, M4 after Manning (1981)

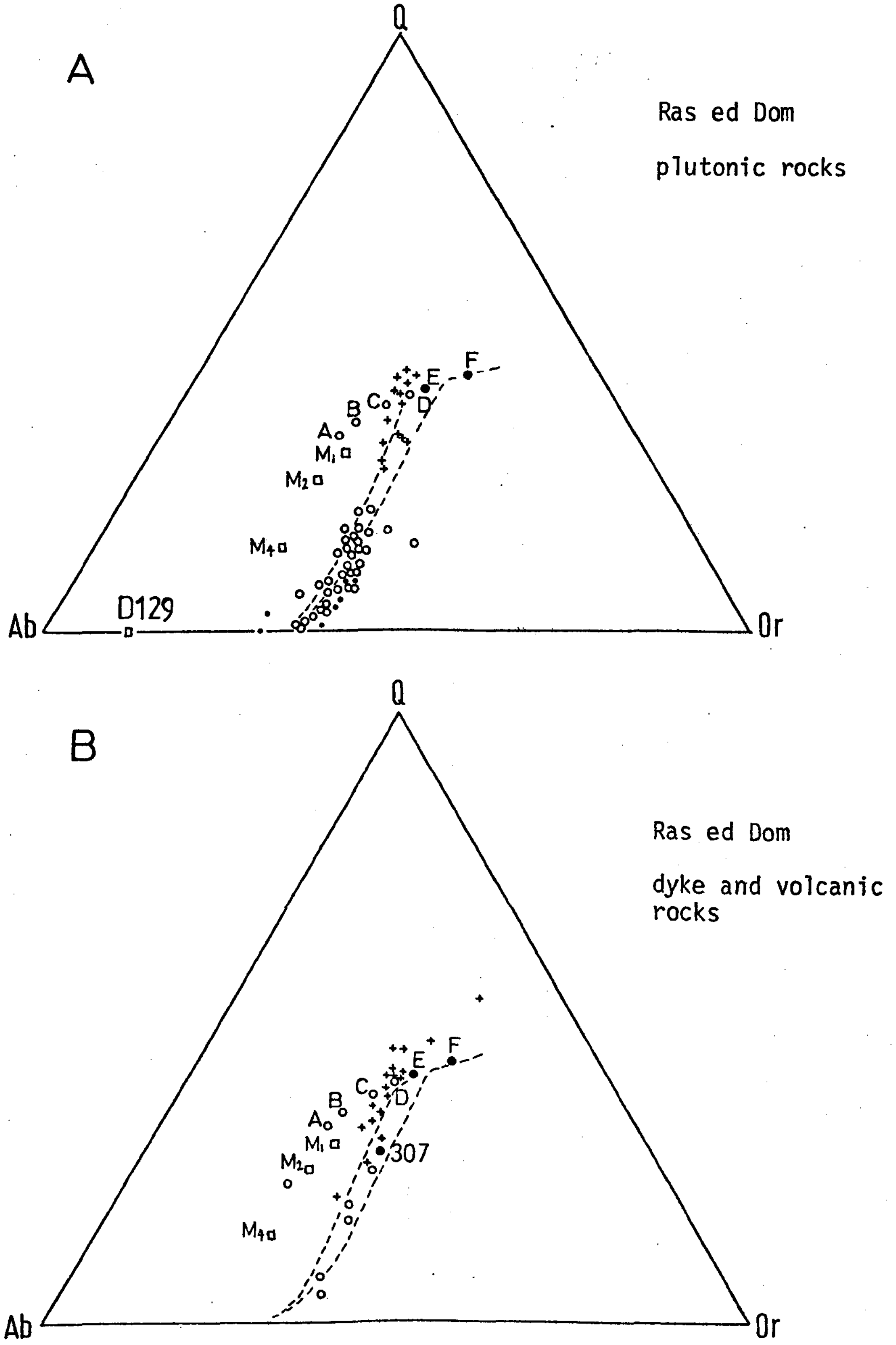

Fig. 6.10 : YOUNGER GRANITE ANALYSIS PLOTTED IN THE GRANITE SYSTEM. (AFTER TUTTLE AND BOWEN, 1958)
see opposite for explanation

Fig. 6.11 (opposite) : Younger Granite analyses plotted in the Granite System of Tuttle and Bowen (1958)

Plot C : PLUTONIC ROCKS - ABU DOM

- ● early syenite
- ○ alkali syenite
- + alkali granite

Plot D : DYKE AND VOLCANIC ROCKS - ABU DOM

- ○ syenitic dykes
- + granitic dykes

D860 and
D861 : silicified dykes
R101 : ignimbrite

other symbols as for Fig. 6.10, preceeding page.

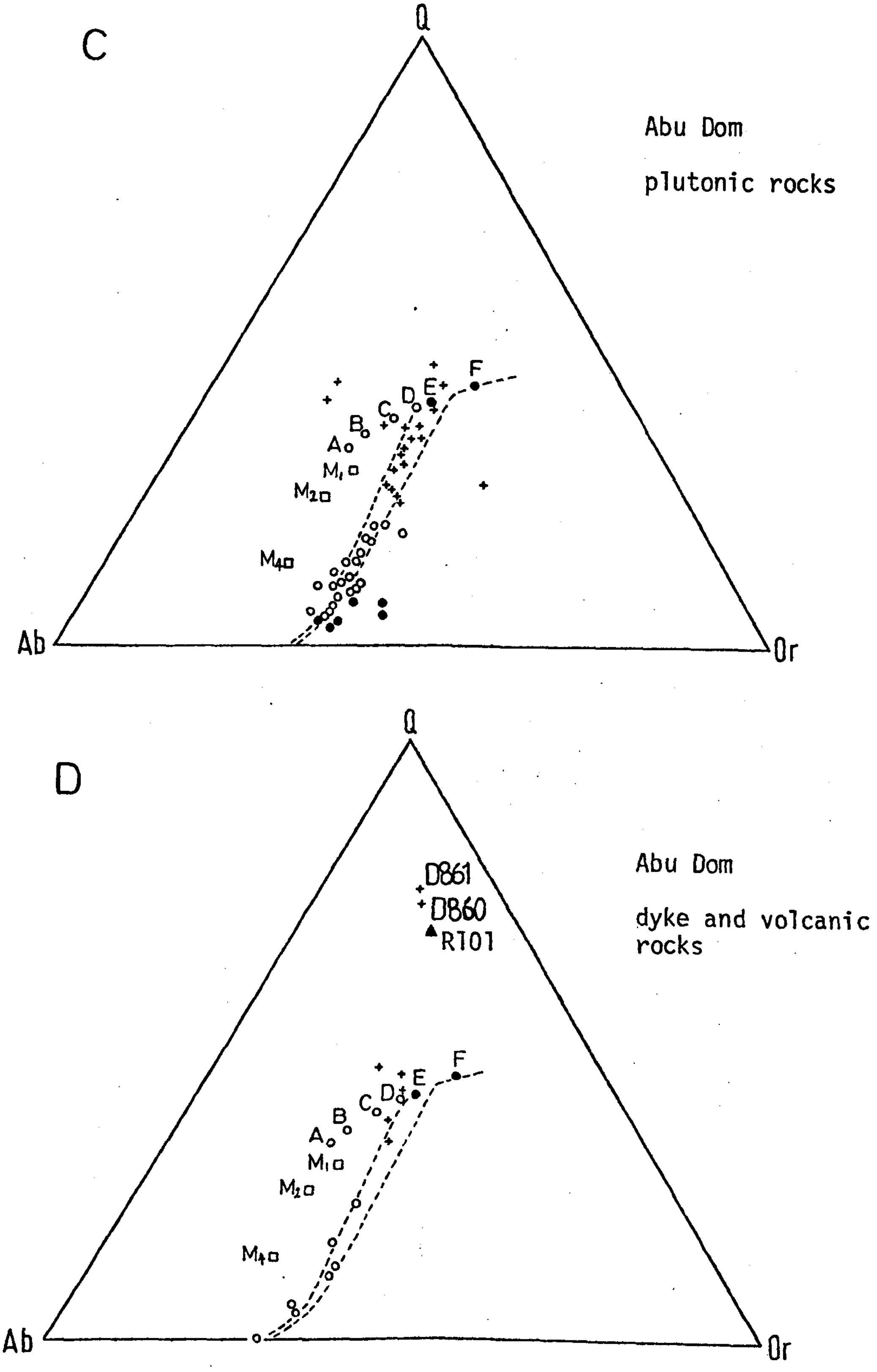

Fig. 6.11 : YOUNGER GRANITE ANALYSIS PLOTTED IN THE GRANITE SYSTEM (AFTER TUTTLE AND BOWEN, 1958) (Cont.)
see opposite for explanation.

composition. The expected compositions are Or 30-40, which are close to those reported in chapter 5 for the more evolved syenites (table 5.2). The work of Thompson and MacKenzie (1967) amplifies Bailey and Schairer's (1964) concept of an 'orthoclase effect' i.e. fractionation of K-rich alkali-feldspar. Bailey (1976), however, concludes that this alone does not fully explain the evolution of perlkaline magmas and that volatiles may play a crucial role. Mustart (1972) has shown that excess alkali in the form of sodium disilicate enhances the solubility of water in the liquid, and that for a wide range of compositions there is a continuum between silicate liquid and vapour.

Despite the above reservations the Bayuda rocks are plotted in the Granite System in figs. 6.10 and 6.11, since few of the rocks contain normative sodium metasilicate (c.f. Curtis 1979). The early syenites, alkali syenites and alkali granites plot as a continuous trend whose position is close to the thermal valley of Carmichael and MacKenzie (1963). The trend is thus consistent with the formation of the rocks at successively lower temperatures by magmatic processes. As expected the trend shows little relation to the simple Granite System minima of Tuttle and Bowen (1958). More surprising is the lack of correlation with the recently determined minima for F-rich systems (Manning, 1981). Although no F data are known for these rocks, alkali granites are typically F-enriched (Bailey, 1977; Harris, 1981). Thus it is apparent that the minima of Manning (1981) do not relate to systems enriched in both alkalies and flourine.

iii. The SiO_2-Al_2O_3-(Na_2O + K_2O) Plot

Over 80% of an analysis of most of the rock compositions under discussion is accounted for by molecular SiO_2, Al_2O_3, Na_2O and K_2O. Recognising this, Bailey & Macdonald (1969) examined alkali-feldspar fractionation in the system Na_2O - K_2O - Al_2O_3 - SiO_2. Any liquid composition in the system must, together with the Ab and Or end-members, define a plane within it. Separation of feldspar cannot remove the residual liquid away from the plane since the latter contains the feldspar join. Removal from the plane requires the intervention of,

Fig. 6.12 (opposite) : $SiO_2 - Al_2O_3 - (Na_2O + K_2O)$ plot
(after Bailey and Macdonald, 1969)

A : Plutonic rocks - Ras ed Dom
B : Dyke and volcanic rocks - Ras ed Dom
C : Plutonic rocks - Abu Dom
D : Dyke and volcanic rocks - Abu Dom

Line KK' is the quartz-alkali feldspar cotectic
Line NN' is the quartz-albite cotectic

Points 1 and 2 represent the minima for the granite system with 4.5% and 8% of both acmite and sodium metasilicate respectively added (Carmichael and Mackenzie, 1963)

Plots A and C :
• early syenite
○ alkali syenite
\+ alkali granite

Plots B and D :
○ syenitic dykes
\+ granitic dykes
▲ D307 volcanic tuff
■ R101 ignimbrite

Points 3, 4, 5, 6 after Thompson and MacKenzie (1967), representing the location of the quartz - feldspar minimum under the conditions specified below, and with pH_2O equal to 1kb.

3 : Granite System + 5% Na_2SiO_3
4 : Granite System + 5% $NaFeSi_2O_6$
5 : Granite System + 5% K_2SiO_3
6 : Granite System + 5% $NaKSiO_3$

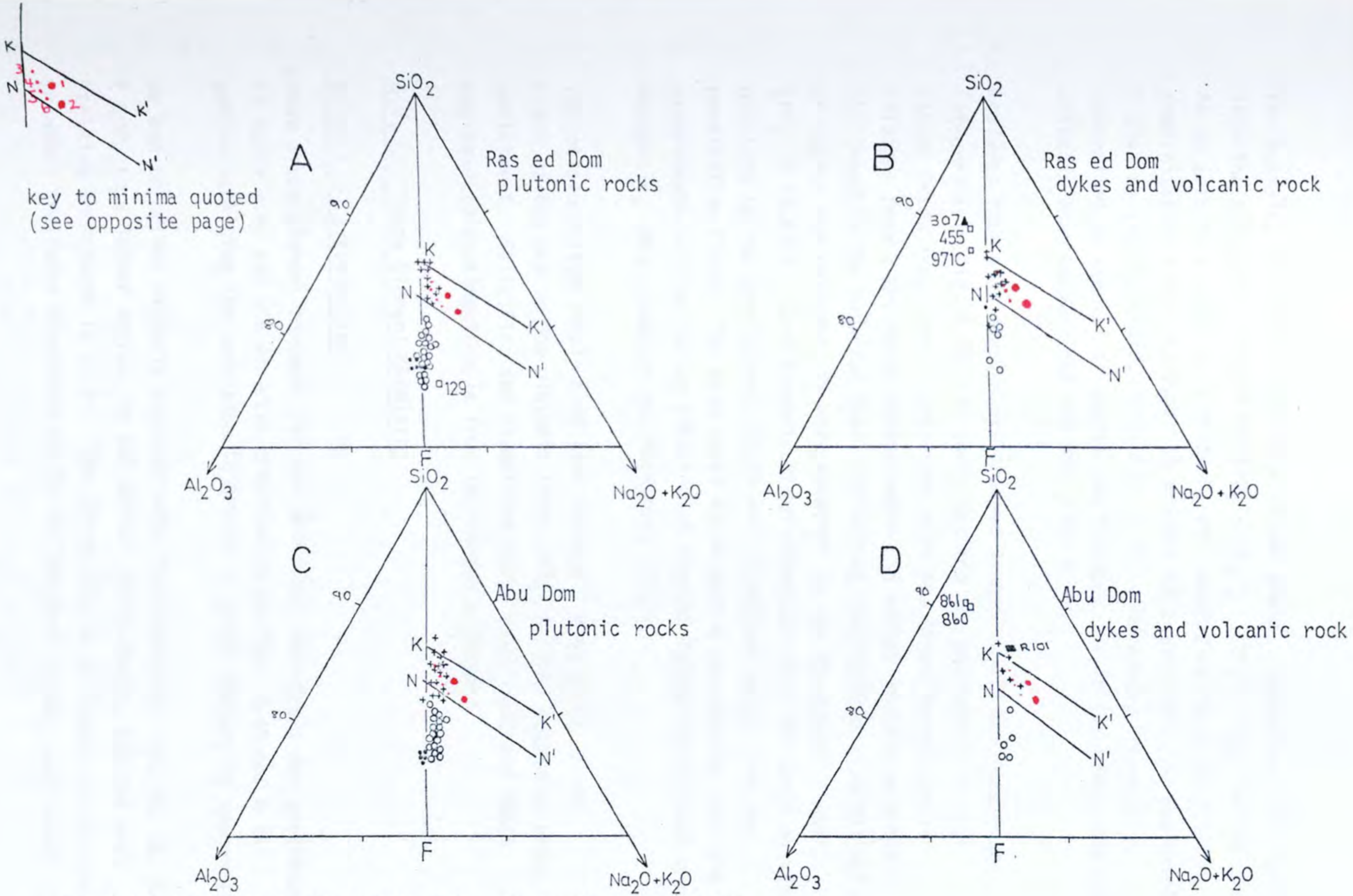

Fig. 6.12 : SiO_2 Al_2O_3 (Na_2O+K_2O) PLOT. see opposite for explanation.

for example, crystallisation of a second phase. Condensing this system into the triangular projection SiO_2 - Al_2O_3 - (Na_2O + K_2O) causes the Ab-Or join to project as a point F, and successive residual liquids precipitating alkali-feldspar to project as a straight line radiating from F (Bailey and Macdonald, 1969; fig. 6.12). Moreover, compositions controlled by removal of quartz and feldspar lie in the quartz-feldspar cotectic zone between KKI and NNI (fig. 6.12).

Analyses from each complex are grouped into plutonic and hypabyssal categories in fig. 6.12. In each instance the analyses plot in a linear trend away from F consistent with fractionation of alkali-feldspar from a trachytic parent magma. A slight broadening out of the trend in the cotectic zone, reflecting simultaneous crystallisation of quartz and feldspar, is more apparent in the hypabyssal trends (fig. 6.12-B+D). Each plutonic trend commences with the early syenites plotting in the peraluminous field and thereafter moves into the peralkaline field. The acid rocks again show a correlation with the experimental minima for an alkali-rich Granite System (Carmichael and MacKenzie, 1963; Thompson and MacKenzie (1967).

The metasomatised sample D129 (see section 4.5.B) plots to the right of the Ras ed Dom plutonic trend (fig. 6.12-A) recording sodic enrichment. Silicified and haematised dykes (e.g. D860 and D861) are readily distinguishable from the magmatic trends.

6.3. : Trace Element Chemistry

6.3.A. : Introduction

Mean trace element contents for the principal rock-types are presented in table 6.8. and are depicted graphically in figs. 6.13 and 6.14. Before examining the variation in detail a brief summary is appropriate.

Ba and Sr become markedly depleted with fractionation. Ce, Nb, La, Rb Y and, to a lesser degree, Ga all behave incompatably, but the most striking enrichment is in Zr. The sharp rise in Zr levels in the alkali granites indicates concentration in the residual magma, and Curtis (1979)

1. EARLY SYENITES

	Ras ed Dom (n=9)				Abu Dom (n=6)			
	max.	min.	$\bar{x}$	σn	max.	min.	$\bar{x}$	σn
Ga	43	35	38	3	41	36	39	2
Rb	74	42	55	11	72	34	47	14
Sr	284	67	189	88	279	137	207	60
Y	56	25	38	11	39	27	31	5
Zr	776	264	433	182	620	305	394	121
Nb	93	41	62	19	88	41	57	17
Ba	1025	540	793	166	1473	779	1081	297
La	79	40	55	15	74	51	64	8
Ce	179	91	123	37	513	109	192	158
Nd	90	46	63	15	76	59	67	7
K/Rb	1089	553	787	171	1282	693	1028	225

2. ALKALI SYENITES

	Ras ed Dom (n=40)				Abu Dom (n=23)			
	max.	min.	$\bar{x}$	σn	max.	min.	$\bar{x}$	σn
Ga	58	37	46	5	57	42	50	4
Rb	153	17	80	23	97	43	76	17
Sr	133	0	27	23	329	8	47	68
Y	87	13	50	18	91	25	58	20
Zr	1835	136	793	366	2082	304	1029	499
Nb	197	24	102	39	262	52	134	47
Ba	1620	0	177	285	1400	25	267	358
La	169	21	85	34	214	46	104	40
Ce	353	40	177	73	427	100	224	80
Nd	144	24	85	27	185	50	102	32
K/Rb	1120	305	581	164	1135	430	607	186

3. ALKALI GRANITES

	Ras ed Dom (n=14)				Abu Dom (n=20)			
	max.	min.	$\bar{x}$	σn	max.	min.	$\bar{x}$	σn
Ga	53	47	50	2	57	39	48	5
Rb	195	92	139	37	199	46	132	33
Sr	23	0	9	7	30	3	14	7
Y	190	35	96	44	130	32	83	27
Zr	3036	470	1589	709	3357	983	1755	547
Nb	283	61	169	72	445	58	191	94
Ba	68	0	18	21	131	7	57	34
La	297	56	139	71	365	44	165	88
Ce	594	86	300	144	489	73	319	134
Nd	270	57	145	65	378	49	157	82
K/Rb	832	183	332	168	491	191	316	75

Table 6.8: Mean trace element concentrations in the principal rock-types of Ras ed Dom and Abu Dom.
All values in ppm, except K/Rb.

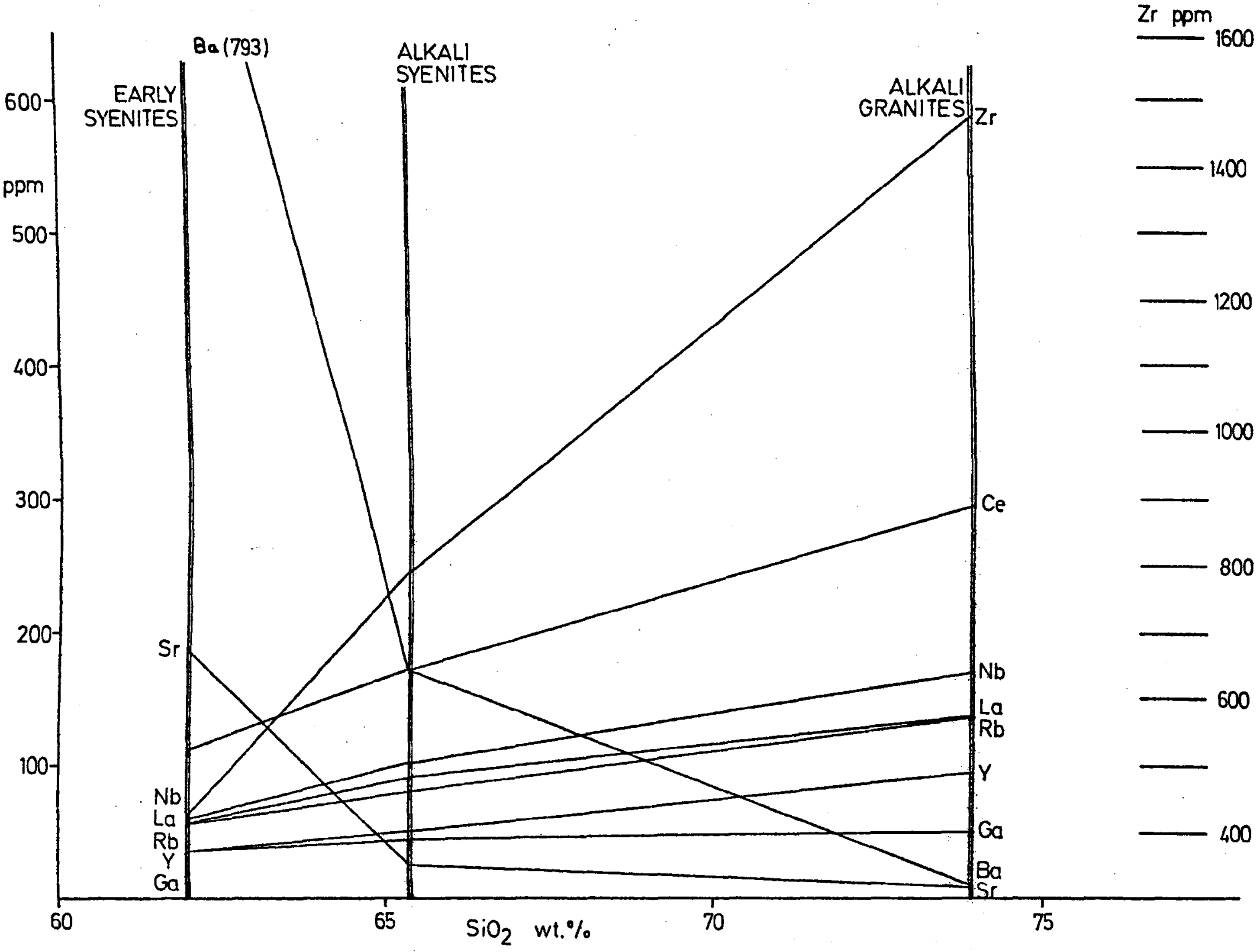

Fig. 6.13 : MEAN TRACE ELEMENT CONTENT VERSUS MEAN SiO_2. SEE TABLE 6.8. RAS ED DOM

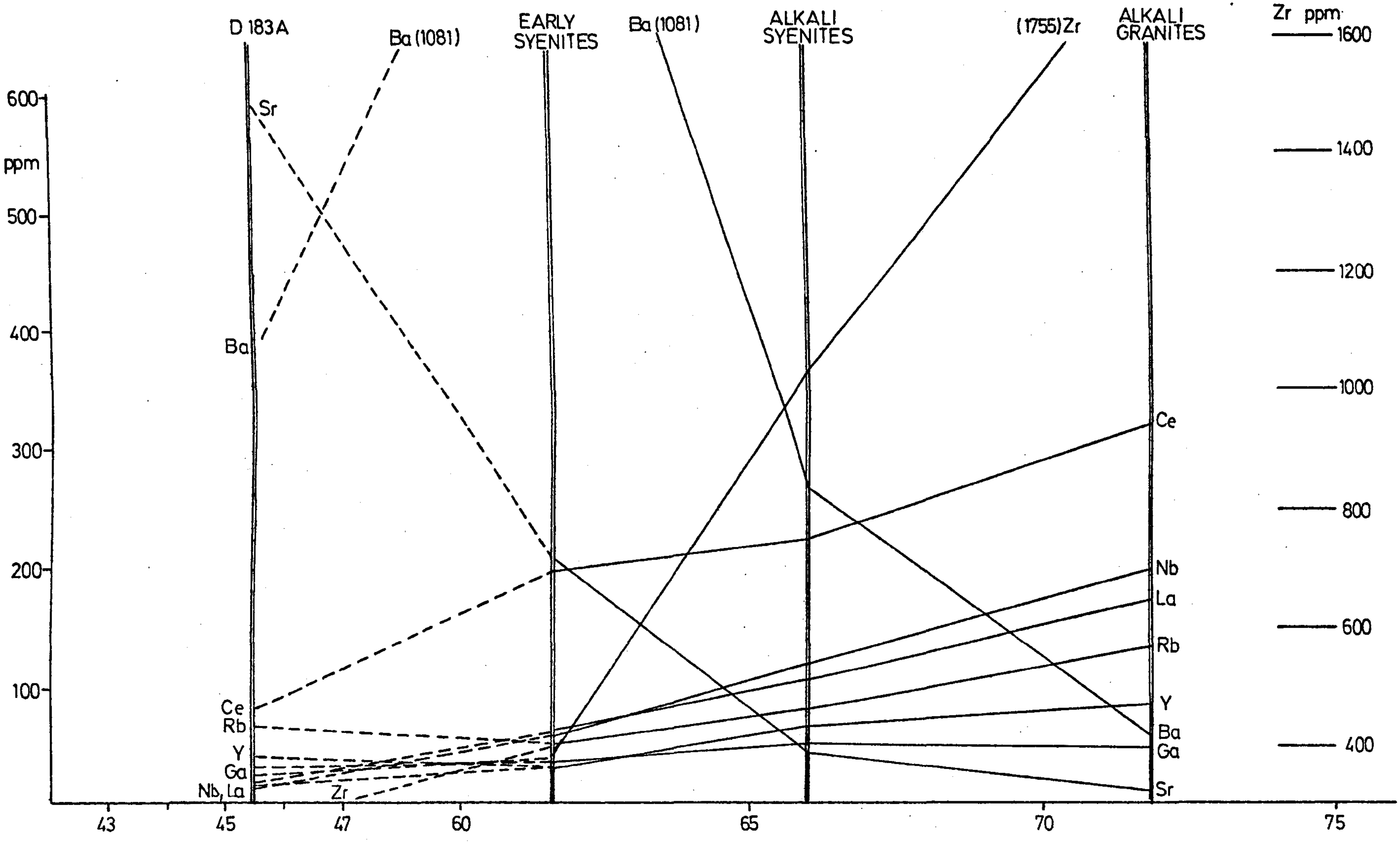

Fig. 6.14 : MEAN TRACE ELEMENT CONTENT VERSUS MEAN SiO_2 SEE TABLE 6.8. ABU DOM

Fig. 6.15. (opposite) : Trace element variation relative to SiO_2.

A : RAS ED DOM - PLUTONIC ROCKS

▲ S1
▼ S2
△ S3
◆ S4
▽ S5
○ S6
⦶ S7
● S8

⊖ S9
◒ S10
▬ S11
⊘ S12
◐ S13
◑ S14
⦸ S15
◇ IT1

• IT2
· IT3
⬘ D209 - early syenite raft in S6
+ G1
× G2
✚ MG1
✖ MG2

B : RAS ED DOM AND ABU DOM - DYKE AND VOLCANIC ROCKS

Ras ed Dom	Abu Dom
○ syenitic dykes	⊙ syenitic dykes
+ granitic dykes	× granitic dykes
● rafted sample of tuff, loc. 307	▲ ignimbrite, Abu Dom Volcanic Group, R101

C : ABU DOM - PLUTONIC ROCKS

▲ S1
△ S2
▽ S3
○ S4
⊙ S5
× G1
+ G2

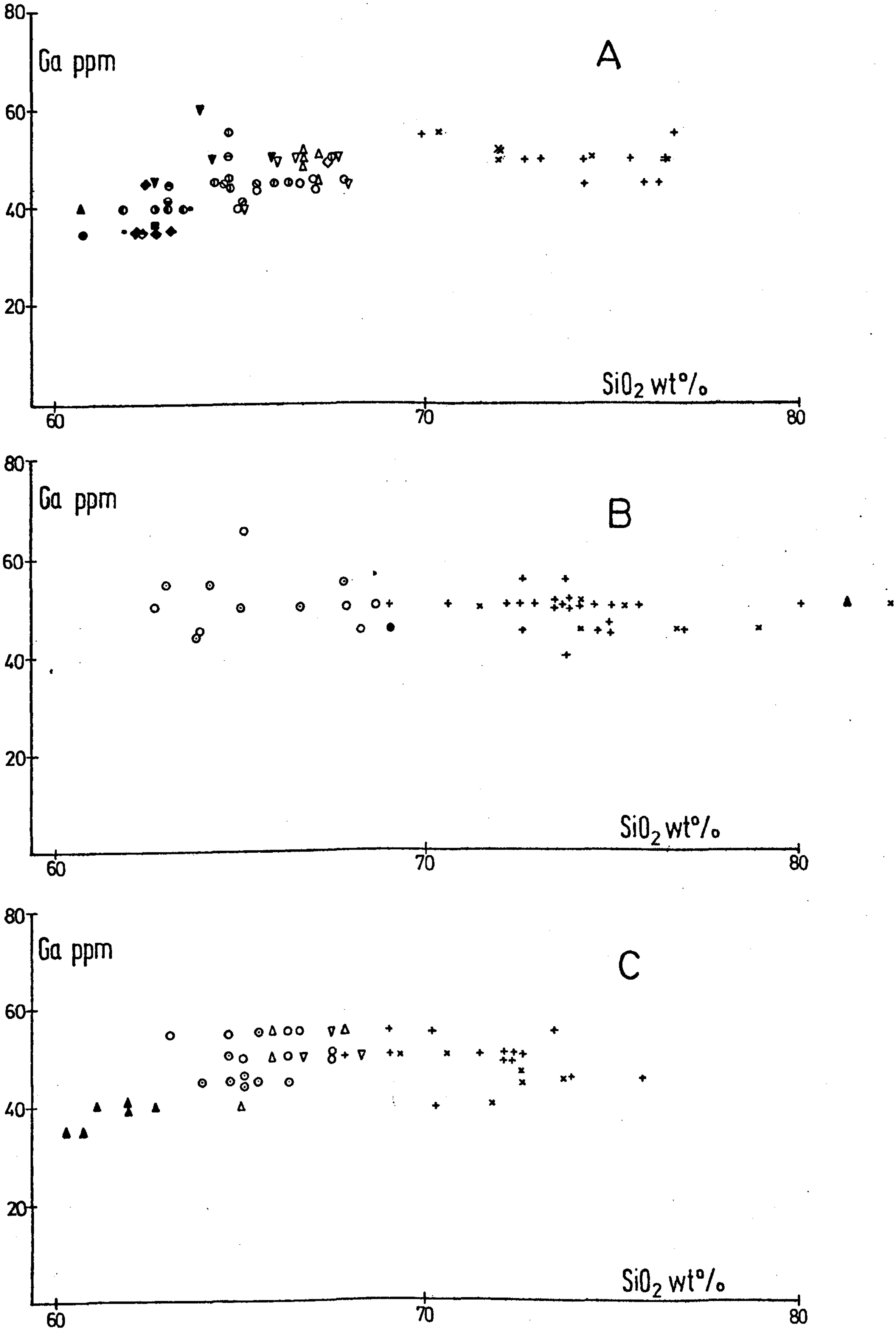

fig.6.15 : Trace element variation relative to SiO_2 (explanation opposite).

Fig. 6.15. (opposite) : Trace element variation relative to SiO_2.

A : RAS ED DOM - PLUTONIC ROCKS

- ▲ S1
- ▼ S2
- △ S3
- ◆ S4
- ▽ S5
- ○ S6
- ⦶ S7
- ◓ S8
- ⊖ S9
- ◒ S10
- ▬ S11
- ⊘ S12
- ◐ S13
- ◑ S14
- ⦸ S15
- ◇ IT1
- ● IT2
- • IT3
- ◈ D209 - early syenite raft in S6
- + G1
- × G2
- ✚ MG1
- ✖ MG2

B : RAS ED DOM AND ABU DOM - DYKE AND VOLCANIC ROCKS

Ras ed Dom	Abu Dom
○ syenitic dykes	⊙ syenitic dykes
+ granitic dykes	× granitic dykes
● rafted sample of tuff, loc. 307	▲ ignimbrite, Abu Dom Volcanic Group, R101

C : ABU DOM - PLUTONIC ROCKS

- ▲ S1
- △ S2
- ▽ S3
- ○ S4
- ⊙ S5
- × G1
- + G2

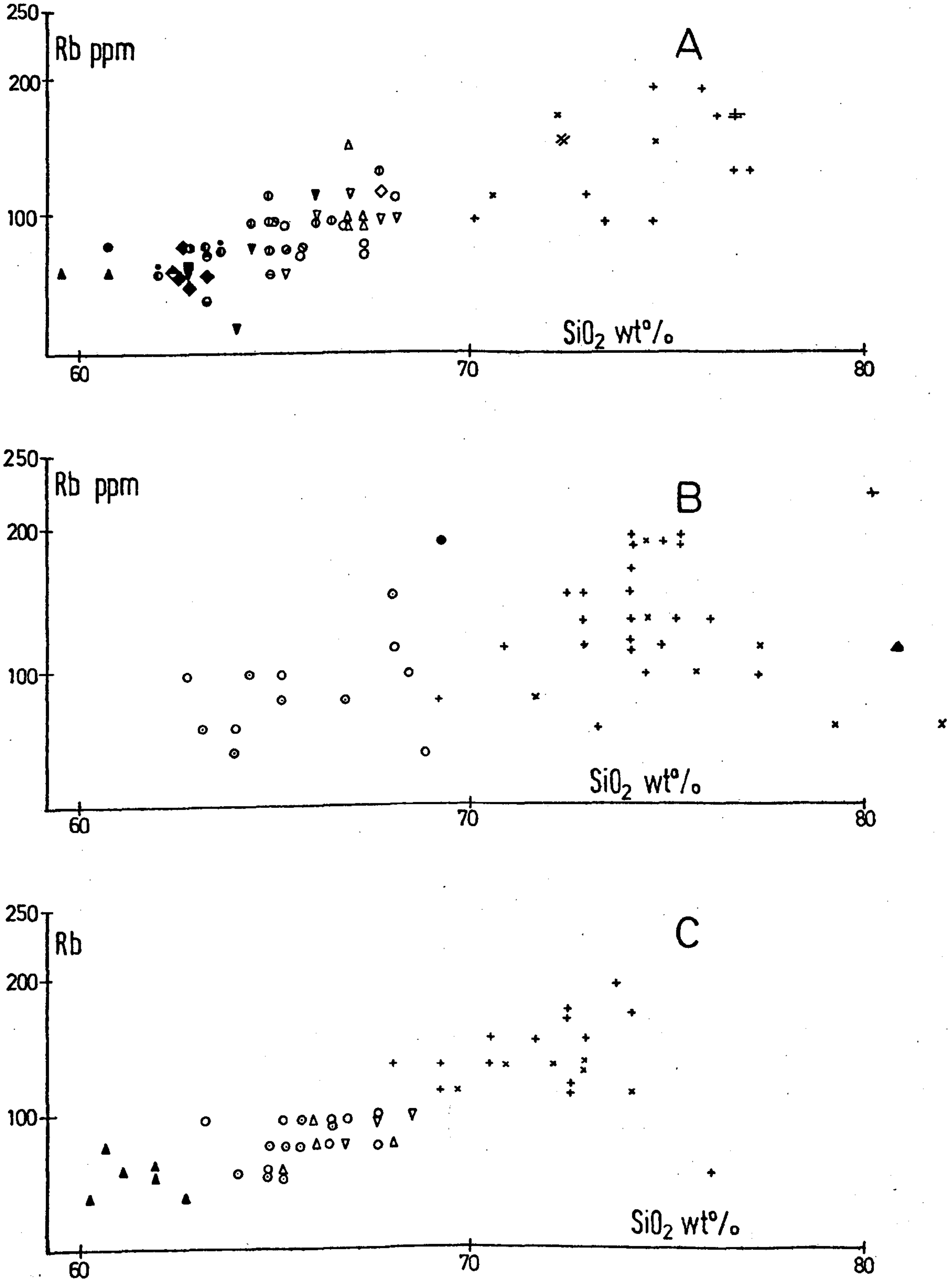

fig.6.15 (contd.) : trace element variation relative to SiO$_2$ (explanation opposite).

Fig. 6.15. (opposite) : Trace element variation relative to SiO_2.

A : RAS ED DOM - PLUTONIC ROCKS

▲ S1
▼ S2
△ S3
◆ S4
▽ S5
○ S6
⦶ S7
◓ S8
⊖ S9
◒ S10
▬ S11
⊘ S12
◐ S13
◑ S14
⊗ S15
◇ IT1
• IT2
· IT3
◈ D209 - early syenite raft in S6
+ G1
× G2
+ MG1
× MG2

B : RAS ED DOM AND ABU DOM - DYKE AND VOLCANIC ROCKS

Ras ed Dom
○ syenitic dykes
+ granitic dykes
● rafted sample of tuff, loc. 307

Abu Dom
⊙ syenitic dykes
× granitic dykes
▲ ignimbrite, Abu Dom Volcanic Group, R101

C : ABU DOM - PLUTONIC ROCKS

▲ S1
△ S2
▽ S3
○ S4
⊙ S5
× G1
+ G2

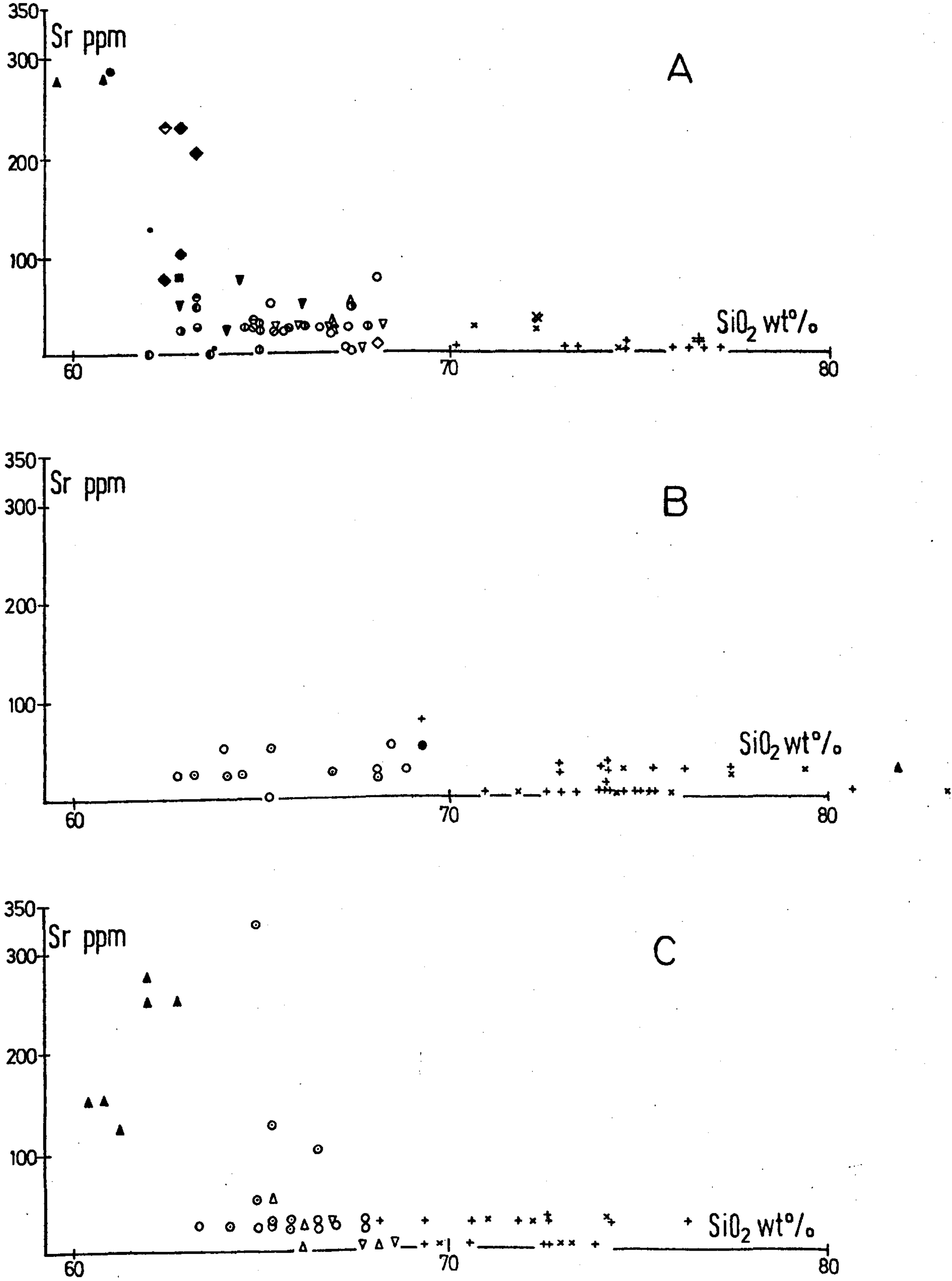

fig.6.15 (contd.) : Trace element variation relative to SiO_2 (explanation opposite).

Fig. 6.15. (opposite) : Trace element variation relative to SiO_2.

A : RAS ED DOM - PLUTONIC ROCKS

▲ S1
▼ S2
△ S3
◆ S4
▽ S5
○ S6
⦶ S7
● S8
⊖ S9
◒ S10
▬ S11
⊘ S12
◐ S13
◑ S14
⦸ S15
◇ IT1
• IT2
· IT3
⬘ D209 - early syenite raft in S6
+ G1
× G2
✚ MG1
✗ MG2

B : RAS ED DOM AND ABU DOM - DYKE AND VOLCANIC ROCKS

Ras ed Dom	Abu Dom
○ syenitic dykes	⊙ syenitic dykes
+ granitic dykes	× granitic dykes
● rafted sample of tuff, loc. 307	▲ ignimbrite, Abu Dom Volcanic Group, R101

C : ABU DOM - PLUTONIC ROCKS

▲ S1
△ S2
▽ S3
○ S4
⊙ S5
× G1
+ G2

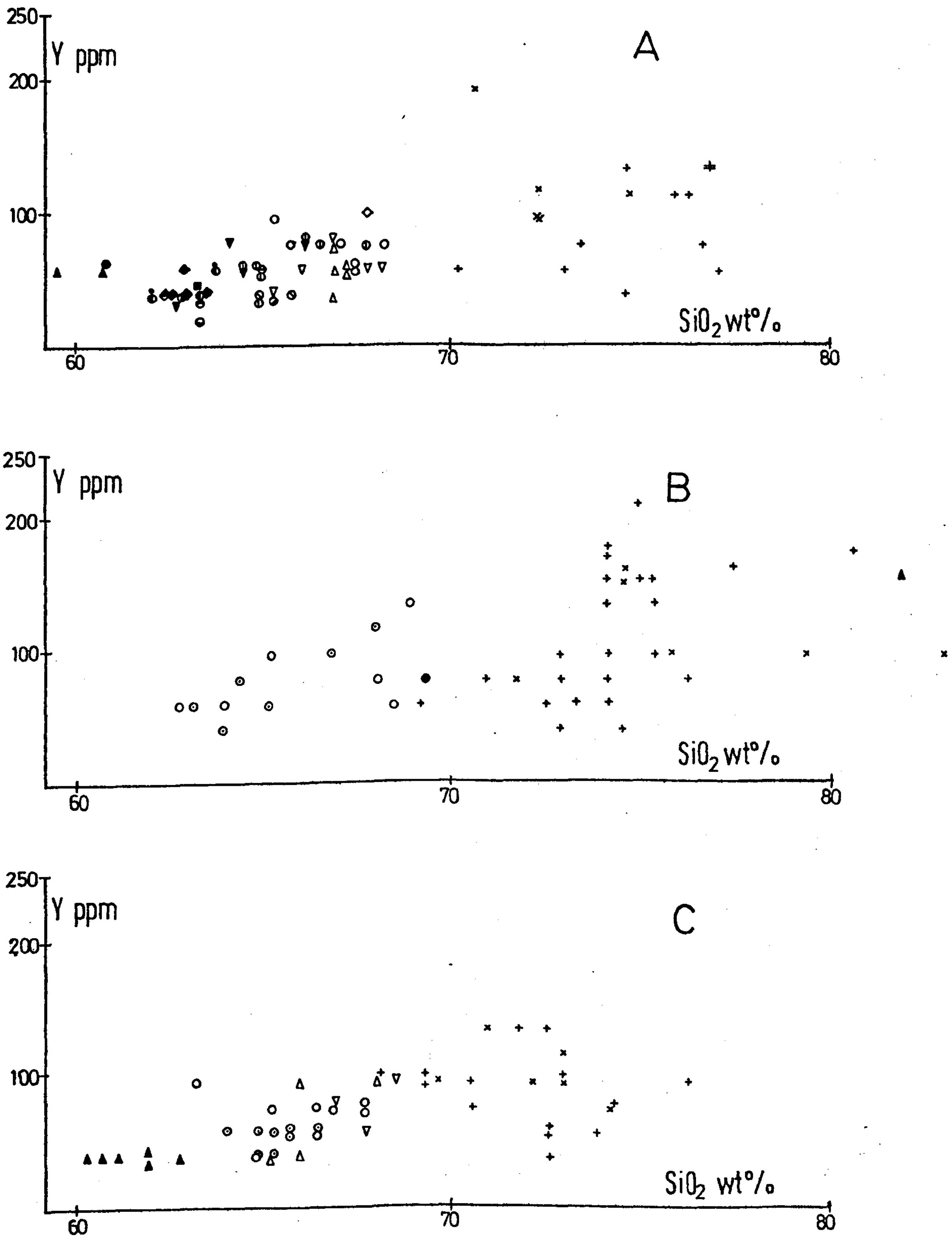

fig.6.15 (contd.) : Trace element variation relative to SiO_2 (explanation opposite).

Fig. 6.15. (opposite) : Trace element variation relative to SiO_2.

A : RAS ED DOM - PLUTONIC ROCKS

▲ S1
▼ S2
△ S3
◆ S4
▽ S5
○ S6
⦶ S7
● S8

⊖ S9
◓ S10
▬ S11
⊘ S12
◐ S13
◑ S14
⊙ S15
◇ IT1

● IT2
• IT3
⬘ D209 - early syenite raft in S6
+ G1
× G2
✛ MG1
✕ MG2

B : RAS ED DOM AND ABU DOM - DYKE AND VOLCANIC ROCKS

Ras ed Dom	Abu Dom
○ syenitic dykes	⊙ syenitic dykes
+ granitic dykes	× granitic dykes
● rafted sample of tuff, loc. 307	▲ ignimbrite, Abu Dom Volcanic Group, R101

C : ABU DOM - PLUTONIC ROCKS

▲ S1
△ S2
▽ S3
○ S4
⊙ S5
× G1
+ G2

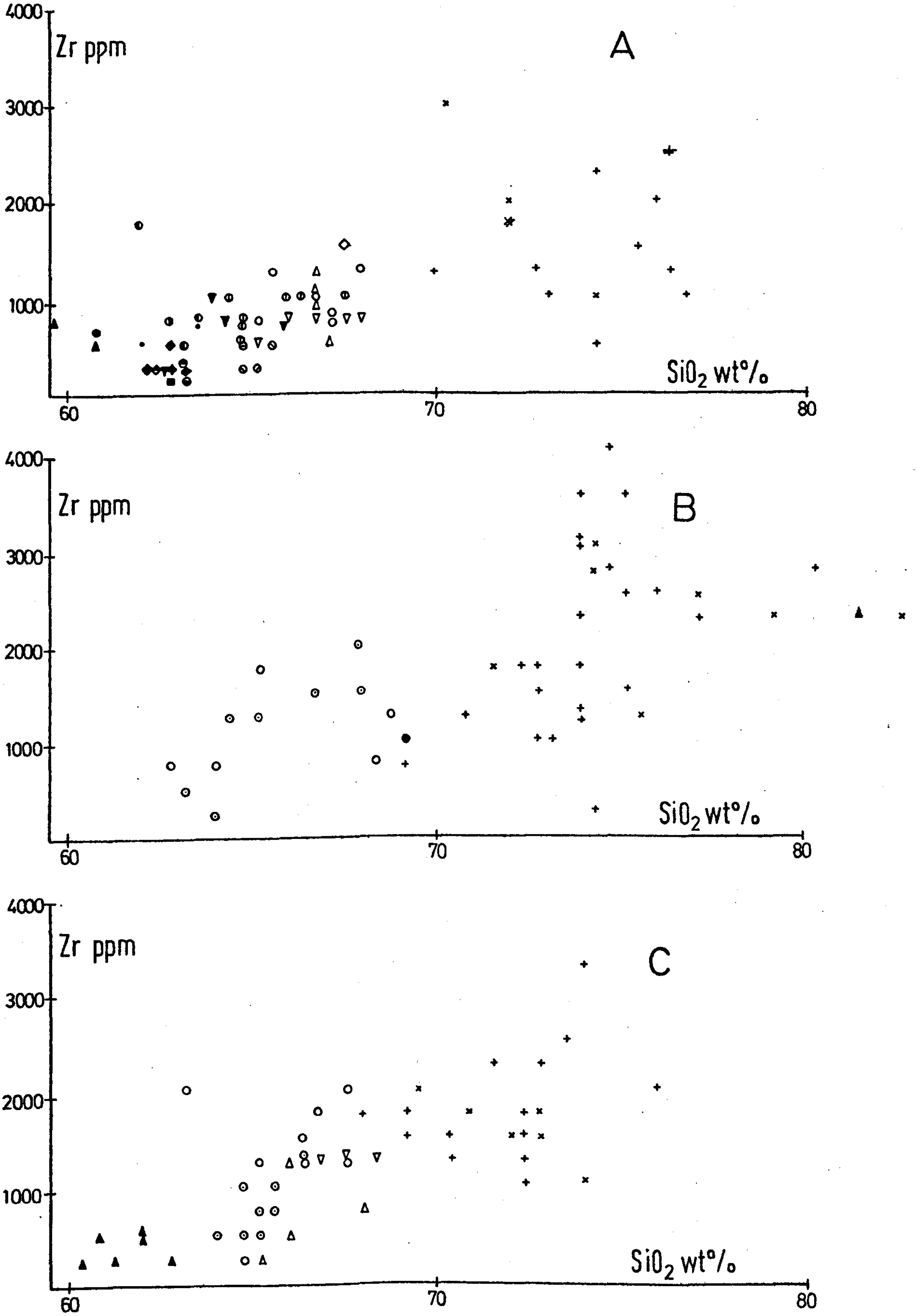

fig.6.15 (contd.) : Trace element variation relative to SiO_2 (explanation opposite).

Fig. 6.15. (opposite) : Trace element variation relative to SiO_2.

A : RAS ED DOM - PLUTONIC ROCKS

- ▲ S1
- ▼ S2
- △ S3
- ◆ S4
- ▽ S5
- ○ S6
- ⦶ S7
- ● S8
- ⊖ S9
- ◒ S10
- ▬ S11
- ⊘ S12
- ◐ S13
- ◑ S14
- ⊗ S15
- ◇ IT1
- • IT2
- · IT3
- ⬘ D209 - early syenite raft in S6
- + G1
- × G2
- ✚ MG1
- ✕ MG2

B : RAS ED DOM AND ABU DOM - DYKE AND VOLCANIC ROCKS

Ras ed Dom	Abu Dom
○ syenitic dykes	⊙ syenitic dykes
+ granitic dykes	× granitic dykes
• rafted sample of tuff, loc. 307	▲ ignimbrite, Abu Dom Volcanic Group, R101

C : ABU DOM - PLUTONIC ROCKS

- ▲ S1
- △ S2
- ▽ S3
- ○ S4
- ⊙ S5
- × G1
- + G2

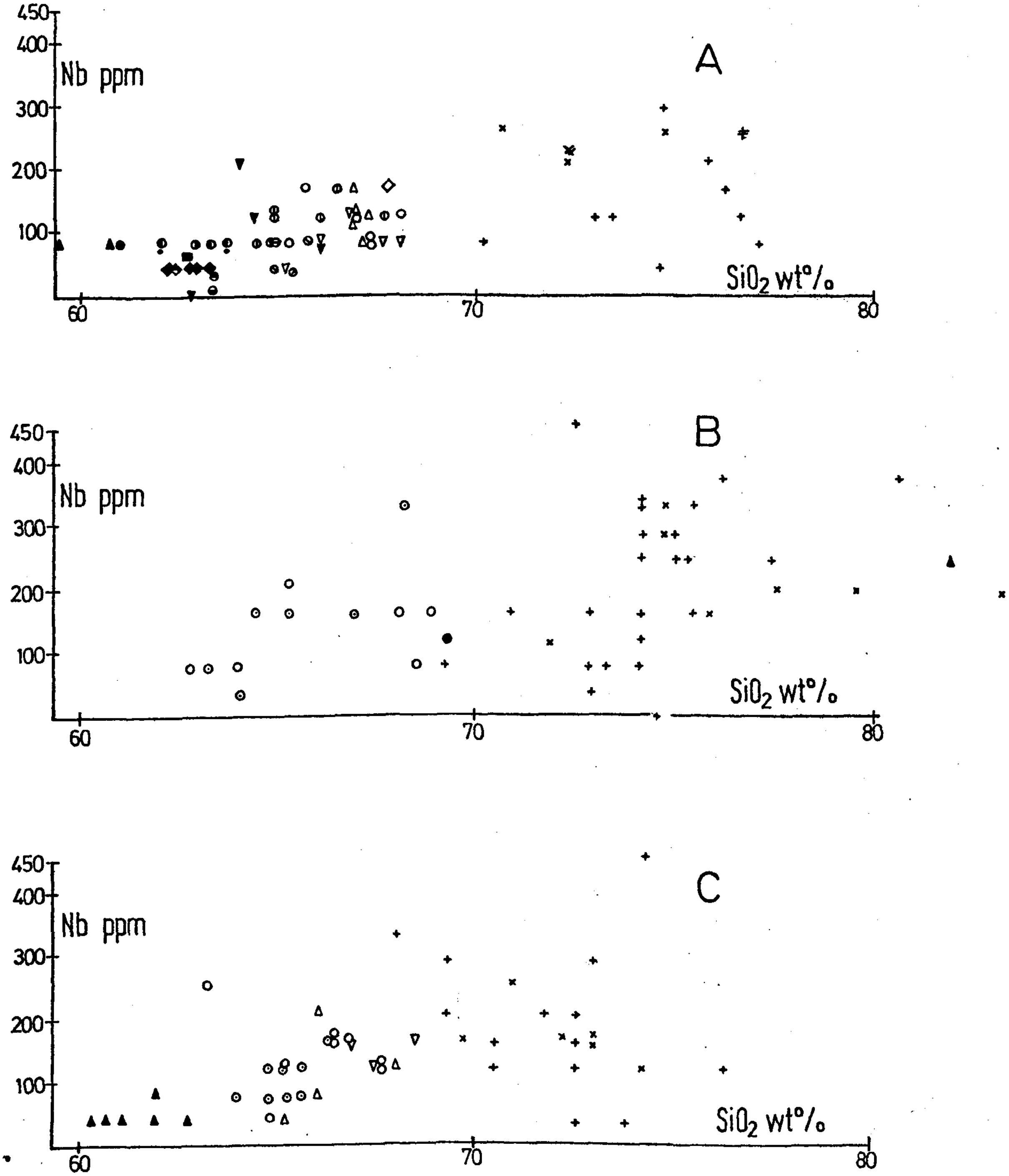

fig.6.15 (contd.) : Trace element variation relative to SiO_2 (explanation opposite).

Fig. 6.15. (opposite) : Trace element variation relative to SiO_2.

A : RAS ED DOM - PLUTONIC ROCKS

- ▲ S1
- ▼ S2
- △ S3
- ◆ S4
- ▽ S5
- ○ S6
- ⦶ S7
- ● S8
- ⊖ S9
- ◓ S10
- ▬ S11
- ⊘ S12
- ◐ S13
- ◑ S14
- ⦸ S15
- ◇ IT1
- • IT2
- · IT3
- ⬘ D209 - early syenite raft in S6
- + G1
- × G2
- ✚ MG1
- ✱ MG2

B : RAS ED DOM AND ABU DOM - DYKE AND VOLCANIC ROCKS

Ras ed Dom	Abu Dom
○ syenitic dykes	⊙ syenitic dykes
+ granitic dykes	× granitic dykes
● rafted sample of tuff, loc. 307	▲ ignimbrite, Abu Dom Volcanic Group, R101

C : ABU DOM - PLUTONIC ROCKS

- ▲ S1
- △ S2
- ▽ S3
- ○ S4
- ⊙ S5
- × G1
- + G2

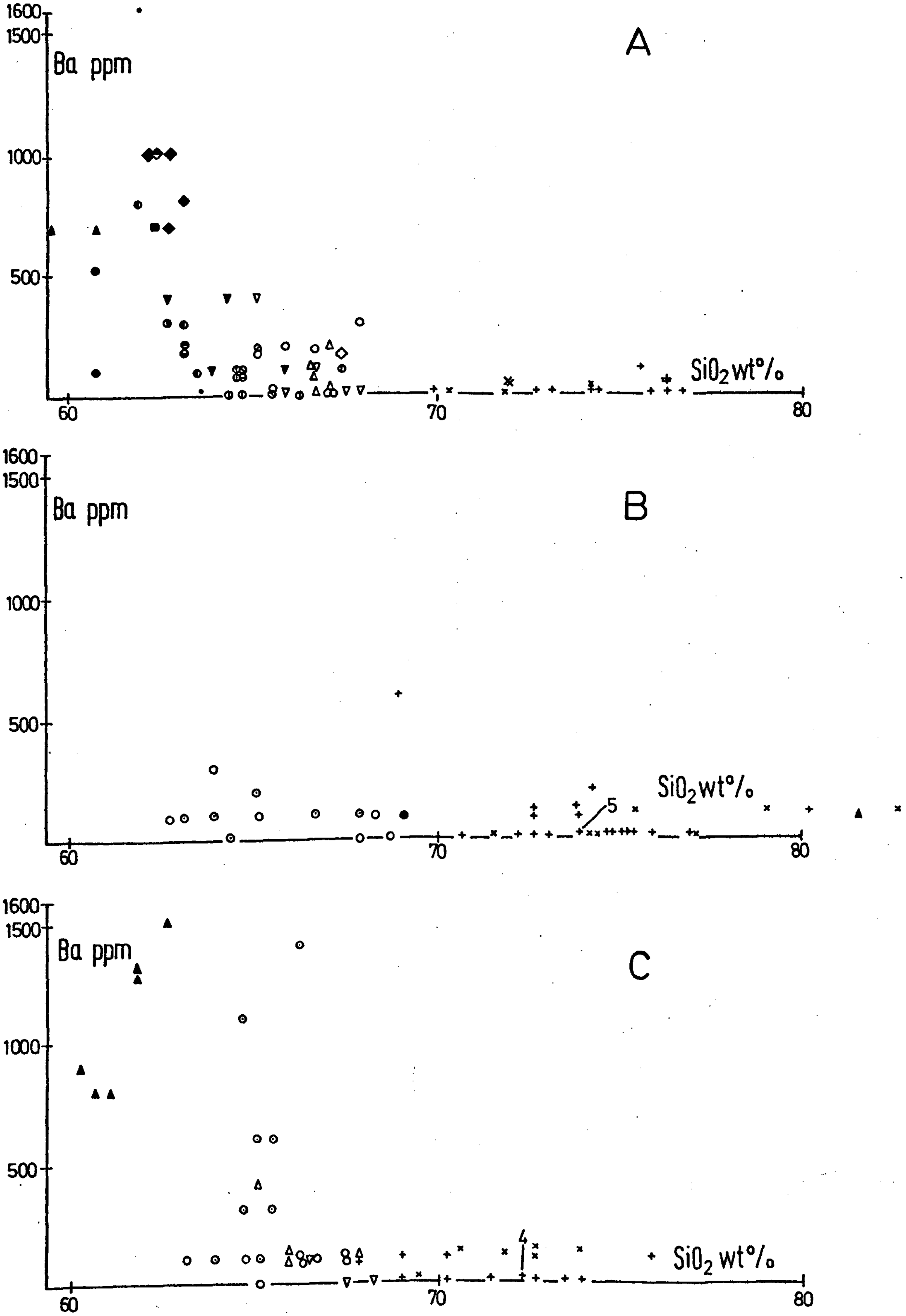

fig.6.15 (contd.) : Trace element variation relative to SiO_2 (explanation opposite).

Fig. 6.15. (opposite) : Trace element variation relative to SiO_2.

A : RAS ED DOM - PLUTONIC ROCKS

▲ S1
▼ S2
△ S3
◆ S4
▽ S5
○ S6
⦶ S7
● S8

⊖ S9
◒ S10
■ S11
⊘ S12
◐ S13
◑ S14
⊗ S15
◇ IT1

• IT2
· IT3
⬖ D209 - early syenite raft in S6
+ G1
× G2
✛ MG1
✕ MG2

B : RAS ED DOM AND ABU DOM - DYKE AND VOLCANIC ROCKS

Ras ed Dom
○ syenitic dykes
+ granitic dykes
• rafted sample of tuff, loc. 307

Abu Dom
⊙ syenitic dykes
× granitic dykes
▲ ignimbrite, Abu Dom Volcanic Group, R101

C : ABU DOM - PLUTONIC ROCKS

▲ S1
△ S2
▽ S3
○ S4
⊙ S5
× G1
+ G2

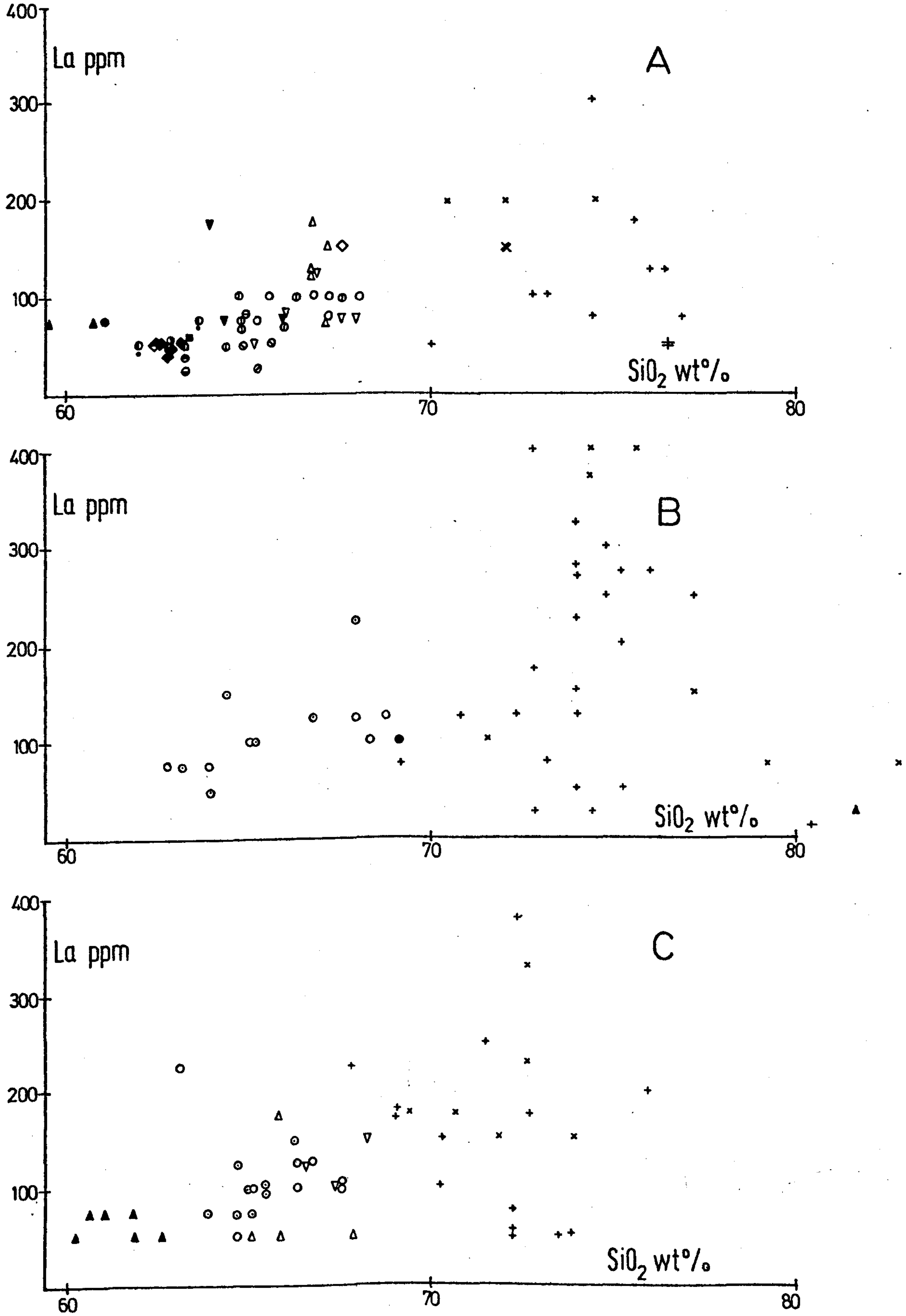

fig.6.15 (contd.) : Trace element variation relative to SiO_2 (explanation opposite).

Fig. 6.15. (opposite) : Trace element variation relative to SiO_2.

A : RAS ED DOM - PLUTONIC ROCKS

▲ S1
▼ S2
△ S3
◆ S4
▽ S5
ȯ S6
⦶ S7
◓ S8
⊖ S9
◒ S10
▬ S11
⊘ S12
◐ S13
◑ S14
⊗ S15
◇ IT1
● IT2
· IT3
⬙ D209 - early syenite raft in S6
+ G1
× G2
+ MG1
✕ MG2

B : RAS ED DOM AND ABU DOM - DYKE AND VOLCANIC ROCKS

Ras ed Dom	Abu Dom
○ syenitic dykes	⊙ syenitic dykes
+ granitic dykes	× granitic dykes
● rafted sample of tuff, loc. 307	▲ ignimbrite, Abu Dom Volcanic Group, R101

C : ABU DOM - PLUTONIC ROCKS

▲ S1
△ S2
▽ S3
○ S4
⊙ S5
× G1
+ G2

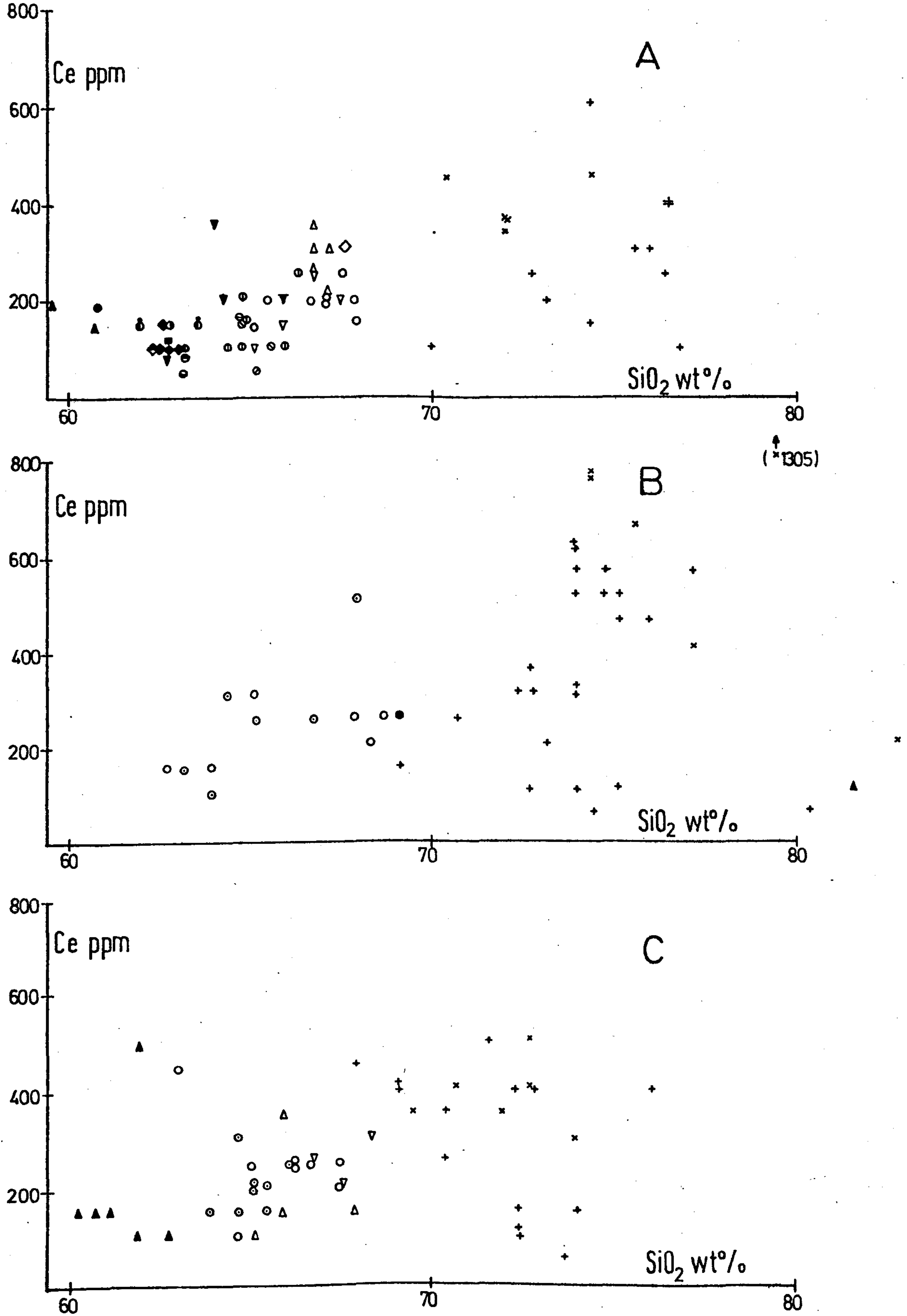

fig.6.15 (contd.) : Trace element variation relative to SiO$_2$ (explanation opposite).

Fig. 6.15. (opposite) : Trace element variation relative to SiO_2.

A : RAS ED DOM - PLUTONIC ROCKS

- ▲ S1
- ▼ S2
- △ S3
- ◆ S4
- ▽ S5
- ȯ S6
- ⦶ S7
- ● S8
- ⊖ S9
- ● S10
- ▬ S11
- ⊘ S12
- ◐ S13
- ◑ S14
- ⊘ S15
- ◇ IT1
- • IT2
- · IT3
- ⬘ D209 - early syenite raft in S6
- + G1
- × G2
- ✚ MG1
- ✕ MG2

B : RAS ED DOM AND ABU DOM - DYKE AND VOLCANIC ROCKS

Ras ed Dom	Abu Dom
○ syenitic dykes	⊙ syenitic dykes
+ granitic dykes	× granitic dykes
● rafted sample of tuff, loc. 307	▲ ignimbrite, Abu Dom Volcanic Group, R101

C : ABU DOM - PLUTONIC ROCKS

- ▲ S1
- △ S2
- ▽ S3
- ○ S4
- ⊙ S5
- × G1
- + G2

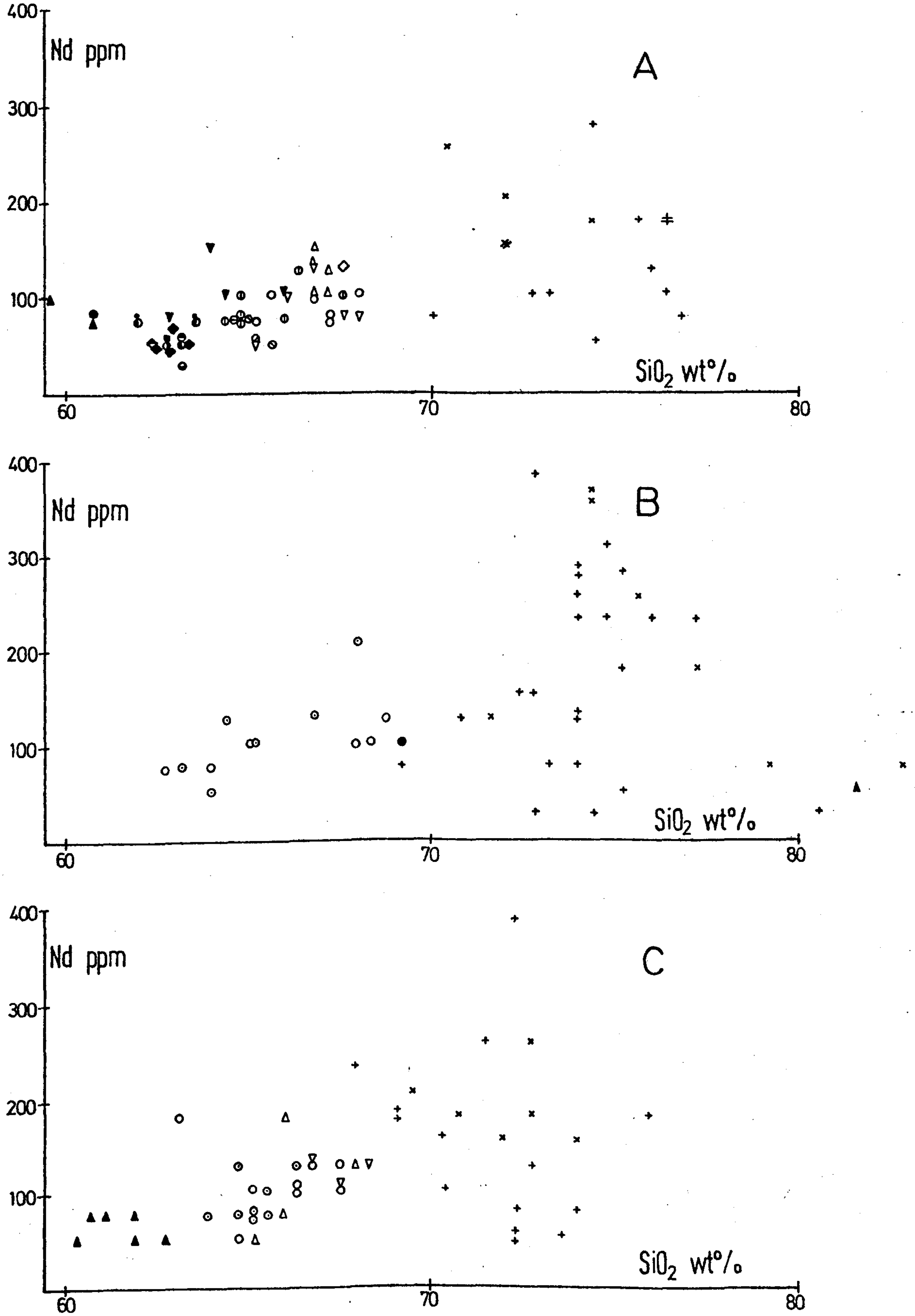

fig.6.15 (contd.) : Trace element variation relative to SiO$_2$ (explanation opposite).

Fig. 6.16. (opposite) : Trace element variation relative to Zr.

A : RAS ED DOM - PLUTONIC ROCKS

- ▲ S1
- ▼ S2
- △ S3
- ◆ S4
- ▽ S5
- ○ S6
- ⦶ S7
- ◓ S8
- ⊖ S9
- ● S10
- ▬ S11
- ⊘ S12
- ◐ S13
- ◑ S14
- ⦸ S15
- ◇ IT1
- ● IT2
- • IT3
- ⬘ D209 - early syenite raft in S6
- + G1
- × G2
- + MG1
- ⋇ MG2

B : RAS ED DOM AND ABU DOM - DYKE AND VOLCANIC ROCKS

Ras ed Dom	Abu Dom
○ syenitic dykes	⊙ syenitic dykes
+ granitic dykes	× granitic dykes
• rafted sample of tuff, loc. 307	▲ ignimbrite, Abu Dom Volcanic Group

C : ABU DOM - PLUTONIC ROCKS

- ▲ S1
- △ S2
- ▽ S3
- ○ S4
- ⊙ S5
- × G1
- + G2

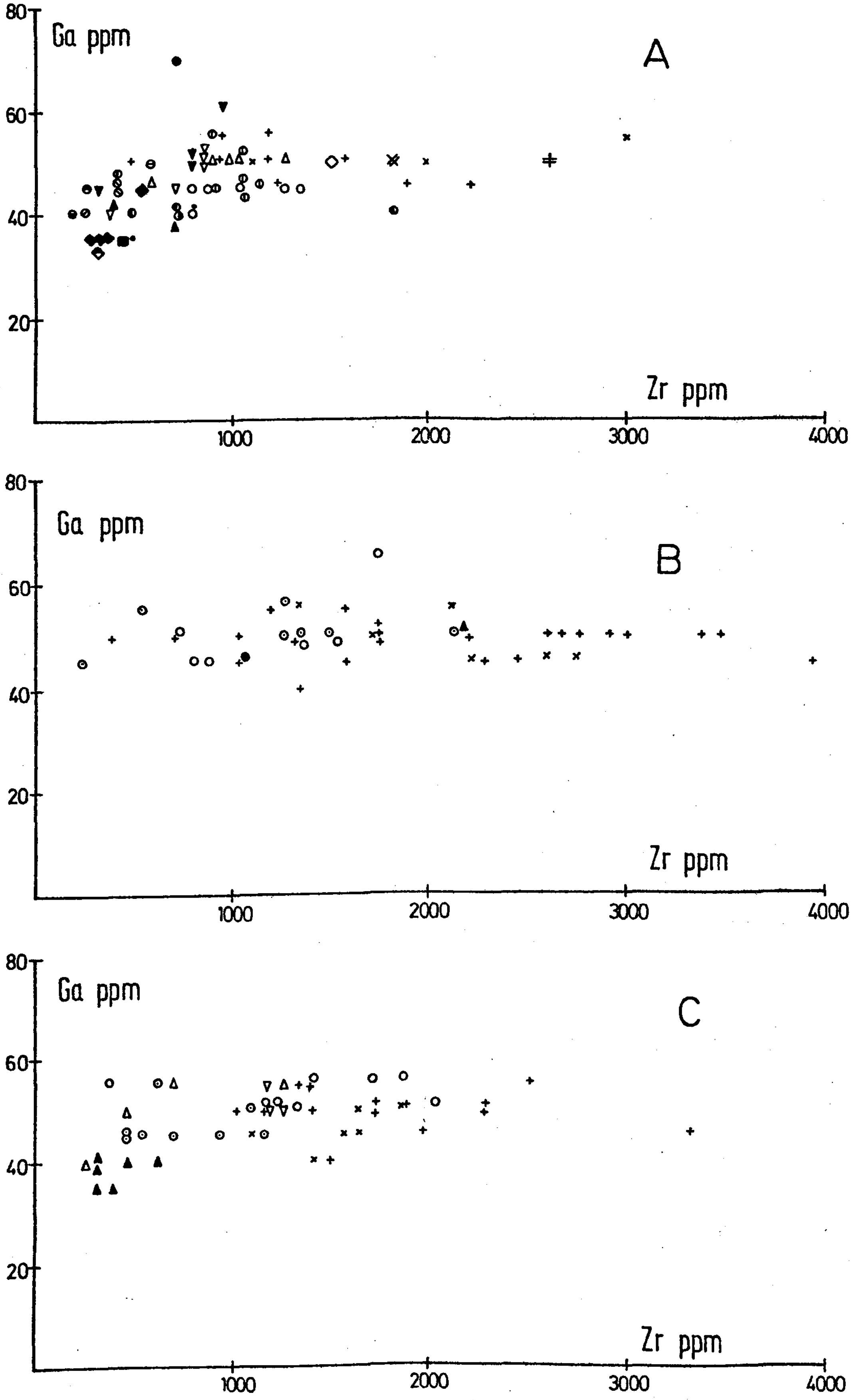

fig.6.16 : Trace element variation relative to Zr (explanation opposite).

Fig. 6.16. (opposite) : Trace element variation relative to **Zr.**

A : RAS ED DOM - PLUTONIC ROCKS

▲ S1
▼ S2
△ S3
◆ S4
▽ S5
○ S6
⦶ S7
◒ S8
⊖ S9
● S10
▬ S11
⊘ S12
◐ S13
◑ S14
⦸ S15
◇ IT1
● IT2
• IT3
⬘ D209 - early syenite raft in S6
+ G1
× G2
+ MG1
⋇ MG2

B : RAS ED DOM AND ABU DOM - DYKE AND VOLCANIC ROCKS

Ras ed Dom
○ syenitic dykes
+ granitic dykes
• rafted sample of tuff, loc. 307

Abu Dom
⦶ syenitic dykes
× granitic dykes
▲ ignimbrite, Abu Dom Volcanic Group

C : ABU DOM - PLUTONIC ROCKS

▲ S1
△ S2
▽ S3
○ S4
⊙ S5
× G1
+ G2

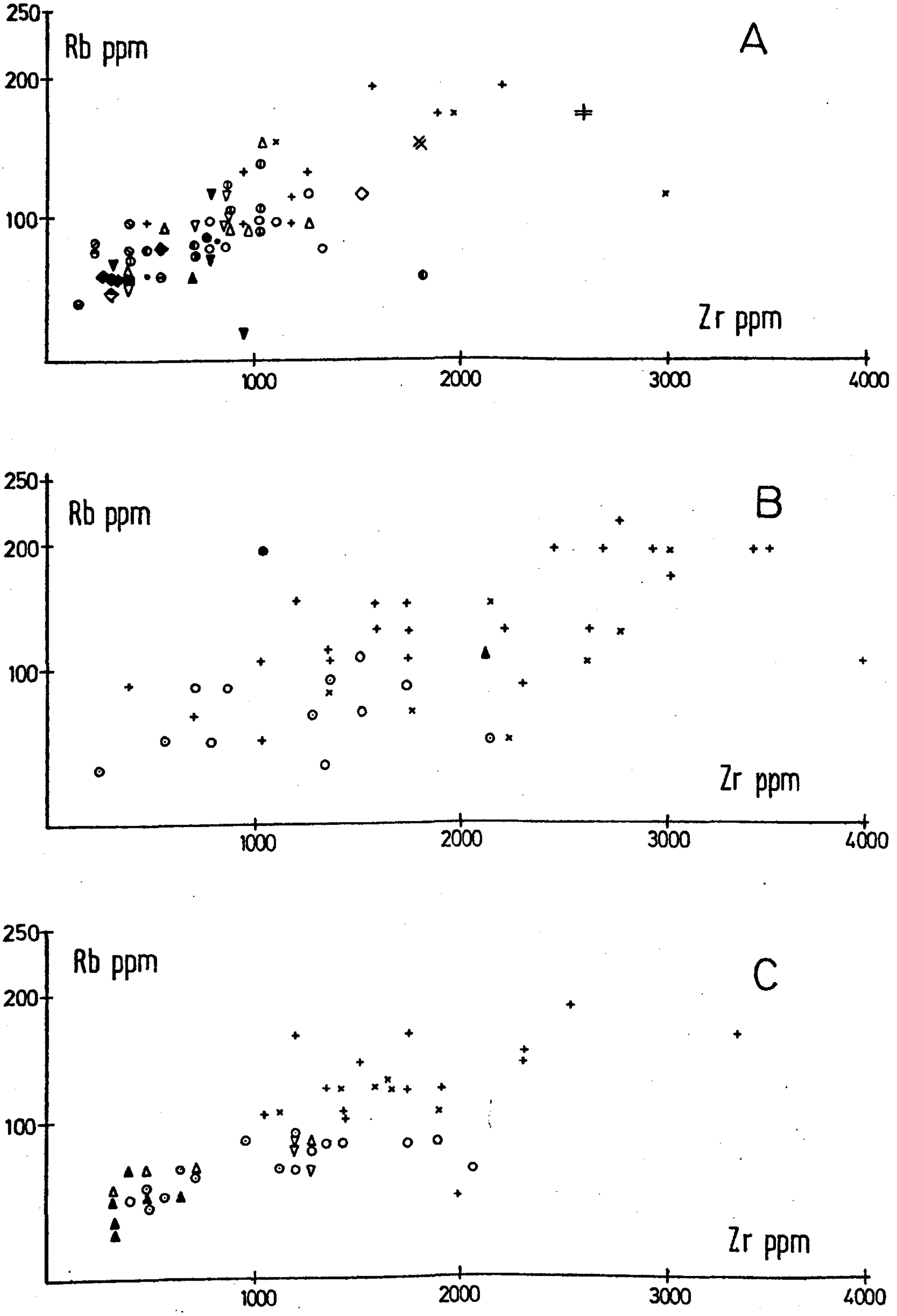

fig.6.16 (contd.) : Trace element variation relative to Zr (explanation opposite).

Fig. 6.16. (opposite) : Trace element variation relative to **Zr.**

A : RAS ED DOM - PLUTONIC ROCKS

- ▲ S1
- ▼ S2
- △ S3
- ◆ S4
- ▽ S5
- ○ S6
- ⦶ S7
- ◒ S8
- ⊖ S9
- ● S10
- ▬ S11
- ⊘ S12
- ◐ S13
- ◑ S14
- ⦸ S15
- ◇ IT1
- • IT2
- · IT3
- ⬘ D209 - early syenite raft in **S6**
- + G1
- × G2
- + MG1
- ✕ MG2

B : RAS ED DOM AND ABU DOM - DYKE AND VOLCANIC ROCKS

<u>Ras ed Dom</u>	<u>Abu Dom</u>
○ syenitic dykes	⊙ syenitic dykes
+ granitic dykes	× granitic dykes
• rafted sample of tuff, loc. 307	▲ ignimbrite, Abu Dom Volcanic Group

C : ABU DOM - PLUTONIC ROCKS

- ▲ S1
- △ S2
- ▽ S3
- ○ S4
- ⊙ S5
- × G1
- + G2

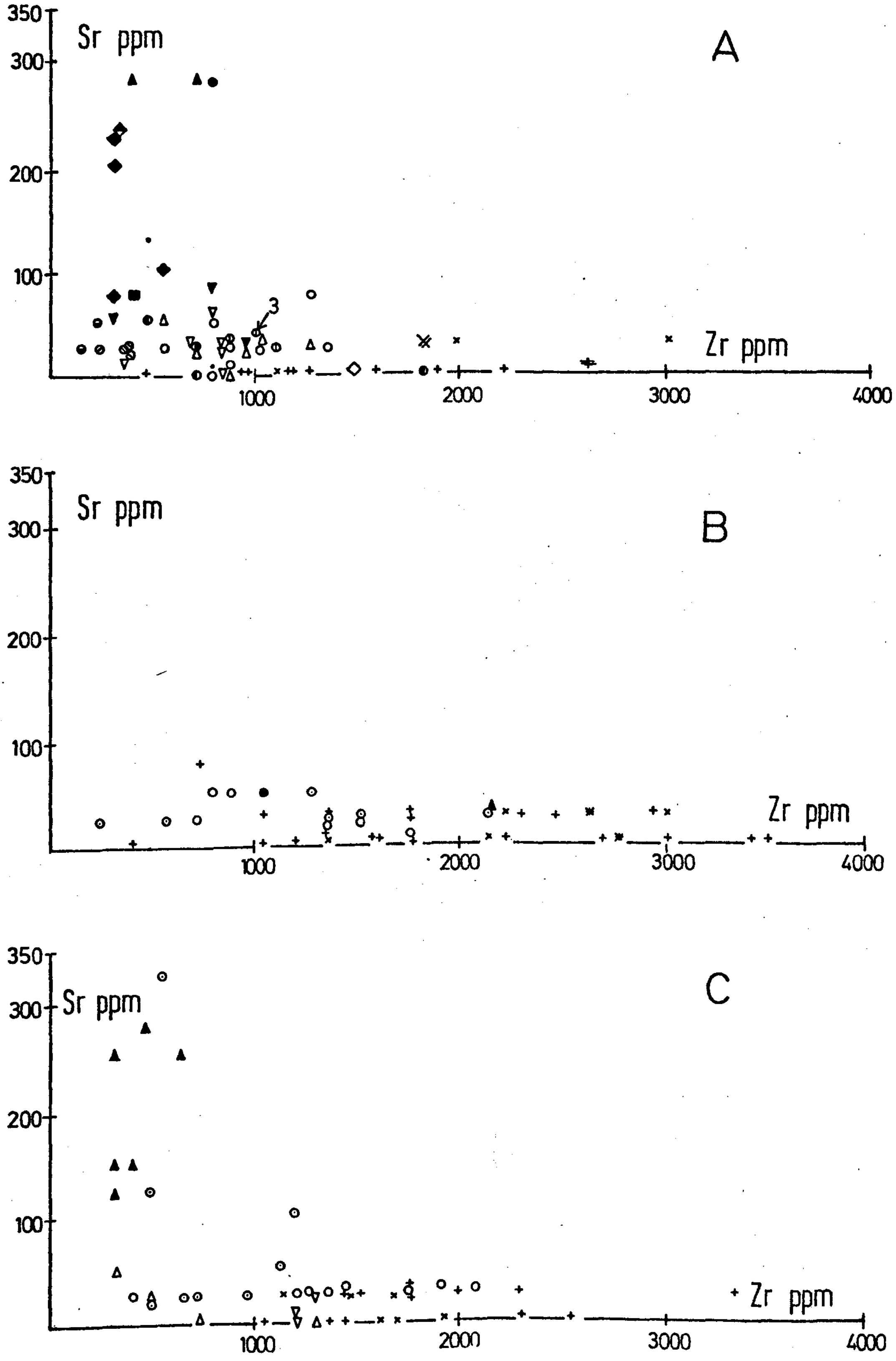

fig.6.16 (contd.) : Trace element variation relative to Zr (explanation opposite).

Fig. 6.16. (opposite) : Trace element variation relative to Zr.

A : RAS ED DOM - PLUTONIC ROCKS

▲ S1
▼ S2
△ S3
◆ S4
▽ S5
○ S6
⦶ S7
◒ S8

⊖ S9
● S10
▬ S11
⊘ S12
◐ S13
◑ S14
⦸ S15
◇ IT1

• IT2
· IT3
⬘ D209 - early syenite raft in S6
+ G1
× G2
+ MG1
⋇ MG2

B : RAS ED DOM AND ABU DOM - DYKE AND VOLCANIC ROCKS

Ras ed Dom	Abu Dom
○ syenitic dykes	⊙ syenitic dykes
+ granitic dykes	× granitic dykes
• rafted sample of tuff, loc. 307	▲ ignimbrite, Abu Dom Volcanic Group

C : ABU DOM - PLUTONIC ROCKS

▲ S1
△ S2
▽ S3
○ S4
⊙ S5
× G1
+ G2

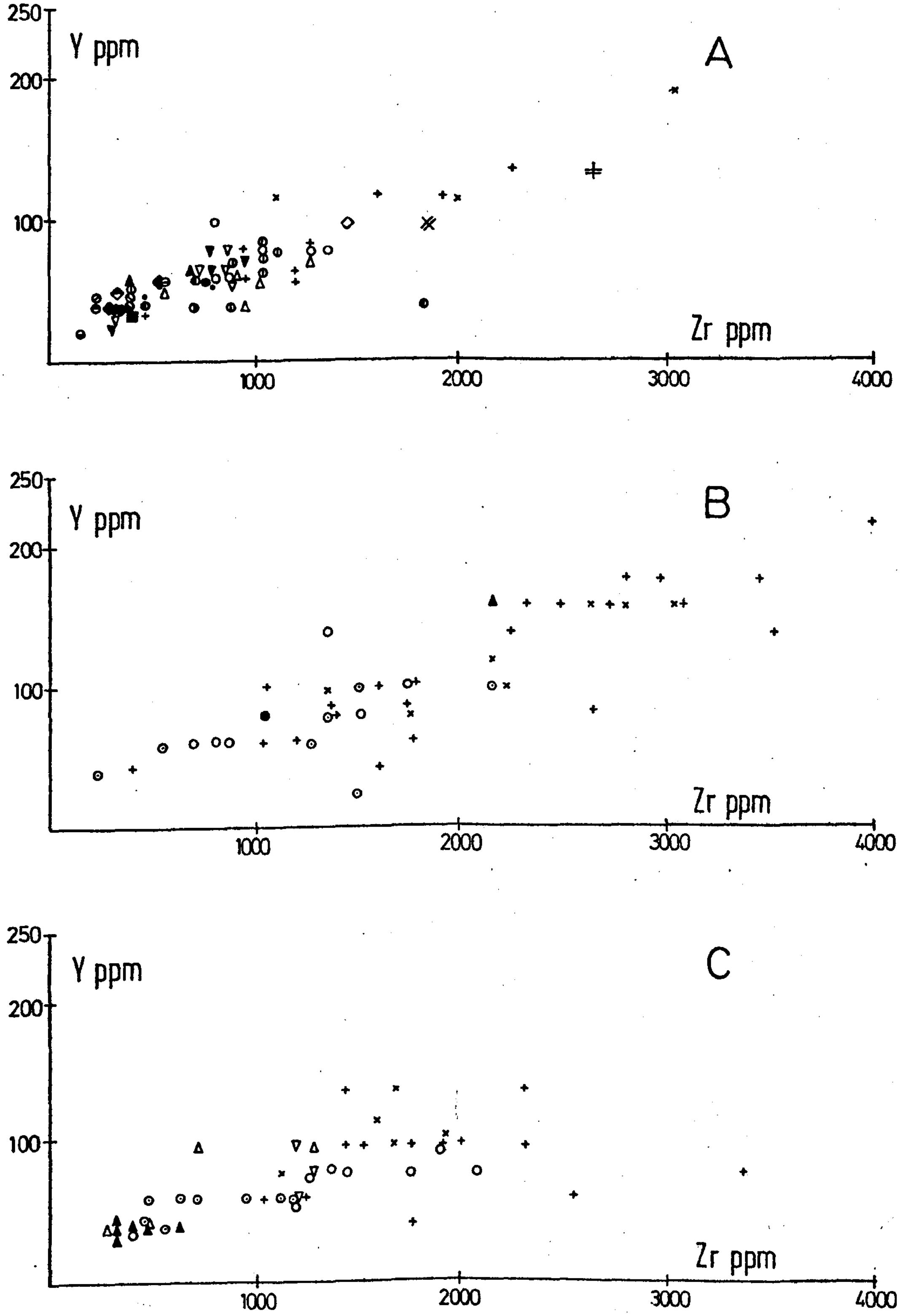

fig.6.16 (contd.) : Trace element variation relative to Zr (explanation opposite).

Fig. 6.16. (opposite) : Trace element variation relative to **Zr.**

A : RAS ED DOM - PLUTONIC ROCKS

▲ S1
▼ S2
△ S3
◆ S4
▽ S5
○ S6
⦶ S7
◓ S8

⊖ S9
● S10
▬ S11
⊘ S12
◐ S13
◑ S14
⦸ S15
◇ IT1

• IT2
· IT3
⬘ D209 - early syenite raft in **S6**
+ G1
× G2
+ MG1
⋇ MG2

B : RAS ED DOM AND ABU DOM - DYKE AND VOLCANIC ROCKS

<u>Ras ed Dom</u>

○ syenitic dykes
+ granitic dykes
• rafted sample of tuff, loc. 307

<u>Abu Dom</u>

⊙ syenitic dykes
× granitic dykes
▲ ignimbrite, Abu Dom Volcanic Group

C : ABU DOM - PLUTONIC ROCKS

▲ S1
△ S2
▽ S3
○ S4
⊙ S5
× G1
+ G2

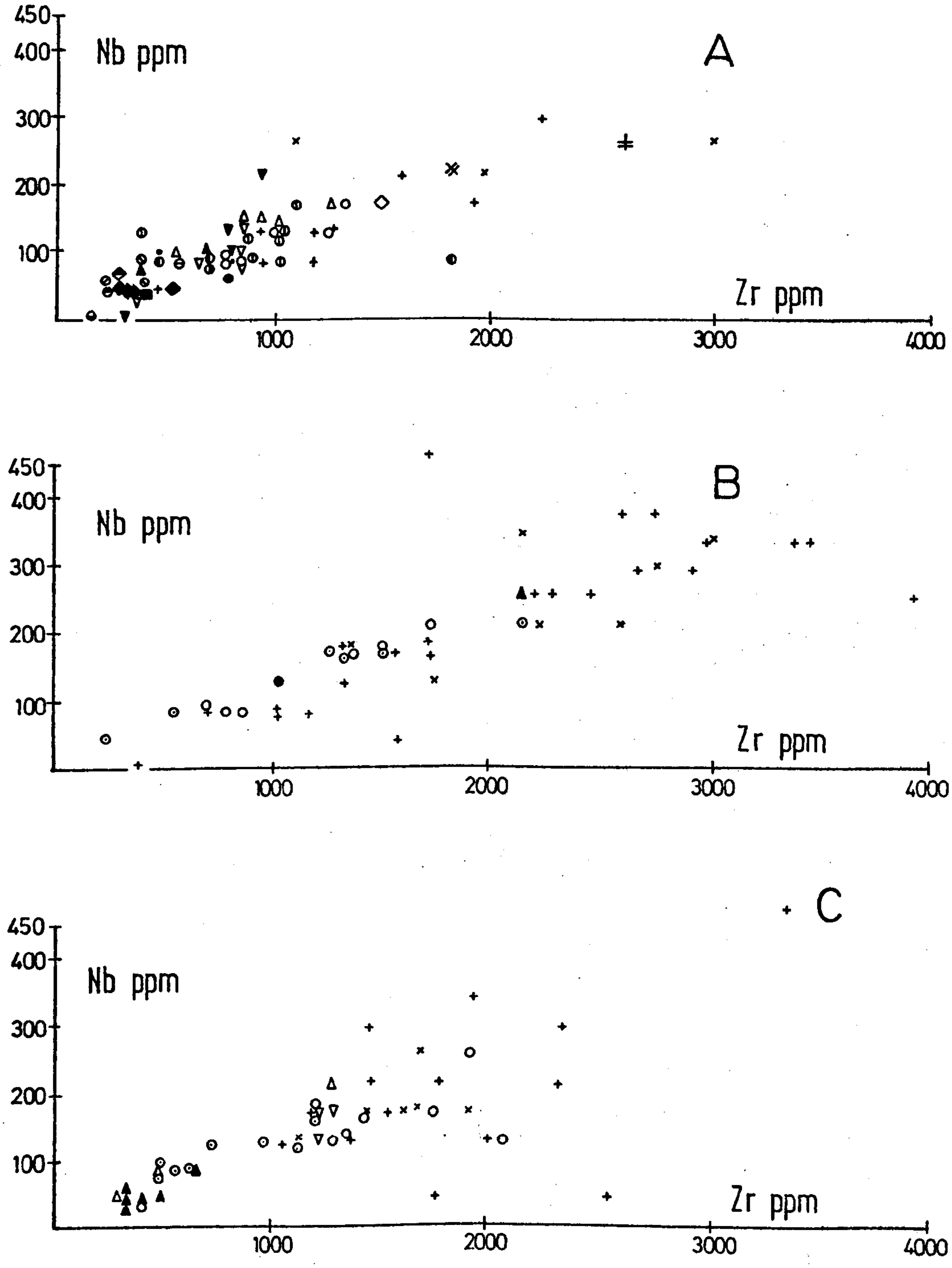

fig.6.16 (contd.) :Trace element variation relative to Zr (explanation opposite).

Fig. 6.16. (opposite) : Trace element variation relative to **Zr.**

A : RAS ED DOM - PLUTONIC ROCKS

▲ S1
▼ S2
△ S3
◆ S4
▽ S5
○ S6
⦶ S7
◒ S8

⊖ S9
● S10
▬ S11
⊘ S12
◐ S13
◑ S14
⦸ S15
◇ IT1

• IT2
· IT3
⬘ D209 - early syenite raft in **S6**
+ G1
× G2
+ MG1
✗ MG2

B : RAS ED DOM AND ABU DOM - DYKE AND VOLCANIC ROCKS

Ras ed Dom	Abu Dom
○ syenitic dykes	⊙ syenitic dykes
+ granitic dykes	× granitic dykes
• rafted sample of tuff, loc. 307	▲ ignimbrite, Abu Dom Volcanic Group

C : ABU DOM - PLUTONIC ROCKS

▲ S1
△ S2
▽ S3
○ S4
⊙ S5
× G1
+ G2

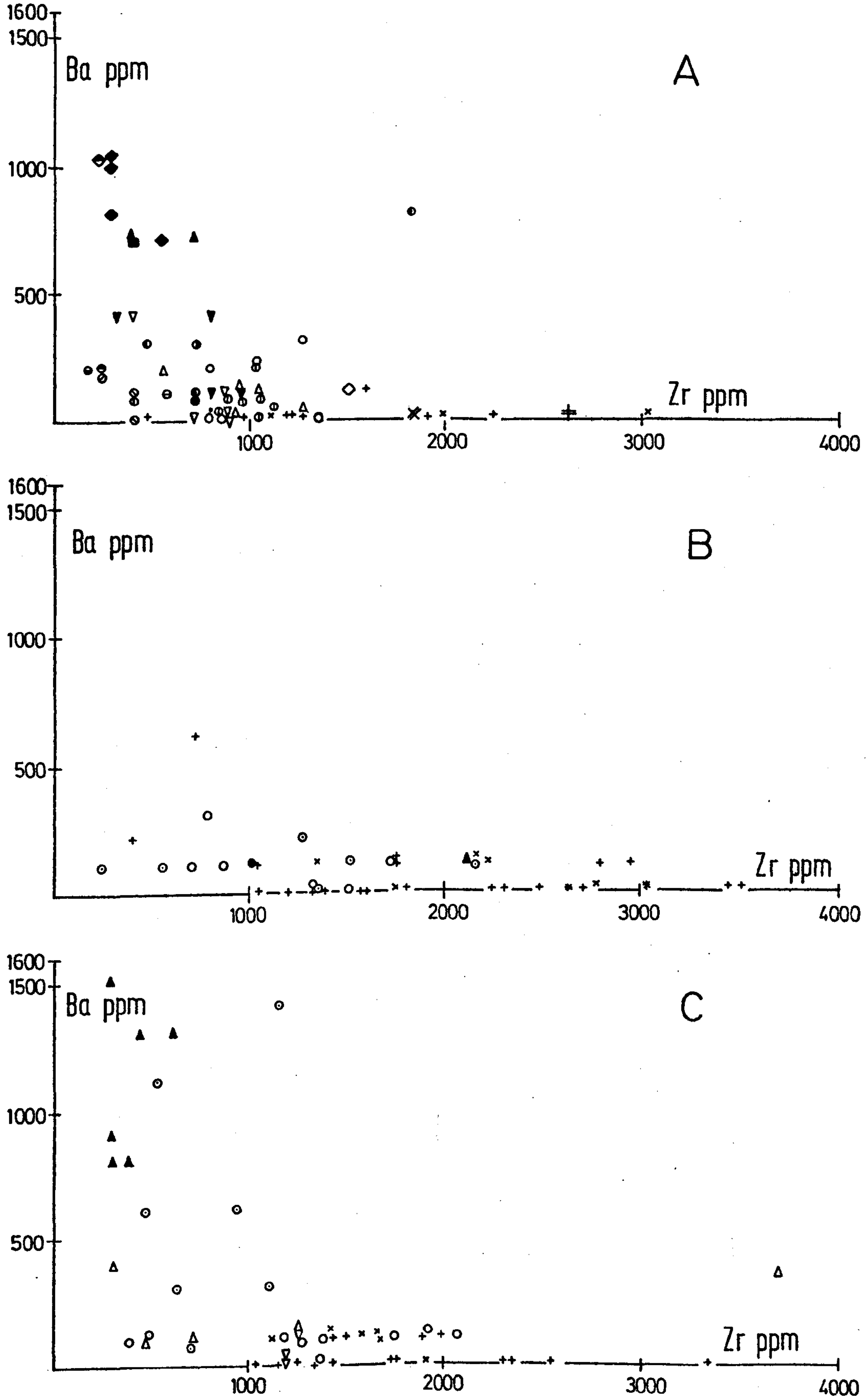

fig.6.16 (contd.) : Trace element variation relative to Zr (explanation opposite).

Fig. 6.16. (opposite) : Trace element variation relative to Zr.

A : RAS ED DOM - PLUTONIC ROCKS

- ▲ S1
- ▼ S2
- △ S3
- ◆ S4
- ▽ S5
- ○ S6
- ⦶ S7
- ◒ S8
- ⊖ S9
- ● S10
- ▬ S11
- ⊘ S12
- ◐ S13
- ◕ S14
- ⦸ S15
- ◇ IT1
- ● IT2
- • IT3
- ⬖ D209 - early syenite raft in **S6**
- + G1
- × G2
- ✛ MG1
- ✖ MG2

B : RAS ED DOM AND ABU DOM - DYKE AND VOLCANIC ROCKS

Ras ed Dom	Abu Dom
○ syenitic dykes	⊙ syenitic dykes
+ granitic dykes	× granitic dykes
● rafted sample of tuff, loc. 307	▲ ignimbrite, Abu Dom Volcanic Group

C : ABU DOM - PLUTONIC ROCKS

- ▲ S1
- △ S2
- ▽ S3
- ○ S4
- ⊙ S5
- × G1
- + G2

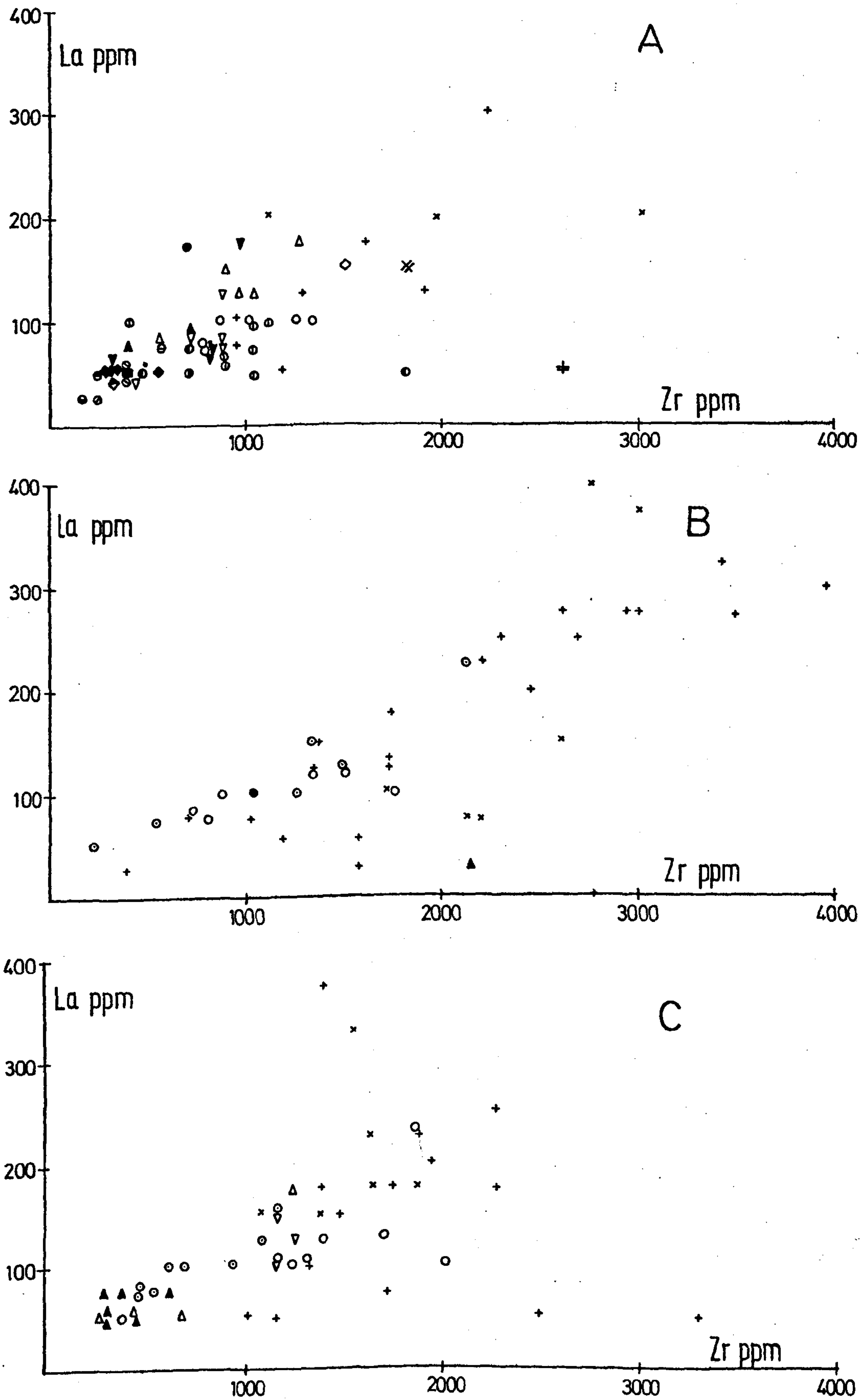

fig.6.16 (contd.) : Trace element variation relative to Zr (explanation opposite).

Fig. 6.16. (opposite) : Trace element variation relative to **Zr.**

A : RAS ED DOM - PLUTONIC ROCKS

▲ S1
▼ S2
△ S3
◆ S4
▽ S5
○ S6
⦶ S7
● S8
⊖ S9
● S10
▬ S11
⊘ S12
◐ S13
◑ S14
⦸ S15
◇ IT1
• IT2
· IT3
⬘ D209 - early syenite raft in S6
+ G1
× G2
+ MG1
⋇ MG2

B : RAS ED DOM AND ABU DOM - DYKE AND VOLCANIC ROCKS

Ras ed Dom	Abu Dom
○ syenitic dykes	⊙ syenitic dykes
+ granitic dykes	× granitic dykes
• rafted sample of tuff, loc. 307	▲ ignimbrite, Abu Dom Volcanic Group

C : ABU DOM - PLUTONIC ROCKS

▲ S1
△ S2
▽ S3
○ S4
⊙ S5
× G1
+ G2

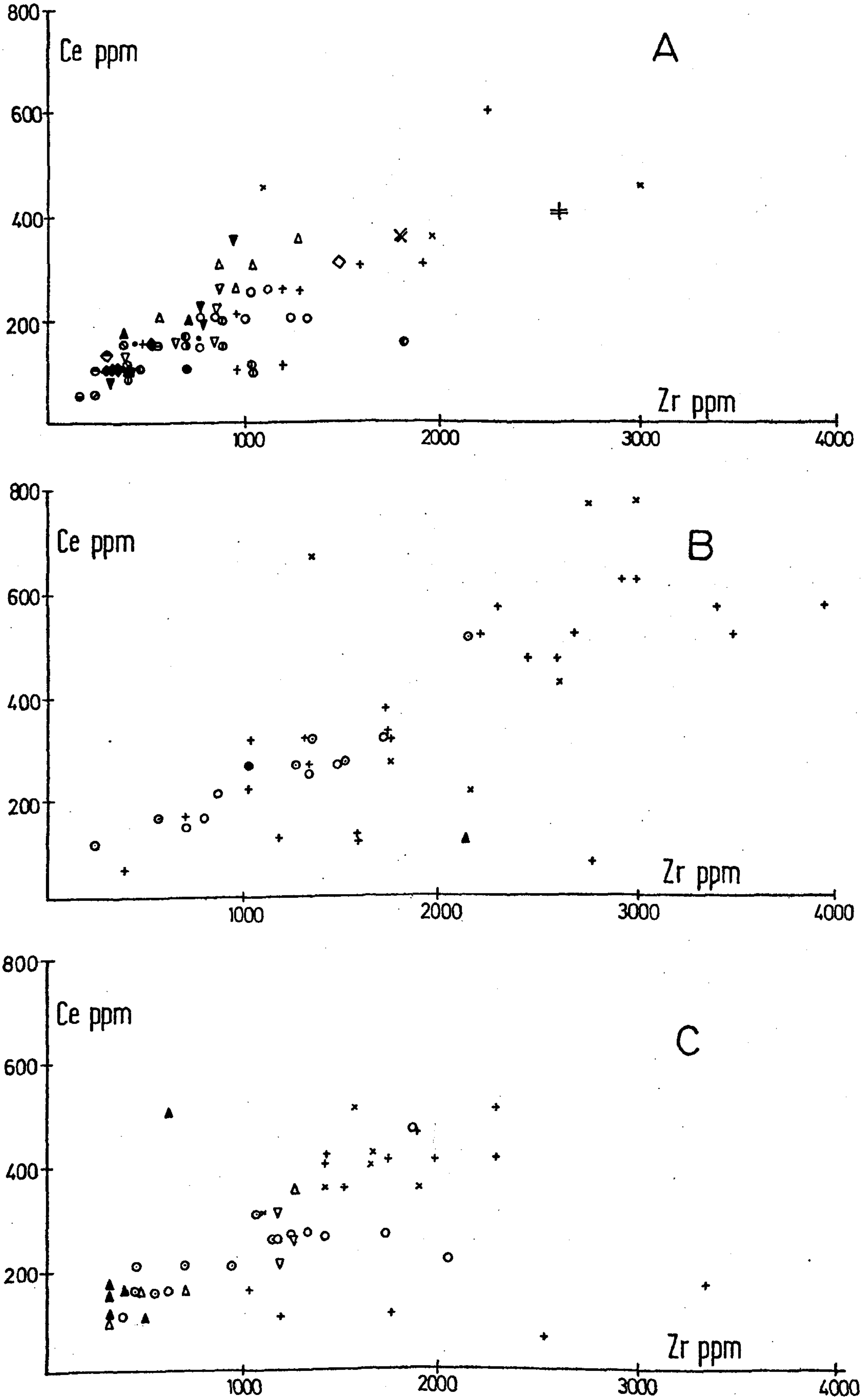

fig.6.16 (contd.) : Trace element variation relative to Zr (explanation opposite).

Fig. 6.16. (opposite) : Trace element variation relative to Zr.

A : RAS ED DOM - PLUTONIC ROCKS

- ▲ S1
- ▼ S2
- △ S3
- ◆ S4
- ▽ S5
- ○ S6
- ⦶ S7
- ◒ S8
- ⊖ S9
- ◓ S10
- ▬ S11
- ⊘ S12
- ◐ S13
- ◑ S14
- ⦸ S15
- ◇ IT1
- ● IT2
- • IT3
- ⬘ D209 - early syenite raft in S6
- + G1
- × G2
- ✛ MG1
- ✕ MG2

B : RAS ED DOM AND ABU DOM - DYKE AND VOLCANIC ROCKS

Ras ed Dom	Abu Dom
○ syenitic dykes	⊙ syenitic dykes
+ granitic dykes	× granitic dykes
● rafted sample of tuff, loc. 307	▲ ignimbrite, Abu Dom Volcanic Group

C : ABU DOM - PLUTONIC ROCKS

- ▲ S1
- △ S2
- ▽ S3
- ○ S4
- ⊙ S5
- × G1
- + G2

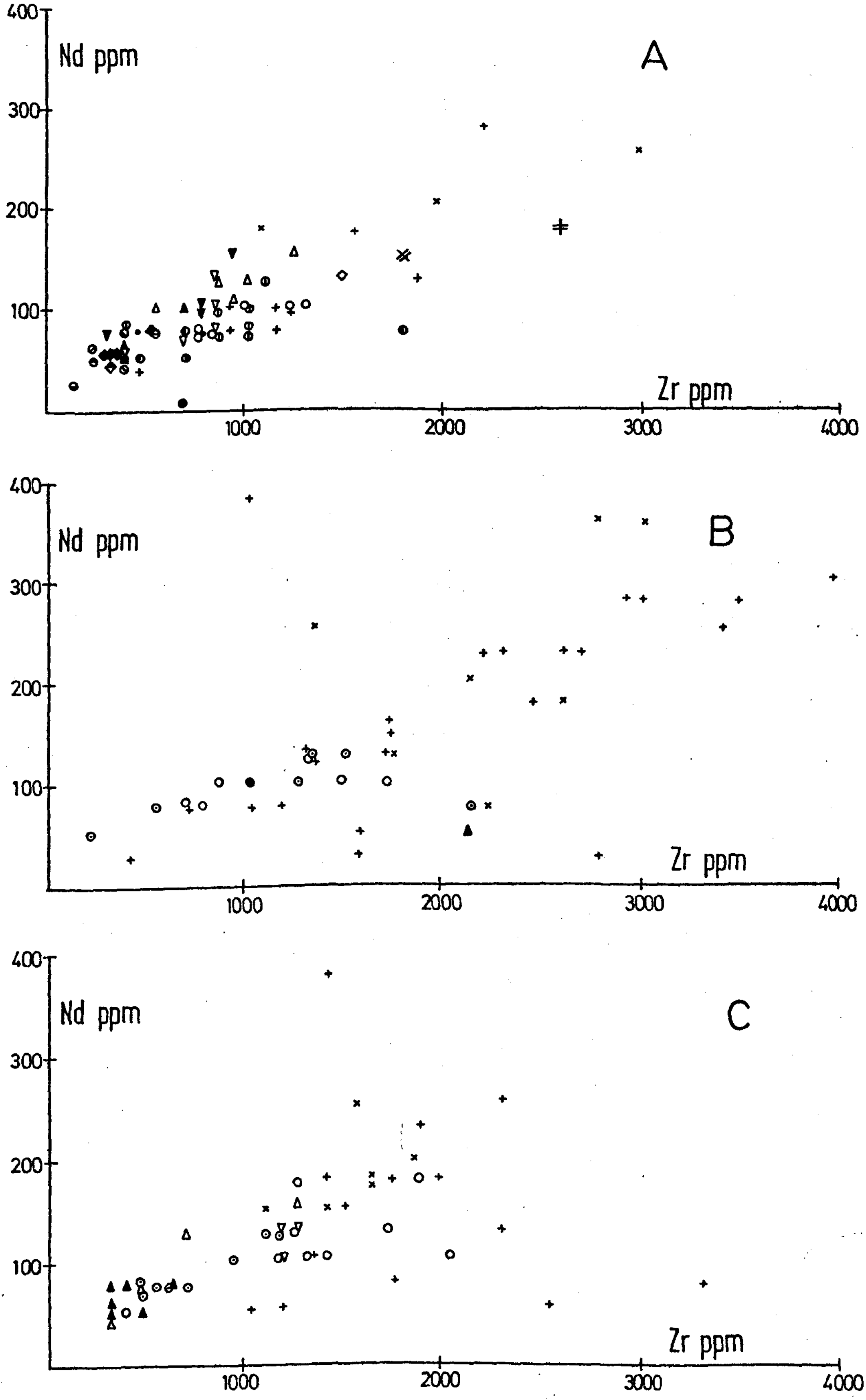

fig.6.16 (contd.) : Trace element variation relative to Zr (explanation opposite).

has reported a similar feature in the Sultaniyat complex. The full trace element variation relative to SiO_2 and Zr is depicted in figs. 6.15 and 6.16. Data for the single basic dyke, D183A (section 4.6) are included in fig. 6.14. Extrapolating back to D183A the patterns of enrichment and depletion are similar, with the exception of Ba which increases sharply from D183A to the early syenites (section 6.3.D. below). How typical the D183A values are, however, is impossible to assess in the absence of further analyses from basic lithologies.

6.3.B. : Gallium

Ga-levels are relatively low in the early syenites, whereas levels in the later alkali rocks are higher but constant, i.e. there is no enrichment from the alkali syenites to alkali granites (table 6.8; figs 6.13, 6.14, 6.15, 6.16). Gallium is camouflaged in aluminous minerals, but as it is less tightly bonded than Al, it may become concentrated relative to Al in later magmatic fractions, so that the Al/10 Ga ratio decreases (Borisenok and Sukov, 1960). Moreover Ga can enter Fe3+ sites (Taylor, 1964), and this may account for the fact that although Al_2O_3 falls from the alkali syenites to granites Ga-levels remain constant. Similar variation characterises Sultaniyat complex (Curtis, 1979), and the Nigerian Younger Granites (Bowden, 1964).

6.3.C. : Rubidium

In the plutonic rocks Rb rises steadily with differentiation (figs. 6.15 and 6.16). Rb can substitute for K in K-bearing minerals, and the larger ironic radius of Rb (1.49A) can cause it to concentrate in late magma fractions (Goldschmidt, 1954). K/Rb ratios for the Bayuda rocks decrease with fractionation (figs. 6.17 and 6.18) and as potash values vary only slightly, the variation effectively reflects Rb enrichment is the suite. Taylor et al. (1956) suggested that low K/Rb ratios characterise highly fractionated rocks of magmatic origin, but subsequent studies suggest that the ratio cannot be used as a general index of magmatic evolution (Carmichael et al., 1974). None the less, the K/Rb ratio is known to decrease with increasing fractionation in several well-documented alkaline provinces e.g. Paresis, Namibia (Siedner, 1965); Gardar (Ferguson, 1970; Macdonald and Edge, 1970) and Nigeria (Butler et al., 1962; Bowden and van Breeman, 1972). It is now appreciated, moreover,

Fig. 6.17. (opposite) : K/Rb ratios versus SiO_2 wt.% values.

A : RAS ED DOM - PLUTONIC ROCKS

▲ S1
▼ S2
△ S3
◆ S4
▽ S5
○ S6
⦶ S7
◓ S8
⊖ S9
◒ S10
▬ S11
⊘ S12
◐ S13
◑ S14
⦸ S15
◇ IT1
• IT2
· IT3
⬘ D209 - early syenite raft in S6
+ G1
× G2
+ MG1
✕ MG2

B : RAS ED DOM AND ABU DOM - DYKE AND VOLCANIC ROCKS

Ras ed Dom

○ syenitic dykes
+ granitic dykes
• rafted sample of tuff, loc. 307

Abu Dom

⊙ syenitic dykes
× granitic dykes
▲ ignimbrite, Abu Dom Volcanic Group, R101

C : ABU DOM - PLUTONIC ROCKS

▲ S1
△ S2
▽ S3
○ S4
⊙ S5
× G1
+ G2

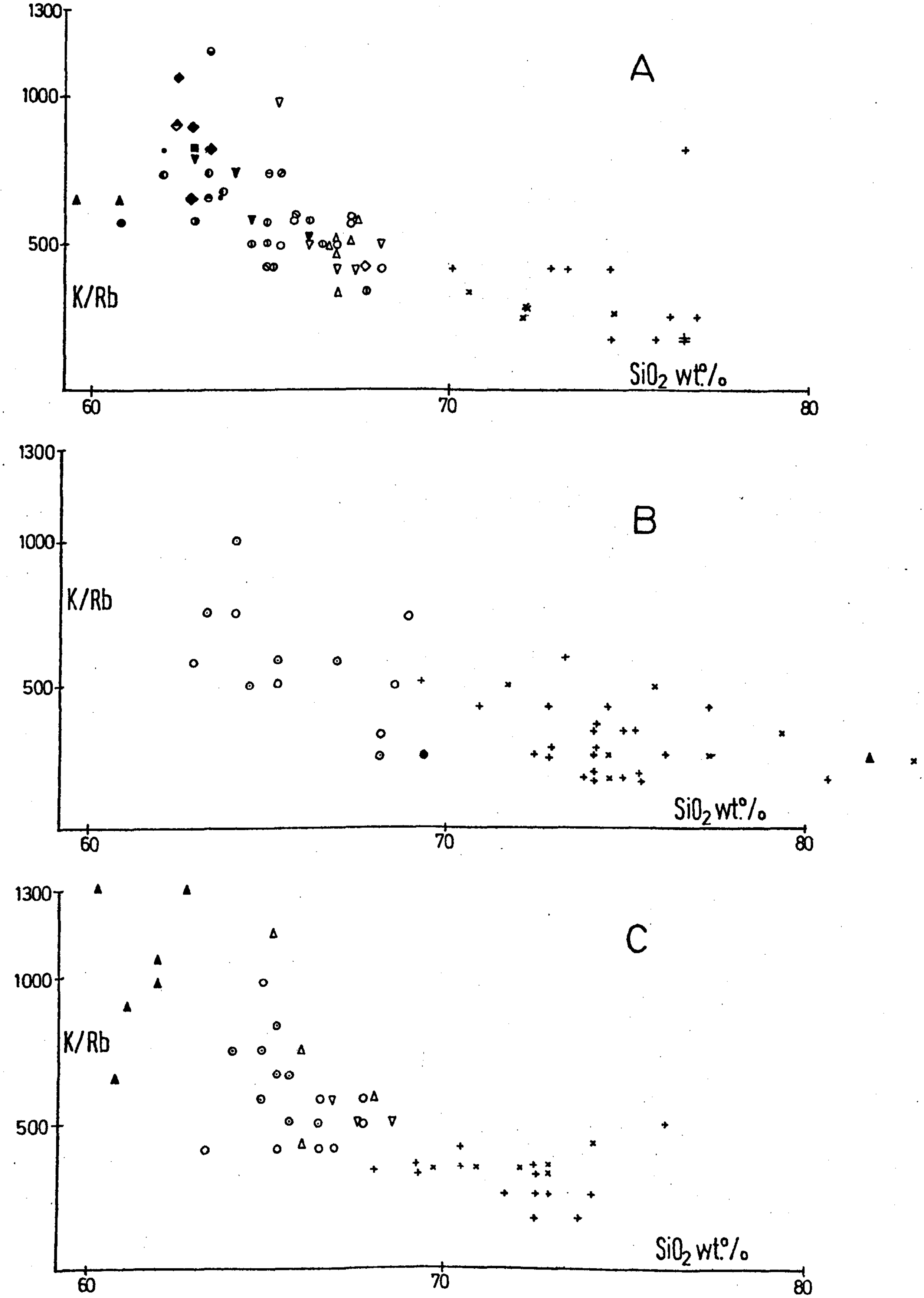

fig.6.17 : K/Rb ratios versus SiO$_2$ wt.% values (explanation opposite).

Fig. 6.18. (opposite) : K/Rb ratios versus Zr.

A : RAS ED DOM - PLUTONIC ROCKS

▲ S1
▼ S2
△ S3
◆ S4
▽ S5
○ S6
⦶ S7
◓ S8
⊖ S9
● S10
▬ S11
◐ S12
◉ S13
◑ S14
⊘ S15
◇ IT1
• IT2
· IT3
⬖ D209 - early syenite raft in S6
+ G1
× G2
✚ MG1
✖ MG2

B : RAS ED DOM AND ABU DOM - DYKE AND VOLCANIC ROCKS

Ras ed Dom	Abu Dom
○ syenitic dykes	⊙ syenitic dykes
+ granitic dykes	× granitic dykes
● rafted sample of tuff, loc. 307	▲ ignimbrite, Abu Dom Volcanic Group, R101

C : ABU DOM - PLUTONIC ROCKS

▲ S1
△ S2
▽ S3
○ S4
⊙ S5
× G1
+ G2

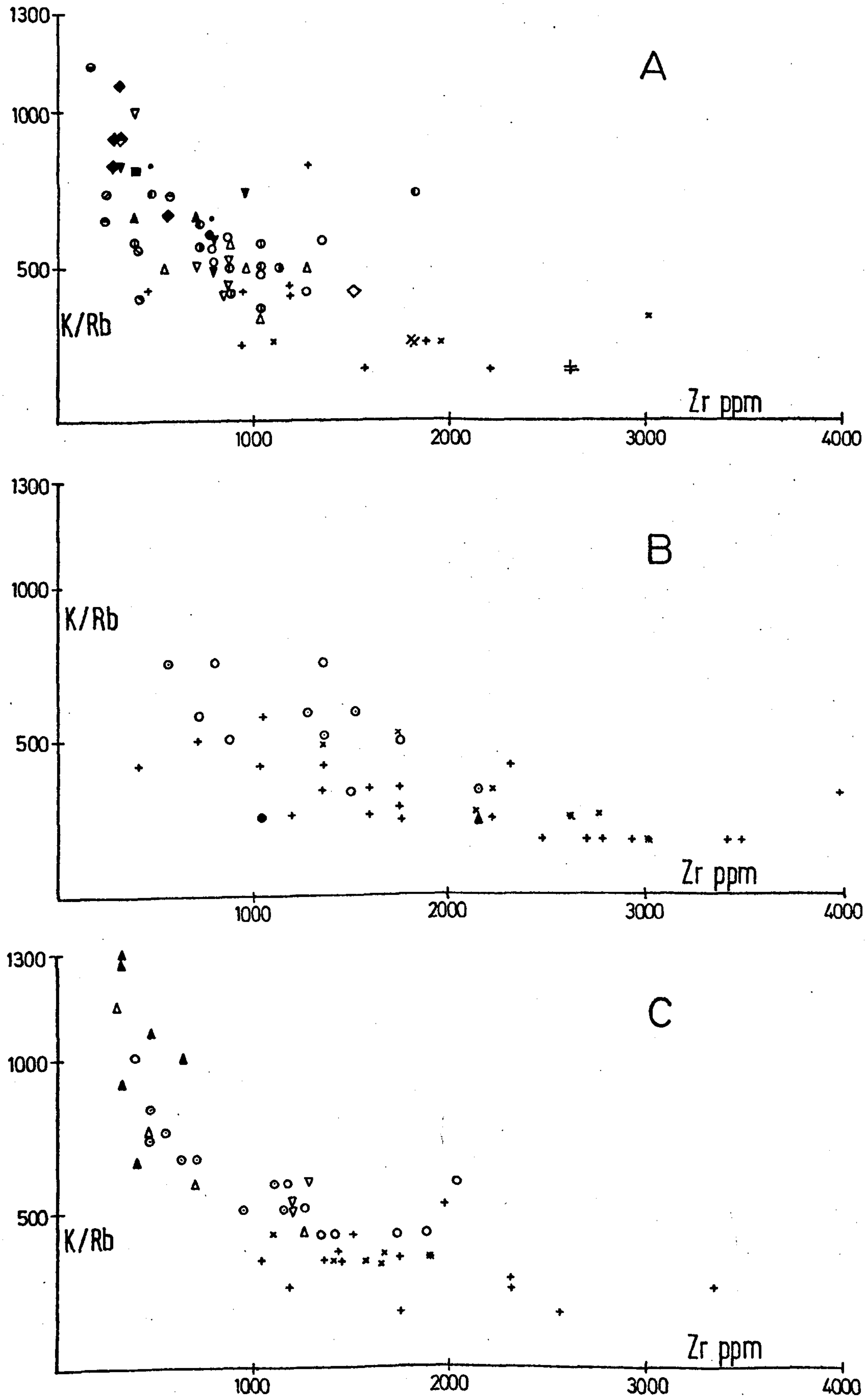

fig.6.18 : K/Rb ratios versus Zr (explanation opposite).

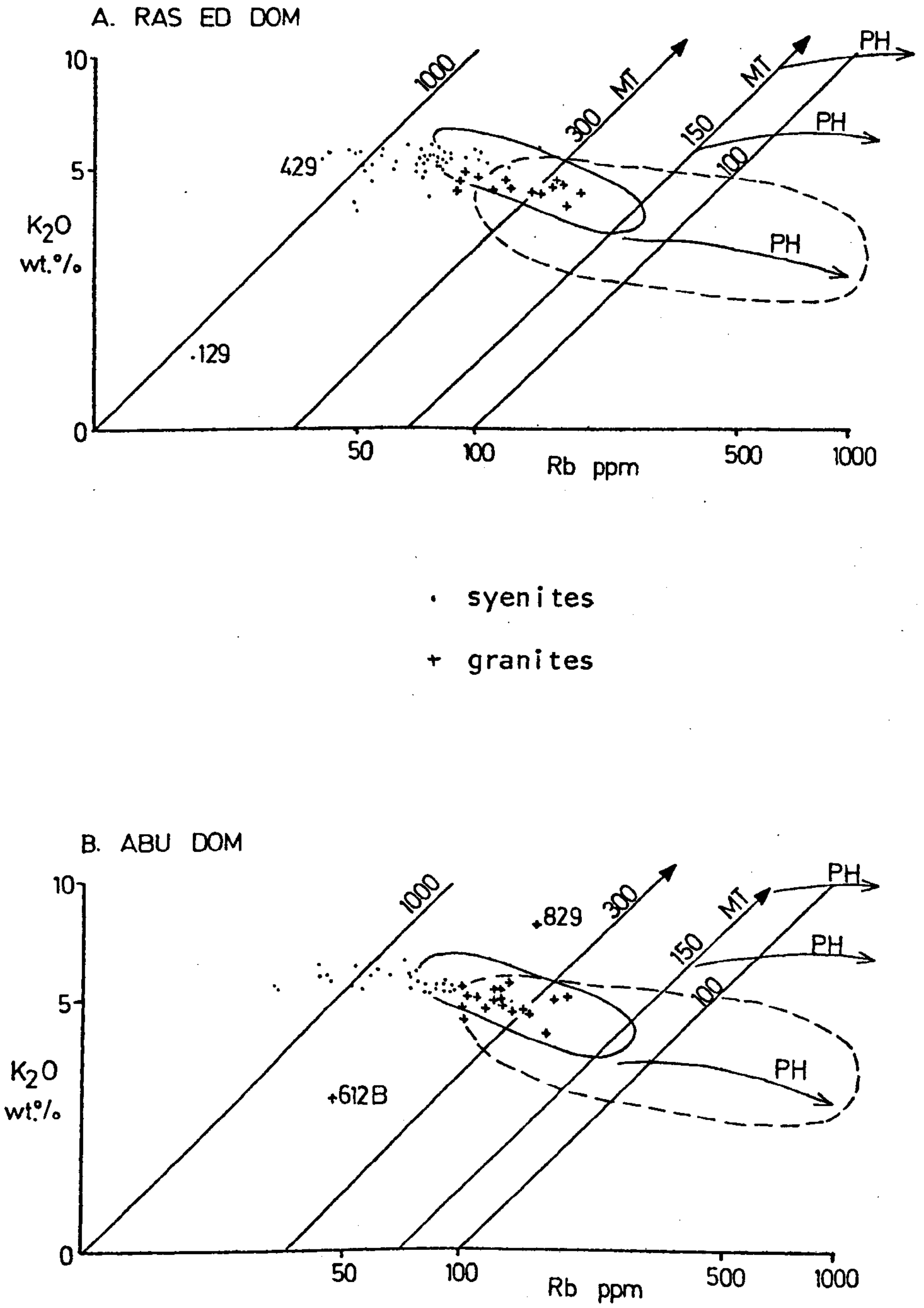

Fig. 6.19 : K_2O v Rb PLOT FOR THE PLUTONIC ROCKS OF RAS ED DOM AND ABU DOM.

MT: MAIN TREND. PH: PEGMATITIC–HYDROTHERMAL TREND. (SHAW 1968) KERGULEN (SOLID LINE) AND NIGERIAN (DASHED LINE) FIELDS AFTER VIDAL ET AL. (1979)

that extremely low K/Rb ratios (< 100) may reflect substantial recrystallisation during albitisation (Bowden and van Breeman, 1972). As values in the Bayuda alkali granites rarely fall below 200, this supports the conclusion, based on petrographic observation (section 4.7.B), that albitisation in the Bayuda rocks is of limited extent.

The degree of Rb enrichment is apparent in fig. 6.19, where K_2O wt.% is plotted against Rb. Vidal et al (1979) have employed this plot to illustrate the abnormal trend displayed by the peralkaline rocks of Kergulen and Nigeria. The observed trends are closer to Shaw's (1968) pegmatitic-hydrothermal trend than to his main magmatic trend. Vidal et al (1979) attribute this to post-magmatic readjustment in response to autometasomatic fluids. The Ras ed Dom and Abu Dom trends are compared with the Kergulen and Nigerian trends in fig. 6.19. It is immediately apparent that the degree of Rb-enrichment is far greater in Nigeria than in Bayuda. Moreover, the bulk of the Bayuda compositions lie above the 300 K/Rb line, suggesting that autometasomatism has not greatly affected the rocks.

6.3.D. : Sr and Ba

Ba and Sr (figs. 6.15 and 6.16) become strongly depleted with fractionation. Sr, in the range 1000-300ppm in the early syenites, falls abruptly to less than 100ppm in the peralkaline rocks. Ba values decline from 1300-1500ppm to less than 250ppm over a small interval of SiO_2.

Ionic radius is the main control over the substitution of Sr and Ba for K. Ba substitutes mainly into alkali-feldspar (Ferrara and Treuil, 1974), and it seems likely that Sr follows it. The dual depletion coincides with a sharp fall in CaO, and is strongly suggestive of fractionation of alkali-feldspar. Partitioning of Sr into early-formed apatite would not be favoured by the strong Ca-bonding encountered at this stage, but preferential capture and incorporation into early-formed Ca-bearing feldspar is to be expected (Goldschmidt, 1952). Similar dual depletions characterise the peralkaline rocks of Nigeria (Bowden and van Breeman, 1972), Namibia (Siedner, 1965), Oslo (Dietrich and Heier, 1967), Gardar (Macdonald and Edge, 1970) and Mull (Walsh et al., 1979).

Fractionation vectors, based on Arth (1976) and adapted from Walsh et al., 1979, are shown in fig. 6.20. The plot suggests that the early syenites (low Rb/Sr ratios) and later peralkaline rocks (higher Rb/Sr ratios) are linked by fractionation of alkali-feldspar. The figures on the vectors refer to the percentage of crystals removed, and are 20%, 20-60% and > 60% for the early syenites, alkali syenites and alkali granites respectively.

6.3.E. : Zirconium

Zr values in the early syenites (table 6.8) are in the range 300-450ppm, but rise steadily in the alkali syenites. The granites show further, but highly variable, enrichment (fig. 6.15). Zr is concentrated in residual liquids during fractionation (Goldschmidt, 1954) and peralkaline suites are especially enriched (Bowden, 1966). A broad correlation with increasing alkalinity, as recorded by the agpaitic ratio, is evident from fig. 6.4. for the plutonic rocks. Alteration and devitrification obscure this relation in the dyke rocks.

Zr-enrichment in alkaline suites is not simply equatable with an abundance of zircon (Chao and Fleischer, 1960), and Zr enters other phases. Most of the Zr in the Nigerian Younger Granites is thought to reside in amphibole and aegirine (Borley, 1963; Bowden, 1966). In Ras ed Dom its appearance in pyroxene coincides with Na-enrichment in the early pyroxene group (section 5.3.B). The amphiboles, however, are Zr-free but the element is present in the late pyroxenes. Watson (1979) studied the behaviour of Zr in the experimental system SiO_2 - Al_2O_3 - Na_2O - K_2O. He found that saturation levels in felsic, non-peralkaline melts are low, and this accounts for the presence of zircon in the early syenites (section 4.3.D). In peralkaline melts Zr solubility increases linearly with increase in agpaicity, and zircon becomes unstable. Moreover, the melt can never regain zircon saturation by continued feldspar crystallisation, and recrossing the saturation line can be achieved only by precipitation of a phase such as aegirine or sodic amphibole (Watson, 1979). These relations could account for the association of zircon and aegirine in the peralkaline rocks (section 4.5.E).

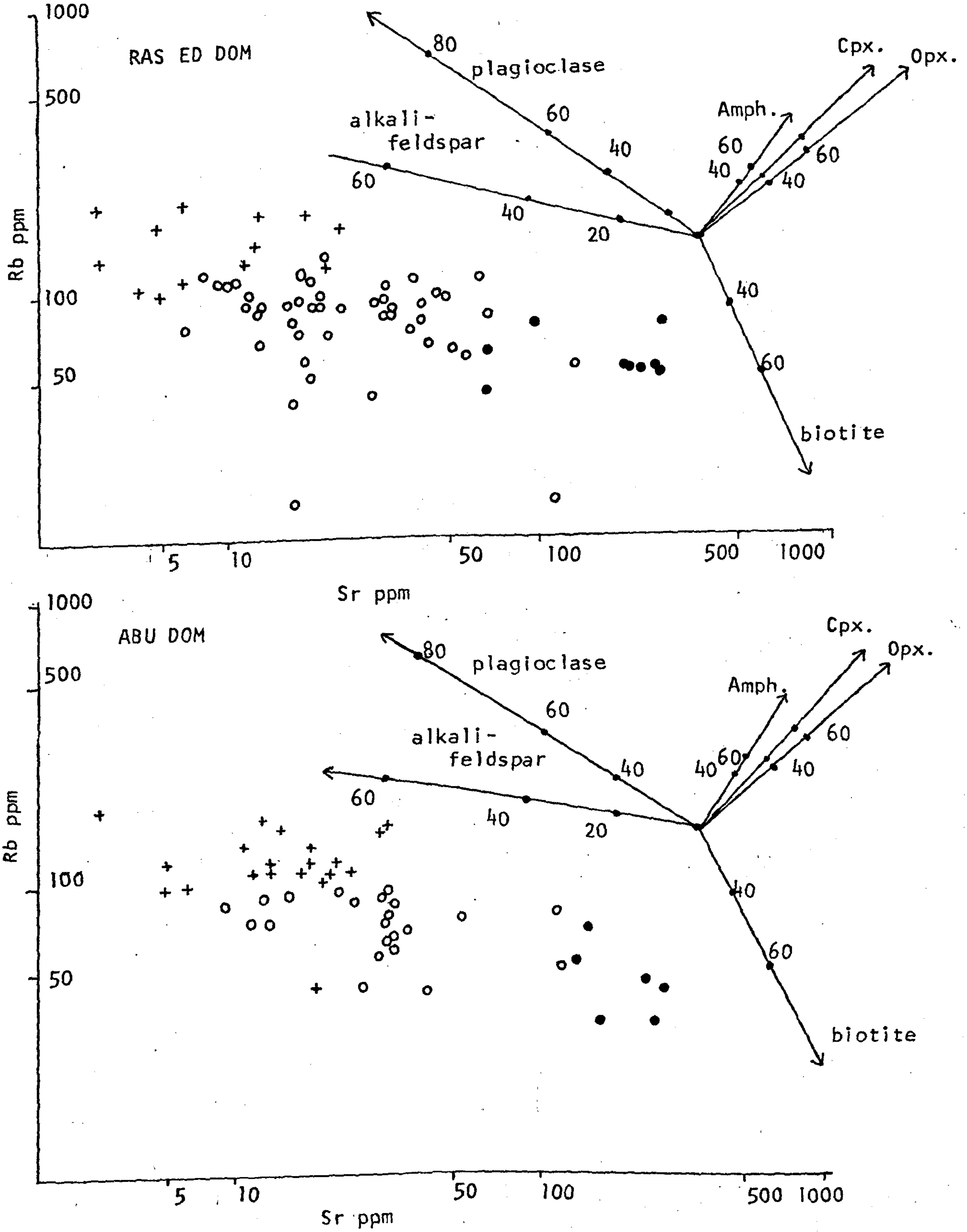

Fig.6.20 : Rb versus Sr plots for the plutonic rocks of Ras ed Dom and Abu Dom, together with fractionation vectors after Arth (1976). • early syenite, ∘ alkali syenite, + alkali granite. The arrows indicate change in composition of melts due to fractional crystallisation of the specified phenocryst phases. The figures indicate % of crystals removed

The marked variability of Zr-levels in the alkali-granites (fig. 6.15) merits comment. Tugarinov et al., (1968) noted that Zr-enrichment under peralkaline conditions can extend into the hydrothermal stage, thereby blurring the distinction between magmatic and post-magmatic processes. Bowden and Turner (1974) have shown that Zr-enrichment and post-magmatic fluid activity are characteristically related in the Nigerian Younger Granites. The association of zircon with late aegirine, and the sporadic spread of Zr-levels in the granites of Bayuda, may accordingly reflect localised overprinting by post-magmatic fluids. However, in the absence of firm petrographic criteria for distinguishing between aegirine of late-magmatic and sub-solidus origin (section 4.5.D) such speculations remain unproven. This problem is discussed further in section 7.5.

6.3.F. : Rare Earth Elements - La, Ce, Nd, (Y)

The Rare Earth Elements (REE) form a strongly coherent group, but partial fractionations do occur in nature and this variation is at its greatest in silicic and alkaline rocks (Koljonen and Rosenberg, 1974). The limited applicability of X.R.F. methods to REE detection meant that only lanthanum, cerium and neodymium were determined in this study. The results are normalised to the Leedy (L6) chondrite values (Nankamura and Masuda, 1973) in the Coryell plot presented in fig. 6.21. Yttrium is known to behave much as a heavy REE (HREE), and is used as a proxy for ytterbium. The normalisation value used for Y is 1.8 (Haskin et al., 1968).

Partial REE patterns for Ras ed Dom and Abu Dom are presented in fig. 6.21. Mean REE levels increase from the early syenites, through the alkali syenites to the granites, and the trends are parallel to each other, leaving little doubt that the suite is cogenetic. The light REE (LREE) are enriched relative to the HREE. This pattern is apparent in the earliest rocks (early syenites) suggesting that the parental melt was likewise LREE enriched. A source rock containing a HREE-rich phase, such as garnet, could account for this (Hanson, 1978; Harris, 1982). The overall patterns are typical of granitic rocks (Koljonen and Rosenberg, 1974) and similar to REE patterns in non-albitised Nigerian Younger Granites (Bowden and Whitley, 1974).

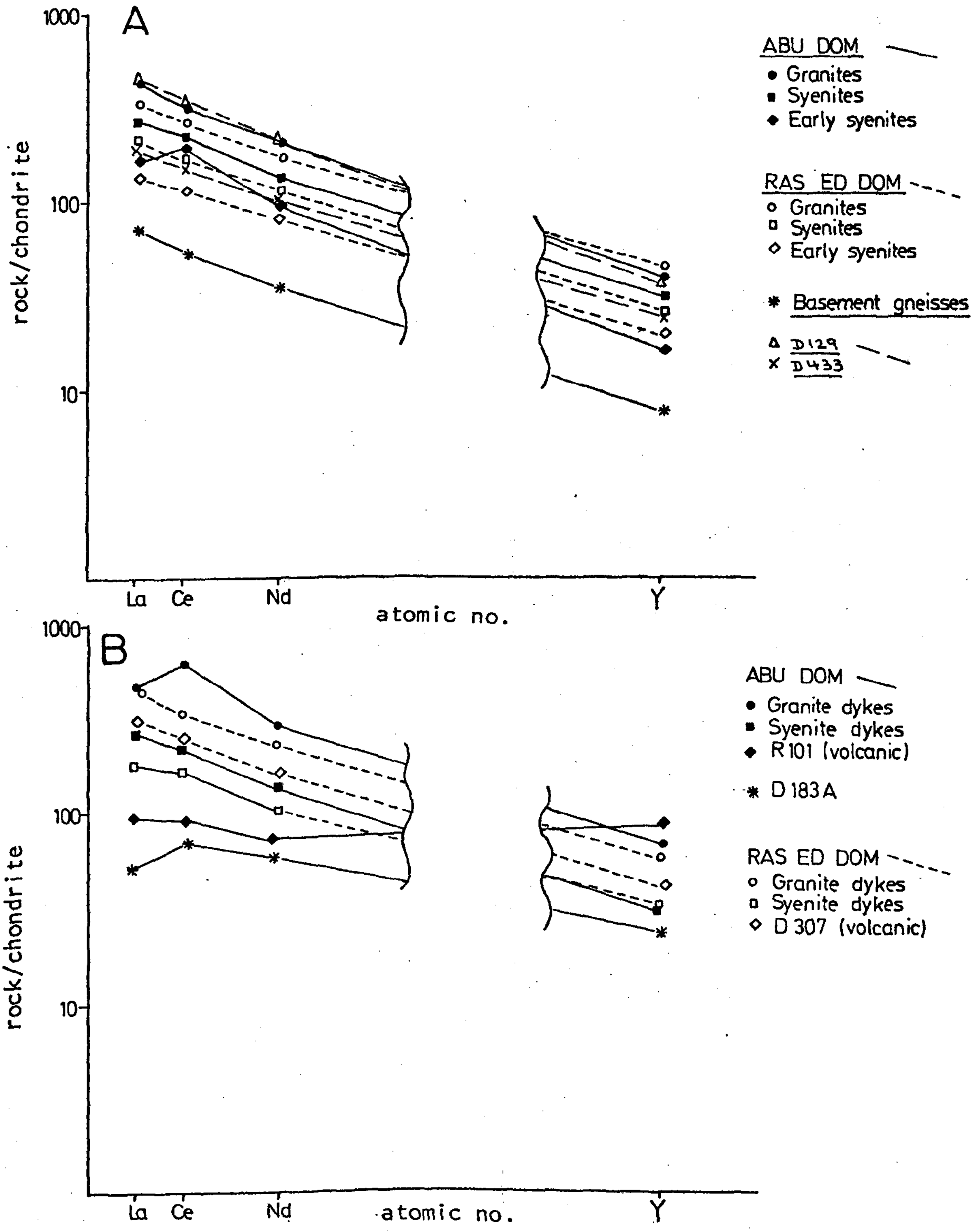

Fig. 6.21 : MEAN REE PARTIAL PATTERNS, TOGETHER WITH SELECTED INDIVIDUAL REE PARTIAL PATTERNS, FOR THE YOUNGER GRANITE ROCKS

A - MAJOR INTRUSIONS

B - DYKE ROCKS AND VOLCANICS

The REE patterns for the dyke rocks (fig. 6.21-B) are closely similar to the plutonic patterns. The D183A (basic dyke, Abu Dom) profile is also typical, but shows lower values consistent with a less fractionated state. Of the volcanic rocks, D307 shows a typical profile, whilst that of R101 shows an almost horizontal pattern, with relative HREE enrichment. However, in the absence of further data from the volcanics of Bayuda, the significance of this horizontal pattern cannot be properly assessed. The major drawback of the partial REE patterns is the absence of Eu data. Eu is known to substitute for Ca, and accordingly can throw light on feldspar fractionation in these rocks. A negative Eu anomaly is to be expected where plagioclase or alkali-feldspar fractionation has occurred (Bowden *et al.*, 1980), and a positive anomaly would characterise feldspar cumulates. Bowden *et al.*, (1980) studied a Nigerian equivalent of what is termed early syenite in this work and found that no Eu anomaly was present. The syenite accordingly could not have evolved from a more basic parent by plagioclase fractionation, nor could it have formed as a cumulate from a granitic liquid. They concluded that the syenite represents an unfractionated parental syenite magma. The granites, which do show a Eu depletion, are thought to have formed from a syenite magma by fractionation of alkali-feldspar (Bowden *et al.*, 1980). The Tuleih syenite of Sabaloka complex, Sudan, is also similar in composition to the early syenites of this work, and has a slight negative Eu anomaly indicating a small degree ($< 20\%$) of feldspar fractionation (Harris *et al.*, 1982). If the estimates of fig. 6.20 are correct a similar degree of fractionation can be inferred from the Rb/Sr ratios for the Bayuda early syenites.

It has generally be considered that the REE are inert to any mobilisation at sub-solidus temperatures (Koljonen and Rosenberg, 1974; Thorpe *et al.*, 197 but opinion is now shifting towards greater REE mobility during non-magmatic processes (Mineyev, 1963; Aleksiyev, 1970; Bowden and Whitley, 1974; Martin *et al.*, 1978). Most especially, albitised peralkaline granites show relative HREE enrichment (Mineyev, 1963; Bowden *et al.*, 1980; Harris and Marriner, 1980) possibly due to HREE retention through halide complexing in a volatile phase (Harris and Marriner, 1980). A full REE coverage would be needed before applying such considerations to the Bayuda rocks.

6.3.G. : Uranium

Uranium was determined in a total of thirty samples (eighteen from RED, twelve from AD), and details of the analytical method (I.N.A.A.) are given in Appendix IIIA.

	Ras ed Dom			Abu Dom		
	x	n	n	x	n	n
Early Syenites	2.3	0.0	1	1.5	0.4	2
Alkali Syenites	2.2	1.0	11*	3.0	1.1	5
Alkali Granites	4.3	1.7	3	3.9	1.4	3
Granitic Dykes	10.5	0.5	2	8.3	1.1	2
Syenitic Dykes	n.d.			n.d.		

n.d. = not determined.

* does not include metasomatised sample D129

All values in ppm.

Table 6.9. : Mean Uranium Values for the Principal Rock-Types of Ras ed Dom and Abu Dom.

Table 6.9 (above) establishes that the U content increases slightly with fractionation, reaching mean values of 4 ppm in the granites. The acidic dykes have significantly larger mean values of 9 ppm. Uranium is known to behave incompatibly in peralkaline rocks from many provinces (Upton, 1960; Harris and Marriner, 1980; Bowden and Turner, 1974). Bowden et al., (1976) stress the similarities between the behaviour of U and Zr, and suggest that U is a possible index of peralkalinity. In this context it is significant that the metasomatised syenite D129 (sections 4.5.D., and 6.4) is U-enriched with 5.9 ppm.

6.3.H. : Niobium

The incompatable behaviour of Nb in the suite is apparent from figs. 6.15 and 6.16. Mean values for Abu Dom are 57 ppm (early syenites), 134 ppm (alkali syenites) and 191 (alkali granites). The range for Bayuda (24-611 ppm) records a strong enrichment comparable with that of the Tugtutoq dykes (20-695 ppm: Macdonald and Edge, 1970) and Nevadan pantelleriates (Noble, 1965). The Bayuda average (141 ppm) is greater than the Nigerian average value (101 ppm: Kovalenko *et al.*, 1972), but extreme values in excess of 1000 ppm, such as characterise the albitised Nigerian granites, are not found. Nb can replace Ti in Ti-minerals, but more generally, as in the present instance, it is concentrated in the residual liquid (Taylor, 1965).

6.4. : Sodic Metasomatism

At loc. 129 in S2, RED, an area of several tens of square metres has been metasomatised and cut by aegirine-augite rich veins. In thin section both discrete veins and recrystallised 'channels' between perthite grains in the host syenite, are composed of aegirine-augite, Fe-Ti oxide and subordinate feldspar and quartz. The feldspar is commonly albitic. Textural relations indicate introduction of fluids along veins and permeation through the host rock along grain boundaries.

Compared to the adjacent unaltered syenites, the matasomatised rocks is enriched in Na_2O, MgO, and Fe_2O_3 relative to FeO, (table 6.10), with concommitant depletion in K_2O and CaO. The latter depletions suggest that complimentary potassic metasomatism might be expected elsewhere in the vicinity, but no evidence for this was found. Such depletions do not characterise the albitic metasomatism found in the Nigerian Younger Granites (Bowden *et al.*, 1976). Zr and Nb are enriched, as are the REE which approach the levels of the alkali granites (fig. 6.21). Sr and Ba are strongly depleted, as is Rb. The latter depletion is surprising as in the suite as a whole a strong Rb-enrichment occurs with increasing alkalinity (fig. 6.19), and would be expected in a metasomatised sample. The peralkaline nature of the metasomatising fluids is however clearly indicated by the high values of the agpaitic ratio, alkalinity ratio, normative albite, normative acmite (12.16) and Ab/Or ratio (table 6.10).

wt.%	1	2	3
SiO_2	64.16	64.33	1.19
Al_2O_3	16.06	15.74	0.75
Fe_2O_3	5.02	4.22	0.52
FeO	1.17	1.89	0.54
MgO	1.10	0.30	0.04
CaO	0.85	1.43	0.06
Na_2O	10.40	5.82	0.51
K_2O	1.52	5.47	0.16
TiO_2	0.47	0.53	0.09
MnO	0.20	0.14	0.02
P_2O_5	0.05	0.11	0.03
Ga ppm	58	47	2
Rb	17	78	18
Sr	15	55	12
Y	65	52	11
Zr	974	606	241
Nb	197	84	44
Ba	69	331	136
La	169	70	11
Ce	338	161	38
Nd	144	83	8
Agpaitic Ratio	1.17	0.99	
Norm. Albite	73.16	49.03	
Ab/Or Ratio	8.14	1.5	

1. D129, Syenite 2, Ras ed Dom. Metasomatised alkali syenite.
2. Average of 3 unaltered analyses. Syenite 2, Ras ed Dom.
3. Standard deviation for column 2.

Table 6.10 : Effects of sodic metasomatism upon bulk rock chemistry.

6.5. : Geochemistry of the Basement Gneisses

The basement gneisses, into which the Younger Granites have been emplaced, are a possible upper crustal source from which the Younger Granites may have been derived by partial melting. The geochemistry of the gneisses is now examined with this possibility in mind. In table 6.11 an average basement composition, based on eight analyses (Appendix IIIB), is compared with averages of all analysed plutonic rocks from Ras ed Dom and Abu Dom. As it has already been proposed that the early syenites may be close in composition to the parental anatectic melts (section 6.3.F.), mean compositions of the early syenites of both complexes are also included in table 6.11.

The basement gneisses are silica-oversaturated rocks, with Q and Hy in the norm (Appendix III). They range from metaluminous to slightly peraluminous compositions (table 6.3) and An values are approximately double those of the early syenites. In major element terms, the gneisses are more aluminous than the Younger Granites and are richer in MgO and CaO. In contrast the Younger Granites are enriched in Fe_2O_3, alkalies, TiO_2 and MnO. Differences in trace element abundances are even more striking. Values of Y and the LREE are 3-4 times higher in the Younger Granites and Ga-levels are roughly twice the basement value. Zr enrichment in the ring-complexes is 4 to 5-fold. The major depletions relative to the gneisses are in Sr and Ba, and these are extreme (table 6.11). Only mean Rb values are comparable in the two suites.

In fig. 6.21 a mean partial REE pattern for the basement gneisses is shown. Concentrations are lower than in the Younger Granites, but the two trends are closely parallel, and suggest that the gneisses could be the anatectic source of the Younger Granites. However there are several objections to such an hypothesis. Firstly, while concentration factors of 4-5, such as those shown by the incompatable elements, are consistent with partial melting and subsequent high-level fractionation of basement-derived melts, the depletions in Sr and Ba are sufficiently extreme (e.g. x16) as to appear to preclude this possibility. Secondly, the early syenites are only slightly oversaturated (see norms in Appendix III), and this implies a low-silica source, whereas the gneisses

wt.%	BA	RA	AA	ERA	EAA
SiO_2	71.05	67.83	66.77	61.95	61.56
Al_2O_3	15.17	13.38	14.43	16.13	16.37
Fe_2O_3	0.80	4.05	5.53	3.68	4.80
FeO	1.29	1.82	1.03	2.61	1.80
MgO	0.70	0.29	0.39	1.11	0.70
CaO	1.69	0.88	1.04	2.15	2.46
Na_2O	4.73	5.27	5.70	5.84	5.50
K_2O	4.20	5.08	5.07	5.09	5.51
TiO_2	0.26	0.49	0.52	0.95	0.85
MnO	0.03	0.16	0.13	0.15	0.16
P_2O_5	0.09	0.09	0.10	0.32	0.31
ppm					
Ga	25	46	49	38	39
Rb	98	90	96	55	47
Sr	626	46	54	189	207
Y	17	59	65	38	31
Zr	221	919	1247	433	394
Nb	2	111	148	62	57
Ba	1116	230	281	793	1081
La	32	93	124	55	64
Ce	62	197	259	123	192
Nd	29	95	120	63	67

Table 6.11 : Comparison between the average major and trace element compositions of the Basement and Younger Granite rocks

BA : average of 8 Basement gneiss analyses
RA : average composition, Ras ed Dom
AA : average composition, Abu Dom
ERA : average Early Syenite, Ras ed Dom
EAA : average Early Syenite, Abu Dom

are SiO_2-rich (table 6.11). Thirdly, it is difficult to envisage how upper crustal melting could occur without even greater melt generation at depth.

To conclude, the gneisses are not thought a likely source for the anatectic Younger Granite parental magma. The early syenites are similar in composition to the Tuleih Syenite, Sabaloka complex, for which an alkalic garnet eclogite source has recently been proposed by Harris et al., (1982), on the basis of REE data and other considerations.

6.6. : Summary

Major element variation in the Younger Granite rocks supports the inference that the sequence early syenite ⟶ alkali syenite ⟶ alkali granite constitutes a fractionation sequence, in which the main changes are an increase in alkalinity due to Al_2O_3 depletion relative to alkalies and enrichment in Fe_2O_3 relative to FeO. Early depletions in CaO, P_2O_5 and TiO_2 are attributable to fractionation of calcic pyroxene, apatite and Fe-Ti oxide. Relations to alkali-enriched analogues of the 'granite system' confirm a magmatic origin, and trends in terms of SiO_2 - Al_2O_3 - (Na_2O + K_2O) suggest that fractionation of alkali-feldspar is the major process contributing to the evolution of the rock-series. Major depletions in Sr and Ba support this hypothesis, as do variations in Rb/Sr ratios, In common with other alkaline provinces, the Bayuda rocks exhibit strong enrichments in incompatable elements such as Zr, Nb, Y and the REE group. Partial REE trends are consistent with a cogenetic origin for the rocks and are characterised by LREE enrichment.

CHAPTER 7 : PETROGENESIS

7.1. : Introduction

In this chapter the petrogenesis of the Ras ed Dom and Abu Dom complexes, and of peralkaline oversaturated plutonic rocks in general, is considered. The relative contributions of fractional crystallisation of basaltic magma and crustal anatexis to the Younger Granite melts are assessed first. Thereafter the magmatic evolution of the Younger Granite magmas is discussed, and inferences concerning variations in temperature and oxygen fugacity are made. The importance of late-magmatic mineral transformations, and the influence of tectonic setting, are reviewed. In the final section of the chapter a petrogenetic synthesis is presented.

No petrogenetic consensus exists as to the origin of peralkaline granites, or indeed of alkalinity in general (Sorensen, 1974). Proposals range from crystallisation of basaltic magma (e.g. Upton, 1974; Barberi et al., 1975), partial melting (e.g. Bailey and Schairer, 1966; Bowden and Turner, 1974), ingress of volatiles (Bailey, 1970), to liquid immiscibility (Philpotts, 1978). There is, however, general agreement that no single parent magma is responsible for the varied alkaline associations. For these reasons, and in view of the lack of detailed isotopic investigations on the Bayuda Younger Granites, this chapter must inevitably pose as many questions as it provides answers.

In the ensuing discussion frequent analogies are made with the Nigerian Younger Granites (Bowden and Turner, 1974), the Gardar province (Emeleus and Upton, 1976) and the Permian Oslo Graben plutonic rocks (Neumann, 1980). The reader is referred to the above-mentioned reviews for further details of these associations.

7.2. : The Role of Fractional Crystallisation of Basaltic Magma

The East African petrochemical series, basalt — trachyte — pantellerite, has long been considered as representing a liquid line of descent (Bowen, 1937), and the pantellerites may thus be viewed as the salic members of the alkali-basalt association. The possibility that peralkaline granites are likewise derived through fractionation of a basic magma must therefore be examined. Especially crucial in this context are the minor basic rocks associated with Younger Granite type intrusions.

In Ras ed Dom and Abu Dom only minor occurrences of volcanic rocks are found (sections 2.2.B and 2.3.B), and apart from a few trachytic xenoliths, they are acidic in composition. However, large areas of caldera-preserved volcanic rocks characterise the other ring-complexes of the Ban Gidid - Ras ed Dom chain (Map 3, rear pocket). The Sultaniyat Volcanic Group consists of over 2000m of lavas and pyroclastic rocks (Curtis, 1979). The succession is dominantly acidic and peralkaline in composition, but minor trachytic and mugearitic lava fragments occur. The Meigil Volcanic Group of Muweilih complex (McCormac, pers. comm.) is also acidic in character, but the older Musran Volcanic Group is a basic - intermediate sequence extending from hawaiite through mugearite and benmoreite to alkali-feldspar trachytes.

The Sabaloka complex, 80km N. of Khartoum, is a Younger Granite complex characterised by acidic volcanic and intrusive rocks, largely peraluminous to metaluminous in composition (Almond, 1977). The oldest rocks, however, are a thin succession (20m) of basic lavas. The primary mineralogy is not always preserved, but observed phenocryst phases include plagioclase (labradorite-oligoclase range), augite, Fe-Ti oxides, and pseudomorphs after olivine. Some of the lavas are transitional towards trachyte. Although Almond (1977) reports only one analysis, it is transitional between alkali-basalt and tholeiite in composition.

The early basic rocks associated with the Sudanese Younger Granites are not necessarily extrusive. An early-formed, mildly alkaline gabbro occurs in J. Qeili complex (Ahmed, 1975). The dolerite dyke at loc. 183 in Abu Dom (section 4.6) is a further instance, and is characterised by strong normal zonation of the plagioclase (labradorite to oligoclase).

Similar basic volcanic sequences characterise the earliest volcanic rocks of the Nigerian Younger Granites. In the Ningi Massif the full sequence is basalt - trachybasalt- mugearite - trachyandesite - quartz trachyte - rhyolite (Turner and Bowden, 1979). Although liquid compositions are difficult to define, the sequence is thought to represent a differentiation series involving high-pressure fractional removal of olivine. The series is not of markedly alkaline character. Ike (1979), however, reports a similar early basic sequence from the nearby Tibchi complex, which is mildly alkaline and becomes more so with fractionation. Minor hybrid gabbroic masses, such as the net-veined basic-acid units of Sara-Fier complex (Turner, 1963) also occur. Most significant are rare sheet-like anorthosite bodies, associated with the northern ring-complexes in Niger (Bowden and Turner, 1974), which are of cumulus origin (Black, 1965).

The basic volcanic sequences described above are similar to those of the Quaternary Boina volcano in Ethiopia (Barberi et al., 1975). The Boina series spans the basalt — trachybasalt — trachyte — pantellerite range, and the basalts are transitional, mildly alkaline, types. Fractionation of plagioclase generated an increase in alkalinity, and fractionation in the peralkaline field was dominated by alkali-feldspar.

The question, therefore, must be posed as to whether the later intermediate and acid intrusive rocks of the Sudanese and Nigerian provinces are differentiates of such transitional basic magmas. Before answering this question it is appropriate to consider two instances for which the majority of workers accept such a genesis, namely the Early Precambrian Gardar province (Emeleus and Upton, 1976) and the Permian Oslo province (Barth, 1945; Neumann, 1980).

In both the Gardar and Oslo instances early extrusive rocks consist of transitional basalts, trachytes and rhyolites. Early-stage evolution of the magmas was controlled by fractionation of plagioclase, but later differentiates diverge at larvikite (augite-syenite) compositions into two trends. One trend is undersaturated, controlled by fractionation of nepheline and sodalite, and leads to nepheline syenites and phonolites. The other trend is oversaturated, and through fractionation of alkali-feldspar produced peralkaline granites and commendites (Upton, 1974; Neumann, 1980). Implicit in these schemes is the equivalence in magmatic terms of the intrusive and extrusive rocks. The abundances of rock-types do not at first sight support the proposed fractionation schemes. At Gardar compositions between the gabbros and syenites are rare (Upton, 1974), while at Oslo the proportion of basic/acid rocks is 1:24 (Oftedahl, 1978). Geophysical studies, however, indicate the existence of large masses of basic rocks at depths of 20-34km in the Oslo graben (Ramberg and Spjeldnaes, 1978), and Bridgwater and Harry (1968) have postulated a similar body at depth in the Gardar area. The dense rocks at depth are believed to represent hidden cumulates complimentary to the felsic rocks (Neumann, 1980). Certainly in the Gardar province anorthosite xenoliths are common, lending support to this notion of a 'basic batholith' at depth. The failure of the basic rocks to reach the surface is attributed to the crust acting as a density filter in tectonically quiescent periods (Ramberg, 1970; Roberts, 1970; Gill, 1973).

Returning to the Sudanese and Nigerian Younger Granites, the question must be asked whether similar arguments to those outlined for Gardar and Oslo apply. Four considerations suggest not.

i. The large volumes of rhyolitic volcanics and intermediate-acid intrusive rocks, with only minor basic associates, seem to preclude a basic parentage (Almond, 1977; Turner and Bowden, 1979).

ii. Whilst no gravity evidence is available for Bayuda, studies at Sabaloka complex indicate an absence of any basic bodies at high crustal levels (Sadig et al., 1974), although no inferences as to deep-crustal structure were made. Likewise in Nigeria, gravity studies confirm that the ring-complexes are isolated and extend to depths of 3-12 km, and that basic rocks are unimportant to similar depths (Ajakaiye, 1976).

iii. No anorthosites have been found associated with the Sudanese Younger Granites, although minor anorthosites occur associated with the Niger Younger Granites.

iv. In contrast to the Oslo and Gardar areas, undersaturated felsic rocks are not found in the Nigerian and Sudanese provinces, and this difference appears to be fundamental.

To invoke the presence of a lower crustal 'basic batholith' is accordingly considered unwarranted, and this point is discussed further in section 7.6 below. Thus although Younger Granite magmatism is associated in space and time with a differentiated basalt sequence, its main characteristics do not derive from the latter. Following Turner and Bowden (1979) the writer suggests that the early basic magmatism served as a heat source for a lower crustal anatectic event that produced an intermediate parent magma for the Younger Granite rocks. Large volumes of this second-stage magma reached the surface as compared with the mantle-derived basic material, thereby accounting for the present-day proportion of rock-types. The nature of the anatectic event is discussed in the next section.

7.3. : The Role of Crustal Anatexis

In the preceeding section the conclusion was reached that, in order to account for the observed geologic relations in the Bayuda complexes, it was necessary to postulate a crustal anatectic event. The available evidence indicates that the deep crust is mafic-rich, anhydrous, and presumably inhomogeneous (Bailey, 1974b) and that trachytic, rhyolitic and phonolitic melts, similar to those in Petrogeny's Residua System, are the kind of low-temperature fractions that would be produced by partial melting of such source rocks (op.cit.). In the Bayuda complexes under examination the least fractionated major rock-type is early syenite, and as suggested in sections 4.7.F., and 6.3.F., it is reasonable to infer that the parental partial melt was of comparable composition, i.e. hedenbergite syenite or monzonite composition. Harris (1982) has suggested that, on REE and other grounds, an alkalic garnet-eclogite source rock is likely for melts of this type. As the early syenites are essentially metaluminous (table 6.3), there is no reason to invoke a primary peralkaline melt composition, as suggested by Bailey and Schairer (1966). The passage of mantle-derived basic magma, as described in the previous section, is though to have triggered partial melting in the lower crust, but it is likely that mantle degassing further promoted anatexis (Bailey, 1970; 1974 1978). Degassing of the underlying mantle reduces the melting temperature of the basic source rocks, introduces volatiles which carry heat with them and focus it efficiently, and in addition may contribute to the distinctly alkaline character of later differentiates. Volatile influx would also help account for the limited variation found in alkaline rocks, a regularity that is difficult to reconcile with a heterogeneous source region (Bailey, 1974

An alternative anatectic model might involve upper crustal source areas. Bowden (1970) proposed that the Nigerian Younger Granites originated by partial melting, at high crustal levels, of Precambrian granites. As with the Bailey and Schairer (1966) model, the initial melt envisaged was peralkaline, with progressive melting yielding metaluminous and peraluminous compositions. Bowden has subsequently abandoned this proposal (Bowden, 1974) but Borley (1979) has advanced a similar scheme. Apart from difficulties in reconciling this with reported REE data (Bowden et al., 1979), it is difficult to imagine such high-level melting occurring without concomittant greater degrees of melting at depth. Moreover, the proposed sequence of rock-compositions is the reverse of that encountered in Ras ed Dom and Abu Dom, where metaluminous compositions characterise the earliest magmas.

Sr-isotope systematics have a bearing on the discussion. Barth and Meinhold (1979) report Sr-isotope determinations for 12 ring-complexes in the Bayuda Desert. The range in initial $^{87}Sr/^{86}Sr$ ratios is 0.7036 - 0.712, with the bulk of the results clustering about 0.704. Barth and Meinhold do not distinguish the metaluminous syenites as a separate category, but five alkali syenite and granite units contributed to a 4-point isochron for the combined Abu Dom - Sultaniyat - Ras ed Dom complexes. This yielded an isotopic age of 234±6 MA, and an initial ratio of 0.7063. More detailed data from each complex are clearly needed but the ratio is consistent with a lower crustal source, as proposed in this thesis, or indeed with a mantle signature that has undergone limited crustal contamination.

Significantly, in the present context, the lowest $^{87}Sr/^{86}Sr$ initial ratios in the Nigerian Younger Granites come from syenites, and suggest that the syenitic liquids had initial ratios of 0.7048, i.e. close to mantle values (van Breeman *et al*., 1975). The transition syenite — fayalite granite — peralkaline granite is marked by increasing initial ratios, consistent with increasing degrees of crustal contamination. However, van Breeman *et al*., (1975) noted that the increase might equally well be controlled by increasing peralkalinity in the melt. Peralkaline fluids or vapours, or indeed circulating groundwaters, may have leached ^{87}Sr from the basement country rocks.

In the Oslo and Gardar provinces the basic and syenitic rocks have low $^{87}Sr/^{86}Sr$ initial ratios, averaging about 0.704, while the peralkaline rocks yield higher ratios of up to 0.707 (Sundvoll, 1978; Blaxland *et.al*., 1978).

Further studies are needed to clarify Sr-isotope systematics in alkaline rocks (Faure and Powell, 1972). Post-magmatic alteration, such as albitisation, is now known to give anomalously high initial ratios (e.g. 0.752 in the Liruei albitised granite, van Breeman *et al*., 1975). Bowden *et al*., 1976 conclude on a note of caution, by observing "that the sialic crust, the lower crust, and even the upper mantle may all have contributed in some way to the evolution of the granitic liquids in the Nigerian province". In the case of Bayuda further studies are clearly needed, but the available data are consistent with the lower crustal anatectic model suggested in this chapter.

The magmatic evolution of the parental syenite magma is considered in the following section.

7.4. : Magmatic History of the Younger Granite Rocks

7.4.A. : Introduction

In preceeding chapters it has been proposed that the sequence early syenite ⟶ transitional syenite ⟶ alkali syenite ⟶ alkali granite, represents a fractionation sequence. Chemical evidence (chapter 6) supports this interpretation, and indicates that fractionation of alkali-feldspar is the driving mechanism in fractionating the magma and promoting increasing alkalinity. In this section a combination of petrographic, mineral-chemical and whole-rock chemical data, is used to qualitatively infer the behaviour of intensive variables, such as temperature and oxygen fugacity, with fractionation in the Bayuda magma.

Several indications of the variation in pressure can be recognised as follows:-

i. the occurrence of clear orthoclase grains in some of the early and transitional syenites (sections 4.3.B and 4.4.B) is consistent with relatively 'dry' conditions, with $pH_2O < pTotal$ (Parsons, 1981).

ii. in alkaline volcanic rocks, such as trachytes, continuous variation from Ca-rich to Na-rich pyroxenes can occur in one sample and the absence of amphibole is thought to reflect volatile loss upon extrusion (Ferguson, 1978). In the Bayuda plutonic rocks, however, an interval of amphibole crystallisation occurs between the early and late pyroxenes (section 5.3.A), and is consistent with a gradual build up in pH_2O in the residual liquids.

iii. the development of pegmatitic grain size, with large prisms of arfvedsonite-riebeckite and aegirine (see plate 2.4 and section 2.2.1), in the alkali syenites and granites suggests that in these instances pH_2O = pTOT.

For the purposes of referring to experimental data a pTOT of the order of 1kb is assumed in the following account. This is consistent with the sub-volcanic intrusive level of the ring-complexes.

7.4.B. : Early Syenite Magma

A few fresh grains of fayalite, and more common iddingsitic relicts occur in the early syenites (section 4.3.C). No analyses are available, but by analogy with similar rocks at Sabaloka complex (Almond, pers. comm.) compositions close to the pure end-member may be anticipated. Barker (1974, quoted in Larsen, 1976) conducted melting experiments on a fayalite-bearing agpaitic rock from the Trans-Pacos province, Texas. The results show fayalite to be stable above 800°C for the WM buffer at 1kb, but unstable where fO_2 approaches the QFM butter. (figure 7.1). Data concerning ferrohedenbergite stability are lacking, but hedenbergite is known to break down above 965°C (Bowen et al., 1933). The absence of mosaic textures in the ferrohedenbergites, indicative of inversion from ferrobustamite (Lindsley et al., 1969;Huebner, 1980), suggests an upper limit of ~ 930°C (fig. 7.3). Only sparse details on edenite stability are available (Peto, 1976). Peto located the upper stability limits for Mg-rich edenite at 925°C, 890°C and 875°C at 2, 1 and 0.5kb respectively, but did not specify buffer conditions. Upper stability limits for Mg end-members are commonly much higher than those for Fe-rich end-members (Ernst, 1962) and this suggests that Peto's values are probably considerably in excess of those for ferroedenite.

An estimate of maximum temperature, where pH_2O = pTOT, can be made using the pH_2O-T curve for the binary alkali-feldspar solidus minimum (Tuttle and Bowen, 1958). The effect of An-content on this curve is assumed to be negligible, an assumption supported by the close agreement between feldspar compositions and the thermal minimum in Ab-Or-An (fig. 5.1; c.f. Parsons, 1981). Feldspar stability in terms of An content, T^o and P is summarised diagrammatically in fig. 7.2,

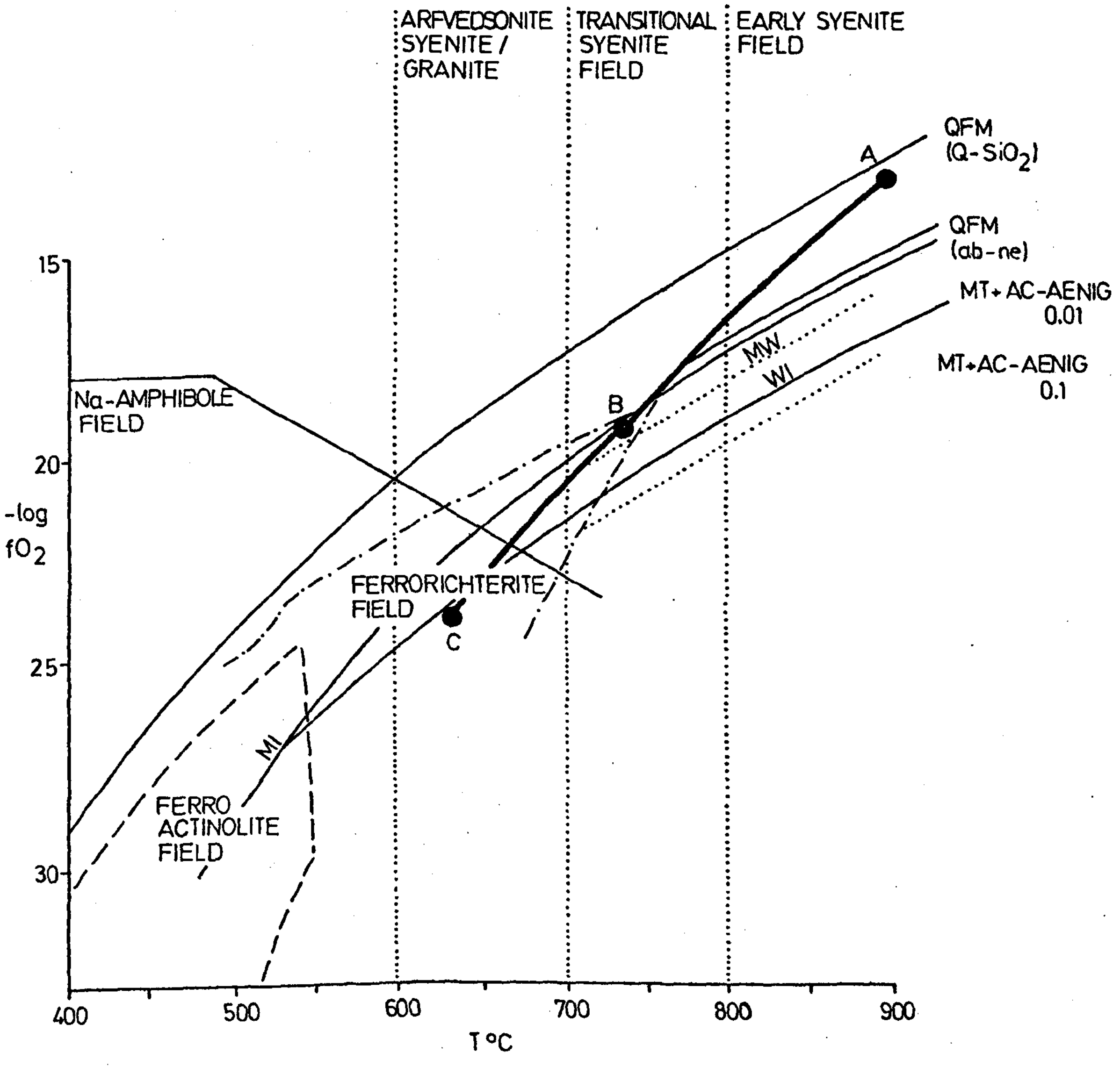

Fig. 7-1 : fO$_2$ - T °C DIAGRAM SHOWING POSSIBLE EVOLUTIONARY PATH (ABC) OF THE YOUNGER GRANITE MAGMAS. SEE TEXT FOR SOURCES OF THE MINERAL STABILITY FIELDS. SUBSOLIDUS MINERAL CHANGES NOT INCLUDED.

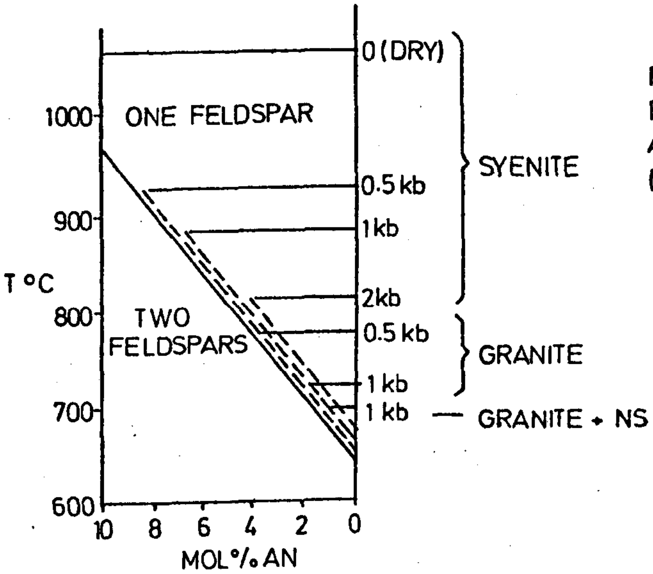

Fig. 7.2 :
FELDSPAR STABILITY IN TERMS OF AN CONTENT, T° AND P
(after Parsons 1978)

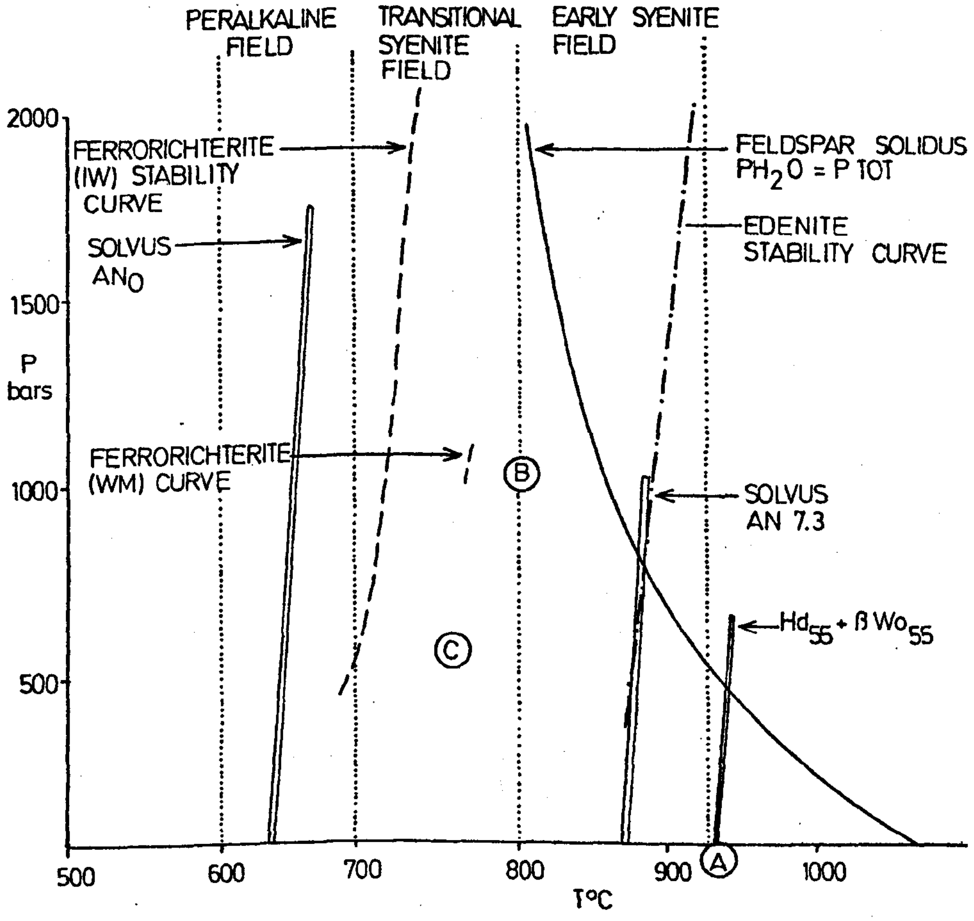

Fig. 7.3 : APPROXIMATE MAGMA STABILITY FIELDS IN P-T° SPACE, TOGETHER WITH RELATED MINERAL STABILITY DATA (FOR SOURCES SEE TEXT)

A - HEDENBERGITE OUT

B - FAYALITE OUT (WM BUFFER)

C - AENIGMATITE OUT (QFM BUFFER)

after Parsons (1978).

In fig. 7.3. the 7.3% An solvus, corresponding to the most calcic feldspar analysed (see table 5.2), is plotted. As the most calcic feldspar it yields the highest (and therefore most nearly magmatic) temperature for the early syenites. The minimum temperature of crystallisation for this composition is defined by the intersection of the solvus with the alkali-feldspar solidus i.e. 870°C (fig. 7.3). The corresponding pH_2O is 0.75kb where pH_2O = pTOT. However, as mentioned earlier, pH_2O was probably somewhat lower than pTOT in the early syenite magma.

The occurrence of modal quartz in the early syenites indicates that activity of silica ($aSiO_2$) lay above the albite-nepheline (Ab-Ne) silica buffer (fig. 7.1; c.f. Mitchell and Platt, 1978).

Summarising the above data, it is reasonable to infer that these early magmas began to crystallise at temperatures in the range 800-900°C (fig. 7.3) and that fO_2 was in the range defined by the QFM and WM buffers (fig. 7.1).

The occurrence of ferrowinchite-ferrobarroisite-ferroactinolite amphiboles as hydrothermal phases, can be used to infer temperatures for this late event. Actinolite is stable below 460°C at 1kb where fO_2 is defined by the MI and MW buffers (Ernst, 1962; fig. 7.1). Annitic biotite (unanalysed) also occurs and the stability data of Eugster and Wones (1962) are applicable. At 1035 bars, annite and quartz can co-exist between 545°C (MI buffer) and 685°C (QFM buffer), although the presence of flourine might decrease the stability limit (op.cit.). On the basis of these considerations the hydrothermal event occurred below 550°C under conditions of low fO_2.

7.4.C. : Transitional Syenite Magma

As the feldspars of the transitional and later alkali rocks are An-poor, they do not define a restricted P-T region and it is difficult to infer the conditions of formation. The petrographic relations (section 4.4.C) indicate that olivine reacted out of the magma as Na-enrichment commenced in the pyroxenes, a situation comparable to that at Ilimaussaq (Larsen, 1976). The enclosure of the pyroxene in ferrorichterite and aenigmatite provides some indication of conditions of formation, as discussed below.

At 1kb the upper stability limit for ferrorichterite is 760°C with fO_2 at the WM buffer (Charles, 1975; fig. 7.1). The stability curves for the QFM and IW buffers, and a partial curve for the WM buffer, are shown in fig. 7.3. Within its stability field (fig. 7.1) the amphibole is on the ferrorichterite bulk composition only at low fO_2 (IW buffer). At higher fO_2 the ferrorichterite is accompanied by acmitic pyroxene which approaches 30-40% of the experimental charge at the QFM buffer (Charles, 1975). This is consistent with the petrographic association of the ferrorichterite with aegirine-augite in these rocks (section 4.4.C).

Lindsley (1971) and Marsh (1975) have provided preliminary results on aenigmatite stability. Aenigmatite can be synthesised at 500-750°C, under moderate pO_2 (0.5kb), where fO_2 is at or below fugacities defined by the QFM buffer. Petrographic observations from many alkaline provinces suggest an antipathetic relationship betwen magnetite and aenigmatite, and this holds true for the Ras ed Dom rocks (section 5.6). This relationship has been used to infer the existence of a 'no-oxide' field in both oversaturated (Nicholls and Carmichael, 1969) and undersaturated magmas (Marsh, 1975). A possible equation to model this reaction is as follows:

$$\underset{\text{aenigmatite}}{\tfrac{3}{2}\,Na_2Fe_5TiSi_6O_{20}} + \underset{\text{gas}}{O_2} \rightleftharpoons \underset{\substack{\beta\text{-phase}\\ \text{solid soln.}}}{\tfrac{3}{2}\,Fe_2TiO_4 + \tfrac{1}{2}Fe_3O_4} + \underset{\text{quartz}}{3SiO_2} + \underset{\text{acmite}}{3NaFeSi_2O_6}$$

Mitchell and Platt (1978) evaluated this equation assuming aenigmatite activities of 0.1 and 0.01 at the start of crystallisation. The resultant curves (fig. 7.1) intersect the ferrorichterite stability field, in agreement with the petrographic association of the two phases. However, the uncertainties in the estimated free energies of aenigmatite and acmite are large. Moreover, it is quite possible that the limit to Fe-Ti oxide crystallisation is determined by equilibria involving ferrorichterite and aenigmatite (Mitchell and Platt, 1978), or an aenigmatite-arfvedsonite buffer which acts as an alkaline hydrous analogue of the QFM buffer (Larsen, 1977). If either of these is the case then the 'no-oxide field' concept may be unnecessary.

To summarise, whilst initial temperatures may have been close to those pertaining to the early syenite magma, later-formed phases reflect lower temperatures (700-800°C), and lower fO_2 in the range bracketed by the WM and IW buffers (fig. 7.1).

7.4.D. : Peralkaline Magma

The amphiboles of the alkali syenites and granites are zoned from cores of ferrorichterite to arfvedsonite rims (section 4.5.D.). Ernst (1962) found that solid-solutions of arfvedsonite-riebeckite are favoured by relatively low fO_2, and that at 1kb such phases are stable up to 695°C (IW buffer). In addition quartz can co-exist with sodic amphibole at oxidation states lower than the HM buffer. The stability field of sodic amphiboles is shown in fig. 7.1.

Aegirine replaces arfvedsonite in the alkali rocks (section 4.5.D). If internal oxygen buffering continued to operate it probably involved an arfvedsonite-acmite equilibrium. However, Larsen (1977) notes that exsolution of a separate gas phase may have involved a change to an external gas control, possibly with resultant discontinuities in fO_2 conditions. Moreover, as pointed out in section 4.5.D. textural evidence suggests that late aegirine and riebeckite are, in part at least, of sub-solidus development. This transition to post-magmatic conditions must be borne in mind in the following discussion.

Ernst (1962) found that the upper stability limit of riebeckite is 496°C (HM buffer) at 1kb, indicating that pure riebeckite cannot form directly from a melt, and requires conditions of high fO_2. Riebeckite may be stabilised magmatically by substitutions (e.g. Mg for Fe, or F^- for OH^-) away from the end-member, although the details of such effects are largely unknown (Ernst, 1962). Considerable solid solution towards riebeckite is evidenced by the Ras ed Dom (section 5.4.D) and Sultaniyat amphiboles (Curtis, 1979) and can be accounted for in terms of falling temperature and increasing fO_2 and $a\,Na_2O$ (Ernst, 1962; Kovalenko, 1968).

Popp and Gilbert (1972) examined the system $NaFeSi_3O_8$ (acmite+quartz) - $NaAlSi_3O_8$ (albite, or jadeite+quartz), and found that acmitic pyroxenes can form over a wide temperature range (350-600°C) at low pressure (1kb). Bailey (1969) examined acmite stability in the presence of H_2O, and found that its production involved incorporation of O_2, i.e. was favoured by high fO_2. Thus acmite is unstable under the IW and WM buffer conditions, and at 1kb its upper stability limit is 880°C, 850°C and 800°C for conditions governed by the HM, NNO and QFM buffers respectively. These studies suggest that the aegirines of the alkali rocks could have formed in the range 300-800°C. Fortunately, the composition of sodic pyroxenes, co-existing with quartz and/or albite, can be used to indicate temperature of formation if pressure can be independantly estimated (Popp and Gilbert, 1972). The estimate is based on the Fe-rich part of the acmite-jadeite join, using the convention $Fe^{3+}/(Fe^{3+} + (Al^{vi} - Al^{iv})) = \%$ acmite (fig. 7.4). The proportion of the jadeite component increases with higher pressure and lower temperature.

Applying the Popp and Gilbert (1972) method to the pyroxenes of the alkali syenites (D1057) and granites (D145, D447) indicates almost pure acmite compositions (> 98% acmite), which for an assumed pressure of 1kb, suggests temperatures of formation in excess of 600°C. This suggests a magmatic origin for the aegirines. However, the results are dependent upon estimates of Fe^{3+} content and pressure, and uncertainties remain in both. Moreover, as pointed out in section 4.5.D., the textural relations of the late pyroxenes are not unequivocally magmatic. In the recrystallised pyroxenes of D433 jadeite

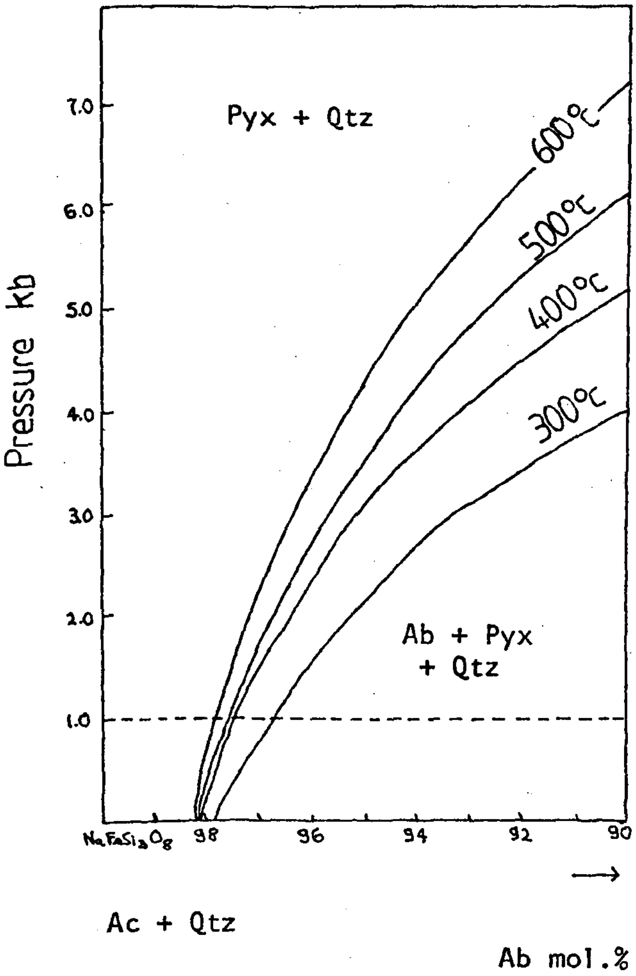

Fig. 7.4 : Relations for the Fe-rich portion of the join $NaAlSi_3O_8$ - $NaFeSi_3O_8$, after Popp and Gilbert (1972).

solid solution is greater (0-7%) suggesting formation in the range 300°C to 600°C. Albite and quartz are absent from this rock, but a normative Q value of 0.19 confirms that the rock is slightly over-saturated.

In summary, the richterite arfvedsonite solid solutions suggest formation under conditions of falling temperature and fO_2 (fig. 7.1). The assemblage aegirine + riebeckite in contrast, requires conditions of relatively high fO_2 and aNa_2O (Kovalenko, 1968; Ernst, 1962). Uncertainties remain, however, as regards the temperatures involved, and for this reason the assemblage is omitted from figs. 7.1 and 7.2.

7.4.E. : Discussion

The mineral stabilities described suggest a crystallisation range from 900°C to 500°C for the Bayuda magmas, and a crystallisation path, A-B-C, in T-fO_2 space is proposed (fig. 7.1). Estimates for other alkaline provinces, based on similar considerations, and employing pressures of 1-1.5kb, are as follows:-

1.	Ilimaussaq (Larsen, 1976)	800-900°C to 500°C
2.	Coldwell Syenite (Mitchell and Platt, 1978)	800-900°C to 500-550°C
3.	Pikes Peak Batholith (Barker <u>et al</u>., 1975)	900°C to 700°C
4.	Nigerian Younger Granites (Borley, 1976)	900°C to 600°C

These estimates suggest that the crystallisation interval proposed for Ras ed Dom and Abu Dom is reasonable. Moreover, melting experiments on undersaturated alkaline rocks (Piotrowski and Edgar, 1970; Sood and Edgar, 1970) indicate that at 1kb the range of crystallisation is approximately 900-580°C. A linear correlation between rocks with high agpaitic ratios and large melting intervals was found, and Sood and Edgar (1970) suggest that such long crystallisation histories may be attributed to enrichment in volatiles. McDowall and Wyllie (1971) determined the melting relationships for three saturated subaluminous syenites and two aegirine-riebeckite granites from Kungnat complex, Gardar. The crystallisation intervals for the syenites and granites are 900-700°C, and 800-650^{o}C respectively. The latter result is somewhat at odds with the long crystallisation history indicated by Sood and Edgar (1970).

7.5. : The Late- to Post-Magmatic Stages

Petrographic evidence (section 4.5.D. and 4.7.A+B) indicates that late-stage mineral transformations are recorded in the alkali rocks. The exsolution features of the alkali-feldspars and the growth of discrete albite are believed to reflect the passage of late fluids through the rocks. Aegirine is developed at the expense of arfvedsonite and minor riebeckite is encountered. Both of these minerals occur as tiny grains in 'channels' of recrystallised perthite, and in such instances appear to be of sub-solidus origin. Aegirine has commonly crystallised along quartz-quartz boundaries, and is associated with zircon, calcite and more rarely flourite.

If these features are indeed attributable to the action of late fluids, then it is reasonable to envisage the latter as being acmite-albite rich (Bowden, 1974; Bowden and Turner, 1974), with high concentrations of volatiles, REE, Zr and Nb (Kogarko, 1974). In the Bayuda examples the effects are confined within primary intrusive boundaries, and thus must be viewed as the result of a regressive autometasomatism, consequent upon falling temperatures, in which the residual fluids permeate through the largely crystallised rock. The Q-Ab-Or (figs. 6.10 and 6.11) and SiO_2 - Al_2O_3 - (Na_2O + K_2O) (fig. 6.12) plots support such a view. In these plots the granites are evidently co-magmatic with the earlier rocks, suggesting that the late fluids are consanguineous with the melt, and are not externally derived fenitising fluids. With the exception of locality D129 (section 4.5.D. and 6.5.), fenites are absent.

The theme of late fluid activity, which has modified the mineralogy and chemistry of the alkali rocks, is central to current ideas on the origin of the Nigerian Younger Granites (Bowden and Kinnaird, 1978; Bowden et al., 1979; Bowden, 1982). Where fluid-rock interaction is extreme, as in the albite-riebeckite granites of Nigeria, a distinctive mineralogy and chemistry results (Bowden, 1974; Bowden et al., 1976)

The rocks are characterised by such features as HREE enrichment and K/Rb ratios of less than 100. Such rocks are not found in Ras ed Dom or Abu Dom, and the assessment of the importance of fluid activity is difficult for several reasons, as follows:-

i. The relative contributions of late-magmatic or sub-solidus growth in, for example, the development of the late aegirine, are difficult to assess on textural criteria alone (section 4.5.D.).

ii. A spectrum of intermediate stages, involving escape, interaction or retention of residual fluid or vapour, can be envisaged (Bowden, 1982). The effects of these various possibilities on the resultant trace element chemistry remain to be established.

To summarise, in the writer's opinion the petrographic evidence (section 4.5.D) indicates a significant contribution by late- to post-magmatic fluids to the mineralogy and, by inference, to the chemistry of the alkali rocks. As indicated above, however, such views are speculative given the present state of the art (see section 7.7). Before leaving this topic, some observations as to the role played by volatiles are appropriate.

Tuttle (1961), on the basis of studies in the experimental system $Na_2O - K_2O - Al_2O_3 - SiO_2 - H_2O$, concluded that in peralkaline melts a gradual change from melt to aqueous fluid is possible at low pressure. Moreover, a continuum between silicate liquid and vapour may exist, without the normal liquid-vapour immiscibility relations expected on cooling (Tuttle, 1961; Mustart, 1972). These experimental considerations help account for the complexity of the late- to post-magmatic transition as described above. On the basis of experimental studies in liquidus-solidus relations of natural obsidians (Bailey and Cooper, 1978), and synthetic compositions in the peralkaline granite system (Luth, 1976), Bowden (1982) has inferred the actual composition of the fluid (vapour) phase. He suggests that, at near liquidus conditions, the fluid (vapour) phase in equilibrium with alkaline silicate melts is H_2O undersaturated and rich in F, Cl and CO_2. On cooling towards the alkali granite solidus the H_2O content and the alkalinity of the residual liquid is increased, with eventual partitioning of H_2O, alkalies and silicate into the vapour phase. Employing the experimental results of Koster Van Groos and Wyllie (1968, 1969), Harris (1981) suggests that Cl partitions into a CO_2-rich volatile phase, whereas F partitions into the residual liquids. Harris (1981) further proposes that enrichment in incompatabile elements in the melt may involve flouride and alkali complexes, whilst in the vapour phase carbonate complexing is more important. In this context a detailed study of volatile contents in the Bayuda rocks would be a rewarding line of future investigation.

Attention can be drawn to three features of the Bayuda rocks which may be related to volatile behaviour.

i. The development of secondary amphibole during the hydrothermal event in the early syenites (section 4.3.C), indicates that the early syenitic, metaluminous magmas exsolved an aqueous vapour phase. This is in agreement with expected relations for such compositions (Tuttle, 1961).

ii. The general absence of chilled margins in the syenites contrasts with the flow-textured chilled selvages invariably found in the granites. This may reflect higher volatile concentrations, with concommitant lower temperatures and viscosities, in the granite melts. However, other variables such as composition could equally account for the contrast in behaviour.

iii. The late pyroxenes of the granites commonly exhibit a high degree of crystal shape (section 4.5.D). Kogarko (1974) suggests that OH^- and F^- ions may substitute for O^{2-} ions, thereby protecting the growing surfaces from resorbtion. These effects occur even where the mineralisers do not enter a particular crystal lattice.

7.6. : The Relationship with Extensional Tectonics

A close relationship has been demonstrated between alkaline magmatism and areas of anorogenic, continental uplift and rifting (Bailey, 1974 ; Gass et al., 1978). The East African Rift system provides numerous illustrations of this, especially the Kenyan, Ethiopian and Afar sectors (Mohr, 1968; Baker et al., 1972; Barberi et al., 1975). More broadly, the siting of Tertiary and later alkaline magmatism in the African continent shows a strong correlation with the location of crustal swells (Le Bas, 1971). This relationship is apparent in Bayuda where Tertiary uplift, testified to by stripping off of the Nubian cover rocks, has been accompanied by alkaline basaltic magmatism (fig. 1.1).

Further back in geological time such a relationship is less easily proven but up-arching and rifting has been described from the Gardar (Steward, 1970; Upton, 1974) and Oslo (Ramberg and Neumann, 1978) provinces. The Nigerian Younger Granites are believed to be broadly related to abortive rifting associated with the Benue Trough aulacogen (Black, 1965; Burke et. al., 1971), although the precise nature of this relationship has not been detailed. The peralkaline granites of Corsica (Bonin et al., 1978) are in close proximity to buried rifts to the west of the island (Glangeaud et al., 1966). Repeated episodic peralkaline silicic magmatism characterised E. North America from the Silurian to the Jurassic, with the emplacement under extensional regimes of the Newfoundland, New Hampshire (White Mountain Magma Series), Massachusetts and Gulf of Maine peralkaline granites (Taylor, 1979; Taylor et al., 1980).

In Bayuda no direct evidence of uplift, and none at all of rifting, is found during the Palaeozoic and Mesozoic. Pre-Nubian sedimentary deposits in the area are sparse (Almond et al., 1969), but their absence is not necessarily related to doming. Nonetheless, it seems more probable that the Bayuda Younger Granites may have a relation to crustal doming rather than to active rifting. This may also explain the restricted compositional range of the Bayuda rocks as compared to the more varied magmatism found at Oslo and Gardar, where rifting is known to have been more advanced. It would also account for the absence of any evidence for a lower crustal basic batholith, such as has been proposed for those provinces (see section 7.2). Moreover, de Gruyter and Vogel (1981) suggest that reactivated basement shears and fractures have been more important controls on the siting of the Egyptian alkaline ring-complexes than updoming. Unfortunately, exposure of the basement rocks in Bayuda is poor, and they have not been studied in sufficient detail to test this notion.

The preliminary isotopic ages for the Bayuda ring-complexes (Barth and Meinhold, 1979) suggest that magmatism commenced in the south in Silurian times and moved northwards with time, the more northerly complexes being Jurassic in age (see section 1.4.C). In the Nigerian-Niger province isotopic ages for the ring-complexes young southwards, from Silurian-Devonian in Niger to Jurassic in Nigeria (Bowden et al., 1976) and Cretaceous-Tertiary in the Camerouns (Lassere, 1969). Rhodes (1971) and van Breeman et al., (1975) have suggested that this age trend may record the passage of the continental plate over a hot-spot or mantle plume (Morgan, 1971). However, the extent of migration of igneous activity is small compared to the northerly drift of Africa in the Phanerozoic (Creer, 1970). More detailed age data from the Sudanese Younger Granites must be awaited before such a mantle plume model can be fully evaluated for the Bayuda area.

7.7. : Petrogenetic Synthesis for Ras ed Dom and Abu Dom

The full cycle of magmatism that produced the Ras ed Dom and Abu Dom complexes, may be briefly outlined as follows:-

i. Arching of the African crustal plate, in response to radial compressive forces (Bailey, 1964) or mantle plumes (Morgan, 1971), induced decompression melting in the lower crust and an influx of volatiles from the upper mantle.

ii. Minor quantities of mantle-derived basaltic liquids penetrated to high-crustal levels producing the basic rocks of the complexes.

iii. The early basic episode was followed by a more extensive acidic volcanism, best seen in adjacent complexes but evidenced by the minor volcanic occurrences in Ras ed Dom and Abu Dom. In contrast to the early volcanics the source magma was a lower crustal anatectic melt.

iv. Emplacement of large volumes of intermediate and acid magma as sub-volcanic intrusions. The parental anatectic melt, generated in the lower crust, was of metaluminous syenitic-monzonitic composition. The subsequent differentiation of this magma at higher levels was controlled by low pressure fractional crystallisation of alkali-feldspar, which generated increasing alkalinity in the residual melts and produced the peralkaline syenites and granites.

v. Late-stage activity of sodic residual fluids further emphasised the peralkaline character of the later differentiates, especially the granites.

The scheme is depicted in fig. 7.6 and is characterised by the evolutionary rock-series early syenite → transitional syenite → alkali syenite → alkali granite. A broadly similar model has been proposed by Curtis (1979) for nearby Sultaniyat complex. Extension of the scheme to the earlier Muweilih complex (Map 3; rear pocket) encounters difficulties as biotite-granites are common there. McCormac (1979) proposes a separate fractionation scheme, pyroxene-biotite syenite → hastingsite-biotite granite → biotite-granite for these rocks. The potassic-aluminous trend and the sodic-peralkaline trend both originate from similar metaluminous parental syenites, however, and are thus complimentary divergent lineages.

Jacobson et al., (1958) recognised similar Al-rich and Al-poor trends in the Nigerian Younger Granites, and the divergence is central to the most recent petrogenetic scheme proposed for the province (Bowden and Kinnaird, 1978; Bowden et al., 1979). As shown in fig. 7.5 the model recognises that the early basic rocks are distinct from the later rocks. The latter derive from a parental anatectic syenite magma which differentiated to yield fayalite-granite compositions. Thereafter, Bowden and Kinnarid (1978), in what represents a radical departure from earlier ideas, propose that the divergence into peralkaline and peraluminous trends may be entirely due to sub-solidus recrystallisation engendered by the interaction of fayalite-granite and hydrothermal fluids.

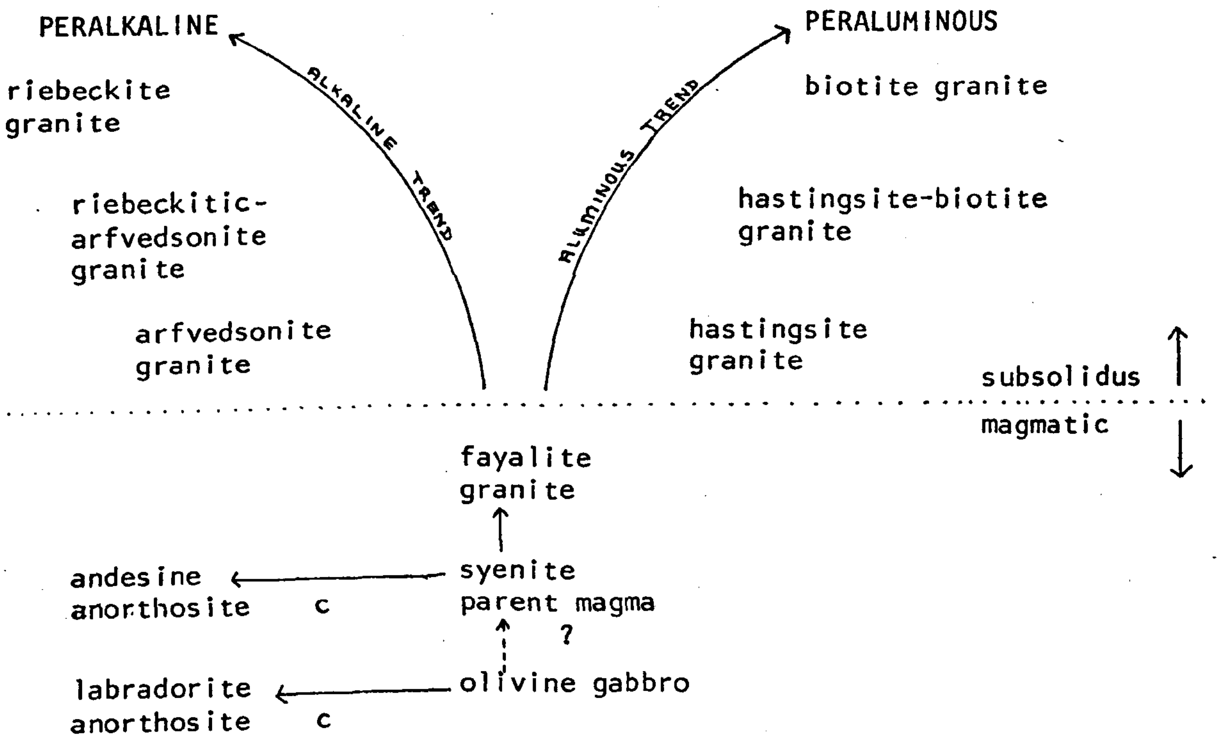

Fig.7.5 : Petrogenetic scheme for the Nigerian Younger Granites,after Bowden and Kinnaird (1978). ← c refers to cumulate formation.

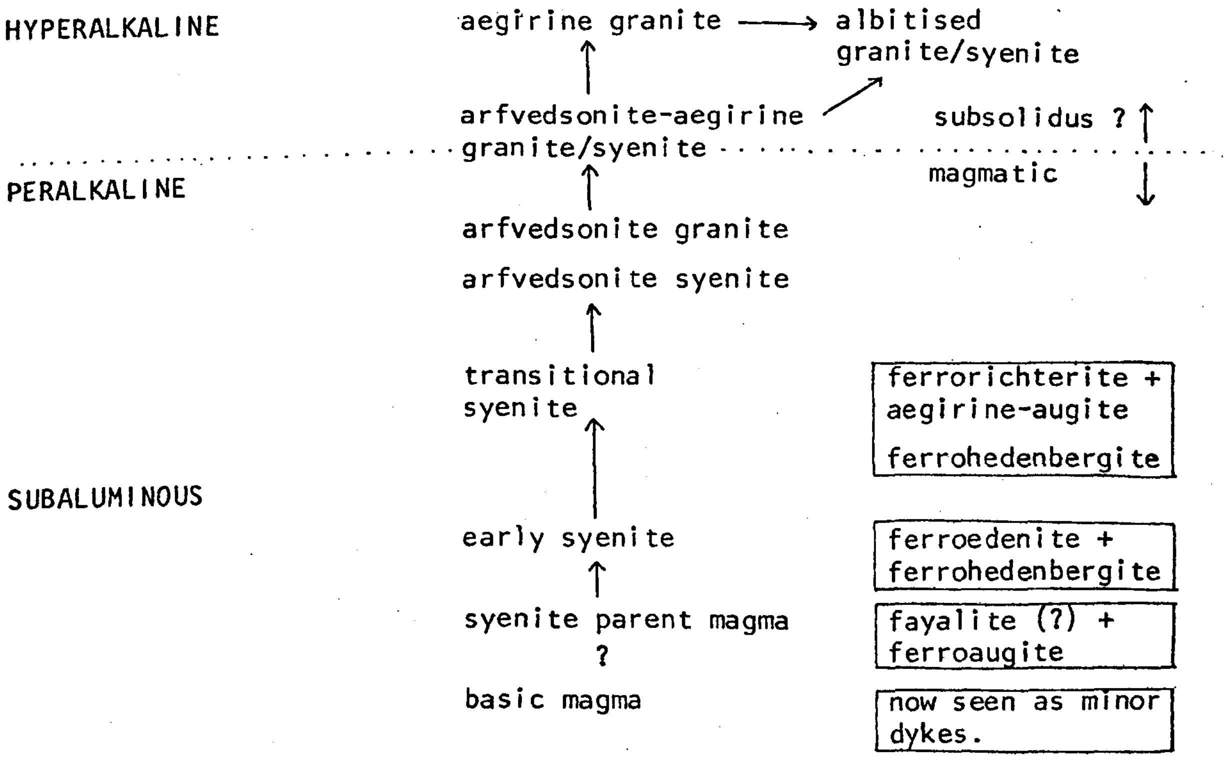

Fig.7.6 : Proposed petrogenetic scheme for Ras ed Dom and Abu Dom. Mineral assemblages and other comments detailed in boxes.

They argue that the importance of sub-solidus adjustment has been neglected, even though stable isotope studies have shown the need to re-examine petrogenetic hypotheses from such a viewpoint (Forester and Taylor, 1977; Bowden _et al_., 1979). The scheme has much in common with that proposed for Bayuda but the writer believes that the formation of arfvedsonite is more appropriately referred to the late-magmatic stage, rather than to the sub-solidus condition. The difficulties encountered in assessing the contributions of late- and post-magmatic fluid activity to the mineralogy and chemistry of the alkali rocks have been discussed in section 7.5., and a stimulating discussion of this and related matters is provided by Bowden (1982).

CHAPTER 8 : SUMMARY AND CONCLUSIONS

8.1. : Introduction

A major cluster of over twenty igneous ring-complexes is located in the Bayuda Desert of Northern Sudan (fig. 1.1)(Almond et al., 1976; Almond et al., 1982). The complexes pierce Precambrian basement rocks, and range from Silurian to Jurassic in age (Barth and Meinhold, 1979). They consist of sub-volcanic ring-intrusions and associated caldera-preserved volcanic rocks (Map 3, rear pocket), and belong to the Younger Granite association (Almond, 1979) which occurs widely in the Sudan (see sections 1.4.C and 8.6). The association is predominantly composed of oversaturated felsic volcanic and plutonic rocks, and is closely similar to the Younger Granites of Nigeria (Jacobson et al., 1958). The five complexes of the Ban Gidid - Ras ed Dom chain have been systematically studied (Map 3; Almond et al., 1982) and the geology of two of them, namely Ras ed Dom and Abu Dom, is the subject of this thesis.

8.2. : Field Relations

Although large areas of caldera-preserved volcanic rocks characterise the nearby Muweilih (McCormac; in. prep.) and Sultaniyat complexes (Curtis, 1979), only minor occurrences of volcanic rocks are found in the two complexes under discussion. They comprise a small faulted block near Abu Dom, and a raft and xenoliths in Ras ed Dom. The lithologies encountered are acid lavas, tuffs and ignimbrites.

Ras ed Dom and Abu Dom are closely similar lithologically. The three principal rock-types present are as follows:-

i. Early Syenite : typically the oldest units in a given structural centre, they are rather dark, hedenbergite-bearing syenites. They account for less than 5% of the total area of intrusive rocks.

ii. Alkali Syenite : This is the most abundant rock-type (55% of the total area) in both complexes, and is aegirine and arfvedsonite-bearing.

iii. Alkali Granite : aegirine- and arfvedsonite-rich granites.

Finer-grained equivalents of these three main categories are also recognised. In the cone-sheet swarms encircling the complexes microgranites predominate.

The essential structure of Ras ed Dom (Map 1, rear pocket) is one of semi-circular intrusions, successively overlapping each other and youging eastwards. The diameters of the units decrease in the same direction so that east-west variation reflects both migration of the centre of activity and decline in its strength with time. Eight distinct structural centres are recognised in the complex as described in section 3.2.B and shown in fig. 3.2. A small northward shift in the focus of magmatism with time is apparent in Abu Dom, but the most striking structural feature is the concentricity of the units in the northern part of the complex (Map 2).

Although it is believed that most of the intrusions were emplaced along ring-faults, most of the contacts are 'healed' intrusive contacts, and only rarely is evidence of faulting preserved. In Ras ed Dom the dominant intrusive form is one of sub-circular stocks. Contacts are often poorly exposed but the available evidence suggests that they are vertical to steeply outward dipping. It is possible that the stocks may constitute roofed 'bell-jars' at depth, but confirmatory evidence of this is not seen at the present level of erosion. Nested plutons are found in both Abu Dom and Ras ed Dom. Narrow annular intrusions, and crescentic sheets that wedge out laterally, are also present. In these instances steep outward dips establish an essential ring-dyke structure, and in some cases inward facing roof pendants are preserved. Granite 2 in Abu Dom is a bifurcating, double ring-dyke. The structures of the complexes typically reflect permissive emplacement, but in some instances it is apparent that fluidisation and hybridisation of adjacent rocks have played a role in the fracture widening process. The early syenites are structurally distinct in having been variably disrupted during the emplacement of later intrusions, a process which involved partial foundering.

Minor joint sets, which are related to the local intrusive pattern have an origin through cooling, and can be distinguished from major joints. The latter are of post-consolidation origin and are related to a regional stress field.

8.3. : Petrography and Mineral Chemistry

The early syenites are a group of slightly oversaturated syenites characterised by hedenbergite enclosed in later ferroedenite. Iddingsitic relicts after fayalite, and plagioclase (oligoclase-andesine) cores to alkali-feldspar grains, are occasionally present. Secondary ferrowinchite, of hydrothermal origin , is abundant. Fe-Ti oxides and apatite are modally significant, and their ubiquitous presence in the mafic clusters constitutes a diagnostic feature of this rock-type.

Under the microscope it is possible to recognise a further rock-type, in addition to the three main categories named above. This is the transitional syenite type in which the early pyroxene has rims of aegirine-augite, and is enclosed in sodic-calcic amphibole (ferrorichterite). Only two such units are known, and they are restricted to Centre 1, Ras ed Dom.

The mineralogy of the alkali syenites and granites reflects the importance of two common processes. The first of these is the increasing importance of modal quartz, whose presence serves to promote greater xenomorphism of the alkali-feldspars. The second feature is the replacement of arfvedsonite by late aegirine. Textural relations indicate that the aegirine and riebeckite of these rocks is, in part at least, of sub-solidus origin. Fe-Ti oxide is rare in the alkali rocks. Aenigmatite is occasionally present in some of the alkali syenites.

Two major variants of alkali-feldspar characterise this typically hypersolvus suite. In the early syenites the feldspar commonly consists of clear, transparent orthoclase, whereas the feldspars of the alkali rocks are invariably turbid micro- and macro-perthites.

There is, moreover, a progressive increase in the coarseness of exsolution features, and a decrease in the regularity of grain boundaries in passing from the early to later lithologies. Discrete, minute grains of albite are commonly developed in 'channels' between perthite grains, especially in the granites. These features are thought to reflect the passage of late-stage residual fluids along grain boundaries in the alkali rocks, and the late aegirine may have a similar origin.

Two further important conclusions are as follows:-

i. It is possible to distinguish two periods of pyroxene crystallisation. The early pyroxene stage involves hedenbergite to aegirine-augite compositions, whereas the late pyroxene stage is characterised by aegirine. The two periods are separated by an interval of amphibole crystallisation and the full mafic mineral reaction series is shown in fig. 4.3.

ii. Field relations, especially in Centre 1, Ras ed Dom, suggest that the sequence early syenite → transitional syenite → alkali syenite → alkali granite constitutes a fractionation sequence in the two complexes.

All the principal plutonic rock-types have counterparts in the dyke rocks. Of interest are a few occurrences of biotite-hedenbergite microsyenites. Only one basic dyke was found and it occurred in Syenite 3 of Abu Dom complex. The rock is a dolerite characterised by strong normal zoning of the plagioclase (labradorite-oligoclase) but the primary mafic minerals have been replaced by secondary amphibole.

Microprobe analysis has provided information as to the cryptic variation in the mineral phases.

Average bulk compositions for the alkali-feldspars cluster near the low-temperature termination of the plagioclase-alkali feldspar join in the Ab-Or-An triangular plot. Molecular anorthite values decrease from 7% in the early rocks to 0% in the alkali rocks. The late albite is almost pure, with six of the eight analyses containing over 99% Ab.

The early pyroxenes are zoned from cores of ferroaugite and ferrohedenbergite through to rims of aegirine-augite, and reflect progressive depletion in Ca and Mg and enrichment in Na and Fe. The late pyroxenes range from aegirine-augite to aegirine, and are Ti-rich. They are depleted in Ca, Mg and Fe^{2+} and show degrees of Na and Fe^{3+} enrichment comparable with the acmites of the Nigerian Younger Granites.

The hydrothermal amphiboles of the early syenites consist of ferrowinchite, ferrobarroisite and ferroactinolite, and are quite distinct chemically from the magmatic amphiboles of the suite. The latter show continuous variation from ferroedenite through ferrorichterite to arfvedsonite and minor riebeckite. The dominant substitution is of Na for Ca, together with substitution of Si for Al. Fe^{3+} becomes progressively dominant over Fe^{2+} with fractionation.

The Fe-Ti oxides were not studied in detail, but consist of both ilmenites and ilmenomagnetites. MnO values are often high, as much as 5%. The aenigmatite is Na- and Mn-rich, and depleted in Al, Ca and Mg.

A recrystallised syenite assemblage, characterised by aegirine-augite + Fe-Ti oxide + biotite, is thought to reflect the passage of late fluids. The biotite is Fe-rich, near annite in composition.

8.4. : Geochemistry

Major element variation in the Younger Granite rocks supports the inference that the sequence early syenite → alkali syenite → alkali granite constitutes a fractionation sequence, in which the main features are:-

i. increase in SiO_2 with fractionation,

ii. increasing alkalinity due to Al_2O_3 depletion relative to total alkalies, and

iii. enrichment in Fe_2O_3 relative to FeO.

In terms of aluminium saturation the early syenites are meta- and sub-aluminous, whereas the alkali rocks are peralkaline with agpaitic ratios greater than or equal to unity. In terms of the Macdonald and Bailey (1973) classification, the dyke rocks range from comendites (intermediate rocks) to pantelleritic (the acid rocks). The available evidence for the Bayuda area shows that, as regards SiO_2-levels, the suite is markedly bimodal , with a major peak at granitic compositions and a lesser peak at syenitic compositions. Compared to other peralkaline provinces the suite is rather low in CaO and MgO, and the predominance of Fe_2O_3 over FeO is marked. Within the suite early depletions in CaO, P_2O_5 and TiO_2, are attributable to fractionation of calcic pyroxene, alkali-feldspar, apatite and Fe-Ti oxide. Relations to alkali-enriched analogues of the 'granite system' confirm a magmatic origin for the rocks. The variation in terms of SiO_2 - Al_2O_3 - (Na_2O + K_2O) suggests that fractionation of alkali-feldspar is the major process contributing to the evolution of the rock-series. Major depletions in Sr and Ba support this notion, as does the variation in Rb/Sr ratios. The K/Rb declines steadily with fractionation. In common with other alkaline provinces, the Bayuda rocks exhibit strong enrichment in incompatabile elements such as Zr, Nb, Y and the REE group. The LREE are enriched relative to the HREE elements, and although only partial patterns are reported (La, Ce, Nd, Y) the trends are parallel, with mean values rising from the early to late rocks. The basement gneisses of the area have a similar REE trend with concentrations lower than in the granites. The gneisses are too silica-rich, however, to be the source of the Younger Granite magmas.

8.5. : Petrogenesis

A reasoned discussion of the petrogenesis of peralkaline granites is presented in Chapter 8. The full cycle of magmatism that produced the rocks of Ras ed Dom and Abu Dom may be briefly outlined as follows:-

i. Arching of the African crustal plate in response to radial compressive forces (Bailey, 1964) or mantle plumes (Morgan, 1971), induced decompression melting in the lower crust and an influx of volatiles, alkalies and rare elements.

ii. Minor quantities of mantle-derived basaltic liquids penetrated to high crustal levels producing the minor basic rocks of the complexes, e.g. the dolerite dyke in Abu Dom.

iii. The early basic episode was followed by a more extensive acidic volcanism, best seen in adjacent complexes but evidenced by the minor volcanic occurrences of Ras ed Dom and Abu Dom. The source magma in this instance is thought to have been a lower crustal anatectic melt.

iv. Emplacement of large volumes of intermediate to acid magma as sub-volcanic intrusions. The parental melt, generated in the lower crust, was of metaluminous syenitic-monzonitic composition. The subsequent differentiation of such magmas at higher crustal levels was controlled by low pressure fractional crystallisation of alkali-feldspar, which generated increasing alkalinity in the residual liquids and produced the peralkaline syenites and granites. The consolidation of the magmas at low pressure, occurred over the range $900^{o}C$ - $c500^{o}C$, and involved conditions of decreasing fO_2.

v. Late-stage activity of volatile-enriched, sodic residual fluids further emphasised the peralkaline character of the later differentiates, especially the granites. The appearance of late aegirine and riebeckite, favoured by increased fO_2, may in part have occurred under sub-solidus conditions.

8.6. : The Sudanese Younger Granite Association

In recent years the use of aerial and satellite photographs has vastly increased the number of known ring-complexes in the Sudan and adjacent areas. In a series of papers Vail (1972, 1973, 1976) has reported the location of one hundred and thirty two such complexes of which about eighty are within the Sudan's borders. Almond (1979) has suggested that at least three distinct petrographic associations may be distinguished amongst them, as follows (see fig. 8.1).

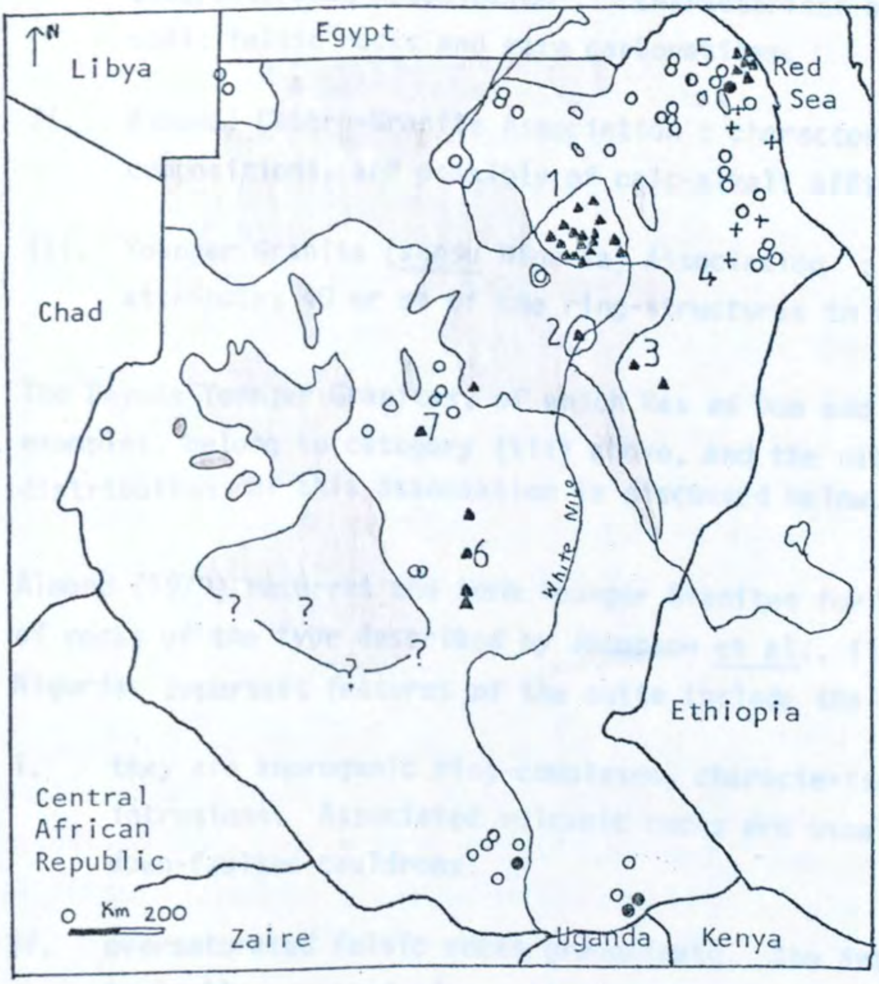

Fig.8.1 : Location of ring-complex associations in Sudan (after Vail,1976 and Almond, 1979).

- ▲ Younger Granite Association
- ● Undersatured Association
- \+ Gabbro-Granite Association
- ○ affinity unknown

1-Bayuda, 2-Sabaloka, 3-Qeili, 4-Tehilla, 5-Dunganab, 6-Nuba Mts., 7-Northern Khordofan.

outcrop of the Nubian Sandstone Formation in the Sudan.

i. Undersaturated Association : characterised by undersaturated, sodic felsic rocks and rare carbonatites.

ii. Bimodal Gabbro-Granite Association : characterised by aluminous compositions, and possibly of calc-alkali affinity.

iii. Younger Granite (sensu Nigeria) Association : Almond (1979) attributes 40 or so of the ring-structures to this category.

The Bayuda Younger Granites, of which Ras ed Dom and Abu Dom are examples, belong to category (iii) above, and the nature and distribution of this association is discussed below.

Almond (1979) reserves the term Younger Granites for an association of rocks of the type described by Jacobson et al., (1958) from Nigeria. Important features of the suite include the following;

i. they are anorogenic ring-complexes, characterised by sub-volcanic intrusions. Associated volcanic rocks are usually preserved in down-faulted cauldrons.

ii. oversaturated felsic rocks predominate. The intrusions are typically composed of syenites and granites, ranging from aluminous to peralkaline compositions. The volcanic rocks exhibit a similar variation. Basic lithologies are distinctly subordinate.

iii. Silica-undersaturated felsic rocks do not occur, although associated basic rocks are often mildly undersaturated.

iv. The suite is characterised by consistently low contents of CaO and MgO. The peralkaline rocks are especially enriched in trace elements such as Zr, Nb and REE.

It is apparent from fig. 8.1 that the Bayuda rings are probably part of a larger cluster linked with the complexes near Khartoum by further occurrences hidden beneath Nubian sediments. Neary et al., (1976) reported some forty or so 'Younger Granites' in the Dunganab region of the northern Red Sea Hill (fig. 8.1) and many appear to be Younger Granites sensu Almond (1979). Isotopic ages suggest emplacement in three episodes, at c700 Ma, 500 Ma and 100 Ma. A third cluster of possible Younger Granites occurs in the Nuba Mountains although the presence of adjacent complexes, in which undersaturated syenites occur, complicates such an ascription.

On a broader scale the recurrence of Younger Granite type magmatism over a vast region of West and North Africa and Arabia at various times is intriguing, and Jacobson et al., (1958) considered the African occurrences as defining an enormous petrographic province. In view of the wide variety of ages involved, this concept now seems untenable but Almond (1979) has suggested that the constant character of the association may be tied to compositional features of the underlying crust and upper mantle.

8.7. : Mineral Potential

Although the peralkaline granites of Ras ed Dom and Abu Dom show high concentrations of Zr, Nb and REE, highly mineralised rock-types, of either dispersed or vein-controlled nature, were not found. The albitised riebeckite-granites of the Nigerian Younger Granite province exhibit dispersed albite-cryolite-pyrochlore mineralisation (Kinnaird, 1977). As the granites of Ras ed Dom and Abu Dom do not show such intense albitisation the absence of significant mineralisation is not surprising. Economic cassiterite placer deposits are associated with the biotite-granites of the Nigerian Younger Granite province (Kinnaird, 1977). The discovery of a tin-tungsten stockwork associated with a muscovite-biotite granite at Sabaloka complex, near Khartoum (Almond, 1967), proves that such mineralisation can occur in the Sudanese Younger Granites. Complexes such as Ras ed Dom and Abu Dom, in which peralkaline lithologies predominate and biotite-granites are absent, are accordingly unlikely to have significant tin-bearing potential. Cassiterite, moreover, has not been found in the biotite-granites of Muweilih complex (Map 3, rear pocket; McCormac, pers. comm).

However, as only four of the twenty or so Younger Granite complexes of Bayuda have been mapped in detail the possibility remains that mineralisation of either Sn or U-Nb types may indeed be present in the area.

8.8. : Suggestions for Further Investigation

It is useful, in conclusion, to consider outstanding problems which remain concerning the nature and origin of the Bayuda Younger Granites. The writer considers that three potentially profitable lines of future investigation are as follows:-

i. A study of the volatile contents of the rocks, in order to assess further the influence of volatiles during both magmatic and late- to post-magmatic stages.

ii. An investigation to assess the importance of sub-solidus, hydrothermal changes in the peralkaline rocks. Petrographic and trace element criteria for evaluating the degree of rock-residual sodic fluid interaction need to be established (Bowden, 1982).

iii. Detailed isotopic and REE data are needed to model more rigourously the petrogenesis and evolution of the suite.

BIBLIOGRAPHY

ABBOTT, M.J. 1969. Petrology of the Nandewar volcano, N.S.W. Australia. Contrib.Mineral.Petrol. 20, 115-134

AHMED, F. 1975. The geology of J.Qeili igneous complex, Central Sudan. Geol.Rdsch. 64, 835-846

AJAKAIYE, D. 1976. A gravity survey over the Nigerian Younger Granite province. In: KOGBE, C.A. (ed.) The Geology of Nigeria. Elizabethan Press, Lagos. 207-224

ALMOND, D.C. 1967. Discovery of a tin-tungsten mineralisation in northern Khartoum Province, Sudan. Geol.Mag. 104, 1-12

ALMOND, D.C. 1974. The composition of basaltic lavas from Bayuda, Sudan and their place in the Cainozoic volcanic history of north-east Africa. Bull.Volcanol. 38, 345-360

ALMOND, D.C. 1977. The Sabaloka igneous complex, Sudan. Philos. Trans.R.Soc.London. 287, 595-633

ALMOND, D.C. 1979. Younger Granite complexes of Sudan. In: AL-SHANTI, A.M.S. (ed.), Evolution and mineralisation of the Arabian-Nubian shield, I.A.G. Bulletin 3, 151-164

ALMOND, D.C., AHMED, F. and KHALIL, B.E. 1969. An excursion to the Bayuda volcanic field of northern Sudan. Bull. Volcanol. 33, 549-565

ALMOND, D.C., O'HALLORAN, D., AHMED, F., CURTIS, P., McCORMAC, M. and VAIL, J.R.V. 1976. Concentrations of Younger Granite ring complexes and of small Cainozoic volcanic fields in the Bayuda Desert, Sudan. Annu.Rep.res.Inst.Afr.Geol.Leeds. 20, 61-65

ALMOND, D.C., CURTIS, P., McCORMAC, M., O'HALLORAN, D. and VAIL, J.R. 1982. Migrating Younger Granite ring-complexes in the Bayuda desert, northern Sudan. Precambrian Res. 16, No.4. A5 Abstract.

ANDERSON, E.M. 1936. The dynamics of the Formation of Cone-sheets, Ring-dykes, and Cauldron-subsidences. Proc.R.Soc. Edinburgh, 56, 128-157

ANDREW, G. 1948. Geology of the Sudan. In: TOTHILL, J.D. (ed.), Agriculture in the Sudan. Oxford University Press. London. 84-128

AOKI, K. 1964. Clinopyroxenes from alkaline rocks of Japan. Am.Mineral. 49, 1199-1223

ARTH, J.G. 1976. Behaviour of trace elements during magmatic processes - a summary of theoretical models and their applications. J.Res.U.S.Geol.Surv. 4, 41-47

BAHAT, D. 1979. A Hertzian quasi-oval fracture model for ring-complexes. J.Geol.Chicago. 88, 271-284

BAHAT, D. 1980. Hertzian fracture, a principal mechanism in the emplacement of the British Tertiary intrusive centres. Geol.Mag. 117, 463-470

BAILEY, D.K. 1964. Crustal warping - a possible tectonic control of alkaline magmatism. J.geophys.Res. 69, 1103-1111

BAILEY, D.K. 1969. The stability of Acmite in the presence of H20. Am.J.Sci. Schairer Vol. 267-A, 1-16

BAILEY, D.K. 1970. Volatile flux, heat focusing and the generation of magma. Geol.J. Special Issue 2, 177-186

BAILEY, D.K. 1974. Continental rifting and alkaline magmatism. In: SØRENSEN, H. (ed.) The Alkaline Rocks, John Wiley and Sons, New York. 148-159

BAILEY, D.K. 1974b. Origin of alkaline magmas as a result of anatexis. (b) Melting in the deep crust. In: SØRENSEN, H. (ed.) The Alkaline Rocks. John Wiley and Sons, New York. 436-442

BAILEY, D.K. 1974c. Experimental Petrology Relating to Oversaturated Peralkaline Volcanics: a Review. Bull.volcanol. 38, 637-652

BAILEY, D.K. 1976. Applications of Experiments to Alkaline Rocks. In: BAILEY, D.K. and MACDONALD, R. (eds.) The Evolution of the Crystalline Rocks. Academic Press, London. 419-471

BAILEY, D.K. 1978. Continental Rifting and Mantle Degassing. In: NEUMANN, E.-R. and RAMBERG, I.B. (eds.) Petrology and Geochemistry of Continental Rifts. D.Reidel, Dordrecht. 1-13

BAILEY, D.K. and COOPER, J.P. 1978. Comparison of the crystallisation of pantelleritic obsidian under hydrous and anhydrous conditions. In: MACKENZIE, W.S. (ed.) Progress in Experimental Petrology. NERC publication series D, no.11, 230-233

BAILEY, D.K. and MACDONALD, R. 1969. Alkali-feldspar fractionation trends and the derivation of peralkaline liquids. Am.J.Sci. 267, 242-248

BAILEY, D.K. and MACDONALD, R. 1975. Flourine and chlorine in peralkaline liquids and the need for magma generation in an open system. Mineralog.Mag.London. 40, 405-414

BAILEY, D.K. and MACDONALD, R. 1976. The Evolution of the Crystalline Rocks. Academic Press, London. 484pp

BAILEY, D.K. and SCHAIRER, J.R. 1964. Feldspar-liquid equilibria in peralkaline liquids - the orthoclase effect. Am.J.Sci. 262, 1198-1206

BAILEY, D.K. and SCHAIRER, J.R. 1966. The system Na_2O - Al_2O_3 - Fe_2O_3 - SiO_2 at 1 athmosphere, and the petrogenesis of alkaline rocks. J.Petrol. 7, 114-170

BAILEY, E.B., CLOUGH, C.T., WRIGHT, M.B. RICHEY, J.E., WILSON, G.V. and others. 1924. The Tertiary and post-Tertiary geology of Mull, Loch Aline and Oban. Mem.geol. Surv.Scotland

BAILEY, J.C. 1977. Flourine in granitic rocks and melts: a review. Chem.Geol. 19, 1-42

BAIN, A.D.N. 1934. The younger intrusive rocks of the Kudaru Hills, Nigeria. Q.J.geol.Soc.London. 90, 201-239

BAKER, B.H., MOHR, P.A., and WILLIAMS, L.A.J., 1972. Geology of the Eastern Rift System of Africa. Spec.Paper.Geol. Soc.Am. 136

BAKER, I. 1968. The Geology of St.Helena, South Atlantic. Unpublished Ph.D. thesis, University of London.

BALK, R. 1937. Structural behaviour of igneous rocks. Geol.Soc.Am. Memoir. 5, 177pp

BARBIERI, F., SANTACROCE, R., FERRARA, G., TREUIL, M. and VARET, J. 1975. A transitional basalt-pantellerite sequence of fractional crystallisation, the Boina Centre (Afar Rift, Ethiopia). J.Petrol. 16, 22-56

BARBOUR, K.M. 1961. The Republic of the Sudan. University of London Press. 292pp

BARKER, F., WONES, D.R., SHARP, W.N. and DESBOROUGH, G.A. 1975. The Pikes Peak Batholith, Colorado Front Range, and a model for the origin of the gabbro-anorthosite-syenite-potassic granite suite. Precambrian Res. 2, 97-160

BARTH, H. and MEINHOLD, K.-D. 1979. Sudanese-German exploration project technical report, Part 1: Mineral Prospecting in the Bayuda Desert. Vol.A Investigation of Mineral Potential. Fed.Inst.Geosci. Nat.Resour.Hannover. 366pp

BARTH, T.F.W. 1945. Studies on the igneous rock complex of the Oslo Region. II systematic petrography of the plutonic rocks. Skr.Nor.vidsk.-Akad. Oslo I. Mat-Naturv.kl. 1-104

BILLINGS, M. 1928. The chemistry, optics and genesis of the hastingsite group of amphiboles. Am.Mineral. 13, 287-296

BILLINGS, M.P. 1943. Ring dikes and their origin. Trans.N.Y.Acad.Sci. 5, 131-144

BIZOUARD, H. and DI PAOLA, G.M. 1978. Mineralogy of the Tullu Moje active volcanic area (Arussi: Ethiopian Rift Valley). In: NEUMANN, E.-R. and RAMBERG, I.B. (eds.) Petrology and Geochemistry of Continental Rifts. D.Reidel. Dordrecht. 87-100

BLACK, R. 1965. Sur la signification pétrogénetique de la découverte d'anorthosites associées aux complexes annulaires subvolcaniques du Niger. C.r.Seances Acad.Sci.Paris. 260, 5829-5832

BLAXLAND, A.B., VAN BREEMAN, O., EMELEUS, C.H. and ANDERSON, J.G. 1978. Age and origin of the major syenite centres in the Gardar province of South Greenland: Rb-Sr studies. Bull-geol.Soc.Am. 89, 231-244

BONIN, B., GRELOU-ORSINI, D. and VIALETTE, Y. 1978. Age, Origin and Evolution of the anorogenic complex of Evisa (Corsica) : a K-Li-Rb-Sr study. Contrib.Mineral. Petrol. 65, 425-432

BORG, I.Y. 1967. Optical Properties and Cell Parameters in the Glaucophane-Riebeckite Series. Contrib.Mineral. Petrol. 15, 67-92

BORISENOK, L.A. and SAUKOV, A.A. 1960. Geochemical cycle of gallium. 21st Int.Geol.Congr.Norden. part 1, 96-105

BORLEY, G.D. 1963. Amphiboles from the Younger Granites of Nigeria. Part I. Chemical classification. Mineralog.Mag. London. 33, 358-376

BORLEY, G.D. 1976. Ferromagnesian Mineralogy and Temperatures of Formation of the Younger Granites of Nigeria. In: KOGBE, C.A. (ed.). Geology of Nigeria. Elizabethan Press, Lagos. 159-176

BORLEY, G.D. 1979. Written contribution to "Younger Granites of Nigeria - a zinc-rich tin province" by BOWDEN, P. KINNAIRD, J.A. Trans.Instn.Ming.Metall.(Sect.B: Appl.earth sci.) 88, B73

BOWDEN, P. 1964. Gallium in the Younger Granites of Northern Nigeria. Geochim.cosmochim.Acta. 28, 1981-1988

BOWDEN, P. 1966. Zirconium in the Younger Granites of northern Nigeria. Contrib.Mineral.Petrol. 30, 985-993

BOWDEN, P. 1970. Origin of the Younger Granites of northern Nigeria. Contrib.Mineral.Petrol. 25, 153-162

BOWDEN, P. 1974. Oversaturated alkaline rocks; granites, pantellerites and comendites. In: SØRENSEN, H. (ed.) The Alkaline Rocks. John Wiley and Sons, New York. 109-123

BOWDEN, P. 1982. Magmatic Evolution and Mineralisation in the Nigerian Younger Granite Province. In: EVANS, A.M. (ed.) Metallization Associated with Acid Magmatism. John Wiley and Sons, New York. 51-61

BOWDEN, P. and VAN BREEMAN, O. 1972. Isotopic and chemical studies on Younger Granites from Northern Nigeria. In: DESSAUVAGIE,T.F. and WHITEMAN, A.M. (eds.) African Geology, Ibadan 1970. Univ. of Ibadan Press. 105-120.

BOWDEN, P. and TURNER, D.C. 1974. Peralkaline and associated ring-complexes in the Nigeria-Niger Province, West Africa. In: SØRENSEN, H. (ed.) The Alkaline Rocks. John Wiley and Sons, New York. 330-351

BOWDEN, P. and WHITLEY, J.E. 1974. Rare-earth patterns in peralkaline and associated granites. Lithos. 7, 15-21

BOWDEN, P., WHITLEY, J.E. and VAN BREEMAN, O. 1976. Recent geochemical studies on the Younger Granites of Northern Nigeria. In: KOGBE, C.A. (ed.). Geology of Nigeria. Elizabethan Press, Lagos. 177-193

BOWDEN, P. and KINNAIRD, J.A. 1978. Younger Granites of Nigeria - a zinc-rich tin province. Trans.Instn.Ming.Metall. (Sect.B: Appl.earth sci.) 87, B66-B69

BOWDEN, P., BENNETT, J.N., WHITLEY, J.E., and MOYES, A.B. 1979. Rare earths in Nigerian Mesozoic Granites and Related Rocks. In: AHRENS, L.H. (ed.) Origin and Distribution of the Elements 2nd symposium. Pergamon Press, Oxford. 479-491.

BOWEN, N.L. 1937. Recent high temperature research on silicates and its significance in igneous geology. Am.J.Sci. 33, 1-21.

BOWEN, N.L., SCHAIRER, J.F. and POSNJAK, E. 1933. The system CaO-FeO-SiO2. Am.J.Sci. 26, 193-284

BRADY, J.B. 1974. Coexisting actinolite and hornblende from west-central New Hampshire. Am.Mineral. 59, 529-535

BRIDGWATER, D. and HARRY, W.T., 1968. Anorthosite xenoliths and plagioclase megacrysts in Precambrian intrusions of South Greenland. Medd.Gronland. no.2., 243p.

BROGGER, W.C. 1890. Die Mineralien der Syenit-pegmatitgange der sudnorwegischen Augit- und Nephelinsyenite. Z.Kristallogr.Mineral. 16, 1-663

BROGGER, W.C. 1906. Eine Sammlung der wichtigsten Typen der Eruptivgesteine der Kristiania-gebietes. Nyt.Mag. f.Naturv. 44, 2.

BROWN, G.C., HUGHES, D.J. and ESSON, J. 1973. New X.R.F. retrieval techniques and their application to USGS standard rocks. Chem.Geol. 11, 223-229

BROWN, G.N. and VINCENT, E.A. 1963. Pyroxenes from the late stages of fractionation of the Skaergaard intrusion, East Greenland. J.Petrol. 4, 175-197

BUCHANAN, M.S., MACLEOD, W.N., and TURNER, D.C. 1971. The geology of the Jos Plateau. Vol.2 Younger Granite Complexes. Geol.Surv.Nigeria.Bull. 32, 159pp

BUDDINGTON, A.F. and LINDSLEY, D.H. 1964. Iron-titanium oxide minerals and synthetic equivalents. J.Petrol. 5, 310-357

BURKE, K.C., WHITEMAN, A.J. and DESSAUVAGIE, T.F.J. 1971. Opening of the Gulf of Guinea and geological history of the Benue depression and Niger delta. Nature.London 233, 51-55

BUSSEN, I.V. and SAKHAROV, A.S. 1972. Petrology of the Lovozero alkaline massif (in Russian). Nauka, Leningrad. 296pp

BUTLER, J.R., BOWDEN, P. and SMITH, A.Z., 1962. K/Rb ratios in the evolution of the Younger Granites of Northern Nigeria. Geochim.cosmochim.Acta. 226, 89-100

CANNILLO, E., MAZZI, R., FANG, J.H., ROBINSON, P.D. and OHYA, X. 1971. The crystal structure of aenigmatite. Am.Mineral. 56, 427-446

CARMICHAEL, I.S.E. 1960. The pyroxenes and olivines from some Tertiary acid glasses. J.Petrol. 1, 309-336

CARMICHAEL, I.S.E. and MACKENZIE, W.S. 1963. Feldspar-liquid equilibria in pantellerites: an experimental study. Am.J.Sci. 261, 382-396

CARMICHAEL, I.S.E., TURNER, F.J., and VERHOOGEN, J. 1974. Igneous Petrology. McGraw-Hill Inc., New York. 739pp

CAWTHORN, R.G. and COLLERSON, K.D. 1974. The Recalculation of Pyroxene End-Member Parameters and the Estimation of Ferrous and Ferric Iron Content from Electron Microprobe Analyses. Am.Mineral. 59, 1203-1208

CHAMBERS, A.D. 1976. The petrology and geochemistry of the North Qôroq Centre, Igaliko complex, South Greenland. Unpublished Ph.D. thesis, University of Durham.

CHAO, E.C.T. and FLEISCHER, M. 1960. Abundance of Zirconium in Igneous Rocks. 21st.Int.Geol.Congr.Norden. Part 1. 106-131

CHAPMAN, R.W. 1935. Percy ring-dyke complex. Am.J.Sci. 30, p.401-431

CHARLES, R.W. 1975. The Phase Equilibria of Richterite and Ferrorichterite. Am.Mineral. 60, 367-374

CHAYES, F. 1963. Relative abundance of intermediate members of the oceanic basalt-trachyte association. J.geol.Res. 68, No.5, 1519-1534

CLARK, J.R. and PAPIKE, J.J. 1968. Crystal-chemical characterisation of omphacites. Am.Mineral. 53, 840-868

CLOUGH, C.T., MAUFE, H.B. and BAILEY, E.B. 1909. The cauldron-subsidence of Glencoe and the associated igneous phenomena. Q.J.geol.Soc.London. 65, 611-678

COX, K.G., BELL, J.D. and PANKHURST, R.J. 1979. The Interpretation of Igneous Rocks. George Allen and Unwin, London. 450pp

CREER, K.M. 1970. A review of palaeomagnetism. Earth Sci.Rev. 6, 369-466

CURTIS, P.A.S. 1979. The geology of the Sultaniyat ring-complex, Bayuda Desert, Sudan. Unpublished Ph.D. thesis, C.N.A.A. 290pp

DE GRUYTER, P. and VOGEL, T.A. 1981. A model for the origin of the alkaline complexes of Egypt. Nature.London. 291, 571-574

DE LA ROCHE, H., LETERRIER, J., GRANDCLAUDE, P. and MARCHAL, M. 1980. A classification of volcanic and plutonic rocks using R1R2-diagram and major element analyses - its relationship with current nomenclature. Chem.Geol. 29, 183-210

DEER, W.A., HOWIE, R.A., and ZUSSMAN, J. 1963. Rock-forming Minerals Vol.4. Framework Silicates. Longmans, London.

DEER, W.A., HOWIE, R.A. and ZUSSMAN, J. 1978. Rock-forming Minerals Vol.2A: Single-chain silicates. 2nd ed. Longmans, London 668pp

DELANY, F.M. 1954. Recent contributions to the geology of the Anglo-Egyptian Sudan. 19th Int.geol.Congr. 20, 11-18

DELANY, E.M. 1958. Observations on the Sabaloka Series of the Sudan Trans.Proc.geol.Soc.South Afr. 61, 111-124

DIETRICH, R.V. and HEIER, K.S. 1967. Differentiation of quartz-bearing syenite (nordmarkite) and riebeckite-arfvedsonite granite (ekerite) of the Oslo Series. Geochim. cosmochim.Acta. 31, 275-280.

DU TOIT, A.L. 1920. The Karoo dolerites of S.Africa : a study in hypabyssal injection. Trans.Proc.geol.Soc. South Afr. 23, 1.

DUCHESNE, J.-C. 1972. Iron-titanium oxide minerals in the Bjerkrem-Sogndal Massif, south-western Norway. J.Petrol. 13, 57-81

DURRANCE, E.M. 1967. Photo-elastic stress studies and their application to a mechanical analysis of the Tertiary ring-complex of Ardnamurchan, Argyllshire. Proc.Geol.Assoc.London. 78, 289-318

EDGAR, A.D. 1974. Experimental Studies. In: SORENSEN, H. (Ed.) The Alkaline Rocks, John Wiley and Sons, New York. 355-389

EDWARDS, W.N. 1926. Fossil plants from the Nubian Sandstone of eastern Darfur. Q.J.geol.Soc.London. 82, 94-100

EMELEUS, C.H. and UPTON, B.G.J. 1976. The Gardar period in southern Greenland. In: ESCHER, A. and WATT, W.S. (eds.) Geology of Greenland. Gronland Geologiske Undersogelse, Denmark. 152-181.

ENGELL, J. 1973. A closed system crystal-fractionation model for the agpaitic Ilímaussaq intrusion, South Greenland, with special reference to the lujavrites. Medd.Dansk geol.Foren. 22, 334-362

ERNST, W.G. 1962. Synthesis, Stability Relations, and Occurrence of Riebeckite and Riebeckite-Arfvedsonite Solid Solutions. J.Geol.Chicago. 70, 689-736

ERNST, W.G. 1968. Amphiboles, Crystal Chemistry, Phase Relations and Occurrence. Springer-Verlag, New York. 125pp

ERNST, W.G. 1979. Coexisting sodic and calcic amphiboles from high-pressure metamorphic belts and the stability of barroisitic amphibole. Mineralog.Mag.London. 43, 269-278

ESSENE, E.J. and FYFE, W.S. 1967. Omphacite in Californian metamorphic rocks. Contrib.Mineral.Petrol. 15, 1-23

EUGSTER, H.P. and WONES, D.R. 1962. Stability relations of the ferruginous biotite, annite. J.Petrol. 3, 82-125

FAURE, G. and POWELL, J.J. 1972. Strontium Isotope Geology. Springer-Verlag, New York. 140pp

FERGUSON, A.K. 1977. The Natural Occurrence of Aegirine-Neptunite Solid Solution. Contrib.Mineral.Petrol. 60, 247-253

FERGUSON, A.K. 1978. The Crystallisation of Pyroxenes and Amphiboles in Some Alkaline Rocks and the Presence of a Pyroxene Compositional Gap. Contrib.Mineral. Petrol. 67, 11-15

FERGUSON, J. 1970. The differentiation of agpaitic magmas: the Ilímaussaq intrusion, South Greenland. Can.Mineral. 10, 335-349

FERRARA, G. and TREUIL, M. 1974. Petrological implications of Trace Element and Sr Isotope Distributions in Basalt-Pantellerite Series. Bull.Volcanol. 38, 548-574

FINGER, L.W. 1972. The Uncertainty in the Calculated Ferric Iron Content of a Microprobe Analysis. Carnegie Inst. Washington.,Ann.Rept.Dir.Geophys.Lab.1971-1972. 600-603

FIRMAN, R.J. 1960. The relationship between joints and fault patterns in the Eskdale Granite, Cumberland and the adjacent Borrowdale Volcanic Series. Q.J.geol.Soc.London 116, 317-347.

FITTON, J.G. and GILL, R.C.O. 1970. The oxidation of ferrous iron during mechanical grinding. Geochim.cosmochim.Acta. 34, 518-524

FLANAGAN, F.J. 1976. 1972 compilation of data on U.S.G.S. standards. In: FLANAGAN, F.J. (ed.) Description and Analyses of eight new U.S.G.S. Rock Standards. U.S.G.S.prof.paper 840, 131-183

FORESTER, R.W. and TAYLOR, H.P.Jr. 1977. $^{18}O/^{16}O$, D/H and $^{13}C/^{12}C$ studies of the Tertiary igneous complex of Skye, Scotland. Am.J.Sci. 277, 136-177

GARSON, M.S. 1959. Stress pattern of carbonatitic and alkaline dykes at Tundulu ring structure, southern Nyasaland. Int.geol. Congr. 20, 309-323

GASS, I.G., CHAPMAN, D.S., POLLACK, H.N. and THORPE, R.S. 1978. Geological and geophysical parameters of mid-plate volcanism. Philos.Trans.R.Soc.London.ser.A. 288, 581-597

GIBB, F.G.F. 1973. The zoned clinophyroxenes of the Shiant Isles Sill, Scotland. J.Petrol. 14, 203-230

GILBERT, M.C. 1969. High-pressure stability of acmite. Am.J.Sci. Schairer vol.267-A. 145-159

GILL, R.C.O. 1973. Mechanism for the salic magma bias of continental alkaline provinces. Nature (phys.Sci.) 242, 41-42

GINDY, A.R. and ANDRAWOS, A.S. 1969. Complex calderas and ring structures in the Bayouda Desert, Northern Sudan. Proc.Acad.Sci.Egypt. 21, 77-86

GINDY, A.R. and ANDRAWOS, A.S. 1970. Discovery of a late-Precambrian volcanic ring-complex at Jebel Abu Nahl, Bayouda Desert, northern Sudan. Bull.Volcanol. 34, 240-253

GLANGEAUD, L., ALINAT, J., POLVECHE, J., GUILLAUME, A., and LEENHARDT, D., 1966. Grandes structures de la mer Ligure, leurs évolutions et leurs relations avec les chaînes continentales. Bull.Soc.geol.Fr. 7, 291-937.

GOLDSCHMIDT, V.M. 1930. Elemente und Minerale pegmatitischer Gesteine. Nach.Gesellsch.Wiss.Göttingen.Math.Phys. Kl, 370-378

GOLDSCHMIDT, V.M. 1954. Geochemistry. Clarendon Press, Oxford, 730pp

GOMES, C. de B., MORO, S.L. and DUTRA, C.V. 1970. Pyroxenes from the alkaline rocks of Itapirapua, Sao Paolo, Brazil. Am.Mineral. 55, 224-230.

GRABHAM, G.W. 1920. The Bayuda volcanic fields. Sudan Notes and Records. 8, 133-136

GRAPES, R., YAGI, K. and OKUMURA, K. 1979. Aenigmatite, Sodic Pyroxene, Arfvedsonite and Associated Minerals in Syenites from Morotu, Sakhalin. Contrib.Mineral.Petrol. 69, 97-103.

GREENWOOD, H.T. 1979. Thermodynamic properties of edenite. Geol.Surv. Canada. Current Research, Part B. Paper 79-1B, 365-370.

GREGORY, J.W. 1920. The "Times" Africa flight. Discovery of a new volcanic field. Nature.London. 104, 667-668

HANSON, G.N. 1978. The Application of Trace Elements to the Petrogenesis of Igneous Rocks of Granitic Composition. Earth Planet. Sci.Lett. 38, 26-43

HARKER, A. 1904. The Tertiary igneous rocks of Skye. Mem.geol.Surv. Scotland. 481pp

HARRIS, N.B.W. 1981. The role of Flourine and Chlorine in the petrogenesis of a peralkaline complex from Saudi Arabia. Chem.Geol. 31, 303-310

HARRIS, N.B.W. 1982. Possible source regions for 'within-plate' magmatism in N.E. Africa and Arabia. Precambrian Res. 16, no.4. A23.Abstract.

HARRIS, N.B.W. and MARRINER, G.F. 1980. Geochemistry and petrogenesis of peralkaline granite complex from the Midian Mountains, Saudi Arabia. Lithos. 13, 325-337

HARRIS, N.B.W., DUYVERMAN, H.J. and ALMOND, D.C. 1982. (in press) The trace element and isotope geochemistry of the Sabaloka Igneous complex, Sudan.

HASKIN, L.A., FREY, F.A. and WILDEMAN, T.R. 1968. Relative and absolute terrestrial abundances of the rare earths. In: AHRENS, L.H. (ed.) Origin and Distribution of the Elements. Pergamon Press, Oxford. 889-912.

HERMANN, A.G. 1970. Yttrium and the lanthanides In: WELDEPOHL, K.H. (Ed.) Handbook of Geochemistry Vol.II-2, chapter 39

HILLS, E.S. 1972. Elements of Structural Geology. Chapman and Hall, London. 502pp

HOBBS, B.E., MEANS, W.D. and WILLIAMS, P.F. 1976. An Outline of Structural Geology. John Wiley and Sons, New York. 571pp

HOLLAND, J.G. and BRINDLE, D.W. 1966. A self-consistent mass absorption correction for silicate analysis by X-ray flouresence. Spectrochim.Acta. 22, 2083-2093

HUEBNER, J.S. 1980. Pyroxene phase equilibria at low pressure. In: PREWITT, C.T. (ed.) Pyroxenes. Reviews in Mineralogy, vol.7. Mineralog.Soc.Am. 213-288

IKE, E.C. 1979. The Structure, Petrology and Geochemistry of the Tibchi Younger Granite ring-complex, Nigeria. Unpublished PhD. thesis, University of St. Andrews

ISSAWI, B. 1973. Nubian Sandstone : type section. Bull.Am.Assoc. Petrol.Geol. 57, 741-745

JACOBSON, R.R.E., MACLEOD, W.M. and BLACK, R. 1958. Ring-complexes in the Younger Granite province of Northern Nigeria. Mem.geol.Soc.London. 1, 72pp

JACOBSON, R.R.E. and MACLEOD, W.N. 1977. Geology of the Liruei, Banke and adjacent Younger Granite ring-complexes. Bull. geol.Surv.Nigeria. 33, 117pp

JEFFREYS, H. 1936. Note on fracture. Proc.R.Soc.Edinburgh. 56, 158-163

JENSEN, B.B. 1973. Patterns of trace element partitioning. Geochim. cosmochim.Acta. 37, 2227-2242

KABESH, M.L. 1959. Geology of the Rubatub area, Berber District, Sudan. Unpublished M.Sc. thesis, Univ.Cairo.

KABESH, M.L. 1960. Mica deposits in northern Sudan. Bull.geol.surv.Sudan. 7, 55pp

KABESH, M.L. 1962a. Petrography of the Basement Complex Mograt area, Northern Province, Sudan. J.Geol.U.A.R. 6, 1-44

KABESH, M.L. 1962b. Geology of the Mograt area, Abu Hamed District, Sudan. Unpublished Ph.D. thesis, Univ.Cairo.

KELSEY, C.H. and McKIE, D. 1964. The unit cell of aenigmatite. Mineralog.Mag.London. 33, 986-1001

KENNEDY, W.Q. 1964. The structural differentiation of Africa in the Pan-African (±500 million years) tectonic episode. Annu.Rep.res.Inst.Afr.Geol.Leeds. 8, 48-49

KHEIRALLA, M.K. 1966. A study of the Nubian Sandstone Formation of the Nile Valley between 14'N and 17'42°N with reference to the groundwater geology. M.Sc. Thesis, Univ. of Khartoum.

KINGSLEY, L. 1931. Cauldron subsidence of the Ossipee Mountains. Am.J.Sci. 22, 139-169

KINNAIRD, J.A. 1977. A geological investigation of some Nigerian Jurassic granites and their mineralisation. Unpublished M.Sc. thesis, University of St. Andrews. Vol.1. 172pp

KNOX, G.J. 1974. The structure and emplacement of the Rio Fortaleza Centred acid complex, Ancash, Peru. J.geol.Soc. London. 130, 295-308

KOGARKO, L.N. 1974. Role of Volatiles. In: SØRENSEN, H. (ed.) The Alkaline Rocks. John Wiley and Sons, New York. 474-487

KOIDE, H. and BHATTACHARGI, S. 1975. Formation of Fractures Around Magmatic Intrusions and Their role in Ore Localisation. Econ.Geol.Alberta. 70, 781-799

KOLJONEN, T. and ROSENBERG, R.J. 1974. Rare earth elements in granitic rocks. Lithos. 7, 249-261

KOSTER VAN GROOS, A.F. and WYLLIE, P.J. 1968. Melting relationships in the system $NaAlSi_3O_8$ - NaCl - H_2O at 1 k'bar pressure with petrological applications. J.Geol.Chicago. 77, 581-605

KOVALENKO, V.I. 1968. On the chemical composition, properties and mineral paragenesis of riebeckite and arfvedsonite. In: I.M.A. Symp.II 1966 : Amphiboles and Pyroxenes. 261-284

KOVALENKO, V.I., FIN'KO, V.I., LETNIKOV, F.A. and KUZ'MIN, M.I. 1972. Certain effusive and subvolcanic rocks with relatively high concentrations of rare elements. Int.geol.Rev. 14, 599-608

KRESTEN, P. 1980. The Alno complex: tectonics of dyke emplacement. Lithos. 13, 153-158

LARSEN, L.M. 1976. Clinopyroxenes and Coexisting Mafic Minerals from the Alkaline Ilímaussaq Intrusion, South Greenland. J.Petrol. 17, 258-290

LARSEN, L.M. 1977. Aenigmatites from the Ilímaussaq intrusion, south Greenland: Chemistry and petrological implications. Lithos. 10, 257-270

LASSERE, M. 1969. Cameroun : Examen des résultats géochronologiques obtenus depuis 1967. Ann.Fac.Sci.Clermont-Ferrand. 41, ser.Geol. 19, 29-33

LE BAS, M.J. 1971. Peralkaline volcanism, crustal swelling and rifting. Nature (Phys.Sci.) 230, 85.

LE MAITRE, R.W. 1976. The Chemical Variability of some Common Igneous Rocks. J.Petrol. 17, 589-637

LEAKE, B.E. 1968. A Catalog of Analysed Calciferous and Subcalciferous Amphiboles Together with Their Nomenclature and Associated Minerals. geol.Soc.Am. Special Paper No.98. 210pp.

LEAKE, B.E. 1978. Nomenclature of amphiboles. Mineralog.Mag.London. 42, 533-563

LINDSLEY, D.H. 1971. Synthesis and preliminary results on the stability of aenigmatite ($Na_2Fe_5TiSi_6O_{20}$). Carnegie.Instn. Washington. Annu.Rep.Dir.Geophys.Lab. 1969-70. 188-190

LINDSLEY, D.H., BROWN, G.M. and MUIR, I.D. 1969. Conditions of the ferrowolastonite-ferrohedenbergite inversion in the Skaergaard Intrusion, East Greenland. Spec.Pap. Mineralog.Soc.Am. 2, 193-201

LUTH, W.C. 1976. Granitic Rocks. In: BAILEY, D.K. and MACDONALD, R. (eds.) The Evolution of the Crystalline Rocks. Academic Press, London. 335-417

McCORMAC, M. (in prep.) An investigation of a ring-complex and associated igneous rocks in the Bayuda Desert, Sudan. Ph.D. thesis, Portsmouth Polytechnic

McCORMAC, M. 1979. Observations on alkali-feldspars in a peralkaline environment. 10th Colloq.Afr.Geol.Montpellier. Abstract. 93.

McDOWELL, S.D. and WYLLIE, P.J. 1971. Experimental studies of igneous rock series : the Kûngnât syenite complex of southwest Greenland. J.Geol.Chicago. 79, 173-194

MACDONALD, R. 1968. Petrological studies on some peralkaline acid rocks from the Gardar province, south Greenland. Unpublished Ph.D. thesis, University of Edinburgh

MACDONALD, R. 1969. The petrology of alkaline dykes from the Tugtutôq area, South Greenland. Medd.Dansk.geol.Foren. 19, 257-282

MACDONALD, R. and EDGE, R.A. 1970. Trace element distribution in alkaline dykes from the Tugtutôq region, south Greenland. Medd.Dansk. geol.Foren. 20, 33-58

MACDONALD, R. and BAILEY, D.K. 1973. The Chemistry of the Peralkaline Oversaturated Obsidians. In: FLEISCHER, M. (ed.) Data of Geochemistry, 6th ed., chapter N : Chemistry of Igenous Rocks. Prof. Paper 440-N-1, 37pp

MANNING, D.A.C. 1981. The Effect of Flourine on Liquidus Phase Relationships in the System Qz-Ab-Or with Excess Water at 1kb. Contrib.Mineral.Petrol. 76, 206-215

MARSH, J.S. 1975. Aenigmatite stability in silica-undersaturated rocks. Contrib.Mineral.Petrol. 50, 135-144

MARTIN, R.F. 1969. The hydrothermal synthesis of low albite. Contrib.Mineral.Petrol. 23, 323-329

MARTIN, R.F. and BONIN, B. 1976. Water and magma genesis: the association hypersolvus granite - subsolvus granite. Can.Mineral. 14, 228-237

MARTIN, R.F., WHITLEY, J.E. and WOOLEY, A.R. 1978. An investigation of rare earth mobility: fenitised quartzites, Borralon complex, N.W. Scotland. Contrib.Mineral. Petrol. 66, 69-73

MEINHOLD, K.-D. 1979a. The Precambrian Basement Complex of the Bayuda Desert, Northern Sudan. Rev.Geogr.phys. Geol.dyn.Paris. 21, 395-401

MEINHOLD, K.D. 1979b. Contribution to the geology of the Bayuda Desert, Sudan. 10th Colloq.Afr.Geol.Montpellier, Abstract. 68-69

MINEYEV, D.A. 1963. Geochemical differentiation of the rare earths. Geochem.Int. 12, 1129-1150

MITCHELL, R.H. and PLATT, R.G. 1978. Mafic Mineralogy of Ferroaugite Syenite from the Coldwell Alkaline Complex, Ontario, Canada. J.Petrol. 19, 627-651

MOHR, P.A. 1968. The Cainozoic Volcanic Succession in Ethiopia. Bull.Volcanol. 32, 5-14

MORGAN, W.J. 1971. Convection plumes in the lower mantle. Nature (phys.Sci.) 230, 42-43

MUIR-WOOD, R. 1980. Compositional zoning in sodic amphiboles from the blueschist facies. Mineralog.Mag.London. 43, 741-752

MUSTART, D.A. 1972. Phase Relations in the peralkaline Portion of the System Na_2O-Al_2O_3-SiO_2-H_2O. Unpublished Ph.D. thesis, Stanford University.

NANKAMURA, N. and MASUDA, A. 1973. Chondrites with peculiar rare-earth patterns. Earth planet.Sci.Lett. 19, 429-437

NASH, W.P. and WILKINSON, J.F.G. 1970. Shonkin Sag Laccolith Montana. I. Mafic minerals and estimates of temperature, pressure, oxygen fugacity and silica activity. Contrib.Mineral.Petrol. 25, 241-269

NEARY, C.R., GASS, I.G. and CAVANAGH, B.J. 1976. Granitic association of northeastern Sudan. Bull.geol.Soc.Am. 87, 1501-1512

NEUMANN, E.-R. 1976. Compositional Relations among pyroxenes, amphiboles and other mafic phases in the Oslo Region plutonic rocks. Lithos. 9, 85-109

NEUMANN, E.-R. 1976b. Two refinements for the calculation of structural formulae for pyroxenes and amphiboles. Nor.geol.Tiddskr. 56, 1-6

NEUMANN, E.-R. 1980. Petrogenesis of the Oslo Region Larvikites and Associated Rocks. J.Petrol. 21, 499-531

NICHOLLS, J. and CARMICHAEL, I.S.E. 1969. The mineralogy and petrology of Mount Suswa, Kenya. J.Petrol. 10, 409-439

NOBLE, D.C. 1965. Gold Flat Member of the Thirsty Canyon Tuff - a pantellerite ash-flow sheet in Southern Nevada. U.S.Geol.Surv.Prof.Pap.525B, B85-B90

NOCKOLDS, S.R. 1954. Average chemical composition of igneous rocks. Bull.geol.Soc.Am. 65, 1007-1032

NORRISH, K. and HUTTON, J.T. 1969. An accurate X-ray spectrographic method for the analysis of a wide range of geological samples. Geochim.cosmochim.Acta. 33, 431-453

ODE, H. 1957. Mechanical analysis of the dike pattern of the Spanish Peaks area, Colorada. Bull-geol-Soc.Am. 68, 567-576

OFTEDAHL, C. 1952. Cauldron subsidences of the Oslo region. Int.geol.Congr. 18, 205-213

OFTEDAHL, C. 1978. Main geologic features of the Oslo Graben. In: RAMBERG, I.B. and NEUMANN, E.-R. (eds.) Tectonics and Geophysics of Continental Rifts. D.Reidel, Dordrecht. 149-165

OSTLE, D., COLEMAN, R.F. and BALL, T.K. 1972. Neutron Activation analysis as an aid to geochemical prospecting for uranium. In: BOWIE, S.H.U., DAVIS, M. and OSTLE, D. (eds.) Uranium Prospecting Handbook. Institution of Mining and Metallurgy, London. 95-109

PAPIKE, J.J., CAMERON, K.L. and BALDWIN, K. 1974. Amphiboles and Pyroxenes: characterisation of other than quadrilateral components and estimates of ferric iron from microprobe data. Abstr.geol.Soc.Am.Progr. 6, 1053-1054

PARSONS, I. 1978. Feldspars and fluids in cooling plutons. Mineralog.Mag. London. 42, 1-17

PARSONS, I. 1979. The Klokken Gabbro-Syenite Complex, South Greenland: Cryptic Variation and Origin of Inversely Graded Layering. J.Petrol. 20, 653-694

PARSONS, I. 1980. Alkali feldspar and Fe-Ti oxide exsolution textures as indicators of the distribution and subsolidus effects of magmatic 'water' in the Klokken layered syenite intrusion, South Greenland. Trans.R.Soc. Edinburgh. 71, 1-12

PARSONS, I. 1981. The Klokken Gabbro-Syenite Complex, South Greenland: Quantitative Interpretation of Mineral Chemistry J.Petrol. 22, 233-260

PETO,P. 1976. Synthesis and stability of edenitic hornblende. Progress in Experimental Petrology: N.E.R.C. publications, Series D. 6, 27-28

PETROV, A.I., PLOTNIKOV, L.M. and YUREVICH, G.G. 1972. Formation mechanism of magmatic structures of central type. Int.geol.Rev. 14, 311-318

PHILLIPS, W.J. 1974. The dynamic emplacement of cone sheets. Tectonophysics. 24, 69-84

PHILPOTTS, A.R. 1978. Rift-associated igneous activity in eastern North America. In: NEUMANN, E.-R. and RAMBERG, I.B. (eds.) Petrology and Geochemistry of Continental Rifts. D.Reidel, Dordrecht. 133-154

PIOTROWSKI, J.M. and EDGAR, A.D. 1970.Melting relations of undersaturated alkaline rocks from South Greenland compared to those of Africa and Canada. Medd.Gronland. 181, 62p

PITCHER, W.S. 1979. The nature, ascent and emplacement of granitic magmas. J.geol.Soc.London. 136, 627-662

POLDEVAART, A. and HESS, H.H. 1951. Pyroxenes in the crystallisation of basaltic magma. J.Geol.Chicago. 59, 472-489

POPP, R.K. and GILBERT, M.C. 1972. Stability of acmite-jadeite pyroxenes at low pressure. *Am.Mineral*. 57, 1210-1231

PUTZER, H. 1958. Das vulkanfeld Bir Sani - Hosh-ed-Dalam in der republik Sudan. *Z.Deutsch.geol.Ges.* 110, 109-116

RAMBERG, H. 1970. Model studies in relation to intrusion of plutonic bodies. *In*: NEWALL, G. and RAST, N. (eds.) *Mechanism of Igneous Intrusion.* Gallery Press, Liverpool. 261-286

RAMBERG, H. 1967. *Gravity deformation and the earth's crust as studied by centrifuged models*. Academic Press, London and New York. 214pp

RAMBERG, I.B. and NEUMANN, E.-R. (Eds.) 1978. *Tectonics and Geophysics of Continental Rifts*. D.Reidel, Dordrecht. 444pp

RAMBERG, I.B. and SPJELDNAES, N. 1978. The tectonic history of the Oslo Region. *In*: RAMBERG, I.B. and NEUMANN, E.-R. (eds.) *Tectonics and Geophysics of Continental Rifts* D.Reidel, Dordrecht. 167-194

REYNOLDS, D.L. 1956. Calderas and ring-complexes. *Nederlandsch. Geol.Mijnbouw.Genoot.Verh*. 16, 355-379

RHODES, R.C. 1971. Structural geometry of sub-volcanic ring complexes as related to pre-Cenozoic motions of continental plates. *Tectonophysics*. 12, 111-117

RICHEY, J.E. 1928. The structural relations of the Mourne granites (Northern Ireland). *Q.J.Geol.Soc.London*. 83, 653-688

RICHEY, J.E. and THOMAS, H.H. 1930. The geology of Ardnamurchan, north-west Mull and Coll. *Mem.geol.Surv.Scotland*. 393pp

ROBERTS, J.L. 1970. The Intrusion of magma into brittle rocks. In: NEWALL, G. and RAST, N. (eds.). Mechanism of Igneous Intrusion Gallery Press, Liverpool. 287-338

ROBSON, G.R. and BARR, K.G. 1964. The effect of stress on faulting and minor intrusions in the vicinity of a magma body. Bull.Volcanol. 27, 315-330

SADIG, A.A., ALMOND, D.C. and QURESHI, I.R. 1974. A gravity study of the Sabaloka igneous complex, Sudan. J.geol.Soc.London. 130, 249-262

SHAND, S.J. 1922. The problem of the alkaline rocks. Trans.Proc.geol. Soc.South Afr. 25, 9-33

SHAW, D.M. 1968. A review of K/Rb fractionation trends by covariance analysis. Geochim.cosmochim.Acta. 32, 573-601

SIEDNER, G. 1965. Geochemical features of a strongly fractionated alkali igneous suite. Geochim.cosmochim.Acta. 29, 113-137

SOOD, M.K. and EDGAR, A.D. 1970. Melting relations of undersaturated alkaline rocks from the Ilímaussaq intrusion and Grønndal-Ika complex, south Greenland, under water vapour and controlled partial oxygen pressure. Medd.Gronland. 181, 41pp

SØRENSEN, H. 1974. The Alkaline Rocks. John Wiley and Sons. New York. 622pp

STATHAM, P.J. 1976. A comparative study of techniques for quantitative analysis of the x-ray spectra obtained with a Si(Li) detector. X-ray.Spectrometry. 5, 16-28

STEPHENSON, D. 1972. Alkali clinopyroxenes from nepheline syenites of the South Qôroq Centre, south Greenland. Lithos. 5, 187-201

STEWART, J.W. 1970. Precambrian alkaline-ultramafic/carbonatite volcanism at Qagssiarsuk, south Greenland. Bull.Gronlands geol.Unders. 84, 70pp

STOUT, J.H. 1972. Phase Petrology and Mineral Chemistry of Coexisting Amphiboles from Telemark, Norway. J.Petrol. 13, 99-145

STRECKEISEN, A. 1967. Classification and nomenclature of igneous rocks. Final report of an inquiry. N.Jahrb.Miner.Abh. 107, 144-144-240

STRECKEISEN, A. 1976. To each plutonic rock its proper name. Earth Sci.Rev. 12, 1-33.

STULL, R.J. 1973. Calcic and Alkali Amphiboles from the Golden Horn Batholith, North Cascades, Washington. Am.Mineral. 58, 873-878

SUNDVOLL, B. 1978. Rb-Sr relationships in the Oslo igneous rocks. In: NEUMANN, E.-R. and RAMBERG, I.B. (eds.) Petrology and Geochemistry of Continental Rifts. D.Reidel. Dordrecht. 181-184

SWEATMAN, T.R. and LONG, J.V.P. 1969. Quantitative electron-probe microanalysis of rock forming minerals. J.Petrol. 10, 332-379

TAYLOR, R.P. 1979. Topsails igneous complex - Further evidence of middle Paleozoic epeirogeny and anorogenic magmatism in the northern Appalachians. Geology. 7, 488-490

TAYLOR, R.P., STRONG, D.F. and KEAN, B.F. 1980. The Topsails igneous complex: Silurian-Devonian peralkaline magmatism in western Newfoundland. Can.J.Earth Sci. 17, 425-439

TAYLOR, S.R., 1965. The application of trace element data to problems in petrology. Phys.Chem.Earth.Oxford. 6, 133-213

TAYLOR, S.R., EMELEUS, C.H. and EXLEY, C.S. 1956. Some anomalous K/Rb ratios in igneous rocks and their petrological significance. Geochim.cosmochim.Acta. 10, 224-229

THOMAS, I.L. and HAUKKA, M.T. 1978. XRF determination of trace and major elements using a single-fused disc. Chem.Geol. 21, 39-50

THOMPSON, R.N. 1976. Alkali amphiboles in the Eocene high-level granites of Skye, Scotland. Mineralog.Mag.London. 40, 891-893

THOMPSON, R.N. and MACKENZIE, W.S. 1967. Feldspar-liquid equilibria in peralkaline acid liquids: an experimental study. Am.J.Sci. 265, 714-734

THORNTON, C.P. and TUTTLE, O.F. 1960. Chemistry of igneous rocks 1. Differentiation Index.1 Am.J.Sci. 258, 664-684

THORPE, R.S., POTTS, P.J. and SARRE, M.B. 1977. Rare earth evidence concerning the origin of granites of the Isle of Skye, northwestern Scotland. Earth planet.Sci.Lett. 36, 111-120

TUGARINOV, A.I., KOVALENKO, V.I., ZNAMENSKY, E.B., LEGEIDO, V.A., SOBATOVICH, E.V., BRANDT, S.B. and TSYHANSKY, V.D. 1968. Distribution of Pb-isotopes, Sn, Zb, Ta, Zr and Hf in the granitoids of Nigeria. In: AHRENS, L.H. (ed.) Origin and Distribution of the Elements. Pergamon Press, Oxford. 687-699

TURNER, D.C. 1963. Ring-structures in the Sara-Fier Younger Granite complex, northern Nigeria. Q.J.geol.Soc.London. 119, 345-366

TURNER, D.C. 1972. Structure and tectonic setting of the Younger Granite ring complexes of Nigeria and Southern Niger. Part I: Ring complexes and their component units. Savanna. 1, 223-236

TURNER, D.C. 1973. Structure and tectonic setting of the Younger Granite ring complexes of Nigeria and Niger. Part II: Structural and tectonic patterns in the Younger Granite province. Savanna. 2, 51-59

TURNER, D.C. 1976. Structure and petrology of the Younger Granite ring complexes. In: KOGBE, C.A. (ed.). Geology of Nigeria. Elizabethan Press, Lagos, 143-158.

TURNER, D.C. and BOWDEN, P. 1979. The Ningi-Burra complex, Nigeria: dissected calderas and migrating magmatic centres. J.geol.Soc.London. 136, 105-118

TUTTLE, O.F. 1961. Residual solution formed by crystallisation. In: Physio-Chemical Problems of the Genesis of Ores and Rocks (in Russian, English summary) Izd.ANSSSR, Moscow. 647-653

TUTTLE, O.F. and BOWEN, N.L. 1958. Origin of granite in the light of experimental studies in the system NaAlSi308-KAlSi308-Si02-H20. Mem.geol.Soc.Am. 74, 153pp

TYLER, R.C. and KING, B.C. 1967. The pyroxenes of the alkaline igneous complexes of eastern Uganda. Mineralog.Mag.London. 36, 5-21

UPTON, B.G.J. 1960. The alkaline igneous complex of Kûngnât Fjeld, South Greenland. Medd.Gronland. 123, 145pp

UPTON, B.G.J. 1964. Geology of Tugtutôq and neighbouring islands, south Greenland, Part II: Normarkitic syenites and related igneous rocks. Bull.Gronland geol.Unders. 44, 62pp

UPTON, B.G.J. 1974. The alkaline province of South West Greenland. In: SØRENSEN, H. (ed.) The Alkaline Rocks. John Wiley and Sons, New York. p221-238

USSING, N.V. 1912. Geology of the Country Around Julianehaab, Greenland. Medd.Gronland. 38, 1-376

VAIL, J.R. 1971. Geological reconnaissance in part of the Berber district, Northern Province, Sudan. Geol.Surv.Sudan,Bull. 18, 76pp Khartoum.

VAIL, J.R. 1972. A ring-complex igneous province in northern Sudan. Proc.Conference.Afr.geol.,Ibadan, 1970. 163-177

VAIL, J.R. 1972b. Pre-Nubian tectonic trends in north-eastern Sudan. J.geol.Soc.London. 128, 21-31

VAIL, J.R. 1973. Distribution of igneous ring-complexes in Sudan and vicinity. Annu.Rep.res.Inst.Afr.Geol.Leeds. 17, 27-30

VAIL, J.R. 1974. Distribution of the Nubian Sandstone Formation in Sudan and vicinity. Bull.Am.Assoc.Petrol.Geol. 58, 1025-1036

VAIL, J.R. 1976. Location and geochronology of igneous ring complexes and related rocks in north-east Africa. Geol.Jahrb.Hannover. B 20, 97-114

VAIL, J.R. 1978. Outline of the geology and mineral deposits of the Democratic Republic of the Sudan and adjacent areas. Overseas Geol.miner.Resour.London. 49, 1-66

VAIL, J.R. 1979. Outline of geology and mineralisation of the Nubian shield east of the Nile valley, Sudan. In: AL-SHANTI, A.M.S. (ed.). Evolution and mineralisation of the Arabian-Nubian shield. I.A.G. Bulletin 3, 97-107

VAN BREEMAN, O., HUTCHINSON, J. and BOWDEN, P. 1975. Age and origin of the Nigerian Mesozoic granites : Rb-Sr isotopic study. Contrib.Mineral.Petrol. 50, 157-172

VARET, J. 1969. Les pyroxènes des phonolites du Cantal (Auvergne, France) Neues Jahrb.Mineral.Abhandlungen. 4, 174-184

VIDAL, P., DOSSO, L., BOWDEN, P. and LAMEYRE, J. 1979. Strontium Isotope Geochemistry in Syenite-Alkaline Granite Complexes. In: AHRENS, L.H. (ed.) Origin and Distribution of the Elements (Int. Series in Earth Sciences, vol.34). 2nd symposium. Pergamon Press, Oxford. 223-231

VILLARI, L. 1974. The Island of Pantelleria. Bull.Volcanol. 38, 680-724

WALKER, G.P.L. 1975. A new concept of the evolution of the British Tertiary intrusive centres. J.geol.Soc.London. 131, 121-141

WALSH, J.N. BECKINSALE, R.D., SKELHORN, R.R. and THORPE, R.S. 1979. Geochemistry and Petrogenesis of Tertiary Granitic Rocks from the Island of Mull, Northwest Scotland. Contrib.Mineral.Petrol. 71, 99-116

WATSON, E.B. 1979. Zircon Saturation in Felsic Liquids: Experimental Results and Applications to Trace Element Geochemistry. Contrib.Mineral.Petrol. 70, 407-419

WHITEMAN, A.J. 1971. The Geology of the Sudan Republic. Clarendon Press, London. 290pp.

WRIGHT, J.B. 1969. A simple alkalinity ratio and its application to questions of non-orogenic granite genesis. Geol.Mag. 106, 370-384

YAGI, K. 1953. Petrochemical studies on the alkalic rocks of the Morotu district, Sakhalin. Bull.geol.Soc.Am. 64, 769-810

YAGI, K. 1966. The system acmite-diopside and its bearing on the stability relations of natural pyroxenes of the acmite-hedenbergite-diopside series. Am.Mineral. 51, 979-1000

ADDITIONAL REFERENCES

ALEKSIYEV, E.I. 1970. Genetic significance of the REE in the Younger Granites of northern Nigeria and the Cameroons. Geochem.Int. 7, 127-132

KOSTER VAN GROOS, A.F. and WYLLIE, P.J. 1969. Melting relationships in the system $NaAlSi_3O_8$ - NaCl - H_2O at 1 k'bar pressure with petrological implications. J.Geol Chicago. 77, 581-605.

UPTON, B.G.J., THOMAS, J.E. and MACDONALD, R. 1971. Chemical variation within three alkaline complexes in south Greenland. Lithos. 4, 163-184.

APPENDIX I

MODAL ANALYSES AND MINERAL OPTICS

APPENDIX IA

MODAL ANALYSES - RAS ED DOM

abbreviations

+	present in trace amounts
-	absent
NA	not applicable

	Ras ed Dom						Abu Dom				
	S1		S4		S11		S1 Milega			S1 Guna	
	1014	236	914	916	R31	165B	685	689	849	752	566B
Alkali-Feldspar	80.1	80.5	76.7	81.4	84.9	90.0	81.2	82.5	78.1	84.4	81.3
Phenocrysts	N.A.	N.A.	31.2	30.2	N.A.	N.A.	26.7	N.A.	35.7	N.A.	N.A.
Groundmass	N.A.	N.A.	45.5	51.2	N.A.	N.A.	54.5	N.A.	42.4	N.A.	N.A.
Albite	3.1	+	-	-	2.6	0.7	-	+	+	+	-
Quartz	1.1	+	5.3	3.8	1.3	1.0	2.8	0.7	3.5	3.2	1.6
Edenitic Amphibole	2.7	-	-	-	4.9	1.9	-	6.0	4.	3.0	-
Winchitic Amphibole	10.9	8.0	7.7	6.7	0.5	0.4	7.9	6.2	6.9	1.2	11.2
Hedenbergitic Pyroxene	0.9	2.1	3.4	3.0	0.8	1.3	1.5	-	2.8	4.1	0.9
Late Sodic Pyroxene	-	-	-	-	-	-	-	1.6	-	-	1
Biotite	+	3.3	+	+	-	1.4	3.7	-	0.5	1.8	2.3
Fe-Ti Oxides	2.8	1.2	5.4	4.1	2.0	1.3	2.5	2.5	3.2	1.6	1.8
Apatite	1.0	1.0	1.0	0.9	0.5	0.3	0.4	0.5	0.7	0.5	0.7
Zircon	+	-	+	+	-	-	+	+	+	-	-
Calcite	+	0.8	+	+	+	+	+	+	+	-	+
Fayalite(?)	?+	?+	-	-	-	-	-	-	-	-	-

Modal Analyses of the Early Syenites of Ras ed Dom and Abu Dom

	Ras ed Dom					Ras ed Dom					
	S2					S3					
	1026*	1028*	1077*	131*	132*	462	1057	458	247A	275^{m*}	1073B^{m*}
Alkali Feldspar	81.4	87.2	78.6	79.2	76.6	78.4	76.8	78.5	78.2	71.8	74.7
Phenocrysts		N.A.	N.A.	N.A.	N.A.	N.A.	N.A.	N.A.	N.A.		
Groundmass		N.A.	N.A.	N.A.	N.A.	N.A.	N.A.	N.A.	N.A.		
Albite	-	+	-	-	-	+	+	+	+	7.9	5.6
Quartz	3.0	0.5	8.2	4.6	5.3	8.6	10.2	10.8	9.8	6.5	6.6
Richterite	4.0	0.7	5.4	9.2	9.7	-	-	-	-	9.2	8.2
Arfvedsonite	-	-	-	-	-	8.3	8.1	8.1	7.6	-	-
Aegirine-Augite (Early)	9.9	8.3	5.6	4.9	5.0	0.4	1.1	0.7	0.4	3.9	1.6
Aegirine (Late)	-	-	-	-	-	1.6	2.5	1.2	1.7	-	-
Fe-Ti Oxides	+	1.6	0.6	0.9	0.4	+	+	+	+	+	+
Apatite	+	0.4	+	+	+	+	-	+	+	+	+
Zircon	+	+	+	0.4	0.8	+	+	+	+	+	+
Fayalite?	-	-	0.9	0.6	0.9	-	-	-	-	+	-

*Transitional Syenite

m = chilled margin

Modal Analyses of S2 and S3, Ras ed Dom

Ras ed Dom

S5

	190*	193*	R56	R58	204^c	188^m	195^m	907^c	904*
Alkali-Feldspar	70.0	75.8	79.0	76.8	70.5	70.9	72.8	89.5	82.1
Phenocryst								24.8	27.8
Groundmass								54.7	54.3
Albite	3.4	2.3	1.2	-	1.1	1.3	3.1	-	-
Quartz	4.7	9.3	5.1	6.6	11.5	7.0	15.6	5.1	2.7
Edenitic Amphibole	6.9	3.6	-	-	-	-	-	-	-
Winchitic Amphibole	9.9	5.2	-	-	-	-	-	-	-
Arfvedsonite	-	-	6.3	7.5	5.0	1.5	1.5	8.0	5.7
Calcic Pyroxene (Early)	3.9	1.1	0.9	1.1	-	-	-	0.7	7.1
Sodic Pyroxene (Late)	-	-	-	5.2	7.7	18.8	6.7	4.6	-
Aenigmatite	-	-	-	-	2.9	-	-	-	-
Fe-Ti Oxides	1.8	1.4	1.5	1.5	0.2	0.4	-	1.6	1.8
Apatite	0.9	0.9	0.8	0.5	0.4	+	+	0.4	0.6
Zircon	+	+	+	+	+	+	+	+	+
Calcite	+	-	+	-	-	-	-	-	+
Flourite	-	-	-	-	-	-	-	-	-

*Transitional

m = chilled margin

c = coarse core to unit

Modal Analyses of Syenite 5, Ras ed Dom

	Ras ed Dom									R.E.D.
	S6									IT1
	290	293	348	362	374A	352A	397^c	$311B^c$	402^c	364
Alkali-Feldspar	71.7	71.5	79.6	77.8	74.1	79.3	77.5	77.8	84.5	74.6
Phenocryst	18.6	21.6	20.0	20.3	26.2	12.5	N.A.	N.A.	N.A.	15.6
Groundmass	53.1	49.9	59.6	57.5	47.9	66.8	N.A.	N.A.	N.A.	59.0
Albite	1.8	+	+	-	1.0	-	1.3	2.0	2.1	-
Quartz	12.3	16.5	10.0	6.8	9.2	5.1	5.6	10.6	7.6	2.3
Edenitic Amphibole	-	-	-	-	-	-	-	-	-	-
Winchitic Amphibole	-	-	-	-	-	-	-	-	-	-
Arfvedsonite	11.1	10.4	7.7	10.8	9.8	9.1	8.3	1.0	5.2	
Calcic Pyroxene (Early)	-	-	-	-	-	-	-	-	-	
Sodic Pyroxene (Late)	0.5	-	0.8	3.0	5.2	4.2	5.7	7.1	-	20.7
Aenigmatite	-	-	-	-	-	-	-	-	-	
Fe-Ti Oxides	1.5	0.9	1.2	1.3	0.5	1.7	1.0	0.6	0.4	1.6
Apatite	+	0.2	+	0.3	0.2	+	+	+	+	+
Zircon	+	0.5	+	-	-	-	0.2	+	+	0.6
Calcite	0.8	-	-	-	+	-	0.2	-	+	
Flourite	+	+	-	-	-	-	-	-	-	

m = chilled margin
c = coarse core to unit

Modal Analyses of S6 and IT1, Ras ed Dom.

		Ras ed Dom	
		IT2	
		310	309
Phenocryst Assemblage	Alkali-Feldspar	21.7	18.6
	Hedenbergite	0.7	0.6
	Fe-Ti Oxides	0.2	0.1
	Total	22.4	19.2
Groundmass Assemblage	Alkali-Feldspar and Quartz	48.8	49.4
	Winchitic Amphibole	21.4	21.6
	Fe-Ti Oxides	7.0	9.5
	Apatite	0.2	0.1
	Calcite	+	+

\+ Present in Trace Amounts

Modal Analyses of IT2, Ras ed Dom.

	Ras ed Dom						Ras ed Dom		R.E.D.	R.E.D.
	S7						S8		S9	S10
	378	340	966	334	417^m	$R3^m$	426	R27	428	429
Alkali-Feldspar	71.6	64.6	71.7	71.5	73.4	68.7	84.9	77.8	81.8	85.8
Albite	6.4	2.5	4.9	5.0	3.5	3.8	-	0.6	2.4	1.9
Quartz	8.7	12.5	7.6	6.9	10.4	8.2	-	3.2	0.7	1.0
Arfvedsonite	1.8	5.1	8.6	9.1	5.9	7.3	7.1	8.5	2.9	6.1
Aegirine-Augite Aegirine	10.3	12.6	6.6	6.4	6.6	10.9	5.3	8.7	10.9	2.8
Fe-Ti Oxides	0.4	+	+	+	+	+	1.6	1.0	0.2	0.5
Apatite	+	0.4	+	+	+	0.3	0.7	+	0.6	0.8
Zircon	+	+	+	+	+	+	+	-	+	-
Calcite	-	1.0	+	-	-	0.4				
Biotite	-	-	-	-	-	-	0.5	-	-	0.5

m = chilled margin

Modal Analyses of the Alkali Syenites, S7-S10 Inclusive, Ras ed Dom.

	Ras ed Dom	Ras ed Dom				Ras ed Dom	Ras ed Dom		
	S12	S13				S14	S15		
	R41	430B	R33	432	433	R40	R35	180B	435
Alkali-Feldspar	86.6	86.5	82.2	84.9	85.1	82.5	83.0	81.2	79.8
Albite	3.8	1.2	0.9	2.4	-	1.0	-	0.7	-
Quartz	2.5	0.4	-	-	-	0.3	5.9	0.4	3.1
Arfvedsonite	3.4	3.7	2.1	-	1.5	0.5	6.8	5.2	8.9
Calcic Pyroxene (Early)	-	2.4	-	-	-	-	+	+	+
Sodic Pyroxene (Late)	3.1	4.0	10.4	9.3	8.3	12.0	3.5	12.5	3.0
Fe-Ti Oxides	0.5	1.0	2.1	1.5	1.4	1.7	+	+	+
Apatite	+	0.7	0.8	0.8	1.1	0.6	+	+	+
Zircon		-	-	-	0.5		+	+	+
Biotite	-	+	1.1	1.1	1.9	1.1			
Calcite							+	+	+

Modal Analyses of Syenites 12-15 inclusive, Ras ed Dom.

	Ras ed Dom								
	G1								
	146	145	278	447	159	273	231	142B2	460
Alkali-Feldspar	52.0	54.6	56.3	54.6	58.2	51.4	55.6	55.5	44.3
Albite	4.8	4.9	8.8	10.5	3.9	7.2	5.1	2.6	4.9
Quartz	26.6	25.9	23.5	22.8	28.9	30.7	31.2	31.7	32.3
Arfvedsonite	11.4	9.0	7.2	7.9	-	0.5	1.1	3.7	7.3
Aegirine	3.2	4.7	3.1	3.2	8.2	9.8	6.5	5.5	10.5
Fe-Ti Oxides	+	+	+	+	-	-	+	+	-
Apatite	+	+	+	+	-	-	+	-	-
Zircon	+	+	+	-	+	-	-	+	0.5
Flourite	-	-	-	-	-	-	+	-	-

Modal Analyses of the Alkali Granites, Ras ed Dom

	Ras ed Dom					
	MG2			G2		
	344	399	401	291A	289	291D
Alkali-Feldspar	52.8	58.8	70.5	59.8	59.3	55.0
Albite	3.4	1.4	4.4	1.8	0.2	0.4
Quartz	25.4	22.6	10.9	24.4	22.7	23.3
Arfvedsonite	1.1	10.6	9.7	3.5	2.1	+
Aegirine	16.6	5.9	2.2	10.1	14.5	21.0
Fe-Ti Oxides	0.3	0.2	+	+	0.8	+
Apatite	+	+	0.2	-	+	-
Zircon	0.3	0.3	+	+	+	0.3
Flourite	-	-	+	-	-	-

	Ras ed Dom	
	MG1	
	300	300A
Alkali-Feldspar	76.3	73.3
Phenocrysts	24.5	16.8
Groundmass	51.8	56.5
Albite	+	+
Quartz	16.9	19.6
Aegirine*	6.7	6.9
Fe-Ti Oxides	+	+
Apatite	-	-
Zircon	+	+

*Altered to Fe-Ti Oxide

I-11

Modal Analyses of the Alkali Granites and Microgranites, Ras ed Dom

APPENDIX IB

MODAL ANALYSES - ABU DOM

abbreviations

+	present in trace amounts
-	absent
NA	not applicable

	Ras ed Dom						Abu Dom				
	S1		S4		S11		S1 Milega			S1 Guna	
	1014	236	914	916	R31	165B	685	689	849	752	566B
Alkali-Feldspar	80.1	80.5	76.7	81.4	84.9	90.0	81.2	82.5	78.1	84.4	81.3
Phenocrysts	N.A.	N.A.	31.2	30.2	N.A.	N.A.	26.7	N.A.	35.7	N.A.	N.A.
Groundmass	N.A.	N.A.	45.5	51.2	N.A.	N.A.	54.5	N.A.	42.4	N.A.	N.A.
Albite	3.1	+	-	-	2.6	0.7	-	+	+	+	-
Quartz	1.1	+	5.3	3.8	1.3	1.0	2.8	0.7	3.5	3.2	1.6
Edenitic Amphibole	2.7	-	-	-	4.9	1.9	-	6.0	4.	3.0	-
Winchitic Amphibole	10.9	8.0	7.7	6.7	0.5	0.4	7.9	6.2	6.9	1.2	11.2
Hedenbergitic Pyroxene	0.9	2.1	3.4	3.0	0.8	1.3	1.5	-	2.8	4.1	0.9
Late Sodic Pyroxene	-	-	-	-	-	-	-	1.6	-	-	1
Biotite	+	3.3	+	+	-	1.4	3.7	-	0.5	1.8	2.3
Fe-Ti Oxides	2.8	1.2	5.4	4.1	2.0	1.3	2.5	2.5	3.2	1.6	1.8
Apatite	1.0	1.0	1.0	0.9	0.5	0.3	0.4	0.5	0.7	0.5	0.7
Zircon	+	-	+	+	-	-	+	+	+	-	-
Calcite	+	0.8	+	+	+	+	+	+	+	-	+
Fayalite(?)	?+	?+	-	-	-	-	-	-	-	-	-

Modal Analyses of the Early Syenites of Ras ed Dom and Abu Dom

	Abu Dom		Abu Dom					
	S2		S3					
	570	858	528	562B	769	730	643	840
Alkali-feldspar	73.1	83.8	65.4	73.2	68.4	80.8	67.9	71.9
Albite	0.4	3.0	3.4	2.5	2.9	1.2	4.4	3.9
Quartz	5.5	1.4	10.4	12.6	4.4	4.8	10.8	13.1
Arfvedsonite	9.6	7.1	10.5	4.1.	9.1	4.6	7.9	6.7
Calcic Pyroxene (Early)	+	+	-	+	-	-	-	-
Aegirine (Late)	6.0	4.0	9.4	6.7	13.3	8.0	8.5	3.7
Fe-Ti Oxides	4.2	0.2	0.5	0.4	+	-	+	+
Apatite	0.7	0.3	0.4	0.3	+	+	+	+
Zircon	+	-	+	0.3	-	-	+	+
Calcite	+	-	-	-	1.7	-	+	-

Modal Analyses of the Alkali Syenites, Abu Dom

	Abu Dom							Abu Dom
	S4							S5
	740^{m}	524A	504	524B	809^{m}	721^{m}	526^{m}	1190^{m}
Alkali-feldspar	82.8	92.5	70.0	89.5	72.8	69.1	72.1	71.9
Albite	0.4	0.8	7.3	0.5	4.3	4.6	5.0	4.1
Quartz	7.3	1.2	7.0	2.9	9.9	6.1	7.4	5.4
Arfvedsonite	4.8	2.0	5.7	1.5	3.6	7.8	8.0	4.7
Calcic Pyroxene (Early)	0.9	1.0	+	+	-	-	-	1.9
Aegirine (Late)	3.2	2.3	8.8	3.9	8.6	11.9	7.4	11.2
Fe-Ti Oxides	0.3	+	+	0.4	+	+	+	+
Apatite	+	+	+	+	0.2	+	+	+
Zircon	+	+	0.6	+	0.2	+	-	-
Calcite	-	-	0.3	-	-	+	-	0.3

m = Marginal

Modal Analyses of the Alkali Syenites, Abu Dom

	Abu Dom					Abu Dom						
	G1					G2						
	S48	701	848	781	558	573	828	527B	808	532	565	540
Alkali-Feldspar	67.6	57.1	60.4	54.0	59.2	48.8	59.3	43.8	43.1	51.3	44.2	53.8
Albite	4.2	2.9	3.7	1.2	2.0	4.0	3.7	2.1	3.8	4.7	2.2	2.3
Quartz	12.9	31.5	23.1	23.9	21.6	27.9	15.2	28.8	26.8	17.9	25.1	27.1
Arfvedsonite	4.4	1.3	4.8	7.2	7.8	1.8	7.5	14.0	-	1.3	2.2	5.0
Aegirine	9.8	6.1	7.5	13.2	4.4	16.8	12.8	10.5	26.0	24.6	26.0	9.9
Fe-Ti Oxides	0.7	0.6	+	+	3.0	0.3	+	0.4	0.3	+	+	1.8
Apatite	-	+	-	-	+	+	+	-	+	-	-	+
Zircon	-	+	+	+	0.2	+	+	+	-	-	-	-
Flourite	-	-	-	-	-	-	+	-	-	-	-	+
Calcite	0.3	0.4	-	-	1.1	-	-	-	-	-	-	-

Modal Analyses of the Alkali Granites, Abu Dom.

APPENDIX IC

MINERAL OPTICS

APPENDIX IC : MINERAL OPTICS

The optical properties of the principal mafic mineral species are listed below. In most instances the selected examples correspond with microprobe analyses provided in Appendix II. 2V values are approximate as no Universal Stage determinations were attempted. All the examples are from Ras ed Dom complex.

i. AMPHIBOLES

FERROEDENITE (sample 1014, early syenite)

Pleochroism : moderate to strong
X pale brown; Y smokey brown - deep brown; Z olive green.
$X<Y\leqslant Z$. OAP(010). Extinction $Z\wedge c$ 25°.
Birefringence 0.025. $2V\sim 50°$. Optically -ve.
Dispersion $r<v$, strong.

FERROWINCHITE-FERROBARROISITE (sample 1014, early syenite)

Hydrothermal paragenesis. Moderate pleochroism.
X colourless; Y pale blue-green; Z blue-green.
$X<Y<Z$. OAP(010). Extinction $Z\wedge c$ 16°.
Birefringence 0.025. 2V moderate, $\sim 40°$. Optically -ve.
Dispersion $r<v$.

FERRORICHTERITE (sample 275, transitional syenite)

Strong pleochroism.
X pale brown; Y smokey brown; Z dark brown, commonly with greenish tinge. $X<Y<Z$. OAP(010).
Extinction $Z\wedge c$ 22°, often incomplete on 110 sections.
Birefringence 0.026. 2V large, in excess of 60°.
Optically -ve. Dispersion $r<v$, strong.

ARFVEDSONITE (sample 145, alkali granite)

Strong pleochroism.
X dark blueish brown, often virtually opaque;
Y light brown; Z dark brown - smokey brown.
$Y < X > Z$. OAP$\perp$(010). Extinction difficult to determine.
Birefringence low, 0.006. 2V large, in excess of 60°.
Optically -ve. Dispersion $r < v$, strong.

RIEBECKITE (sample 142B1, alkali granite)

Strong pleochroism. X prussian blue; Y smokey blue;
Z yellow brown. $X > Y > Z$. OAP$\perp$(010). Extinction $X \wedge c \leq 10°$.
Birefringence 0.008. 2V large, in excess of 60°.
Optically -ve. Dispersion $r < v$, strong.

ii. PYROXENES

FERROAUGITE (sample 110, transitional syenite)

Pleochroism absent to weak. Colourless to faint green.
High relief. $Z \wedge c$ 45°. Birefringence 0.022.
2V~50°. Optically +ve. Dispersion $r > v$, moderate.

AEGIRINE (sample 145, alkali granite)

Zoned grains:		Cores	Rims
	X	grass green	blue-green
$X > Y > Z$	Y	pale green	pale green
	Z	yellow	colourless - golden yellow
Birefringence :		0.050	0.033

2V large, in excess of 60°. Optically -ve.
Dispersion $r > v$, moderate.

iii. BIOTITES

ANNITE (sample 433, recrystallised alkali syenite)

Pleochroism strong. X orange-red; Y dark brown; Z dark brown. X Y=Z. OAP(010). Extinction $X\wedge c$ 3°. Birefringence 0.05. 2V small, ~10°. Optically -ve.

APPENDIX II

MINERAL ANALYSES

APPENDIX IIA

MACHINE RUN CONDITIONS, RECALCULATION OF ANALYSES AND ESTIMATION OF FERRIC IRON

APPENDIX IIA : MACHINE RUN CONDITIONS, RECALCULATION OF ANALYSES AND ESTIMATION OF FERRIC IRON

The mineral analyses were obtained using the automatic Energy Dispersive Microprobe at the Department of Earth Sciences, Cambridge University. Run conditions involved an accelerating voltage of 20kv, a beam current of 45nA, and a live count time of 80 seconds. The analytical procedure follows Sweatman and Long (1969), and the raw data **were** processed using programs developed by Statham (1976).

As electron microprobe analysis does not provide a determination of the Fe2+/Fe3+ ratio in minerals, the recalculation procedures used must estimate the ratio.

Considering first the pyroxenes, several methods have been proposed (Cawthorn and Collerson, 1974; Essene and Fyfe, 1967; Finger 1972). The method adopted here is the charge difference method of Neumann (1976) which assumes stoichiometry. The principle is that if the pyroxene structural formula is calculated on the number of the cations and not the number of oxygens, then Fe3+= ideal charge - actual positive charge. The calculated ratios are within 20% of the analytical values with this method (op.cit). The method can be applied to any mineral with a fixed number of cations and oxygens and is also used in this thesis for the Fe-Ti oxides (ilmenites based on 2 cations and 6 oxygens; magnetites based on 3 cations and 4 oxygens) and aenigmatites (based on 14 cations and 20 oxygens). For the feldspars all Fe is assumed to be in the ferric state (Deer et al., 1963). For the partial analyses of biotites the commonly accepted convention of calculating on the basis of 22 oxygens, without correcting for Fe3+, is observed.

Estimation of Fe3+ content of amphiboles is more complex as,

1. possible vacancies in the A-site may exist,
2. Leake (1968) showed that there may be between 1 and 3 hydroxyl groups present instead of the ideal two.

However, following current practise an anion content of 23 oxygens is assumed, and taken as representing conventional if not empirical truth (Leake, 1978; Muir-Wood, 1980). Considering possible vacancies numerous recalculation methods have been proposed (Stout, 1972; Brady, 1974; Papike et al., 1974; Neumann, 1976; Ernst, 1980; Muir-Wood, 1980) but no one method is clearly superior.

In the recalculations used in this thesis no single method was found to work for all amphiboles. The 3 different methods used reflect the following criteria, which follow the recommendations of Leake (1968) where possible.

1. The sum of C+T sites should be close to 13. Leake (1968) recommended the range 12.67 - 13.33 as acceptable. Borley (1963) proposed that minor Na (0.97A) may substitute into the C-site, but modern opinion concludes that an ionic radius of about 0.90A represents a divide between the C-site cations and the 2-3 larger cations of the A and B-sites (Jensen, 1973; Neumann, 1976; Stout, 1972), and accordingly such a Na substitution may be discounted.

2. Accepting that Ca, Na and K are confined to the A and B-sites, then the raw cation values (i.e. merely normalised to 46 oxygens, all Fe as FeO), when summed give an indication of the degree of site occupancy).

--- where A+B is less than or about 2.0 the results are recalculated on the basis of C+T=13.0 (Leake, 1978; Stout, 1972). Such a recalculation provides the maximum possible Fe3+ consistent with stoichiometry and a maximum amount of Na enters the B-site. This method has been applied to the calcic, sodic-calcic (low Na) amphiboles of D1014 and D916, and also the the riebeckites of D204 and D433

--- where A+B is in excess of 2.0 then recalculation is based on a cation total of 16.0, which assumes the A-site to be full and maximum reduction. Both assumptions seem justified when one examines the wet-chemical analyses of Borley (1963). C+T totals by this method are close to 13.0, further reinforcing confidence in the results. This scheme is used for the sodic-calcic (high Na) ferrorichterites and arfvedsonites of D275, D204, D433, D1057, D145 and D447. The ferrorichterites of ~~D275~~ D110 are quoted on the C+T=13 basis, but results by the total = 16 method are virtually identical for this sample.

--- Recalculation by either of the above methods may yield a negative Fe3+ value. If the value is less than -0.5 the result is taken as zero. In a few instances however both above methods yielded negative Fe3+ values outside that permitted limit. In such cases the analysis is marked by an asterisk in the Fe3+ position, and is left normalised to 23 oxygens with all Fe as FeO.

--- An analysis quoted is charge balanced, irrespective of which of the three options was employed in the recalculation.

--- Moreover in each case the total Fe cation value is within the range defined by the 'all ferric' and 'all ferrous' assumptions, as it must be if it is to have any validity.

The use of different recalculation methods for different amphibole species is clearly undesirable, but perhaps equally unavoidable if the realities of variable site occupancy are acknowledged (Stout, 1972; Neumann, 1976; Muir-Wood, 1980; Ernst, 1980). The author suggests that the tests employed here, namely, C+T=13; total Fe values within the range defined by 'all ferric' or 'all ferrous', and maintenance of charge balance, testify to the rigourousness of the correction procedures. However, caution must be exercised when comparing the two main groups of amphiboles (i.e. the C+T=13 group, and the total cations = 16 group) from Ras ed Dom, or indeed when comparing either group with a third group recalculated by some other method (Stout, 1972). Clearly international agreement on appropriate procedures for each amphibole sub-group would be desirable.

APPENDIX IIB

FELDSPARS - 34 analyses

Key to abbreviations

OLIG	Oligoclase
AND	Andesine
LAB	Labradorite

ALKALI FELDSPARS

	D1014				D916		D110			
Wt.%	1	2	3	4	1	2	1	2	3	4
SiO2	67.09	66.71	65.53	65.04	66.05	66.45	65.58	65.71	65.78	65.19
AL203	20.15	19.73	19.78	20.00	18.77	19.11	19.00	18.71	19.29	19.42
TiO2	0.04	0.03	-	0.18	0.10	0.07	0.09	0.03	0.15	-
ΣFe as Fe_2O_3	0.17	0.24	0.27	0.45	0.23	0.23	1.64	0.34	0.30	0.20
MnO	-	-	-	-	-	-	-	-	-	-
CaO	0.91	0.88	1.24	1.45	0.38	0.55	0.45	0.27	0.55	0.91
Na20	5.82	7.14	7.45	7.49	4.64	6.00	7.34	6.16	5.75	7.56
K20	5.43	4.50	4.00	3.98	9.72	7.57	4.97	7.15	6.32	4.88
TOTAL	99.61	99.23	98.27	98.59	99.89	99.98	99.07	98.37	98.14	98.16
	number of ions on the basis of 32 oxygens									
Si	11.917	11.902	11.817	11.720	11.954	11.926	11.822	11.964	11.931	11.828
Al	4.220	4.150	4.205	4.248	4.005	4.043	4.038	4.016	4.124	4.154
Ti	0.006	0.004	-	0.024	0.014	0.009	0.012	0.004	0.021	-
Fe+3	0.023	0.032	0.037	0.061	0.031	0.031	0.223	0.047	0.041	0.027
Mn	-	-	-	-	-	-	-	-	-	-
Ca	0.173	0.168	0.240	0.280	0.074	0.106	0.087	0.053	0.107	0.177
Na	2.005	2.470	2.605	2.617	1.628	2.088	2.566	2.175	2.022	2.660
K	1.231	1.024	0.920	0.915	2.244	1.733	1.143	1.661	1.462	1.130
Mol % OR	36.3	28.1	24.3	23.9	56.7	44.0	30.3	42.8	40.6	28.6
AB	58.7	67.2	69.4	68.8	41.3	53.3	67.4	55.8	56.4	67.0
AN	5.0	4.7	6.3	7.3	1.9	2.8	2.4	1.4	3.0	4.4
No. of Points Averaged	3	5	2	4	6	2	3	4	4	3

ALKALI FELDSPARS

	D275					D204			
wt.%	1	2	3	4	5	1	2	3	4
SiO2	67.52	68.16	67.35	66.65	67.17	67.02	66.97	66.63	66.94
AL2O3	18.62	18.58	18.77	18.87	18.78	18.94	18.59	18.57	18.33
TiO2	0.04	-	-	-	-	-	-	-	-
ΣFe as Fe_2O_3	0.34	0.63	0.20	1.43	0.21	0.16	0.20	-	0.44
MnO	-	-	-	-	-	-	-	-	0.02
CaO	0.03	0.06	-	0.07	-	0.32	0.25	0.29	0.08
Na2O	7.26	6.96	7.03	7.99	7.41	6.83	6.32	6.89	5.98
K2O	6.14	4.75	7.04	5.18	6.09	5.80	7.59	7.05	8.20
TOTAL	99.95	99.14	100.39	100.19	99.66	99.07	99.92	99.43	99.99
	number of ions on the basis of 32 oxygens								
Si	12.044	12.136	12.012	11.888	12.018	12.023	12.021	12.006	12.039
Al	3.915	3.900	3.946	3.968	3.961	4.005	3.934	3.945	3.886
Ti	0.005	-	-	-	-	-	-	-	-
Fe+3	0.046	0.084	0.027	0.191	0.028	0.022	0.027	-	0.060
Mn	-	-	-	-	-	-	-	-	-
Ca	0.006	0.011	-	0.013	-	0.062	0.048	0.056	0.003
Na	2.511	2.403	2.431	2.763	2.571	2.376	2.200	2.407	2.086
K	1.397	1.079	1.602	1.179	1.390	1.327	1.738	1.621	1.882
Mol% OR	35.7	30.8	39.9	29.8	35.1	35.4	43.8	39.8	47.4
AB	64.2	68.9	60.1	69.9	64.9	62.9	55.1	58.9	52.3
AN	0.1	0.3	-	0.3	-	1.7	1.1	1.3	0.3
No. of Points Averaged	4	3	4	2	2	4	4	4	5

ALBITES

	447		447		447		447	
wt.%	1A	1B	2A	2B	3A	3B	4A	4B
Si02	68.50	69.60	67.16	68.22	69.26	69.88	71.94	82.46
AL203	19.22	19.20	18.27	18.73	18.81	18.78	16.67	10.50
ΣFe as Fe_2O_3	-	-	0.50	0.23	-	-	-	-
Ca	-	-	0.10	-	-	-	-	-
Na	10.49	11.03	10.80	10.44	11.90	11.17	10.67	6.30
K	1.90	0.09	0.61	-	-	0.10	0.10	-
TOTAL	100.13	99.94	97.48	97.64	99.99	99.94	99.40	99.27
	number of ions on the basis of 32 oxygens							
Si	12.018	12.110	12.060	12.131	12.089	12.162	12.526	13.917
Al	3.976	3.939	3.869	3.927	3.871	3.853	3.423	2.089
Ti	-	-	-	-	-	-	-	-
Fe+3	-	-	0.069	0.031	-	-	-	-
Ca	-	-	0.021	-	-	-	-	-
Na	3.572	3.721	3.762	3.602	4.029	3.771	3.603	2.062
K	0.427	0.021	0.141	-	-	0.023	0.024	-
Mol% OR	10.58	0.56	3.85	-	-	0.55	0.58	-
AB	89.42	99.44	95.60	100.00	100.00	99.45	99.42	100.00
AN	-	-	0.55	-	-	-	-	-

PLAGIOCLASE FELDSPARS

	D183A	D183A			D183A		
wt.%	1	2A	2B	2C	3A	3B	3C
SiO2	55.22	53.86	60.03	61.51	53.44	54.15	55.39
AL2O3	25.88	28.09	24.64	23.40	28.30	27.77	26.20
TiO2	-	0.17	-	-	0.21	0.15	0.16
ΣFe as Fe_2O_3	1.73	0.80	0.57	0.78	0.82	0.84	1.04
CaO	8.79	11.34	6.84	4.04	12.06	11.39	6.97
Na2O	5.92	4.86	7.82	7.54	4.50	5.11	5.42
K2O	0.66	0.08	0.16	1.05	0.13	0.23	1.78
CL	0.08	-	-	-	-	-	0.09
TOTAL	98.31	99.23	100.07	98.35	99.49	99.68	97.09
	——— number of ions on the basis of 32 oxygens-						
Si	10.170	9.821	10.712	11.082	9.740	9.848	10.280
Al	5.619	6.038	5.184	4.971	6.082	5.956	5.733
Ti	-	0.024	-	-	0.029	0.022	0.023
Fe+3	0.241	0.111	0.078	0.107	0.113	0.116	0.146
Ca	1.735	2.216	1.309	0.780	2.356	2.222	1.387
Na	2.114	1.720	2.708	2.636	1.593	1.805	1.953
K	0.156	0.019	0.038	0.243	0.032	0.055	0.423
Mol% OR	3.9	0.6	1.0	6.5	1.1	1.6	11.2
AB	52.9	43.7	66.7	72.2	40.0	44.3	52.1
AN	43.2	55.8	32.3	21.3	58.9	54.1	36.7
LOCUS:		core ——→		rim	core ——→		rim
NAME:	AND	LAB	AND	OLIG	LAB	LAB	AND

APPENDIX IIC

EARLY PYROXENES - 29 analyses

Key to Abbreviations

FE-AUG	Ferroaugite
FE-HED	Ferrohedenbergite
A-A	Aegirine-augite

EARLY PYROXENES

	D916	D110			D110				D110	
wt.%	1A	1A	1B	1C	2A	2B	2C	2D	3A	3B
SiO2	51.516	50.963	48.809	49.110	50.652	50.055	50.274	49.684	50.099	50.833
AL2O3	0.548	0.325	-	-	0.741	0.505	0.741	0.270	0.468	0.251
TiO2	0.401	0.335	0.286	0.216	0.542	0.384	0.493	0.328	0.465	0.323
ΣFe as FeO	19.392	28.039	28.878	26.466	18.854	20.878	19.845	25.761	21.789	27.200
MgO	7.760	0.924	0.761	1.187	6.996	6.196	6.581	2.614	5.034	1.682
MnO	0.979	0.862	0.960	0.871	0.958	1.023	1.022	0.989	0.917	0.882
CaO	20.102	13.988	14.254	15.380	20.224	19.649	19.755	15.987	19.242	14.929
Na2O	-	4.397	4.637	3.474	0.463	-	0.858	2.695	1.467	3.770
K2O	-	-	-	-	-	-	-	-	-	-
Cr2O3	-	-	-	-	-	-	-	-	0.124	-
ZrO2	-	0.209	0.435	0.561	-	-	-	-	-	-
TOTAL	100.697	100.043	99.019	97.263	99.430	98.691	99.569	98.238	99.606	99.871

NUMBER OF IONS ON THE BASIS OF 6 OXYGENS AND 4 CATIONS

	D916 1A	D110 1A	D110 1B	D110 1C	D110 2A	D110 2B	D110 2C	D110 2D	D110 3A	D110 3B
Si	2.008	2.023	1.997	2.017	1.996	2.011	1.979	2.010	1.983	2.020
AL	0.025	0.015	-	-	0.034	0.024	0.034	0.013	0.022	0.012
Ti	0.012	0.010	0.009	0.007	0.016	0.012	0.015	0.010	0.014	0.010
Fe+3	-	0.249	0.332	0.207	-	-	0.044	0.159	0.093	0.220
Fe+2	0.632	0.682	0.603	0.702	0.621	0.702	0.609	0.713	0.628	0.684
Mg	0.451	0.054	0.046	0.073	0.411	0.371	0.386	0.158	0.297	0.100
Mn	0.032	0.029	0.033	0.030	0.032	0.035	0.034	0.034	0.031	0.030
Ca	0.840	0.594	0.612	0.677	0.854	0.846	0.833	0.693	0.816	0.636
Na	-	0.338	0.361	0.277	0.035	-	0.066	0.211	0.113	0.290
K	-	-	-	-	-	-	-	-	-	-
Cr	-	-	-	-	-	-	-	-	0.004	-
Zr	-	0.004	0.009	0.011	-	-	-	-	-	-
LOCUS:		core	→	rim	core	→	→	rim	core →	rim
NAME:	FE-AUG.	A-A.	A-A.	A-A.	FE-AUG.	FE-AUG.	FE-AUG.	A-A.	FE-AUG.	A-A.

EARLY PYROXENES

	D110		D110		D110	D110	D275	D275	
wt.%	4A ✓	4B	5A	5B	6	7	1 ✓	2A	2B
SiO2	50.663	49.976	50.969	50.766	50.131	49.508	50.271	50.366	49.239
AL2O3	0.491	0.267	0.527	0.616	0.669	0.882	0.357	0.242	0.444
TiO2	0.489	-	0.543	0.461	0.446	0.485	0.260	0.497	0.308
ΣFe as FeO	19.801	26.107	19.664	19.823	20.382	20.416	26.581	26.907	27.232
MgO	6.846	1.573	6.960	6.356	6.484	5.953	1.998	-	0.211
MnO	0.851	0.594	0.992	0.941	1.044	0.989	1.034	0.648	0.807
CaO	19.604	16.374	19.681	19.405	19.547	19.602	18.171	13.008	14.913
Na2O	0.551	3.554	0.537	0.872	0.637	0.561	1.889	6.344	4.773
K2O	-	0.099	-	-	-	-	-	-	0.110
Cr2O3	-	-	-	-	-	0.147	-	0.126	0.118
ZrO2	-	-	-	-	-	-	-	0.696	0.471
TOTAL	99.296	98.544	99.874	99.241	99.340	98.543	100.561	98.834	98.627

NUMBER OF IONS ON THE BASIS OF 6 OXYGENS AND 4 CATIONS

	4A	4B	5A	5B	6	7	1	2A	2B
Si	2.001	2.011	2.003	2.007	1.985	1.982	2.009	2.000	1.980
AL	0.023	0.013	0.024	0.029	0.031	0.042	0.017	0.011	0.021
Ti	0.015	-	0.016	0.014	0.013	0.015	0.008	0.015	0.009
Fe+3	-	0.243	-	-	0.022	0.004	0.096	0.417	0.356
Fe+2	0.660	0.636	0.646	0.655	0.653	0.680	0.792	0.476	0.560
Mg	0.403	0.094	0.408	0.375	0.383	0.355	0.119	-	0.013
Mn	0.029	0.020	0.033	0.032	0.035	0.034	0.035	0.022	0.028
Ca	0.830	0.706	0.829	0.822	0.829	0.841	0.778	0.553	0.643
Na	0.042	0.277	0.041	0.067	0.049	0.044	0.146	0.488	0.372
K	-	0.055	-	-	-	-	-	-	0.006
Cr	-	-	-	-	-	0.005	-	0.004	0.004
Zr	-	-	-	-	-	-	-	0.014	0.009
LOCUS	core ⟶ rim		core ⟶ rim					non-dir.	
NAME:	FE-AUG.	A-A.	FE-AUG.	FE-AUG.	FE-AUG.	FE-AUG.	FE-HED.	A-A.	A-A.

EARLY PYROXENES

	D275		D275		D275		D275		D275	
wt.%	3A	3B	4A	4B ✓	5A ✓	5B ✓	6A	6B	7A	7B
SiO2	50.605	50.353	49.888	49.247	49.902	50.451	50.573	50.478	50.707	51.058
AL203	0.211	0.212	-	-	0.317	0.214	0.202	-	0.299	-
TiO2	0.291	0.506	0.277	0.308	0.186	0.196	0.576	0.330	0.251	0.573
ΣFe as FeO	27.595	27.284	25.579	27.414	27.712	28.032	27.395	27.748	27.333	27.117
MgO	0.306	-	0.334	1.211	1.098	1.221	-	-	-	-
MnO	1.104	0.593	1.104	0.951	0.930	0.912	0.590	0.687	0.868	0.561
CaO	16.077	12.738	15.567	17.882	18.513	17.680	12.939	15.016	11.627	11.194
Na2O	3.990	6.008	3.910	2.031	1.267	2.113	6.065	4.890	7.650	7.120
K2O	-	-	-	-	-	0.131	-	-	-	-
Cr2O3	-	-	0.128	-	-	-	-	-	-	-
ZrO2	0.215	0.636	0.210	-	-	-	0.759	0.189	0.183	0.965
TOTAL	100.394	98.331	99.946	99.044	99.924	100.950	99.099	99.338	98.918	98.589

NUMBER OF IONS ON THE BASIS OF 6 OXYGENS AND 4 CATIONS

	3A	3B	4A	4B	5A	5B	6A	6B	7A	7B
Si	2.012	2.016	2.050	2.008	2.030	2.016	2.010	2.016	1.984	2.024
AL	0.010	0.010	-	-	0.015	0.010	0.010	-	0.014	-
Ti	0.009	0.015	0.007	0.009	0.006	0.006	0.017	0.010	0.007	0.017
Fe+3	0.248	0.369	0.185	0.126	0.013	0.116	0.374	0.320	0.577	0.428
Fe+2	0.669	0.544	0.694	0.809	0.930	0.821	0.536	0.606	0.318	0.471
Mg	0.018	-	0.021	0.074	0.067	0.073	-	-	-	-
Mn	0.037	0.020	0.038	0.033	0.032	0.031	0.020	0.023	0.029	0.019
Ca	0.685	0.546	0.685	0.781	0.807	0.757	0.551	0.642	0.488	0.475
Na	0.308	0.466	0.312	0.161	0.100	0.164	0.467	0.379	0.580	0.547
K	-	-	-	-	-	0.007	-	-	-	-
Cr	-	-	0.004	-	-	-	-	-	-	-
Zr	0.004	0.012	0.004	-	-	-	0.015	0.004	0.004	0.019
LOCUS:	non-dir.		rim ← core		core → rim		rim ← core		rim ← core	
NAME:	A-A.	A-A.	A-A.	FE-HED.	FE-HED.	FE-HED.	A-A.	A-A.	A-A.	A-A.

APPENDIX IID

LATE PYROXENES - 82 analyses

Key to Abbreviations

A-A	Aegirine-augite
AEG	Aegirine
tit	titanian

LATE PYROXENES

	D204	D204			D204		D204		D204		
wt.%	1	2A	2B	2C	3A	3B	4A	4B	5A	5B	5C
SiO2	52.231	53.316	53.632	53.186	51.486	51.537	51.240	51.357	52.170	52.055	52.763
AL203	-	-	-	-	-	-	-	-	0.243	0.249	-
TiO2	0.274	0.518	0.527	0.526	0.279	0.343	0.383	0.280	0.204	0.280	0.398
ΣFe as FeO	29.716	29.670	29.691	29.927	28.895	29.223	29.868	30.626	29.209	29.504	29.230
MgO	-	-	-	-	-	-	-	-	-	-	-
MnO	0.651	0.339	0.331	0.370	0.420	0.569	0.541	0.294	0.551	0.531	0.315
CaO	7.548	3.889	3.474	3.996	5.561	6.030	6.601	3.041	6.739	5.766	4.740
Na2O	9.469	11.971	12.565	11.896	10.774	10.293	10.205	11.890	10.394	10.982	11.319
K2O	-	-	-	-	0.075	-	-	-	0.078	0.078	-
Cr2O3	-	-	-	-	0.126	-	-	-	-	-	-
ZrO2	-	0.525	0.857	0.498	0.391	-	-	-	-	0.237	0.801
TOTAL	99.888	100.229	101.077	100.400	97.976	97.994	98.837	97.488	99.589	99.682	99.565

NUMBER OF IONS ON THE BASIS OF 6 OXYGENS AND 4 CATIONS

	1	2A	2B	2C	3A	3B	4A	4B	5A	5B	5C
Si	2.003	2.004	1.993	1.997	1.992	1.999	1.974	1.980	1.988	1.976	2.006
AL	-	-	-	-	-	-	-	-	0.011	0.011	-
Ti	0.008	0.015	0.015	0.015	0.008	0.010	0.011	0.008	0.006	0.008	0.011
Fe+3	0.682	0.817	0.859	0.824	0.791	0.757	0.792	0.912	0.774	0.824	0.769
Fe+2	0.271	0.116	0.064	0.116	0.144	0.191	0.170	0.075	0.157	0.113	0.160
Mg	-	-	-	-	-	-	-	-	-	-	-
Mn	0.021	0.011	0.010	0.012	0.014	0.019	0.018	0.010	0.018	0.017	0.010
Ca	0.310	0.157	0.138	0.161	0.231	0.251	0.273	0.126	0.275	0.235	0.193
Na	0.704	0.872	0.905	0.866	0.806	0.774	0.762	0.889	0.768	0.808	0.835
K	-	-	-	-	0.004	-	-	-	0.004	0.004	-
Cr	-	-	-	-	0.004	-	-	-	-	-	-
Zr	-	0.010	0.016	0.009	0.007	-	-	-	-	0.004	0.015
LOCUS:		core	→	rim	non-dir.		core →	rim	core	→	rim
NAME:	A-A	AEG	AEG	AEG	AA	A-A	A-A	AEG	A-A	A-A	AEG

LATE PYROXENES

	D204	D204			D204				D433	
wt.%	6	7A	7B	7C	8A	8B	8C	8D	1A	1B
SiO2	51.629	52.444	52.625	53.359	51.487	51.405	51.842	51.586	52.006	52.496
Al2O3		-	-	-	-	-	-	-	0.858	0.810
TiO2	0.347	0.423	0.684	0.514	0.308	0.291	0.342	0.385	0.671	0.495
ΣFe as FeO	29.490	29.744	29.436	29.149	28.982	28.791	28.856	28.935	24.477	24.577
MgO	-	-	-	-	-	-	-	-	1.865	1.860
MnO	0.571	0.408	0.348	0.271	0.420	0.533	0.494	0.432	0.509	0.577
CaO	7.276	4.500	4.368	3.756	5.770	6.440	5.654	5.990	9.781	9.583
Na2O	9.636	11.342	11.736	12.148	10.754	9.927	10.967	10.601	8.581	8.452
K2O	-	-	-	-	-	-	-	-	-	-
Cr2O3	-	-	-	-	-	-	-	-	-	-
ZrO2	-	0.848	0.384	0.621	0.540	0.227	0.455	0.246	0.382	0.465
TOTAL	98.950	99.710	99.582	99.817	98.261	97.613	98.609	98.177	99.129	99.314

NUMBER OF IONS ON THE BASIS OF 6 OXYGENS AND 4 CATIONS

	6	7A	7B	7C	8A	8B	8C	8D	1A	1B
Si	1.995	1.994	1.992	2.009	1.988	2.008	1.990	1.993	1.991	2.009
AL	-	-	-	-	-	-	-	-	0.039	0.037
Ti	0.010	0.012	0.020	0.015	0.009	0.009	0.010	0.011	0.019	0.014
Fe+3	0.712	0.793	0.824	0.817	0.791	0.711	0.799	0.777	0.564	0.527
Fe+2	0.241	0.153	0.108	0.101	0.144	0.230	0.127	0.158	0.219	0.260
Mg	-	-	-	-	-	-	-	-	0.106	0.106
Mn	0.019	0.013	0.011	0.009	0.014	0.018	0.016	0.014	0.017	0.019
Ca	0.301	0.183	0.177	0.152	0.239	0.270	0.233	0.248	0.401	0.393
Na	0.722	0.836	0.861	0.887	0.805	0.752	0.816	0.794	0.637	0.627
K	-	-	-	-	-	-	-	-	-	-
Cr	-	-	-	-	-	-	-	-	-	-
Zr	-	0.016	0.007	0.011	0.010	0.004	0.009	0.005	0.007	0.009
LOCUS:		core	⟶	rim	rim ⟵	core	⟶	rim	rim ⟵	core
NAME:	A-A.	AEG.	AEG.	AEG.	A-A.	A-A.	A-A.	A-A.	A-A.	A-A.

LATE PYROXENES

	D433		D433				D433		
wt.%	2A	2B	3A	3B	3C	3D	4A	4B	4C
SiO2	51.731	51.843	51.875	52.333	51.927	52.557	53.201	52.325	52.264
AL2O3	0.669	0.744	0.327	0.649	0.676	0.405	1.012	0.881	0.441
TiO2	0.447	0.502	0.437	0.552	0.421	0.436	0.648	0.581	0.401
ΣFe as FeO	24.447	25.286	26.385	26.256	26.776	26.337	25.184	25.915	26.783
MgO	1.881	1.335	0.888	0.918	0.806	1.410	1.867	1.300	0.829
MnO	0.669	0.826	0.503	0.609	0.519	0.617	0.583	0.557	0.541
CaO	10.866	10.254	8.390	9.011	8.622	8.708	9.483	8.943	8.762
Na2O	7.782	8.179	9.180	9.107	9.614	9.346	8.997	9.150	9.227
ZrO2	0.432	0.573	0.484	0.239	-	0.510	0.479	0.430	0.230
TOTAL	98.924	99.542	98.469	99.674	99.360	100.328	101.455	100.082	99.479

NUMBER OF IONS ON THE BASIS OF 6 OXYGENS AND 4 CATIONS

	2A	2B	3A	3B	3C	3D	4A	4B	4C
Si	1.970	1.993	2.006	1.998	1.979	1.989	1.988	1.985	1.999
AL	0.084	0.034	0.015	0.029	0.030	0.018	0.045	0.039	0.020
Ti	0.013	0.015	0.013	0.016	0.012	0.012	0.018	0.017	0.012
Fe+3	0.509	0.540	0.618	0.609	0.698	0.647	0.578	0.614	0.635
Fe+2	0.270	0.273	0.236	0.229	0.156	0.187	0.209	0.209	0.222
Mg	0.107	0.077	0.051	0.052	0.046	0.080	0.104	0.074	0.047
Ma	0.022	0.027	0.017	0.020	0.017	0.020	0.019	0.018	0.018
Ca	0.443	0.422	0.348	0.368	0.352	0.353	0.380	0.364	0.359
Na	0.575	0.610	0.688	0.674	0.711	0.686	0.652	0.673	0.684
Zr	0.008	0.011	0.009	0.004	-	0.009	0.009	0.008	0.004
LOCUS:	non-dir.		rim ⟵ core ⟶ rim						
NAME:	A-A.	A-A.	A-A.	A-A.	A-A.	A-A.	A-A.	A-A.	A-A.

LATE PYROXENES

	D433			D433			
wt. %	4D	4E	4F	5A	5B	5C	5D
SiO2	51.873	51.807	51.730	51.463	51.588	50.881	51.697
AL2O3	0.496	0.531	0.607	-	0.224	0.324	0.615
TiO2	0.343	0.184	0.385	0.272	0.211	0.304	0.737
ΣFe as FeO	26.786	26.515	26.453	26.805	26.059	25.848	25.107
MgO	1.303	1.257	0.897	0.731	0.919	0.924	1.412
MnO	0.670	0.632	0.496	0.553	0.493	0.637	0.536
CaO	10.141	9.234	9.151	9.737	8.865	9.422	8.286
Na2O	8.238	9.152	8.942	8.620	9.051	8.540	9.461
ZrO2	0.219	0.544	0.438	-	0.595	0.856	0.739
TOTAL	100.068	99.857	99.099	98.182	98.005	97.735	98.590

NUMBER OF IONS ON THE BASIS OF 6 OXYGENS AND 4 CATIONS

	4D	4E	4F	5A	5B	5C	5D
Si	1.984	1.973	1.990	2.003	2.005	1.993	1.986
AL	0.022	0.024	0.028	-	0.010	0.015	0.028
Ti	0.010	0.005	0.011	0.008	0.006	0.009	0.021
Fe+3	0.592	0.676	0.621	0.629	0.627	0.596	0.634
Fe+2	0.265	0.168	0.231	0.243	0.220	0.251	0.172
Mg	0.074	0.071	0.051	0.042	0.053	0.054	0.081
Mn	0.022	0.020	0.016	0.018	0.016	0.021	0.017
Ca	0.416	0.377	0.377	0.406	0.369	0.396	0.341
Na	0.611	0.676	0.667	0.650	0.682	0.649	0.705
Zr	0.004	0.010	0.008	-	0.011	0.016	0.014
LOCUS:				rim ←		core →	rim
NAME:	A-A.	A-A.	A-A.	A-A.	A-A.	A-A.	A-A.

LATE PYROXENES

	D1057		D1057		D1057				D1057	
wt.%	1A	1B	2A	2B	3A	3B	3C	3D	4A	4B
SiO2	54.605	53.062	52.901	53.372	53.374	53.501	53.489	53.985	53.421	53.926
AL2O3	0.946	-	0.542	-	0.232	0.250	-	0.504	0.230	-
TiO2	0.332	2.414	1.420	1.884	2.408	1.201	1.260	1.583	2.050	1.889
ΣFe as FeO	29.408	28.585	27.587	27.466	28.036	29.569	29.160	29.058	28.449	28.525
MnO	0.272	0.495	1.058	0.601	0.387	0.281	0.386	0.315	0.411	0.431
CaO	0.374	0.275	0.891	0.997	1.364	1.338	1.066	0.948	0.876	1.380
Na2O	14.930	14.419	13.965	14.311	13.901	13.918	14.441	14.473	14.121	14.034
K2O	0.092	-	0.099	0.090	-	-	-	-	-	-
ZrO2	-	-	0.182	1.673	0.173	-	-	-	-	0.214
TOTAL	100.959	99.250	98.645	100.393	99.876	100.057	99.802	100.866	99.559	100.399

NUMBER OF IONS ON THE BASIS OF 6 OXYGENS AND 4 CATIONS

	1A	1B	2A	2B	3A	3B	3C	3D	4A	4B
Si	1.981	1.975	1.981	1.977	1.982	1.980	1.976	1.974	1.984	1.991
AL	0.041	-	0.024	-	0.010	0.011	-	0.022	0.010	-
Ti	0.009	0.068	0.040	0.053	0.067	0.033	0.035	0.044	0.057	0.052
Fe+3	0.892	0.890	0.864	0.851	0.871	0.915	0.901	0.888	0.884	0.881
Fe+2	-	-	-	-	-	-	-	-	-	-
Mn	0.008	0.016	0.034	0.019	0.012	0.009	0.012	0.010	0.013	0.014
Ca	0.015	0.011	0.036	0.040	0.054	0.053	0.042	0.037	0.035	0.055
Na	1.050	1.041	1.014	1.028	1.001	0.999	1.034	1.026	0.017	1.005
K	0.004	-	0.005	0.004	-	-	-	-	-	-
Zr	-	-	0.003	0.030	0.003	-	-	-	-	0.004
LOCUS:	core ⟶	rim	core ⟶	rim	rim ⟵		core	rim ⟵	core ⟶	rim
NAME:	AEG.	AEG.	AEG.	AEG.	AEG.	AEG.	AEG.	AEG.	AEG.	AEG.
ADJECTIVAL MODIFIER:		tit	tit	tit	tit	tit	tit	tit	tit	tit

LATE PYROXENES

	D1057			D1057		D145					D145		
wt.%	5A	5B	5C	6A	6B	1A	1B	1C	1D	1E	2A	2B	2C
SiO_2	52.709	52.969	52.760	51.997	53.231	53.606	52.758	51.978	53.220	51.932	52.549	53.034	53.821
AL_2O_3	0.477	0.333	0.617	0.273	-	0.287	0.194	-	-	0.325	0.310	0.294	-
TiO_2	1.763	1.748	0.924	1.581	1.919	2.045	1.687	1.475	1.696	0.917	3.415	3.911	0.499
ΣFe as FeO	28.121	29.257	27.763	28.267	28.699	27.580	28.233	28.018	27.785	28.971	26.551	26.192	30.521
MnO	0.377	0.288	0.519	0.847	0.245	0.595	0.644	0.604	0.588	0.397	0.644	0.813	-
CaO	0.763	0.881	0.355	1.041	0.323	0.754	0.445	0.436	0.683	0.348	0.371	0.361	-
Na_2O	13.643	13.921	14.351	13.291	13.940	14.872	14.632	13.632	13.987	13.877	13.822	14.660	14.794
K_2O	-	-	0.080	-	-	-	-	-	0.073	-	0.087	-	-
ZrO_2	-	-	-	-	-	0.410	0.477	0.543	0.751	-	-	0.202	-
TOTAL	97.853	99.397	97.369	97.297	98.358	100.148	99.069	96.686	98.783	96.767	97.750	99.467	99.636

NUMBER OF IONS ON THE BASIS OF 6 OXYGENS AND 4 CATIONS

	5A	5B	5C	6A	6B	1A	1B	1C	1D	1E	2A	2B	2C
Si	1.995	1.974	1.988	1.986	2.00	1.969	1.963	1.995	1.998	1.981	1.992	1.967	1.986
AL	0.021	0.015	0.027	0.012	-	0.012	0.009	-	-	0.015	0.014	0.013	-
Ti	0.050	0.049	0.026	0.045	0.054	0.057	0.047	0.043	0.048	0.026	0.097	0.109	0.014
Fe+3	0.890	0.912	0.875	0.903	0.901	0.847	0.879	0.900	0.872	0.924	0.828	0.813	0.942
Fe+2	-	-	-	-	0.002	-	-	-	-	-	0.013	-	-
Mn	0.012	0.009	0.017	0.027	0.008	0.019	0.020	0.020	0.019	0.013	0.021	0.026	-
Ca	0.031	0.035	0.014	0.043	0.013	0.030	0.018	0.018	0.028	0.014	0.015	0.014	-
Na	1.001	1.006	1.049	0.984	1.018	1.059	1.056	1.015	1.018	1.027	1.016	1.055	1.058
K	-	-	0.004	-	-	-	-	-	0.004	-	0.004	-	-
Zr	-	-	-	-	-	0.007	0.009	0.010	0.014	-	-	0.004	-
LOCUS:	core	⟶	rim	core ⟶	rim	rim	⟵	core	⟶	rim	core	⟶	rim
NAME:	AEG.	AEG.	AEG.	AEG.	AEG.	AEG.	AEG.	AEG.	AEG.	AEG.	AEG.	AEG.	AEG.
ADJECTIVAL MODIFIER:	tit	tit		tit	tit	tit	tit	tit	tit		tit	tit	

LATE PYROXENES

	D145		D145		D145	D145	D145		D145	
wt.%	3A	3B	4A	4B	5	6	7A	7B	8A	8B
SiO2	53.754	52.932	50.870	51.817	48.695	54.124	52.946	54.417	52.787	53.467
AL2O3	0.423	0.422	0.294	0.346	0.229	0.296	0.358	0.435	-	0.283
TiO2	0.371	1.611	0.995	0.649	1.629	1.439	3.323	4.343	3.110	3.307
ΣFe as FeO	30.571	28.490	29.648	30.239	27.332	28.724	26.902	26.472	27.519	27.042
MnO	-	0.452	0.239	0.166	0.200	0.486	0.291	0.420	0.514	0.621
CaO	0.392	1.007	4.401	0.358	7.019	0.264	0.657	0.609	0.426	0.571
Na2O	14.737	13.690	11.292	13.048	12.370	14.434	14.836	14.502	14.078	14.234
K2O	0.081	0.076	-	0.183	-	-	-	0.077	-	-
ZrO2	-	-	-	-	-	0.365	0.416	0.694	0.190	0.178
TOTAL	100.330	98.680	97.739	96.806	97.474	100.133	99.729	101.969	98.625	99.703

NUMBER OF IONS ON THE BASIS OF 6 OXYGENS AND 4 CATIONS

	3A	3B	4A	4B	5	6	7A	7B	8A	8B
Si	1.969	1.987	1.965	1.992	1.860	1.997	1.956	1.981	1.984	1.985
AL	0.018	0.019	0.013	0.016	0.010	0.013	0.016	0.019	-	0.012
Ti	0.010	0.046	0.029	0.019	0.047	0.040	0.092	0.119	0.088	0.092
Fe+3	0.937	0.894	0.845	0.945	0.873	0.886	0.831	0.785	0.865	0.840
Fe+2	-	-	0.112	0.027	-	-	-	0.021	-	-
MN	-	0.014	0.008	0.005	0.007	0.015	0.009	0.013	0.016	0.020
Ca	0.015	0.041	0.182	0.015	0.287	0.010	0.026	0.024	0.017	0.023
Na	1.047	0.996	0.846	0.972	0.916	1.032	1.063	1.024	1.026	1.025
K	0.004	0.004	-	0.009	-	-	-	0.004	-	-
Zr	-	-	-	-	-	0.007	0.008	0.012	0.004	0.003
LOCUS:			core ——→rim				non-dir.			
NAME:	AEG.	AEG.	AEG.	AEG.	AEG.	AEG.	AEG.	AEG.	AEG.	AEG.
ADJECTIVAL		tit	tit		tit	tit	tit	tit	tit	tit
MODIFIER:										

LATE PYROXENES

	D447				D447				D447			
wt.%	1A	1B	1C	2	3A	3B	3C	3D	4A	4B	4C	4D
SiO2	54.316	53.157	52.752	54.185	51.035	53.832	53.393	53.386	52.296	53.151	52.638	52.964
AL2O3	-	-	-	-	-	0.240	0.281	0.289	-	-	0.211	-
TiO2	2.876	4.346	4.007	-	5.308	5.392	1.905	1.555	3.439	3.625	2.026	0.475
ΣFe as FeO	27.295	25.512	26.264	29.316	25.318	25.490	27.920	28.140	26.305	26.012	26.856	27.853
MnO	0.228	0.226	0.240	0.498	0.285	0.208	0.246	0.212	0.173	0.281	0.248	0.888
CaO	0.309	1.069	1.681	0.182	1.957	1.671	0.926	0.719	0.860	0.866	0.155	-
Na2O	15.332	14.056	13.575	14.839	12.843	13.638	14.262	14.090	14.222	14.074	14.816	14.921
K2O	-	-	-	-	-	-	0.121	-	0.086	-	-	-
ZrO2	0.614	0.639	0.916	-	0.374	-	0.886	0.667	0.829	0.947	0.817	-
TOTAL	100.790	99.004	99.435	99.020	97.121	100.471	99.941	99.069	98.209	98.957	97.767	97.102

NUMBER OF IONS ON THE BASIS OF 6 OXYGENS AND 4 CATIONS

Si	1.974	1.993	1.981	2.005	1.970	1.996	1.979	1.995	1.973	1.995	1.979	1.993
AL	-	-	-	-	-	0.011	0.012	0.013	-	-	0.009	-
Ti	0.079	0.123	0.113	-	0.154	0.150	0.053	0.044	0.098	0.102	0.057	0.013
Fe+3	0.833	0.767	0.766	0.907	0.699	0.678	0.865	0.879	0.830	0.794	0.845	0.877
Fe+2	-	0.033	0.059	-	0.118	0.112	-	-	-	0.022	-	-
Mn	0.007	0.007	0.008	0.016	0.009	0.007	0.007	0.007	0.006	0.009	0.008	0.028
Ca	0.012	0.043	0.068	0.007	0.081	0.066	0.037	0.029	0.035	0.035	0.006	-
Na	1.084	1.022	0.989	1.065	0.961	0.980	1.025	1.021	1.040	1.025	1.080	1.089
K	-	-	-	-	-	-	0.006	-	0.004	-	-	-
Zr	0.011	0.012	0.017	-	0.007	-	0.016	0.012	0.015	0.017	0.015	-
LOCUS:	rim ←		core		core →			→ rim	rim ←		core →	rim
NAME:	AEG.	AEG.	AEG.	AEG.	AEG.	AEG.	AEG.	AEG.	AEG.	AEG.	AEG.	AEG.
ADJECTIVAL	tit	tit	tit		tit	tit	tit	tit	tit	tit	tit	
MODIFIER:												

APPENDIX IIE

AMPHIBOLES - 129 partial analyses

<u>Key to Abbreviations</u>

FE-ED	Ferro-edenite
FE-ACT-HO	Ferro-actinolitic-hornblende
FE-BAR	Ferro-barroisite
KATO	Katophorite
FE-RICH	Ferro-richterite
FE-WIN	Ferro-winchite
FE-ACT	Ferro-actinolite
ARFV	Arfvedsonite
RIEB	Riebeckite
CROSS	Crossite
sub-cal	sub-calcic
sodian	
tit	titanian
pot	potassian
calc	calcian

AMPHIBOLES

	D1014						D1014			
wt.%	1A	1B	1C	1D	1E	1F	2A	2B	2C	2D
SiO2	48.710	48.573	49.041	45.576	47.875	47.576	49.293	48.694	48.927	48.411
AL2O3	3.296	3.535	3.797	3.599	3.574	3.383	2.497	2.663	2.548	3.166
TiO2	1.557	1.581	1.698	1.763	1.646	1.596	1.386	1.455	1.064	1.544
ΣFe as FeO	24.253	23.919	22.160	22.293	24.485	24.004	25.773	25.380	24.845	24.417
MgO	8.111	8.314	8.999	8.534	7.948	7.616	7.078	6.919	7.818	7.897
MnO	0.398	0.471	0.423	0.441	0.514	0.440	0.532	0.508	0.471	0.561
CaO	8.534	8.763	8.923	8.715	8.319	8.581	7.933	8.095	8.612	8.137
Na2O	3.513	3.360	3.398	3.217	3.617	2.958	3.448	3.242	2.745	3.660
K2O	1.019	1.045	1.052	1.015	0.948	0.996	0.786	0.901	0.872	0.961
CL	0.078	0.085	-	-	0.111	0.073	0.085	0.084	-	0.090
TOTAL	99.469	99.647	99.491	97.153	99.036	97.224	98.810	97.942	97.273	98.845

NUMBER OF IONS ON THE BASIS OF 23 OXYGENS AND C + T = 13 CATIONS

Si	7.323	7.281	7.320	7.149	7.230	7.314	7.466	7.457	7.393	7.321
AL	0.584	0.625	0.668	0.666	0.636	0.613	0.446	0.481	0.460	0.564
Ti	0.176	0.178	0.191	0.208	0.187	0.184	0.158	0.168	0.123	0.176
Fe+3	0.450	0.465	0.273	0.510	0.596	0.486	0.568	0.476	0.700	0.540
Fe+2	2.600	2.534	2.493	2.414	2.496	2.600	2.697	2.774	2.481	2.540
Mg	1.817	1.857	2.002	1.995	1.789	1.745	1.598	1.579	1.783	1.780
Mn	0.051	0.060	0.054	0.059	0.066	0.057	0.068	0.066	0.061	0.072
Ca	1.375	1.408	1.427	1.465	1.346	1.414	1.287	1.328	1.413	1.318
Na	1.024	0.977	0.983	0.978	1.059	0.882	1.013	0.963	0.815	1.073
K	0.195	0.200	0.200	0.203	0.183	0.195	0.152	0.176	0.170	0.185
LOCUS:	non-dir		rim ←	core →		rim	rim ←	core →		rim
NAME:	FE-ED	FE-ED	FE-ED	FE-ED	FE-ED	FE-ACT-	FE-BAR	FE-BAR	FE-ACT-	KATO
ADJECTIVAL	sodian	sub-cal	sub-cal	sub-cal	sodian	HO			HO	
MODIFIER:	sub-cal				sub-cal	sub-cal			sub-cal	

AMPHIBOLES

	D1014		D1014			D1014		
wt.%	3A	3B	4A	4B	4C	5A	5B	5C
Si02	49.843	48.648	48.353	49.490	49.264	52.079	52.839	51.895
AL203	2.470	3.113	2.571	2.099	2.285	0.314	0.517	0.489
Ti02	1.471	1.594	1.304	1.298	1.235	0.288	0.297	0.267
ΣFe as Fe0	25.602	24.536	25.830	26.075	26.393	29.467	27.902	27.969
Mg0	7.039	7.772	6.803	7.323	6.923	6.293	6.553	6.184
Mn0	0.514	0.454	0.585	0.598	0.576	1.519	1.222	1.373
Ca0	7.899	8.297	7.379	7.918	7.672	6.257	6.691	6.736
Na20	3.762	3.272	2.965	3.572	3.144	2.427	2.652	2.495
K20	0.820	0.909	0.850	0.821	0.770	0.417	0.445	0.412
CL	0.081	0.099	0.066	0.081	-	-	-	-
TOTAL	99.502	98.694	96.711	99.276	98.263	99.061	99.117	97.820

NUMBER OF IONS ON THE BASIS OF 23 OXYGENS AND C + T = 13 CATIONS

	3A	3B	4A	4B	4C	5A	5B	5C
Si	7.517	7.353	7.430	7.466	7.467	7.696	7.823	7.804
AL	0.439	0.555	0.466	0.373	0.408	0.055	0.090	0.087
Ti	0.167	0.181	0.151	0.147	0.141	0.032	0.033	0.030
Fe+3	0.382	0.554	0.892	0.636	0.811	1.735	1.230	1.267
Fe+2	2.847	2.548	2.427	2.654	2.535	1.907	2.225	2.251
Mg	1.582	1.751	1.558	1.647	1.564	1.386	1.446	1.386
Mu	0.066	0.058	0.076	0.076	0.074	0.190	0.153	0.175
Ca	1.277	1.344	1.215	1.280	1.246	0.991	1.061	1.086
Na	1.100	0.959	0.883	1.045	0.924	0.695	0.761	0.728
K	0.158	0.175	0.617	0.158	0.149	0.079	0.084	0.079
LOCUS:	non-dir		rim ←	core	→ rim	non-dir		
NAME:	FE-RICH	FE-ACT-	FE-BAR	FE-BAR	FE-BAR	FE-WIN	FE-WIN	FE-WIN
ADJECTIVAL		HO						
MODIFIER:		sub-cal						

AMPHIBOLES

	D1014				D1014		D916		
wt.%	6A	6B	6C	6D	7A	7B	1A	1B	1C
SiO2	51.651	50.263	50.483	51.835	51.534	52.285	51.029	49.972	49.466
AL2O3	0.613	0.511	0.513	0.428	0.611	0.335	1.608	1.802	1.599
TiO2	0.189	0.256	0.257	0.316	0.306	0.145	1.223	1.462	1.537
ΣFe as FeO	27.522	27.285	27.395	26.864	26.023	26.355	27.8790	30.345	31.107
MgO	5.610	5.680	5.705	6.560	6.791	7.099	5.217	3.813	3.180
MnO	1.023	0.898	0.901	0.942	0.607	0.602	0.562	0.569	0.579
CaO	6.852	7.116	7.146	8.021	10.112	9.908	7.391	6.847	6.393
Na2O	3.020	3.379	3.393	2.614	1.260	1.410	3.282	4.038	4.343
K2O	0.590	0.621	0.624	0.381	0.360	0.348	1.001	1.063	1.128
CL	-	-	-	-	-	-	0.068	0.113	-
TOTAL	97.072	96.008	96.417	97.962	97.305	98.488	99.260	100.024	99.332

NUMBER OF IONS ON THE BASIS OF 23 OXYGENS AND C + T = 13 CATIONS

	6A	6B	6C	6D	7A	7B	1A	1B	1C
Si	7.922	7.863	7.864	7.870	7.874	7.911	7.767	7.666	7.678
AL	0.111	0.094	0.094	0.077	0.111	0.060	0.289	0.326	0.293
Ti	0.022	0.030	0.030	0.036	0.035	0.017	0.140	0.169	0.179
Fe+3	0.736	0.586	0.584	0.657	0.293	0.392	0.324	0.344	0.335
Fe+2	2.794	2.984	2.985	2.754	3.052	2.943	3.225	3.550	3.803
Mg	1.282	1.324	1.324	1.484	1.556	1.601	1.183	0.872	0.736
Mn	0.133	0.119	0.119	0.121	0.080	0.077	0.073	0.074	0.076
Ca	1.126	1.193	1.193	1.305	1.665	1.606	1.205	1.126	1.063
Na	0.898	1.025	1.025	0.770	0.376	0.414	0.969	1.201	1.307
K	0.115	0.124	0.124	0.074	0.071	0.067	0.194	0.208	0.223
LOCUS:	rim ← core → rim				non-dir		rim ← core → rim		
NAME:	FE-WIN	FE-WIN	FE-WIN	FE-WIN	FE-ACT	FE-ACT	FE-WIN	FE-RICH	FE-RICH
ADJECTIVAL MODIFIER:								Sodian	Sodian

AMPHIBOLES

	D916				D916			
wt.%	2A	2B	2C	2D	3A	3B	3C	3D
SiO2	52.769	49.777	49.677	49.612	50.227	49.430	51.804	50.912
AL203	1.091	1.837	1.559	1.679	1.760	1.469	0.349	1.474
TiO2	0.556	1.225	1.251	1.482	1.409	1.446	-	0.679
ΣFe as FeO	27.411	27.296	26.882	27.814	29.942	28.972	32.369	30.528
MgO	4.606	4.925	5.822	5.518	4.117	4.388	3.965	3.863
MnO	1.215	0.485	0.487	0.556	0.463	0.481	1.744	1.031
CaO	7.438	7.221	7.282	7.324	7.079	7.064	6.823	7.330
Na20	1.686	3.181	3.333	3.038	3.737	3.401	1.379	2.277
K20	0.393	1.082	1.013	0.868	1.064	0.952	0.166	0.786
CL	-	0.068	0.100	-	0.102	0.075	0.093	0.110
TOTAL	97.164	97.095	97.407	97.892	99.899	97.678	98.693	98.991

NUMBER OF IONS ON THE BASIS OF 23 OXYGENS AND C + T = 13 CATIONS

	2A	2B	2C	2D	3A	3B	3C	3D
Si	8.043	7.755	7.686	7.618	7.688	7.703	7.770	7.757
AL	0.196	0.337	0.284	0.304	0.318	0.270	0.062	0.265
Ti	0.064	0.144	0.146	0.171	0.162	0.170	-	0.078
Fe+3	0.586	0.279	0.439	0.633	0.343	0.411	1.772	0.847
Fe+2	2.908	3.278	3.039	2.939	3.490	3.365	2.288	3.044
Mg	1.046	1.444	1.342	1.263	0.939	1.019	0.886	0.877
Mn	0.157	0.064	0.064	0.072	0.060	0.064	0.222	0.133
Ca	1.215	1.205	1.207	1.205	1.161	1.180	1.097	1.197
Na	0.498	0.961	1.000	0.905	1.109	1.028	0.40	0.673
K	0.076	0.215	1.000	0.170	0.208	0.189	0.032	0.153
LOCUS:	rim ←	core		→ rim	rim ←	core		→ rim
NAME:	FE-ACT	FE-WIN	FE-WIN	FE-WIN	FE-WIN	FE-WIN	FE-ACT	FE-WIN
ADJECTIVAL	sub-cal						sub-cal	
MODIFIER:								

AMPHIBOLES

	D110			D110			D110		
wt.%	1A	1B	1C	2A	2B	2C	3A	3B	3C
SiO_2	50.327	51.230	51.264	50.795	49.696	50.919	49.167	49.955	49.347
AL_2O_3	1.434	1.345	1.424	1.309	1.253	1.147	1.236	1.225	1.260
TiO_2	1.974	2.123	1.938	2.276	2.220	2.313	2.416	2.586	2.546
ΣFe as FeO	26.007	26.336	26.159	27.608	27.876	28.356	31.413	31.117	31.305
MgO	5.774	5.897	5.566	4.894	4.629	4.619	1.695	2.264	2.347
MnO	0.490	0.570	0.632	0.638	0.640	0.609	0.872	0.892	0.993
CAO	6.086	5.900	5.569	5.535	5.539	5.204	4.697	5.060	4.657
Na_2O	5.087	5.262	5.473	5.666	5.481	5.726	5.222	5.580	5.538
K_2O	1.178	1.175	1.233	1.249	1.229	1.272	1.198	1.260	1.165
Cr_2O_3	-	-	-	-	-	-	-	-	-
CL	-	-	-	0.068	-	0.095	0.083	-	0.086
TOTAL	98.357	99.836	99.258	100.037	98.562	100.260	97.999	99.938	99.444

NUMBER OF IONS ON THE BASIS OF 23 OXYGENS AND C + T = 13 CATIONS

	1A	1B	1C	2A	2B	2C	3A	3B	3C
Si	7.764	7.770	7.830	7.771	7.728	7.776	7.797	7.778	7.717
AL	0.261	0.241	0.256	0.236	0.230	0.207	0.231	0.225	0.231
Ti	0.229	0.242	0.223	0.262	0.260	0.266	0.288	0.303	0.298
Fe^{+3}	-	0.042	-	-	0.052	0.063	0.155	-	0.280
Fe^{+2}	3.355	3.299	3.342	3.532	3.573	3.558	4.012	4.052	3.798
Mg	1.327	1.333	1.267	1.116	1.073	1.051	0.401	0.525	0.545
Mn	0.064	0.073	0.082	0.083	0.084	0.079	0.117	0.118	0.131
Ca	1.006	0.959	0.912	0.907	0.923	0.852	0.798	0.844	0.777
Na	1.522	1.548	1.621	1.681	1.653	1.696	1.606	1.685	1.673
K	0.232	0.227	0.240	0.244	0.244	0.248	0.242	0.250	0.232
Cr	-	-	-	-	-	-	-	-	-
LOCUS:	core	→	rim	core	→	rim	core	→	rim
NAME:	FE-RICH	FE-RICH	FE-RICH	FE-RICH	FE-RICH	FE-RICH	FE-RICH	FE-RICH	FE-RICH
ADJECTIVAL				tit	tit	tit	tit	tit	tit
MODIFIER:								pot	

AMPHIBOLES

	D110		D110	
wt.%	4A	4B	5A	5B
Si02	49.092	49.346	50.073	48.963
AL203	1.428	1.356	1.337	1.211
Ti02	2.613	2.464	2.135	1.978
ΣFe as FeO	32.493	31.463	27.637	28.855
MgO	1.563	1.633	4.570	3.699
MnO	0.964	0.673	0.831	0.854
CaO	4.583	4.494	5.562	5.444
Na20	5.510	5.838	5.061	4.408
K20	1.171	1.262	1.171	1.182
Cr203	-	-	-	0.121
CL	0.080	-	-	0.070
TOTAL	99.495	98.528	98.377	96.785

NUMBER OF IONS ON THE BASIS OF 23 OXYGENS AND C + T = 13 CATIONS

	4A	4B	5A	5B
Si	7.683	7.812	7.760	7.730
AL	0.26	0.253	0.244	0.225
Ti	0.30	0.293	0.249	0.235
Fe+3	0.311	-	0.138	0.400
Fe+2	3.94	4.166	3.444	3.410
Mg	0.36	0.385	1.056	0.830
Mn	0.12	0.090	0.109	0.114
Ca	0.76	0.762	0.924	0.921
Na	1.672	1.792	1.521	1.349
K	0.23	0.255	0.232	0.238
Cr	-	-	-	0.015
LOCUS:	core →	rim	core →	rim
NAME:	FE-RICH	FE-RICH	FE-RICH	FE-RICH
ADJECTIVAL	tit	tit	tit	
MODIFIER:		pot		

AMPHIBOLES

	D275		D275	D275		D275	D275	
wt.%	1A*	1B	2A*	3A	3B	4A	6A	6B
SiO2	48.916	48.477	48.998	49.382	49.331	49.370	47.230	48.496
AL2O3	1.638	1.674	1.875	1.523	1.364	1.454	1.722	1.466
TiO2	2.087	2.008	2.066	1.841	1.853	1.914	2.047	2.029
ΣFe as FeO	32.149	32.291	31.819	32.623	32.490	32.617	31.818	31.408
MgO	0.523	0.441	0.790	0.505	0.703	0.444	0.991	1.201
MnO	1.102	1.064	0.999	1.121	1.166	1.162	1.013	1.097
CaO	5.710	5.673	4.847	4.863	4.582	4.881	5.181	4.590
Na2O	5.666	6.508	6.482	6.479	6.492	6.675	6.312	6.478
K2O	1.159	1.188	1.326	1.505	1.542	1.490	1.333	1.475
CL	-	0.074	-	-	-	-	0.078	-
TOTAL	98.949	99.398	99.203	99.842	99.524	100.124	97.725	98.242
NUMBER OF IONS ON THE BASIS OF 23 OXYGENS AND 16 CATIONS								
Si	7.769	7.700	7.751	7.804	7.814	7.770	7.615	7.752
AL	0.307	0.313	0.350	0.284	0.255	0.270	0.327	0.276
Ti	0.249	0.240	0.246	0.219	0.221	0.226	0.248	0.244
Fe+3	*	0.05	*	-	-	0.101	0.194	0.041
Fe+2	4.270	4.236	4.211	4.312	4.304	4.190	4.100	4.158
Mg	0.124	0.104	0.186	0.119	0.166	0.104	0.238	0.286
Mn	0.148	0.143	0.134	0.150	0.157	0.155	0.138	0.149
Ca	0.972	0.966	0.829	0.824	0.778	0.822	0.895	0.786
Na	1.745	2.004	1.989	1.985	1.994	2.063	1.973	2.008
K	0.235	0.24	0.268	0.303	0.312	0.299	0.274	0.301
C + T	12.8671	12.7896	12.8780	12.8876	12.9167	12.8151	12.8573	12.9053
LOCUS:	non-dir			non-dir			non-dir	
NAME:	FE-RICH	FE-RICH	FE-RICH	FE-RICH	FE-RICH	FE-RICH	FE-RICH	FE-RICH
ADJECTIVAL	tit		pot	pot	pot	pot	pot	pot
MODIFIER:							tit	

*Normalised to 23 oxygens only

AMPHIBOLES

	D275		D275					D275		
wt.%	8A	8B	5A	5B*	5C	5D*	5E*	7A*	7B	7C
SiO2	48.914	48.695	47.574	47.450	47.474	48.432	48.222	48.692	47.744	48.423
AL2O3	1.201	1.314	1.717	1.695	1.801	1.560	1.614	1.518	1.610	1.652
TiO2	1.753	1.494	1.988	2.024	1.962	2.091	2.255	1.927	2.063	2.068
ΣFe as FeO	32.485	32.590	31.455	31.449	31.953	31.919	31.749	30.981	31.706	31.666
MgO	0.540	0.594	1.165	0.509	0.934	1.283	0.880	1.211	0.933	0.853
MnO	1.051	1.238	1.125	1.077	1.002	1.092	1.098	1.133	1.043	1.007
CaO	5.324	5.354	5.737	5.191	4.861	5.712	5.750	5.278	5.151	5.372
Na2O	6.428	6.402	6.226	6.168	6.098	5.825	6.077	6.149	6.266	6.475
K2O	1.246	1.173	1.259	1.245	1.439	1.150	1.140	1.416	1.412	1.389
CL	-	-	-	-	0.081	-	0.093	0.071	0.069	0.076
TOTAL	98.943	98.855	98.250	96.808	97.606	99.064	98.882	98.377	97.998	98.975

NUMBER OF IONS ON THE BASIS OF 23 OXYGENS AND 16 CATIONS

	8A	8B	5A	5B*	5C	5D*	5E*	7A*	7B	7C
Si	7.805	7.775	7.619	7.726	7.680	7.693	7.688	7.769	7.681	7.700
AL	0.226	0.247	0.324	0.325	0.344	0.292	0.303	0.286	0.305	0.310
Ti	0.210	0.179	0.239	0.248	0.239	0.250	0.270	0.231	0.250	0.247
Fe+3	-	0.064	0.150	*	0.029	*	*	*	0.078	0.074
Fe+2	4.335	4.288	4.063	4.283	4.294	4.240	4.233	4.134	4.188	4.138
Mg	0.128	0.141	0.278	0.124	0.225	0.304	0.209	0.288	0.224	0.202
Mn	0.142	0.167	0.153	0.149	0.137	0.147	0.148	0.153	0.142	0.136
Ca	0.910	0.916	0.984	0.906	0.843	0.972	0.982	0.902	0.888	0.915
Na	1.989	1.982	1.933	1.947	1.913	1.794	1.879	1.902	1.955	1.997
K	0.254	0.239	0.257	0.259	0.297	0.233	0.232	0.288	0.290	0.282
C + T	12.8472	12.8630	12.8253	12.8543	12.9477	12.9255	12.8525	12.8600	12.8676	12.8063
LOCUS:	non-dir			non-dir		core ⟶ rim			non-dir	
NAME:	FE-RICH	FE-RICH	FE-RICH	FE-RICH	FE-RICH	FE-RICH	FE-RICH	FE-RICH	FE-RICH	FE-RICH
ADJECTIVAL	pot	pot	pot	pot	pot	tit	tit	pot	pot	pot
MODIFIER:				tit					tit	tit

*Normalised to 23 oxygens only

AMPHIBOLES

	D275			D204			D204	
wt.%	9A*	9B*	9C	1A	1B	1C	2A	2B
SiO2	47.922	46.150	46.061	49.299	49.681	50.593	52.265	52.117
AL2O3	1.648	1.727	1.651	0.329	0.414	0.552	0.612	-
TiO2	2.052	1.950	1.929	1.045	1.218	1.064	0.319	0.370
ΣFe as FeO	32.008	31.486	31.245	33.637	33.366	33.790	34.425	36.580
MgO	0.530	0.864	0.733	0.544	0.549	0.465	0.234	0.281
MnO	1.076	1.000	0.977	1.360	1.380	1.271	0.851	0.276
CaO	5.537	5.374	4.990	2.050	2.029	1.954	1.604	0.876
Na2O	6.185	5.713	6.686	7.278	7.969	7.677	6.703	7.115
K2O	1.187	1.115	1.297	1.350	1.452	1.498	0.539	0.252
CL	0.070	0.082	0.080	-	-	-	-	-
TOTAL	98.215	95.461	95.649	96.893	98.058	98.864	97.553	97.867

NUMBER OF IONS ON THE BASIS OF 23 OXYGENS AND 16 CATIONS (ARFV) OR C+T = 13 CATIONS (RIEB)

	9A*	9B*	9C	1A	1B	1C	2A	2B
Si	7.708	7.650	7.561	8.000	7.913	8.018	8.178	8.100
AL	0.313	0.338	0.320	0.063	0.078	0.103	0.113	-
Ti	0.248	0.243	0.239	0.128	0.146	0.127	0.038	0.043
Fe+3	*	*	0.483	0.252	0.561	0.270	0.778	1.227
Fe+2	4.301	4.365	3.807	4.314	3.884	4.209	3.727	3.529
Mg	0.127	0.213	0.180	0.132	0.130	0.120	0.055	0.065
Mn	0.147	0.140	0.136	0.187	0.186	0.171	0.113	0.036
Ca	0.954	0.954	0.878	0.357	0.346	0.332	0.269	0.144
Na	1.929	1.836	2.128	2.290	2.461	2.359	2.034	2.144
K	0.244	0.236	0.272	0.280	0.295	0.303	0.108	0.050
C + T	12.8474	12.9484	12.7227	13.0739	12.8975	13.0063		
LOCUS:	core →		rim	rim ←	core	→ rim	non-dir	
NAME:	FE-RICH	FE-RICH	FE-RICH	ARFV	ARFV	ARFV	RIEB	RIEB
ADJECTIVAL MODIFIER:	tit		pot					

*Normalised to 23 oxygens only.

AMPHIBOLES

	D433		D433			D433			
wt.%	1A	1B	2A	2B	2C	3A	3B	3C	3D
SiO2	48.804	46.734	47.355	47.042	46.912	46.548	46.977	47.666	49.481
AL2O3	2.937	4.313	4.282	4.473	4.354	4.192	4.549	4.277	2.937
TiO2	1.545	2.098	2.466	2.363	2.546	2.267	2.428	2.324	2.055
ΣFe as FeO	25.812	26.668	27.368	27.096	27.605	27.062	27.740	27.957	27.263
MgO	4.994	4.185	3.894	4.237	3.890	3.763	4.116	3.801	4.692
MnO	1.241	1.190	1.186	1.143	1.142	1.000	1.172	1.244	1.131
CaO	3.556	3.685	4.057	4.089	3.822	3.949	4.208	4.130	3.745
Na2O	6.920	6.844	6.871	7.248	7.113	6.749	6.944	7.108	7.378
K2O	1.582	1.522	1.576	1.525	1.615	1.521	1.545	1.452	1.684
Cr2O3	-	-	-	-	-	-	-	-	-
ZrO2	-	-	-	-	-	-	-	0.190	-
TOTAL	97.392	97.240	99.055	99.216	99.000	97.151	99.678	100.147	100.365

NUMBER OF IONS ON THE BASIS OF 23 OXYGENS AND 16 CATIONS

Si	7.599	7.323	7.311	7.208	7.234	7.335	7.199	7.284	7.490
AL	0.539	0.797	0.779	0.808	0.792	0.779	0.822	0.771	0.524
Ti	0.181	0.247	0.286	0.272	0.295	0.269	0.280	0.267	0.234
Fe+3	0.304	0.446	0.393	0.682	0.595	0.383	0.586	0.489	0.520
Fe+2	3.057	3.049	3.141	2.790	2.966	3.184	2.967	3.084	2.932
Mg	1.159	0.977	0.896	0.968	0.894	0.884	0.940	0.866	1.058
Mn	0.164	0.158	0.155	0.148	0.149	0.134	0.152	0.161	0.145
Ca	0.593	0.619	0.671	0.671	0.632	0.667	0.691	0.676	0.607
Na	2.089	2.080	2.057	2.154	2.127	2.062	2.062	2.106	2.165
K	0.314	0.304	0.310	0.298	0.318	0.306	0.302	0.283	0.325
Cr	-	-	-	-	-	-	-	-	-
Zr	-	-	-	-	-	-	-	0.014	-
C + T	13.0031	12.9974	12.9615	12.8770	12.9241	12.9654	12.9451	12.9347	12.9020
LOCUS:	non-dir		rim ←	core	→ rim		core	→	→ rim
NAME:	ARFV	ARFV	KATO	KATO	ARFV	KATO	KATO	KATO	ARFV
ADJECTIVAL	pot	pot	pot	pot	pot	pot	pot	pot	pot
MODIFIER:	calc	calc tit	tit	tit	calc tit	tit	tit	tit	calc

AMPHIBOLES

	D433			D433	D433	
wt.%	4A	4B	4C	5	6A	6B
Si02	46.719	48.116	47.571	47.521	52.365	51.155
AL203	4.216	4.079	4.034	4.159	2.324	1.744
Ti02	1.611	1.708	1.690	2.092	0.198	0.794
ΣFe as Fe0	27.625	28.315	28.025	27.429	27.840	29.965
Mg0	4.012	4.079	4.034	4.042	3.224	3.276
Mn0	1.042	1.025	1.015	1.181	0.893	0.941
Ca0	3.697	3.814	3.773	3.957	2.484	2.382
Na20	6.616	7.378	7.301	7.094	5.386	6.428
K20	1.580	1.562	1.545	1.517	1.464	0.763
Cr203	-	0.117	0.116	-	-	-
Zr02	-	-	-	-	-	-
TOTAL	97.120	100.193	99.103	98.993	96.180	97.448

	NUMBER OF IONS ON THE BASIS OF 23 OXYGENS AND 16 CATIONS				NUMBER OF IONS ON THE BASIS OF 23 OXYGENS AND C + T = 13 CATIONS	
Si	7.352	7.310	7.307	7.320	8.095	7.866
AL	0.782	0.731	0.731	0.755	0.424	0.316
Ti	0.191	0.195	0.195	0.242	0.023	0.092
Fe+3	0.468	0.721	0.729	0.532	0.615	0.918
Fe+2	3.168	2.876	2.871	2.993	2.984	2.935
Mg	0.941	0.924	0.923	0.928	0.743	0.751
Mn	0.139	0.132	0.132	0.154	0.117	0.123
Ca	0.623	0.621	0.621	0.653	0.411	0.392
Na	2.019	2.173	2.174	2.118	1.614	1.916
K	0.317	0.303	0.303	0.298	0.289	0.150
Cr	-	0.014	0.014	-	-	-
Zr	-	-	-	-	-	-
C + T	13.0406	12.9030	12.9020	12.9305		
LOCUS:		non-dir				
NAME:	ARFV	ARFV	ARFV	ARFV	CROSS	RIEB
ADJECTIVAL	pot	pot	pot	pot	pot	
MODIFIER:	calc	calc	calc	calc		

AMPHIBOLES

	D1057		D1057			D1057	
wt.%	1A	1B	2A	2B	2C	3A	3B
Si02	50.448	50.020	50.324	49.740	50.980	48.766	42.274
AL203	0.374	0.541	0.548	0.575	0.563	0.888	1.004
Ti02	1.927	1.691	1.972	1.898	1.568	1.525	1.739
ΣFe as Fe0	33.954	33.325	33.529	33.179	33.363	33.481	32.859
Mg0	0.252	0.395	0.278	-	0.247	-	0.251
Mn0	1.139	1.094	0.983	1.069	1.179	1.1400	1.089
Ca0	3.186	3.496	3.417	2.945	2.771	5.318	5.258
Na20	7.922	7.638	7.685	7.995	7.947	6.315	6.069
K20	1.551	1.552	1.673	1.531	1.557	1.146	1.176
Cr203	-	-	-	-	-	-	-
CL	-	-	-	-	-	-	0.081
TOTAL	100.753	99.754	100.428	98.931	100.176	98.579	96.800

NUMBER OF IONS ON THE BASIS OF 23 OXYGENS AND 16 CATIONS

	1A	1B	2A	2B	2C	3A	3B
Si	7.850	7.858	7.860	7.871	7.961	7.855	7.762
AL	0.069	0.100	0.101	0.107	0.104	0.169	0.194
Ti	0.226	0.200	0.232	0.22	0.184	0.185	0.215
Fe+3	0.479	0.422	0.376	0.461	0.322	-	0.030
Fe+2	3.939	3.956	4.004	3.930	4.035	4.510	4.482
Mg	0.058	0.093	0.065	-	0.058	-	0.061
Mn	0.150	0.146	0.130	0.143	0.156	0.156	0.152
Ca	0.531	0.590	0.572	0.499	0.464	0.918	0.925
Na	2.390	2.327	2.328	2.453	2.406	1.972	1.932
K	0.308	0.311	0.333	0.309	0.310	0.235	0.246
Cr	-	-	-	-	-	-	-
C + T	12.7707	12.7740	12.7673	12.7385	12.8199	12.8742	12.8963
LOCUS:	core ——→	rim	rim ←——	core ——→	rim	core ——→	rim
NAME:	ARFV	ARFV	ARFV	ARFV	ARFV	FE-RICH	FE-RICH
ADJECTIVAL	calc	calc	calc	calc			
MODIFIER:	pot	pot	pot	pot	pot		

AMPHIBOLES

	D1057			D1057	
wt.%	4A	4B	4C	5A	5B
SiO_2	47.758	47.984	48.904	48.343	48.850
AL_2O_3	1.321	0.914	0.761	1.481	1.520
TiO_2	1.914	1.683	1.487	2.045	2.184
ΣFe as FeO	33.847	33.800	33.496	32.913	32.426
MgO	0.233	0.271	0.230	1.330	1.243
mnO	1.120	1.281	1.125	0.932	0.841
CaO	5.605	5.292	4.758	6.384	6.299
Na_2O	6.348	6.394	6.302	5.745	6.120
K_2O	1.148	1.229	1.302	1.100	1.172
Cr_2O_3	0.120	-	-	-	-
CL	-	-	0.094	0.104	-
TOTAL	99.414	98.847	98.458	100.378	100.756

NUMBER OF IONS ON THE BASIS OF 23 OXYGENS AND 16 CATIONS

Si	7.624	7.699	7.887	7.635	7.657
AL	0.249	0.173	0.145	0.276	0.281
Ti	0.230	0.203	0.180	0.243	0.257
Fe+3	0.228	0.264	-	-	-
Fe+2	4.291	4.272	4.518	4.347	4.251
Mg	0.055	0.065	0.055	0.313	0.290
Mn	0.151	0.174	0.154	0.125	0.112
Ca	0.959	0.910	0.822	1.080	1.058
Na	1.965	1.989	1.971	1.759	1.860
K	0.234	0.252	0.268	0.222	0.234
Cr	0.015	-	-	-	-
C + T	12.843	12.8494	12.9392	12.9387	12.8478
LOCUS:	core	→	rim		
NAME:	FE-RICH	FE-RICH	FE-RICH	FE-RICH	FE-RICH
ADJECTIVAL		pot	pot		tit
MODIFIER:					

AMPHIBOLES

	D145					D145				
wt.%	1A	1B	1C	1D	1E	2A	2B	2C	2D	2E
Si02	50.025	49.848	49.452	49.855	49.393	49.414	51.236	50.705	51.450	51.074
AL203	0.460	0.261	0.311	-	0.227	-	-	-	-	0.292
Ti02	1.348	1.239	0.990	1.567	1.437	1.486	1.524	1.035	1.731	1.366
ΣFe as FeO	35.052	35.033	35.175	34.300	34.161	33.716	34.412	35.363	34.270	34.680
Mn0	0.861	0.677	0.660	0.647	0.828	1.257	1.357	0.646	0.669	0.653
Ca0	2.513	2.692	3.590	1.549	1.797	2.197	1.593	1.917	1.580	1.747
Na20	7.102	7.471	7.503	7.654	7.960	8.265	8.000	8.260	8.251	8.303
K20	1.704	1.691	1.421	1.830	1.713	1.784	1.976	1.584	1.960	1.511
CL	-	-	-	-	-	-	-	-	-	0.075
TOTAL	99.065	98.913	99.102	97.402	97.515	98.118	100.099	99.511	99.911	99.701
NUMBER OF IONS ON THE BASIS OF 23 OXYGENS AND 16 CATIONS										
Si	7.983	7.937	7.854	8.049	7.938	7.871	8.033	7.997	8.057	8.019
AL	0.087	0.049	0.058	-	0.043	-	-	-	-	0.054
Ti	0.162	0.148	0.118	0.190	0.174	0.178	0.180	0.123	0.204	0.161
Fe+3	0.168	0.431	0.597	0.295	0.565	0.818	0.402	0.638	0.375	0.415
Fe+2	4.510	4.235	4.075	4.337	4.026	3.674	4.110	4.015	4.113	4.139
Mn	0.116	0.091	0.089	0.089	0.113	0.170	0.180	0.086	0.08	0.087
Ca	0.430	0.459	0.611	0.268	0.309	0.375	0.268	0.323	0.265	0.294
Na	2.198	2.307	2.311	2.396	2.481	2.553	2.432	2.520	2.505	2.528
K	0.347	0.344	0.288	0.377	0.351	0.363	0.395	0.317	0.392	0.303
C + T	13.0257	12.8907	12.7907	12.9591	12.8589	12.7128	12.9051	12.8591	12.8379	12.8755
LOCUS:	rim ←		core		→ rim	rim ←		core		→ rim
NAME:	ARFV	ARFV	ARFV	ARFV	ARFV	ARFV	ARFV	ARFV	ARFV	ARFV
ADJECTIVAL	pot	pot	pot	pot	pot	pot	pot	pot	pot	pot
MODIFIER:			calc							

AMPHIBOLES

	D145				D447				
wt.%	3A	3B	3C	3D	1A	1B	1C	1D	1E
SiO2	50.362	47.260	50.133	50.217	49.318	49.826	49.566	49.748	50.016
AL2O3	0.215	0.671	0.363	-	0.325	0.225	-	0.256	0.486
TiO2	1.277	1.008	0.962	1.486	1.402	1.488	1.490	1.533	1.567
ΣFe as FeO	35.085	34.523	34.213	34.841	33.452	33.818	34.236	33.859	33.863
MnO	0.929	0.846	0.930	0.693	0.975	0.661	0.670	0.863	0.982
CaO	1.919	3.794	2.945	1.796	3.379	2.621	2.411	2.852	2.746
Na2O	8.164	6.249	7.341	7.516	7.741	7.829	7.899	7.638	7.679
K2O	1.663	1.332	1.700	1.801	1.527	1.565	1.617	1.571	1.598
CL	-	-	-	-	-	-	-	-	-
TOTAL	99.613	95.684	98.586	98.349	98.119	98.033	97.889	98.321	98.934
NUMBER OF IONS ON THE BASIS OF 23 OXYGENS AND 16 CATIONS									
Si	7.922	7.854	8.002	8.046	7.880	7.969	7.943	7.950	7.940
AL	0.040	0.132	0.068	-	0.061	0.042	-	0.048	0.091
Ti	0.151	0.126	0.116	0.179	0.169	0.179	0.180	0.184	0.187
Fe+3	0.638	0.205	0.315	0.253	0.551	0.409	0.541	0.370	0.343
Fe+2	3.978	4.593	4.252	4.416	3.919	4.115	4.047	4.155	4.153
Mn	0.124	0.119	0.126	0.094	0.132	0.090	0.091	0.11	0.132
Ca	0.324	0.676	0.504	0.308	0.579	0.449	0.414	0.488	0.467
Na	2.490	2.014	2.272	2.335	2.398	2.428	2.454	2.36	2.364
K	0.334	0.282	0.346	0.368	0.311	0.319	0.331	0.320	0.324
C + T	12.8527	13.0285	12.8782	12.9884	12.7119	12.804	12.8011	12.8245	12.9052
LOCUS:	rim ←	core	→	rim	rim ←		core	→	rim
NAME:	ARFV	FE-RICH	ARFV	ARFV	ARFV	ARFV	ARFV	ARFV	ARFV
ADJECTIVAL	pot	pot	pot	pot	pot	pot	pot	pot	pot
MODIFIER:			calc		calc				

AMPHIBOLES

wt.%	D447						D447		
	2A	2B	2C	2D	2E	2F	3A	3B	3C
SiO2	51.414	50.685	49.336	49.335	48.156	51.476	50.513	50.010	49.947
AL203	0.208	-	0.695	0.693	0.725	0.290	0.433	0.573	0.428
TiO2	1.564	1.561	1.431	1.345	1.465	1.532	1.466	1.579	1.480
ΣFe as FeO	33.749	34.216	33.985	34.480	33.597	34.149	34.281	34.505	34.071
MgO	-	-	-	-	-	0.301	-	-	-
MnO	0.690	0.854	0.950	0.859	0.849	0.904	0.917	0.868	0.962
CaO	1.314	1.742	4.070	4.326	3.801	2.585	3.216	3.552	3.430
Na20	9.153	8.458	6.810	6.917	6.851	8.430	7.838	7.458	7.656
K20	1.684	1.504	1.370	1.368	1.480	1.618	1.576	1.459	1.460
TOTAL	99.775	99.019	98.645	99.324	96.923	101.284	100.241	100.004	99.434

NUMBER OF IONS ON THE BASIS OF 23 OXYGENS AND 16 CATIONS

	2A	2B	2C	2D	2E	2F	3A	3B	3C
Si	7.991	7.999	7.912	7.853	7.848	7.925	7.906	7.876	7.892
AL	0.038	-	0.131	0.30	0.139	0.053	0.080	0.106	0.080
Ti	0.183	0.185	0.173	0.161	0.180	0.177	0.173	0.187	0.176
Fe+3	0.707	0.523	0.098	0.255	0.278	0.577	0.456	0.338	0.424
Fe+2	3.679	3.993	4.460	4.335	4.301	3.820	4.031	4.207	4.079
Mg	-	-	-	-	-	0.069	-	-	-
Mn	0.091	0.114	0.129	0.116	0.117	0.118	0.122	0.116	0.129
Ca	0.219	0.295	0.699	0.738	0.664	0.426	0.539	0.599	0.581
Na	2.758	2.588	2.117	2.135	2.165	2.517	2.379	2.278	2.346
K	0.334	0.303	0.280	0.278	0.308	0.318	0.314	0.293	0.294
C + T	12.6889	12.8144	12.9028	12.8494	12.8636	12.7392	12.7674	12.8289	12.7792
LOCUS:	rim ←			core		→ rim	rim ←	core	→ rim
NAME:	ARFV	ARFV	FE-RICH	FE-RICH	FE-RICH	ARFV	ARFV	ARFV	ARFV
ADJECTIVAL	pot	pot	pot	pot	pot	pot	pot	pot	pot
MODIFIER:							calc	calc	calc

APPENDIX IIF

BIOTITES - 6 partial analyses

BIOTITES

	D433		D433		D433	
wt.%	1A	1B	2A	2B	3A	3B
SiO2	37.340	37.668	39.862	40.623	37.629	38.764
AL2O3	9.646	9.183	8.884	8.965	9.689	8.732
TiO2	4.212	3.846	2.358	2.360	4.070	2.735
ΣFe as FeO	32.160	30.586	25.636	25.651	32.347	31.152
MgO	4.099	4.687	7.667	7.913	3.825	4.574
MnO	0.897	1.035	1.321	1.279	0.988	0.939
CaO	-	-	0.122	0.165	-	0.336
Na2O	-	-	-	-	-	0.666
K2O	9.065	8.834	8.962	9.004	8.877	8.784
CL	-	-	-	-	-	0.073
TOTAL	97.418	95.840	94.811	95.960	97.426	96.754

NUMBER OF IONS ON THE BASIS OF 22 OXYGENS

Si	5.969	6.074	6.317	6.343	6.009	6.209
AL	1.818	1.746	1.660	1.650	1.824	1.649
Ti	0.506	0.466	0.281	0.277	0.489	0.329
Fe+2	4.299	4.125	3.398	3.350	4.320	4.173
Mg	0.976	1.126	1.811	1.841	0.910	1.092
Mn	0.121	0.141	0.177	0.169	0.134	0.127
Ca	-	-	0.021	0.028	-	0.058
Na	-	-	-	-	-	0.207
K	1.849	1.817	1.812	1.794	1.809	1.795

APPENDIX IIG

AENIGMATITES - 12 analyses

AENIGMATITES

	D204		D204									
wt.%	1A	1B	2A	2B	2C	2D	2E	2F	2G	2H	2I	2J
SiO2	42.011	42.430	41.784	40.783	41.953	41.852	42.093	41.405	41.557	40.147	41.530	41.691
AL2O3	-	-	-	0.221	-	-	-	-	-	0.204	-	0.305
TiO2	8.575	8.772	8.534	8.189	8.427	8.248	8.861	9.040	9.003	8.622	8.760	8.472
ΣFe as FeO	40.074	39.847	40.157	41.652	40.325	41.013	40.291	40.685	39.661	39.793	39.715	39.783
MnO	1.558	1.482	1.598	1.671	1.614	1.683	1.681	1.613	1.558	1.572	1.522	1.440
CaO	0.118	0.116	-	0.262	-	-	-	0.187	-	0.204	0.112	0.186
Na2O	7.989	7.420	8.044	7.743	8.055	7.775	7.941	8.035	8.166	7.706	7.662	7.862
K2O	-	-	-	-	-	-	-	-	-	-	-	0.078
TOTAL	100.325	100.067	100.117	100.521	100.374	100.571	100.867	100.965	99.944	98.247	99.301	99.817

NUMBER OF IONS ON THE BASIS OF 20 OXYGENS AND 14 CATIONS

	1A	1B	2A	2B	2C	2D	2E	2F	2G	2H	2I	2J
Si	5.946	6.054	5.931	5.782	5.933	5.927	5.936	5.833	5.898	5.816	5.958	5.928
AL	-	-	-	0.037	-	-	-	-	-	0.035	-	0.051
Ti	0.913	0.941	0.911	0.873	0.896	0.879	0.940	0.958	0.961	0.939	0.945	0.906
Fe+3	0.475	0.062	0.531	0.781	0.551	0.524	0.420	0.613	0.530	0.620	0.327	0.462
Fe+2	4.269	4.693	4.236	4.158	4.218	4.334	4.332	4.180	4.177	4.202	4.438	4.269
Mn	0.187	0.179	0.178	0.201	0.193	0.202	0.201	0.193	0.187	0.193	0.185	0.173
Ca	0.018	0.018	-	0.040	-	-	-	0.028	-	0.032	0.017	0.028
Na	2.193	2.053	2.219	2.129	2.209	2.135	2.171	2.195	2.247	2.165	2.131	2.168
K	-	-	-	-	-	-	-	-	-	-	-	0.014

APPENDIX IIH

FE-TI OXIDES - 22 analyses

Key to Abbreviations

IL	Ilmenite
MAG	Magnetite

FE-TI OXIDES

	D916			D916			
wt.%	1A	1B	1C	2A	2B	2C	2D
SiO2	2.974	3.009	1.451	1.074	1.483	1.170	1.243
Al2O3	0.570	0.577	0.359	0.213	0.929	1.332	0.486
TiO2	12.977	13.100	13.623	50.855	17.815	15.175	22.183
ΣFe as FeO	75.737	76.406	79.308	43.366	72.236	75.670	70.177
MgO	0.399	0.404	-	-	-	-	-
MnO	0.570	0.576	0.438	4.694	2.063	1.637	2.266
CaO	0.305	0.308	-	-	-	-	-
Total	93.532	94.380	95.180	100.20	94.526	94.983	96.354
FeO	44.69	66.69	44.96	42.26	46.85	44.80	50.67
Fe2O3	34.50	10.79	38.18	1.23	28.22	34.30	21.68
Si	0.114	0.098	0.055	0.027	0.057	0.045	0.047
Al	0.026	0.022	0.016	0.006	0.042	0.060	0.022
Ti	0.375	0.759	0.390	0.958	0.514	0.434	0.633
Fe+3	0.997	0.264	1.094	0.023	0.815	0.983	0.619
Fe+2	1.435	1.811	1.431	0.886	1.504	1.426	1.607
Mg	0.023	0.020	-	-	-	-	-
Mn	0.019	0.016	0.014	0.100	0.067	0.053	0.073
Ca	0.013	0.011	-	-	-	-	-
NAME:	MAG	MAG	MAG	IL	MAG	MAG	MAG

magnetites : calculated on the basis of 3 cations and 4 oxygens
ilmenites : calculated on the basis of 2 cations and 6 oxygens

FE-TI OXIDES

	D110		D110	
wt.%	1A	1B	2A	2B
SiO2	1.107	1.231	1.271	1.121
Al2O3	0.251	0.208	0.316	0.228
TiO2	50.991	51.202	51.050	51.400
ΣFe as FeO	45.690	45.360	44.047	43.832
MnO	2.165	2.315	2.373	2.496
Cr2O3	-	-	0.129	-
NiO	-	-	-	0.172
TOTAL	100.20	100.31	99.186	99.249
FeO	44.98	45.17	44.04	43.83
Fe2O3	0.78	0.21	-	-
Si	0.028	0.031	0.032	0.028
Al	0.007	0.006	0.009	0.007
Ti	0.961	0.964	0.972	0.979
Fe+3	0.015	0.004	-	-
Fe+2	0.943	0.946	0.953	0.951
Mn	0.046	0.049	0.051	0.054
Cr	-	-	0.003	-
Ni	-	-	-	0.004
NAME:	IL	IL	IL	IL

ilmenites : calculated on the basis of 2 cations and 6 oxygens

FE-TI OXIDES

	D433			D433	
wt.%	1A	1B	1C	2A	2B
SiO_2	3.982	1.276	10.929	3.406	2.123
Al_2O_3	0.414	0.310	2.866	0.472	0.386
TiO_2	47.799	51.065	36.367	11.181	16.154
ΣFe as FeO	41.968	41.542	38.092	73.078	75.056
MgO	-	-	0.805	-	-
MnO	4.865	6.213	4.805	1.340	1.763
CaO	0.115	-	-	0.131	-
NiO	-	-	-	0.183	-
TOTAL	99.143	100.40	93.864	89.791	95.612
FeO	41.97	41.15	38.09	42.28	46.76
Fe_2O_3	-	0.43	-	34.22	34.22
Si	0.100	0.032	0.277	0.136	0.081
Al	0.012	0.009	0.086	0.022	0.017
Ti	0.901	0.960	0.694	0.337	0.460
Fe^{+3}	-	0.008	-	1.031	0.907
Fe^{+2}	0.880	0.860	0.809	1.416	1.472
Mg	-	-	0.031	-	-
Mn	0.103	0.132	0.103	0.046	0.057
Ca	0.003	-	-	0.006	-
Ni	-	-	-	0.006	-
NAME:	IL	IL	IL	MAG	MAG

ilmenites : calculated on the basis of 2 cations and 6 oxygens

magnetites : calculated on the basis of 3 cations and 4 oxygens

FE-TI OXIDES

	D433		D433		D433	
wt.%	3A	3B	4A	4B	5A	5B
SiO2	1.242	1.237	1.293	1.356	1.377	1.330
Al2O3	-	0.217	0.334	0.277	0.259	0.306
TiO2	50.609	13.812	50.553	50.351	14.582	15.710
ΣFe as FeO	44.133	78.165	42.431	42.089	73.923	73.927
MgO	-	-	-	-	-	-
MnO	5.024	2.229	5.355	5.049	1.809	1.940
CaO	-	-	-	-	-	0.090
NiO	-	-	-	-	-	-
TOTAL	101.08	95.661	99.966	99.122	91.949	92.673
FeO	41.91	43.18	41.58	41.78	43.22	44.35
Fe2O3	2.48	38.88	0.94	0.34	34.12	32.86
Si	0.031	0.047	0.032	0.034	0.054	0.052
Al	-	0.010	0.010	0.008	0.012	0.014
Ti	0.946	0.394	0.954	0.958	0.433	0.463
Fe+3	0.046	1.109	0.018	0.006	1.014	0.956
Fe+2	0.871	1.369	0.872	0.884	1.427	1.447
Mg	-	-	-	-	-	-
Mn	0.106	0.072	0.114	0.108	0.061	0.064
Ca	-	-	-	-	-	0.004
Ni	-	-	-	-	-	-
NAME:	IL	MAG	IL	IL	MAG	MAG

ilmenites : calculated on the basis of 2 cations and 6 oxygens

magnetites : calculated on the basis of 3 cations and 4 oxygens

APPENDIX III

WHOLE-ROCK ANALYSES

APPENDIX IIIA

ANALYTICAL PROCEDURES AND USE OF U.S.G.S.STANDARDS

APPENDIX IIIA : ANALYTICAL PROCEDURES AND THE USE OF U.S.G.S. STANDARDS

1. Crushing Procedure

Sample preparation for whole-rock analysis was as follows. Between one and two KILO/grams of rock were crushed, depending on the grain size. The sample was split with a horizontal splitter and weathered surfaces were removed. Preliminary comminution of the resultant fragments was effected in a mechanical jaw-crusher. The material was transferred to a Tema mill equipped with a tungsten carbide barrel and milled for 15 seconds. Up to 10g of rock powder were then removed and set aside for ferrous iron determination. This procedure is in accordance with the recommendation of Fitton and Gill (1970) who, mindful of the need to obviate oxidation of FeO to Fe_2O_3, suggest 30 seconds as the outside limit for milling when a determination of Fe^{2+} is required. The remaining powder was returned to the mill and further ground until it passed through a 250µm mesh sieve. With resistant silicic rocks this involved up to 80 seconds milling. The sample was then thoroughly homogenised and quartered. Approximately 40g of the quartered material were again milled for another 40-80 seconds, producing a powder fine enough to pass through a 53µm sieve. Finally, the powders were rehomogenised and a 7g sample was used to prepare pressed pellets, backed with a boric acid support, for X.R.F. analysis.

2. X-Ray Flouresence Analysis

Ten major element oxides (SiO_2, Al_2O_3, total iron as Fe_2O_3, MgO, CaO, Na_2O, K_2O, TiO_2, MnO and P_2O_5), together with ten trace elements (Ga, Rb, Sr, Y, Zr, Nb, Ba, La, Ce and Nd), were analysed for using a Phillips PW 1540 x-ray flouresence spectrometer. One pressed pellet per rock sample was used for all determinations. Machine operating conditions and computations of raw count data followed the procedures of Brown *et al*., (1973). The use of pressed pellets for all determinations has been criticised (Norrish and Hutton, 1969; Thomas and Haukka 1978) and a brief discussion is appropriate. Three major sources of error in the method have been noted by Holland and Brindle (1966).

Firstly, the matter of instability in the spectrometer and associated equipment. An air-conditioned environment, together with the counting of each unknown in conjunction with a control standard, enabled drift to be effectively monitored. The computations employed correct the raw count data for instrumental variation by the intensity ratio method (Brown et al., 1973).

Secondly, concerning the questions of sample heterogeneity and surface effects, thorough homogenisation and the use of finely ground powders are considered to have considerably reduced interference. The application, moreover, of quadratic functions to the relationship between concentration and flouresence reduces non-linearity caused by matrix effects (op.cit.).

The third error is that of mass absorption of flouresence by interfering elements in the sample. The computing programme used involves a three-stage least squares regression process, and has the advantage of incorporating all standards during and after mass absorption correction. In the case of major elements the use of quadratic equations enables a three-stage refinement of mass absorption coefficients. Calibrations are developed during the analysis and unlike other methods this does not rely upon independant calibration curves (op.cit.).

The success of the method for major elements depends on the use of a large number of standard rocks (in this case 48 such standards), whose compositional range exceeds that expected from the unknowns. Sixteen combinations of selected standards were tested in refining the results, and the combination finally used comprised 19 standard rocks including the U.S.G.S. rocks G-2, GSP-1 and AGV-1, together with 2 peralkaline granites DUT-23 and WS-13 provided by Dr. P. Bowden, St. Andrews University. An independant check was made by running a sample of riebeckite granite from Corsica as an unknown, and then comparing the result with the published analysis (RT 4958; Bonin et al., 1978).

During trace element analysis two primary synthetic standards are used to correct machine drift. Synthetic secondary standards enable coverage of a range of compositions in excess of that encountered in the unknowns. Mass absorption corrections are deduced from the previously determined major element results. A final analytical result is derived from a least squares fit regression line (Brown et al., 1973).

Data concerning the precision and accuracy of the results obtained for major and minor elements by these procedures are given in tables A3.1 and A3.2. All major element oxide values are normalised to total one hundred percent.

3. Other Methods

Ferrous iron was determined by dissolution of the sample in an acid mixture, followed by direct titration with potassium dichromate. Uranium was determined for 30 rock samples (18 from RED, 12 from AD) by Instrumental Neutron Activation Analysis, courtesy of the Institute of Geological Sciences, London. Details of the method used are reported by Ostle et al. (1972).

Major Element Analyses on U.S.G.S. Standard Rocks, and on Riebeckite Granite 4958.*

	G2			GSP-1			AGV-1			4958*	
wt.%	A	B	C	A	B	C	A	B	C	E	F
SiO2	69.73	68.67	69.26	67.86	68.15	67.72	60.07	59.93	60.54	76.99	76.65
Al2O3	15.54	15.64	15.42	15.37	15.76	15.18	17.56 av.	17.67	17.03	11.71	11.86
**Fe2O3	2.67	2.95	2.82	4.36	3.78	4.40	6.88	6.79	7.11	1.75	1.94
MgO	0.77 av.	1.28	1.13	0.97	1.19	1.04	1.56 av.	1.44	1.60	0.05	0.08
CaO	1.96 av.	1.87	2.00	2.04	1.88	2.07	4.99	5.23	5.02	0.25	0.32
Na2O	4.11 av.	4.01	4.10	2.82	2.85	3.08	4.34	4.17	4.08	4.61	4.28
K2O	4.55	4.91	4.61	5.57	5.44	5.49	2.94	3.04	2.90	4.61	4.76
TiO2	0.50	0.49	0.51	0.66	0.59	0.68	1.06	1.08	1.12	tr.	0.04
MnO	0.03 mag.	0.04	0.02	0.04 av.	0.03	0.02	1.10	0.09	0.10	0.03	0.03
P2O5	0.14	0.15	0.13	0.28	0.33	0.32	0.50	0.56	0.50	tr.	0.02

**Total Iron as Fe_2O_3

All columns normalised to total 100%. A-columns; recommended values from Flanagan (1976)
B-columns; results obtained during the present work. C-columns; results obtained by Brown et al (1973) using the same analytical procedure and computer program as that used during the present work.
av. = average, mag. = magnitude, tr. = trace.
*Column E, Riebeckite granite, Corsica (Bonin et al, 1978). Column F, results from the present work.

TABLE A3.1 : ANALYTICAL ACCURACY AND PRECISION : MAJOR ELEMENTS

*Trace Element Analyses on U.S.G.S. Standard Rocks, and on Riebeckite Granite 4958:**

Trace Element ppm	G-2			GSP-1			AGV-1			BCR-1			4958	
	a	b	c	a	b	c	a	b	c	a	b	c	a	b
Rb	168 rec.	165	158	254 rec.	256	256	67 rec.	66	58	47 rec.	45	39	243	247
Y	12 rec.	10	10	30 av.	25	26	21 av.	18	19	37 av.	34	33		
Sr	479 rec.	481	475	233 rec.	238	240	657 rec.	682	673	330 rec.	336	337	3	3
Zr	300 rec.	314	325	500 rec.	521	536	225 rec.	228	240	190 mag.	184	191		
Ce	150 mag.	163	165	394 av.	330	333	63 av.	73	78	54 rec.	55	55		
Nd	60 av.	61	58	188 av.	158	159	39 av.	37	37	29 rec.	31	33		
La	96 av.	88	92	191 av.	123	137	35 mag.	36	36	26 mag.	18	21		
Ba	1870 rec.			1300 rec.			1208 rec.			675 rec.				
Ga	23 rec.			22 mag.			20 rec.			20 mag.				
Nb	13 rec.			29 rec.			15 rec.			14 rec.				

a - columns: data from Flanagan (1976), identified as rec. = recommended, av. = average, mag.= magnitude.
b + c-columns: results of determinations obtained during the present work.
*4958 : data on Rb and Sr only, from Bonin et al (1978) quoted in column a; column-b, results obtained from present work.

TABLE A3.2 : ANALYTICAL ACCURACY AND PRECISION : TRACE ELEMENTS

APPENDIX IIIB

METAMORPHIC BASEMENT ROCKS

BASEMENT GNEISSES

		R	R	R	R	A	A	A	A
	wt.%	239	342	1005	R19	711	853	613	820
	SiO2	72.04	73.21	68.70	70.51	69.99	73.19	69.52	71.22
	AL2O3	13.24	14.14	15.34	16.20	16.40	14.27	16.31	15.42
	Fe2O3	1.34	0.80	0.86	0.87	0.49	0.42	0.73	0.88
	FeO	2.63	0.99	1.81	0.39	1.44	1.55	0.87	0.63
	MgO	1.08	0.49	0.53	0.61	0.85	0.80	0.55	0.65
	CaO	2.38	1.07	1.89	1.18	1.96	1.21	2.08	1.74
	Na2O	4.40	3.61	4.51	5.60	5.13	3.83	5.53	5.23
	K2O	2.33	5.45	5.81	4.39	3.28	4.39	4.03	3.91
	TiO2	0.40	0.12	0.38	0.15	0.33	0.22	0.26	0.21
	MnO	0.07	0.03	0.04	0.03	0.02	0.02	0.02	0.02
	P2O5	0.09	0.09	0.12	0.07	0.10	0.10	0.10	0.08
	Ag. Ratio	0.74	0.84	0.89	0.86	0.73	0.77	0.82	0.83
ppm	Ga	23	23	31	25	26	23	25	24
	Rb	81	144	196	97	41	112	66	47
	Sr	213	244	273	951	1189	218	923	994
	Y	51	19	27	10	4	15	3	5
	Zr	224	130	344	132	198	356	181	204
	Nb	2	3	14	n.d.	n.d.	n.d.	n.d.	n.d.
	Ba	381	863	1179	1380	1456	985	1325	1356
	La	24	26	75	24	26	32	26	25
	Ce	91	46	158	20	39	52	43	44
	Nd	42	18	72	8	19	27	22	22
	U	-	-	-	-	-	-	-	-
C.I.P.W norm.	Q	30.00	28.09	15.67	17.86	21.60	29.63	17.07	21.50
	C	-	0.56	-	0.24	1.08	1.25	-	-
	OR	13.74	32.18	34.34	25.90	19.41	25.93	23.83	23.14
	AB	37.25	30.58	38.15	47.41	43.39	32.38	46.75	44.29
	AN	9.48	4.72	4.45	5.40	9.08	5.35	7.76	7.03
	DI	1.42	-	3.49	-	-	-	1.53	0.85
	HY	5.17	2.23	1.63	1.52	3.85	4.17	1.23	1.34
	MT	1.94	1.16	1.24	0.92	0.71	0.60	1.06	1.27
	HM	-	-	-	0.23	-	-	-	-
	IL	0.76	0.22	0.72	0.28	0.62	0.41	0.49	0.39
	AP	0.21	0.21	0.28	0.16	0.23	0.23	0.23	0.19

R Adjacent Ras Ed Dom
A Adjacent Abu Dom

APPENDIX IIIC

YOUNGER GRANITE VOLCANIC ROCKS

YOUNGER GRANITE VOLCANIC ROCKS

	wt.%	Ras Ed Dom 307	Abu Dom R101
	Si02	69.29	81.59
	AL203	13.47	10.52
	Fe203	5.62	1.97
	Fe0	0.10	0.29
	Mg0	0.44	0.12
	Ca0	0.84	0.85
	Na20	2.97	1.20
	K20	6.51	3.21
	Ti02	0.51	0.19
	Mn0	0.17	0.01
	P205	0.08	0.04
	Ag. Ratio	0.89	0.52
ppm	Ga	43	50
	Rb	183	113
	Sr	42	30
	Y	61	145
	Zr	1038	2152
	Nb	139	236
	Ba	147	140
	La	109	36
	Ce	238	96
	Nd	107	55
	U	-	-
C.I.P.W. norm	Q	24.87	60.43
	C	0.20	3.62
	OR	38.47	18.97
	AB	25.13	10.15
	AN	3.64	3.95
	HY	1.09	0.29
	MT	-	0.41
	HM	5.61	1.68
	IL	0.57	0.36
	AP	0.18	0.09
	RU	0.20	-

APPENDIX IIID

YOUNGER GRANITE INTRUSIVE ROCKS-RAS ED DOM

EARLY SYENITES

		S2	S1	S4	S4	S4	S4	RAFT IN S6	IT2	S11
	wt.%	1014	236	914	916	285A	285B	209	310	R31
	SiO2	59.59	60.84	63.13	62.75	62.32	62.95	62.25	60.98	62.77
	AL203	15.82	16.29	16.26	16.36	16.22	15.99	16.50	15.05	16.69
	Fe2O3	4.93	3.01	3.55	4.41	3.40	3.38	3.59	3.22	3.59
	FeO	3.21	3.59	2.22	1.54	2.48	2.70	2.55	3.89	1.27
	MgO	1.50	1.22	1.00	1.16	1.06	0.60	0.94	1.98	0.55
	CaO	2.80	2.55	1.74	1.80	1.86	1.61	2.03	3.01	2.02
	Na2O	6.40	6.91	5.47	5.18	5.69	5.99	5.31	5.18	6.49
	K2O	3.89	4.04	5.33	5.50	5.51	5.62	5.50	4.80	5.65
	TiO2	1.17	0.96	0.86	0.84	0.95	0.75	0.92	1.39	0.70
	MnO	0.19	0.16	0.15	0.16	0.17	0.17	0.12	0.13	0.13
	P2O5	0.49	0.42	0.28	0.30	0.34	0.23	0.30	0.37	0.14
	Ag. Ratio	0.93	0.97	0.91	0.88	0.94	1.00	0.89	0.91	1.01
ppm	Ga	40	41	37	36	36	43	37	36	35
	Rb	50	49	52	51	42	74	50	72	57
	Sr	266	270	205	214	67	96	233	284	69
	Y	56	48	30	30	33	46	28	50	25
	Zr	664	414	325	295	286	515	264	776	355
	Nb	93	75	46	45	41	69	43	81	66
	Ba	718	715	837	977	1025	689	965	540	675
	La	79	63	48	47	41	60	40	76	44
	Ce	179	149	98	102	92	131	92	177	91
	Nd	90	72	53	56	51	68	53	82	46
	U	-	-	-	-	-	-	-	2.3	-
C.I.P.W. norm	Q	2.15	-	7.03	7.22	4.33	3.71	5.93	4.91	0.73
	OR	23.01	23.85	31.51	32.49	32.53	33.18	32.48	28.37	33.37
	AB	54.19	58.45	46.31	43.82	48.11	50.66	44.89	43.85	54.37
	AN	2.91	1.50	4.04	5.14	2.49	0.15	4.97	3.61	-
	AC	-	-	-	-	-	-	-	-	0.47
	DI	6.08	6.90	2.15	1.42	3.55	5.21	2.46	7.21	2.95
	WO	—	—	—	—	—	—	—	—	2.22
	HY	1.12	1.11	1.49	3.23	1.44	0.19	1.59	3.86	-
	OL	-	0.98	-	-	-	-	-	-	-
	MT	7.14	4.36	5.13	3.05	4.93	4.89	5.20	4.67	2.49
	HM	-	-	0.01	2.29	-	-	-	-	1.71
	AL	2.23	1.83	1.63	1.59	1.80	1.42	1.75	2.63	1.33
	AP	1.16	0.99	0.66	0.71	0.80	0.54	0.71	0.88	0.33

		SYENITE 2			
	wt.%	129	1028	1026	1077
	SiO2	64.16	62.94	64.21	65.85
	AL2O3	16.06	16.75	15.52	14.96
	Fe2O3	5.02	4.44	4.72	3.50
	FeO	1.17	1.48	1.55	2.65
	MgO	1.10	0.32	0.34	0.25
	CaO	0.85	1.34	1.50	1.45
	Na2O	10.40	6.30	6.05	5.11
	K2O	1.52	5.53	5.26	5.63
	TiO2	0.47	0.60	0.58	0.40
	MnO	0.20	0.16	0.15	0.12
	P2O5	0.05	0.14	0.12	0.07
	Ag. Ratio	1.17	0.98	1.01	0.97
ppm	Ga	58	45	48	49
	Rb	17	57	77	101
	Sr	15	57	69	39
	Y	65	37	56	64
	Zr	974	265	773	780
	Nb	197	24	126	103
	Ba	69	427	427	139
	La	169	55	73	81
	Ce	338	108	196	181
	Nd	144	72	89	89
	U	5.9	-	-	-
C.I.P.W. norm.	Q	-	3.18	7.09	11.76
	OR	8.99	32.67	31.07	33.24
	AB	73.16	53.30	50.53	43.27
	AN	-	1.08	-	1.25
	NE	0.53	-	-	-
	AC	12.16	-	0.58	-
	DI	2.56	1.72	1.83	4.22
	WO	-	1.02	1.80	0.22
	MT	1.17	3.55	3.80	5.08
	HM	-	1.98	1.89	-
	IL	0.89	1.14	1.10	0.76
	AP	0.11	0.33	0.28	0.16

SYENITE 3

	wt.%	461	459	1057	1073B	R80A
	Si02	66.80	66.62	66.73	67.18	67.03
	AL203	15.21	14.77	15.18	15.06	14.88
	Fe203	3.51	4.32	2.26	2.42	2.27
	Fe0	1.88	1.48	2.56	2.34	2.78
	Mg0	0.20	0.24	0.24	0.15	0.22
	Ca0	0.66	0.70	1.30	0.73	0.95
	Na20	5.86	5.64	5.77	5.99	5.74
	K20	5.26	5.62	5.49	5.63	5.54
	Ti02	0.41	0.40	0.31	0.35	0.39
	Mn0	0.15	0.15	0.11	0.12	0.13
	P205	0.05	0.06	0.05	0.04	0.07
	Ag. Ratio	1.01	1.04	1.02	1.06	1.04
ppm	Ga	48	49	49	50	46
	Rb	85	153	85	84	89
	Sr	14	17	27	11	48
	Y	37	56	74	56	55
	Zr	957	1014	1288	861	576
	Nb	128	130	153	121	93
	Ba	74	61	28	6	176
	La	125	129	167	139	86
	Ce	259	285	353	287	188
	Nd	111	122	141	117	91
	U	-	-	4.2	2.5	-
C.I.P.W. norm.	Q	11.62	11.98	9.50	9.48	10.25
	OR	31.09	33.20	32.41	33.29	32.71
	AB	48.91	44.66	47.55	46.09	45.73
	AC	0.61	2.69	1.08	4.01	2.47
	DI	1.71	1.29	5.30	2.95	3.74
	WO	0.35	0.59	-	-	-
	HY	-	-	0.67	1.91	2.14
	MT	4.77	4.10	2.73	1.48	2.04
	HM	-	0.55	-	-	-
	IL	0.78	0.76	0.59	0.66	0.74
	AP	0.11	0.14	0.11	0.09	0.16

SYENITE 5

	wt.%	193	204	283A	195	188
	SiO2	65.06	67.87	67.62	65.88	66.61
	AL2O3	16.02	12.98	13.34	13.68	13.44
	Fe2O3	2.41	4.07	5.85	5.89	5.78
	FeO	2.84	2.87	0.93	1.37	1.30
	MgO	0.45	0.19	0.15	0.14	0.16
	CaO	0.85	1.10	0.79	1.30	0.88
	Na2O	5.82	5.18	5.54	5.83	5.50
	K2O	5.72	5.06	4.95	5.10	5.60
	TiO2	0.54	0.48	0.60	0.58	0.53
	MnO	0.15	0.13	0.18	0.18	0.15
	P2O5	0.13	0.06	0.05	0.05	0.05
	Ag. Ratio	0.98	1.08	1.08	1.10	1.12
ppm	Ga	40	47	52	51	52
	Rb	47	82	92	82	102
	Sr	16	18	10	17	16
	Y	30	45	43	51	61
	Zr	394	716	850	864	869
	Nb	52	78	86	91	126
	Ba	435	50	22	-	57
	La	47	71	87	79	129
	Ce	99	144	182	175	261
	Nd	50	69	85	90	127
	U	-	2.2	-	-	-
C.I.P.W. norm.	Q	6.58	17.00	16.81	12.61	14.05
	OR	33.79	29.88	29.22	30.12	33.08
	AB	49.23	38.62	41.10	41.98	37.96
	AN	0.70	-	-	-	-
	AC	-	4.56	5.05	6.46	7.54
	DI	2.27	4.42	0.80	0.75	0.86
	WO	-	-	1.06	2.15	1.22
	HY	2.57	0.82	-	-	-
	MT	3.49	3.61	1.84	3.32	3.14
	HM	-	-	2.83	1.35	1.00
	IL	1.02	0.91	1.14	1.03	1.00
	AP	0.30	0.14	0.11	0.11	0.11

SYENITE 6

	wt.%	290	293	362	397	401	402*
	Si02	66.85	68.13	65.04	65.62	67.31	67.07
	AL203	13.64	14.36	14.55	14.70	14.40	15.23
	Fe203	3.14	2.67	2.78	5.10	5.31	3.89
	FeO	3.05	2.14	3.51	1.16	-	1.69
	MgO	0.52	0.38	0.62	0.22	0.35	0.20
	CaO	1.51	0.97	1.59	1.17	1.17	0.29
	Na20	5.12	5.27	5.61	5.74	5.51	5.66
	K20	5.30	5.35	5.25	5.42	5.26	5.32
	Ti02	0.59	0.49	0.71	0.60	0.46	0.42
	MnO	0.17	0.13	0.15	0.22	0.16	0.16
	P205	0.12	0.10	0.18	0.06	0.07	0.06
	Ag. Ratio	1.04	1.01	1.02	1.04	1.02	0.99
ppm	Ga	44	44	42	46	45	47
	Rb	86	105	85	78	75	80
	Sr	29	65	41	15	19	11
	Y	64	79	86	74	47	54
	Zr	1034	1243	797	1362	837	774
	Nb	115	147	91	163	99	110
	Ba	237	296	189	-	34	48
	La	96	104	82	97	97	79
	Ce	210	221	169	209	198	186
	Nd	97	96	84	100	87	83
	U	-	4.2	-	-	-	-
C.I.P.W. norm.	Q	13.82	15.04	8.66	10.73	13.88	13.16
	OR	31.30	31.62	31.02	32.00	31.08	31.44
	AB	40.64	44.07	45.59	45.44	44.78	47.90
	AN	-	-	-	-	-	0.43
	AC	2.34	0.46	1.66	2.73	1.62	-
	DI	5.68	3.48	5.69	1.18	1.88	0.48
	WO	-	-	-	1.62	0.81	-
	HY	1.42	0.50	2.38	-	-	0.27
	MT	3.38	3.63	3.19	2.72	-	4.76
	HM	-	-	-	2.27	4.74	0.60
	AL	1.12	0.93	1.35	1.14	0.34	0.79
	AP	0.28	0.23	0.42	0.14	0.16	0.14

* partly haematised mafic minerals

		SYENITE 7							SYENITE 15	
	wt.%	378	966	340	R3	375	996	417	166	435
	SiO2	64.67	65.88	66.46	64.86	64.23	64.69	67.48	65.44	64.68
	AL2O3	14.72	14.71	14.17	14.38	15.68	16.00	14.20	16.06	16.02
	Fe2O3	6.79	5.03	5.34	7.08	6.64	4.17	5.30	4.44	4.43
	FeO	0.48	1.15	1.09	0.19	0.11	1.53	0.67	0.58	1.01
	MgO	0.22	0.36	0.21	0.27	0.28	0.44	0.24	0.16	0.27
	CaO	0.80	1.06	0.84	1.34	0.32	1.16	0.51	1.12	1.44
	Na2O	6.43	5.69	6.13	5.75	6.50	5.56	6.04	6.52	6.17
	K2O	5.20	5.33	5.07	5.23	5.44	5.81	5.07	5.26	5.41
	TiO2	0.52	0.49	0.45	0.56	0.56	0.48	0.31	0.32	0.38
	MnO	0.12	0.24	0.18	0.23	0.19	0.07	0.11	0.16	0.14
	P2O5	0.04	0.07	0.06	0.10	0.05	0.09	0.06	0.04	0.05
	Ag. Ratio	1.10	1.03	1.10	1.05	1.06	0.96	1.09	1.02	1.00
ppm	Ga	56	47	47	47	46	47	52	47	46
	Rb	110	81	91	82	89	79	126	75	98
	Sr	7	21	18	32	15	31	19	14	31
	Y	37	62	71	60	60	48	62	29	30
	Zr	833	990	1098	851	1030	399	987	392	366
	Nb	80	119	160	111	87	119	145	72	60
	Ba	24	155	17	60	41	84	78	5	77
	La	69	75	109	84	52	92	106	50	57
	Ce	142	80	246	189	125	124	234	109	135
	Nd	68	77	115	88	66	87	110	55	77
	U	2.1	-	-	-	-	-	-	1.7	-
C.I.P.W. norm.	Q	7.97	11.32	11.93	10.56	5.96	8.03	13.54	6.30	6.23
	OR	30.74	31.47	29.94	30.91	32.15	34.30	29.97	31.10	31.94
	AB	46.73	45.99	44.67	44.85	50.33	47.00	44.79	53.30	52.18
	AN	-	-	-	-	-	1.58	-	-	0.05
	AC	6.78	1.87	6.32	3.35	4.13	-	5.59	1.67	-
	DI	1.18	1.93	1.13	1.45	0.37	2.37	1.29	0.86	1.45
	WO	0.91	0.96	0.97	1.59	-	0.23	0.20	1.75	2.04
	HY	-	-	-	-	0.52	-	-	-	-
	MT	0.43	3.07	2.80	-	-	3.77	1.62	1.46	2.61
	HM	4.14	2.26	1.22	5.92	5.21	1.56	2.24	2.84	2.62
	IL	0.98	0.93	0.85	0.89	0.63	0.91	0.58	0.60	0.72
	AP	0.09	0.16	0.14	0.23	0.11	0.21	0.14	0.09	0.11
	TN	-	-	-	0.22	0.54	-	-	-	-

INTRUSIVE TRACHYTES

	wt.%	IT1 364	IT3 167	IT3 430A
	Si02	67.62	63.47	61.82
	AL203	13.71	17.46	16.16
	Fe203	5.97	3.10	4.31
	Fe0	0.36	1.77	2.17
	Mg0	0.19	0.35	0.68
	Ca0	0.63	0.94	1.68
	Na20	6.14	6.91	6.91
	K20	4.75	5.40	5.07
	Ti02	0.41	0.41	0.84
	Mn0	0.16	0.11	0.14
	P205	0.05	0.07	0.22
	Ag. Ratio	1.11	0.99	1.04
ppm	Ga	52	40	37
	Rb	101	71	52
	Sr	9	6	133
	Y	87	44	37
	Zr	1532	796	468
	Nb	169	104	76
	Ba	59	4	1620
	La	144	77	62
	Ce	306	163	127
	Nd	130	70	65
	U	-	1.7	-
C.I.P.W. norm.	Q	14.63	0.90	0.45
	OR	28.08	31.91	29.97
	AB	44.04	58.50	54.87
	AN	-	0.67	-
	AC	6.99	-	3.14
	NS	-	-	-
	DI	1.02	2.30	4.00
	WO	0.62	0.27	0.76
	MT	0.49	4.49	4.67
	HM	3.21	-	-
	IL	0.77	0.78	1.59
	AP	0.11	0.16	0.52

* mafic minerals haematised

GRANITE 1

	wt.%	142B1	142B2	186A	186B	187	159	447	460	132*
	SiO2	75.71	76.03	73.33	74.27	70.11	76.83	72.64	74.54	76.39
	AL2O3	10.36	10.49	11.71	10.86	12.07	10.33	12.19	9.46	11.10
	Fe2O3	4.00	2.95	2.53	2.96	5.73	4.00	1.84	4.88	3.54
	FeO	0.74	1.24	2.41	2.21	0.85	0.29	2.78	1.87	0.22
	MgO	0.06	0.06	0.07	0.09	0.08	0.09	0.07	0.10	0.15
	CaO	0.32	0.37	0.27	0.31	0.59	0.35	0.31	0.34	0.28
	Na2O	4.26	4.04	4.74	4.49	5.11	3.64	5.02	4.14	3.34
	K2O	4.30	4.57	4.76	4.47	4.84	4.35	4.87	4.18	4.71
	TiO2	0.16	0.18	0.25	0.23	0.51	0.05	0.19	0.15	0.18
	MnO	0.06	0.06	0.09	0.09	0.07	0.02	0.08	0.11	0.07
	P2O5	0.02	0.02	0.03	0.02	0.03	0.02	0.03	0.02	0.02
	Ag. Ratio	1.13	1.11	1.11	1.12	1.13	1.03	1.11	1.20	0.95
ppm	Ga	50	47	49	48	53	53	51	47	47
	Rb	195	163	93	92	94	125	103	189	121
	Sr	6	5	1	4	5	3	6	3	10
	Y	106	114	67	35	49	41	60	140	77
	Zr	1615	1897	949	470	1211	938	1182	2208	1274
	Nb	193	187	114	61	78	72	122	283	135
	Ba	68	-	-	19	31	14	-	-	32
	La	180	122	98	63	56	79	109	297	117
	Ce	325	278	214	126	123	86	227	594	251
	Nd	180	129	103	57	65	77	100	270	110
	U	-	-	3.9	-	2.4	-	-	-	-
C.I.P.W. norm.	Q	35.59	35.42	26.85	30.78	22.97	38.97	24.04	35.44	38.16
	C	-	-	-	-	-	-	-	-	0.04
	OR	25.43	26.98	28.14	26.42	28.62	25.71	28.74	24.75	27.84
	AB	29.32	28.51	33.72	30.95	35.12	28.96	35.60	25.44	28.27
	AN	-	-	-	-	-	-	-	-	1.26
	AC	5.95	4.97	5.64	6.21	7.19	1.66	5.31	8.51	-
	NS	-	-	-	-	-	-	0.18	-	-
	DI	0.32	1.49	1.01	1.24	0.43	0.48	1.19	1.36	-
	WO	0.43	-	-	-	0.91	0.41	-	-	-
	HY	-	0.45	3.52	2.73	-	-	4.48	1.32	0.37
	MT	2.11	1.78	0.54	1.18	1.49	0.85	-	2.82	0.41
	HM	0.48	-	-	-	2.21	2.83	-	-	0.37
	IL	0.30	0.34	0.47	0.43	0.97	0.09	0.36	0.28	0.34
	AP	0.05	0.05	0.07	0.05	0.07	0.05	0.07	0.05	0.05

*mafic minerals haematised

MICROGRANITES

		MG1	MG2	G2	G2	G2
	wt.%	300*	399	294	289	R54
	SiO_2	76.38	72.04	74.48	71.95	70.20
	AL_2O_3	10.61	10.92	10.50	11.13	10.25
	Fe_2O_3	4.21	3.61	5.02	5.67	5.46
	FeO	0.40	2.65	0.35	0.56	3.24
	MgO	0.07	0.20	0.12	0.24	0.12
	CaO	0.31	0.68	0.37	0.62	0.28
	Na_2O	3.12	4.56	4.26	4.61	5.07
	K_2O	4.54	4.74	4.51	4.71	4.54
	TiO_2	0.23	0.41	0.23	0.39	0.57
	MnO	0.10	0.14	0.13	0.08	0.23
	P_2O_5	0.02	0.04	0.02	0.04	0.04
	Ag. Ratio	0.95	1.16	1.13	1.14	1.29
ppm	Ga	50	49	51	50	57
	Rb	176	156	147	171	115
	Sr	12	23	11	16	19
	Y	137	96	116	113	190
	Zr	2583	1839	1072	1976	3036
	Nb	244	192	244	205	240
	Ba	-	22	-	43	25
	La	62	153	212	207	188
	Ce	407	333	447	335	458
	Nd	174	146	186	188	240
	U	-	-	-	6.5	-
C.I.P.W. norm.	Q	40.13	26.70	33.51	27.96	24.27
	C	0.04	-	-	-	-
	OR	26.84	28.03	26.66	27.84	26.80
	AB	26.41	29.77	28.91	30.99	27.45
	AN	1.40	-	-	-	-
	AC	-	7.79	6.29	7.08	13.59
	DI	-	2.73	0.64	1.29	1.00
	WO	-	-	0.36	0.48	-
	HY	0.17	2.76	-	-	4.58
	MT	0.94	1.32	0.88	0.93	1.09
	HM	3.55	-	2.23	2.57	-
	IL	0.43	0.78	0.43	0.74	1.08
	AP	0.04	0.09	0.04	0.09	0.09

* mafic minerals partly haematised

SYENITES

	wt.%	S9 428	S13 433	S13 R33	S14 R40	S12 R41*	S10 429*	S8 426	S13 430B
	Si02	64.60	63.47	62.11	62.77	65.08	63.29	63.30	63.37
	AL203	15.46	17.32	16.94	16.65	17.18	17.18	17.17	16.58
	Fe203	4.43	3.84	4.26	5.85	4.19	5.06	4.39	3.59
	Fe0	2.13	0.90	1.30	0.40	0.39	0.14	0.98	1.67
	Mg0	0.32	0.41	0.70	0.33	0.13	0.23	0.46	0.53
	Ca0	0.76	0.72	1.49	0.91	0.28	1.34	0.78	1.32
	Na20	7.04	7.28	6.91	6.95	6.17	6.43	6.42	6.70
	K20	4.65	5.26	5.14	5.20	5.83	5.40	5.74	5.33
	Ti02	0.41	0.58	0.82	0.65	0.60	0.65	0.47	0.63
	Mn0	0.13	0.12	0.13	0.17	0.10	0.17	0.14	0.16
	P205	0.07	0.10	0.19	0.12	0.05	0.11	0.09	0.12
	Ag. Ratio	1.07	1.02	1.00	1.03	0.96	0.96	0.98	1.01
ppm	Ga	51	42	41	42	39	40	43	40
	Rb	55	64	55	78	69	40	75	63
	Sr	16	11	-	31	37	27	41	43
	Y	45	41	34	32	24	13	25	31
	Zr	520	694	1835	674	233	136	216	445
	Nb	81	102	79	83	48	26	46	74
	Ba	70	75	822	264	190	207	217	253
	La	82	74	62	60	34	21	46	52
	Ce	129	148	132	128	65	40	106	107
	Nd	84	66	64	60	39	24	56	53
	U	1.8	2.0	1.4	-	-	0.6	-	-
C.I.P.W. norm.	Q	5.43	0.19	-	1.61	6.21	3.14	2.45	2.20
	C	-	-	-	-	0.32	-	-	-
	OR	27.48	31.05	30.35	30.47	34.46	31.91	33.89	31.49
	AB	53.60	59.81	58.19	56.66	52.22	54.41	54.29	55.60
	AN	-	-	0.04	-	1.06	2.06	1.10	-
	NE	-	-	0.15	-	-	-	-	-
	AC	5.22	1.55	-	1.91	-	-	-	0.97
	DI	2.79	2.20	3.76	1.77	-	1.23	1.70	2.85
	WO	-	0.03	0.53	0.58	-	0.51	0.20	0.88
	HY	0.70	-	-	-	0.32	-	0.35	-
	MT	3.80	1.61	2.24	-	-	-	2.25	4.08
	HM	-	2.19	2.71	5.18	4.18	5.05	2.83	0.43
	IL	0.78	1.10	1.56	1.20	1.03	0.65	0.89	1.19
	AP	0.16	0.23	0.45	0.28	0.11	0.26	0.14	0.28
	TN	-	-	-	0.03	-	0.74	-	-
	RU	-	-	-	-	0.05	-	-	-

* mafic minerals partly haematised

		MINOR INTRUSIONS SYENITIC					
	wt.%	108	101	120*	418C	975*	DR.17
	SiO2	63.96	65.03	68.84	67.85	68.25	62.83
	AL2O3	15.65	13.27	13.29	13.40	13.65	15.67
	Fe2O3	3.38	8.83	6.73	4.82	5.82	5.76
	FeO	3.39	0.31	0.12	1.59	1.71	1.20
	MgO	0.33	0.21	0.13	0.26	0.15	0.31
	CaO	1.20	0.56	0.98	0.92	0.34	1.43
	Na2O	5.90	5.85	5.71	5.55	4.31	6.47
	K2O	5.31	4.99	3.49	4.99	5.30	5.53
	TiO2	0.58	0.83	0.46	0.41	0.61	0.59
	MnO	0.15	0.07	0.21	0.14	0.27	0.12
	P2O5	0.13	0.05	0.04	0.06	0.09	0.09
	Ag. Ratio	0.99	1.13	0.99	1.08	0.94	1.06
ppm	Ga	47	65	51	51	46	50
	Rb	57	83	39	116	90	83
	Sr	51	10	14	16	46	29
	Y	51	84	126	71	53	43
	Zr	752	1716	1369	1510	832	682
	Nb	95	217	174	187	106	77
	Ba	281	56	20	33	89	141
	La	68	102	121	117	89	72
	Ce	157	297	274	253	195	155
	Nd	75	105	120	109	93	80
	U	-	-	-	-	-	-
C.I.P.W. norm.	Q	6.34	13.12	21.00	16.51	22.20	3.30
	OR	31.37	29.50	20.62	29.48	31.32	32.66
	AB	49.94	40.44	48.32	41.17	36.45	49.82
	AN	0.52	-	0.32	-	1.10	-
	AC	-	8.00	-	5.10	-	4.31
	DI	3.95	0.80	0.69	1.39	-	1.66
	WO	-	-	1.28	0.99	-	1.82
	HY	1.54	0.14	-	-	0.37	-
	MT	4.90	-	-	4.40	4.63	2.55
	HM	-	6.06	6.72	0.02	2.12	2.51
	IL	1.10	0.80	0.70	0.78	1.16	1.12
	AP	0.30	0.11	0.09	0.14	0.21	0.21
	TN	-	0.99	0.22	-	-	-

* mafic minerals partly haematised

MINOR INTRUSIONS GRANITIC

	wt.%	216	221	239	455	922	383B	409*	317A
	SiO2	69.01	75.25	73.80	74.70	74.13	72.95	75.88	74.90
	AL2O3	13.91	10.86	10.12	9.48	11.88	12.10	10.23	10.07
	Fe2O3	2.65	3.80	3.63	4.89	3.42	3.54	5.23	5.42
	FeO	2.20	0.77	2.78	1.87	0.46	0.73	0.40	0.33
	MgO	0.33	0.12	0.12	0.10	0.10	0.20	0.12	0.06
	CaO	1.15	0.16	0.55	0.34	0.37	0.67	0.12	0.16
	Na2O	5.16	3.94	4.27	4.15	4.65	4.31	2.90	3.84
	K2O	4.84	4.75	4.34	4.19	4.61	5.08	4.53	4.96
	TiO2	0.48	0.25	0.24	0.15	0.28	0.31	0.22	0.17
	MnO	0.13	0.07	0.12	0.11	0.06	0.07	0.05	0.07
	P2O5	0.13	0.02	0.02	0.02	0.03	0.03	0.02	0.02
	Ag. Ratio	0.99	1.07	1.16	1.20	1.06	1.04	0.94	1.16
	Ga	48	47	51	49	42	46	48	45
	Rb	78	129	187	191	110	104	134	110
	Sr	71	3	9	2	14	22	14	10
	Y	57	89	170	143	79	97	67	217
	Zr	700	1619	3428	2694	1361	1034	2603	3978
ppm	Nb	91	159	329	273	133	102	390	240
	Ba	567	22	-	-	33	105	33	-
	La	76	45	332	254	141	391	275	308
	Ce	165	91	548	522	296	311	462	565
	Nd	80	49	262	236	133	385	225	292
	U	-	-	-	-	-	-	-	-
	Q	18.12	34.70	31.64	35.44	29.81	28.00	40.85	35.24
	C	-	-	-	-	-	-	0.02	-
	OR	28.61	28.09	25.66	24.75	27.25	30.04	26.78	29.32
	AB	43.68	29.39	27.88	25.44	35.45	33.93	24.55	24.14
	AN	0.49	-	-	-	-	-	1.45	-
	AC	-	3.50	7.29	8.51	3.44	2.26	-	7.37
C.I.P.W. norm.	DI	3.67	0.51	2.29	1.36	0.53	1.07	-	0.32
	WO	-	-	-	-	0.39	0.73	-	0.10
	HY	0.26	0.06	3.10	1.32	-	-	0.29	-
	MT	3.84	1.98	1.60	2.82	0.86	1.68	0.81	0.80
	HM	-	1.21	-	-	1.63	1.59	4.75	2.31
	IL	0.91	0.47	0.45	0.28	0.53	0.58	0.41	0.32
	AP	0.30	0.04	0.04	0.04	0.07	0.07	0.04	0.04
	TN	-	-	-	-	-	-	-	-

MINOR INTRUSIONS GRANITIC

	wt.%	324	350	951	932	R7A	197	283B
	Si02	73.94	72.84	73.98	72.49	72.80	70.66	73.38
	AL203	9.91	11.39	9.68	10.31	10.65	12.67	11.11
	Fe203	6.45	4.31	5.46	6.61	6.34	4.94	4.76
	Fe0	0.35	1.34	1.63	0.53	0.13	0.64	0.95
	Mg0	0.09	0.25	0.12	0.09	0.11	0.26	0.13
	Ca0	0.34	0.39	0.22	0.25	0.56	0.42	0.43
	Na20	4.31	4.42	4.29	5.07	4.51	4.72	4.57
	K20	4.34	4.60	4.28	4.19	4.58	5.08	3.93
	Ti02	0.19	0.36	0.19	0.25	0.23	0.40	0.59
	Mn0	0.05	0.06	0.14	0.18	0.07	0.14	0.14
	P205	0.02	0.05	0.02	0.02	0.02	0.06	0.02
	Ag. Ratio	1.19	1.08	1.21	1.25	1.16	1.05	1.06
ppm	Ga	53	50	49	50	57	48	51
	Rb	160	136	180	151	141	110	59
	Sr	3	18	5	7	5	9	12
	Y	43	71	141	47	32	80	47
	Zr	1155	1708	3057	1715	1554	1371	990
	Nb	75	161	320	447	57	152	103
	Ba	45	75	-	-	35	34	34
	La	59	186	282	129	27	126	73
	Ce	97	331	606	310	79	264	182
	Nd	68	162	270	153	34	120	78
	U	-	-	-	-	-	-	-
C.I.P.W. norm.	Q	34.00	29.85	34.17	29.60	30.33	23.69	31.94
	C	-	-	-	-	-	-	-
	OR	25.65	27.16	25.27	24.77	27.06	30.04	23.19
	AB	26.81	32.97	25.96	29.67	29.28	36.86	35.26
	AN	-	-	-	-	-	-	-
	AC	8.51	3.87	9.09	11.67	7.82	2.73	2.96
	DI	0.48	1.25	0.82	0.48	0.59	1.31	0.69
	WO	0.39	-	-	0.20	0.77	-	0.46
	HY	-	0.04	0.90	-	-	0.03	-
	MT	0.74	3.47	3.35	1.57	-	1.36	1.81
	HM	3.00	0.57	-	1.49	3.62	3.05	2.48
	IL	0.36	0.68	0.36	0.47	0.42	0.76	1.12
	AP	0.04	0.11	0.04	0.04	0.04	0.14	0.04
	TN	-	-	-	-	0.01	-	-

* mafic minerals partly haematised

MINOR INTRUSIONS GRANITIC

	wt.%	917	976	980	R83	969*	971C*	988*	206
	Si02	75.13	73.83	74.04	74.26	75.30	80.24	77.24	73.99
	AL203	10.41	9.45	9.51	9.76	9.72	11.53	9.96	11.47
	Fe203	4.05	6.01	4.81	5.16	6.05	0.43	3.68	3.29
	Fe0	1.09	1.29	2.29	1.58	0.34	0.15	1.16	1.40
	Mg0	0.07	0.05	0.07	0.08	0.10	0.09	0.07	0.17
	Ca0	0.24	0.25	0.57	0.29	0.85	0.57	0.37	0.39
	Na20	4.27	4.34	4.22	4.21	2.28	1.23	3.05	4.11
	K20	4.47	4.42	4.16	4.39	4.98	5.58	4.20	4.79
	Ti02	0.17	0.19	0.19	0.17	0.19	0.14	0.22	0.28
	Mn0	0.08	0.15	0.13	0.08	0.15	0.01	0.02	0.08
	P205	0.02	0.02	0.02	0.02	0.03	0.02	0.02	0.04
	Ag. Ratio	1.14	1.26	1.20	1.20	0.94	0.70	0.96	1.04
ppm	Ga	49	50	49	51	46	50	47	49
	Rb	191	138	198	95	199	216	90	116
	Sr	5	12	14	6	17	6	23	21
	Y	132	138	165	24	149	167	141	93
	Zr	3531	2182	2917	370	2469	2781	2332	1770
	Nb	311	246	288	18	244	356	239	173
	Ba	-	-	81	151	-	63	42	130
	La	279	223	272	32	192	11	242	116
	Ce	522	502	615	30	427	30	527	311
	Nd	274	236	269	30	183	18	229	118
	U	-	-	10.00	-	-	11.1	-	-
C.I.P.W. norm.	Q	34.41	34.03	33.94	34.30	41.61	50.42	42.71	31.64
	C	-	-	-	-	-	2.47	-	-
	OR	26.38	26.09	24.58	25.92	29.43	32.98	24.78	28.29
	AB	28.69	24.03	25.72	25.76	19.29	10.41	25.83	32.33
	AN	-	-	-	-	1.58	2.69	1.08	-
	AC	6.51	11.14	8.80	8.67	-	-	-	2.12
	DI	0.90	0.96	2.38	1.13	0.53	-	0.37	1.19
	WO	-	-	-	-	0.73	-	0.05	0.07
	HY	0.09	0.17	1.58	0.59	-	0.22	-	-
	MT	2.61	3.13	2.55	3.13	1.03	0.11	3.17	3.70
	HM	-	-	-	-	5.34	0.35	1.49	-
	IL	0.32	0.36	0.36	0.32	0.36	0.26	0.41	0.53
	AP	0.04	0.04	0.04	0.04	0.07	0.04	0.04	0.09
	TN	-	-	-	-	-	-	-	-

APPENDIX IIIE

YOUNGER GRANITE INTRUSIVE ROCKS-ABU DOM

EARLY SYENITES - SYENITE 1

	wt.%	D715	D817	D849	D685	D566B	D596B
	Si02	61.87	62.11	60.85	61.22	62.73	60.56
	AL203	16.35	16.43	15.96	16.27	16.76	16.47
	Fe203	5.13	3.54	4.70	4.17	3.36	7.92
	FeO	0.57	2.01	2.76	3.27	2.16	0.02
	MgO	0.47	0.71	0.77	0.79	0.70	0.76
	CaO	2.98	2.60	2.95	2.23	1.61	2.37
	Na20	5.85	6.01	4.90	4.84	6.21	5.21
	K20	5.37	5.31	6.01	5.89	5.22	5.25
	Ti02	0.90	0.83	0.87	0.82	0.79	0.87
	MnO	0.13	0.14	0.17	0.19	0.17	0.20
	P205	0.27	0.28	0.32	0.31	0.28	0.38
	Ag. Ratio	0.94	0.95	0.91	0.88	0.95	0.87
ppm	Ga	41	39	36	39	40	37
	Rb	45	43	72	54	34	34
	Sr	246	279	162	137	257	162
	Y	39	30	33	27	27	29
	Zr	620	432	379	305	319	310
	Nb	88	65	46	46	55	41
	Ba	1274	1283	779	819	1473	855
	La	74	59	70	66	51	61
	Ce	513	120	143	139	109	128
	Nd	76	61	72	70	59	62
	U	1.9	-	-	1.1	-	-
C.I.P.W. norm.	Q	3.21	2.86	4.34	5.55	3.60	5.72
	OR	31.75	31.39	35.53	34.81	30.86	31.02
	AB	49.52	50.89	41.49	40.93	52.58	44.08
	AN	2.46	2.14	3.78	5.27	2.41	6.04
	DI	2.52	3.82	4.27	3.07	2.96	0.82
	WO	2.88	1.70	1.35	-	-	-
	HY	-	-	-	2.02	0.55	1.51
	MT	-	4.54	6.80	6.04	4.86	-
	HM	5.22	0.42	-	-	-	7.91
	IL	1.48	1.58	1.64	1.56	1.50	0.47
	AP	0.64	0.66	0.76	0.73	0.66	0.90

D715 D827
Mechachita Dykes
D849 D685
Milega Outcrop
D566B
Guna Outcrop
D596B
Isolated Outcrop
Adjacent to
Volcanic Outlier

* mafic minerals haematised

		SYENITE 2				SYENITE 3		
	wt.%	D858*	D604	D857	D792	D562B	D769	D840
	SiO2	65.27	65.81	68.08	65.89	67.78	66.74	68.49
	AL2O3	16.54	12.27	13.48	15.12	12.92	13.55	13.29
	Fe2O3	3.26	8.19	5.50	4.53	6.25	6.35	5.82
	FeO	1.59	0.85	0.54	0.44	0.61	0.19	0.23
	MgO	0.30	0.35	0.16	0.26	0.23	0.23	0.23
	CaO	0.46	0.35	1.07	1.15	0.66	1.42	0.53
	Na2O	5.88	6.16	5.14	6.21	5.62	5.40	5.57
	K2O	5.81	4.93	5.47	5.62	5.20	5.22	5.16
	TiO2	0.58	0.77	0.36	0.54	0.50	0.64	0.45
	MnO	0.16	0.26	0.10	0.16	0.17	0.19	0.16
	P2O5	0.15	0.06	0.04	0.07	0.05	0.06	0.06
	Ag. Ratio	0.96	1.26	1.07	1.12	1.15	1.07	1.11
ppm	Ga	42	53	53	51	56	49	52
	Rb	43	89	79	61	89	79	92
	Sr	41	8	12	32	10	32	11
	Y	27	90	91	36	52	76	81
	Zr	304	1262	729	465	1188	1252	1186
	Nb	52	198	122	81	119	180	164
	Ba	408	55	71	144	40	72	43
	La	46	167	46	60	99	115	154
	Ce	115	348	163	128	222	260	325
	Nd	59	185	120	64	91	117	133
	U	1.0	-	-	-	-	4.1	3.7
C.I.P.W. norm.	Q	7.82	14.09	17.01	8.11	16.48	14.72	17.22
	C	0.09	-	-	-	-	-	-
	OR	34.33	29.10	32.34	33.22	30.75	30.85	30.50
	AB	49.75	35.70	38.85	46.45	37.48	40.64	39.64
	AN	1.30	-	-	-	-	-	-
	AC	-	14.43	4.10	5.39	8.90	4.45	6.60
	NS	-	-	-	-	-	-	-
	DI	-	1.04	0.86	1.39	1.23	1.23	1.23
	WO	-	-	1.64	1.44	0.56	1.80	0.25
	HY	0.74	0.38	-	-	-	-	-
	MT	3.97	1.35	0.004	0.37	1.07	-	-
	HM	0.51	2.26	0.02	2.41	2.42	4.81	3.53
	IL	1.10	1.46	0.004	1.02	0.95	0.80	0.82
	AP	0.35	0.14	0.003	0.16	0.11	0.14	0.14
	TN	-	-	-	-	-	0.52	0.03

SYENITE 4

	wt.%	526	721	184	818	809	837	832	833
	SiO2	66.34	66.76	67.59	63.16	66.49	65.37	67.60	64.62
	AL2O3	14.22	13.88	13.98	13.69	14.40	13.54	13.48	15.34
	Fe2O3	5.64	6.16	4.64	9.01	6.68	7.37	4.61	5.18
	FeO	1.05	0.32	1.39	0.55	0.08	0.16	1.65	0.56
	MgO	0.36	0.30	0.29	0.28	0.17	0.43	0.30	0.41
	CaO	0.66	0.87	0.72	0.83	0.28	1.46	0.74	1.05
	Na2O	5.61	6.04	5.38	6.30	6.16	5.93	5.59	6.71
	K2O	5.27	5.13	5.31	4.92	5.09	4.94	5.24	5.21
	TiO2	0.60	0.32	0.41	1.02	0.38	0.55	0.48	0.71
	MnO	0.17	0.17	0.19	0.15	0.21	0.19	0.19	0.12
	P2O5	0.09	0.05	0.10	0.09	0.06	0.06	0.11	0.08
	Ag. Ratio	1.05	1.12	1.04	1.15	1.09	1.12	1.10	1.09
ppm	Ga	51	54	52	53	57	52	50	53
	Rb	80	97	76	95	96	93	91	45
	Sr	30	20	29	32	14	28	23	24
	Y	57	75	67	90	62	62	70	25
	Zr	1147	1715	2082	1911	1445	1339	1293	356
	Nb	157	165	146	262	157	144	146	60
	Ba	129	94	62	108	65	25	113	121
	La	95	114	92	214	121	106	103	46
	Ce	249	245	213	427	272	237	261	100
	Nd	92	114	98	171	107	102	124	50
	U	-	-		-	3.7	-	-	-
C.I.P.W. norm.	Q	13.28	12.56	15.65	8.87	12.16	11.68	15.31	5.57
	OR	31.11	30.32	31.36	29.09	30.08	29.14	30.95	30.81
	AB	43.80	42.84	42.36	43.00	45.73	42.14	40.18	49.88
	AC	3.20	7.29	2.77	9.03	5.63	7.07	6.26	6.11
	DI	1.93	1.61	1.56	1.50	0.62	2.31	2.42	2.20
	WO	0.08	0.80	0.38	0.31	-	1.39	-	0.77
	HY	-	-	-	-	0.13	-	0.13	-
	MT	2.20	0.65	3.91	-	-	-	3.54	0.13
	HM	3.01	3.18	0.98	5.88	4.73	.03	-	2.97
	IL	1.14	0.60	0.78	1.48	0.61	.004	0.91	1.34
	AP	0.21	0.11	0.23	0.21	0.14	.004	0.26	0.19
	TN	-	-	-	0.58	0.13	.002	-	-

* mafic minerals haematised

SYENITE 5

	wt.%	D533	D525	798	813	800	801 *	812 *	944
	Si02	64.14	65.58	65.61	65.13	66.30	64.61	65.09	64.96
	AL203	16.37	16.17	15.40	15.92	15.81	17.19	16.35	14.47
	Fe203	4.61	3.73	5.41	5.41	4.08	3.54	4.97	6.36
	FeO	0.75	0.80	0.81	0.27	1.01	0.88	0.33	0.59
	MgO	0.41	0.25	0.26	0.21	0.22	0.23	0.32	0.31
	CaO	0.97	0.84	0.58	0.54	0.42	1.25	0.85	1.19
	Na20	6.36	6.70	5.89	6.24	6.49	6.55	5.93	6.27
	K20	5.43	5.44	5.07	5.51	4.98	5.04	5.26	5.00
	Ti02	0.67	0.30	0.61	0.49	0.45	0.48	0.62	0.55
	MnO	0.16	0.12	0.24	0.19	0.16	0.12	0.14	0.22
	P205	0.12	0.06	0.11	0.09	0.09	0.10	0.14	0.08
	Ag. Ratio	1.00	1.05	0.99	1.02	1.02	0.94	0.94	1.09
ppm	Ga	47	54	45	47	43	45	44	48
	Rb	59	72	89	66	81	56	52	76
	Sr	27	35	32	30	112	329	125	54
	Y	51	45	57	46	49	34	40	59
	Zr	426	633	955	713	1196	546	453	1062
	Nb	101	87	144	117	155	94	90	131
	Ba	141	257	619	144	1400	1114	647	271
	La	82	106	108	88	138	76	84	137
	Ce	142	150	213	190	270	149	176	288
	Nd	82	87	96	78	114	68	83	115
	U	-	-	-	2.5	-	-	-	-
C.I.P.W. norm.	Q	4.82	5.47	10.96	7.33	9.17	5.12	8.72	9.18
	OR	32.11	32.17	29.98	32.56	29.39	29.81	31.09	29.56
	AB	53.85	52.88	49.80	51.21	53.60	55.39	50.20	46.56
	AN	0.05	-	0.62	-	-	2.61	2.43	-
	AC	-	3.32	-	1.40	1.13	-	-	5.74
	DI	2.20	1.34	1.19	1.12	1.16	1.23	0.41	1.66
	WO	0.47	0.85	-	0.26	-	0.56	-	1.35
	HY	-	-	0.09	-	0.008	-	0.60	-
	MT	0.99	2.10	1.62	0.07	2.47	1.83	-	1.02
	HM	3.92	1.13	4.29	4.87	1.98	2.27	4.96	3.66
	IL	1.27	0.57	1.16	0.93	0.85	0.91	0.99	1.04
	AP	0.28	0.14	0.26	0.21	0.21	0.23	0.33	0.19
	TN	-	-	-	-	-	-	0.23	-

* mafic minerals haematised

GRANITE 1

	wt.%	845*	558	606	844	848	781A
	SiO2	74.00	72.93	71.81	70.64	72.90	69.70
	AL203	11.70	11.83	11.72	12.85	11.88	9.69
	Fe203	4.62	4.40	5.04	3.07	4.37	9.96
	FeO	0.12	0.67	0.21	1.79	0.68	0.07
	MgO	0.18	0.12	0.19	0.15	0.14	0.09
	CaO	0.40	0.16	1.13	1.02	0.53	0.22
	Na20	3.42	4.38	4.37	4.54	3.97	5.07
	K20	5.16	5.04	5.07	5.47	5.09	4.51
	TiO2	0.26	0.30	0.31	0.33	0.28	0.52
	MnO	0.11	0.13	0.11	0.09	0.12	0.13
	P205	0.03	0.03	0.04	0.05	0.03	0.03
	Ag. Ratio	0.96	1.07	1.08	1.04	1.01	1.36
ppm	Ga	44	43	42	48	44	48
	Rb	107	127	126	135	129	102
	Sr	18	5	16	20	12	5
	Y	67	98	89	130	103	91
	Zr	1106	1689	1404	1633	1585	1915
	Nb	127	186	155	234	174	165
	Ba	90	85	100	60	53	28
	La	157	215	160	182	322	175
	Ce	309	413	337	394	489	335
	Nd	140	184	145	171	260	210
	U	-	5.9	-	-	-	-
C.I.P.W. norm.	Q	33.40	28.81	26.65	22.19	29.75	26.78
	OR	30.49	29.80	29.96	32.33	30.10	26.65
	AB	28.94	32.76	32.06	35.61	32.74	24.73
	AN	1.33	-	-	-	-	-
	AC	-	3.81	4.33	2.46	0.77	16.00
	DI	0.34	0.46	1.02	2.84	0.75	-
	WO	-	-	1.68	0.59	0.61	-
	HY	0.28	0.08	-	-	-	0.22
	MT	-	1.71	0.13	3.21	1.77	-
	HM	4.61	1.89	3.44	-	2.87	4.4
	IL	0.48	0.57	0.58	0.62	0.53	0.42
	AP	0.07	0.07	0.09	0.11	0.07	0.07
	TN	0.007	-	-	-		0.63
	RU	-	-	-	-		0.03

* mafic minerals haematised

		GRANITE 2						
	wt.%	516*	527C	573	612B	826	828	829
	SiO2	72.20	72.48	69.28	76.16	72.29	70.43	70.54
	AL2O3	11.34	10.82	11.79	10.41	10.05	12.15	13.91
	Fe2O3	6.31	5.53	6.96	4.33	7.19	5.47	2.24
	FeO	0.30	1.06	0.22	0.64	0.44	0.81	2.29
	MgO	0.24	0.18	0.24	0.11	0.16	0.21	0.17
	CaO	0.65	0.29	0.55	0.43	0.69	0.24	0.45
	Na2O	3.65	4.38	5.32	4.90	4.93	5.17	2.88
	K2O	4.83	4.78	4.88	2.72	3.92	4.93	7.13
	TiO2	0.36	0.33	0.43	0.20	0.26	0.39	0.28
	MnO	0.08	0.13	0.27	0.07	0.04	0.15	0.08
	P2O5	0.03	0.02	0.06	0.02	0.02	0.04	0.04
	Ag. Ratio	0.99	1.14	1.19	1.06	1.23	1.14	0.89
ppm	Ga	51	50	50	45	42	55	39
	Rb	111	105	128	46	170	129	153
	Sr	19	6	23	17	13	12	29
	Y	122	51	94	96	32	61	89
	Zr	1422	983	1766	1983	1779	1357	1529
	Nb	208	117	196	136	58	115	157
	Ba	46	43	44	60	32	37	112
	La	365	47	182	188	72	92	153
	Ce	415	163	388	414	111	226	336
	Nd	378	53	170	178	71	90	145
	U	-	-	-	-	-	3.0	-
C.I.P.W. norm.	Q	31.39	29.98	21.42	37.32	30.35	22.94	24.49
	C	-	-	-	-	-	-	0.73
	OR	28.55	28.21	28.84	16.08	23.17	29.15	42.12
	AB	30.89	29.07	33.48	38.37	29.88	35.02	24.34
	AN	0.29	-	-	-	-	-	1.97
	AC	-	7.06	10.17	2.74	10.44	7.71	-
	DI	1.29	0.96	1.29	0.59	0.86	0.72	-
	WO	0.45	0.02	0.28	0.52	0.91	-	-
	HY	-	-	-	-	-	0.18	2.45
	MT	0.18	2.88	0.34	1.71	0.79	1.97	3.24
	HM	6.18	1.09	3.20	2.20	3.03	1.44	-
	IL	0.68	0.62	0.81	0.38	0.49	0.74	0.53
	AP	0.07	0.04	0.14	0.04	0.04	0.09	0.09

GRANITE 2

	wt.%	807	808	624	532	539	741	565
	SiO2	73.77	72.38	74.16	69.04	72.79	67.87	71.77
	AL2O3	10.15	9.66	8.76	10.83	8.74	11.43	10.36
	Fe2O3	6.79	7.84	7.87	8.15	8.88	8.25	7.65
	FeO	0.10	0.44	0.71	0.57	0.35	0.33	0.24
	MgO	0.11	0.09	0.14	0.24	0.13	0.31	0.26
	CaO	0.17	0.25	0.41	0.49	0.36	0.69	0.53
	Na2O	3.95	4.16	3.03	5.43	3.88	5.52	4.32
	K2O	4.73	4.81	4.35	4.53	4.51	4.82	4.44
	TiO2	0.16	0.20	0.25	0.45	0.25	0.48	0.29
	MnO	0.05	0.15	0.30	0.23	0.07	0.26	0.12
	P2O5	0.02	0.02	0.02	0.04	0.03	0.04	0.02
	Ag. Ratio	1.14	1.25	1.11	1.28	1.29	1.25	1.15
ppm	Ga	57	48	43	53	49	52	48
	Rb	199	180	163	118	149	128	143
	Sr	3	11	30	10	9	15	16
	Y	41	46	70	82	84	99	122
	Zr	2503	1193	3357	1456	2274	1874	2287
	Nb	61	156	445	295	304	325	211
	Ba	7	18	20	89	39	131	49
	La	44	45	61	184	172	227	247
	Ce	73	97	151	405	392	451	486
	Nd	60	49	73	168	137	219	246
	U	-	2.8	-	-	-	-	-
C.I.P.W. norm.	Q	34.09	32.20	40.35	22.82	35.38	19.52	30.54
	OR	27.94	28.44	25.72	26.78	26.66	28.49	26.24
	AB	25.87	22.87	20.80	30.45	19.85	31.96	28.57
	AC	6.65	10.88	4.27	13.67	11.44	13.00	7.03
	DI	0.55	0.48	0.75	1.29	0.69	1.66	1.39
	WO	-	0.20	0.39	0.21	0.28	0.42	0.29
	HY	0.01	-	-	-	-	-	-
	MT	0.02	1.32	2.54	1.28	0.63	0.52	0.32
	HM	4.47	3.15	4.63	2.53	4.49	3.39	4.98
	IL	0.30	0.38	0.47	0.85	0.47	0.91	0.55
	AP	0.04	0.04	0.04	0.09	0.07	0.09	0.04

		MINOR INTRUSIONS (SYENITIC)							(BASIC)
	wt.%	560	531	803	811	946	722		183A
	SiO2	63.87	66.98	65.16	63.06	64.53	67.97		45.49
	AL2O3	15.65	13.80	15.00	15.00	13.56	12.46		15.38
	Fe2O3	3.64	4.99	6.39	7.35	6.13	5.96		8.87
	FeO	2.40	1.40	-	0.43	2.45	1.85		6.16
	MgO	0.29	0.37	0.22	0.29	0.35	0.29		3.33
	CaO	1.44	0.70	1.07	1.08	0.84	0.50		10.04
	Na2O	6.99	6.12	6.05	7.10	6.35	5.48		4.39
	K2O	4.89	4.82	5.30	4.55	4.84	4.70		1.82
	TiO2	0.54	0.51	0.54	0.85	0.66	0.50		3.44
	MnO	0.17	0.21	0.20	0.20	0.22	0.20		0.23
	P2O5	0.11	0.10	0.07	0.09	0.07	0.07		0.84
	Ag. Ratio	1.07	1.11	1.05	1.11	1.16	1.13		0.60
ppm	Ga	46	51	51	53	56	54		29
	Rb	40	69	80	53	83	147		67
	Sr	15	21	44	27	32	23		594
	Y	21	81	48	42	61	111		43
	Zr	191	1501	1237	511	1362	2114		285
	Nb	31	186	163	96	154	342		29
	Ba	88	129	171	124	46	106		384
	La	41	122	110	78	152	216		21
	Ce	94	262	241	161	311	482		75
	Nd	55	115	107	81	129	209		49
	U	-	-	-	-	-	-		-
C.I.P.W. norm.	Q	2.97	13.53	9.12	4.76	9.57	19.10		
	OR	28.91	28.46	31.31	26.90	28.62	27.76	OR	10.76
	AB	53.26	44.16	47.64	51.79	42.76	37.95	AB	25.79
	AC	5.17	6.70	3.12	7.32	9.63	7.42	AN	16.88
	DI	5.53	1.99	1.18	1.55	3.13	1.60	NE	6.14
	WO	-	0.11	0.93	0.94	-	-	AC	-
	HY	0.17	-	-	-	0.78	0.10	NS	-
	MT	2.68	3.72	-	-	4.06	4.92	DI	17.90
	HM	-	0.10	5.31	4.81	-	-	WO	1.85
	IL	1.02	0.97	0.42	1.33	1.25	0.95	HY	-
	AP	0.26	0.23	0.16	0.21	0.16	0.16	OL	-
	TN	-	-	0.77	0.36	-	-	MT	10.63
								HM	1.54
								IL	6.53
								AP	1.97

* mafic minerals partly haematised

MINOR INTRUSIONS (ACIDIC)

	wt.%	559	860 *	861 *	938	1106 *	856	596
	SiO2	74.33	79.17	82.90	74.40	77.23	71.61	75.60
	AL203	9.06	9.60	10.33	9.63	10.18	10.85	11.37
	Fe203	7.16	6.33	2.67	5.67	4.33	6.58	3.01
	FeO	0.66	0.16	0.25	1.07	0.34	0.27	0.41
	MgO	0.12	0.10	0.02	0.07	0.08	0.07	0.11
	CaO	0.30	0.59	0.05	0.29	0.25	0.71	0.33
	Na20	4.03	1.18	1.14	4.27	3.34	4.80	4.02
	K20	4.06	2.40	2.35	4.33	3.99	4.59	4.85
	TiO2	0.19	0.21	0.25	0.14	0.18	0.34	0.21
	MnO	0.05	0.23	0.01	0.12	0.05	0.14	0.06
	P205	0.03	0.02	0.02	0.02	0.02	0.03	0.03
	Ag. Ratio	1.22	0.47	0.43	1.22	0.96	1.19	1.04
ppm	Ga	44	46	48	48	46	50	49
	Rb	136	58	59	192	114	72	81
	Sr	3	16	4	19	15	10	3
	Y	157	99	91	150	148	74	96
	Zr	2744	2245	2132	3048	2585	1732	1335
	Nb	304	196	230	315	214	121	167
	Ba	-	70	142	-	8	23	51
	La	389	67	82	379	160	103	396
	Ce	728	1305	208	774	385	269	654
	Nd	361	86	64	356	173	136	257
	U	-	7.2	-	9.4	-	-	-
C.I.P.W. norm.	Q	37.18	61.76	67.19	35.08	41.94	27.67	33.75
	C	-	4.03	5.87	-	-	-	-
	OR	24.00	14.18	13.89	25.56	23.58	27.12	28.67
	AB	24.01	9.98	9.64	25.46	28.27	30.26	31.44
	AN	-	2.79	0.11	-	1.00	-	-
	AC	8.90	-	-	9.36	-	9.13	2.27
	DI	0.64	-	-	0.37	0.08	0.37	0.59
	WO	0.19	-	-	0.34	-	1.18	0.28
	HY	-	0.24	0.05	-	0.16	-	-
	MT	1.74	0.65	0.11	3.43	0.73	0.34	0.90
	HM	2.88	5.87	2.59	0.05	3.82	3.19	1.59
	IL	0.36	0.39	0.47	0.26	0.34	0.64	0.39
	AP	0.07	0.04	0.04	0.04	0.04	0.07	0.07

APPENDIX IIIF

CAINOZOIC BASALTS

		CAINOZOIC BASALTS	
	wt.%	973	R86
	Si02	48.97	47.08
	AL203	14.10	14.77
	Fe203	5.90	5.95
	FeO	3.47	3.93
	MgO	8.02	9.10
	CaO	8.60	9.51
	Na20	5.79	4.89
	K20	2.31	1.94
	Ti02	2.13	2.14
	MnO	0.21	0.21
	P205	0.49	0.48
C.I.P.W. norm.	Q	-	-
	C	-	-
	OR	13.64	11.45
	AB	20.79	16.93
	AN	5.63	12.63
	NE	15.28	13.24
	AC	-	-
	NS	-	-
	DI	26.33	24.46
	WO	-	-
	HY	-	-
	OL	5.44	7.94
	MT	5.71	7.14
	HM	1.95	1.02
	IL	4.04	4.06
	AP	1.16	1.14

CONTENTS OF REAR POCKET

MAP 1 : Geology of the Ras ed Dom Younger Granite ring-complex, Bayuda Desert, Sudan.

MAP 2 : Geology of the Abu Dom Younger Granite ring-complex, Bayuda Desert, Sudan.

MAP 3 : Geology of Younger Granite ring-complexes, central Bayuda Desert, Sudan.

MAP 4 : Dyke and Locality map, Ras ed Dom.

MAP 5 : Dyke and Locality map, Abu Dom.

PHOTOMOSAIC A : Ras ed Dom.

PHOTOMOSAIC B : Abu Dom.

MAP 1 GEOLOGY OF THE RAS ED DOM YOUNGER GRANITE RING-COMPLEX, BAYUDA DESERT, SUDAN.

STRUCTURAL CENTRES OF RAS ED DOM COMPLEX

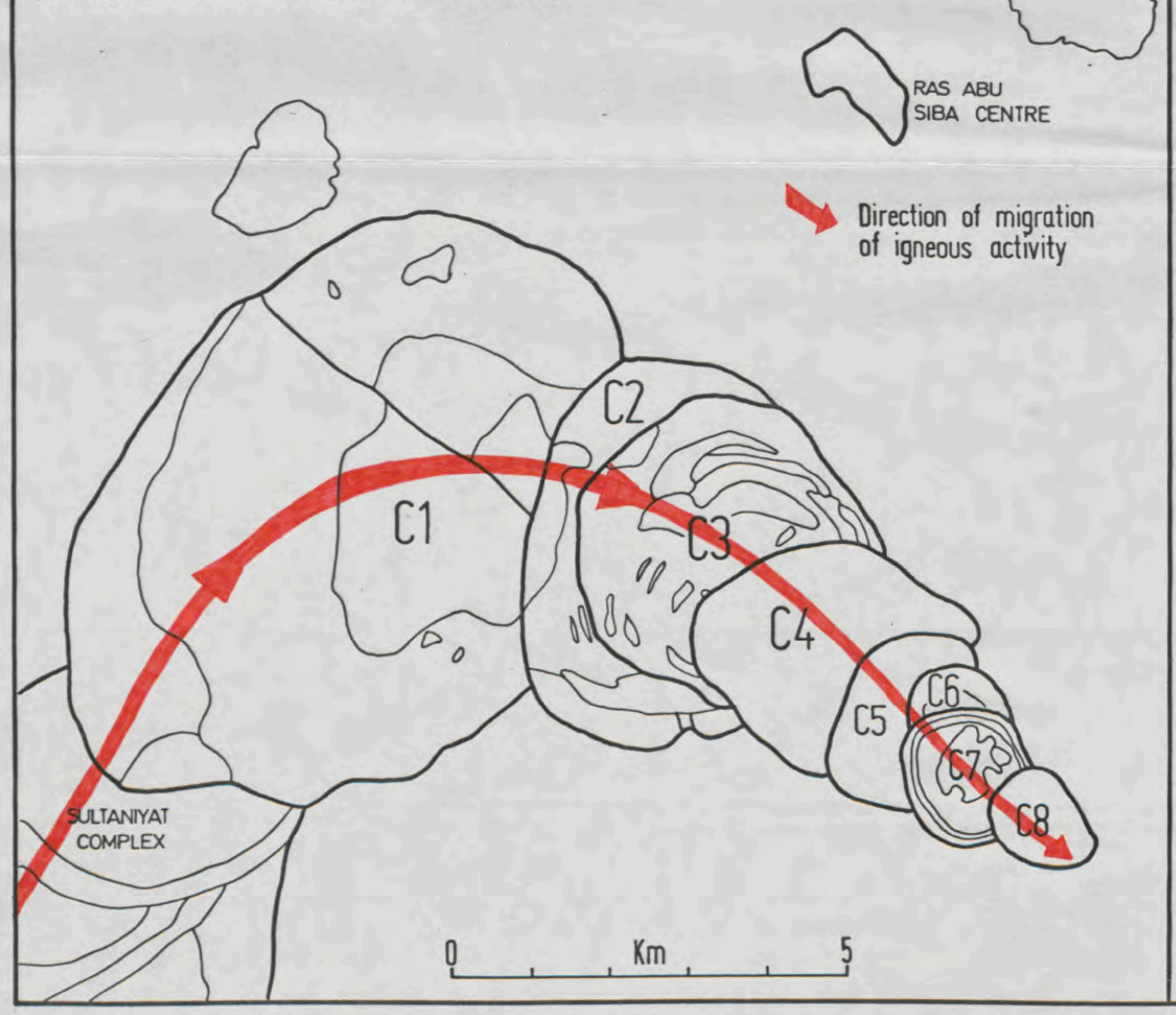

☐	Unconsolidated wadi sands and gravels†
××	Cainozoic basalts
	Younger Granite rocks
⋰	Basement gneisses
╲	Geological boundary
╲	Geological boundary - inferred
╲	Fault
╲	Fault - inferred
╲	Rock outcrop boundary
▨	Younger Granite dykes

† Wadi deposits within areas of younger granite rock are omitted for the purpose of clarity. Their distribution in such instances may, however, be deduced from the rock outcrop boundary lines.

Ras Ed Dom geologically mapped by D. A. O'Halloran, 1976-77

RAS ED DOM COMPLEX

CENTRE 8

▨	Syenite 15. alkali quartz syenite. aegirine < arfvedsonite

CENTRE 7

IT3	Intrusive trachyte 3. alkali trachyte. xenocrysts of hedenbergite - syenite
S14	Syenite 14. alkali syenite. aegirine > arfvedsonite, minor biotite
S13	Syenite 13. alkali syenite. aegirine - augite, katophorite $\xrightarrow{z}$ arfvedsonite, minor riebeckite, biotite ✱
▥	Syenite 12. alkali syenite. aegirine - augite < arfvedsonite
S11	Syenite 11. hedenbergite syenite. sodic amphibole > early hedenbergite, minor late biotite

CENTRE 6

▤	Syenite 10. alkali syenite. arfvedsonite > aegirine - augite
S9	Syenite 9. alkali syenite. aegirine - augite > arfvedsonite

CENTRE 5

S8	Syenite 8. alkali syenite. arfvedsonite > aegirine - augite, minor biotite

CENTRE 4

▧	Syenite 7. alkali quartz syenite. aegirine > arfvedsonite

CENTRE 3

░	Minor microgranite intrusions. alkali microgranites (undifferentiated) aegirine > arfvedsonite
G2	Granite 2. alkali granite. aegirine > arfvedsonite
MG2	Microgranite 2. alkali microgranite. aegirine < arfvedsonite
IT2	Intrusive trachyte 2. feldspar phyric, hedenbergite trachyte
MG1	Microgranite 1. alkali microgranite. aegirine
IT1	Intrusive trachyte 1. alkali trachyte. aegirine - augite
+++	Syenite 6. alkali quartz syenite. aegirine < arfvedsonite

CENTRE 2

S5	Syenite 5. alkali quartz syenite. aegirine - augite $\xrightarrow{z}$ aegirine, arfvedsonite, minor riebeckite ✱
S4	Syenite 4. ferro - augite syenite. ferro - augite, variable calcic and sodic - calcic amphiboles ✱

RAS ABU SIBA CENTRE

A.S.F.	Abu Siba felsite. alkali intrusive felsite. aegirine

CENTRE 1

		Chilled margin → Interior
S3	Syenite 3. alkali quartz syenite.	fe - hedenbergite $\xrightarrow{z}$ aegirine augite → aegirine ✱ fe - richterite $\xrightarrow{z}$ arfvedsonite ✱
G1	Granite 1. alkali granite.	aegirine, fe - richterite $\xrightarrow{z}$ arfvedsonite ✱
☐	Syenite 2. quartz syenite.	fe - augite $\xrightarrow{z}$ aegirine - augite ✱ fe - richterite → arfvedsonite ✱
S1	Syenite 1. ferro - augite syenite.	ferro-augite, calcic and sodic-calcic amphiboles ✱

SULTANIYAT COMPLEX (after Curtis, 1979, with permission)

I.R.G.	Inner ring microgranite. alkali microgranite
O.R.G.	Outer ring microgranite. alkali microgranite
▨	Syenite 2. alkali syenite. calcic clinopyroxene, sodic-calcic amphibole
G2	Granite 2. alkali granite. aegirine, alkali amphibole
▧	Quartz microsyenite. alkali microsyenite. aegirine, alkali amphibole

✱ Electron microprobe identification

→ Mineral zonation

z Extent of zonation observed within individual crystals

MAP 2 GEOLOGY OF THE ABU DOM YOUNGER GRANITE RING-COMPLEX, BAYUDA DESERT, SUDAN.

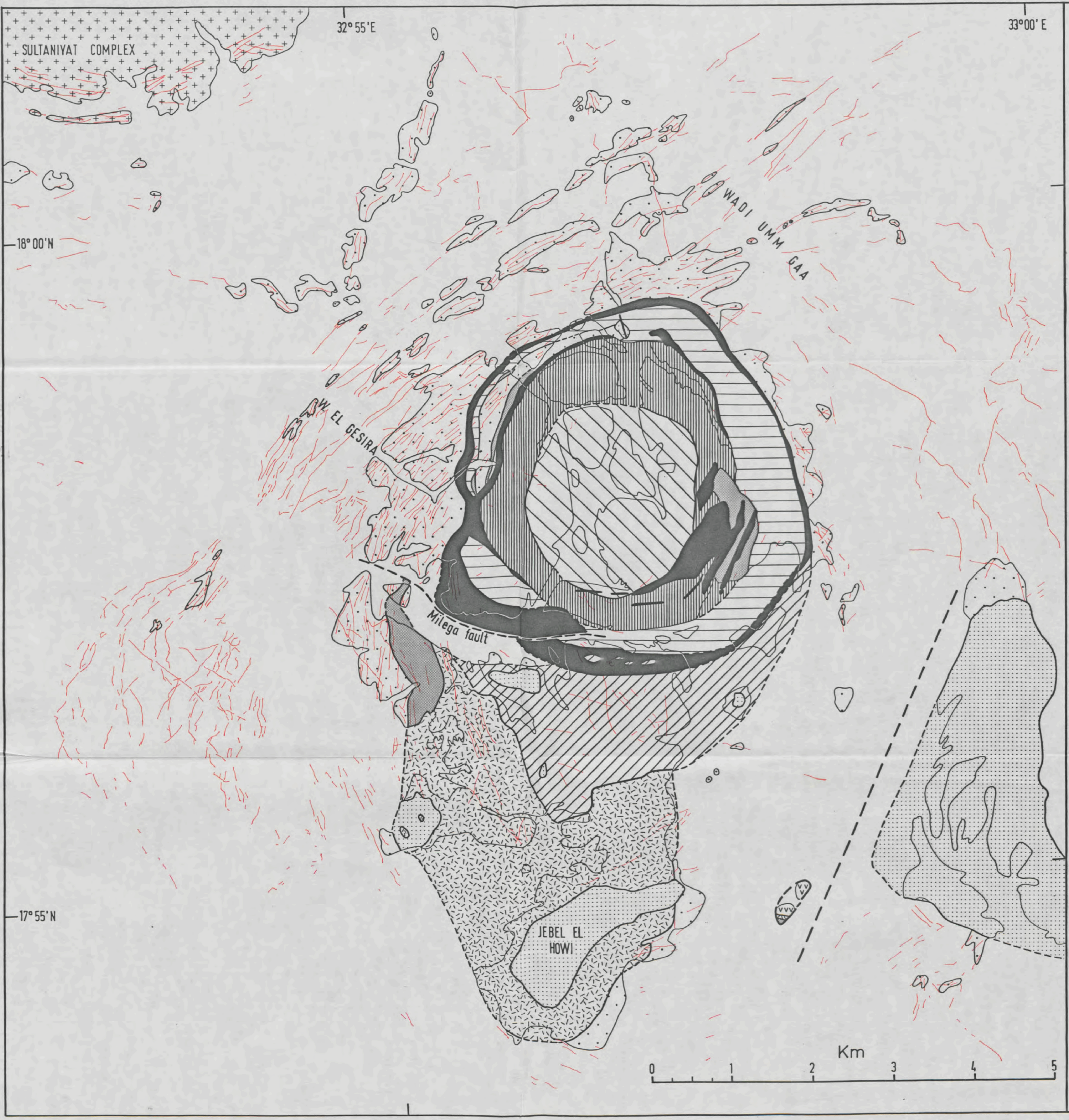

SEQUENCE OF ROCK TYPES

- Unconsolidated wadi sands and gravels[†]
- Nubian Sandstone Formation
- Younger Granite rocks of Sultaniyat Complex
- Granite 2. alkali granite. aegirine > arfvedsonite
- Syenite 5. alkali quartz-syenite. aegirine, arfvedsonite
- Syenite 4. alkali quartz-syenite. aegirine > arfvedsonite
- Syenite 3. alkali quartz-syenite. aegirine ≃ arfvedsonite
- Granite 1. alkali granite. aegirine > arfvedsonite
- Syenite 2. alkali syenite. arfvedsonite > aegirine
- Syenite 1. hedenbergite syenite. hedenbergite < calcic → sodic-calcic amphiboles
- Abu Dom Volcanic Group
- Younger Granite dykes
- Basement gneisses
- Geological boundary
- Geological boundary - inferred
- Fault
- Fault - inferred
- Rock outcrop boundary

[†] Wadi deposits within areas of younger granite rocks are omitted for the purpose of clarity. Their distribution in such instances may, however, be deduced from the rock outcrop boundary lines.

Abu Dom geologically mapped by D.A. O'Halloran, 1976-77

red lines = dykes ?

MAP 3

GEOLOGY OF YOUNGER GRANITE RING-COMPLEXES, CENTRAL BAYUDA DESERT, SUDAN

Scale 1:100,000 (Approx)

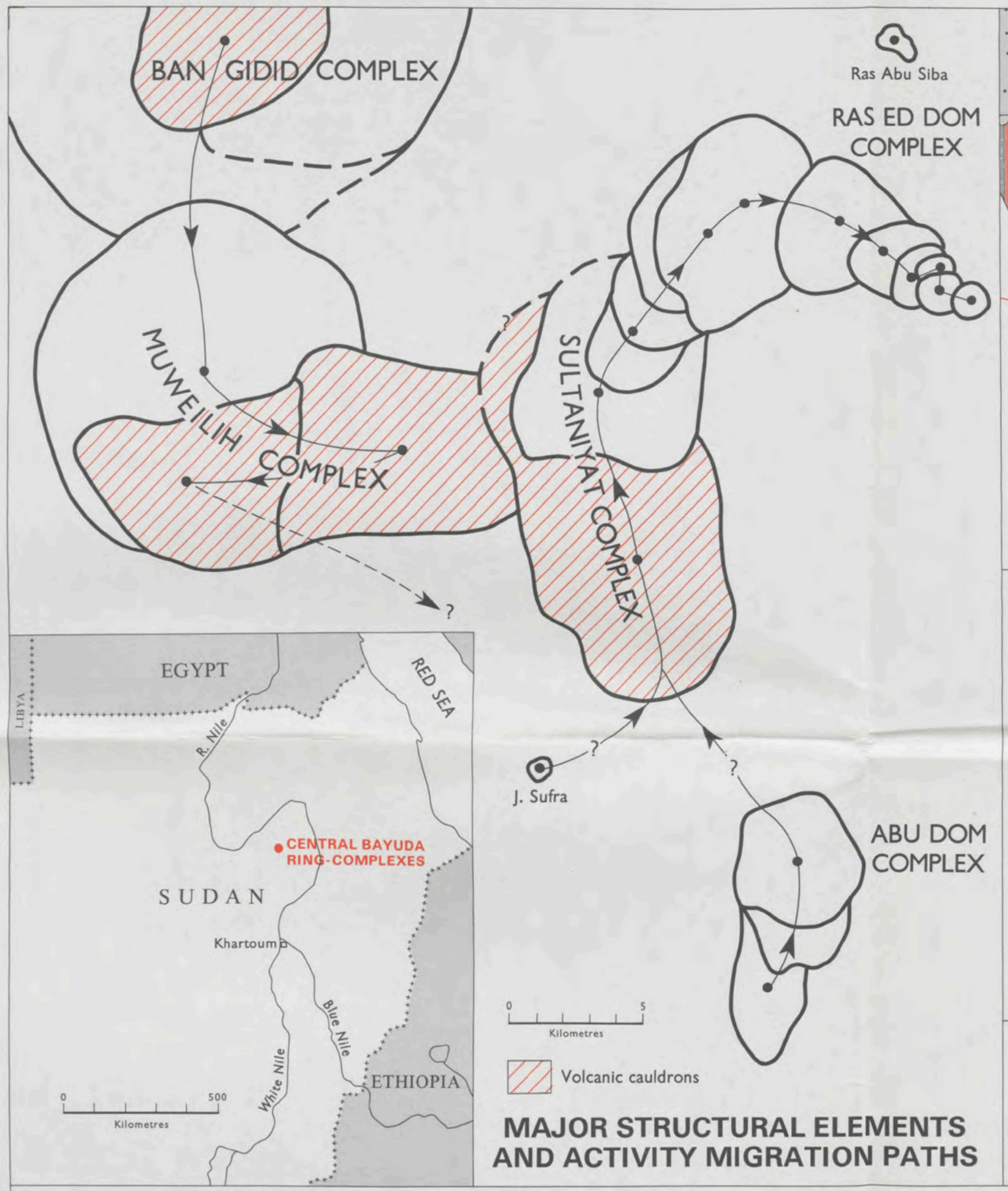

MAJOR STRUCTURAL ELEMENTS AND ACTIVITY MIGRATION PATHS

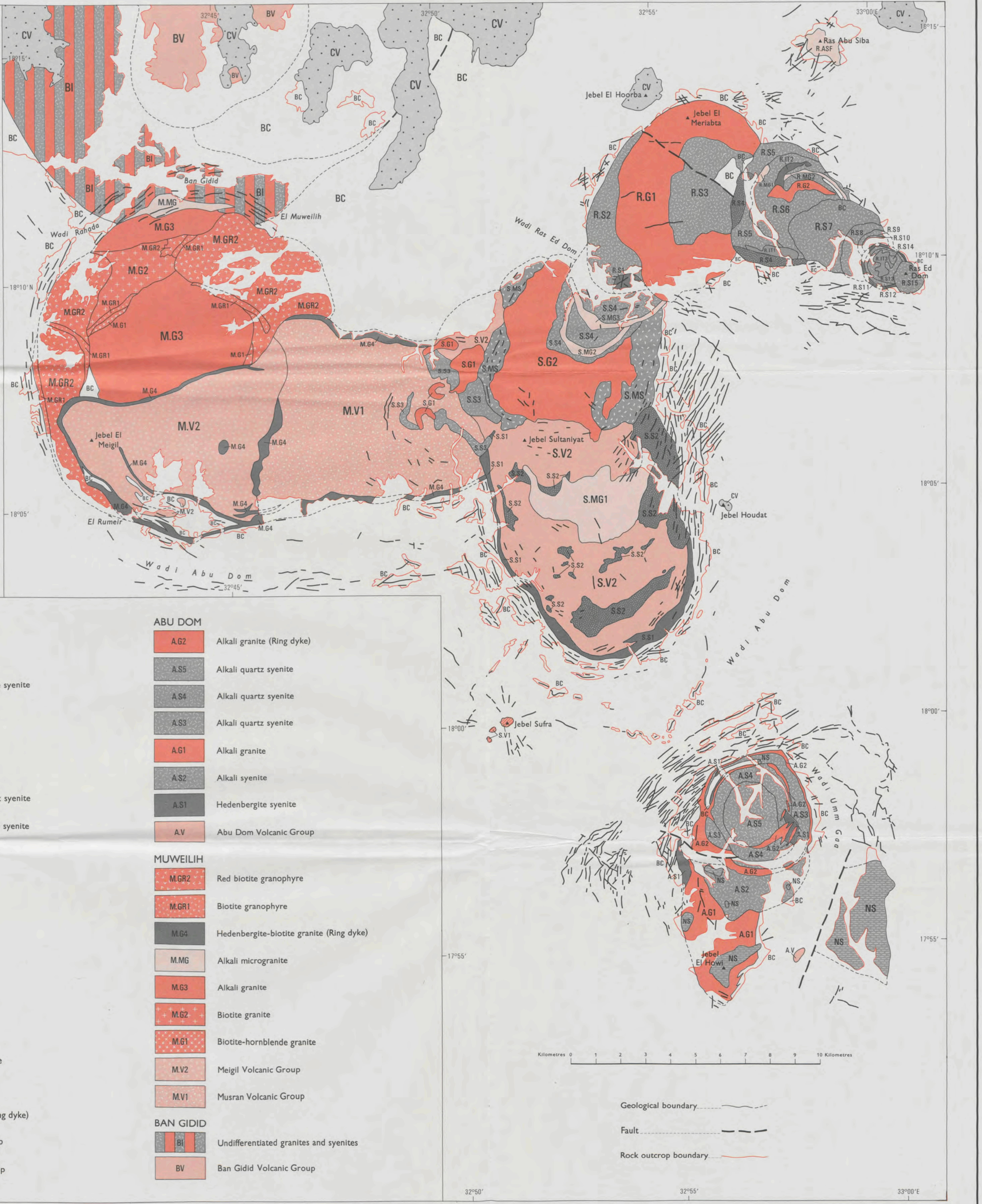

· CV ·	Cainozoic volcanic rocks
NS	Nubian Sandstone Formation
▨	Minor intrusions related to younger granite complexes
BC	Undifferentiated Precambrian country rocks and superficial deposits

RAS ED DOM

R.S15	Alkali quartz syenite
R.IT3	Intrusive alkali trachyte
R.S14	Alkali syenite
R.S13	Alkali syenite
R.S12	Alkali syenite
R.S11	Hedenbergite syenite
R.S10	Alkali syenite
R.S9	Alkali syenite
R.S8	Alkali syenite
R.S7	Alkali quartz syenite
R.G2	Alkali granite
R.MG2	Alkali microgranite
R.IT2	Intrusive hedenbergite trachyte
R.IT1	Intrusive alkali trachyte
R.MG1	Alkali microgranite
R.S6	Alkali quartz syenite
R.S5	Alkali quartz syenite
R.S4	Hedenbergite-hornblende syenite
R.ASF	Alkali felsite of Abu Siba
R.S3	Alkali quartz syenite
R.G1	Alkali granite
R.S2	Augite-hornblende-quartz syenite
R.S1	Hedenbergite-hornblende syenite

SULTANIYAT

S.MG3	Alkali microgranite
S.MG2	Alkali microgranite
S.S4	Alkali syenite
S.G2	Alkali granite
S.MG1	Alkali microgranite
S.G1	Alkali granite
S.S3	Alkali quartz syenite
S.MS	Alkali quartz microsyenite
S.S2	Hedenbergite syenite
S.S1	Hedenbergite syenite (Ring dyke)
S.V2	Sultaniyat Volcanic Group
S.V1	Jebel Sufra Volcanic Group

ABU DOM

A.G2	Alkali granite (Ring dyke)
A.S5	Alkali quartz syenite
A.S4	Alkali quartz syenite
A.S3	Alkali quartz syenite
A.G1	Alkali granite
A.S2	Alkali syenite
A.S1	Hedenbergite syenite
A.V	Abu Dom Volcanic Group

MUWEILIH

M.GR2	Red biotite granophyre
M.GR1	Biotite granophyre
M.G4	Hedenbergite-biotite granite (Ring dyke)
M.MG	Alkali microgranite
M.G3	Alkali granite
M.G2	Biotite granite
M.G1	Biotite-hornblende granite
M.V2	Meigil Volcanic Group
M.V1	Musran Volcanic Group

BAN GIDID

BI	Undifferentiated granites and syenites
BV	Ban Gidid Volcanic Group

Prepared for publication by the British Government's Directorate of Overseas Surveys, 1981.

Field work (1976-1977) and map production financially supported by the British Government's Overseas Development Administration (Research Scheme R2986).

Geologically mapped by P. S. Curtis (Sultaniyat complex), M. McCormac (Ban Gidid, Muweilih complexes) and D. A. O'Halloran (Ras Ed Dom, Abu Dom complexes) under the general supervision of J. R. Vail, Portsmouth Polytechnic, U.K. and D. C. Almond, Kingston Polytechnic, U.K.

Map based on uncontrolled mosaics of air photography supplied by the Sudan Government.

MAP 4 LOCALITY AND DYKE MAP, RAS ED DOM COMPLEX.

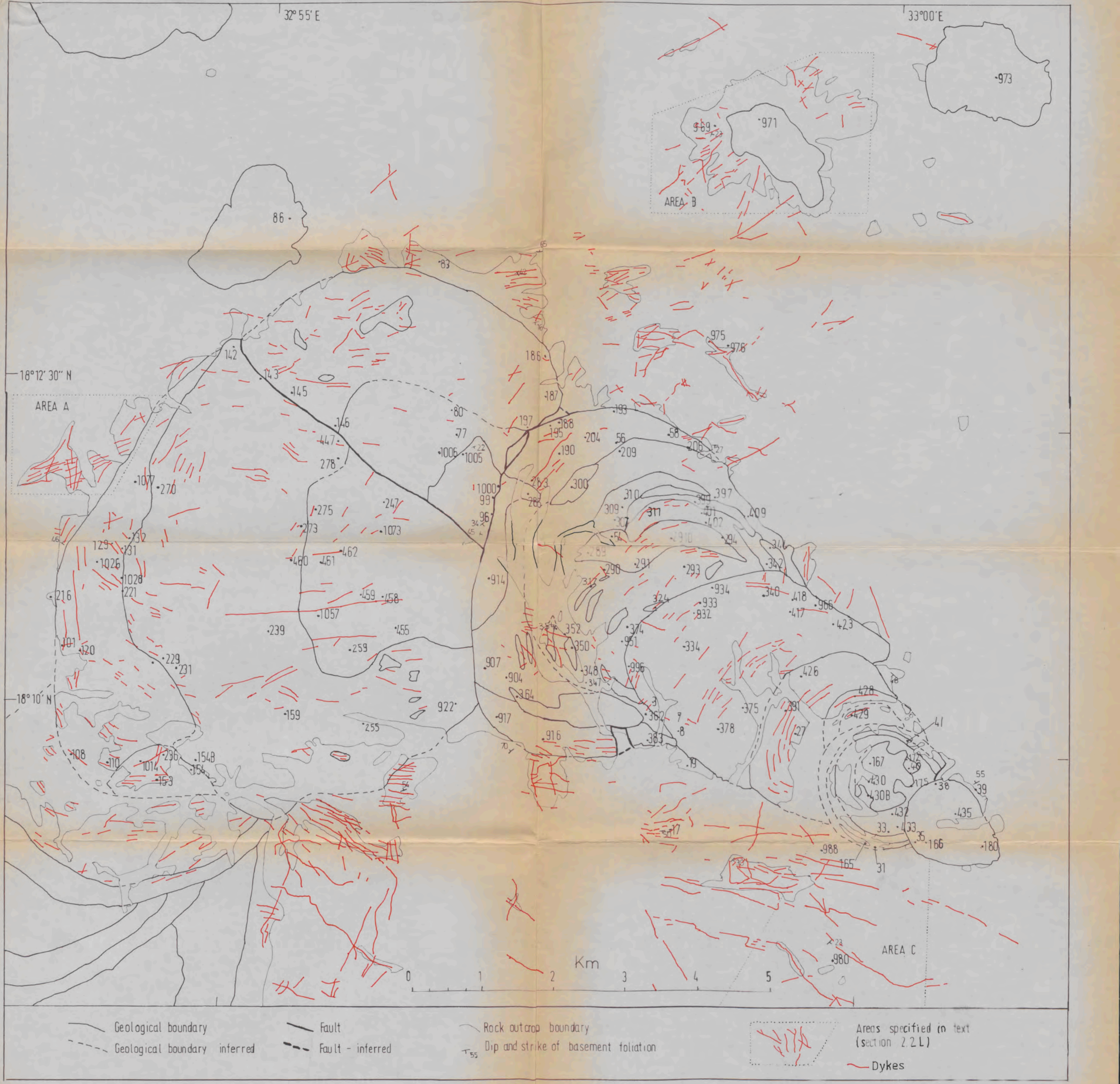

MAP 5 LOCALITY AND DYKE MAP, ABU DOM COMPLEX.

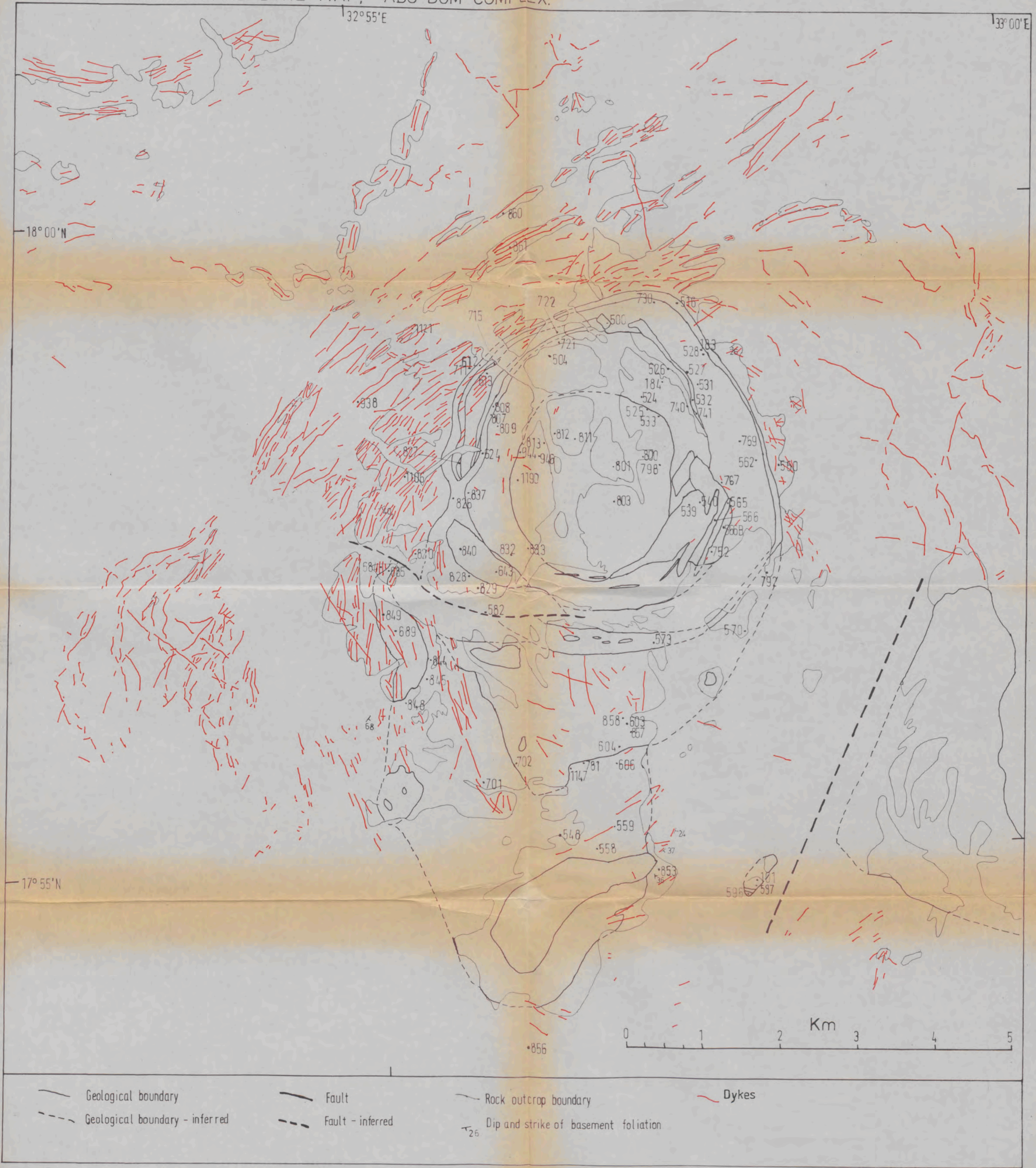

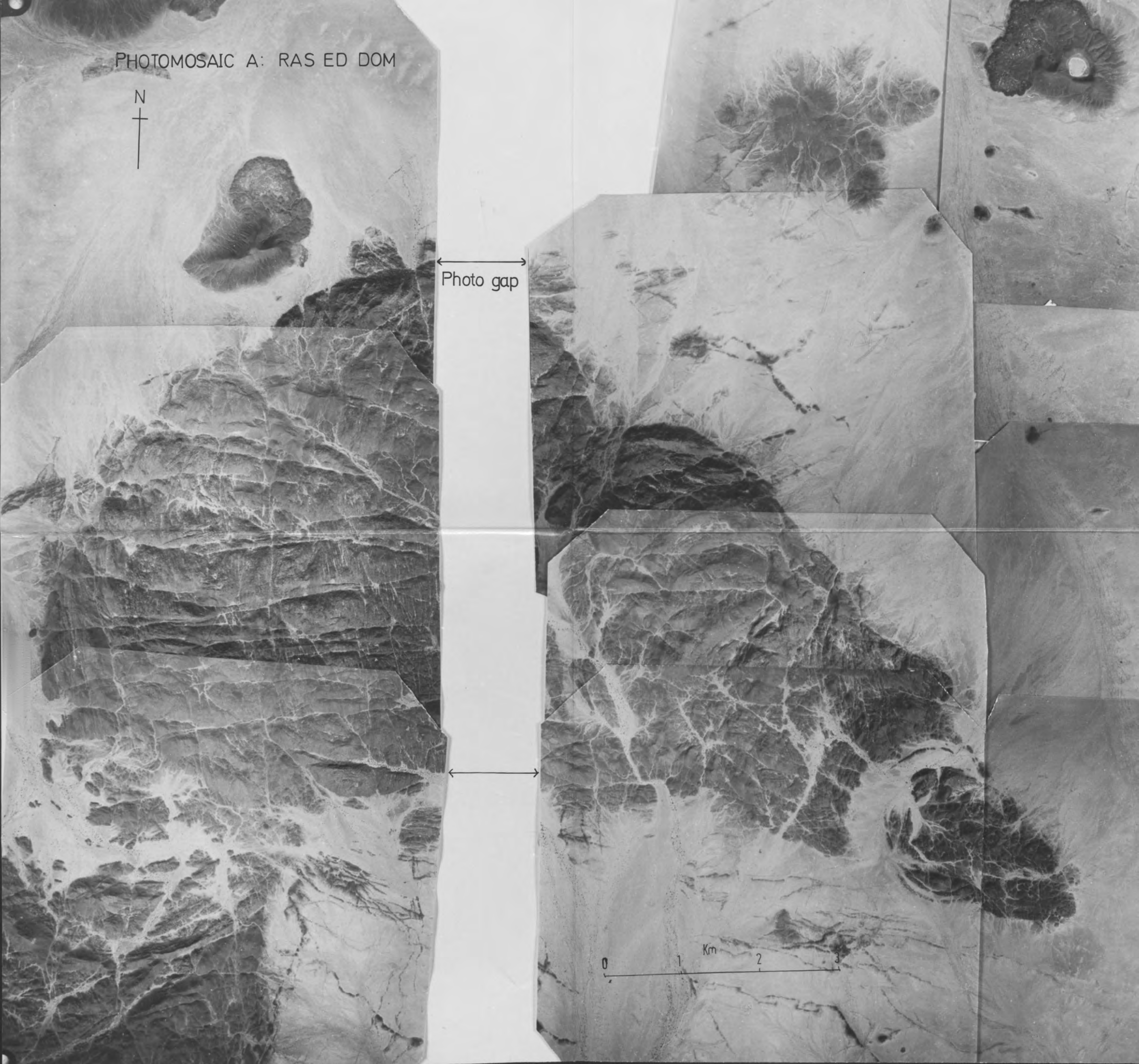
PHOTOMOSAIC A: RAS ED DOM
N
Photo gap
Km
0
1
2
3

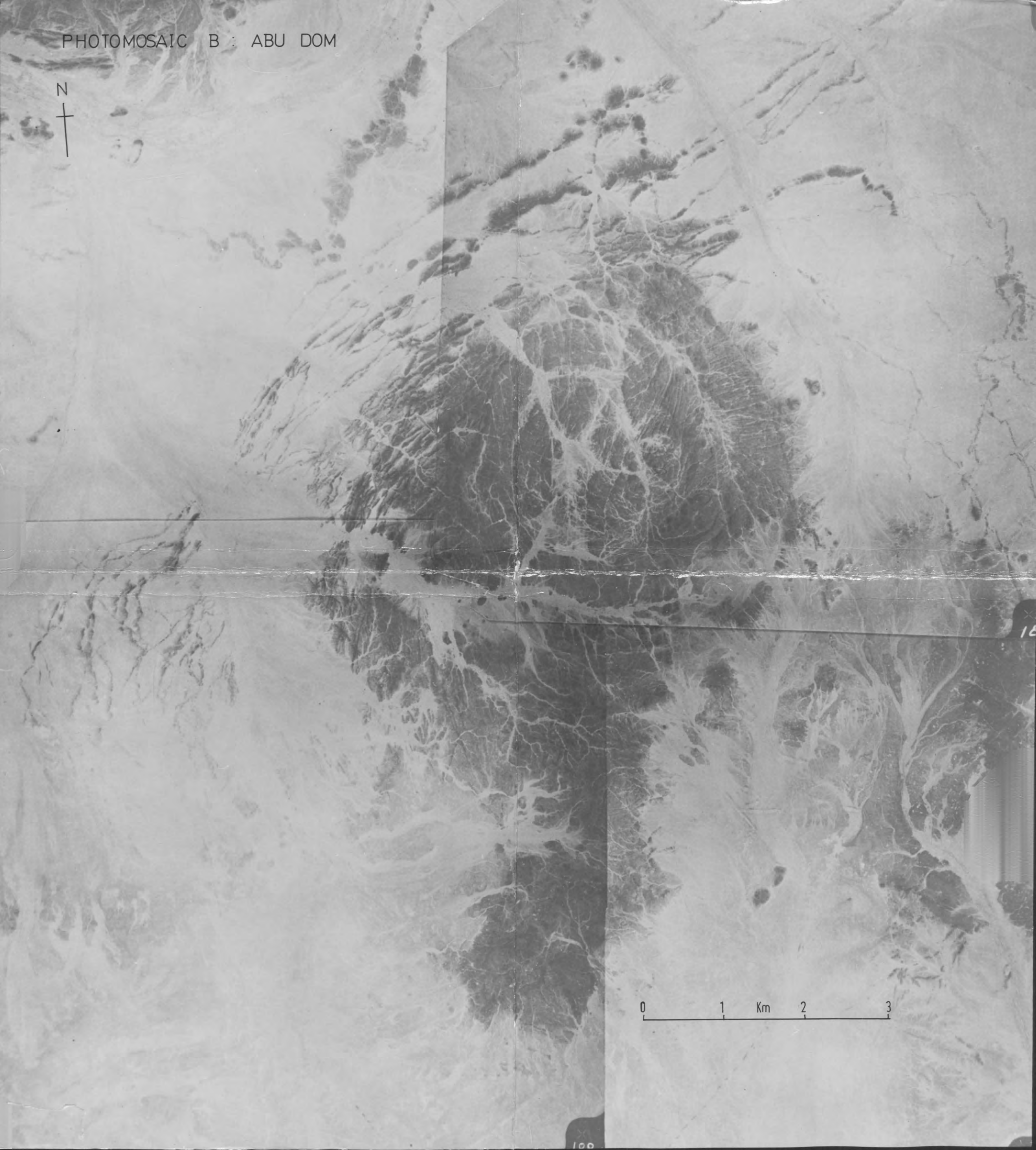

PHOTOMOSAIC B : ABU DOM